

From small scales to large scales –The Gulf of Finland Science Days 2017

9th – 10th October 2017
Estonian Academy of Sciences, Tallinn



**Gulf of Finland
Co-operation**

PRESENTATIONS



CONTENTS

Presentations Day 2 • 10th October 2017

MORNING • SESSION A

- 1 V. Tarbaeva, E. Vorobyeva
“Helcom “Hot spots”. Current status and plans for elimination. Russian overview from the catchment area of the Gulf of Finland
- 2 Y. Polyak
Toxic cyanobacteria of the eastern Gulf of Finland: their ecology, toxicological effects, and control
- 3 S. Golubkov, N. Berezina, Y. Gubelit, A. Demchuk, M. Golubkov, A. Tiunov
Contribution of the carbon from green tides in the coastal food webs in the eastern Gulf of Finland: stable-isotope estimate using Bayesian mixing model
- 4 Y. Gubelit, N. Berezina, Y. Polyak, T. Shigaeva, G. Dembska, G. Pazikowska-Sapota, M. Polyak, V. Kudryavtseva
“Green tides” in the eastern Gulf of Finland: factors affecting the biomass accumulation and its consequences for the coastal zone
- 5 M. Golubkov, S. Golubkov
Influence of weather conditions on midsummer primary production and mineralization of organic matter in the Neva Estuary (eastern Gulf of Finland, Baltic Sea)

MORNING • SESSION B

- 6 A. Giudici, J. Kalda, T. Soomere
Patchiness of the sea surface under the combined effect of winds and currents
- 7 N. Kudryavtseva, K. Pindsoo, T. Soomere
Non-stationary extreme value modeling of trends in extreme water levels in the Gulf of Finland
- 8 V. Ryabchenko, I. Leontyev, D. Ryabchuk, A. Sergeev, A. Dvornikov, S. Martyanov, V. Zhamoïda
Coastal erosion caused by storm surges and protection measures for the Kotlin Island’s coastline in the Gulf of Finland: data analyses and modeling
- 9 V. Zhurbas, J. Laanemets, U. Lips, G. Väli
Eulerian and Lagrangian submesoscale coherent structures on the sea surface driven by coastal upwelling: a case study for the Gulf of Finland

AFTERNOON

- 10 J. Harff
What determines the dynamics of Baltic Sea coasts?
- 11 K. Herkül, R. Aps
Spatial overlap of nature values, protected areas, and human uses in the Baltic Sea
- 12 P. Ekholm, J. Riihimäki, J. Linjama, M. Ollikainen, E. Punttila, S. Puroila, A-K. Koskenius
Reducing agricultural phosphorus load by gypsum: results from the first year after amendment

AFTERNOON

- 13 P. Yli-Hemminki, K. Jörgensen, J. Lehtoranta
Iron–manganese concretions contribute to benthic release of phosphorus and arsenic in anoxic conditions in the Gulf of Finland
- 14 D. Ryabchuk, H. Vallius, V. Zhamoïda, A. Kotilainen, A. Rybalko, N. Malysheva, N. Deryugina, L. Sukhacheva
Sedimentary processes and pollution history of Neva Bay bottom sediments (eastern Gulf of Finland, Baltic Sea)
- 15 S. Kholodkevich, T. Kuznetsova, A. Kurakin, A. Sharov
Development of a new approach in the assessment of biological effects of pollution in the Gulf of Finland
- 16 E. Mikhailova, L. Barabanova
Implication of genetic approaches for biosystem state and dynamics survey of the Gulf of Finland.
- 17 A. Rybalko, O. Korneev, A. Pedchenko, D. Ryabchuk
Facies features (geodiversity) of sedimentation in the Eastern Gulf of Finland and their use for proper assessment of the results of geochemical monitoring of hazardous substances.
- 18 K. Rubtsova, T. Mironenko, E. Daev
Preliminary assessment of water and sediment pollutions in littoral zone of the Kotlin Island.
- 19 G. Frumin, Y. Fetisova
Dynamics of water quality of the transboundary river Narva

From small scales to large scales
–The Gulf of Finland Science Days 2017
9th-10th October 2017
Estonian Academy of Sciences, Tallinn

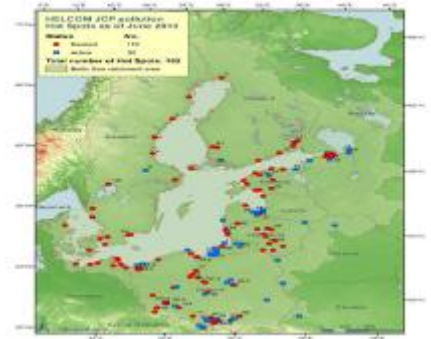
2nd Day



**Gulf of Finland
Co-operation**

V.Tarbaeva, E.Vorobyeva

**“Helcom “Hot spots”. Current status and plans for
elimination. Russian overview from the catchment
area of the Gulf of Finland**



GENERAL INFORMATION

WHY NOW?

Contract with the Ministry of Natural Resources and Environment of the Russian Federation

Lead partner

Russian State Hydrometeorological University

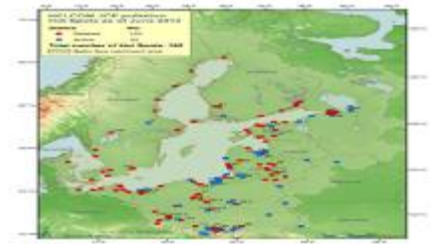
Partners

NGO “Union for conservation of nature” – St-Petersburg and Leningrad region

BIEH (Baltic Institute of hydrosphere ecology) - Kaliningrad

ToR for NGO “Union for conservation of nature”

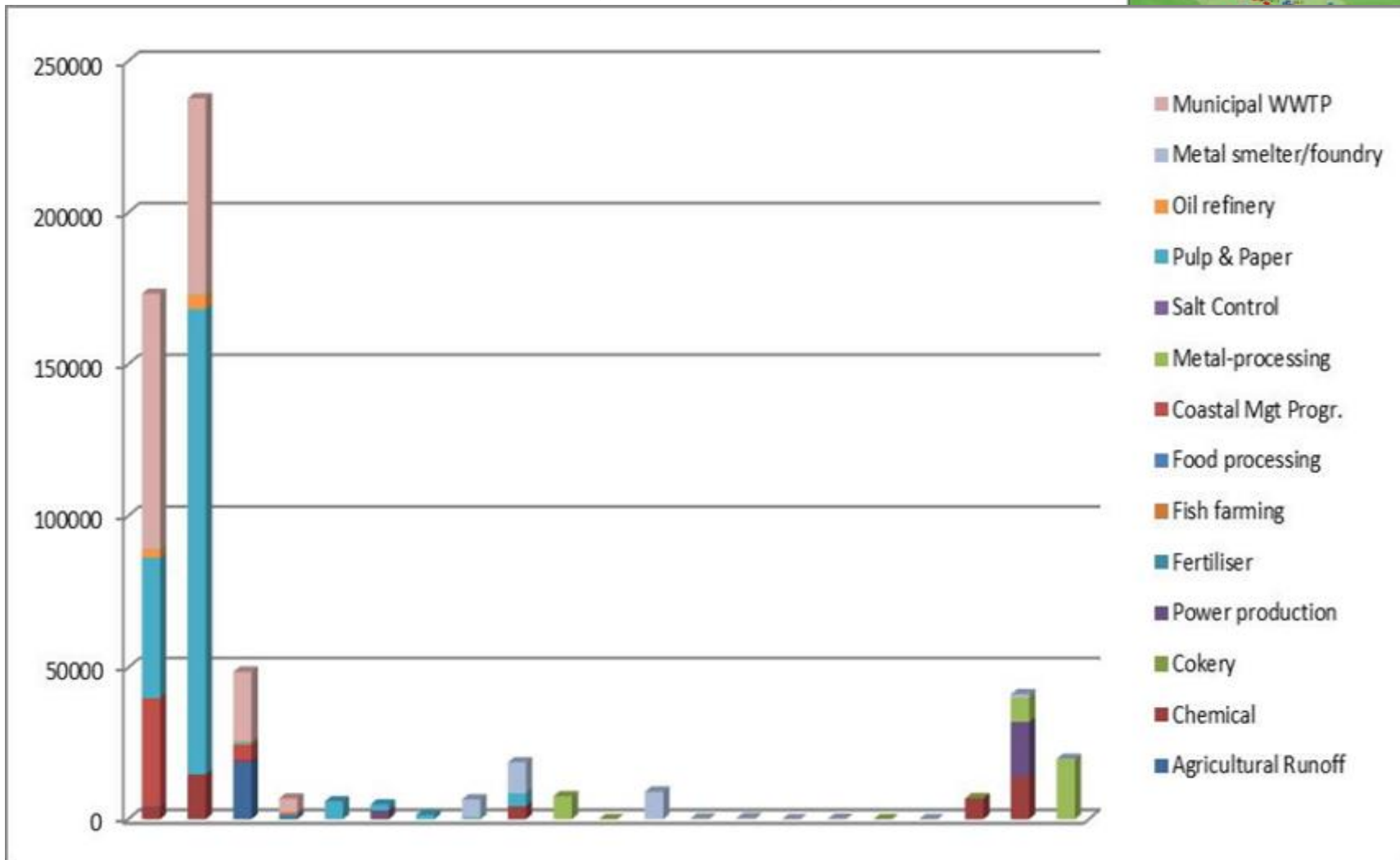
Evaluation of current situation of the Russian “Hot spots” (location in St-Petersburg and Leningrad region) and elaboration applications for elimination.



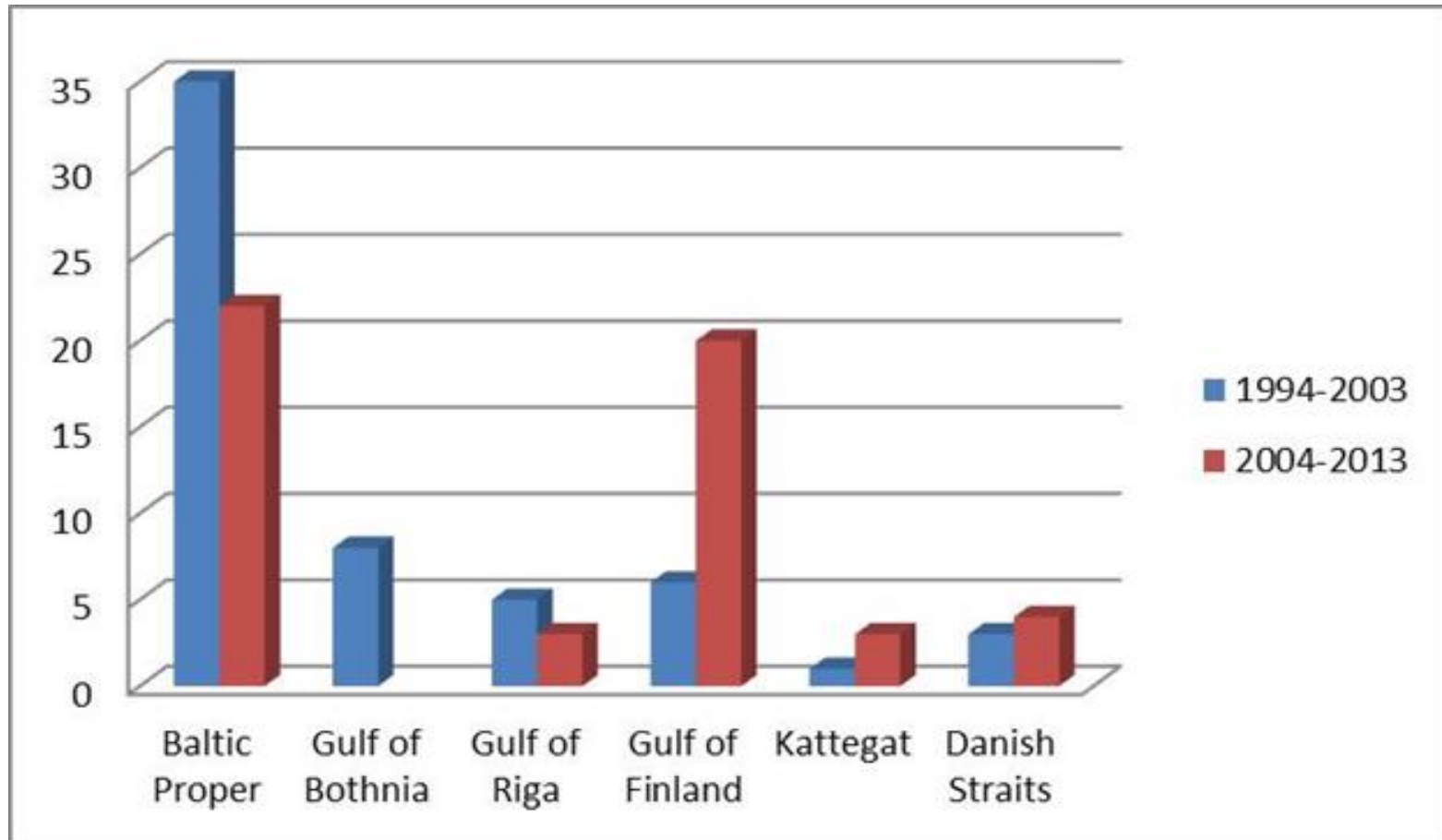
HISTORY. MAIN POINTS

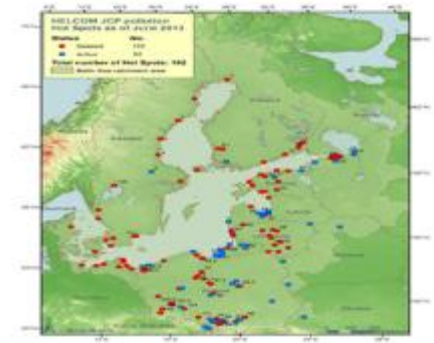
- The Baltic Sea Joint Comprehensive Environmental Action Programme (JCP) was established in 1992 for the long-term restoration of the ecological balance of the Baltic Sea.
- The programme was designed to have been completed by 2012 at the latest.
- With one third of original hot spots still remaining in the list, there is a need to continue the work on remediation of the remaining 52 pollution sites, till the very last of those will be removed from the List.
- HELCOM Ministerial Meeting in Copenhagen assessed the effectiveness of the implementation of the HELCOM JCP (1992--2012) and noted the need for its prolongation. The active hotspots have to be included into national Baltic Sea Action Plans.

POLLUTION LOAD REDUCTIONS FROM DELETED HOT SPOTS (1994-2013)



NUMBER OF DELETED HOT SPOTS PER SUB-BASIN PER PERIOD, 1994- 2003 AND 2004-2013





GULF OF FINLAND

5 hot spots located in St-Petersburg

- №18 (sub-spots 18.1 – 18.19). Municipal waste water treatment
- № 23 Hazardous waste Landfill “Krasniy Bor”

Leningrad region

- № 14 «Sysskiy Pulp and Paper Mill»
- № 15 «Volkhov Aluminium Plant»
- № 24 «Large livestock farm (sewage water treatment and sediment treatment)»

INTERIM RESULTS



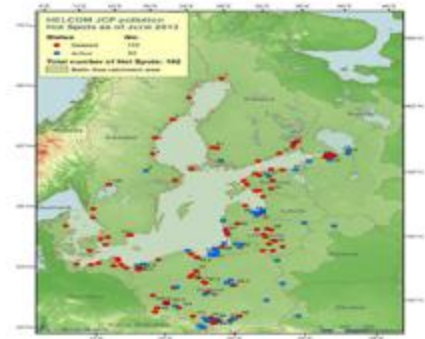
HS #	Hot spot name	Situation in 2013	Progress in 2017
18.1	Municipal sewage water treatment in St. Petersburg, The sewage collectors	The application for exclusion of the hot sub-spot № 18.1 was submitted at the 19 th meeting of the HELCOM LAND Group in 2014.	Was deleted
18.11	Municipal sewage water treatment in St. Petersburg, WWTP Kolpino	To postpone the consideration of exclusion of these hot sub-spots from the list of “hot spots” until commissioning the treatment plants in these settlements after 2015	To postpone the consideration of exclusion after 2019 and 2023
18.15	WWTP Metallostroy		
23	Hazardous Waste Landfill -State Unitary Nature Conservation Enterprise (SUNE) Krasny Bor Landfill	To postpone the consideration of excluding the hot spot from the list of “Hot Spots” until commissioning the plant of hazardous waste treatment after 2015.	Urgent plan to eliminate environmental damage at Krasnyi Bor landfi. Recultivation will be done/



INTERIM RESULTS

HS #	Hot spot name	Situation in 2013	Progress in 2017
14	Syasskiy Pulp and Paper Mill (PPM)	Solution of the enterprise ecological problems is associated with high financial costs. The problem of exclusion of the enterprise from the “hot spots” list cannot be quickly solved now without the investment support.	No any progress
15	Volkhov Aluminium Plant (Limited Liability Company “Metankhim)	As far as the “Volkhov Aluminium Plant” was divided into three independent enterprises: № 15.1 Limited Liability Company “Parosilovoe Hozyaystvo - Volkhov” - № 15.2. VAZ-SUAL of OJSC “SUAL” № 15.3 Limited Liability Company “Metakhim”	15.1 – will be nominated 15.2 – will be nominated 15.3 – wait their answer
24	“Large livestock farms (sewage water treatment and sediment treatment)”	Introduction of the Technological regulations for handling manure and dung at all large livestock enterprises of the Leningrad Region will allow to reduce significantly the nutrients load on the Baltic Sea and to exclude the agricultural sector of the Region from the HELCOM’s List	Progress but it needs time to establish system of manure management for the region.

TS HAVE A PROGRESS AND RUSSIA WILL SHOW POSITIVE TREND IN POLLUTION DECREASING





Welcome your comments and proposals!

priodasouz@yandex.ru

www.nature-union.ru

From small scales to large scales
–The Gulf of Finland Science Days 2017
9th-10th October 2017
Estonian Academy of Sciences, Tallinn

2nd Day



**Gulf of Finland
Co-operation**

Y. Polyak

Toxic cyanobacteria of the eastern Gulf of Finland: their ecology, toxicological effects, and control

Toxic cyanobacteria of the eastern Gulf of Finland: their ecology, toxicological effects, and control

Yulia Polyak

*Saint-Petersburg Scientific-Research Centre for Ecological
Safety, Russian Academy of Sciences*

St. Petersburg State University



Cyanobacterial bloom in the Eastern Gulf of Finland, 2015



Key cyanotoxin exposure routes:

- Oral intake through contaminated water;
- Recreational activities (swimming - dermal contact);
- The bioaccumulation of cyanotoxins in the food web.



Cyanobacteria

✓ Cyanobacteria have been around for 2 billion years and contributed to the generation of oxygen in the Earth's atmosphere;

✓ Cyanobacteria are microscopic but populations can be visible as benthic mats, scums, large gelatinous colonies or blooms;

✓ Research on toxicity of cyanobacteria began in 19th century;

✓ Over the past decades there has been an expansion in the awareness of toxic cyanobacterial blooms and reports of these events.



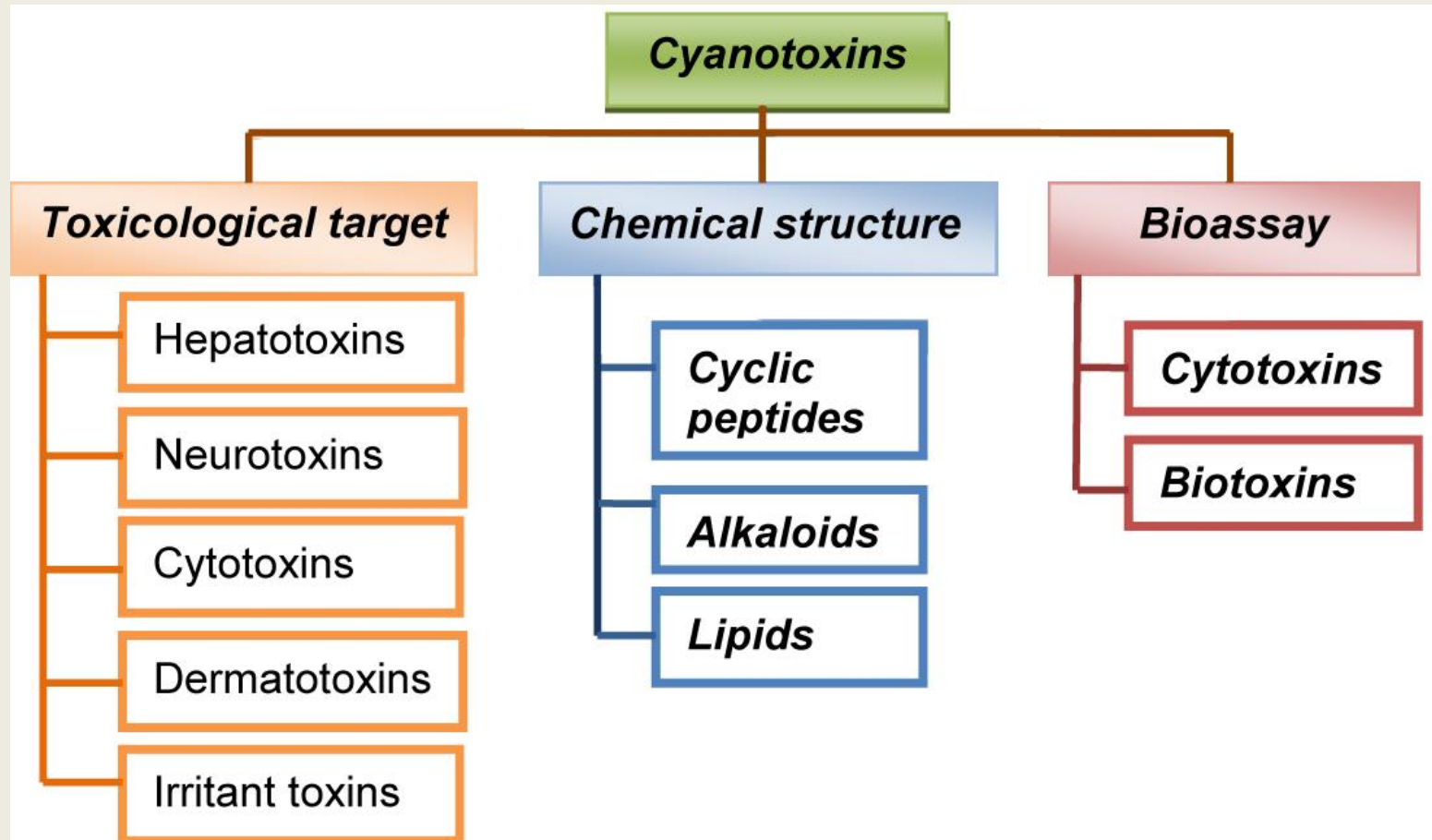


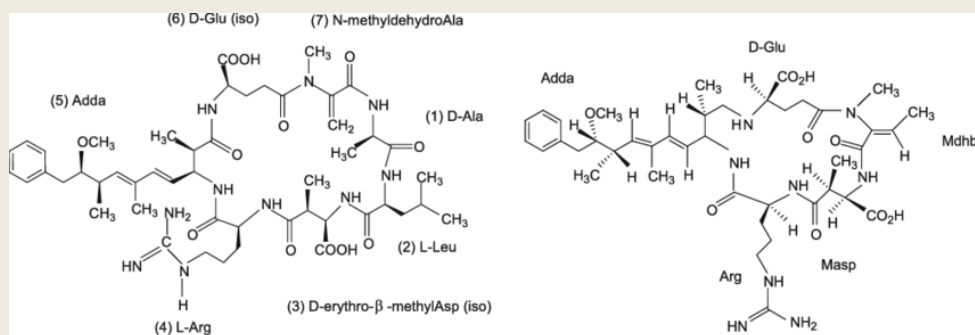
*Cyanobacterial bloom (Microcystis)
in Pavlovsk, St. Petersburg, 2013*

The increasing distribution of toxic cyanobacteria in 20th-21st centuries can be caused by

- Eutrophication of surface water;
- Population pressure;
- Global warming;
- Increased monitoring/awareness;
- Other factors?

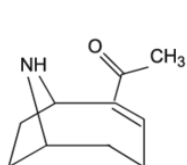
Classification of cyanotoxins on the basis of toxicological target, chemical structure, and bioassay



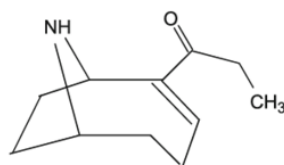


Microcystin-LR

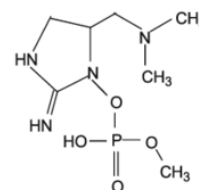
Nodularin



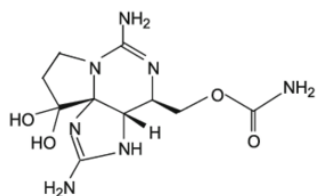
Anatoxin-a



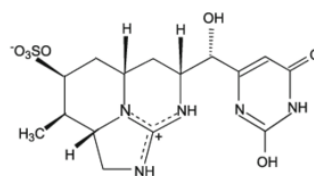
Homoanatoxin



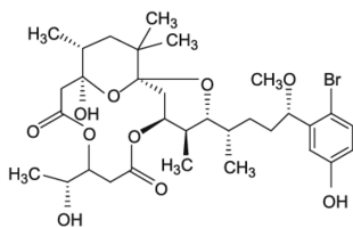
Anatoxin (a)-s



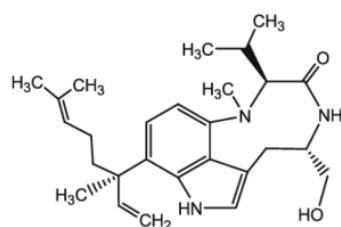
Saxitoxin



Cylindrospermopsin



Aplysiatoxin

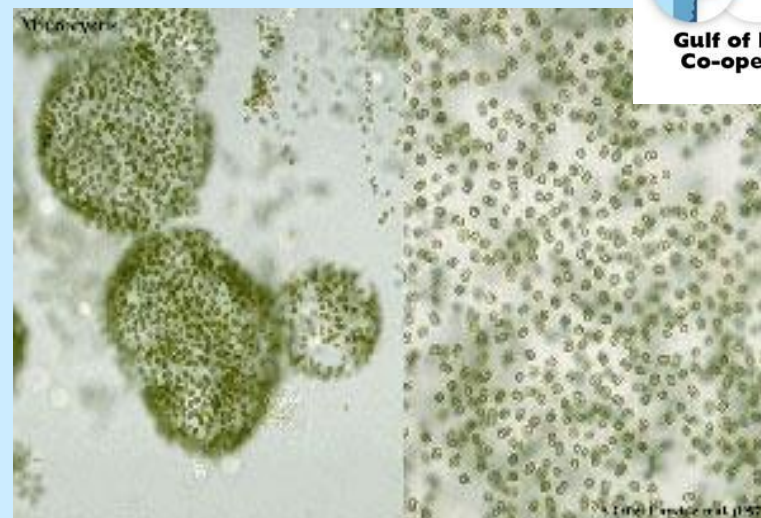


Lyngbiatoxin-a

*Chemical structure of
cyanotoxins*



Anabaena



Microcystis



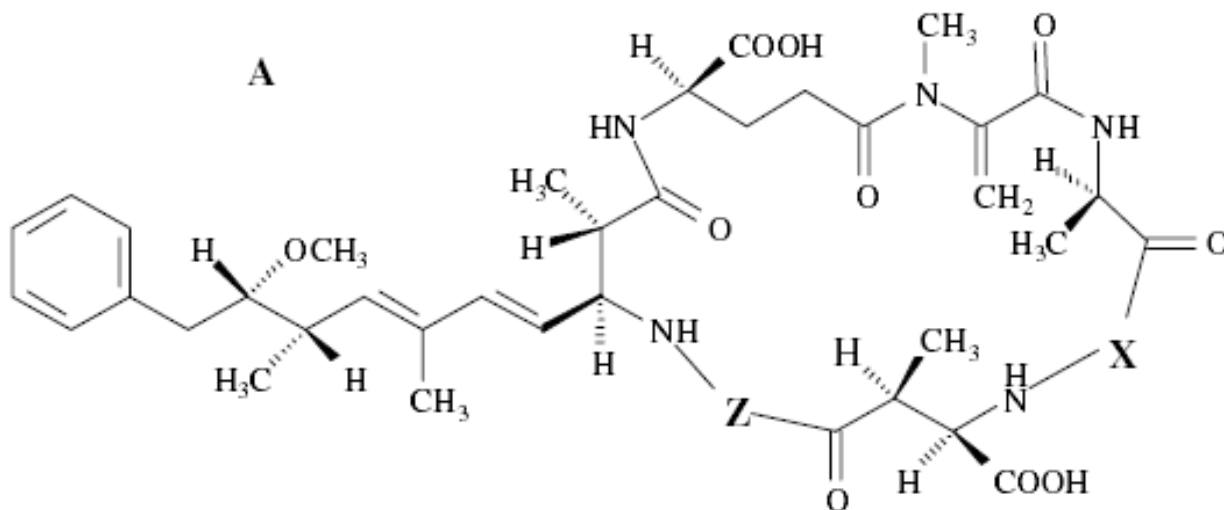
Aphanizomenon



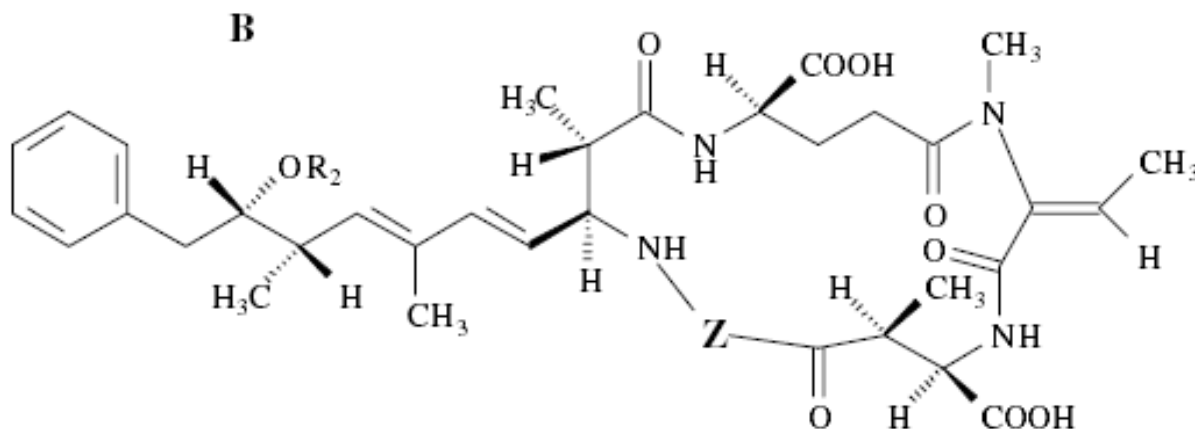
Planktothrix

Cyanobacterial toxins

Cyanobacterial toxin	Producing genera/species	Toxic mechanism	LD ₅₀ (µg/kg)
Microcystin -LR	<i>Microcystis</i> , <i>Oscillatoria</i> (<i>Planktothrix</i>), <i>Anabaena</i> , <i>Nostoc</i> , <i>Phormidium</i> et al.	Hepatotoxic, inhibition of eukaryotic protein phosphatases of type 1 and 2A	50
Microcystin-RR			600
Nodularin			<i>Nodularia spumigena</i>
Anatoxin-a	<i>Anabaena</i> , <i>Aphanizomenon</i> , <i>Oscillatoria</i> (<i>Planktothrix</i>), <i>Phormidium</i>	Neurotoxic, mimics the neurotransmitter acetylcholine	375
Homoanatoxin-a			250
Anatoxin-a(s)			20
Saxitoxin	<i>Anabaena</i> , <i>Aphanizomenon</i> , <i>Cylindrospermopsis</i> , <i>Lyngbya</i> , <i>Planktothrix</i>	Neurotoxic, blocks voltage-gated Na ⁺ channels	10
Cylindrospermopsin	<i>Anabaena</i> , <i>Aphanizomenon</i> , <i>Cylindrospermopsis</i> , <i>Umezakia</i>	Hepatotoxic, cytotoxic, neurotoxic; inhibition of glutathione synthesis, protein synthesis and cytochrome P450	200
Aplysiatoxin	<i>Lyngbya</i> , <i>Oscillatoria</i> (<i>Planktothrix</i>), <i>Schizothrix</i>	Tumor promoting, binds to protein kinase C (PKC)	100
Lyngbyatoxin	<i>Lyngbya</i> , <i>Oscillatoria</i> (<i>Planktothrix</i>), <i>Schizothrix</i>		250



(A) Microcystins:
 MC-RR (Z=Arg, X=Arg);
 MC-YR (Z=Tyr, X=Arg);
 MC-LR (Z=Leu, X=Arg);
 MC-LA (Z=Leu, X=Ala);
 MC-LW (Z=Leu,
 X=Trp);
 MC-LF (Z=Leu,
 X=Phen).



(B) Nodularin-R
 (Z=Arg)

Chemical structures of hepatotoxins (A) microcystins and (B) nodularin
 (X and Z - variable L-amino acids)

Hepatotoxin concentrations in water bodies

Location	Toxic samples (all samples)	Toxins	Concentration ($\mu\text{g}/\text{kg}$ dry biomass)	Reference
Denmark	198 (296)	MC	5-1,900	Henriksen et al., 1996
Germany	385 (533)	MC	1-5,000	Fastner, 1998
Finland	17 (20)	MC-LR	> 10-800	Lahti, 1997
Baltic Sea	6 (16)	Nodularin	300-18,000	Kononen, 1993
Poland	31 (40)	MC	100-6000	Izydorczyk et al, 2008
France	16 (22)	MC	70-3,970	Vezie, 1997
China	5 (10)	MC-RR, MC-LR	200-7,300	Zhang et al., 1991
Australia	4	MC	2,100-4,100	Jones, 1995

Cyanotoxins in the Eastern Gulf of Finland and freshwater ecosystems of Russian Northwest region

Location	Toxins	Dominated cyanobacteria	Reference
Eastern GoF, Neva Bay	Microcystin-LR, [DMAdda ⁵]microcystin-LR	<i>M. aeruginosa</i> , <i>Planktothrix agardhii</i>	Voloshko, Safronova 2015; Voloshko 2016
Eastern GoF, Inner Estuary	Micropeptins, oscillapeptin, anabaenopeptin, aeruginosins	<i>M. aeruginosa</i>	Voloshko, Safronova 2015
Ladoga Lake	Microcystin-LR, microcystin-RR, microcystin-VF, [d-Asp ³ ,Dha ⁷]microcystin-LR	<i>Microcystis</i> spp., <i>Anabaena</i> spp., <i>Aphanizomenon flos-aquae</i>	Voyakina 2007; Voloshko et al. 2008; Voloshko, 2016
Sestroretskij Razliv Lake	14 microcystin variants (microcystin-LR, demethyl- MC -LR, microcystin-RR, microcystin-YR, etc.), anatoxin-a	<i>Microcystis</i> spp., <i>Aphanizomenon flos-aquae</i> , <i>Dolichospermum planctonicum</i>	Chernova et al. 2016; Chernova et al. 2017
Lower Suzdal Lake	9 microcystin variants, anatoxin-a	<i>P. agardhii</i> , <i>A. flos-aquae</i>	Chernova et al. 2016

Toxicity of the most frequently detected cyanotoxins in comparison to other known toxins

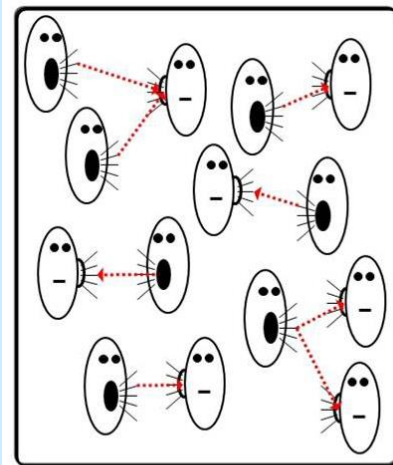
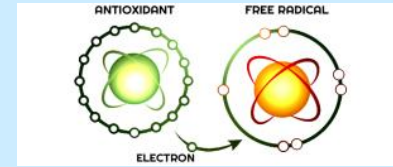
Toxin	Chemical nature	Source	LD ₅₀
Ricin	Glycoprotein	Castor bean <i>Ricinus communis</i>	22
Microcystin-LR	Cyclic peptide	Cyanobacteria	50
Cobra venom	Polypeptide	Egyptian <i>Naja haje</i> cobras	185
Anatoxin-a	Alkaloid	Cyanobacteria	200
Sarin	Organophosphate, war gas	synthetic	218
Microcystin-RR	Cyclic peptide	Cyanobacteria	300-600
Curare	Alkaloids (e.g. d-tubocurarine)	Plants (e.g. <i>Strychnos toxifera</i>)	500
Strychnine	Alkaloid	<i>Strychnos</i> plants	2 500/980
Hydrogen cyanide	HCN	Plants	10 000

LD₅₀ (µg/kg) - the acute toxicity in mice (intra-peritoneal)

Ecological role of cyanotoxin

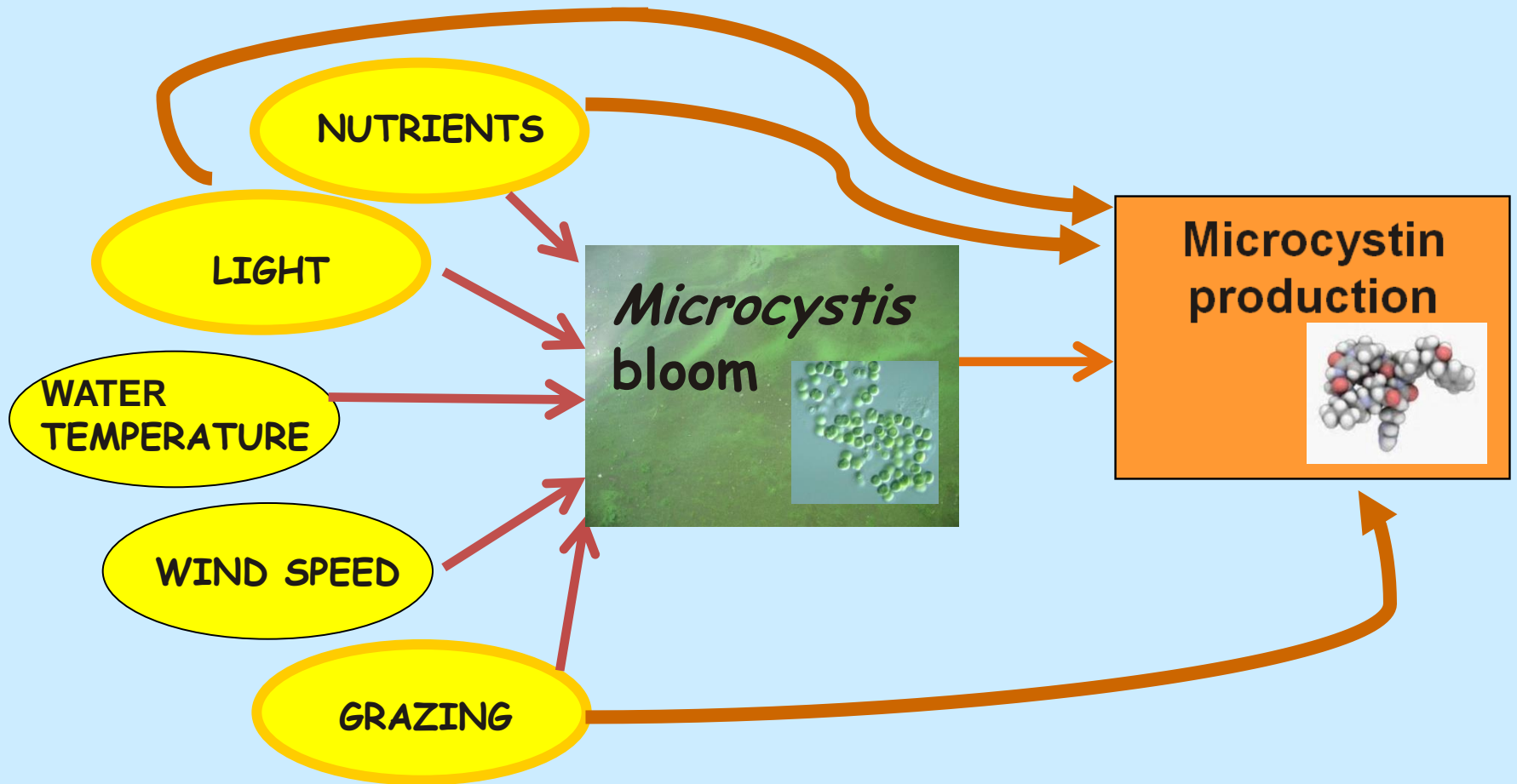
"Competitive advantage" or "physiological aide"?

- ❖ A functional role in protecting proteins from oxidative damage;
- ❖ A role in colony formation by regulating polysaccharide biosynthesis genes;
- ❖ Grazing defense mechanism, allelopathy;
- ❖ May act as a signaling molecule;
- ❖ Other?



  : Cyanobacteria
.....→ : Signal molecules

Environmental factors influencing growth and toxin production in *Microcystis*



Positive impacts on the development of cyanobacteria

- Growth stimulation is observed in response to both N and P additions;
- Warmer temperatures (>25 °C) favor surface bloom-forming cyanobacteria. Microcystin concentrations are generally highest between 20 and 25 °C;
- Vertical stability through stratification and long water replacement times favor cyanobacteria over eukaryotic phytoplankton;
- Salinization can favor some salt-tolerant bloom-forming cyanobacteria (*Microcystis aeruginosa* remain unaffected by salinities up to 10%).

Negative impacts on the development of cyanobacteria

- Decreasing N and P inputs;
- Increasing flushing rates;
- Mixing and phytoplankton entrapment below the photic zone;
- Cold temperatures;
- Among the zooplankton, smaller protozoan species are generally more capable of grazing *Microcystis* than larger grazers (including daphnids and copepods).

Key factors involved in bloom control

Biotic factors

- grazing,
- bacterial interactions,
- viral lysis.

Physical factors

- cooler temperatures,
- water column destratification,
- high turbidity,
- increased wind velocities.

Removal

Cyanobacterial cells

coagulation

flocculation

sedimentation

filtration

disinfection

Toxins

adsorption

photolysis

chlorination

ozonization

ultrasounding

electrochemical
oxidation

biodegradation

Recommendations:

- Monitoring;
- Prevention;
- Increase awareness;
- Continuation of research.

Conclusions

- Cyanobacteria that occur in the Eastern GoF and Northwest region produce dozens of toxic substances. Commonly reported are microcystins, anatoxin-a and a variety of bioactive peptides;
- Microcystins are the most often detected cyanotoxins in the Eastern GoF and freshwater ecosystems of Russian Northwest region;
- Our understanding of the variability in cyanotoxin diversity in the Eastern GoF is relatively unknown, and the ability to predict cyanotoxin concentrations remains obscure.
- The efforts focused solely on microcystins may be inadequate to protect public health.
- To limit health risks, regular monitoring of the eastern Gulf of Finland and risk assessment of cyanotoxins are necessary.



*Thank you
for your attention!*

From small scales to large scales
–The Gulf of Finland Science Days 2017
9th-10th October 2017
Estonian Academy of Sciences, Tallinn

2nd Day



**Gulf of Finland
Co-operation**

S. Golubkov, N. Berezina, Y. Gubelit, A. Demchuk, M. Golubkov, A. Tiunov

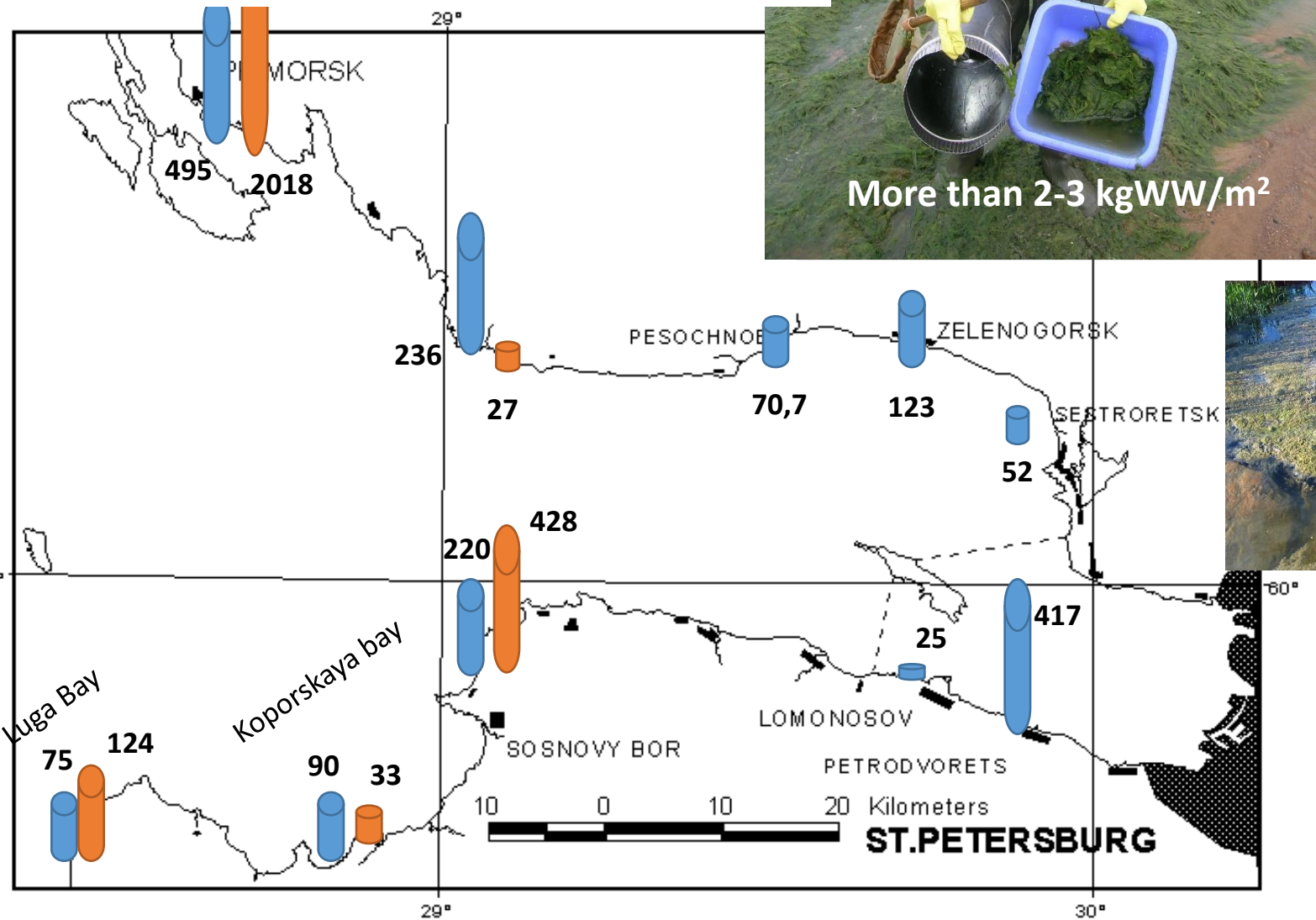
Contribution of the carbon from green tides in the coastal food webs in the eastern Gulf of Finland: stable-isotope estimate using Bayesian mixing model



Contribution of the carbon from green tides in the coastal food webs in the eastern Gulf of Finland: stable-isotope estimate using Bayesian mixing model

**Sergey Golubkov, Nadezhda Berezina,
Yulia Gubelit, Anna Demchuk, Mikhail
Golubkov, Alexei Tiunov**

Biomass of macroalgae (gDW m⁻²) in the eastern Gulf of Finland in 2014



Depth
 0,5 m
 1,5 m

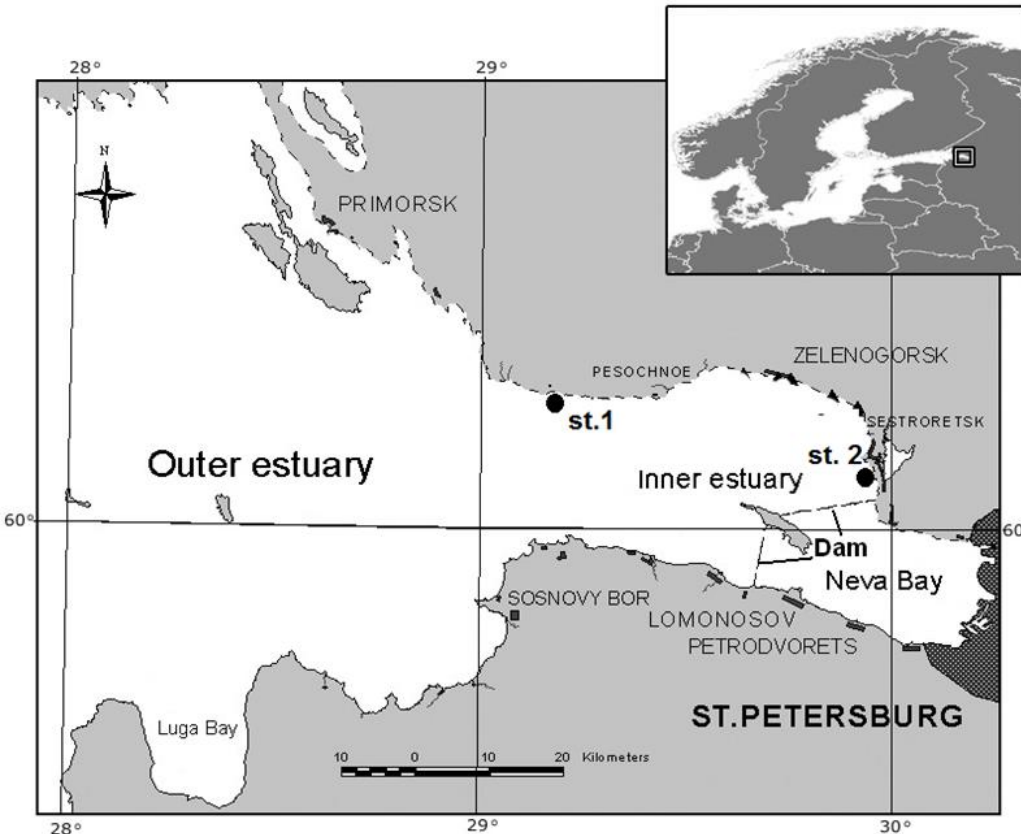


Green tides of macroalgae *Cladophora glomerata* and *Ulva intestinalis* in summer time is one of the major environmental problems in the shallow coastal zone of the eastern Gulf of Finland

Aim of the study and methods

We to test a hypothesis that **organic carbon of macroalgae produced during green tides may be an important source of carbon supporting coastal food webs**

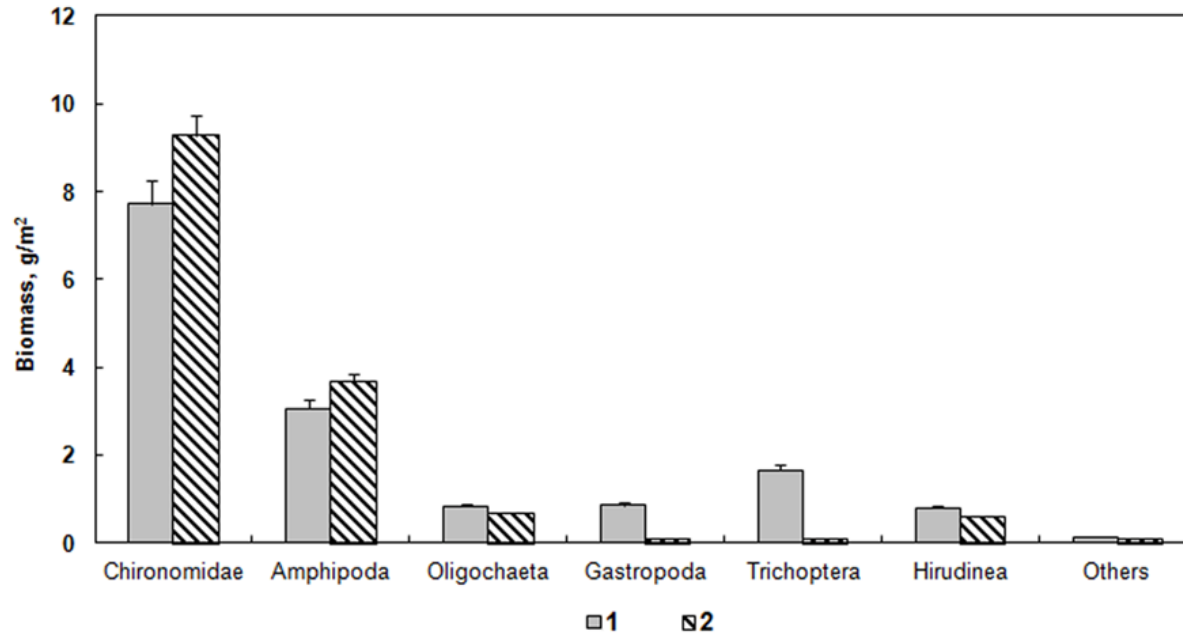
Stable isotope composition of carbon and nitrogen of suspended organic matter (seston) and tissues of macroalgae, macroinvertebrates and fish from two stations were analyzed to quantify basal resources of carbon used by various consumers.. The was used for estimating trophic links of the consumers based on their $\delta^{13}\text{C}$ and $\delta^{15}\text{N}$ values. We applied **Bayesian mixing model** running on R Software SIAR. This approach enables depicting a proportional contribution of different sources in the diet of a consumer relying on inherent isotopic variation between different resources. We also studied feeding patterns of fish to improve interpretation of SIAR's results



Biomass of macroalgae and macroinvertebrates

1. *Ulva intestinalis* dominated at the station 1. Its mean biomass was 200 ± 120 g DW/m². The biomass of *Cladophora glomerata* was 134 ± 21 g DW/m². No attached macroalgae were found at the station 2. Only a small amount of drifting *C. glomerata* was observed.

2



Gmelinoides fasciatus

Chironomids (Tanypodinae and Chironominae), alien amphipods *Gammarus tigrinus* (station 1) and *Gmelinoides fasciatus* (station 2) were abundant. Leeches *Erpobdella octoculata* and *Glossiphonia complanata*, gastropods (*Lymnaea ovata*, *Bithynia tentaculata*, *Theodoxus fluviatilis*) and larvae of caddisflies *Hydropsyche contubernalis* and *Agraylea multipunctata*, alien bivalve mollusks *Dreissena polymorpha* and native *Unio pictorum*, and several species of mayfly's larvae (*Caenis robusta*, *Ephoron virgo*, *Heptagenia sulphurea*) were common.

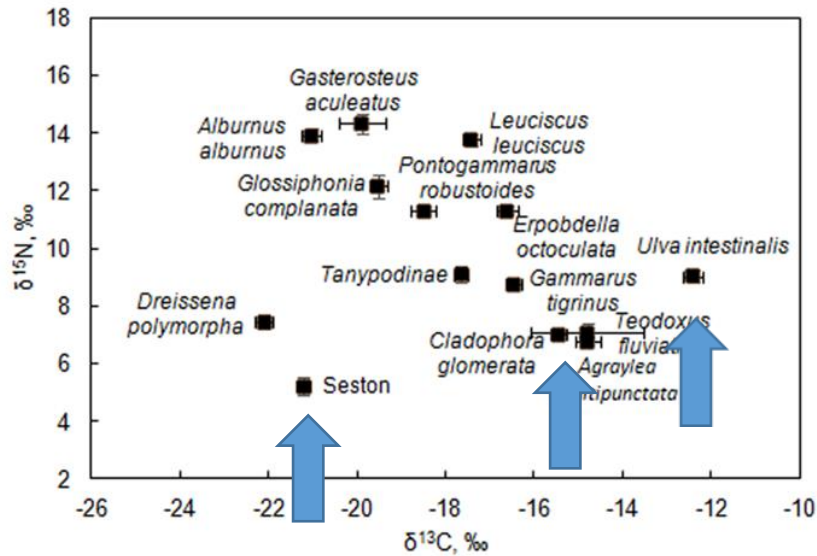
Frequency of occurrence (F) and the relative wet mass (I_i) of different prey in the stomachs of fish from two sampling station

Taxa	<i>Leuciscus leuciscus</i>		<i>Alburnus alburnus</i>		<i>Perca fluviatilis</i>		<i>Gasterosteus aculeatus</i>	
	F (%)	I (%)	F (%)	I (%)	F (%)	I (%)	F (%)	I (%)
<i>Alona</i> sp.	-	-	<10	0,19	-	-	-	-
<i>Eurytemora</i> sp.	-	-	-	-	-	-	40	21.15
<i>Bosmina</i> sp	-	-	40	2.32	-	-	-	-
<i>Daphnia cucullata</i>	-	-	45	89.9	-	-	-	-
<i>Chydorus sphaericus</i>	100	2.11	90	0.92	-	-	-	-
<i>Cricotopus</i> sp.	-	-	20	4.42	-	-	40	7.92
Chironomidae	100	95.67			-	-	-	-
Chironomidae pupae	-	-	<10	2.14	-	-	40	6.15
Diptera (imago)	50	2.22	<10	0.11	-	-		
<i>Gammarus</i> sp.	-	-	-	-	-	-	15	11.1
Gammaridae gen sp. juv	-	-	-	-	50	57.58	-	-
<i>Pontogammarus robustoides</i>	-	-	-	-	-	-	50	48.6
<i>G. aculeatus</i> eggs	-	-	-	-	-	-	25	0.67
<i>Osmerus eperlanus</i> juv.	-	-	-	-	-	-	25	4.41
<i>Perca fluviatilis</i> juv.	-	-	-	-	100	42.42	-	-

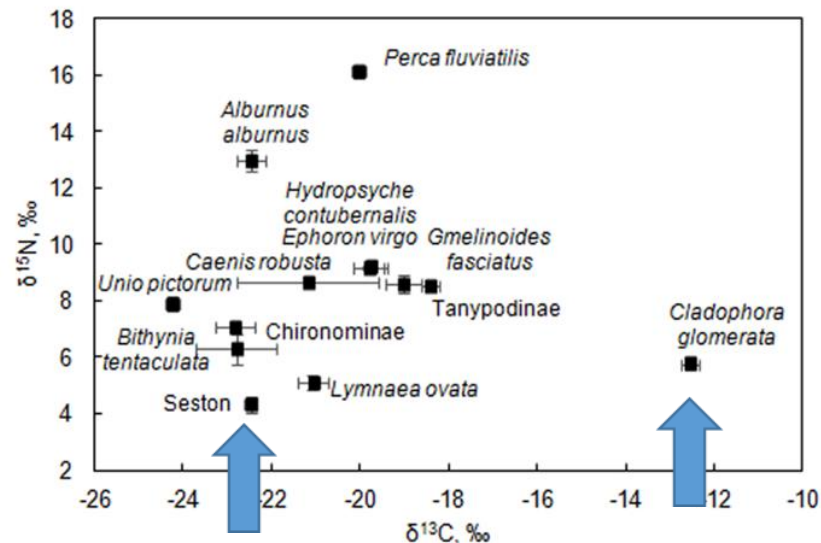
Four fish species were common at the sampling sites. The dace *L. leuciscus* was mostly benthivorous. The bleak *A. alburnus* was mostly planktivorous. Stickleback *G. aculeatus* had mixed type of feeding. Its diet included benthic invertebrates, plankton copepods *Eurytemora* sp. and a small number of juvenile specimens of smelt *Osmerus eperlanus*. The partly piscivorous perch *Perca fluviatilis* consumed gammarids and its own juveniles.

Isotope signatures ($\delta^{13}\text{C}$ and $\delta^{15}\text{N}$) of seston, macroalgae, common species of zoobenthos and fish at station 1 (A) and station 2 (B).

A



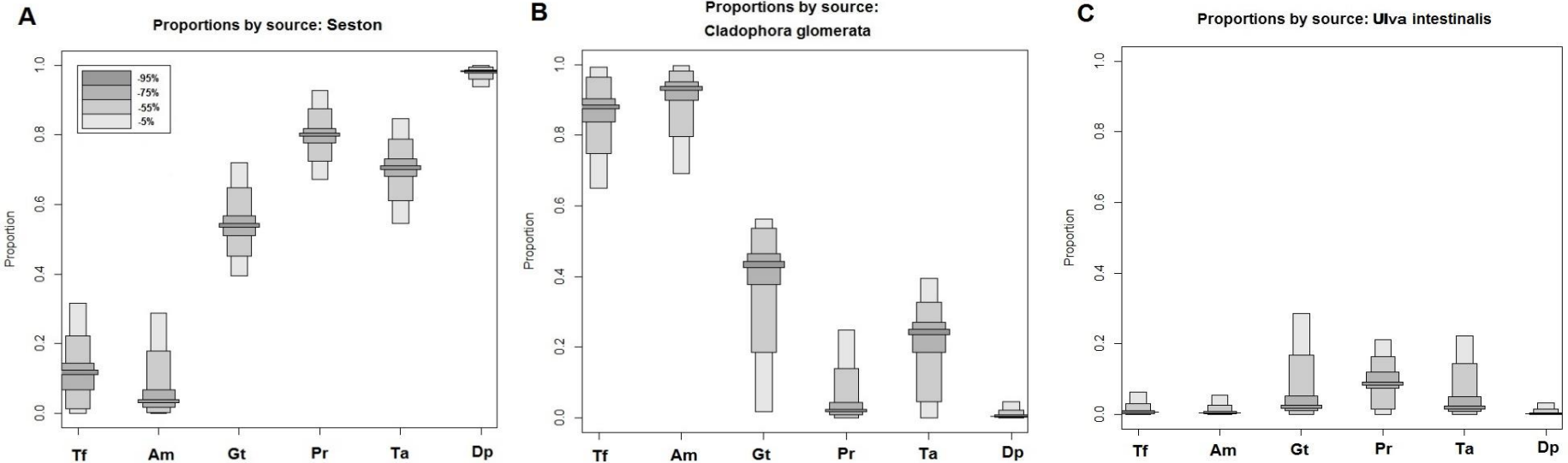
B



Stable isotope ratios of macroalgae varied within and among two sample stations. The $\delta^{13}\text{C}$ values of *Ulva intestinalis* were higher than the carbon isotope signatures of *Cladophora glomerata*. There was a strong isotopic separation between benthic and pelagic sources in the carbon isotope signatures. The $\delta^{13}\text{C}$ values of seston were considerably lower than the carbon isotope signatures of macroalgae at both sample stations.

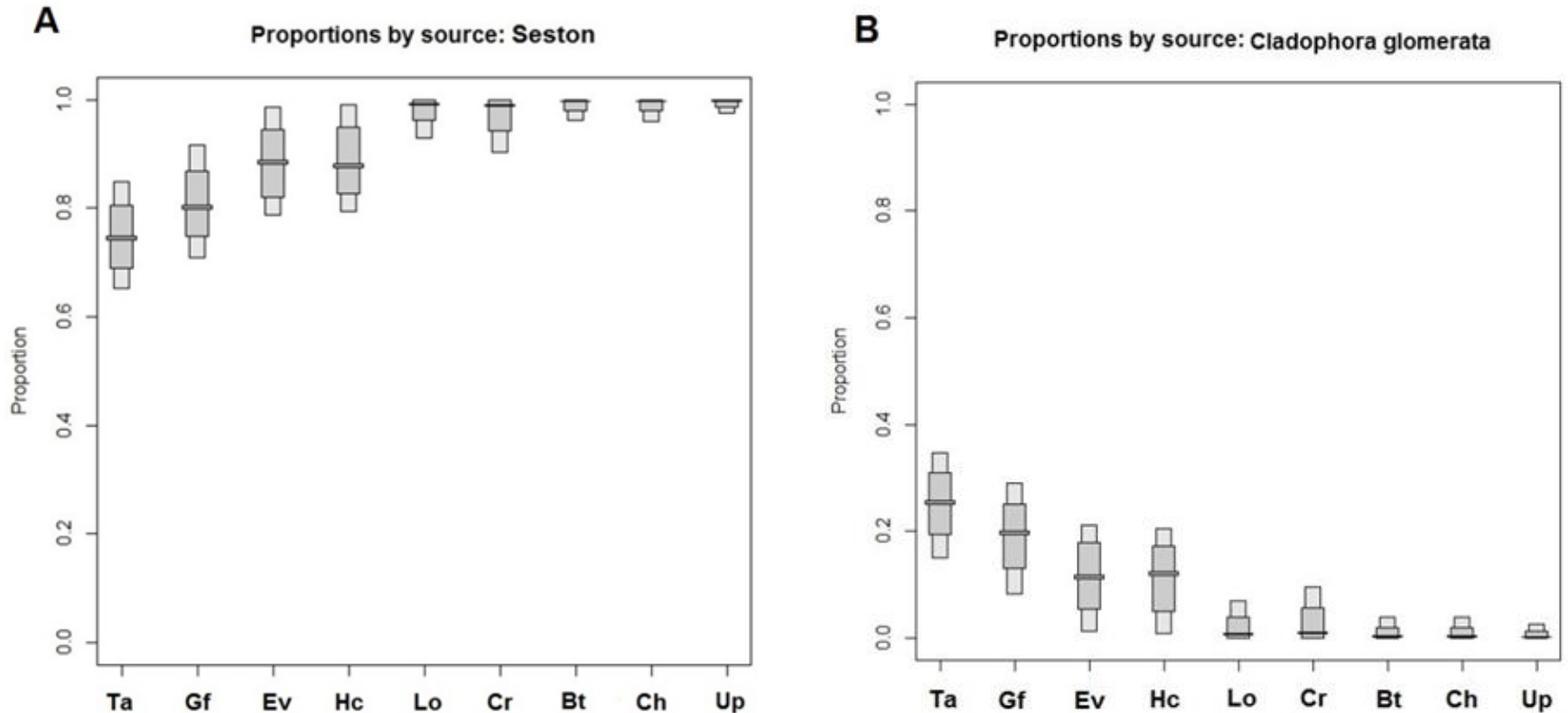
Results of SIAR modelling

Model SIAR estimates of use of different basal resources for non-predatory macroinvertebrate consumers at the station 1. The dark grey, grey, light grey and white are 95%, 75%, 55% and 5% credibility intervals. Tf – *Theodoxus fluviatilis*, Am – *Agraylea multipunctata*, Gt – *Gammarus tigrinus*, Pr – *Pontogammarus robustoides*, Ta – *Tanypodinae*, Dp – *Dreissena polymorpha*.



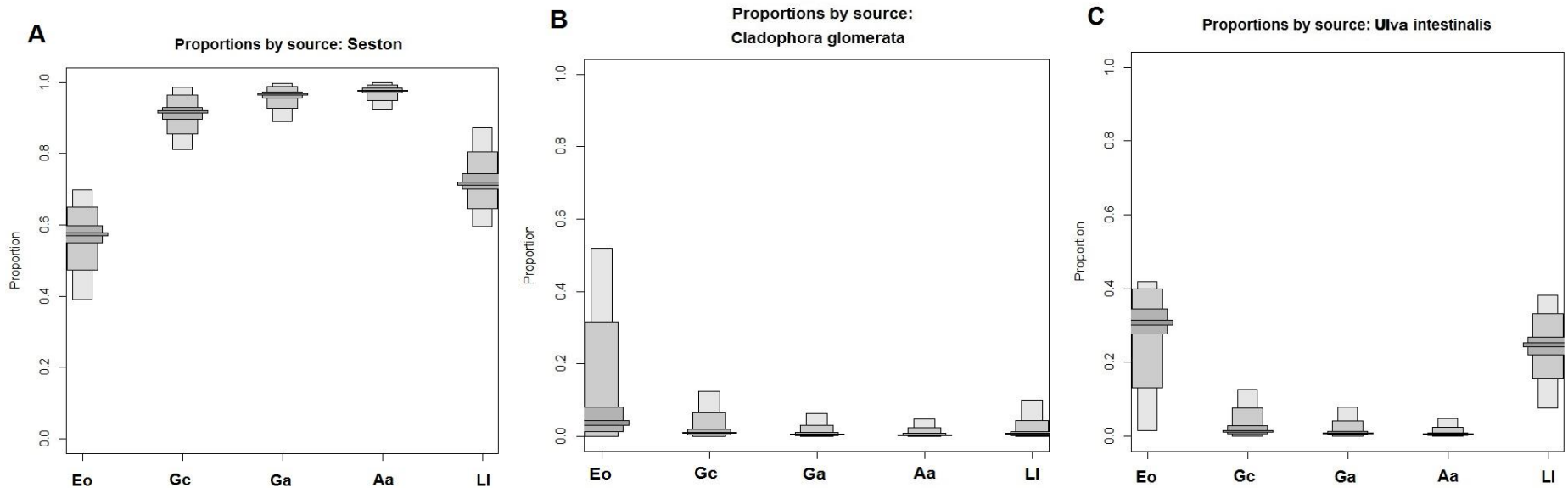
According to the SIAR model, pelagic (seston) inputs were the main source of carbon for the most of non-predatory macroinvertebrates (Fig. A). Only two macroinvertebrates caddisfly *Agraylea multipunctata* and gastropod *Theodoxus fluviatilis* mostly used *C. glomerata* as a basal resource of carbon (Fig. B). *Cladophora* was also significant in the diet of gastropod *Gammarus tigrinus*. The use of *Ulva* was much lower than the use of *Cladophora* (Figs. B, C).

Model SIAR estimates of use of different basal resources for non-predatory macroinvertebrate consumers at the station 2. Ta – Tanypodinae, Gf – *Gmelinoides fasciatus*, Ev – *Ephoron virgo*, Hc – *Hydropsyche contubernalis*, Lo – *Lymnaea ovata*, Cr - *Caenis robusta*, Bt – *Bithynia tentaculata*, Ch – Chironominae, Up – *Unio pictorum*.



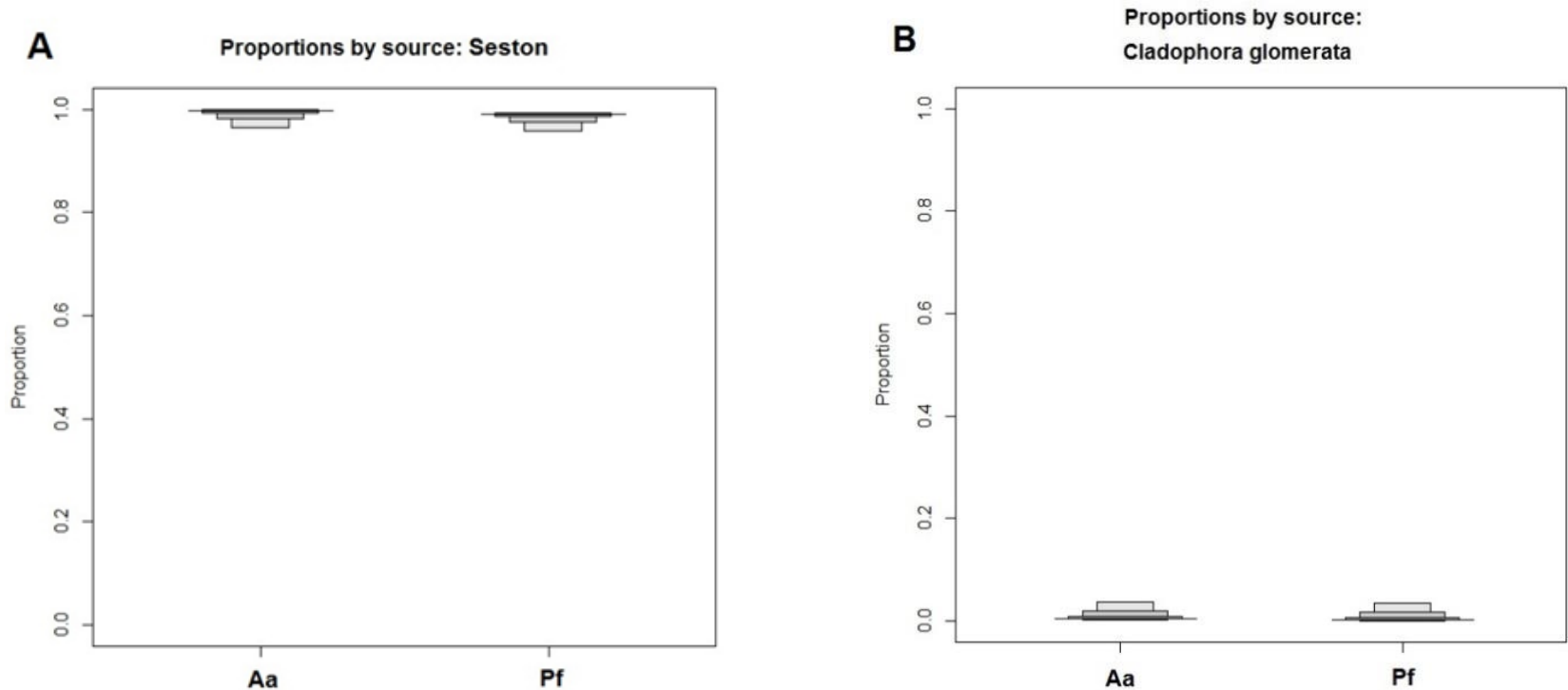
At the station 2, where only a small amount of drifting *C. glomerata* was observed, seston derived carbon was predominant in the diet of macroinvertebrates (Fig. A). Only some species used macroalgae as additional source of carbon (Fig. B).

Model SIAR estimates of use of different resources for predatory macroinvertebrates and fish at the station 1. Eo – *Erpobdella octoculata*, Gc – *Glossiphonia complanata*, Ga – *Gasterosteus aculeatus*, Aa – *Alburnus alburnus*, Ll – *Leuciscus leuciscus*.



According to the SIAR model predatory macroinvertebrates (the leeches *E. octoculata* and *G. complanata*) and fish (secondary consumers, trophic level III) at the station 1 mostly rely on seston carbon as a basal resource (Fig. A). Among them only dice *L. leuciscus* and leech *E. octoculata* showed notable use the macroalgae source (Figs. B, C).

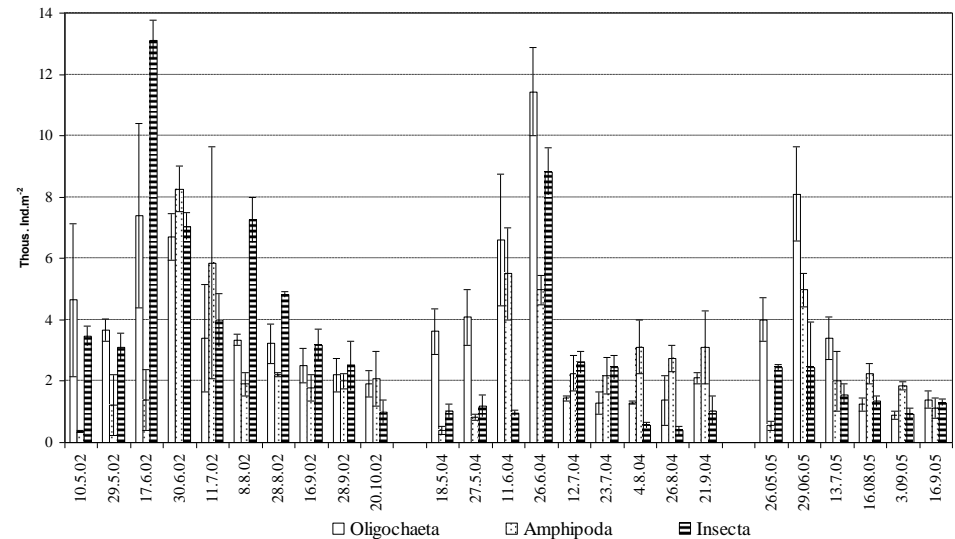
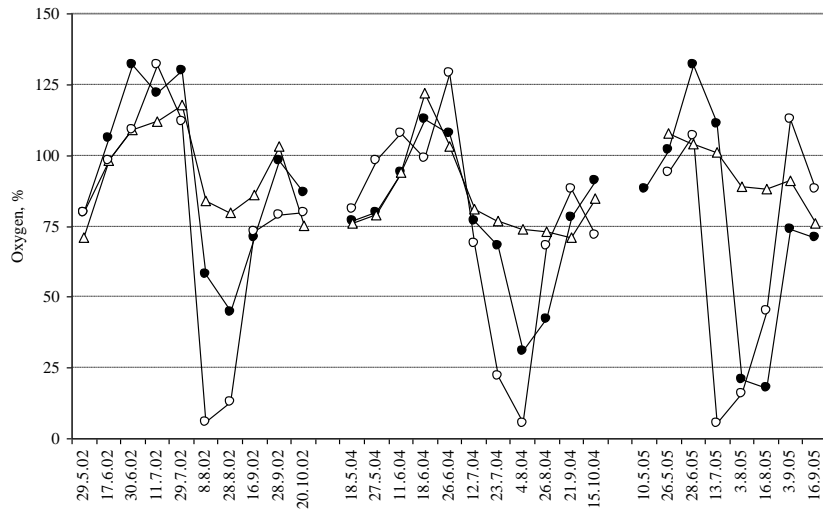
Model SIAR estimates of use of different carbon resources for fish at the station 2. *Aa* – *Alburnus alburnus*, *Pf* – *Perca fluviatilis*.



At the station 2 both fish species used seston as a basal resource of carbon

Dynamics of oxygen in the near bottom water and density of invertebrates in the shallow coastal zone of the eastern Gulf of Finland.


From: Berezina, N.A. & Golubkov, S.M., 2008. *Journal of Marine Systems* 74, S80–S85.



During low oxygen content in the water (0.62–2.8 mg/l) in late July and August, coinciding with the period of intensive decomposition of macroalgae 4–10-fold decrease in the density of amphipods, oligochaetes and aquatic insects was recorded.

Conclusions

- **Stable isotope analysis showed that organic carbon produced by macroalgae is poorly used by consumers**
- **According to SIAR model pelagic derived carbon is a main basal resource supporting coastal food webs**
- **Only few grazers effectively consumed macroalgae**
- **Taking into account that green tides in the Neva Estuary resulted in intensive oxygen depletion and in periodic substantial decrease of abundance of macroinvertebrates, we likely should consider this phenomenon as a negative one, which contaminates coastal zone of the estuary by excessive amount of organic matter and destabilizes benthic communities.**



Thank you for your attention!

From small scales to large scales
–The Gulf of Finland Science Days 2017
9th-10th October 2017
Estonian Academy of Sciences, Tallinn

2nd Day



**Gulf of Finland
Co-operation**

Y. Gubelit, N. Berezina, Y. Polyak, T. Shigaeva, G. Dembska, G. Pazikowska-Sapota, M. Polyak, V. Kudryavtseva

“Green tides” in the eastern Gulf of Finland: factors affecting the biomass accumulation and its consequences for the coastal zone

“Green tides” in the eastern Gulf of Finland: factors affecting the biomass accumulation and its consequences for the coastal zone.

Yu. Gubelit^{1*}, N. Berezina¹, Yu. Polyak², T. Shigaeva², G. Dembska³, G. Pazikowska-Sapota³, M. Polyak⁴, V.Kudryavtseva².

¹ Zoological Institute, Russian Academy of Sciences (RAS), Saint Petersburg, Russia

² The St. Petersburg Research Center for Ecological Safety, RAS, Saint Petersburg, Russia

³ Maritime Institute in Gdansk, Department of Environmental Protection, Gdansk, Poland

⁴ Saint Petersburg State University of Aerospace Instrumentation, St.Petersburg, Russia

In recent years so-called “green tides” has become a widespread phenomenon, reaching a great scale.

Yellow sea



Smetacek, V., Zingone, A. 2013. Green and golden seaweed tides on the rise. *Nature*. 504: 84-88.

France, Bretagne



Great Lakes



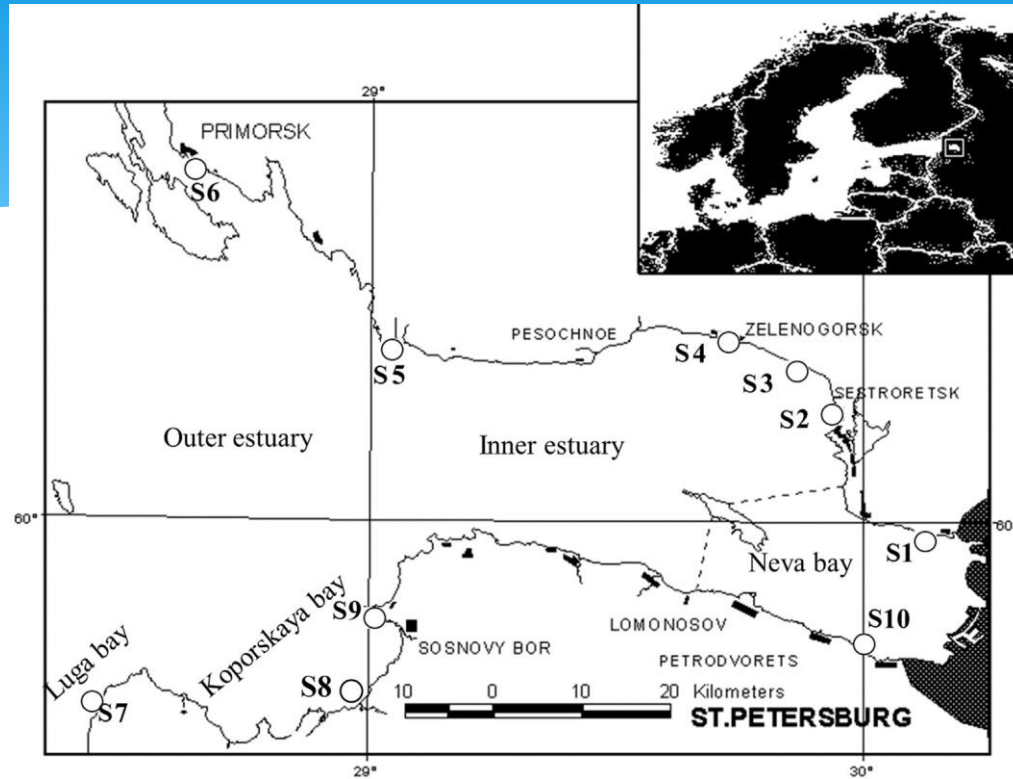
Eastern Gulf of Finlang in the sites of algae accumulation
Cladophora, *Ulva*

Cladophora glomerata-
«Global ecosystem engineer»

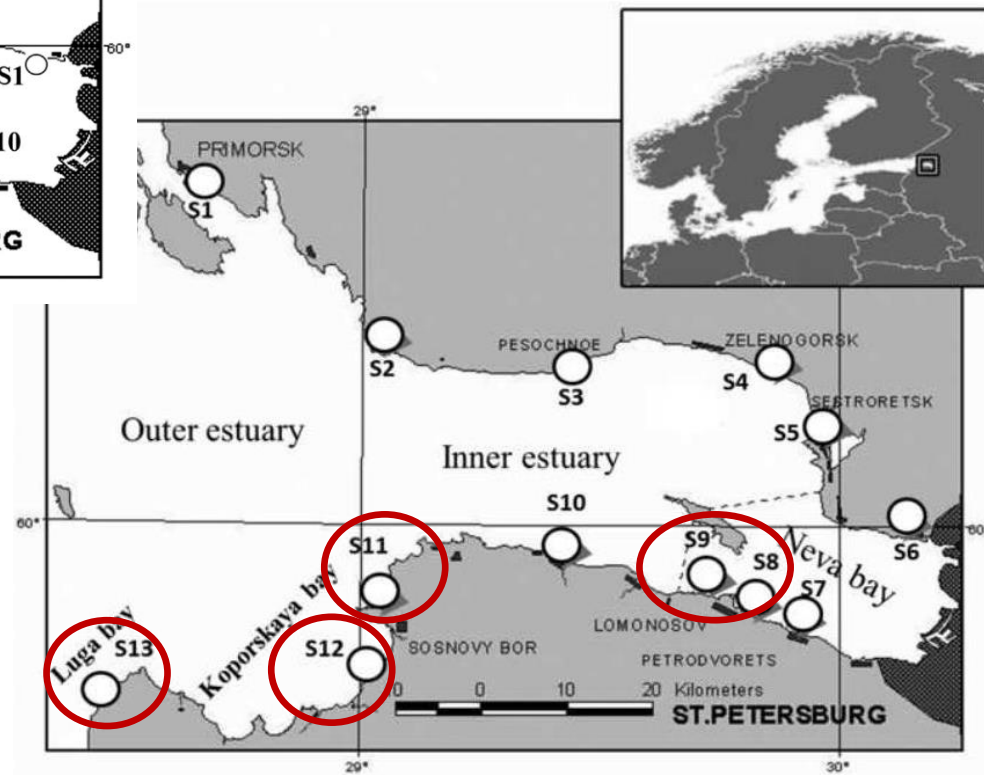
Zulkifly et. al. 2013



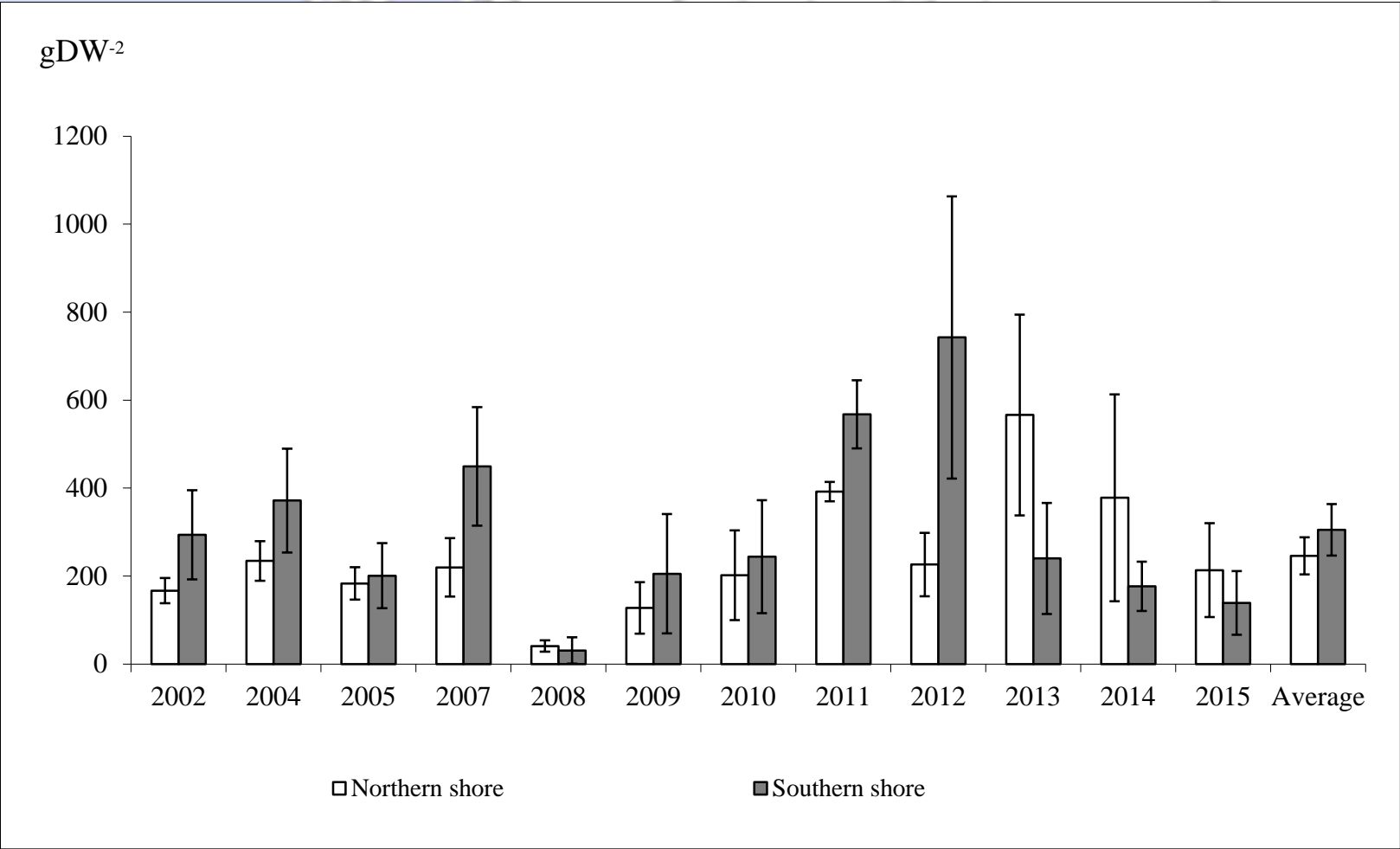
2004-2012



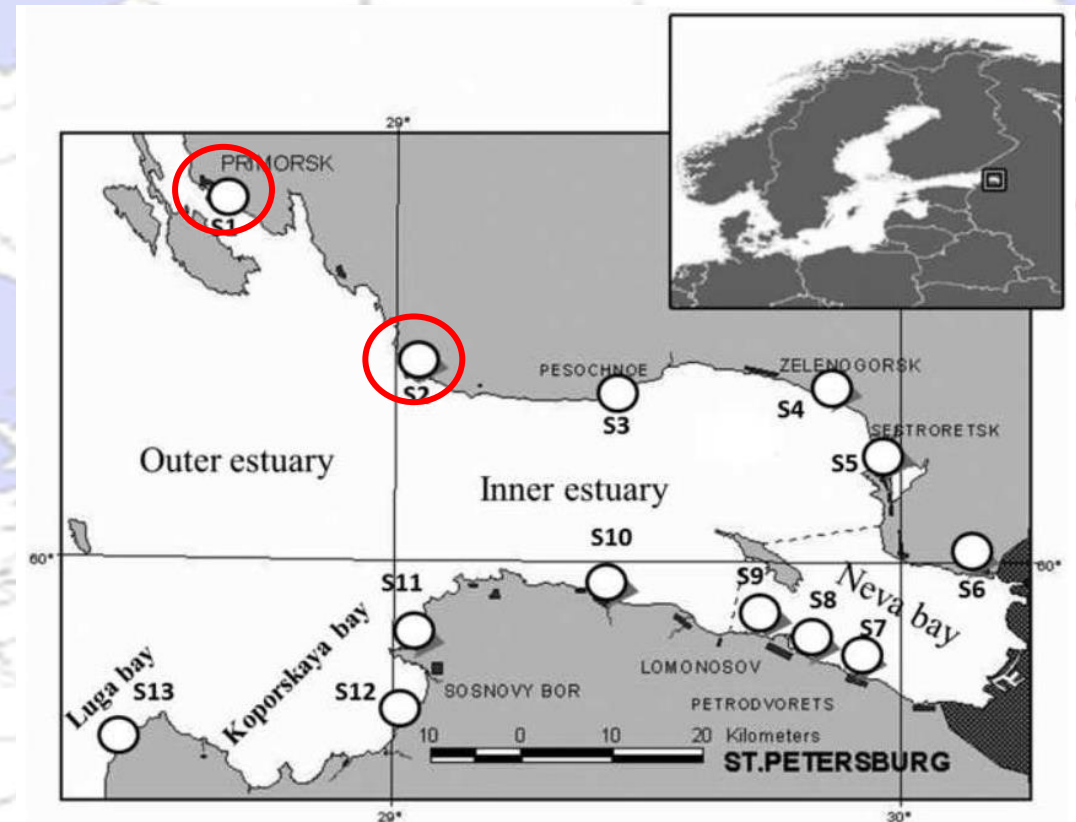
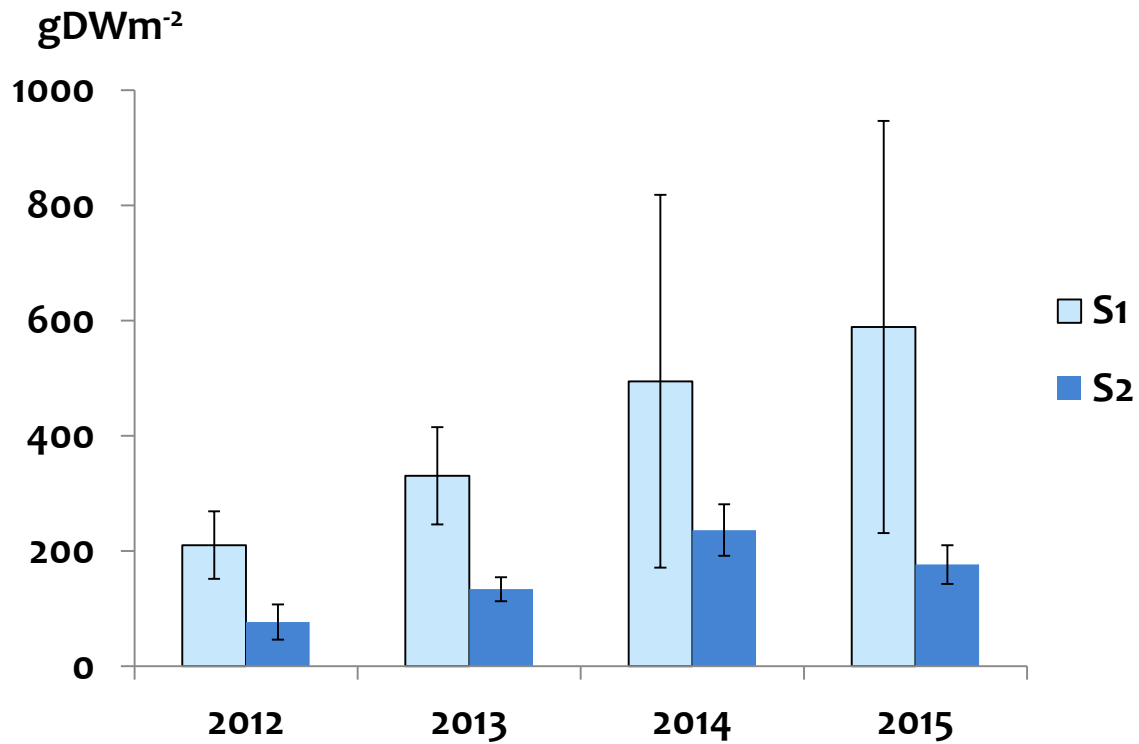
2014-2015



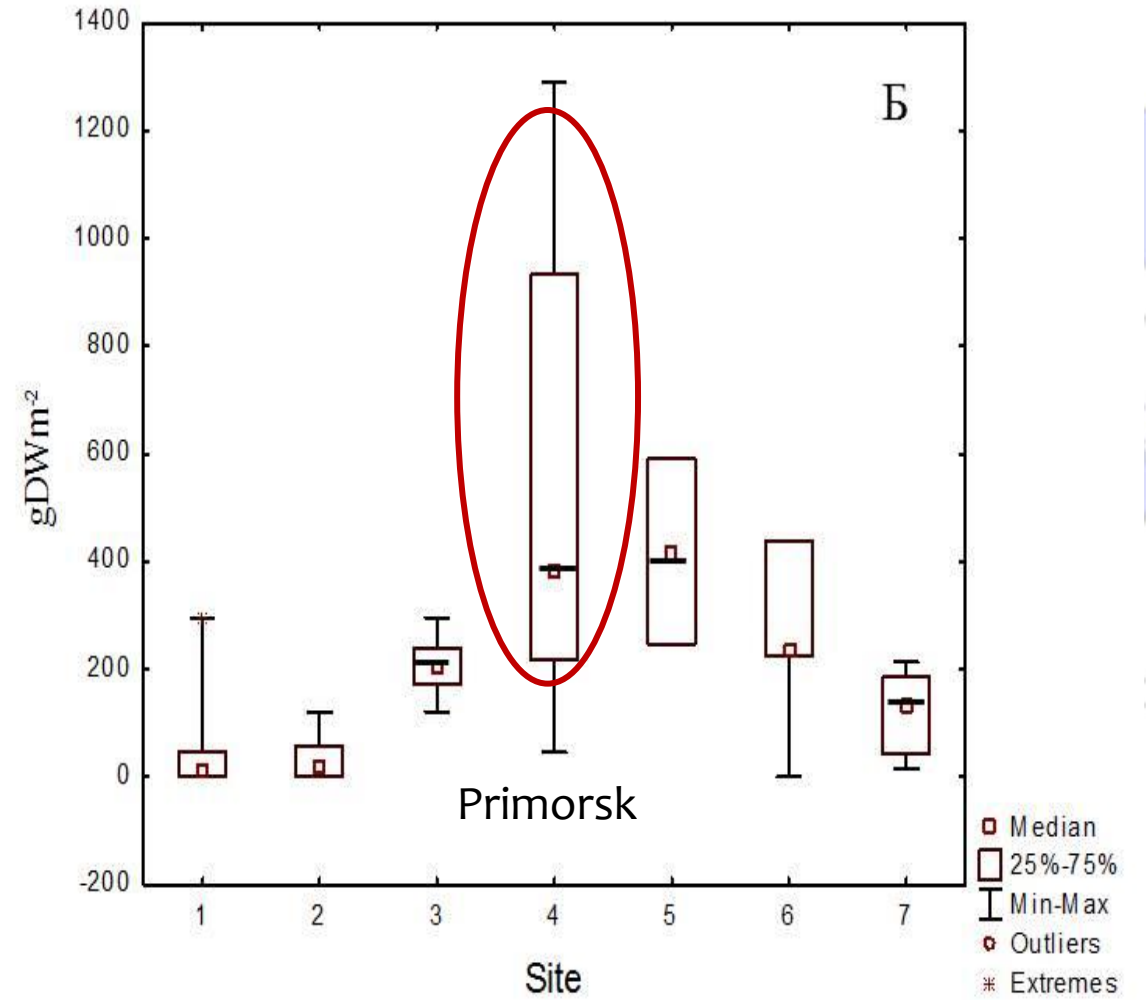
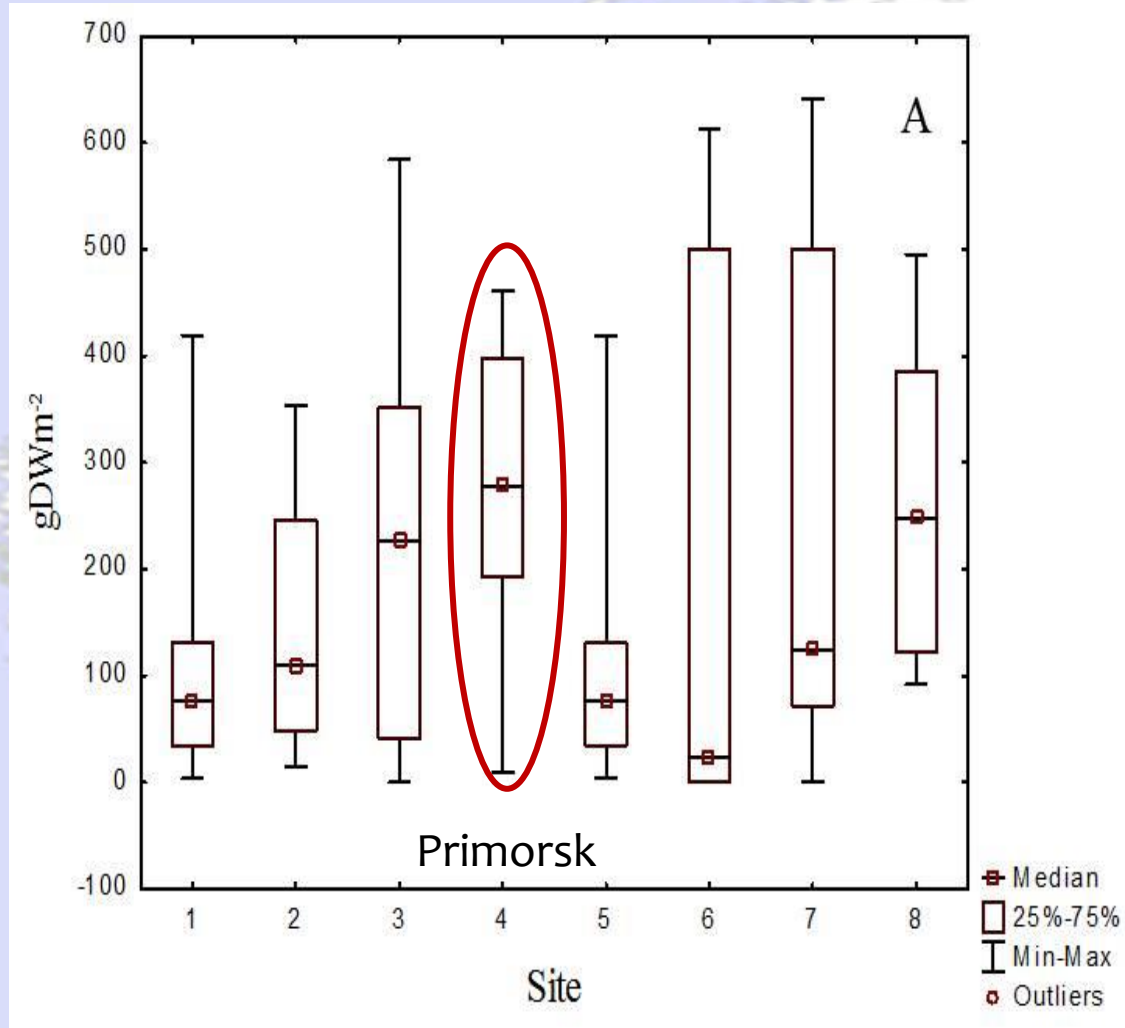
Long-term biomass dynamics of the “green tide” algae in the eastern Gulf of Finland



S1- Primorsk
S2- cape Flotsky

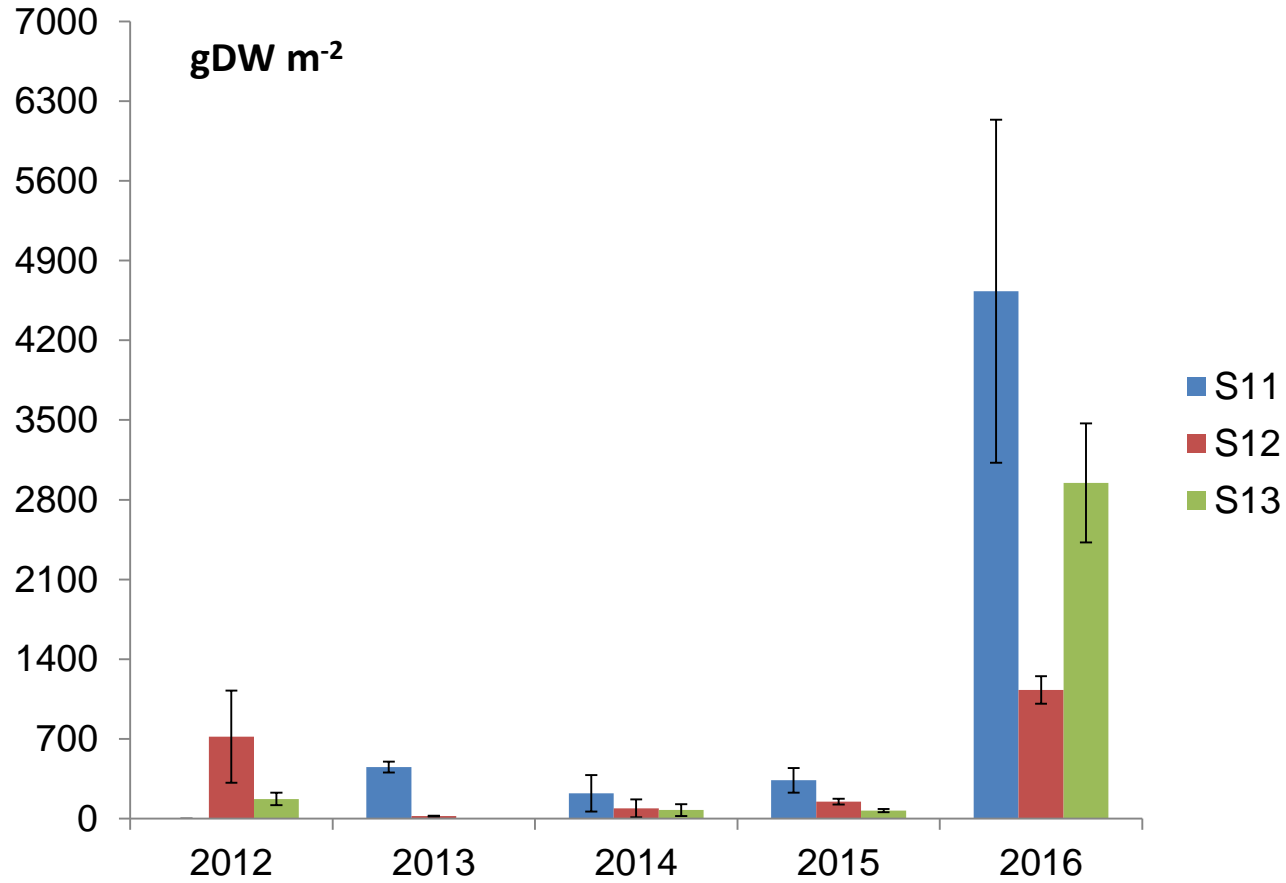


Biomass of the “green tide” algae in the eastern Gulf of Finland . A – 2004-2011 гг, Б - 2014-2015 гг.



Southern Shore

S11 – Grafskaya bay
S12 – Sisto-Palkino
S13 – Luga Bay



Which factors may influence biomass accumulation?

When in some places the biomass arose, in other sites it dropped.



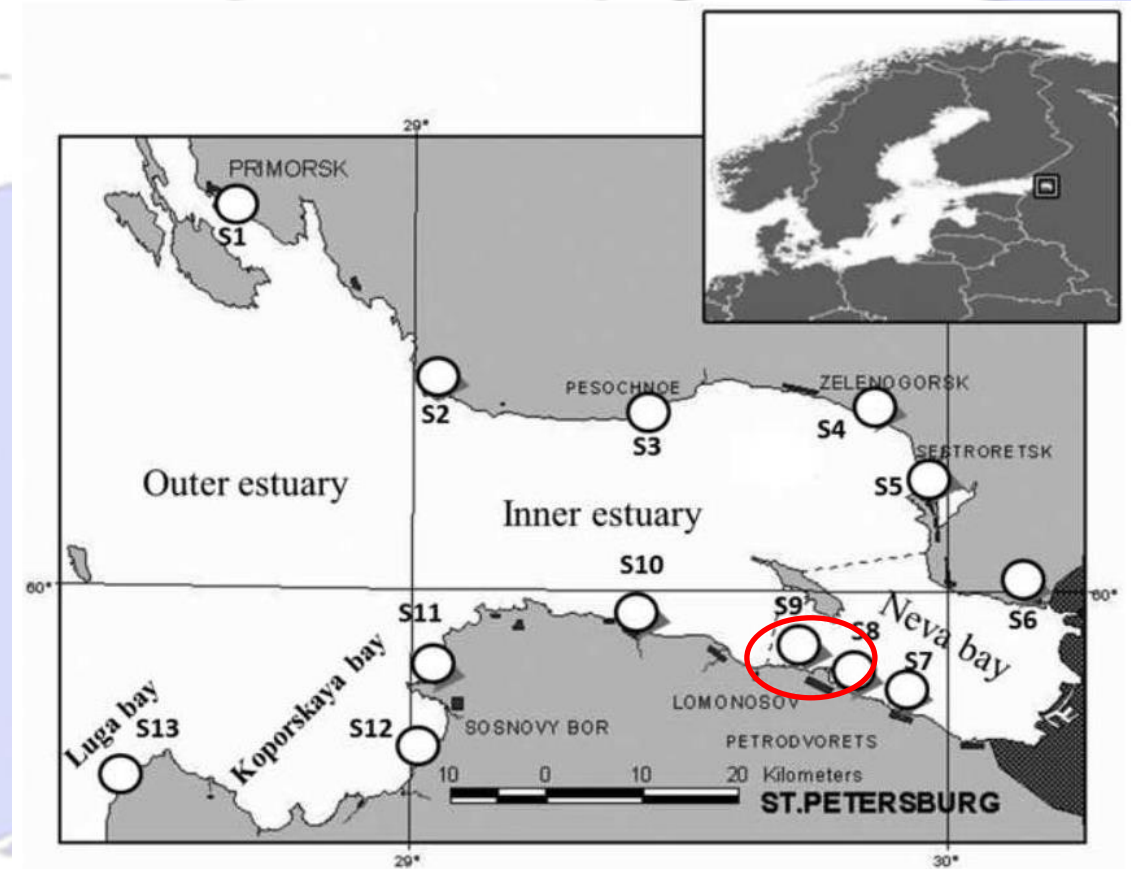
2014

S9 - 176 ± 56 gDW m⁻²

S8 - 26 ± 24 gDW m⁻²

2015-2016 – macroalgae were absent

Water transparency had been less than 30cm



Climate influence

Spearman Rank Order Correlations between biomass of green macroalgae, weather conditions and NAO indices. The values which are marked by asterisk, are significant at $p < 0.05$.

	Northern shore				Southern shore				Seasonal biomass	NAO annual
Site	1	2	3	4	5	6	7	8		
Wind speed	-0.30	-0.71	0.47	-0.10	-0.82*	0.26	-0.19	-0.48	-0.93 ^A	0.79 ^A
Air temperature	0.93*	0.14	0.48	0.70	0.18	0.29	0.18	0.21	0.30 ^A	-0.64 ^A
NAO winter	-0.26	-0.14	-0.62	-0.33	-0.36	0.21	-0.14	-0.11	-0.28	0.59
NAO annual	0.10	-0.29	-0.12	-0.05	-0.33	-0.61	0.18	0.14	-0.76*	1.00

^A – the correlation was calculated for average seasonal (end of May – beginning of September) wind speed and temperature.

Gubelit Yu.I. 2015. Climatic impact on community of filamentous macroalgae in the Neva estuary (eastern Baltic Sea). **Marine Pollution Bulletin.** 91:166–172

In the published literature about “green tides” the main recorded consequences are

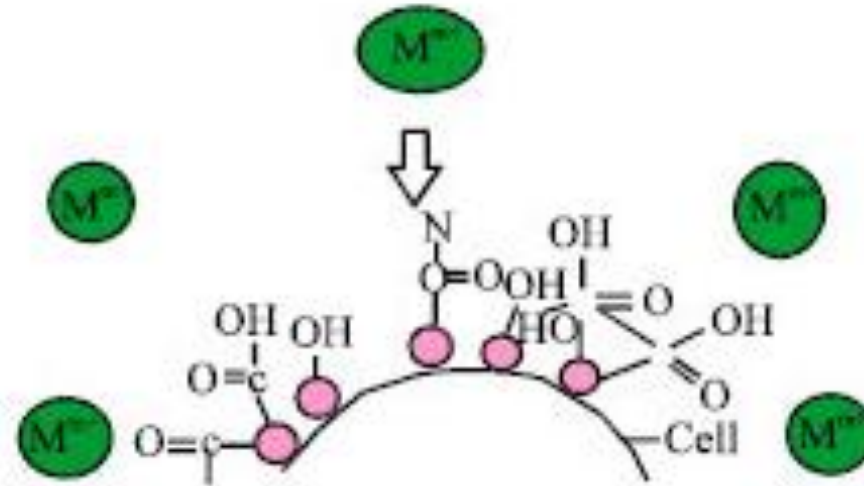
- **substitution of perennial algal species**
- **hypoxia, mass mortality and migration of benthic animals**
- **accumulation enterobacteria in algal biomass**
(Valiela et al. 1997; Berger et al. 2003, etc.).

Confirmed for EGOF

Berezina et al. 2005; 2007; 2009; 2017

Gubelit, Vainshtein, 2011

It's well known that *Ulva* и *Cladophora* have a high ability to accumulate Pb, Zn, Cu, Ni, Cr and Cd.

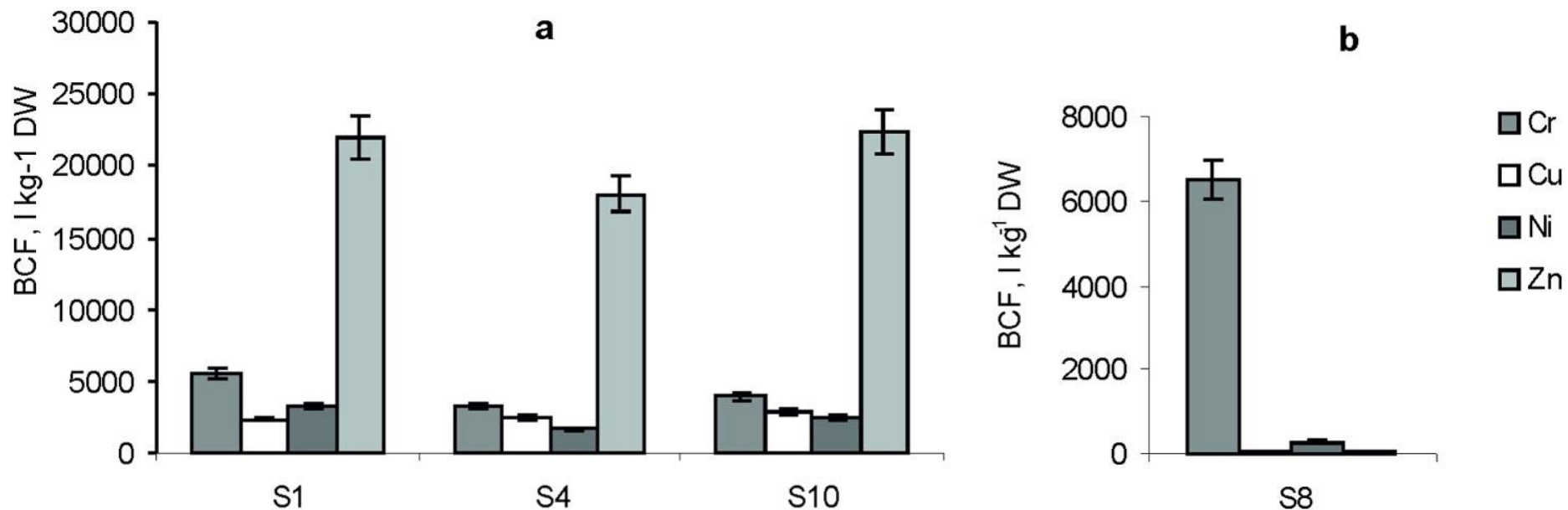


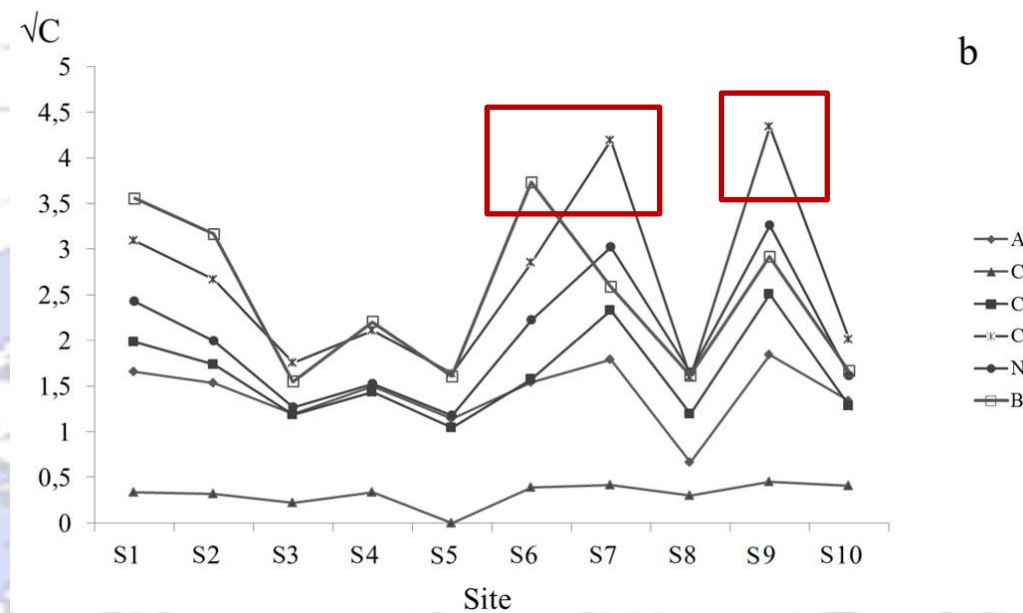
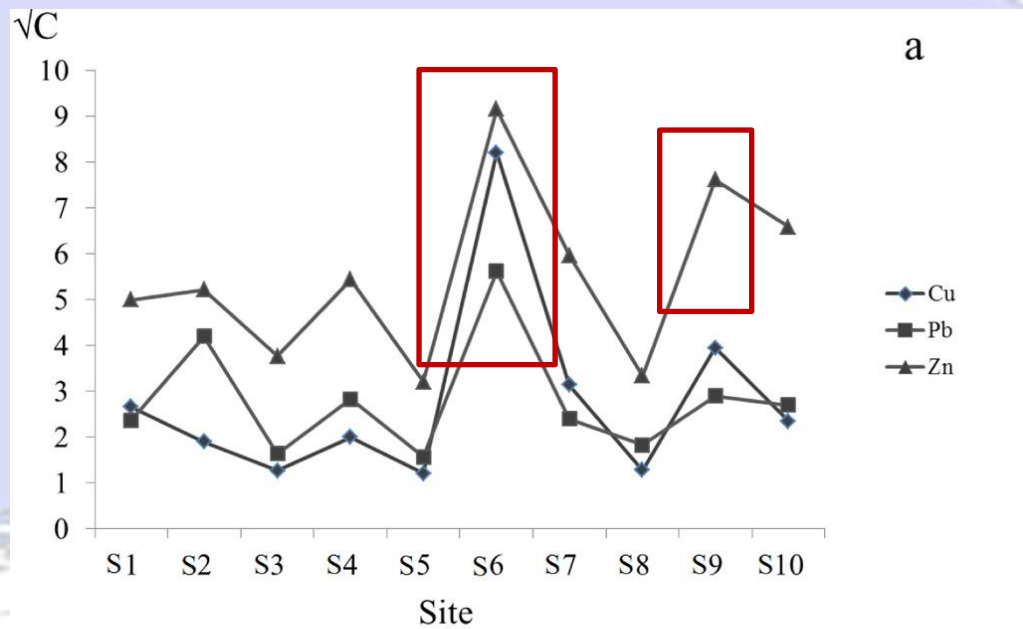
Lamaia et al., 2005; Zbikowski et al., 2007; Tang et al., 2014
и др.

Our recent study confirmed a high degree of metal bioaccumulation in macroalgal biomass.

Gubelit et al. 2016. Science of the Total Environment 550:806–819

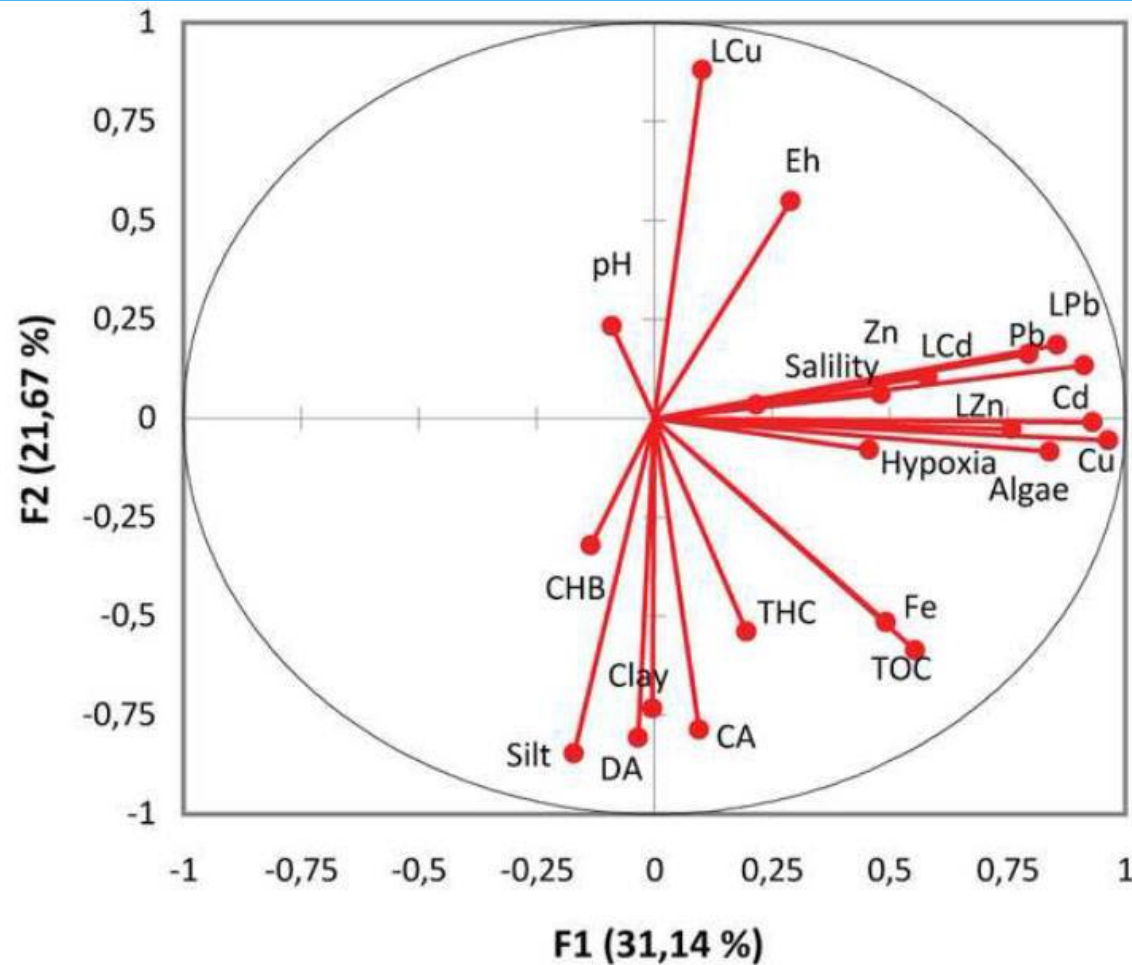
Selected field-measured metal bioconcentration factors (BCF, $\text{l kg}^{-1}\text{DW}$) for chrome (Cr), copper (Cu), nickel (Ni) and zink (Zn) in *Cladophora glomerata* from northern coast of the eastern Gulf of Finland and the Neva Bay (a) and southern coast of the eastern Gulf of Finland (b).





**During the study in 2012
The highest concentrations
of metals had been found at
the sites with highest algal
biomass and strong hypoxic
conditions**

Polyak et al. 2017. Journal of Marine Systems, 171: 101-110, special issue



Correlation between
macroalgae biomass and
Cu-content in sediments
 $R=0.571$

**Estimated nutrient loading from
the biomass may reach
 $0.8-2.51 \text{ g m}^{-2}$ for phosphorus, $4-12 \text{ g m}^{-2}$
for sulfur, $9-27 \text{ g m}^{-2}$ for
nitrogen and $147- 443 \text{ g m}^{-2}$ for
carbon**

Gubelit et al. 2016. Science of the Total Environment

Hypothesis to be checked

- *The mass development of “green tide” algae in the coastal area may contribute to accumulation of organic matter, nutrients and associated metals.*
- *On the other hand decomposition of this biomass through promotion of anoxic conditions may contribute to remobilization of adsorbed metals and enhance the pollution of surface sediments .*

Thank you for attention!

From small scales to large scales
–The Gulf of Finland Science Days 2017
9th-10th October 2017
Estonian Academy of Sciences, Tallinn

2nd Day



**Gulf of Finland
Co-operation**

YM. Golubkov, S. Golubkov

Influence of weather conditions on midsummer primary production and mineralization of organic matter in the Neva Estuary (eastern Gulf of Finland, Baltic Sea)



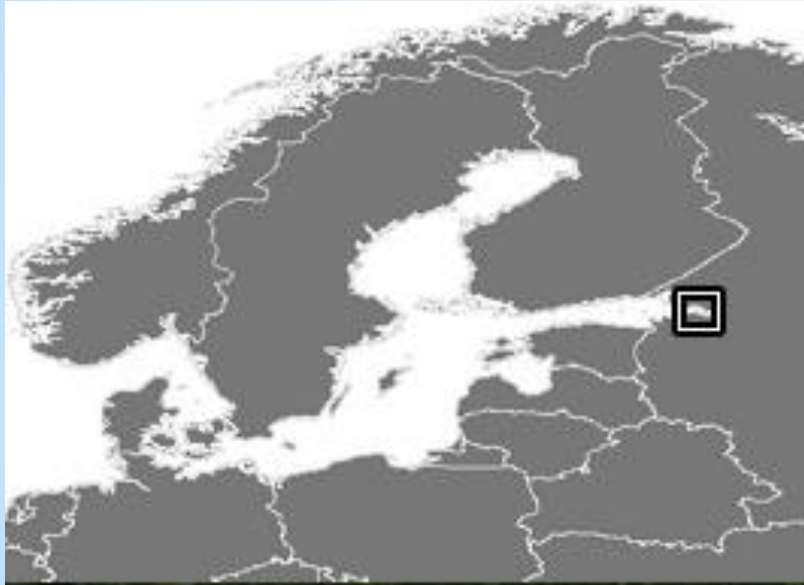
ZOOLOGICAL INSTITUTE OF RUSSIAN ACADEMY OF SCIENCES
St. Petersburg =



Influence of weather conditions on midsummer primary production and mineralization of organic matter in the Neva Estuary (eastern Gulf of Finland, Baltic Sea)

Mikhail Golubkov, Sergey Golubkov

SAMPLING



- **Sampling:**

19 sampling stations were obtained at summer 2003-2017 at the end of July and very beginning of August 2003-2017 in the **Upper part of Neva Estuary** – *freshwater and shallow Neva Bay* and in the **Middle part of Neva Estuary** (*salinity of surface water up to 3 PSU, depth up to 30 m*).

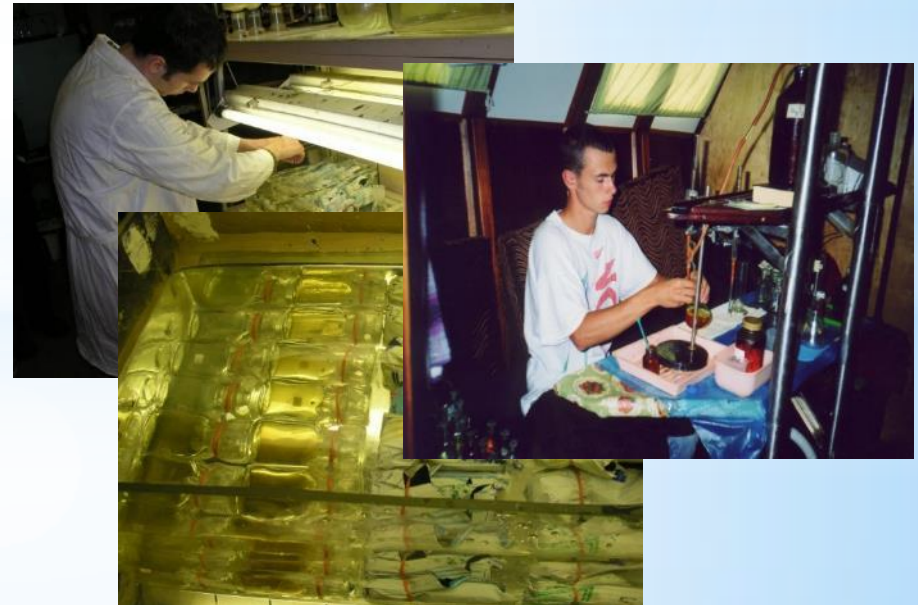


METHODS



To characterize heterogeneity of the waters C6-multisensor platform (TurnersDesigns, USA) and CTD90m probe (Sea&Sun Tech., Germany) were used.

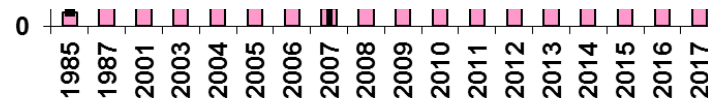
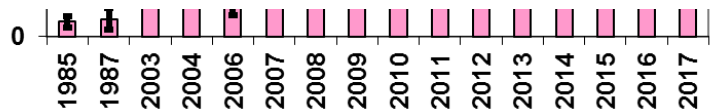
On each sampling station Secchi depth, primary production of phytoplankton and mineralisation of organic matter in water column, concentration of chlorophyll *a*, concentration of total phosphorus were measured.



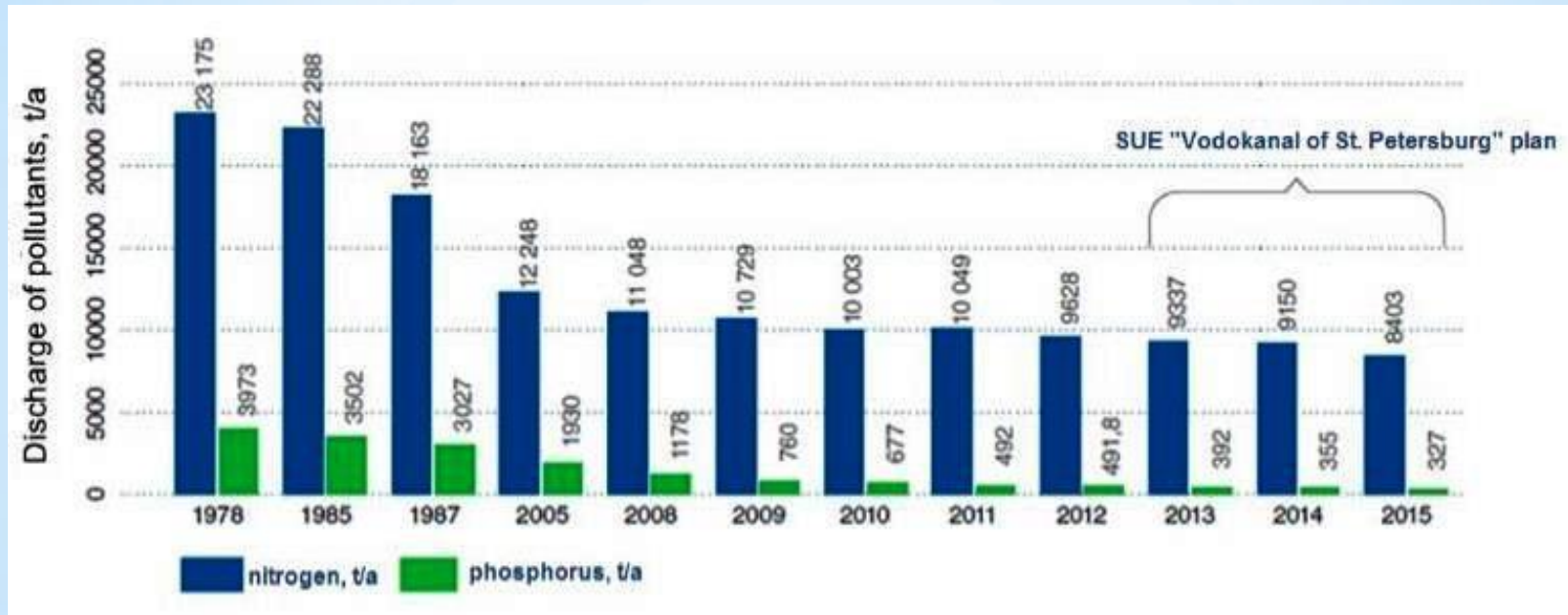
Chlorophyll *a* and ratio between primary production of phytoplankton (PP) and mineralisation of organic matter (D) in the Neva Estuary at the end of July and very beginning of August 2003-2017



- What are the reasons?
- What does it mean?

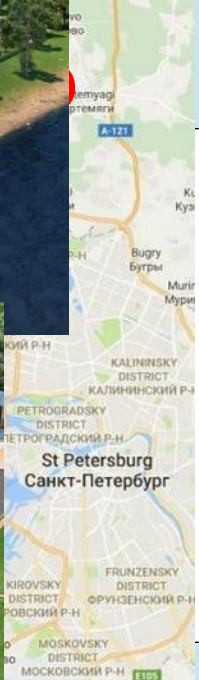
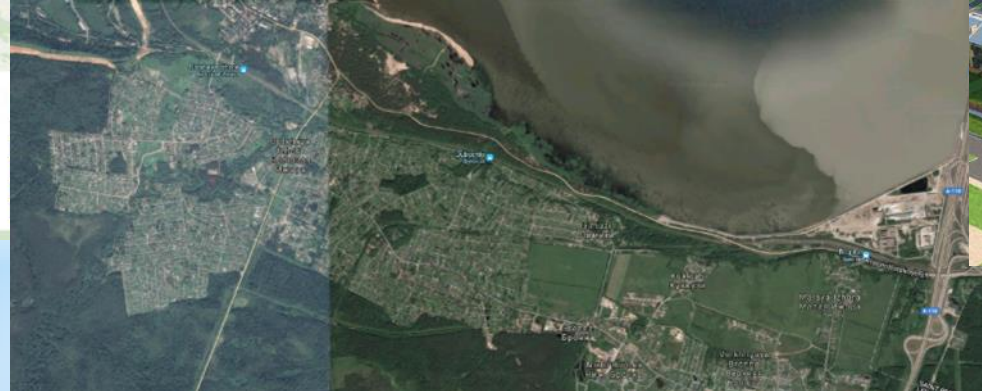


Protection of the Baltic Sea by SUE “Vodokanal of St. Petersburg”



- Within the commitments undertaken by the Russian Federation to fulfil the Helsinki Convention on the Protection of the Marine Environment of the Baltic Sea, St. Petersburg Vodokanal implements large-scale activities targeted to the reduction of untreated wastewater discharges and removal of nutrients (nitrogen and phosphorus) from wastewater.
- To meet new requirements and stabilize nutrient removal process at wastewater treatment plants of St. Petersburg, in 2005, the enhanced biological treatment and chemical phosphorus precipitation were introduced at wastewater treatment plants.
- Today, **98,5%** of wastewater in St.Petersburg is treated.

Concentration of total phosphorus in the Neva Estuary at the end of July and very beginning of August 2003-2016



Precipitation

The reason - rainy weather

- Soil anoxia, which occurs during continuous rains, may result in re-dissolution Fe-P associations in soils to over time (Uusitalo et al., 2015).
- Extreme high flows and flood events will reduce the retention of phosphorus in streams and will enhance the degradation and transport of particulate phosphorus from stream banks; additional phosphorus loads are also expected from more frequent flushing and sewer overflows (Withers and Jarvie, 2008).

Temperature

The reason – air temperature

- Bacterial growth rate in the water must be affected by substrate supply rates and temperature simultaneously (Shiah, Ducklow 1997). In the Neva Estuary, substrate is not a limiting factor to bacteria growth due to high discharge of the Neva River. The concentration of dissolved organic matter in the Neva Estuary is 50–60% higher than in the western part of Gulf of Finland (Aarnos et al., 2012). Therefore, temperature was probably the main factor responsible for interannual variations in mineralization of organic matter in the estuary.

Thank you for your attention!



From small scales to large scales
–The Gulf of Finland Science Days 2017
9th-10th October 2017
Estonian Academy of Sciences, Tallinn

2nd Day



**Gulf of Finland
Co-operation**

A. Giudici, J. Kalda, T. Soomere

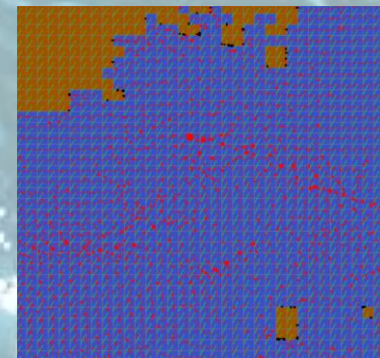
Patchiness of the sea surface under the combined effect of winds and currents

The Gulf Of Finland Science Days 2017
“From small scales to large scales”

Last Reviewed: 10/10/2017 06:45

Patchiness of the sea surface under the combined effect of winds and currents

Giudici, A., Kalda, J., Soomere, T.



Presentation outline

- Introduction
- Description of employed dataset
- Eulerian Simulation Model and Collision Detection
- Simulations Results
- Conclusions

Introduction - The Gulf of Finland



- Estuarine area which shows extremely complex dynamics
- High proportion of vertical motions of water masses [Leppäranta and Myrberg, 2009]
- Frequently hosts up- and downwelling phenomena [Lehmann and Myrberg, 2007]
- Extremely dense ship traffic throughout the year.

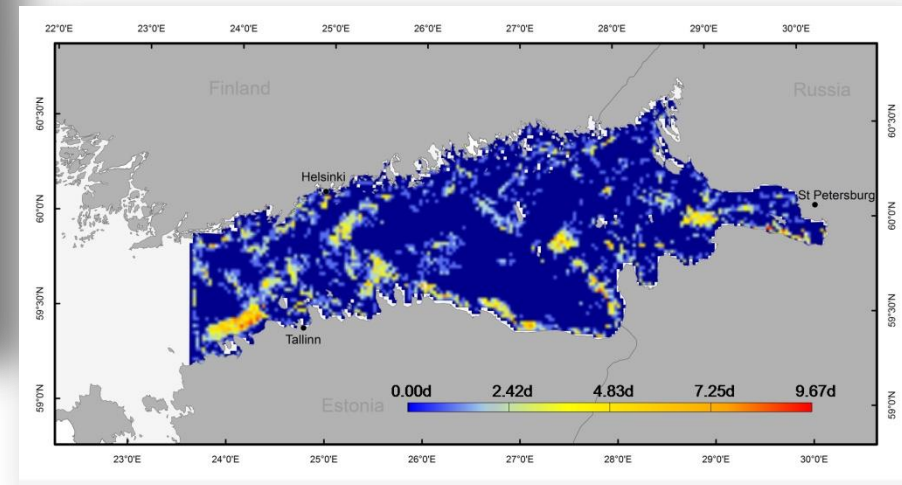
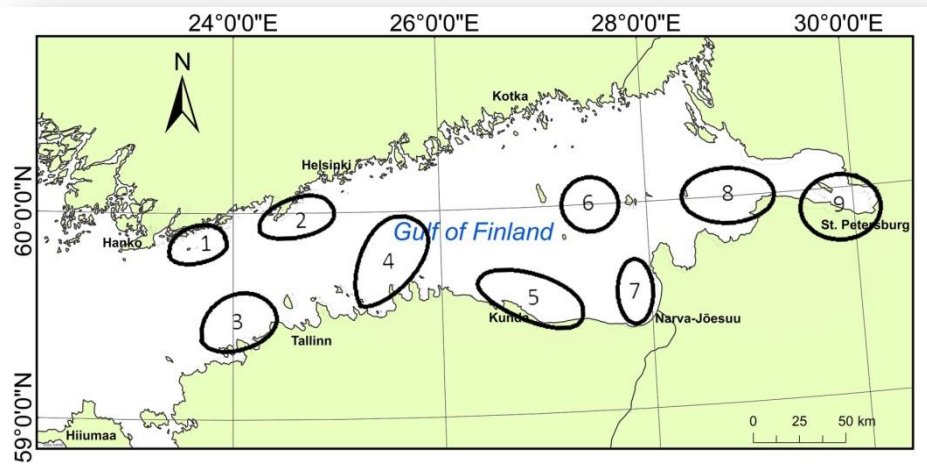
Introduction

- Patchiness in distributions of matter in the ocean is one of the oldest observed phenomena in oceanography
- Despite this, there is little consensus on its causes, and a general theory remains a distant goal ==> some studies even speculate whether such general theory does exist
- Compressibility of surface velocity field is a convenient measure to indicate the possibility of gathering of floating litter into patches on the sea surface.
 - **In some sense, it characterises** the intensity of downwelling and upwelling motions near the surface, equivalently, **whether water parcels can dive**
 - It can be calculated from the 2D velocity pattern
- Its values are from 0 to 1. If it becomes large enough (>0.5 in the case of Kolmogorov turbulence), patch formation accelerates explosively [1]
- In the case of quasi-2D flows (like marine flows in many cases), the surface flow compressibility is strongly suppressed.

Introduction

- Seabed features in specific regions (eg. Gulf of Finland) - may enhance patch generation by supporting up- and downwelling.

==> Previous work has highlighted regions where patches are almost always formed in the Gulf of Finland by the field of currents only [2][3]



[1] Eckhardt, B. and Schumacher, J. "Turbulence and passive scalar transport in a free-slip surface", Phys.Rev.E 64(1), 2001

[2] Kalda, J., Soomere, T. and Giudici, A. "On the finite-time compressibility of the surface currents in the Gulf of Finland, the Baltic Sea", J. Marine Syst. 129, 2012

[3] Giudici, A., Soomere, T. "Finite-time compressibility as an agent of frequent spontaneous patch formation in the surface layer: a case study for the Gulf of Finland, the Baltic Sea", Mar. Poll. Bull. 89, 2014

Introduction

- Other effects may also play a role in increasing effective compressibility, and therefore the clustering rate of floating litter:

==> Surface gravity waves: normally minor effect; they need to be strongly nonlinear in order to play a significant role [4][5][6]

==> Lateral stirring and mixing at sub-mesoscale, which were shown to have a direct effect on the patchiness of phytoplankton distribution [8]

==> Interplay of different phenomena, like waves and currents: an effective mechanism for providing patchiness of pollutants on the ocean surface [9]

[5] Denissenko, P., Falkovich and G., Lukashuck, S. "How waves affect the distribution of particles that float on a liquid surface", Phys. Rev.Lett. 97(1), 2006

[6] Balk, A.M., Falkovich, G. and Stepanov, G. "Growth of density inhomogeneities in a flow of wave turbulence", Phys.Rev.Lett. 92(1), 2004

[7] Vucelja, M., Falkovich, G. and Fouxon, I. "Clustering of matter in waves and currents

[8] Martin, A.P., "Phytoplankton patchiness: the role of lateral stirring and mixing", Prog.Oceanog. 57(2), 2003

[9] Vucelja, M., Falkovich, G., Fouxon, I. "Clustering in waves and currents", Phys.Rev.E Stat. Nonlin. Soft.Matter Phys., 75(6-2), 2007

Introduction

- A potential factor that may increase the effective compressibility is **the interplay of currents and winds**.
- Specifically, the effect of the differences in the wind drift speed of different patches as a function of their size.
- This mechanism is expected to be coupled with the turbulent mixing and the intrinsic compressibility of the flow field.

This work presents an attempt to quantify the effect of such differences in drift speeds by means of an Eulerian tracking model.

Introduction

- The main idea is to **create a model which is able to integrate current data with geostrophic wind information.**
- We know the areas where patch formation usually occurs. We want to know what happens outside of these areas and how we can quantify the process.
- The overlapping region of two data sets (current and wind), covering a large portion of the GoF, is gridded using a uniform 1NM grid.
- Simulated small patches of floating sticky litter (e.g. remnants of plastic bags, or small oil spills) are scattered uniformly across the Gulf.
- The behavior of such patches is simulated in terms of their:
 - => relocation under the effect of winds and currents
 - => colliding trajectories
- We aim at describing the resulting distribution of patches, after they are left at sea for various periods of time.

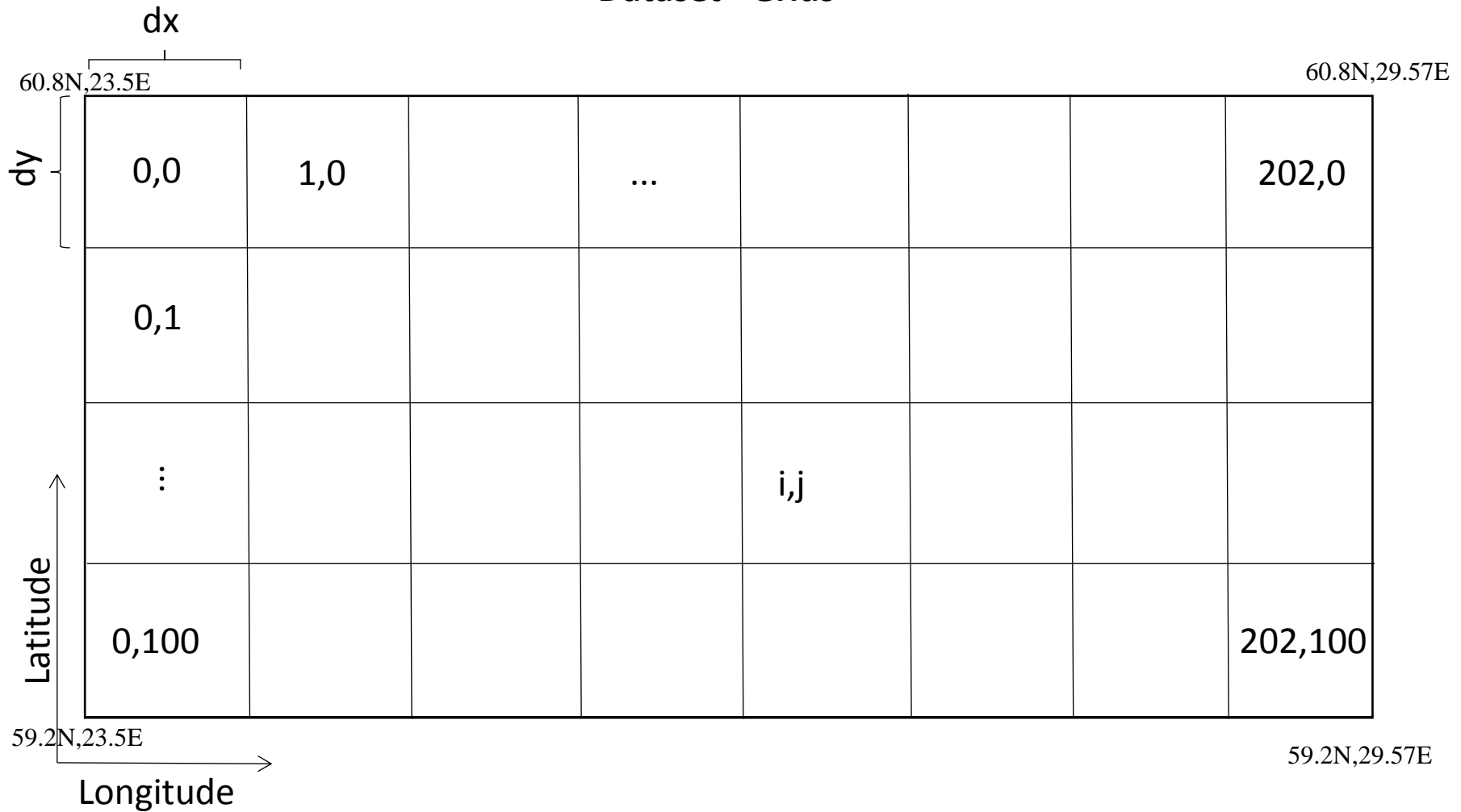
Dataset



Currents data BL (59.2N, 23.5E) @ 0.03dx, 0.016dy → 202x100 grid 1NM res OAAS model

Winds data: BL (58.92, 22.97E) @ 0.19528dx 0.09754dy → 38x26 grid (flipped) calculated from air pressure gradients and rescaled at 10m height

Dataset - Grids



$$\begin{aligned} Lat &= BL_y + (size_y - j)dy \\ Lon &= BL_x + (size_x - i)dx \end{aligned}$$

$$\begin{aligned} i &= \frac{Lon - BL_x}{dx} \\ j &= \frac{BL_y - Lat + dy \cdot size_y}{dx} \end{aligned}$$

Simulation Model - Patches

- A **patch** object is defined by the following properties:

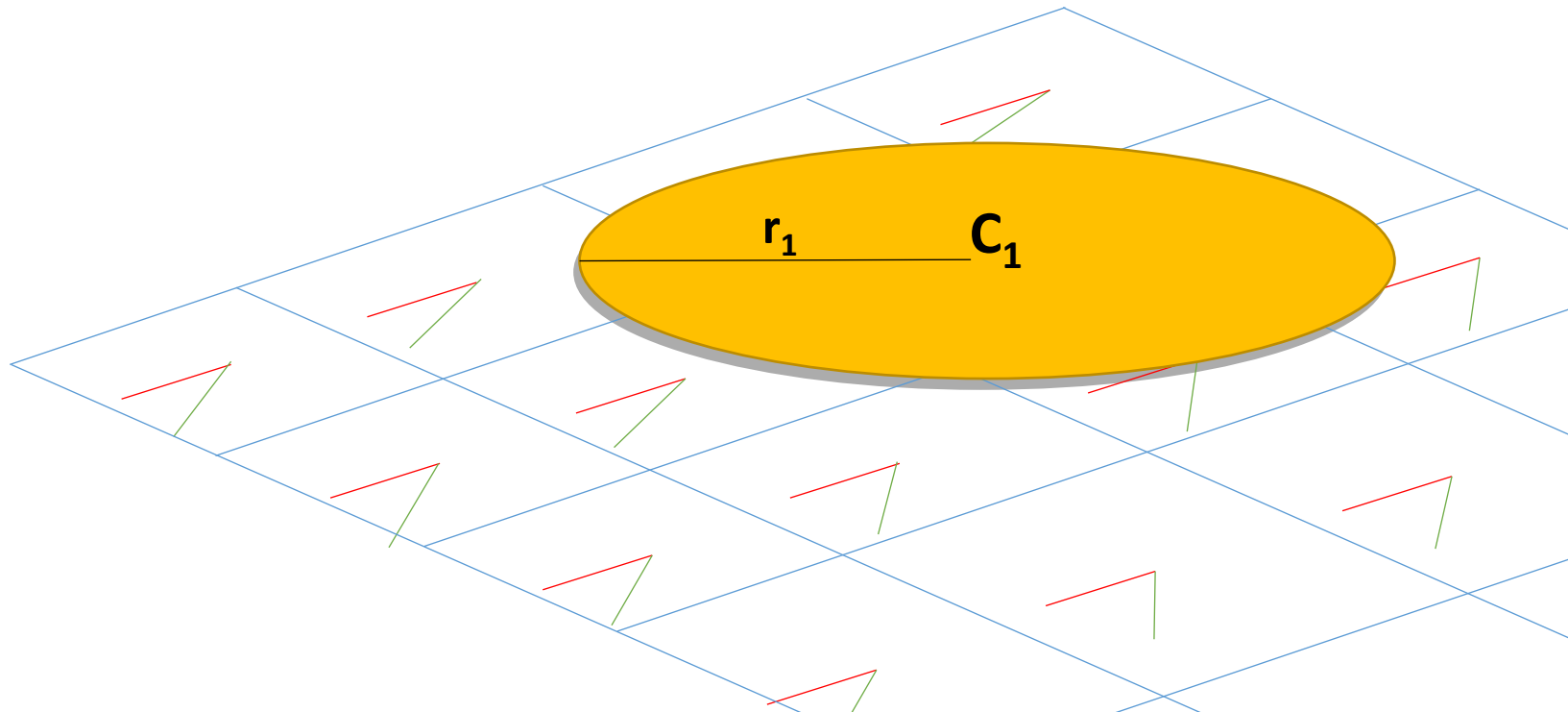
- **Center Coordinates**

- **Radius** (Horizontal Section)

- Vertical Section --> expressed as a function of horizontal section $V_{section} = H_{section}^{\alpha < 1}$

- '**Alive**' status --> whether the patch is at sea or hits the coast

- **Lifetime** --> number of hours the patch is alive for



Simulation Model - Patches

- The model has the following rules for relocating the generated patches:

FOR EACH time step

FOR EACH Patch

GET Interpolated Current Vector **C**

GET Interpolated Wind Vector **W**

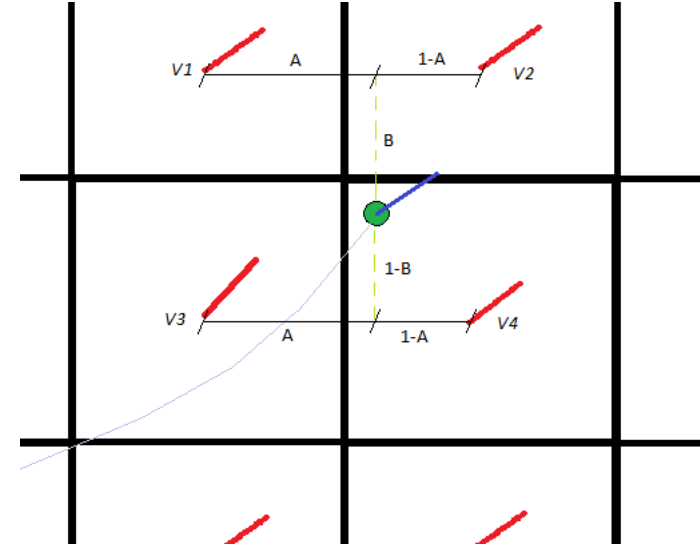
$$\mathbf{x}(t+1) = f(\mathbf{x}(t), \mathbf{W}, \mathbf{C})$$



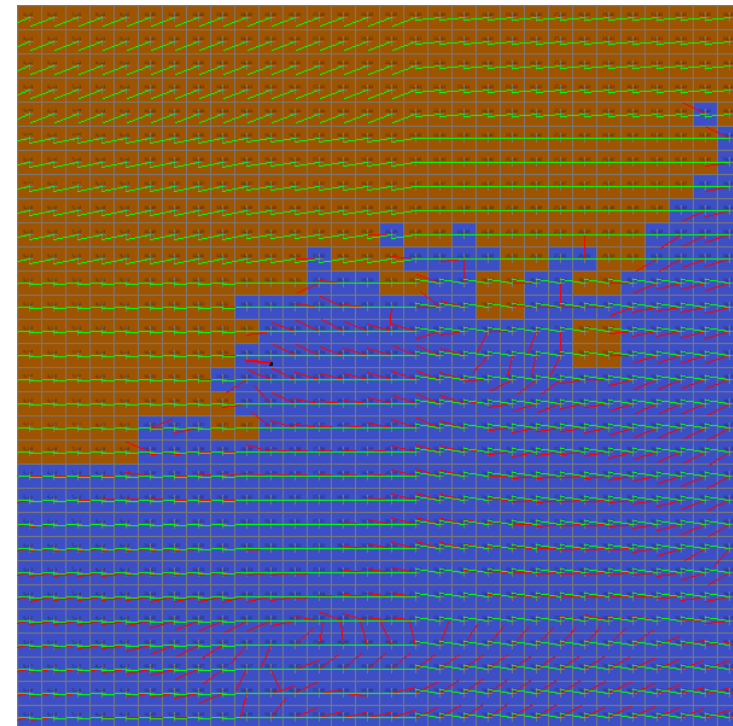
$$x(t+1) = x(t) + v_c \cdot \Delta t + \Delta M$$

$$\frac{\Delta M}{|\Delta M|} = \frac{v_c - v_w}{|v_c - v_w|}$$

$$\Delta M = v_\alpha \cdot \Delta t = \sqrt{\frac{H_{section}}{V_{section}}} \cdot \sqrt{\frac{\rho_{air}}{\rho_{water}}} \cdot (v_c - v_w) \cdot \Delta t$$

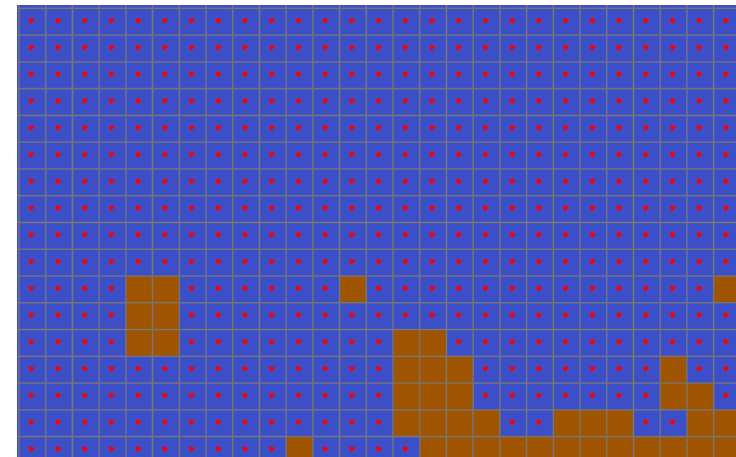
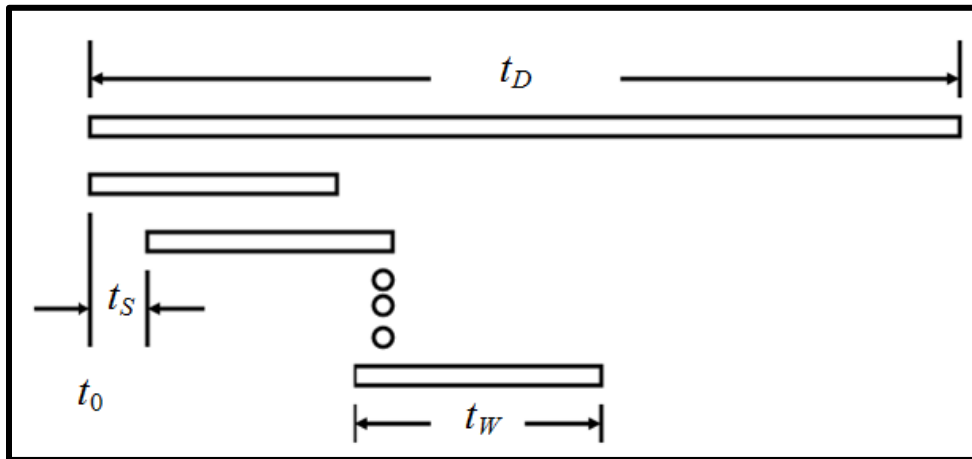


$$V_{Res}^T = B * (A * V_1^T + (1-A) * V_2^T) + (1-B) * (A * V_3^T + (1-A) * V_4^T)$$



Simulation Model - Time Subdivision Scheme

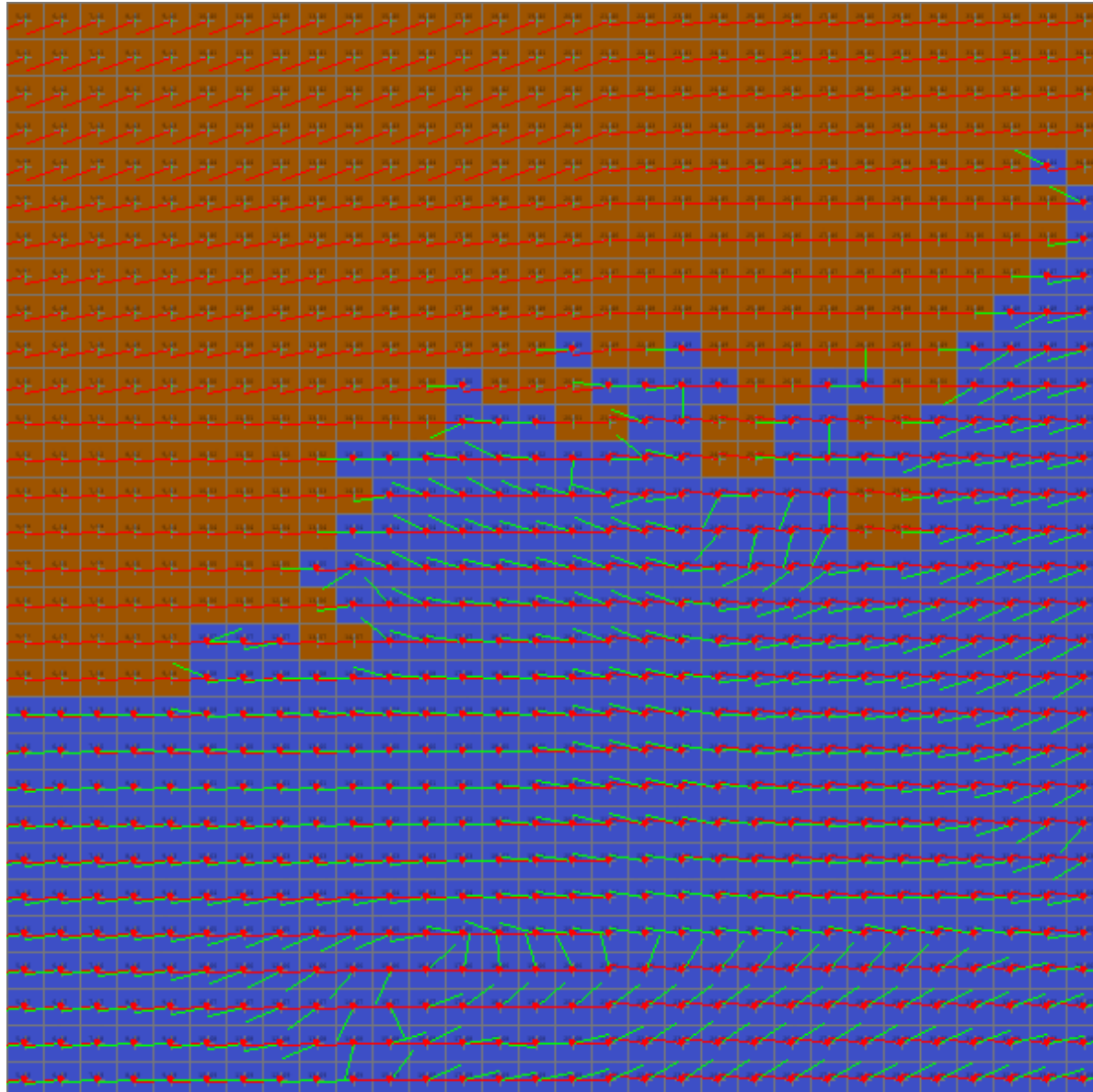
- A time interval of interest t_D is chosen (1 month)
- The time interval is divided into time windows t_W (3 days)
- At the beginning of each time window, a patch of initially small [relative to the grid cell size] size (50, 100, 150, 200, 250, 300 meters) is positioned in the center of each wet grid cell
 - ==> A +/- 15% randomness is added to the initial size of the patches
- The behavior of each patch is simulated throughout the current time window
- At the end of each time window, patch position is reset and the initial time for the next simulation T_0 is advanced by T_s (1 day)



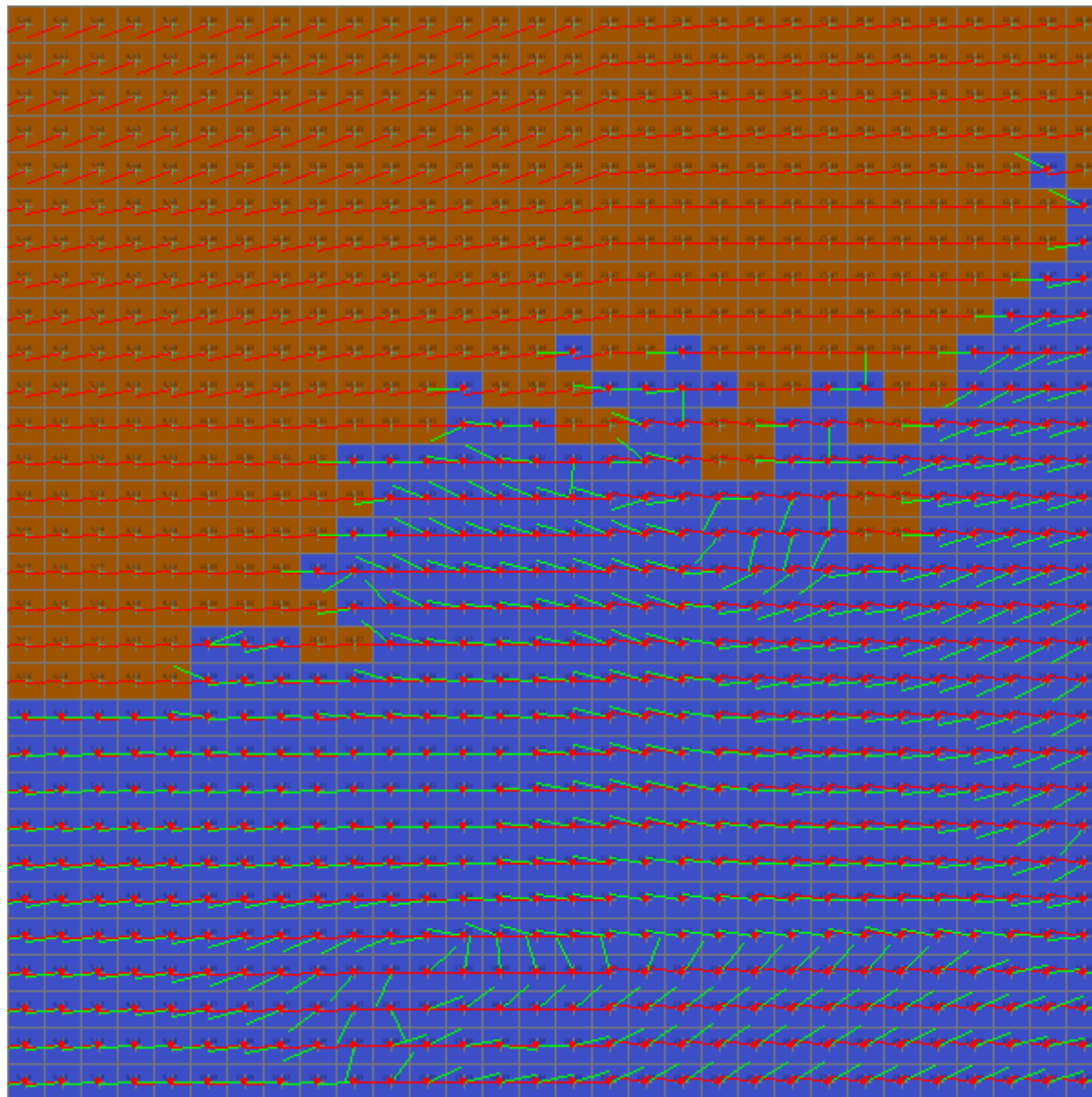
Simulation Model

- Patches are relocated, once per timestep (3 h) throughout the time window, under the combined effect of the interpolated Wind- and Current-fields
 - ==> **Patch relocation model**
- At each timestep, collisions between patches are calculated
 - ==> **Patch collision model**
- Patches properties (lifespan, Hsize, Vsize, coastal hit) are updated
- Set of patches is updated based on collisions (total nr. of patches always diminishes)
- At the end of each time window, statistics are produced (min,max,avg Size, min, max, avg Life, size distribution, N/S coastal hits)
- The process is then repeated by sliding the time-window ahead by an interval (1 day)
- After the last time window is simulated, statistics are averaged over all the available realizations

Simulation Model - Running Simulation [Collisions Disabled]



Simulation Model - Running Simulation [Collisions Enabled]



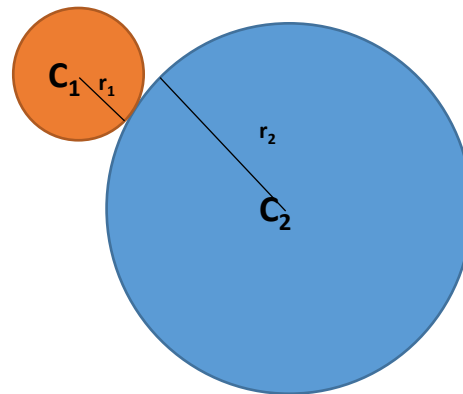
Simulation Model - Collision Detection

- The model has the following rules for collisions among patches:

- 1) When two patches collide, they merge into one patch
- 2) The collision happens whenever the distance between the two patches' centers is less or equal than the sum of the two patches' radii:

$$d(\mathbf{C}_1, \mathbf{C}_2) \leq r_1 + r_2$$

- 3) The patch resulting from the collision has the same area, as the sum of the areas of the two colliding patches
- 4) The bigger patch 'absorbs' the smaller patch and survives -> the resulting patch has the same center and lifespan as the biggest and oldest, of the two colliding patches
- 5) If a patch hits the land, it is marked as landed (N/S) and removed from the simulation



Simulation Model - Collision Detection using BSP Quadtrees

- Collision detection between N patches can be done at high computational cost by checking collisions of each of the N patches, against each other --> $O(N^2)$ [big-O notation, quantifies the amount of time required by a program to run, as a function of the length of the input, and excludes all coefficients and lower order terms]

- While this is perfectly fine for a small number of patches (i.e. a limited sub-region of the area of interest), it becomes computationally unfeasible as the number of patches grows (*36h run-time for one single simulation*).

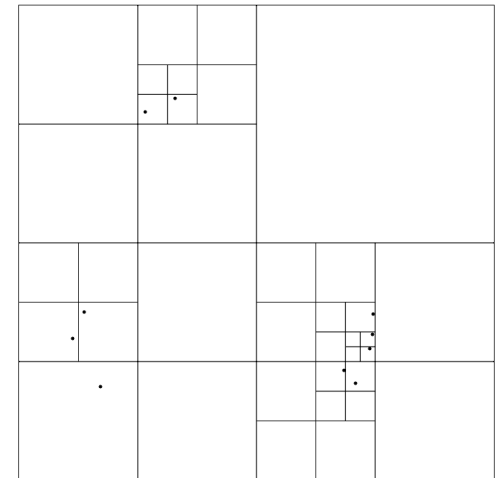
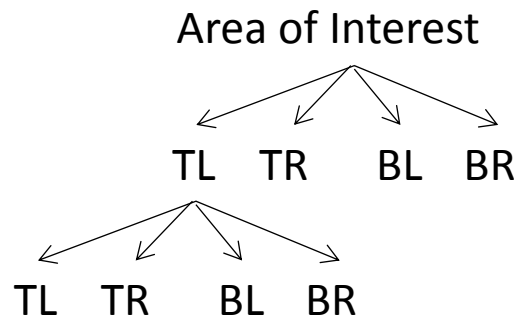
- Binary Space Partitioning (BSP) => Recursively subdivide a space into *convex sets* by using *hyperplanes*

- A **quadtree** structure is used. A quadtree is a 2D-BSP data structure for organizing points on a plane. It's represented tree-shaped data structure, where each internal node has exactly 4 children.

- This allows to bring down computational complexity for collision detection to:

$$O(\log N) \ll O(N^2), N > K$$

(*27s run-time for one single sim.*)



Simulation Results

- Simulations were run with the following parameters:

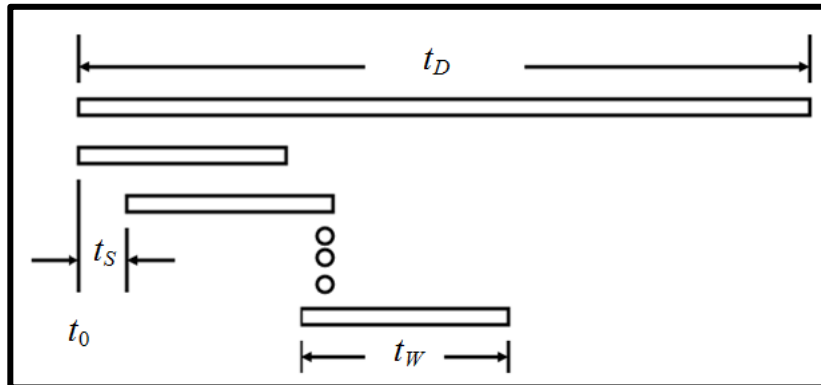
- $T_0 = [1/1/1987, 1/6/1987, 1/12/1987]$

- $T_w = 3$ days

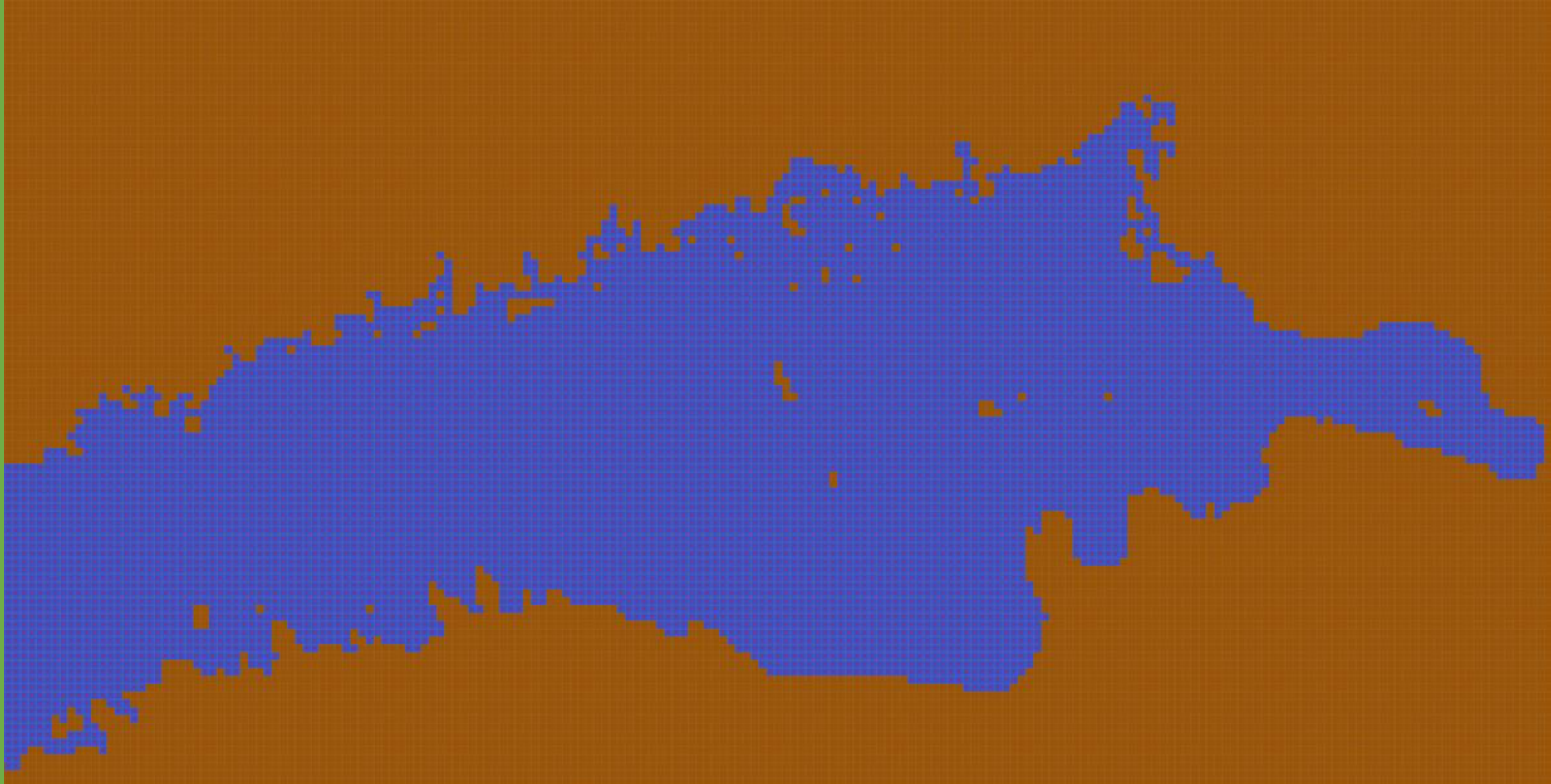
- $T_d = 30$ days

- $T_s = 3$ hours

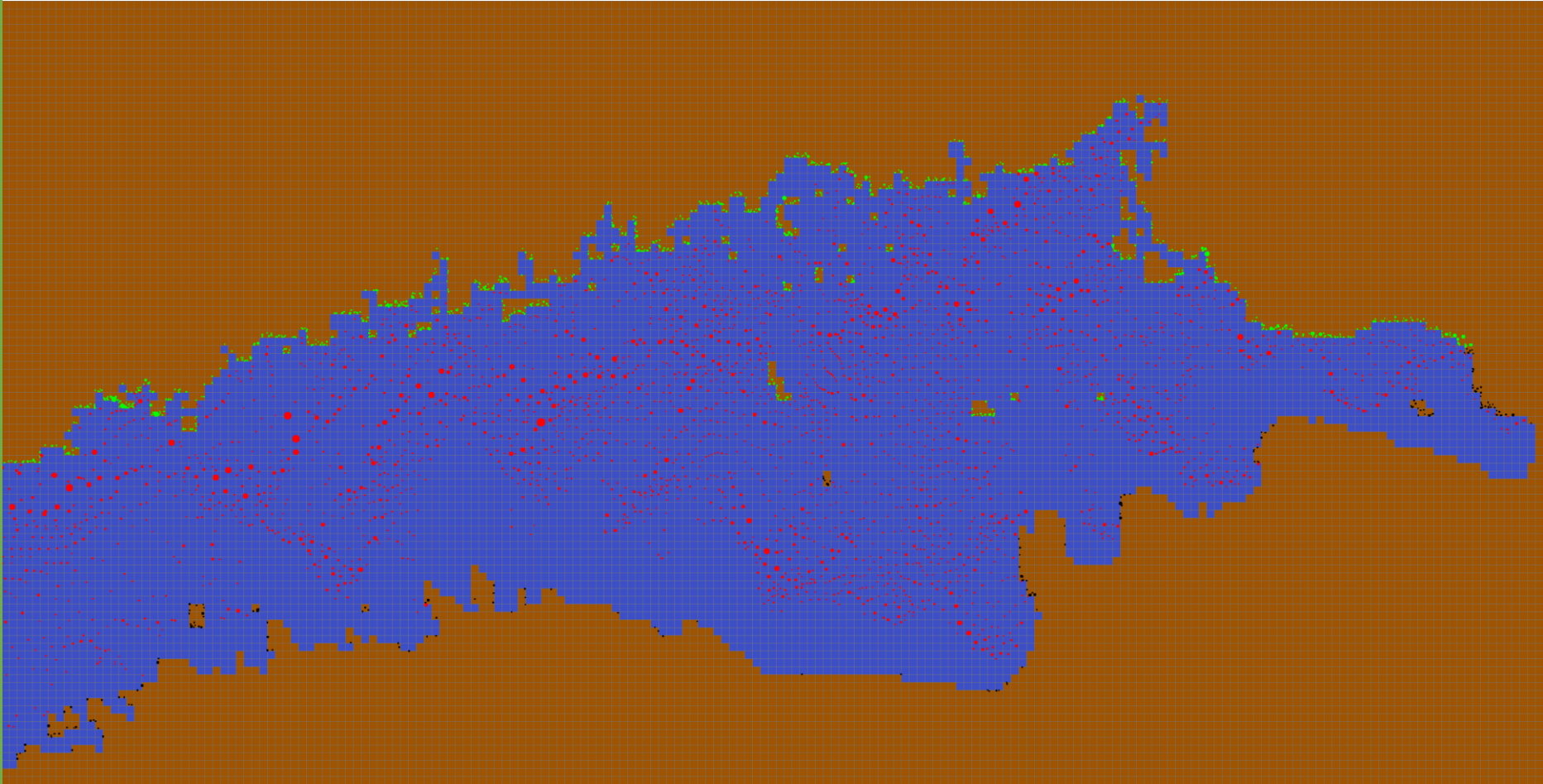
- The entire area of the Gulf of Finland was covered in the simulations



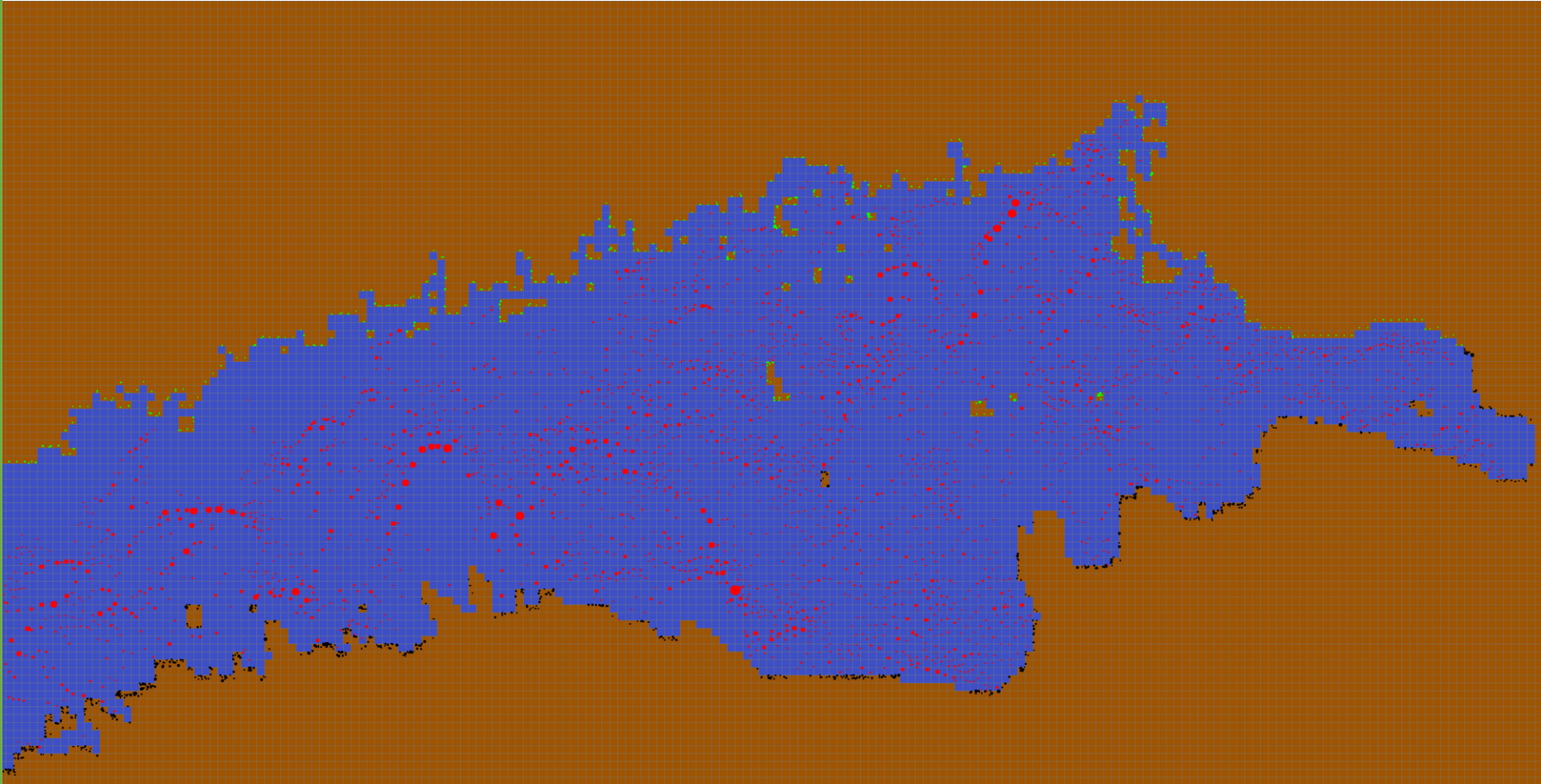
Gulf-wide 3 days run animation



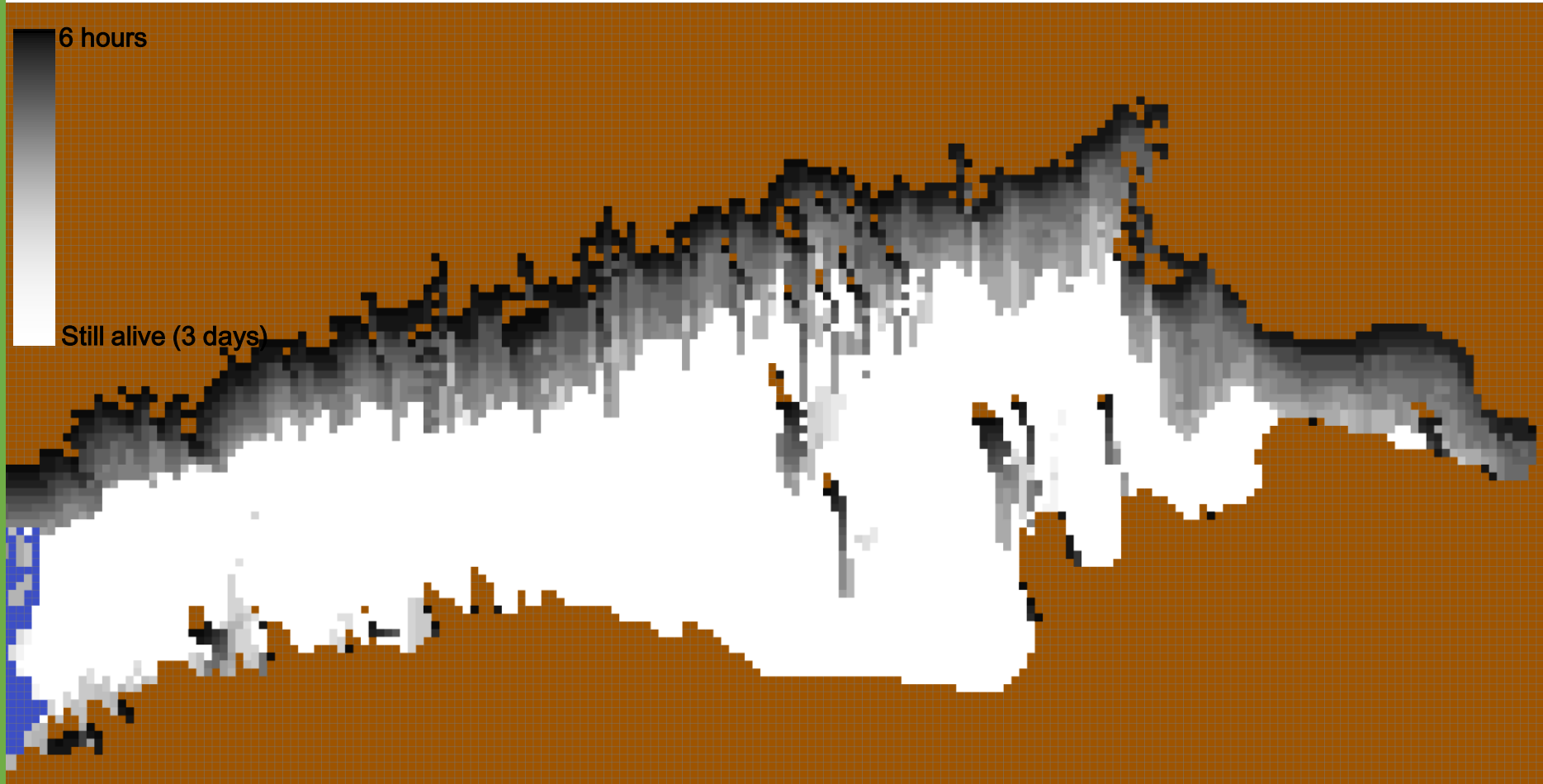
(3 days run final distribution w/ majority of coastal hits to the N coast)



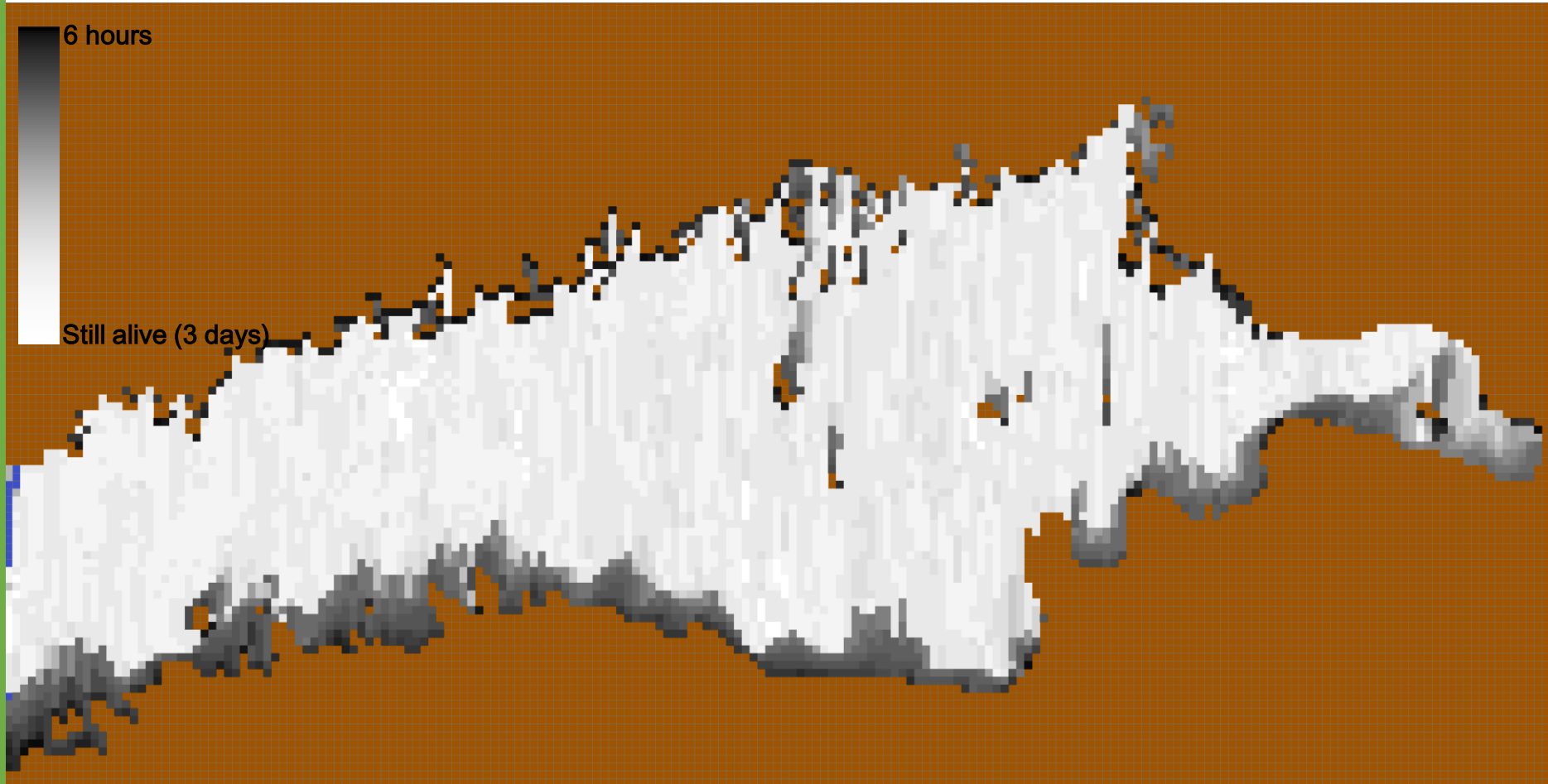
(3 days run final distribution w/ majority of coastal hits to the S coast)



(3 days run, patch max age w/ majority of coastal hits to the N coast)



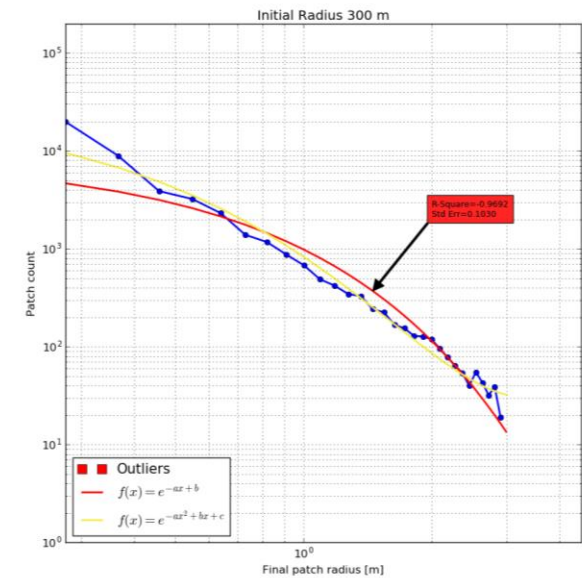
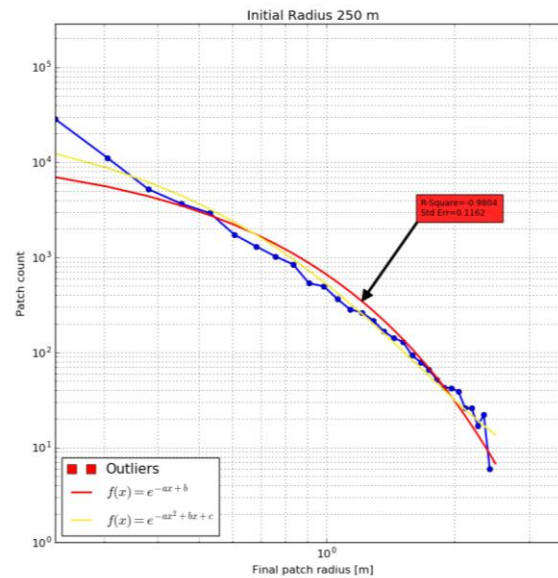
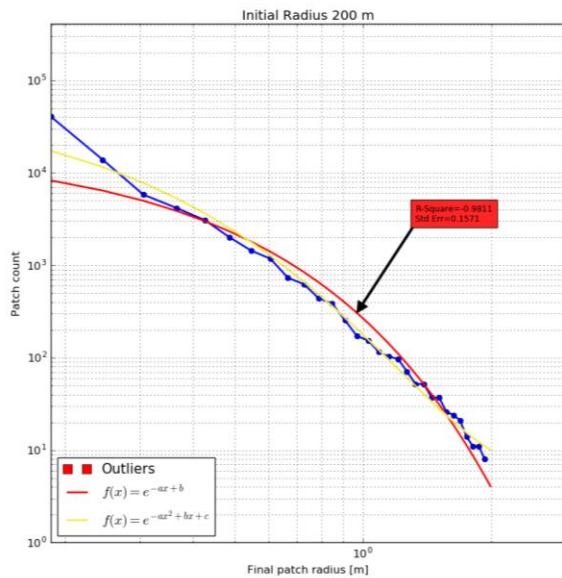
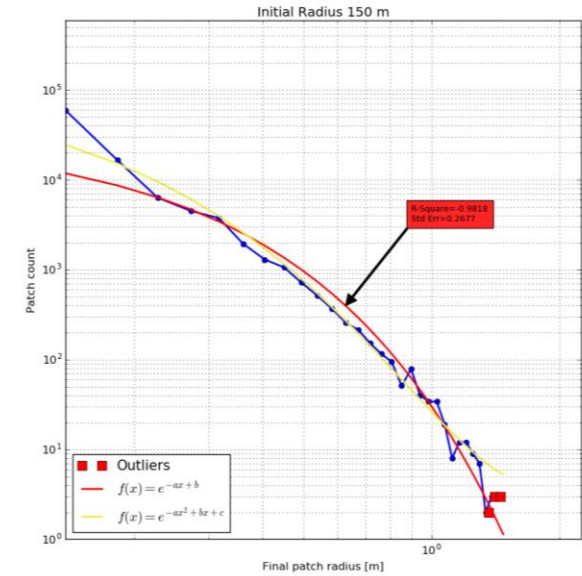
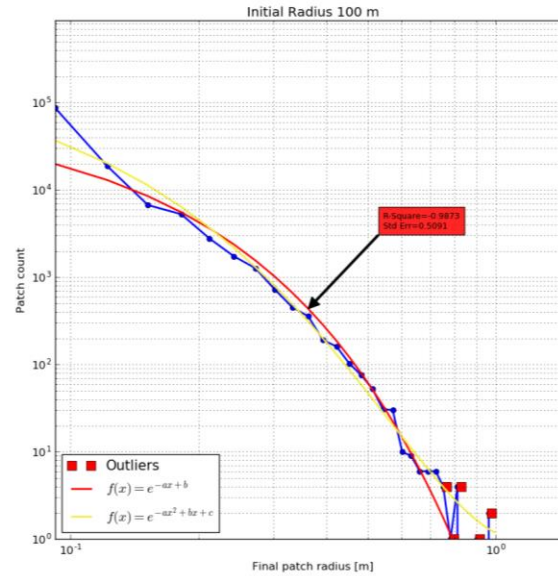
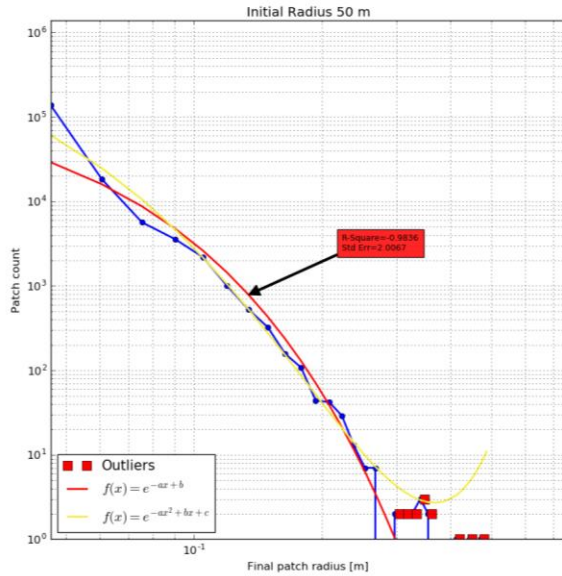
(3 days run, patch max age w/ majority of coastal hits to the S coast)



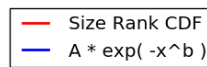
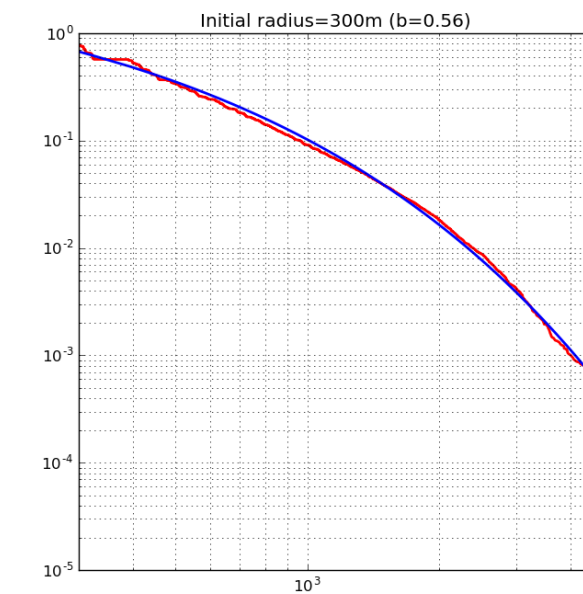
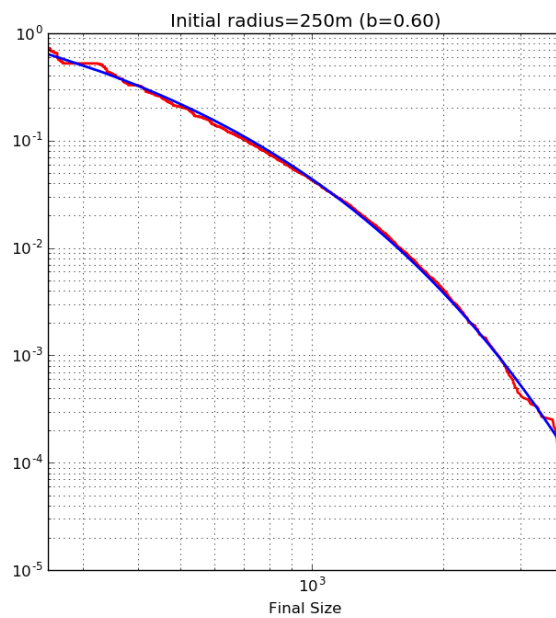
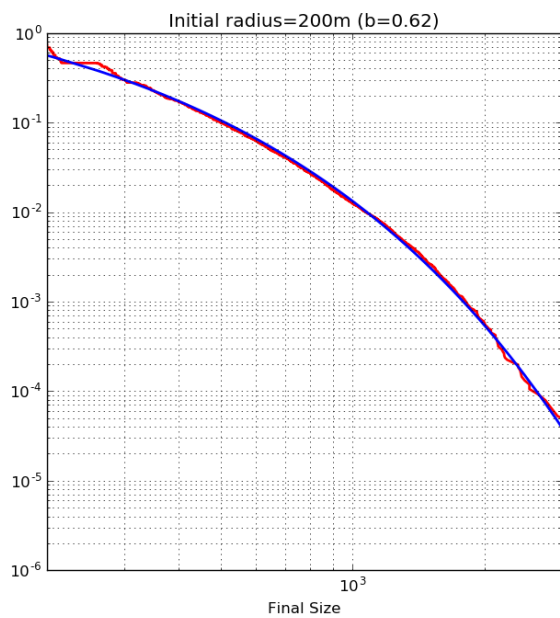
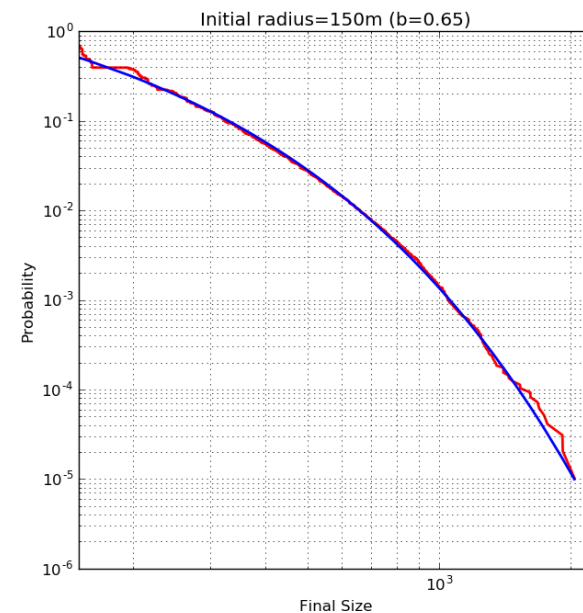
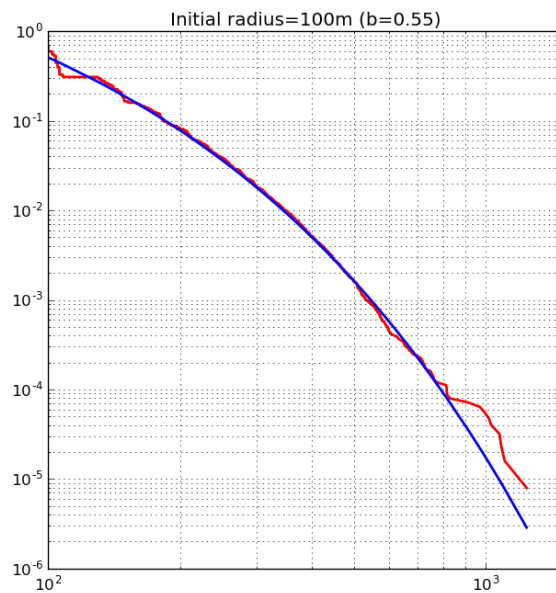
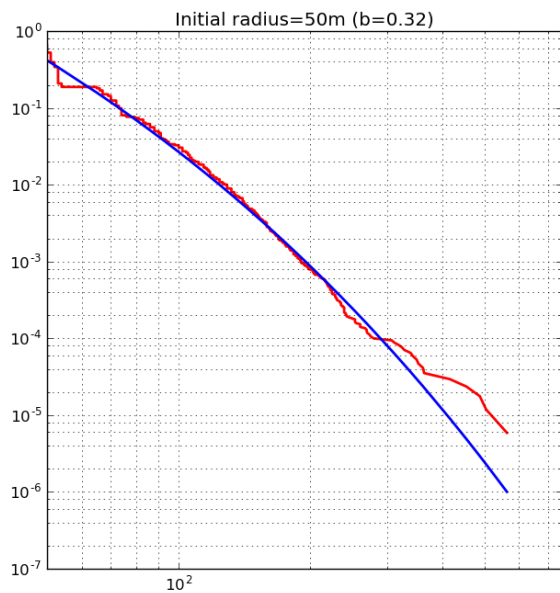
Simulation Statistics (1 month time interval T_d , 31 time windows of 3 days each)

Parameter	Value
Min Min size [m]	150
Max Max size [m]	1573 (+1048%)
Avg Avg size [m]	197 (+131%)
Min Min life span [h]	3
Max Max life span [h]	72
Avg Avg life span [h]	53.2
Avg Coast hits (North)	947
Avg Coast hits (South)	545

Patch size distribution (1 month time interval T_d , 31 time windows of 3 days each)

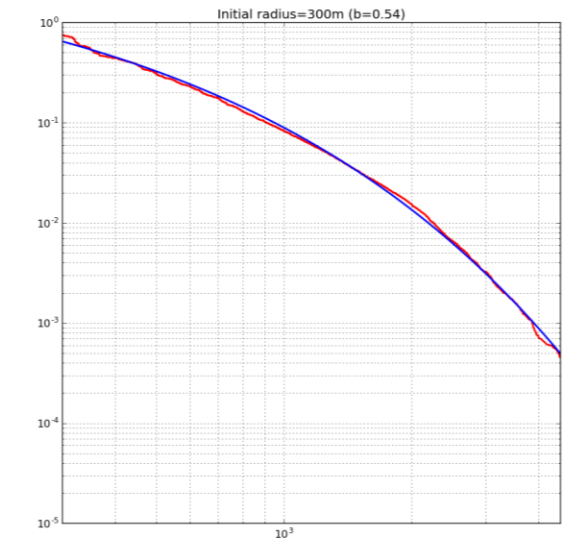
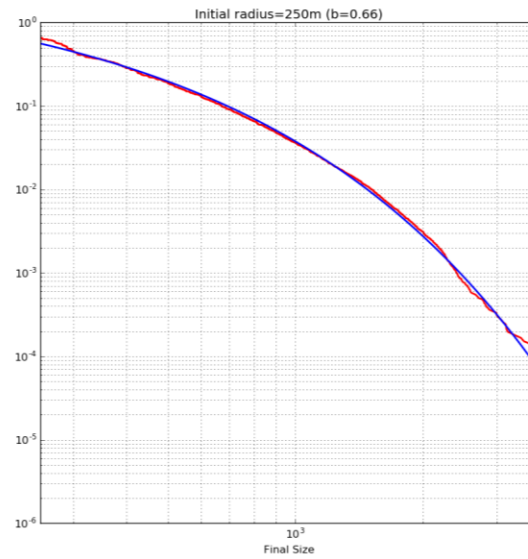
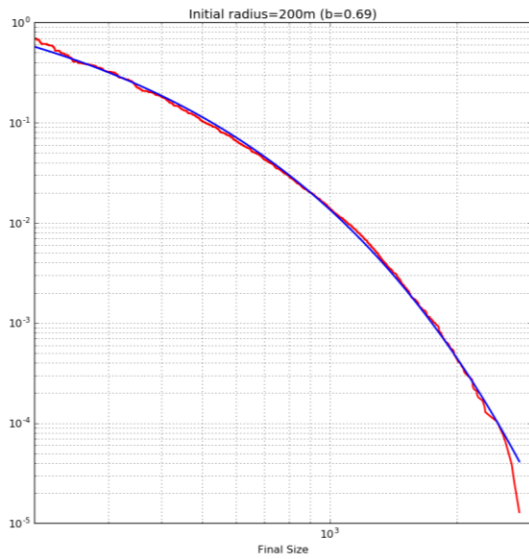
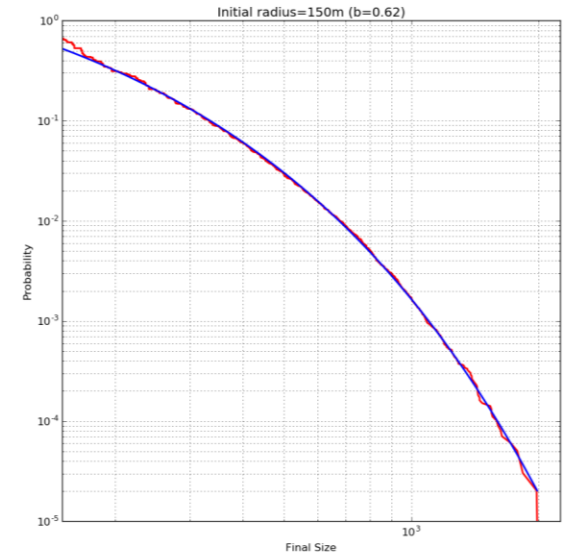
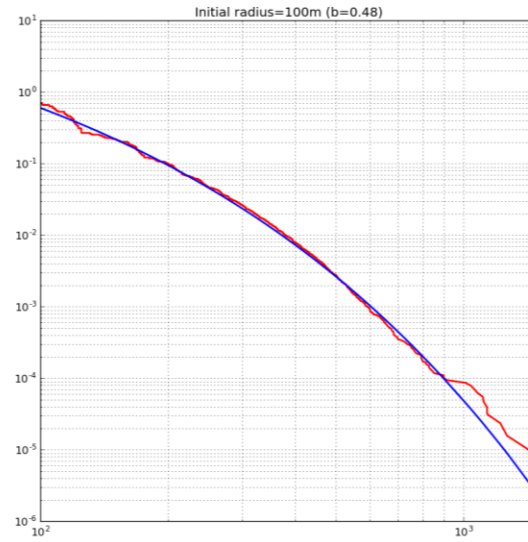
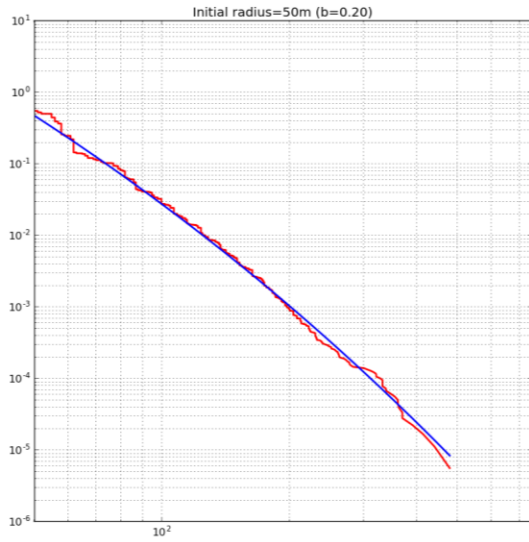


Patch rank CDF (1 month time interval T_d , 31 time windows of 3 days each)



Patch rank CDF (same parameters, uniform wind)

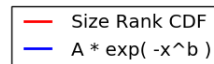
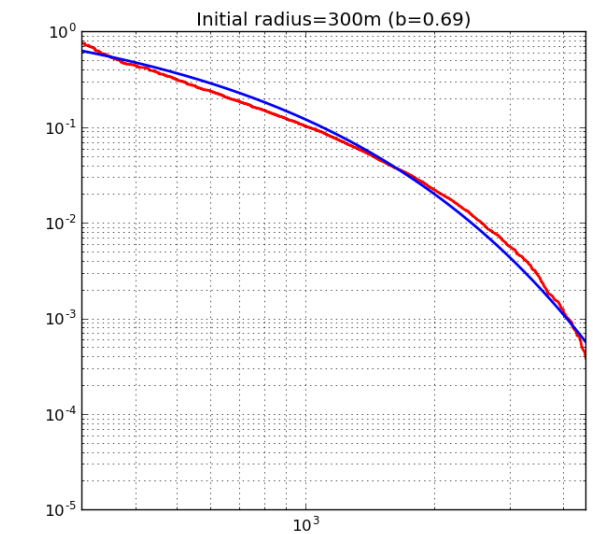
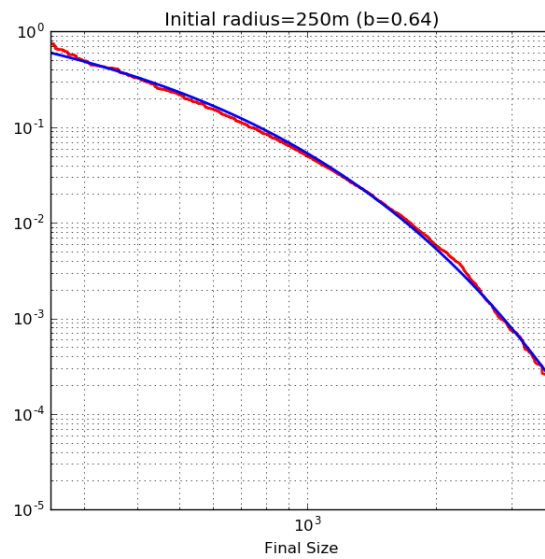
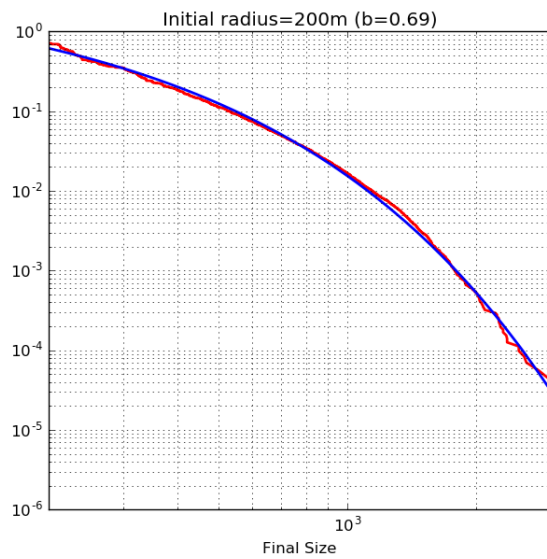
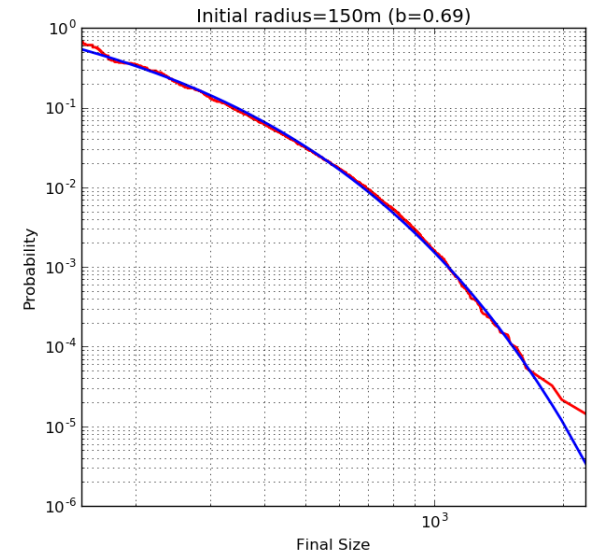
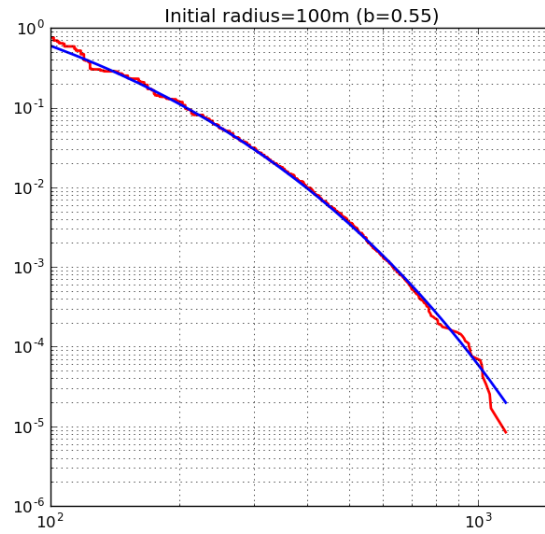
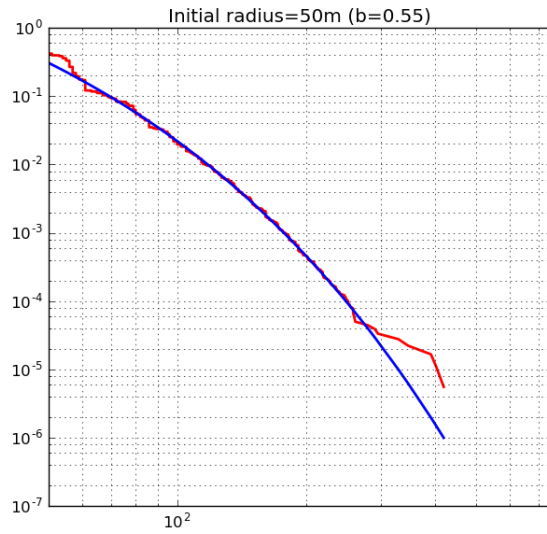
Patch size log-log cumulative probability distribution



— Size Rank CDF
— $A * \exp(-x^b)$

Patch rank CDF (same parameters, flipped wind)

Patch size log-log cumulative probability distribution



Conclusions

- A model is introduced, to simulate the behavior of patches of floatant material on the sea surface, under the combined effect of currents and winds.
- The model employs current data from the OAAS model and wind data calculated from geostrophic wind information.
- The model employs binary-space partitioning of the region of interest to achieve adequate performance when computing collisions between patches in a large-size simulation area.
- The model was run in the area of the Gulf of Finland using a characteristic time subdivision mechanism, during 3 different months.
- The empirical distribution of the number of patches of different size does not really follow an exponential or Gauss/Weibull type of distribution
- **This empirical distribution seems universal and resistant to several parameter changes, and follows a stretched exponential power-law $f\beta(t)=\exp(-t\beta)$**
 - The power β in the exponent losely mirrors the initial patch size
- We regard this as an indicator that such processes on the sea surface are not really random; instead, they exhibit classic self-organisation and scale-invariance properties



Thank you.

Simulation Model - Collision Detection [Naive Approach]

- The easiest way is to check each patch, for collision against every other patch of the set.

==> This means that if there are N total patches, at every time-step, N*N collision checks must be performed

==> In this case the collision-checking algorithm would require a time in the order of

$O(N^2)$ *[big-O notation, quantifies the amount of time required by a program to run, as a function of the length of the input, and excludes all coefficients and lower order terms]*

- While this is perfectly fine for a small number of patches (i.e. a limited sub-region of the area of interest), it becomes computationally unfeasible as the number of patches grows.

Example: computing collisions in the model using this approach takes around 3s/timestep for ~200 patches. Computing the same thing for the entire Gulf of Finland (~8000 patches) takes 3 minutes

==> **Not acceptable**, too many time-steps to compute in a reasonable time
(1 run = 3min x 24timesteps x 30days = 2160 min = 36 hrs run time)

- This approach has the only advantage of offering a simple way to 'store' the patches inside a data structure -> a simple 2D array can be used.

Simulation Model - Collision Detection [BSP Approach]

- A slightly more complex way of storing the patches' positions, allows for a *much* faster way to obtain the collision detection.

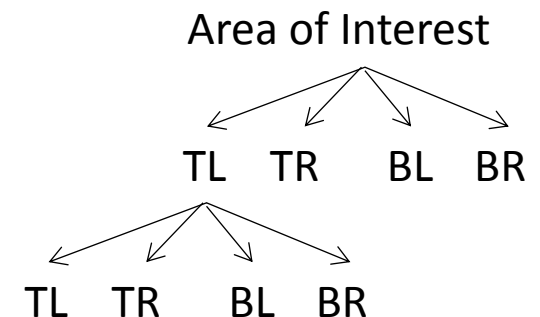
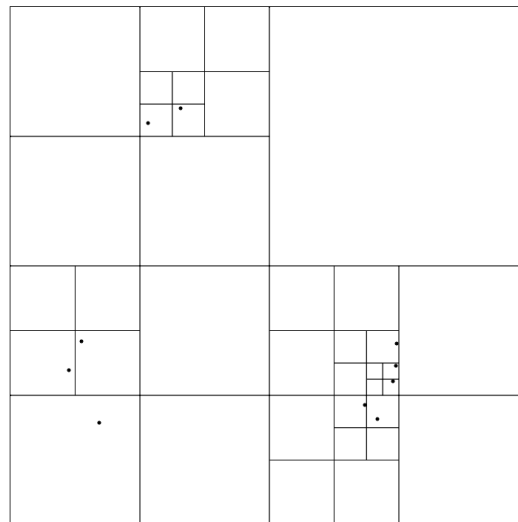
- BSP => Recursively subdivide a space into *convex sets* by using *hyperplanes*

[a region such that, for every pair of points within the region, every point on the straight line segment that joins the pair of points is also within the region]

[subspace of one dimension less than its ambient space]

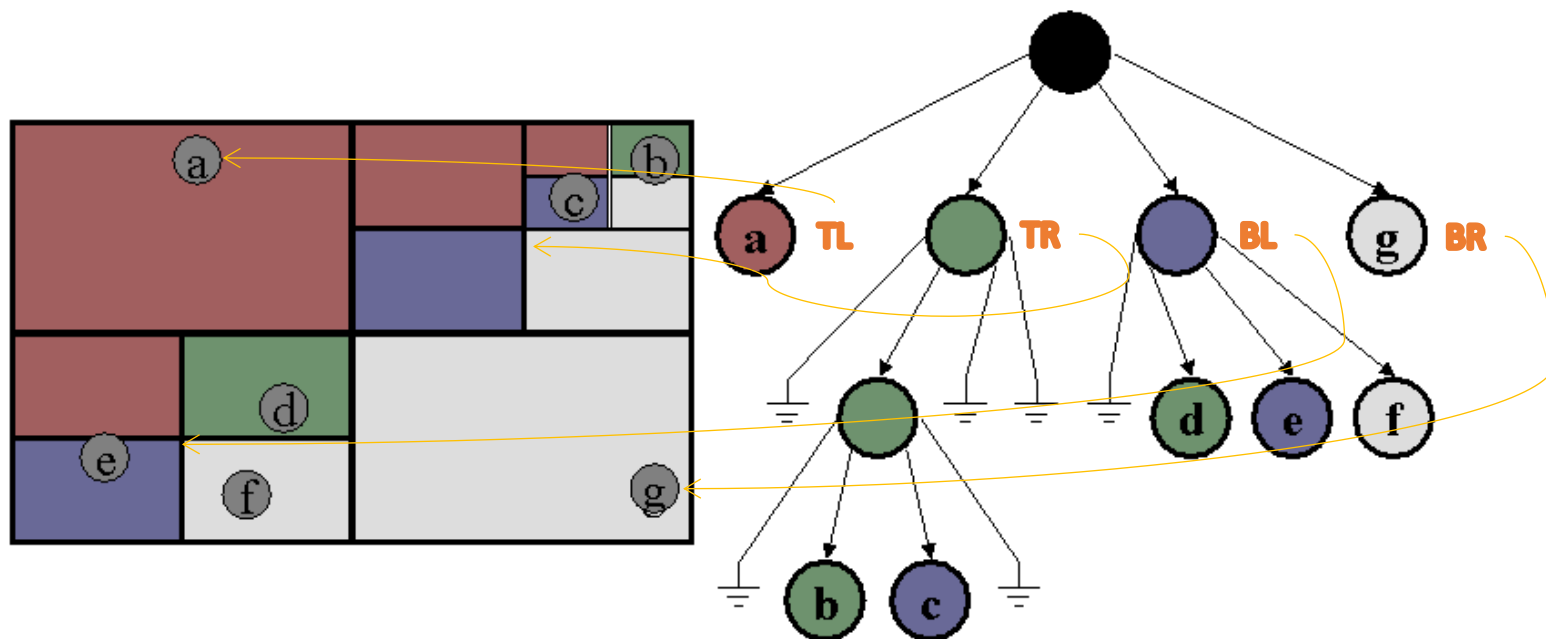
- A **quadtree** structure is used. A quadtree is a 2D-BSP data structure for organizing points on a plane. It's represented tree-shaped data structure, where each internal node has exactly 4 children.

- A region of the 2D plane is decomposed into four equal quadrants, subquadrants, and so on, with each leaf node containing only information about a patch, belonging to a specific subregion.



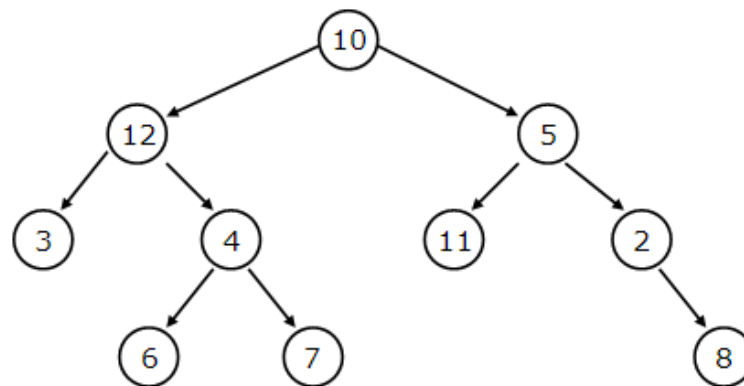
Simulation Model - Collision Detection - Quadtrees

- A quadtree decomposes space into adaptable cells
- Each cell has a maximum capacity of patches. When the max. capacity is reached, a cell is split into 4 sub-elements (a new level is added to the tree)
- The tree directory follows the spatial decomposition of the quadtree
- Notes on balancing the tree / bad cases



Simulation Model - Collision Detection - Quadrees

- With this approach, some 'performance' (= time) is lost while adding patches to the structure, as the tree needs to be traversed every time, to determine which 'leaf' the new patch will be in. This takes $O(N \log N)$ at worst [with the *naive* approach, it takes constant time $O(1)$]
- A lot of time is saved though, when computing collisions, as this can be done only between each patch, and its *closest neighbor* within the spatial structure.
- Note on Recursive Tree Traversing
- **Nearest Neighbor Search (NN)** -> it's an algorithm which aims at finding the point in the tree, that is nearest to a point given as input.
 - This search can be done *efficiently* using the properties of the tree to quickly eliminate large portions of the search space:



Levelorder tree traversal
10, 12, 5, 3, 4, 11, 2, 6, 7, 8

Inorder tree traversal
3, 12, 6, 4, 7, 10, 11, 5, 2, 8

Preorder tree traversal
10, 12, 3, 4, 6, 7, 5, 11, 2, 8

Postorder tree traversal
3, 6, 7, 4, 12, 11, 8, 2, 5, 10

Simulation Model - Collision Detection - Quadrees

- 1) Starting from the root node, the algorithm moves down the tree recursively -> it goes left or right depending on whether the point is lesser or greater than the current node in the split dimension
- 2) Once the algorithm reaches a leaf node, it marks the corresponding patch as the 'current best'
- 3) The algorithm unwinds the recursion on the tree, performing the following steps at each node:
 - 3a) If the current node is closer than the current best, then it becomes the current best
 - 3b) It checks whether there could be any points on the side of the splitting plane that are closer to the search point than the current best.
- 4) When the process is complete starting from the root node, the search is complete.

The nearest point is found in $O(\log N)$ time, given a completely random distribution of points.

$$O(\log N) \ll O(N^2), N > K$$

~~Example: computing collisions in the model using this approach takes around 3s/timestep for ~200 patches. Computing the same thing for the entire Gulf (~8000 patches) takes 3 minutes !!~~



3 seconds / timestep
for the *entire* GoF

From small scales to large scales
–The Gulf of Finland Science Days 2017
9th-10th October 2017
Estonian Academy of Sciences, Tallinn

2nd Day



**Gulf of Finland
Co-operation**

N. Kudryavtseva, K. Pindsoo, T. Soomere

Non-stationary extreme value modeling of trends in extreme water levels in the Gulf of Finland

NON-STATIONARY EXTREME VALUE MODELING OF TRENDS IN EXTREME WATER LEVELS IN THE GULF OF FINLAND

NADIA KUDRYAVTSEVA, KATRI PINDSOO, TARMO SOOMERE

TALLINN UNIVERSITY OF TECHNOLOGY

08.10.2017, THE GULF OF FINLAND SCIENCE DAYS 2017, TALLINN



TALLINN UNIVERSITY OF
TECHNOLOGY



OUTLINE

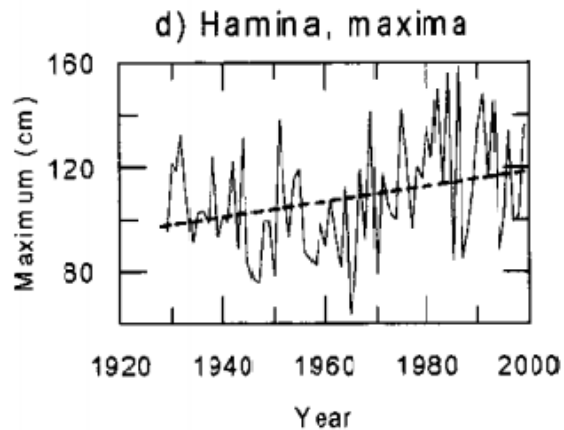
- Introduction
- NEMO model data
- Non-stationary extreme value modelling
- Results

MOTIVATION

- We know that climate is changing. Water levels are increasing by ~ 2 cm/decade – 10 cm/decade in the Baltic Sea
- Is the number of the extremes or its severity changing?
- It is unclear whether there is a positive trend or negative in number of extreme events in the Baltic Sea or is there spatial distribution of the trends

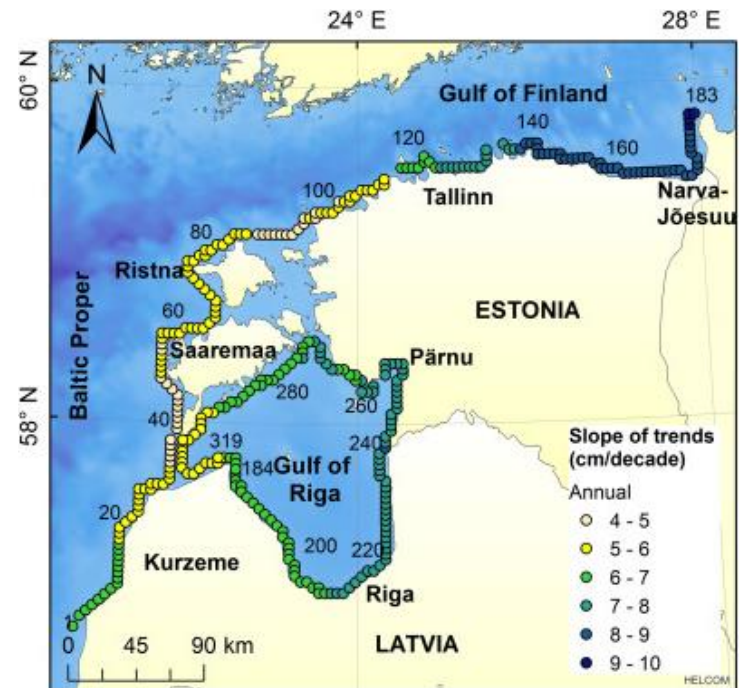


MOTIVATION



14.7 cm / 50 years trend in maxima
 Johansson et al. 2001, Boreal environmental
 Research, 6, 159

- Many previous studies showed different trends in the sea levels and extremes



Soomere & Pindsoo 2016, Continental
 Shelf Research, 115, 53



OUTLINE

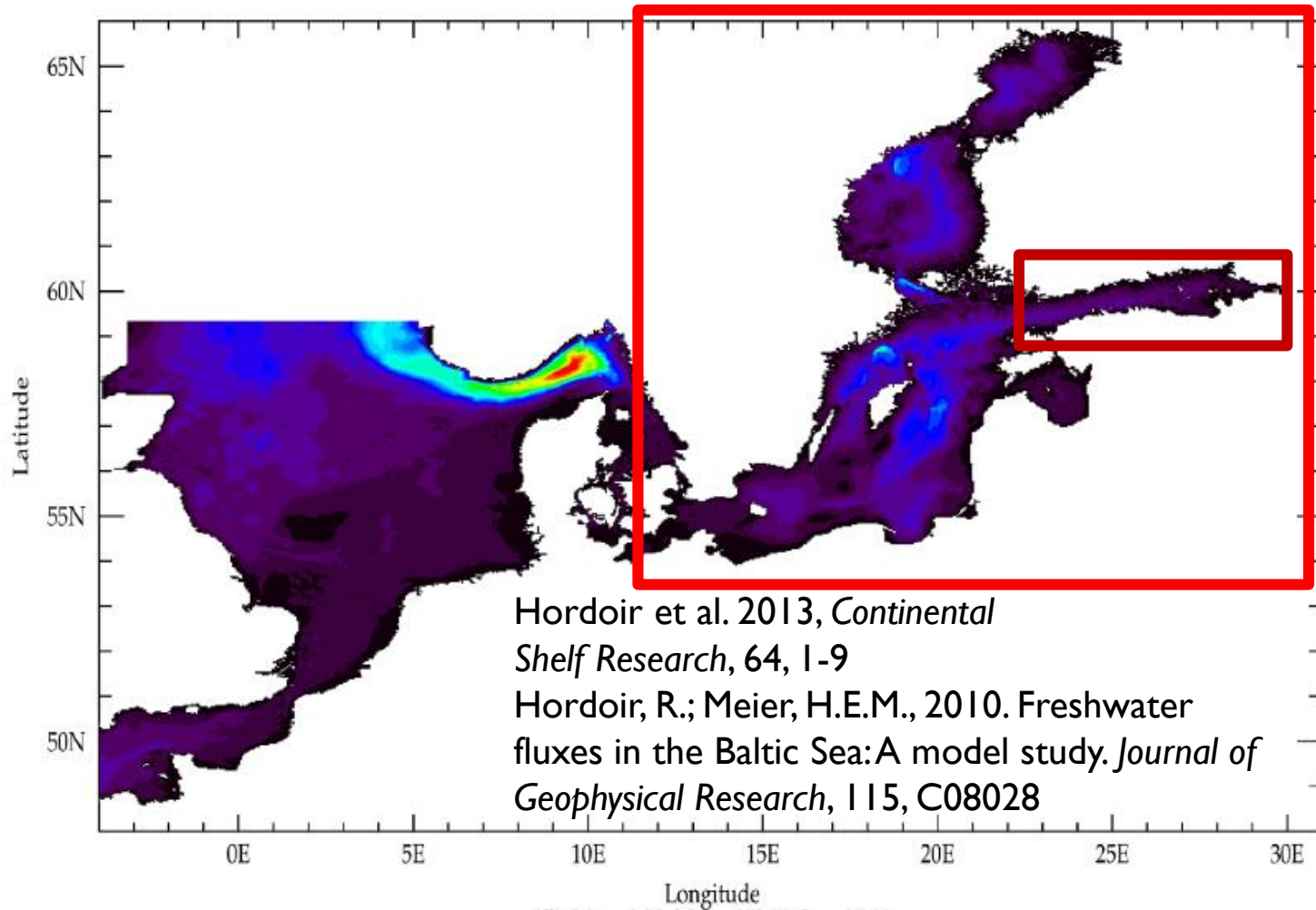
■ Introduction

■ NEMO model data

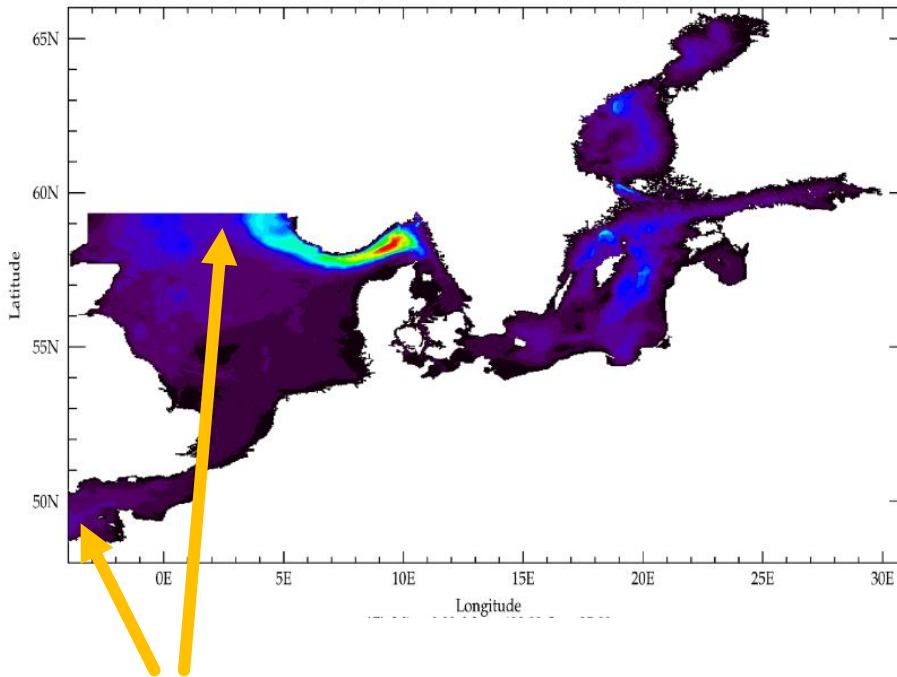
■ Non-stationary extreme value modelling

■ Results

NEMO BALTIX MODEL



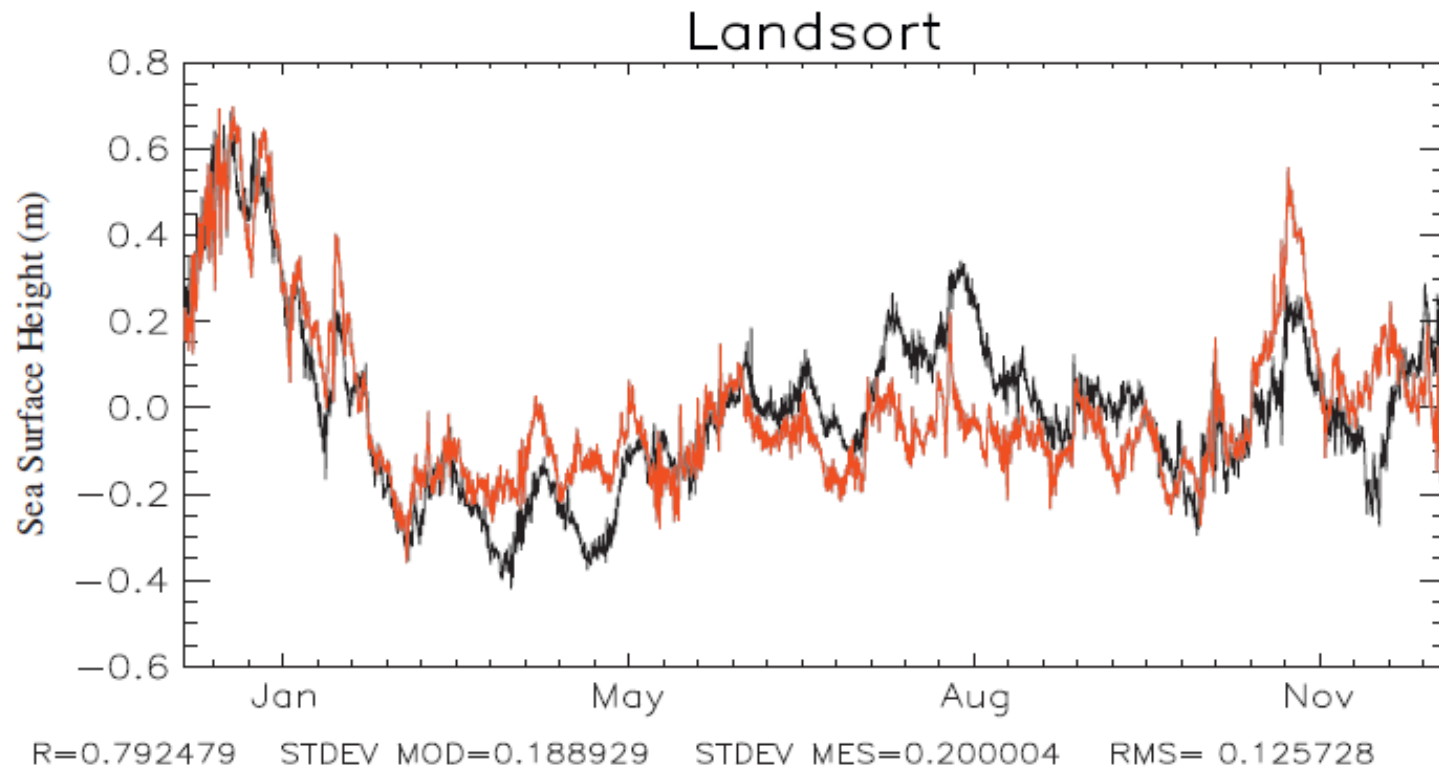
NEMO BALTIX MODEL



ERA 40 reanalysis forcing
RCA Samuelsson et. al. 2011

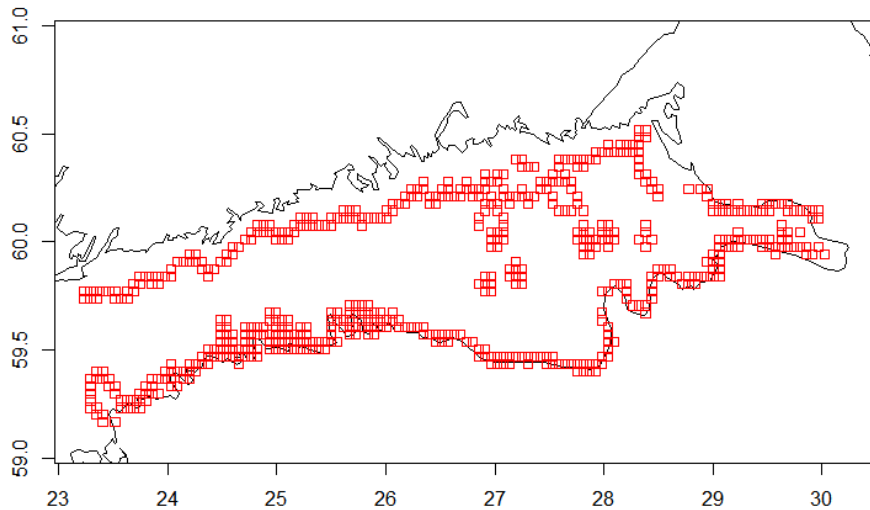
- 1979 – 2012 time period
- BaltiX configuration developed by SMHI
- 2 nautical miles resolution (3.7 km)
- 1 hour time resolution – good to catch extremes, not catching very fast variations
- Joined exchange of water between the North Sea and the Baltic Sea
- River runoff forcing O’dea et al. 2012 and Meier 2007

NEMO MODEL VALIDATION



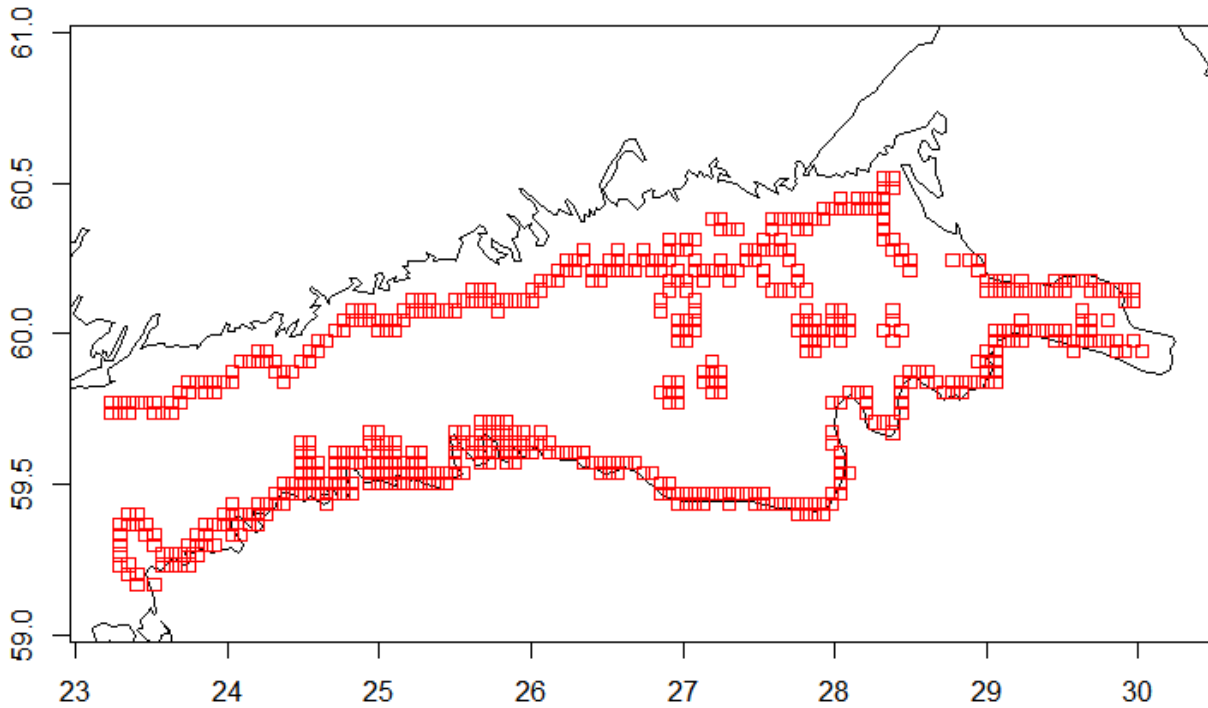
Hordoir et al. 2013, *Continental Shelf Research*, 64, 1-9

COASTLINE POINTS

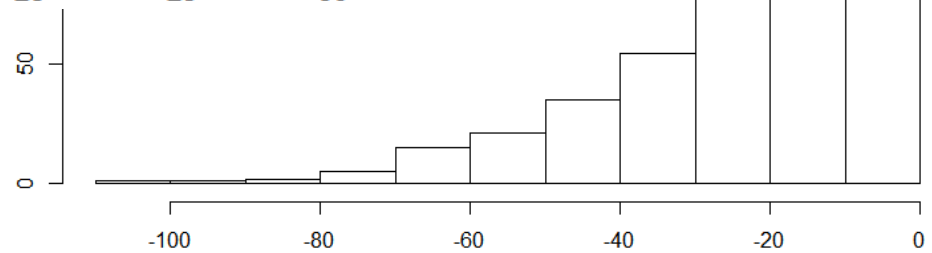


- Model extraction along coastline points
- IOW bathymetry (Seifert et al. 2001) to select points deeper than 4 meters
- For sandy beaches selected edge model grid points
- For rocky coast grid points between 0.06 – 0.1 degrees from coastline polynomial, GSHHG world shoreline Wessel, P., and W. H. F. Smith, A Global Self-consistent, Hierarchical, High-resolution Shoreline Database, *J. Geophys. Res.*, 101, #B4, pp. 8741-8743, 1996.

COASTLINE POINTS



■ Water depths < -4 meters



Water depth [m]

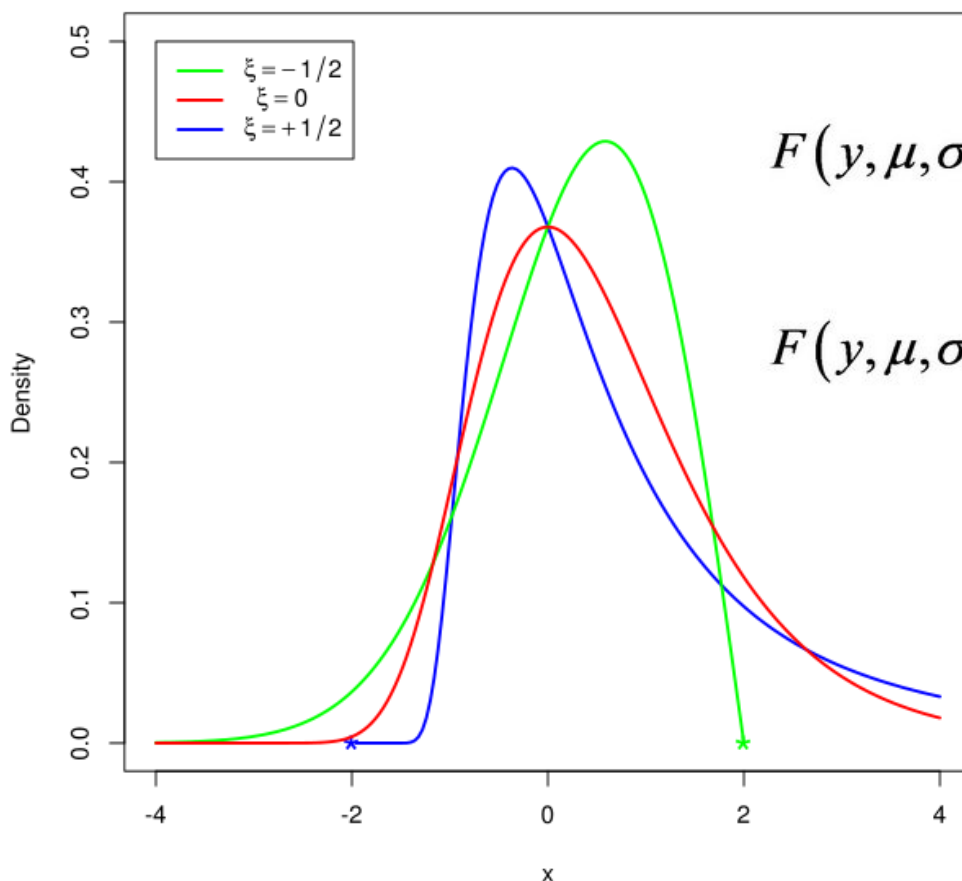


OUTLINE

- Introduction
- NEMO model data
- Non-stationary extreme value modelling
- Results

NON-STATIONARY EXTREME VALUE MODELLING

Generalized extreme value densities

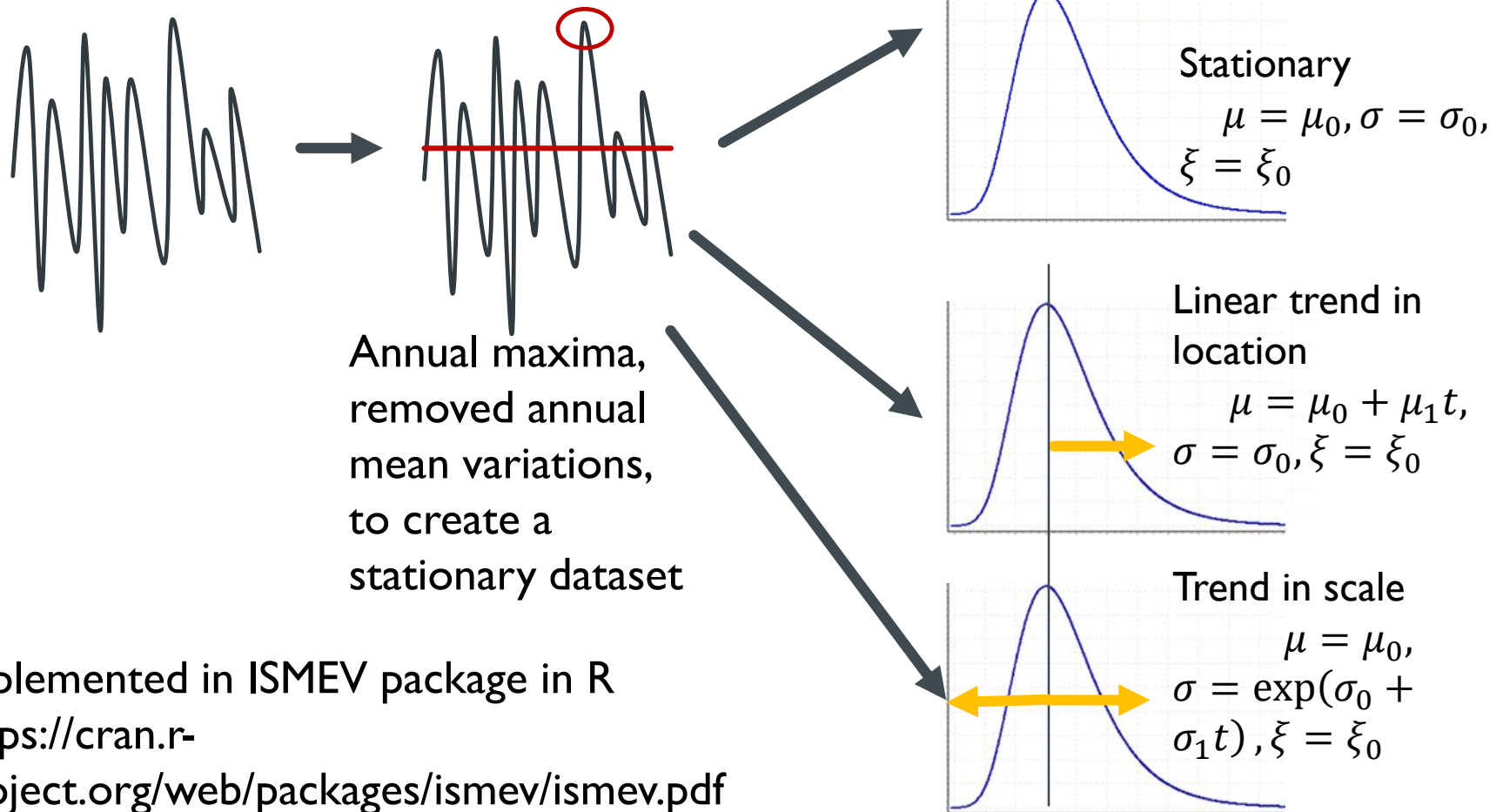


$$F(y, \mu, \sigma, \xi) = \exp \left[- \left(1 + \xi \left(\frac{y - \mu}{\sigma} \right) \right)^{-\frac{1}{\xi}} \right], \quad \xi \neq 0$$

$$F(y, \mu, \sigma, \xi) = \exp \left[- \exp \left(- \frac{y - \mu}{\sigma} \right) \right], \quad \xi = 0$$

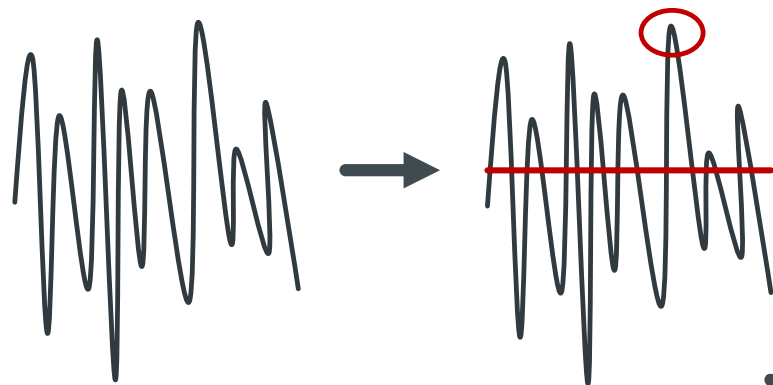
All with $\mu = 0$, $\sigma = 1$. Asterisks mark support-endpoints

NON-STATIONARY EXTREME VALUE MODELLING

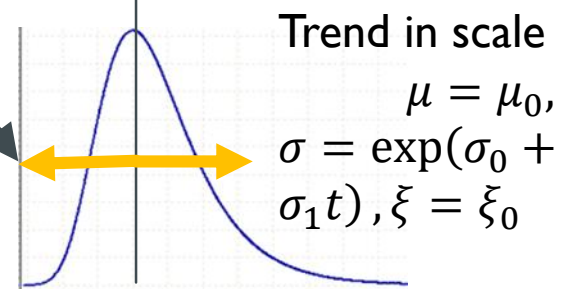
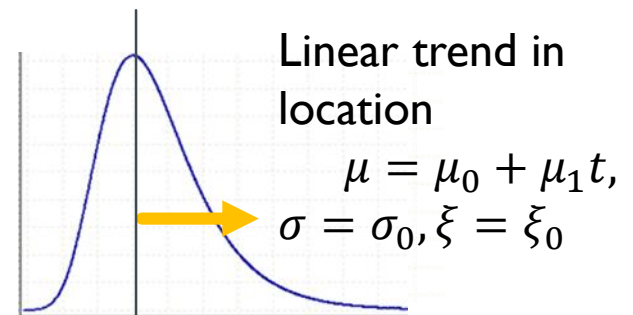
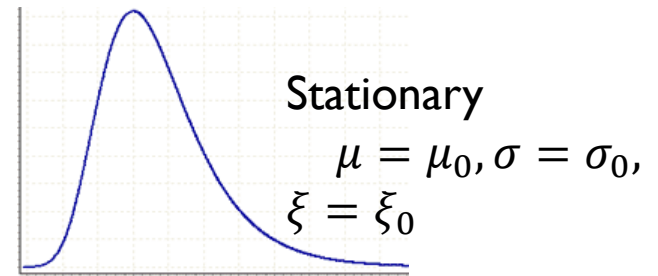


Implemented in ISMEV package in R
<https://cran.r-project.org/web/packages/ismev/ismev.pdf>

NON-STATIONARY EXTREME VALUE MODELLING



Important for engineering construction, allows to build things calculating return periods with linear trends accounted for



STATISTICAL SIGNIFICANCE STATIONARY VS NON-STATIONARY MODEL



- Used a likelihood ratio test to see how significant is non-stationary model to a stationary one
- Comparing goodness of fit for two models, using chi-square approach with $k = 1$ degree of freedom
- $LRT = 1 - pchisq(-2*(fit_non_stationary - fit_stationary))$

$$f(x; k) = \begin{cases} \frac{x^{(k/2-1)} e^{-x/2}}{2^{k/2} \Gamma\left(\frac{k}{2}\right)}, & x > 0; \\ 0, & \text{otherwise.} \end{cases}$$

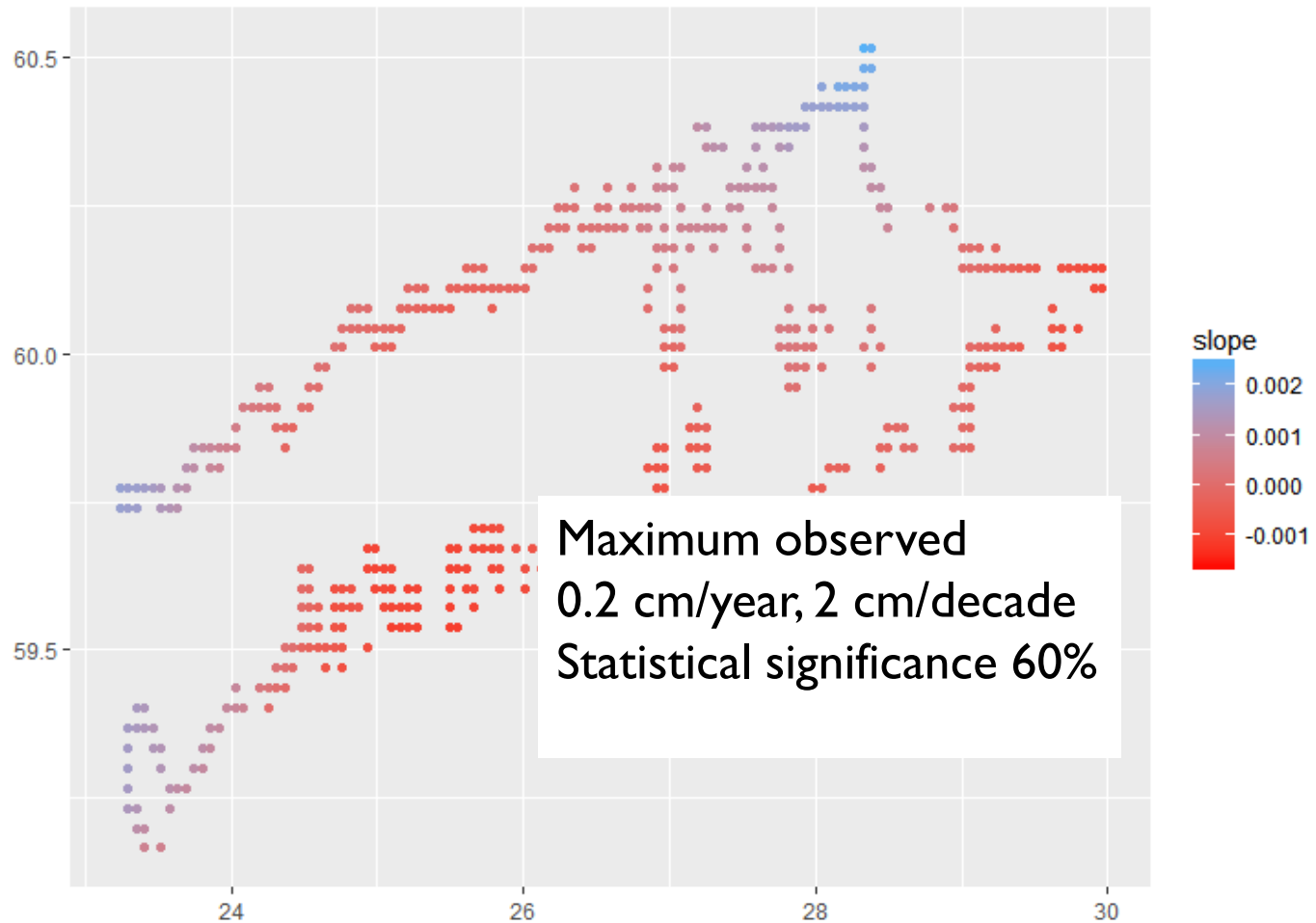


OUTLINE

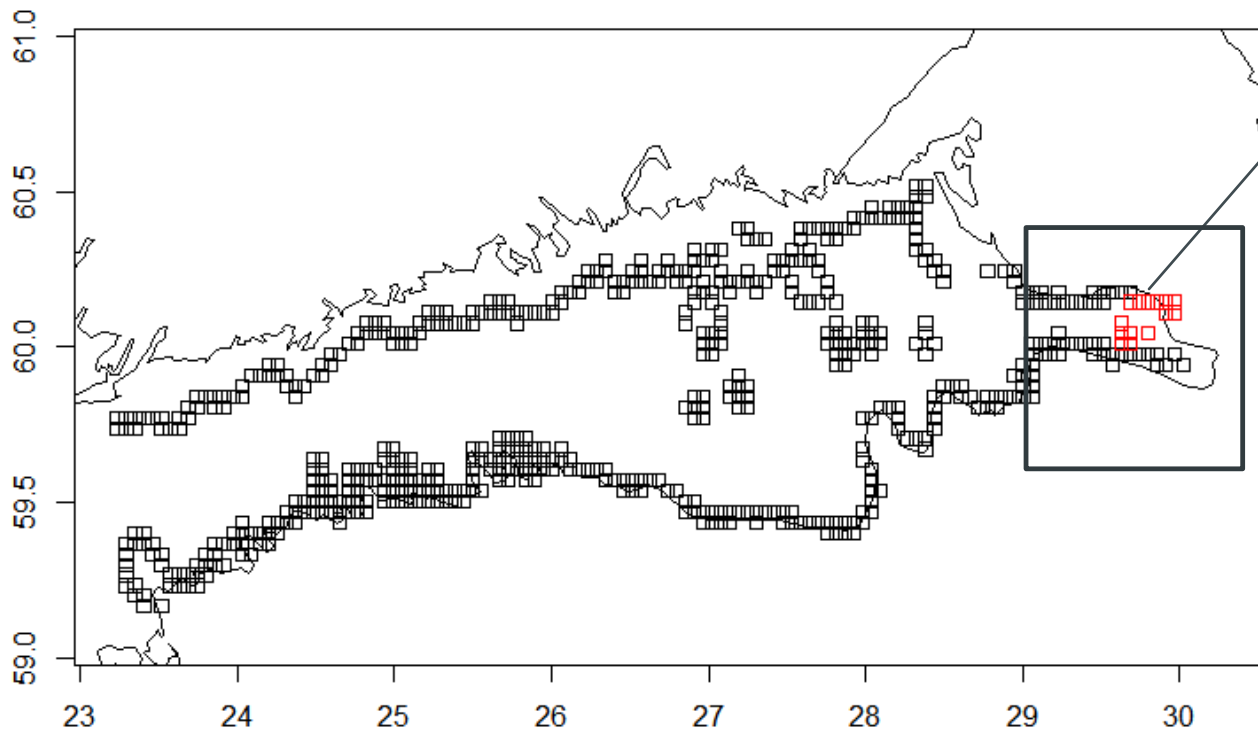
- Introduction
- NEMO model data
- Non-stationary extreme value modelling
- Results



TRENDS IN LOCATION (MU)

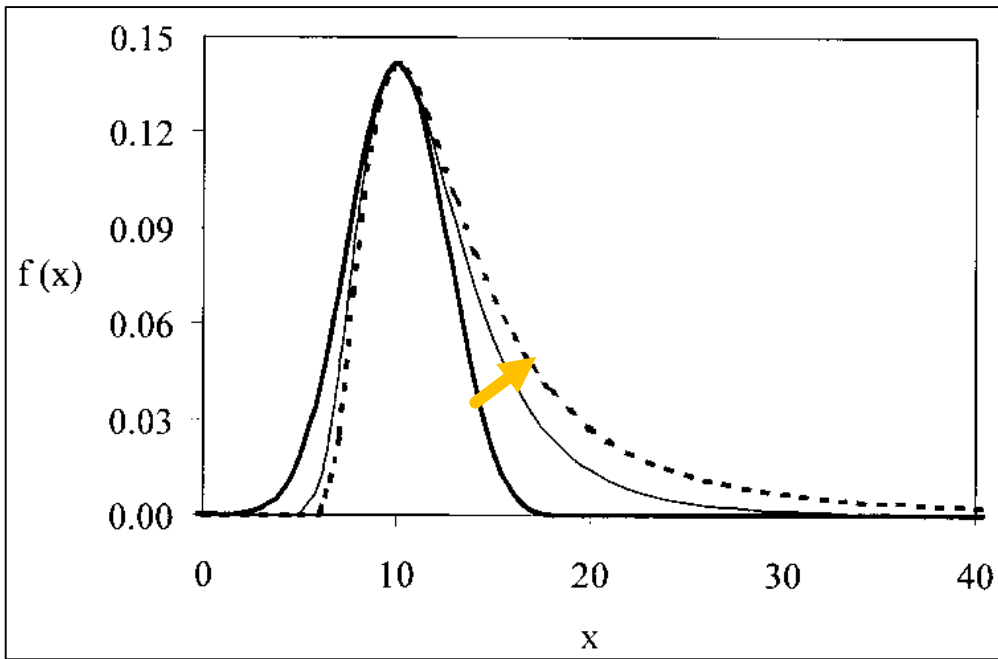


SIGNIFICANT LINEAR TRENDS SIGMA



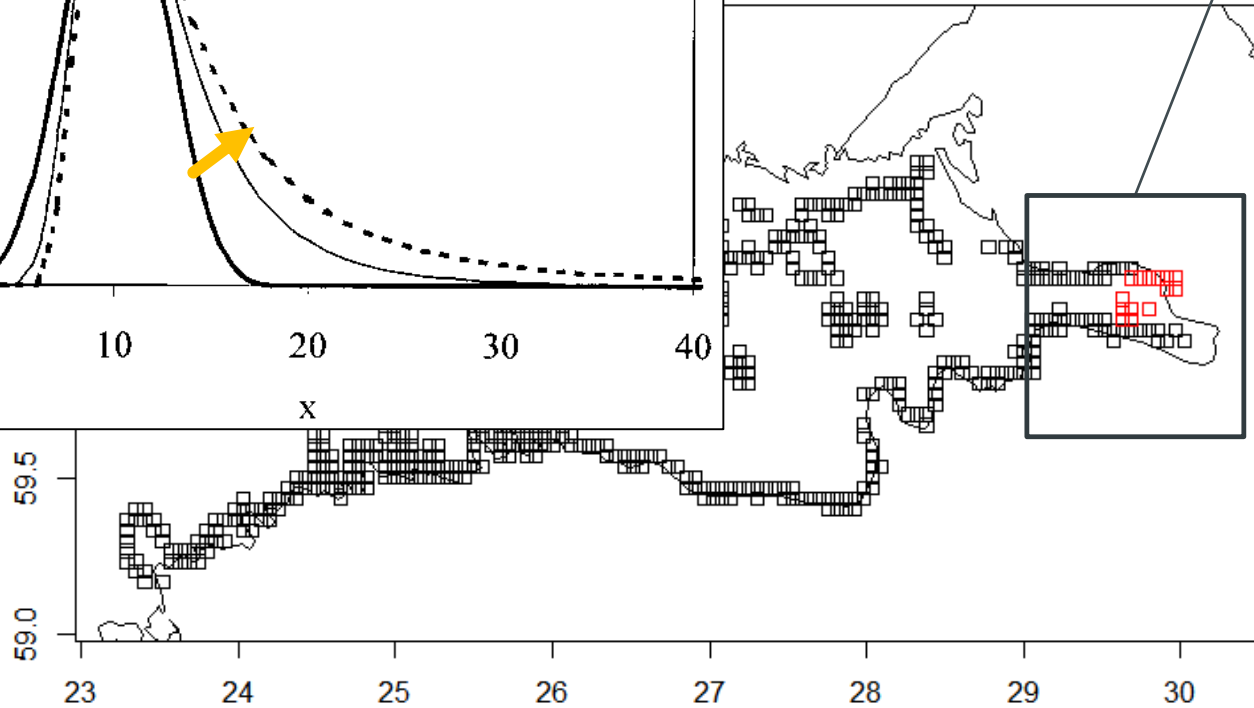
At 75% -
85% significance
level

SIGNIFICANT LINEAR TRENDS SCALE



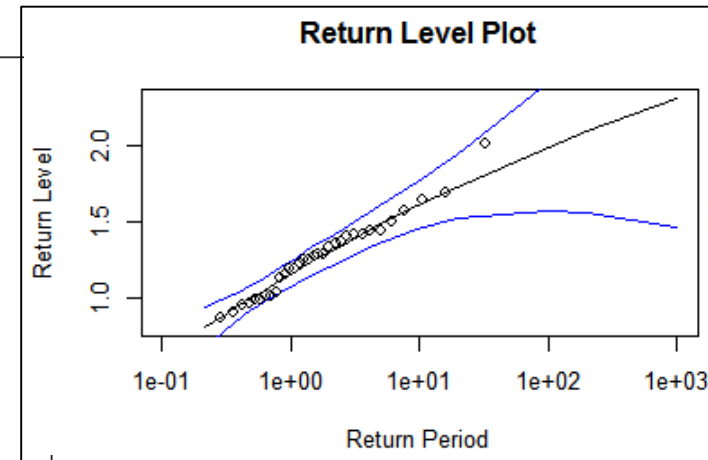
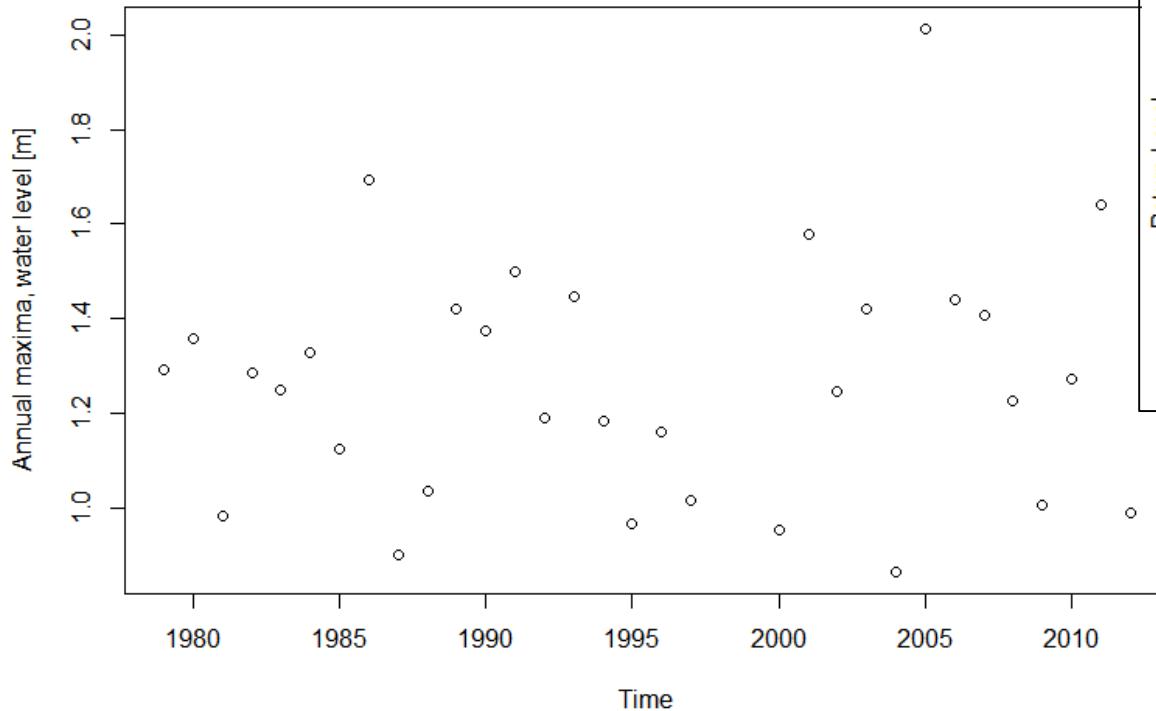
Change in scale parameter, widening of the distribution

At 75% - 85% significance level





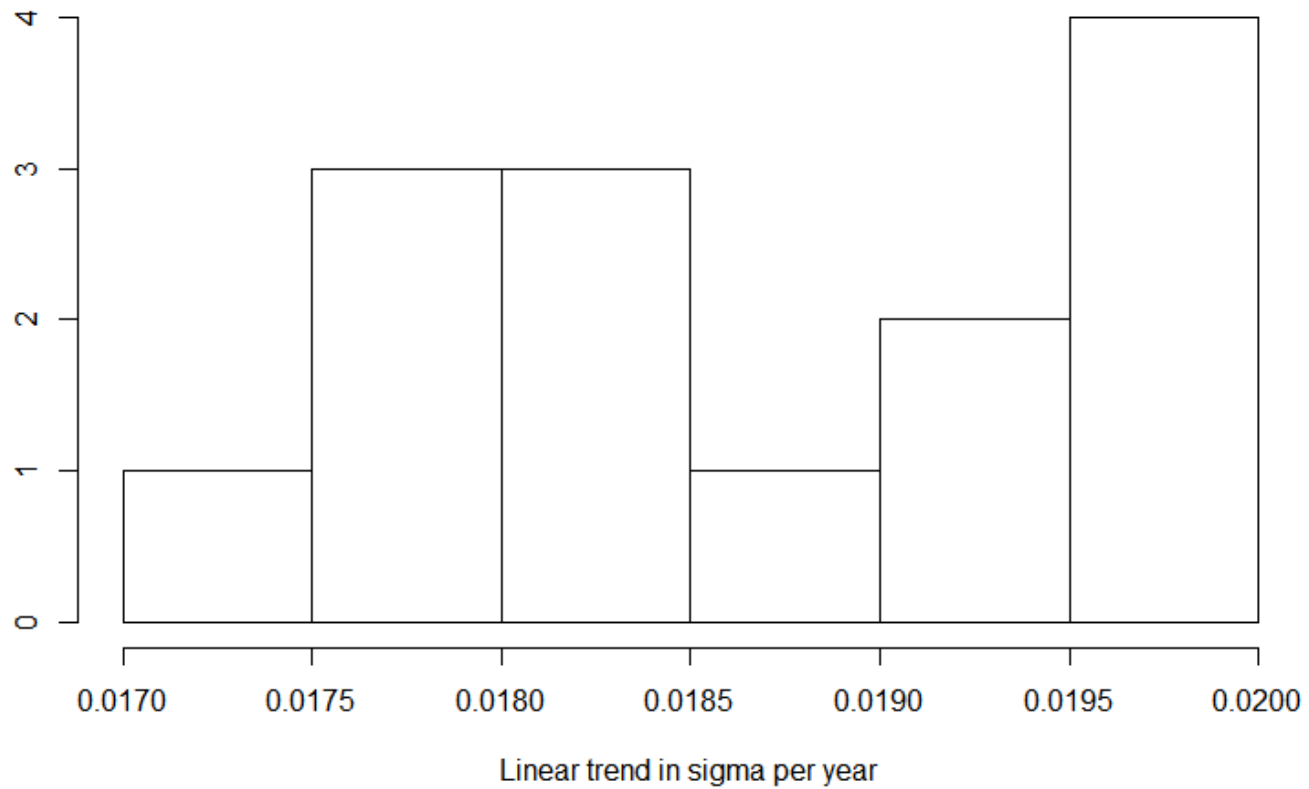
STATIONARY VS NON-STATIONARY FIT



■ $\text{Sigma } 0.255 + 0.014 * \text{time}$

TRENDS IN SCALE PARAMETER

Histogram of slope



SUMMARY

- Performed non-stationary extreme value modelling using NEMO joint Baltic Sea – North Sea water level model data
- An assumption of linear trends in location parameter was not statistically better than stationary fit
- An assumption of linear trends in scale parameter showed a good fit with preference of non-stationary model to stationary one with 85% significance level in the eastern part of Gulf of Finland
- That shows that the “middle-range” extreme values are increasing with time, not the most severe conditions



From small scales to large scales
–The Gulf of Finland Science Days 2017
9th-10th October 2017
Estonian Academy of Sciences, Tallinn

2nd Day



**Gulf of Finland
Co-operation**

V. Ryabchenko, I. Leontyev, D. Ryabchuk, A. Sergeev, A. Dvornikov, S. Martyanov, V. Zhamoida

Coastal erosion caused by storm surges and protection measures for the Kotlin Island's coastline in the Gulf of Finland: data analyses and modeling

Coastal erosion caused by storm surges and protection measures for the Kotlin Island's coastline in the Gulf of Finland: data analyses and modeling

Vladimir A. Ryabchenko¹, Igor O. Leontyev¹, Daria V. Ryabchuk², Alexander Yu. Sergeev², Anton Yu. Dvornikov¹, Stanislav D. Martyanov¹, Vladimir A. Zhamoida²

¹ P.P. Shirshov Institute of Oceanology, Russian Academy of Sciences

² A.P. Karpinsky Russian Geological Research Institute (VSEGEI)

The Gulf of Finland Science Days 2017
Tallinn, Estonia, 9-10 October 2017

Motivation

Analyses of remote sensing data of the western Kotlin coast revealed maximal for the eastern GoF erosion rates of 1.2-1.6 m/y during last 76 years. The trend can lead to the complete disappearance of sandy beaches of the western Kotlin in the future.

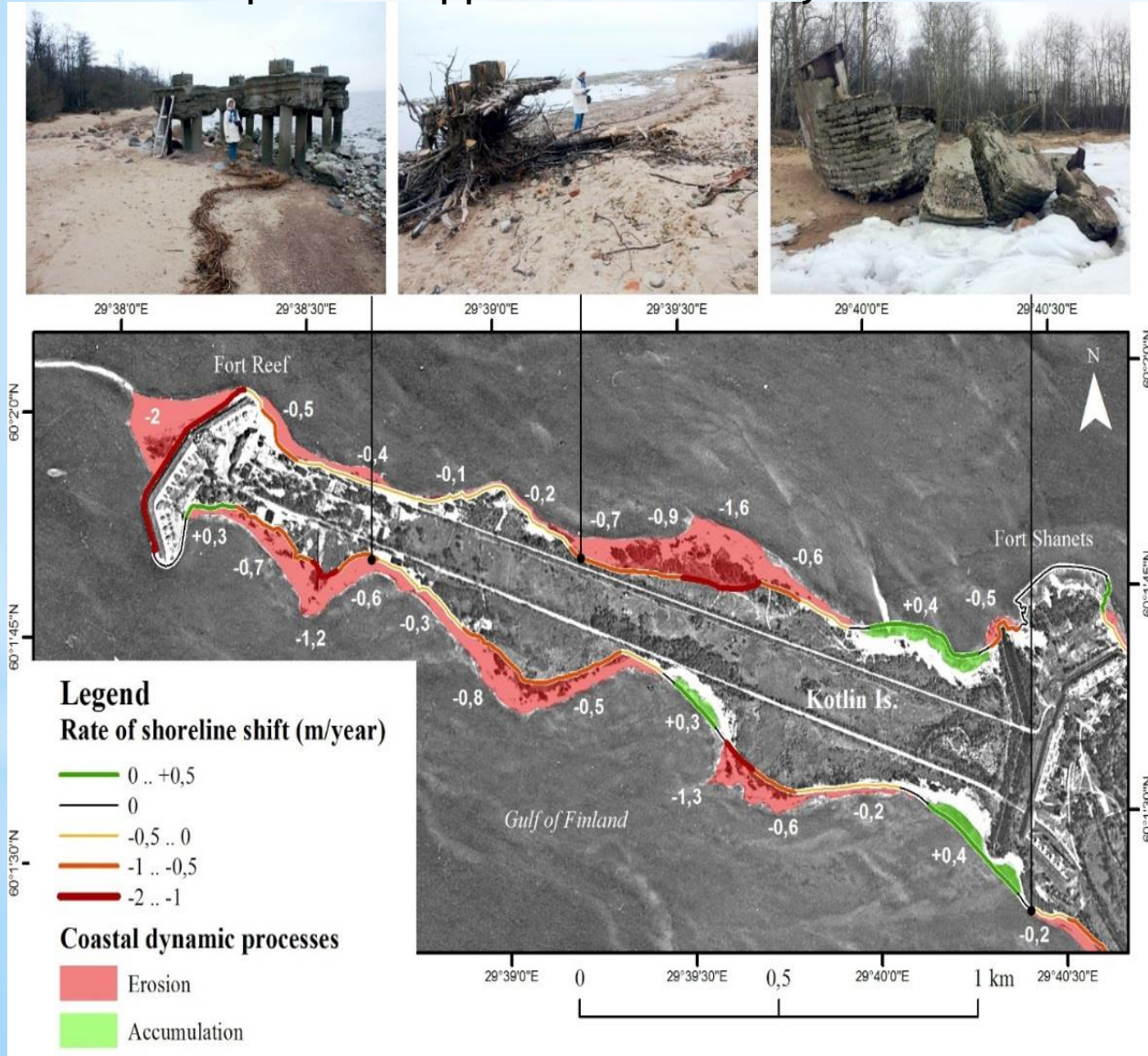
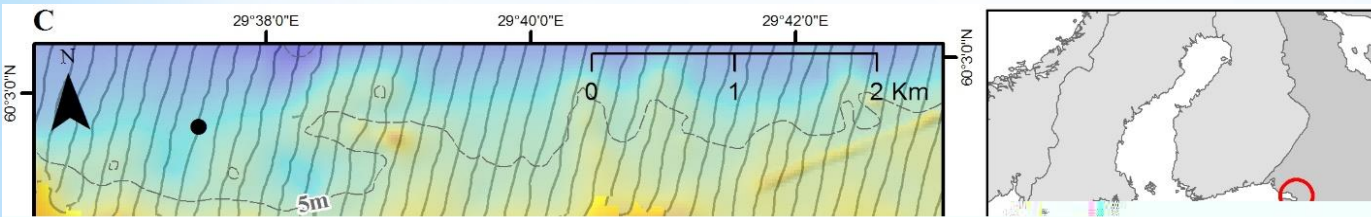


Fig. 1. Scheme of coastal dynamics of the western Kotlin. Analyses carried out using air-photography of 15.08.1939, resol. 2 m. Recent coastal line from Yandex maps, resol. 1 m.

Purposes

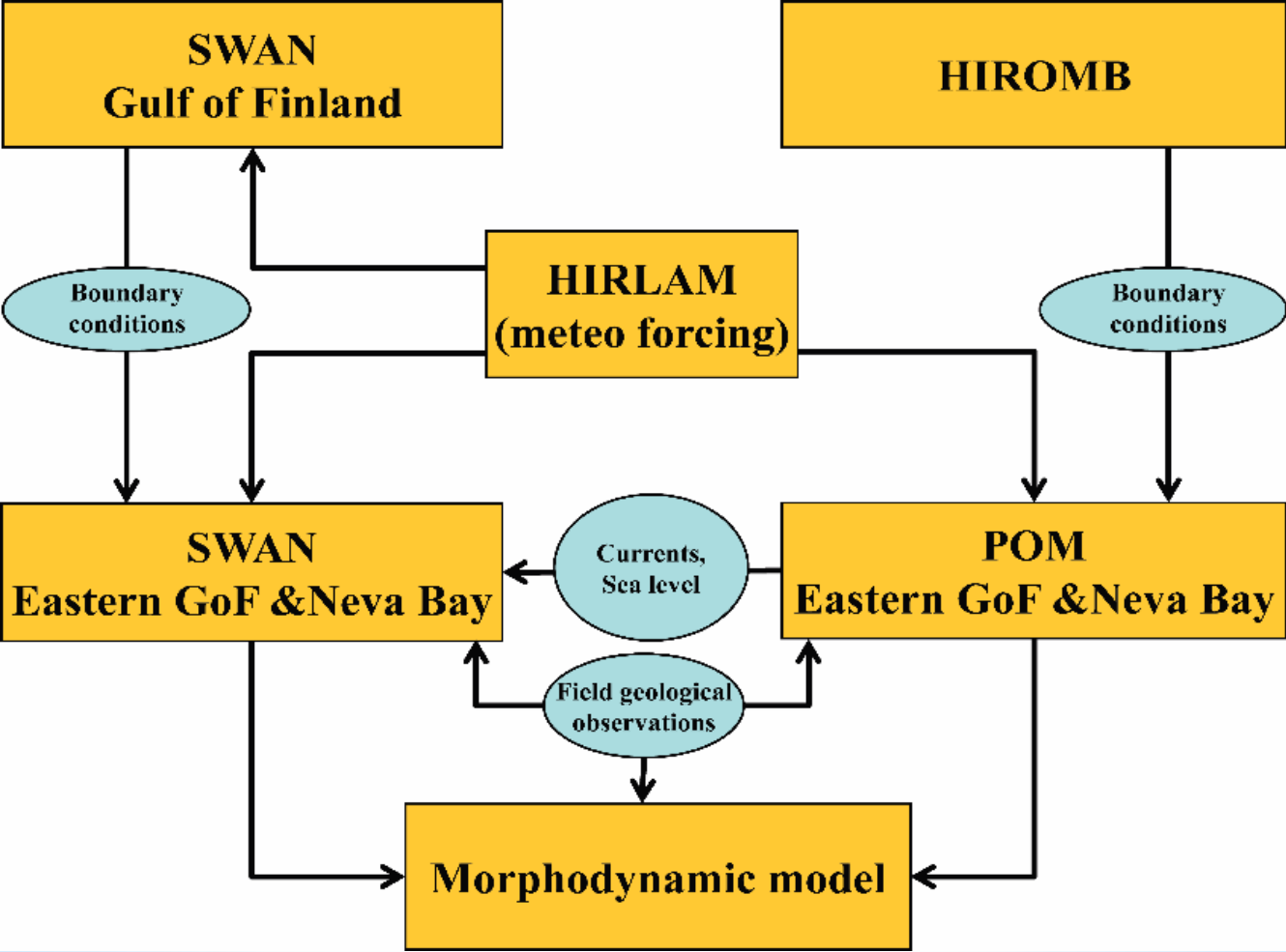
- To develop a method for assessing hazardous destructive geological processes in the coastal zone of the sea on the basis of actual geological and geophysical information on the state of the environment and modeling of the circulation of the sea and wind waves
- To give recommendations for combating these hazardous phenomena.

Study area



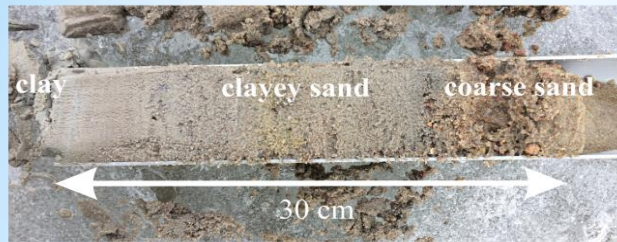
- 1- sediment sampling sites
- 2- side-scan sonar profiles
- 3 - georadar profiles
- 4 - area of remote sensing data analyses
- 5 - isobaths
- 6 - hydrometeorological stations

General scheme of the interaction between different numerical models and data

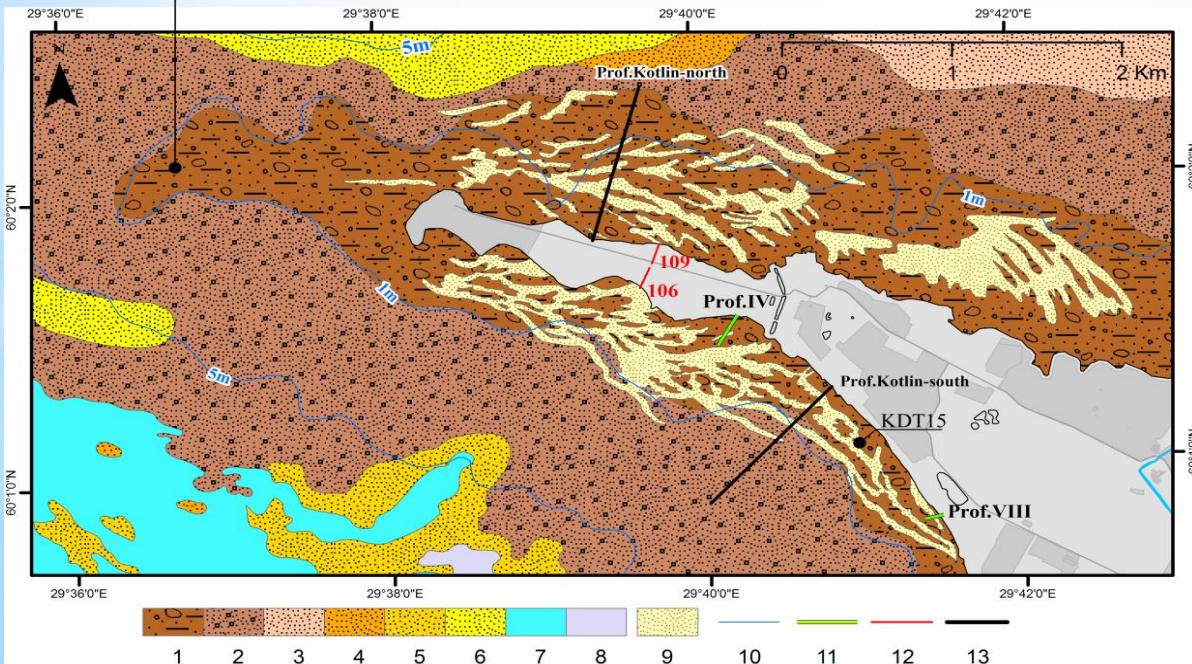
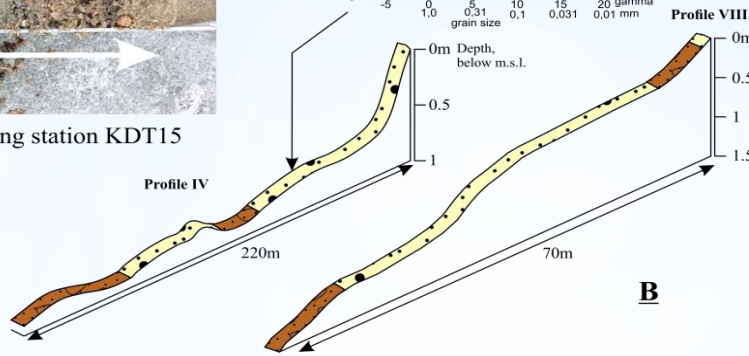
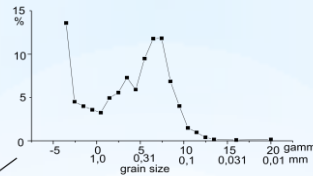


Bottom sediments

Map of bottom sediments of the western Kotlin Island.



sampling station KDT15



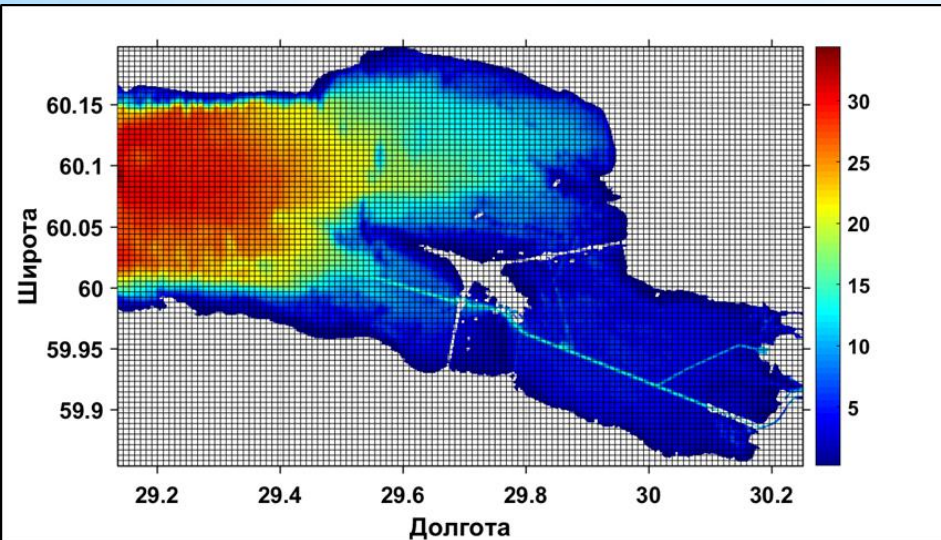
Surface sediment types:

- 1 - boulders, pebbles, gravel
 - 2 - boulders, gravel, sand
 - 3 - unsorted sand
 - 4 - sand with gravel
 - 5 - coarse-grained sand
 - 6 - coarse-medium grained sand
 - 7 - silt
 - 8 - sandy-silty-clayey mud
 - 9 - longshore sand ridges
 - 10 - isobaths
 - 11 - location of cross-shore sea-bed profiles;
 - 12 - location of ground-penetrating radar profiles;
 - 13 - profiles to be used in modeling
- A - drilling core KDT15;
B - cross-shore sea-bed profiles

Recommendation:
to prevent the future erosion artificial sand nourishment can be used as a method of sediment deficiency compensation.

Model domain and bathymetry

Model grid



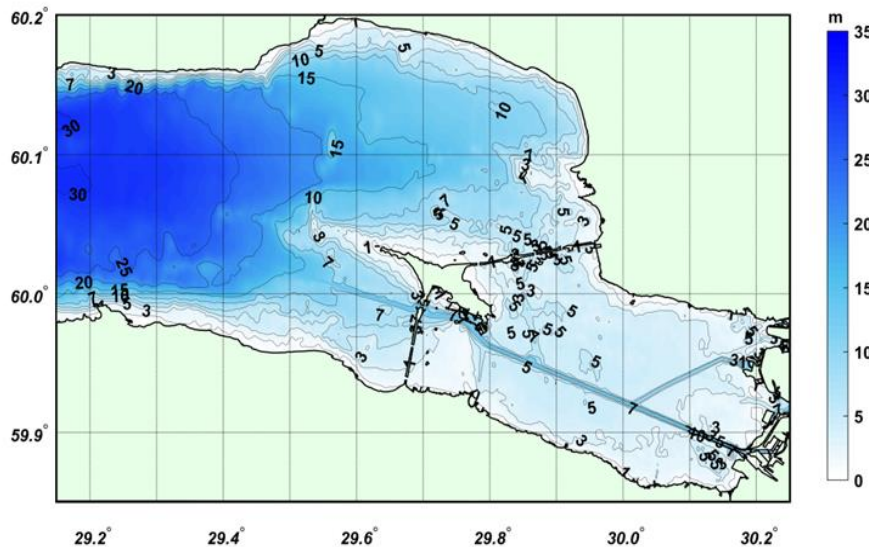
Calculation of current velocities using POM

Calculation of wind waves using SWAN

BC: 1) at the western boundary - hourly sea level from "Shepelevo" , constant T and S;
2) at the eastern boundary - constant T (+2 °C) and S (0 ‰), the river Neva discharge for December of 2030 m³/s.

The entire eastern part of the GoF, $\Delta h=100\text{m}$

Bathymetric depth

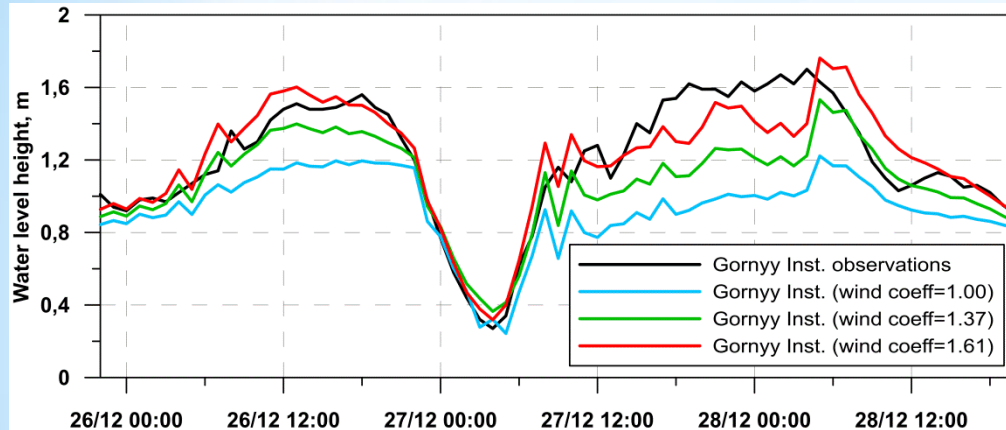


b

Numerical experiments with hydrodynamic models

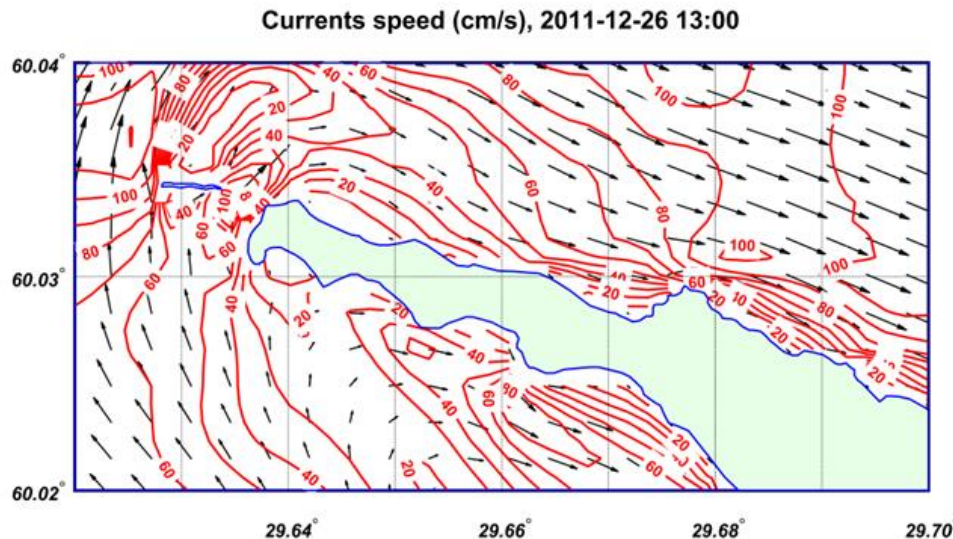
We consider the strongest flood event after putting into operation the St.-Petersburg Flood Protection Barrier, Dec 26-28 2011

Sea level



Water level rise at the "Gorny Institute" station on December 26-28, 2011, based on observations and on model results with different input of wind speed: specified by the HIRLAM model, specified by the HIRLAM model with a wind velocity modulus increased by 1.37 and 1.61 times

Surface current velocity, the case with enforced wind speed ($k=1.61$)

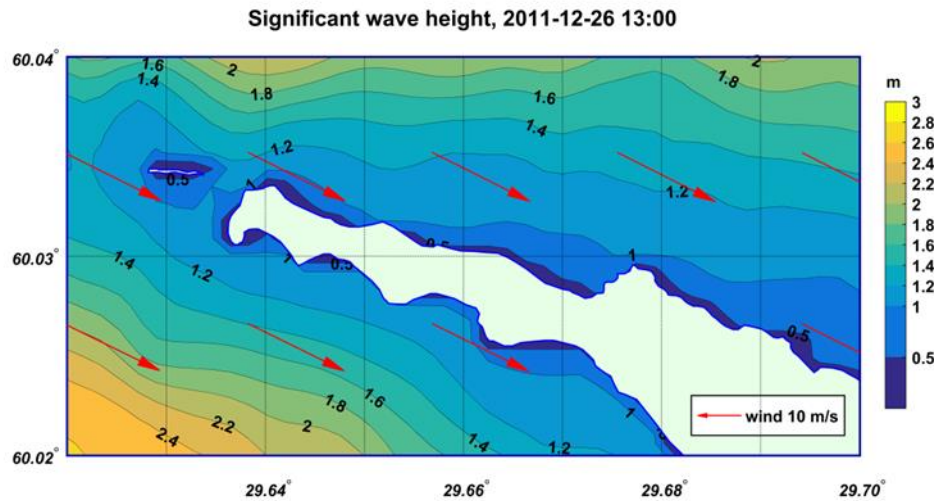


26.12.2011, 13:00

At the maximum water rises on 26 and 28 Dec velocity modules were usually 20-80 cm/s. At the minimum water rise on 27 Dec (between two surges) and at the end of Dec 28 the current velocities along the coasts did not exceed 30-40 cm/s.

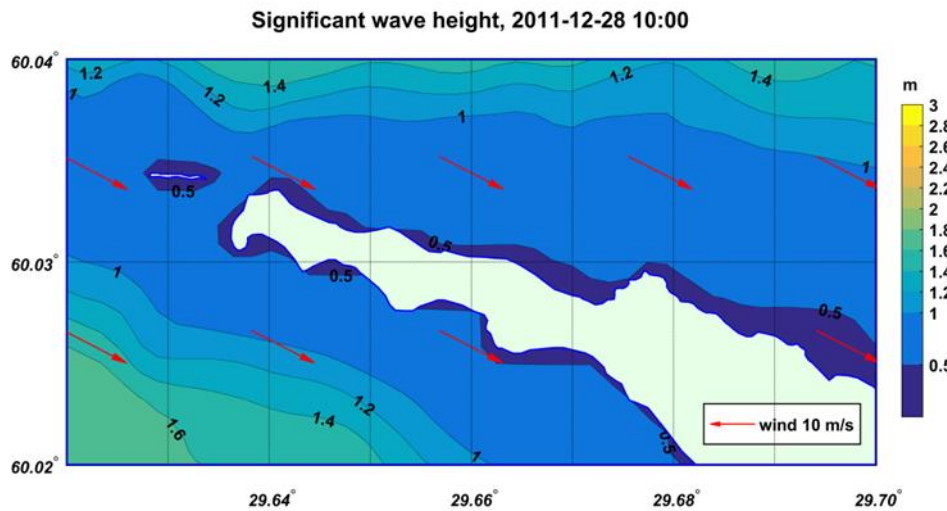
Modeled SWH with enforced wind speed (k=1.61)

26.12.2011, 13:00 the first storm surge



The SWH near the coast during two storm surges was approximately 1.5 times higher than SWH in the end of the considered period on Dec 28

28.12.2011, 10:00 the end of storm surge period

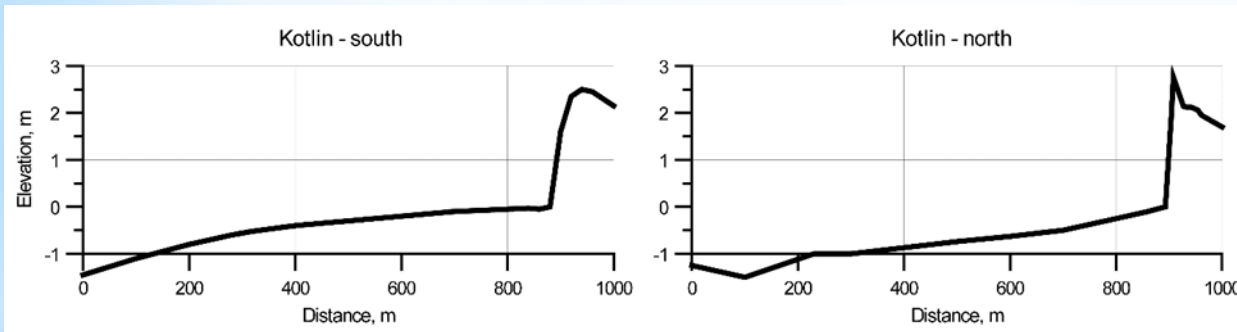


Morphodynamics modeling

Coast deformation due to storms was calculated with using the CROSS-P model (Leontyev I.O., Ryabchuk D.V., Sergeev A.Yu. Oceanology. 2015. V. 55. P. 131-141).

Initial data for these calculations: the initial depth profile, sediment characteristics, wave parameters, wind speed and storm duration, height of the storm surge, current velocity.

1. Two typical initial bottom profiles from the erosion areas of southern and northern Kotlin coasts



A very gentle bottom slope turns into a relatively steep beach and a foredune with a height of about 2.5 m.

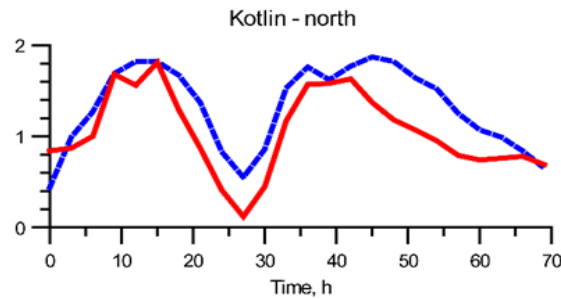
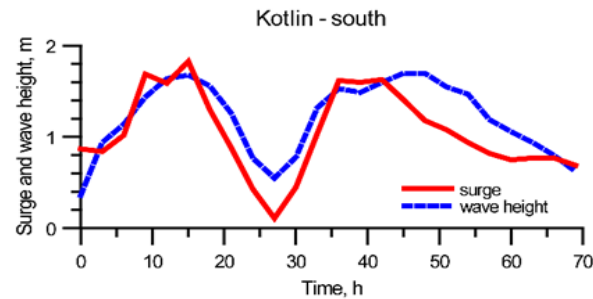
2. The characteristic size of the sand particles is 0.25 mm.

3. Wave parameters are from SWAN model calculations

4. Wind speed and storm duration - from meteorological data

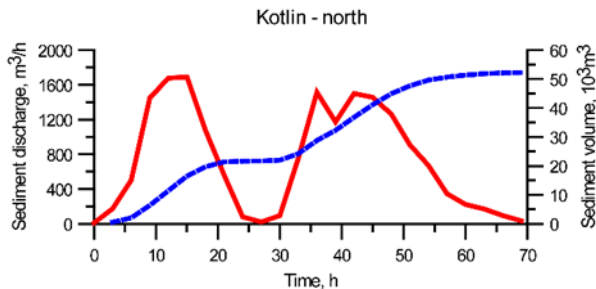
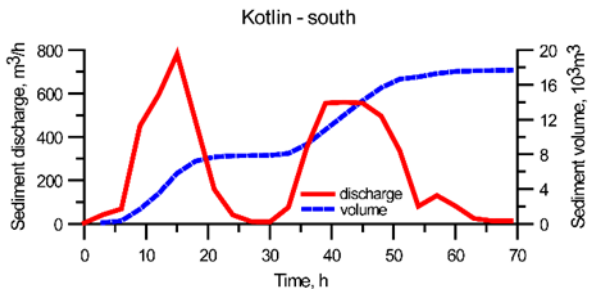
5. Height of the storm surge and current velocity - from hydrodynamic calculations using POM

Changes in water level and SWH during the storm on 26-28.12.2011 at the coastal sections (at depths of about 3 m relative to calm conditions)



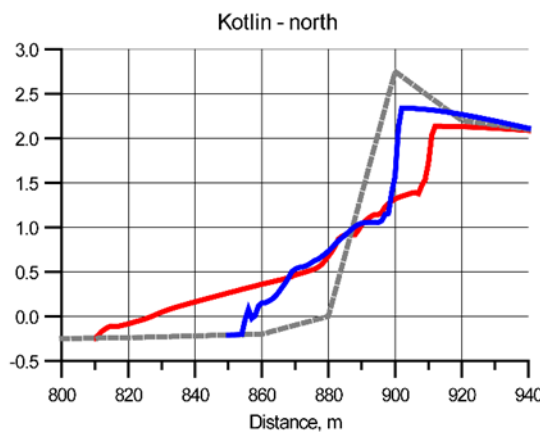
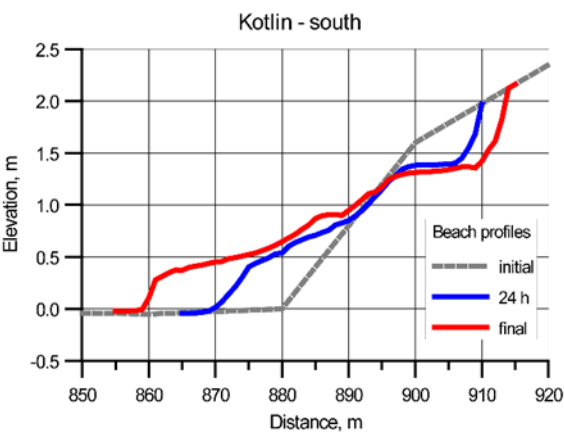
The changes in the water level and SWH during the storm are generally identical for the both sites. At the southern coast current velocity do not exceed 0.3 m/s, at the northern coast it reaches 0.7 m/s

Calculated longshore sediment transport



Due to a higher currents along the northern coast the total sediment amount moved at this section during the storm is three times higher than at the southern one.

Calculated coast profiles deformation due to the storm



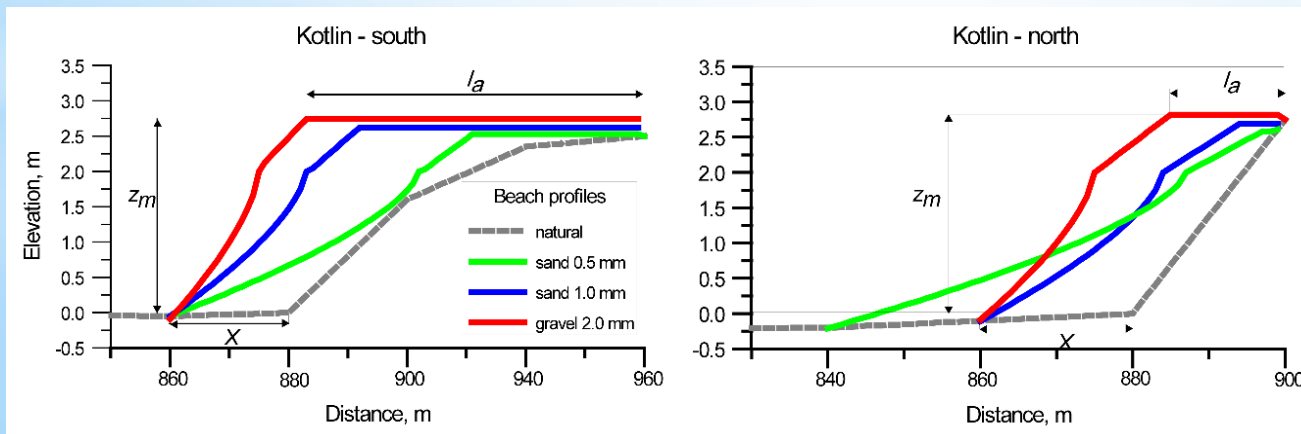
The northern coast is obviously more vulnerable. The foredune crest is actively eroded and its height decreases by 0.6 m by the end of the storm.

Shore-protecting artificial beach

Characteristics of **artificial beach** were estimated using the maximum parameters of the storm of 26-28.12.2011 (an extreme event). The wave height and period H_s and \bar{T} as well as the height of the surge and the extension of the shore X are prescribed (see Table). Three particle size were considered: - medium and coarse sand (0.5 and 1.0 mm), and gravel (2.0 mm).

Table. Initial data and calculated parameters of artificial beach profiles

Section of the coast	H_s , m	\bar{T} , s	η , m	X , m	dg, mm	zm, m	la, m	V, m ³ /m
Kotlin-south	1.7	4.5	2.0	20	0.5	2.53	29.5	22.3
					1.0	2.62	48.4	60.9
					2.0	2.74	56.9	83.1
Kotlin-north	1.9	4.8	2.0	20	0.5	2.58	2.3	39.0
				20	1.0	2.69	6.2	30.8
				20	2.0	2.82	14.9	51.2



* Conclusions

1. The coastline retreat rates reach 1.2-1.6 m / year, which should be taken into account in forecasting the development of the coast reconstructions.
2. The vast geological near-shore zone and onshore geological research revealed the following features of the western KI coastal zone: 1) wide spreading of boulder-pebble benches within near-shore bottom, 2) very small thickness of active sand layer, 3) prevailing of narrow (10-15 m) sand beaches, and 4) low and smooth offshore and onshore relief (foredune height is less than 2 m).
3. A coupled mathematical model including models of water circulation, wind waves, and sediment dynamics was developed. Coast deformation due to storms was calculated with making use of the CROSS-P model. Initial data for these calculations were the initial depth profile, sediment characteristics, wave parameters, height of the storm surge, wind speed, and duration of a storm.
4. The coupled mathematical model was used to determine the parameters of artificial sand nourishment as a method of sediment deficiency compensation for preventing the future erosion. The artificial beach profiles parameters have been calculated at the maximum storm surge and the annual volume of sand necessary for conservation artificial beach has been estimated.

Acknowledgements

This research was a part of the project "Development of General Scheme of Coast Protection of the marine coasts of Saint-Petersburg City" funded by Committee for Natural Use, Environmental Protection and Ecological Safety of St.-Petersburg. V.A. Ryabchenko and S.D. Martyanov were supported by the grant 14-50-00095 of the Russian Science Foundation (RSF). A.Yu. Dvornikov, V.A. Ryabchenko and S.D. Martyanov were supported by the grant 16-55-76021 of the Russian Foundation for Basic Research (RFBR). Also I.O. Leont'yev was supported by the grant 15-05-08239 of the RFBR. A.Yu. Sergeev and D.V. Ryabchuk were supported by the grant 17-77-20041 of the RSF.

From small scales to large scales
–The Gulf of Finland Science Days 2017
9th-10th October 2017
Estonian Academy of Sciences, Tallinn

2nd Day



**Gulf of Finland
Co-operation**

V. Zhurbas, J. Laanemets, U. Lips, G.Väli

Eulerian and Lagrangian submesoscale coherent structures on the sea surface driven by coastal upwelling: a case study for the Gulf of Finland



Eulerian and Lagrangian submesoscale coherent structures on the sea surface driven by coastal upwelling: a case study for the Gulf of Finland

Victor Zhurbas^{1,2}, Jaan Laanemets¹, Urmas Lips¹, Germo Väli¹,

¹ Marine Systems Institute at Tallinn University of Technology, Estonia

² P. P. Shirshov Institute of Oceanology, Russia

Gulf of Finland Trilateral Co-operation Scientific Forum
10 October 2017, Tallinn

Outline

- Background
- Model setup
- Results
- Conclusions

Background

What?

Submesoscale processes in the Gulf of Finland

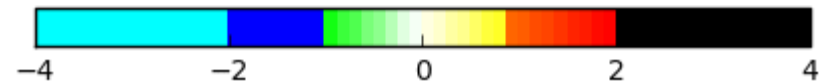
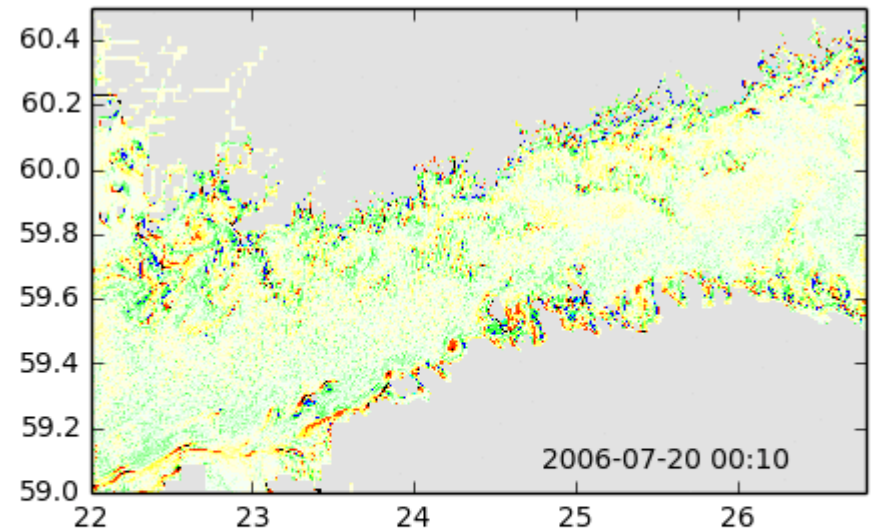
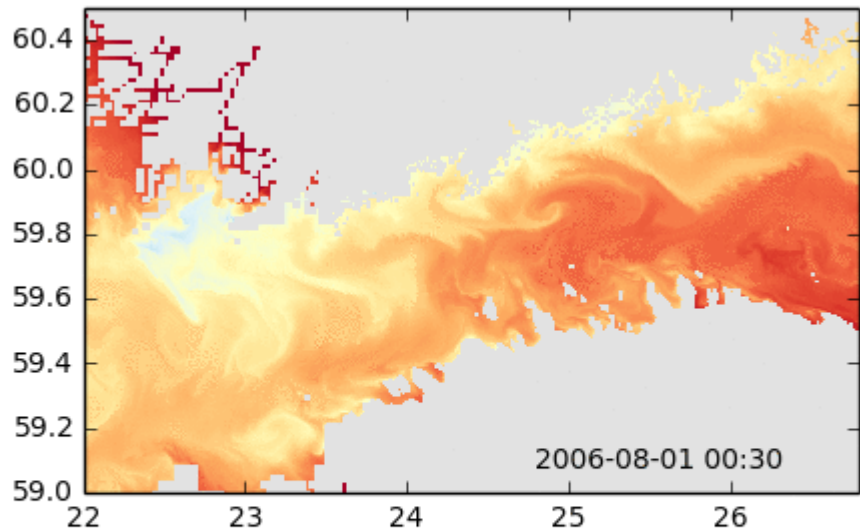
Why?

Vital for transport of vorticity, buoyancy, momentum, matter and biogeochemical properties throughout the upper mixed layer and upper thermocline

How?

Applying 3D primitive equation model with refined horizontal resolution for period of summer upwelling events characterized with enhanced submesoscale activity

Background



Previous work (Väli et al., 2017):

- refinement of the grid step from **0.5** to **0.125** nautical miles (n.m.) showed a **substantial increase** of relative vertical vorticity fluctuations
- 3 types of submesoscale structures in the gulf's surface layer – the high Rossby number **threads**, submesoscale **cyclonic vortices** and **spiral cyclonic eddies** were found
- submesoscale features covered a relatively **large part** of the study area depending on the **wind forcing** and **strength of the baroclinic upwelling front**

Background

Question:

What will happen with Lagrangian floating particles in high resolution current field?

Objectives:

- ❑ To simulate clustering process in the Gulf of Finland based on circulation model of very high resolution
- ❑ To find out the factors determining the clustering rates
- ❑ To study evolution of statistical properties of floating particles concentration in the course of clustering
- ❑ To compare sea surface images „painted“ by the re-distributed floating particles with patterns of submesoscale coherent structures in different Eulerian and Lagrangian fields

Model setup: overall

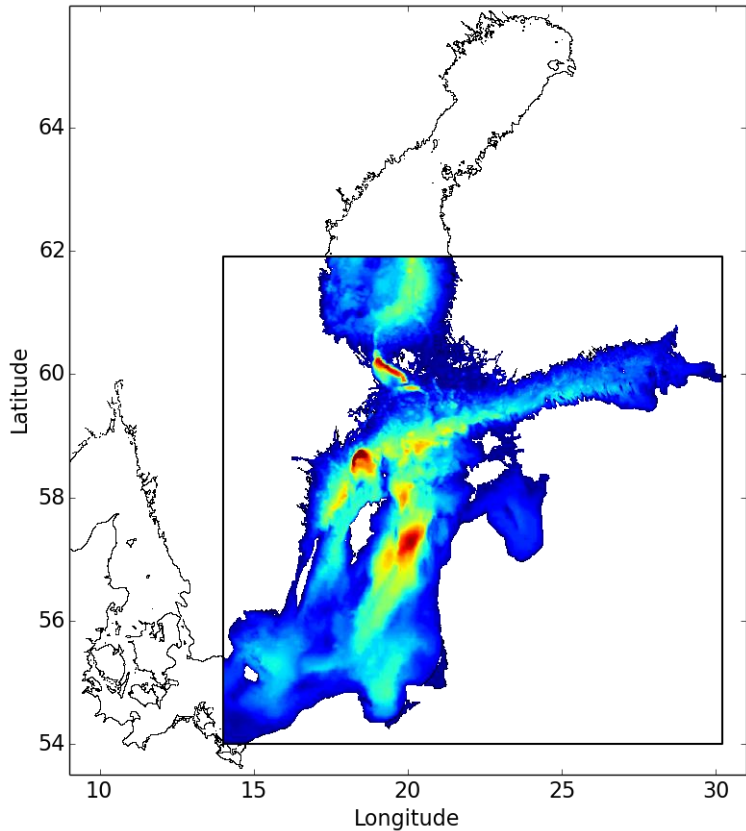
domain: Baltic Proper closed at sounds

initial fields: HIROMB (High Resolution Operational Model for the Baltic), Funkquist, 2001

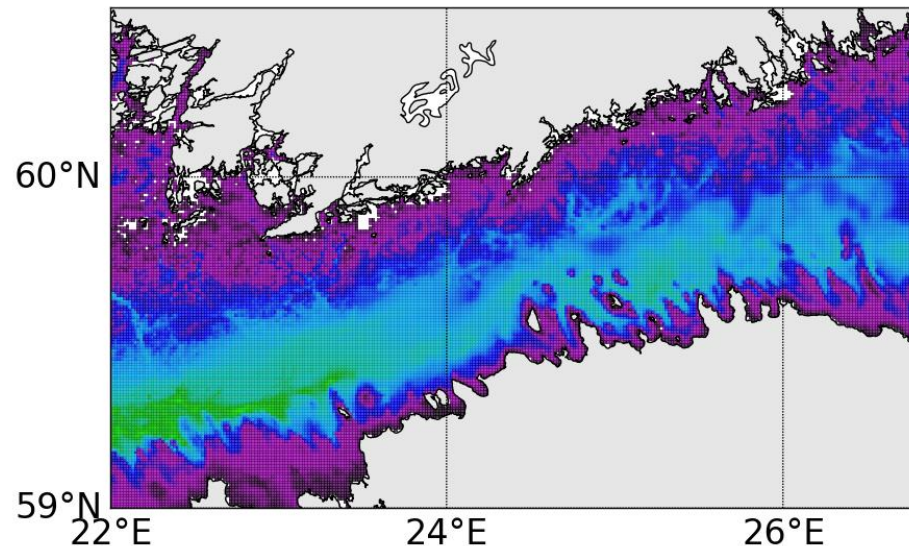
atmospheric forcing: HIRLAM (High Resolution Limited Area Model) version of the EMHI (spatial resolution of 11 km, forecast interval of 1 h (Männik and Merilain, 2007)

runoff: average Neva river inflow of $2460 \text{ m}^3 \text{ s}^{-1}$ (Bergström et al., 2001).

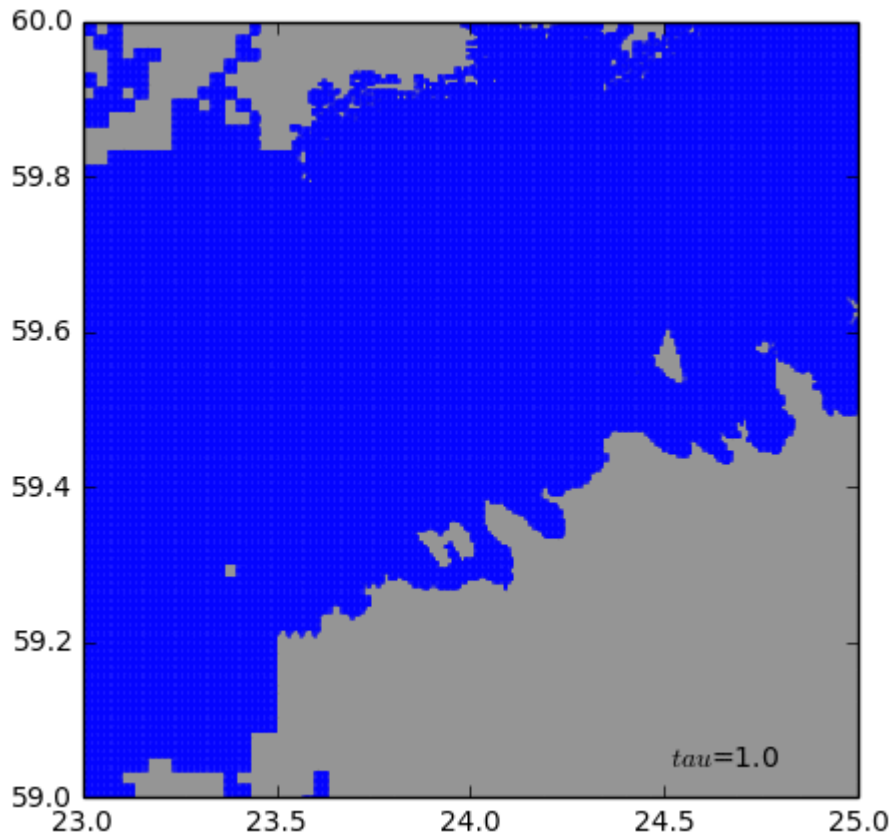
period: summer 2006 (from 10th of July to the end of September)



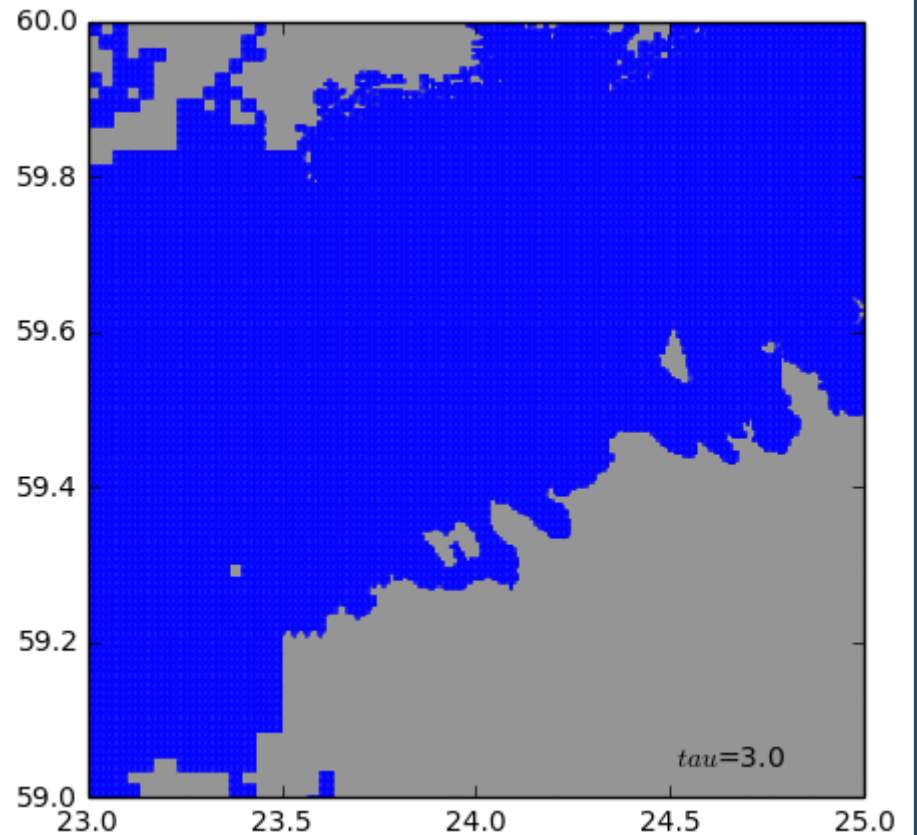
output: near-surface currents with temporal resolution 10 minutes



Results: particles

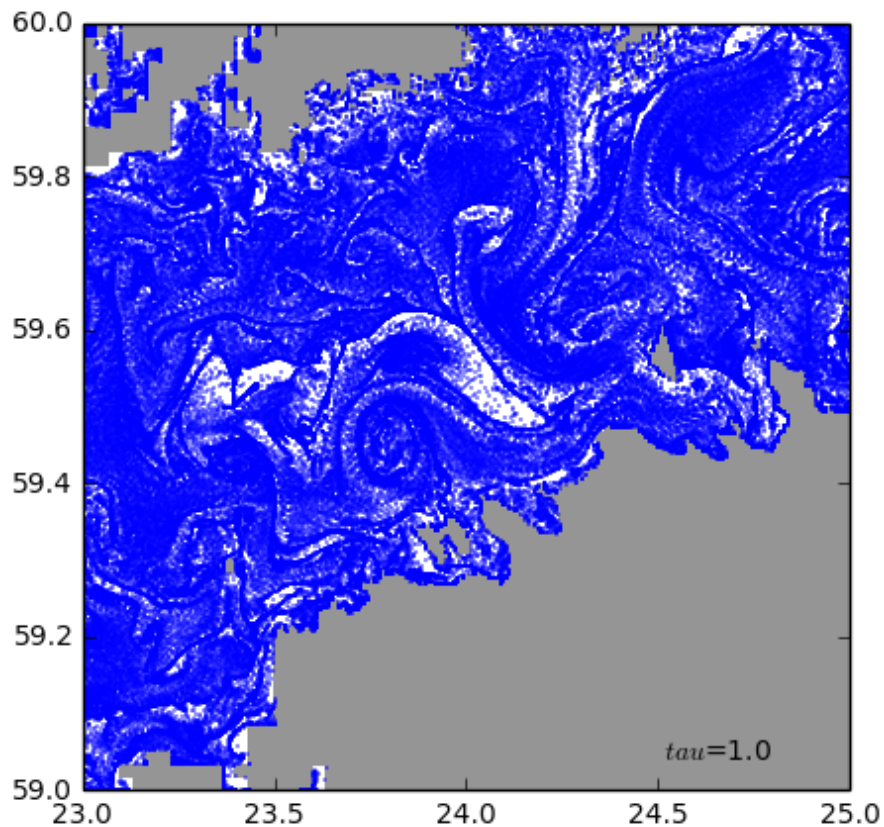


Particle advection time $\tau = 1$ days,
uniformly distributed 18.08.06 13:00
Model resolution: **0.125nm**

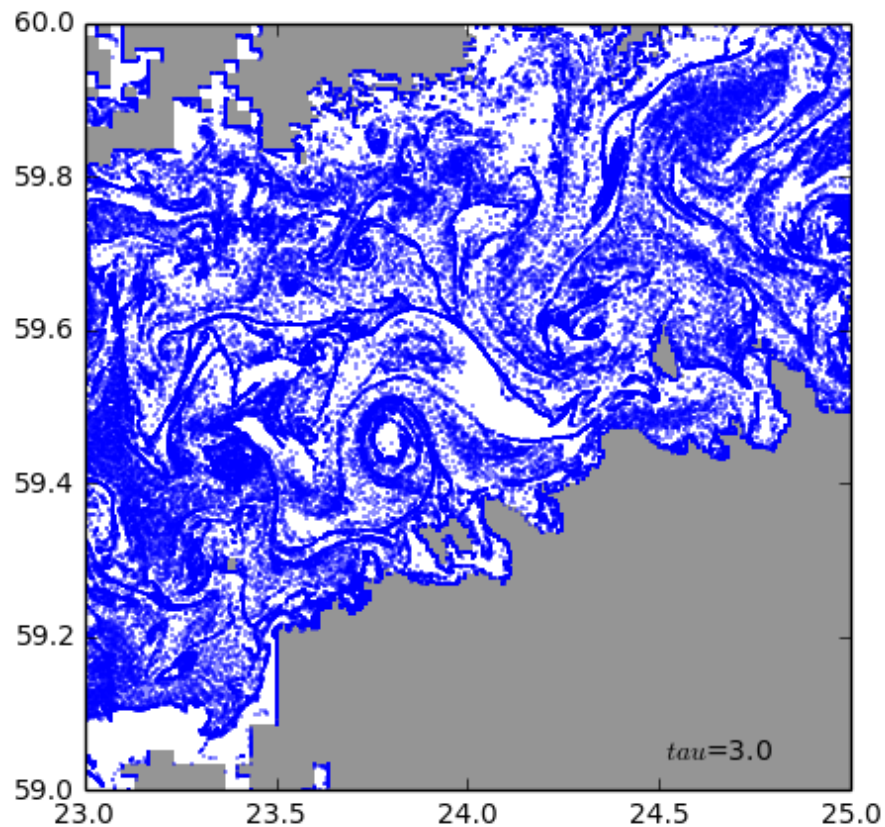


Particle advection time $\tau = 3$ days,
uniformly distributed 16.08.06 13:00
Model resolution: **0.125nm**

Results: particles

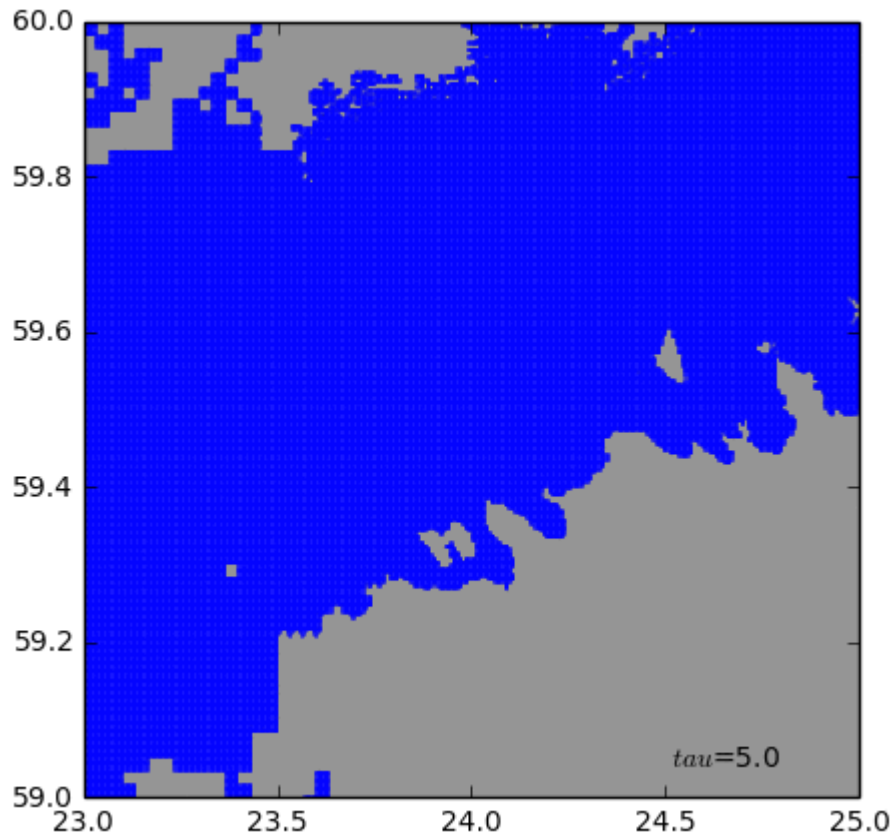


Particle advection time $\tau = 1$ days,
uniformly distributed 18.08.06 13:00
Model resolution: **0.125nm**

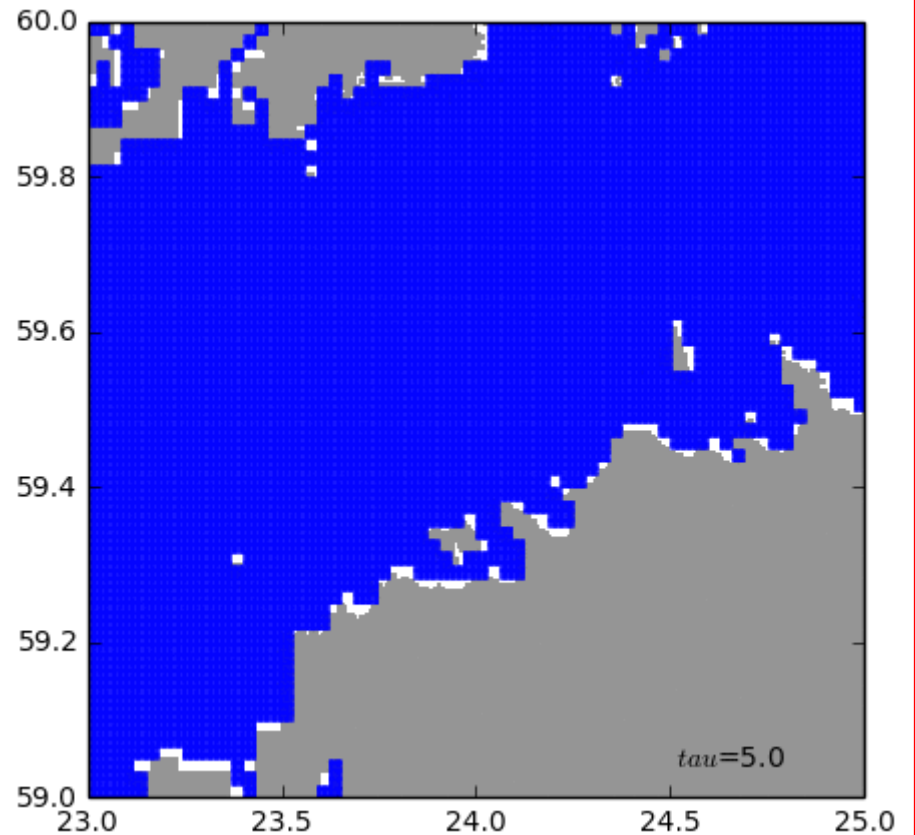


Particle advection time $\tau = 3$ days,
uniformly distributed 16.08.06 13:00
Model resolution: **0.125nm**

Results: particles

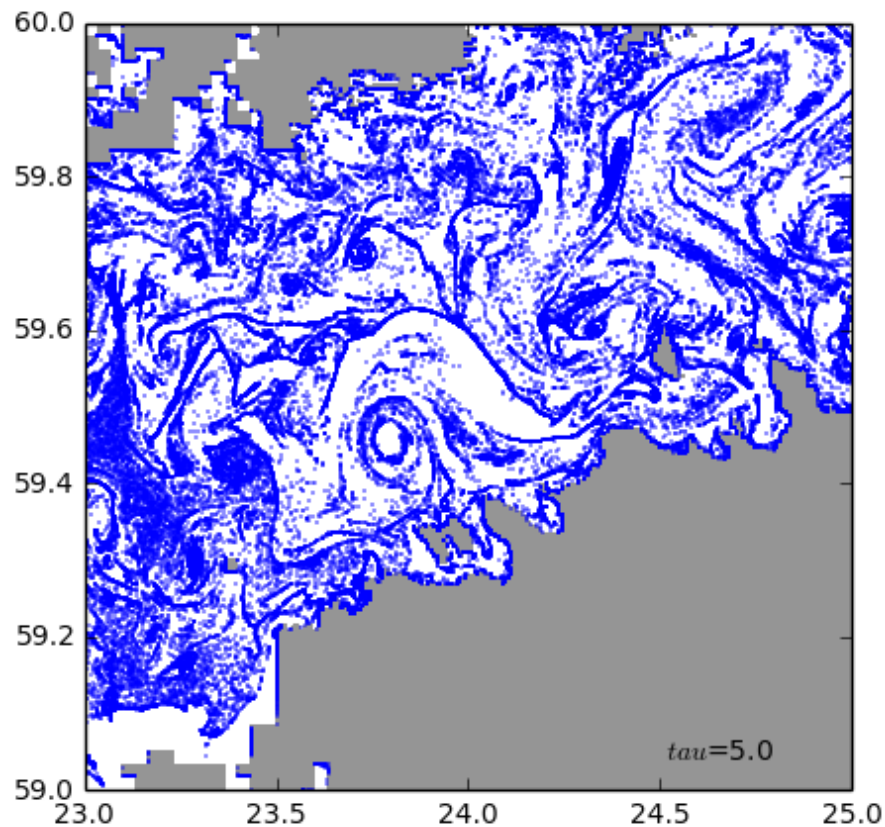


Particle advection time $\tau = 5$ days,
uniformly distributed 14.08.06 13:00
Model resolution: **0.125nm**

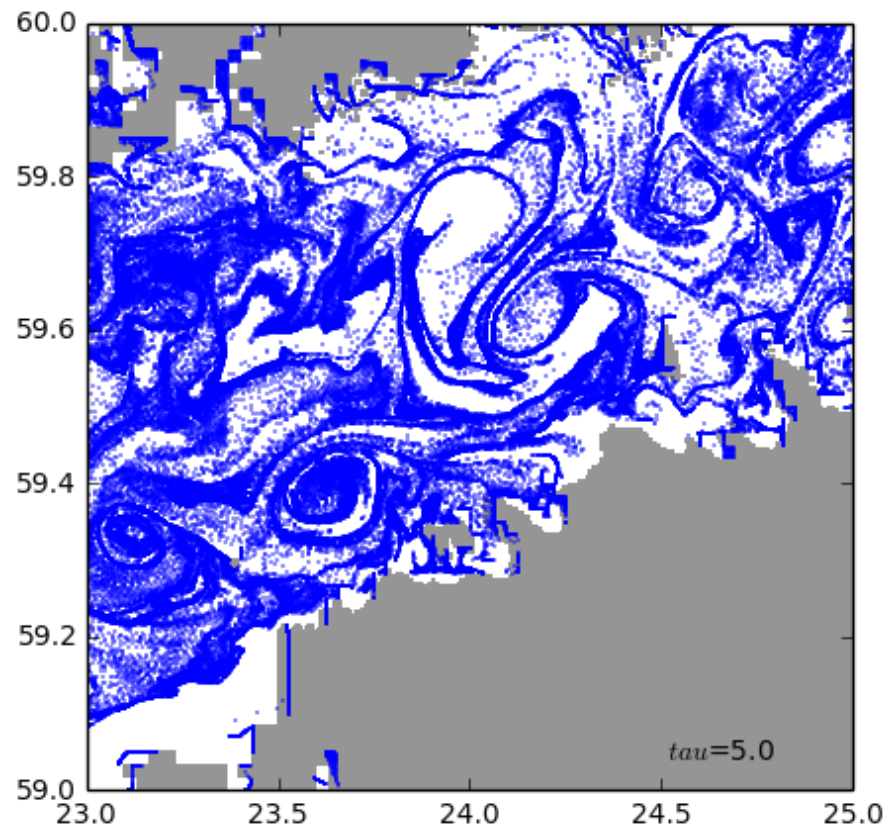


Particle advection time $\tau = 5$ days,
uniformly distributed 14.08.06 13:00
Model resolution: **1.0nm**

Results: particles

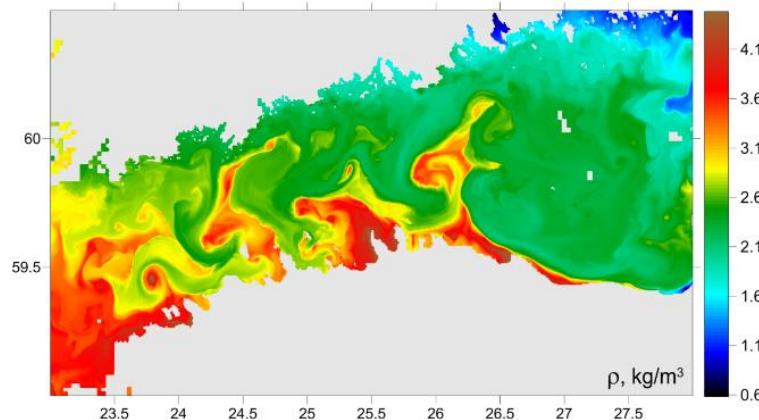
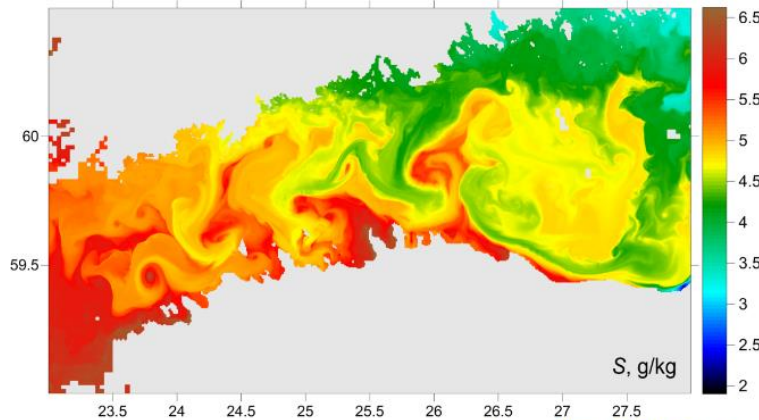
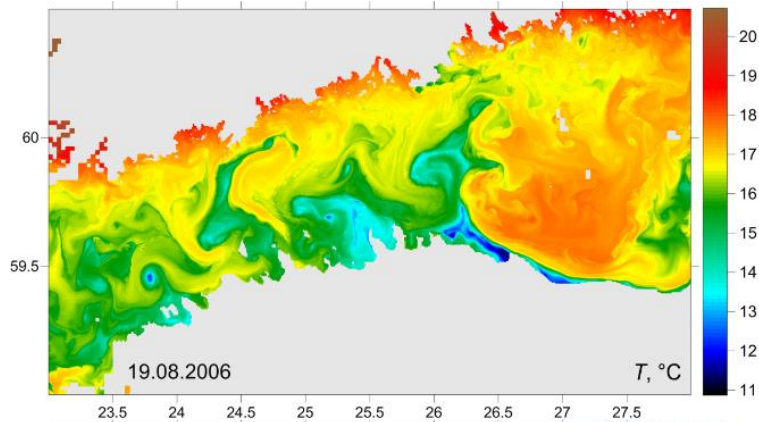


Particle advection time $\tau = 5$ days,
uniformly distributed 14.08.06 13:00
Model resolution: **0.125nm**



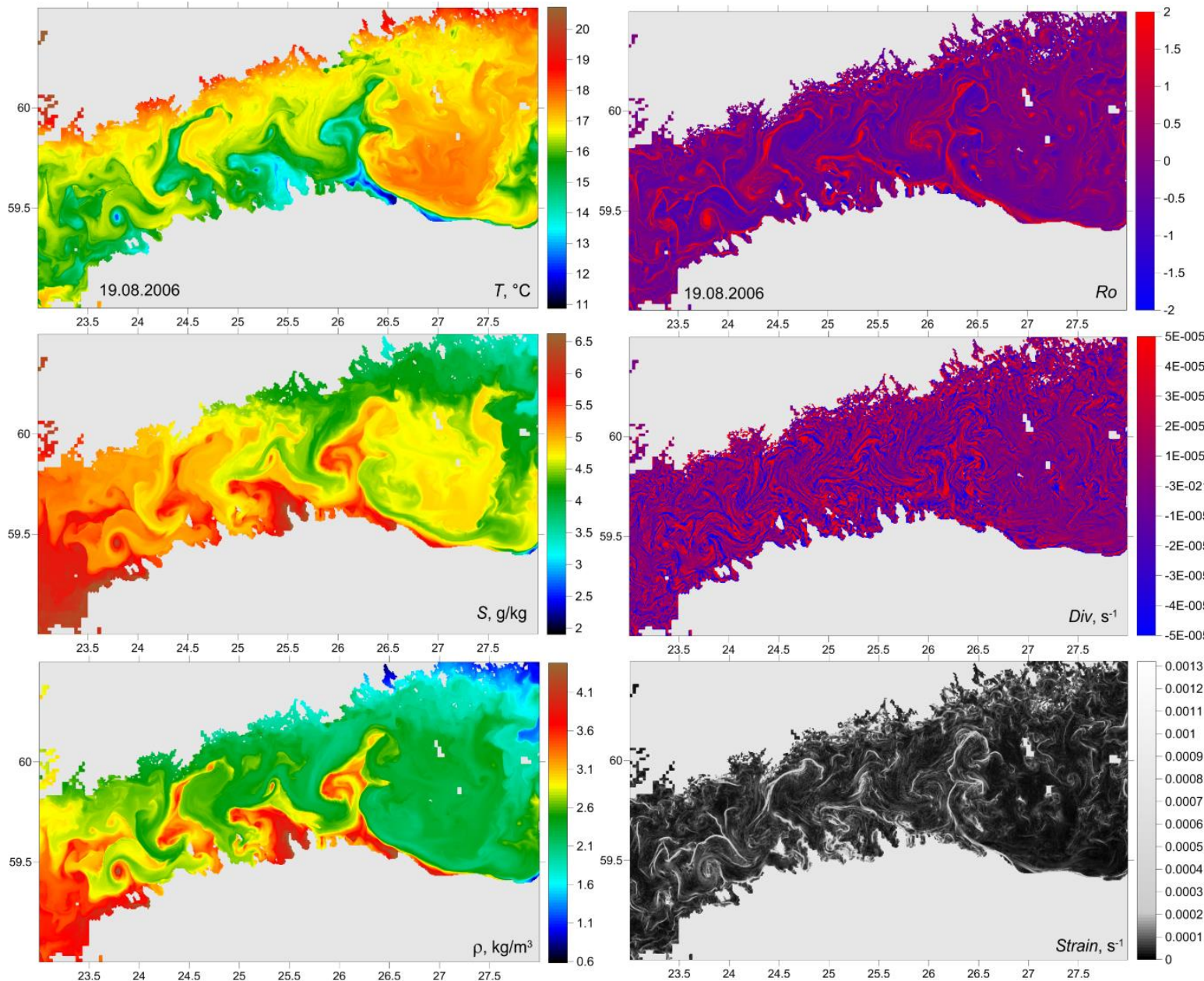
Particle advection time $\tau = 5$ days,
uniformly distributed 14.08.06 13:00
Model resolution: **1.0nm**

Results: tracer fields



- ❑ Relaxation phase of upwelling event along the southern coast of GoF
- ❑ Variability of T, S and ρ characterized by well-defined cold/salt/dense water filaments and isolated spots
- ❑ Outcrops of T, S and ρ contours are concentrated on the lateral boundaries of filaments and isolated spots producing a variety of fronts

Results: flow field

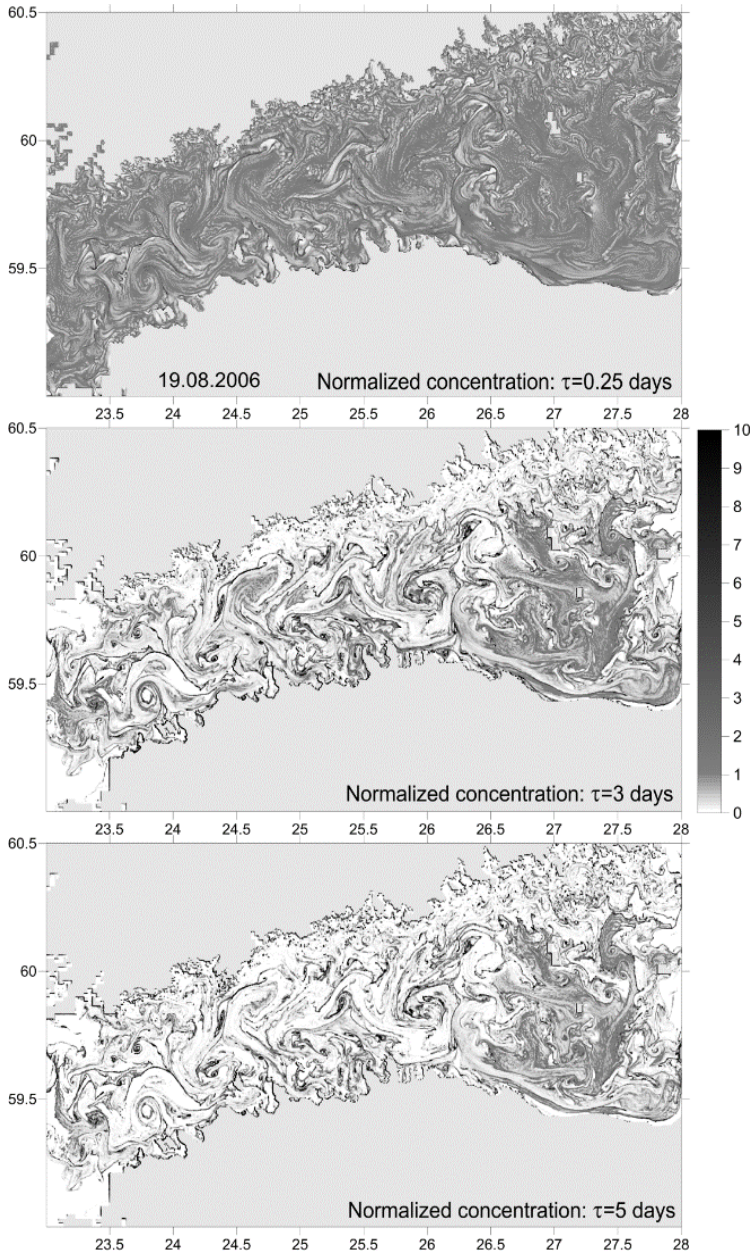


□ Narrow stripes with density outcrops as well as isolated cold/salt/dense water spots always characterized by extremely high positive vorticity

□ Divergence (Div) patchy, but some correspondence between $Ro > 1$ stripes and negative Div suggesting the convergence of near-surface currents taking place preferably on baroclinic fronts with outcropping isopycnals

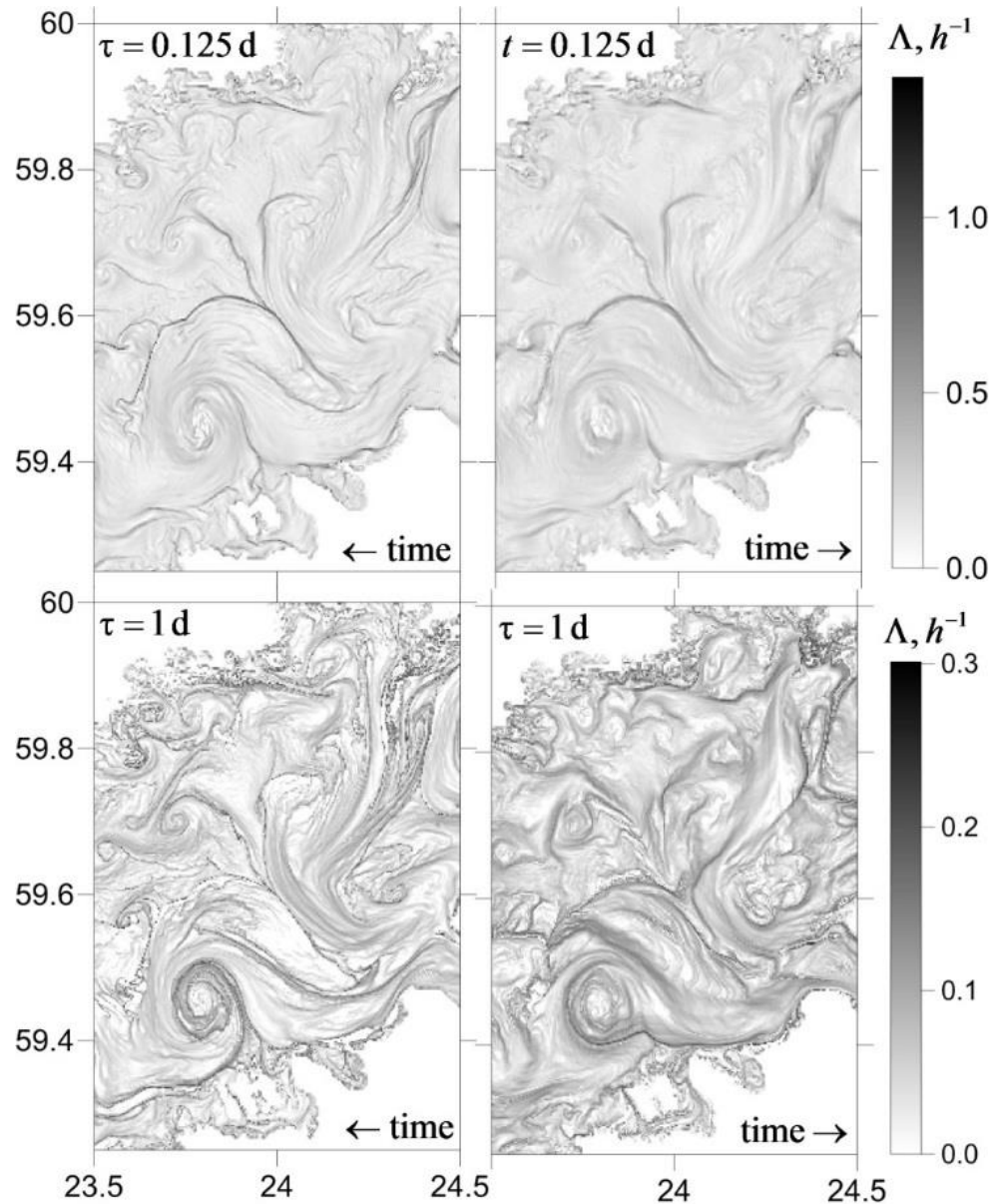
□ High cyclonic vorticity stripes coincide with high deformation rate

Results: particles



- ❑ The normalized concentration and floating particle location images provide similar portraits of submesoscale structures for different values of advection time τ within the examined range of 0.25 to 5 days
- ❑ The distributions of particles display a tendency to be gathered on the high Ro threads with the growth of the advection time
- ❑ The cyclonic eddies are displayed as sites where the high concentration filaments are twisted into cyclonic spirals
- ❑ With smaller τ the normalized concentration images display a tendency to portray the *Div* image

Results: particles

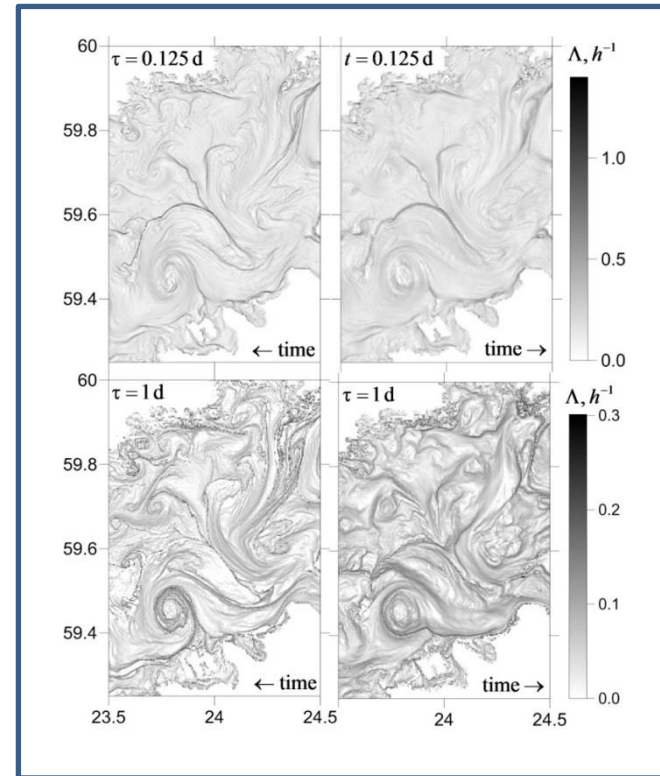
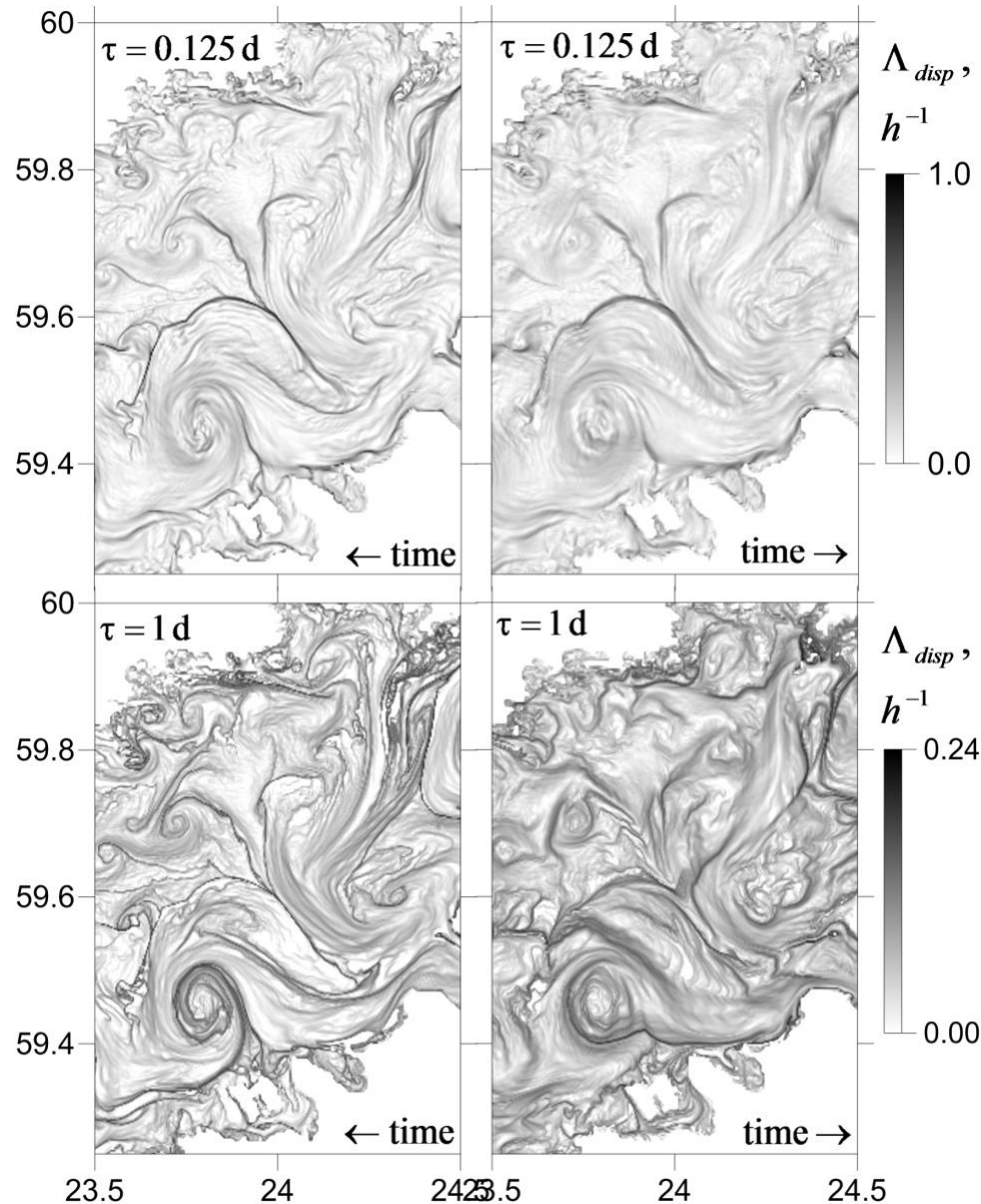


$$\Lambda(\mathbf{X}, t, \tau) = \frac{1}{2\tau} \ln(\lambda_{max}(C(\mathbf{X}, t, \tau)))$$

□ The Finite-Time Lyapunov Exponent (FTLE) Λ is most similar to the particles normalized concentration for advection time up to 1 day.

□ With the growth of the advection time, the similarity between Λ and normalized concentration becomes less pronounced

Results: particles

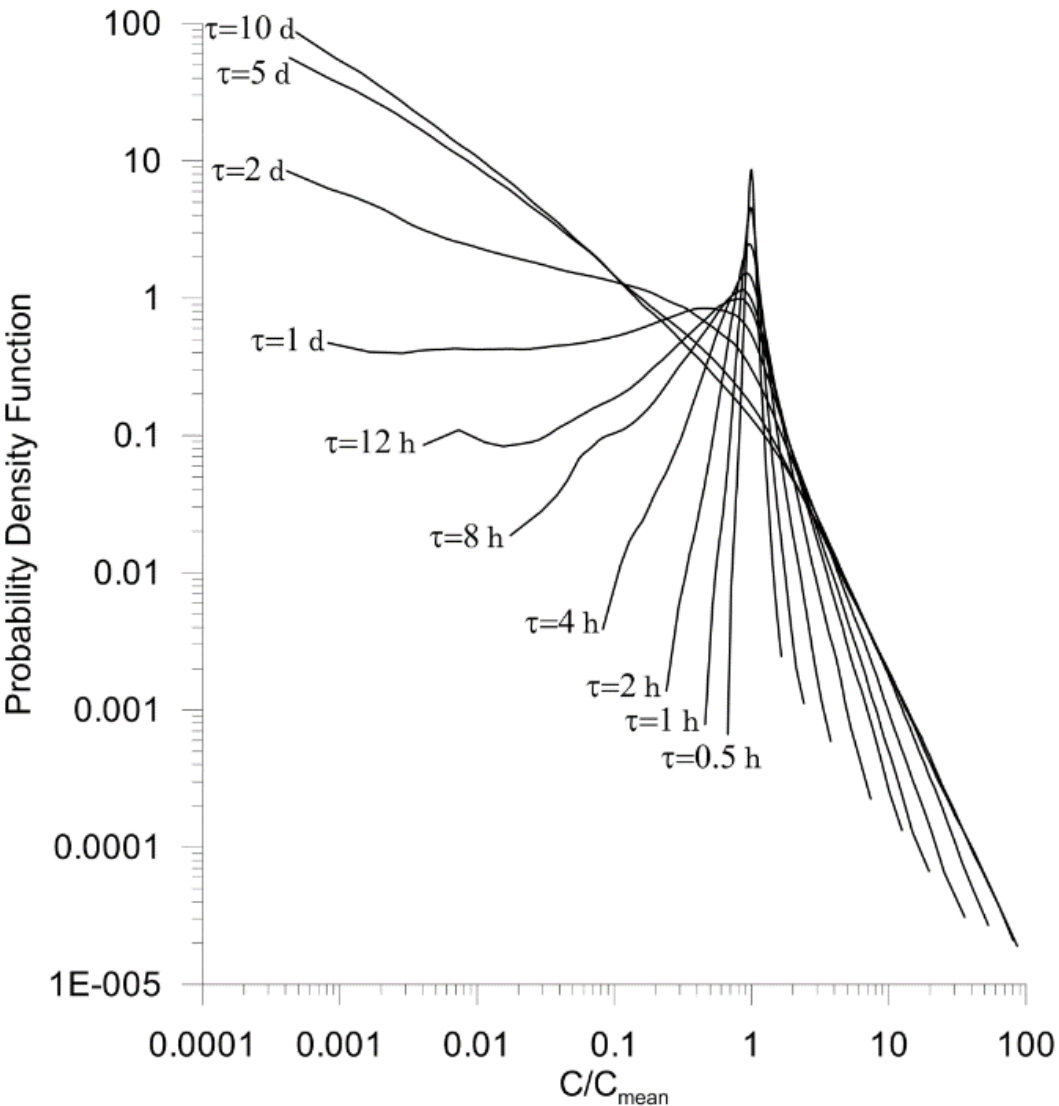


$$\Lambda_{disp}(\mathbf{X}, t, \tau) = \frac{1}{2\tau} \ln(\mu_{max})$$

□ Λ_{disp} is similar to Λ both for small and large values of τ

□ For small τ , the high-concentration threads are characterized by high values of Λ and Λ_{disp}

Results: statistics

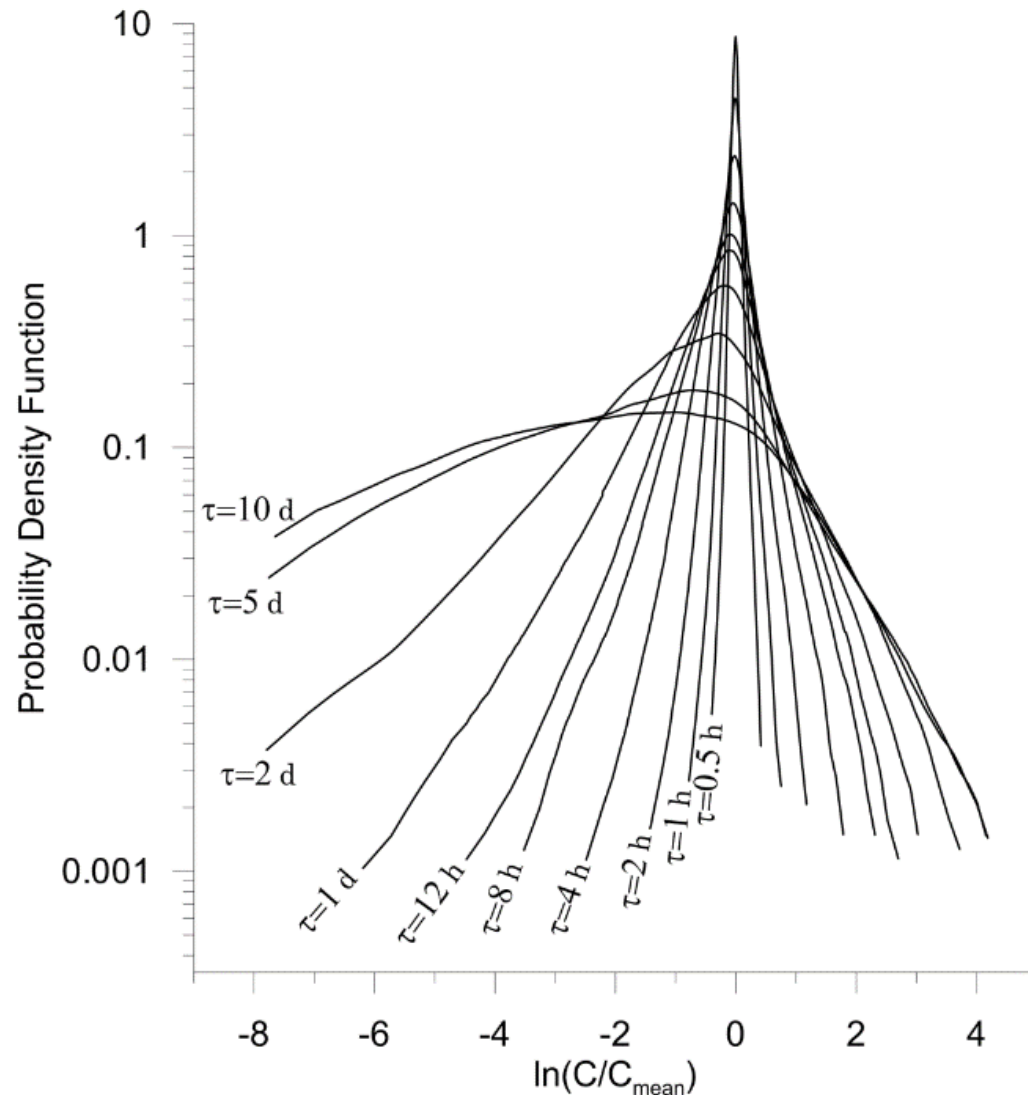


- Probability distribution of C / C_{mean} is characterized by large positive, time-growing values of *Skew* and *Excess*:

$Skew = 1.53$, $Excess = 15.1$, $\tau = 0.5$ h
 $Skew = 314.7$, $Excess = 1.3 \cdot 10^5$, $\tau = 10$ days

- Probability distribution of $\ln (C / C_{mean})$ is characterized by mostly negative, relatively close to zero values of *Skew*, while the kurtosis excess being positive approaches to zero with the growth of the advection time τ
- log-normality of normalized concentration C / C_{mean} at large τ

Results: statistics



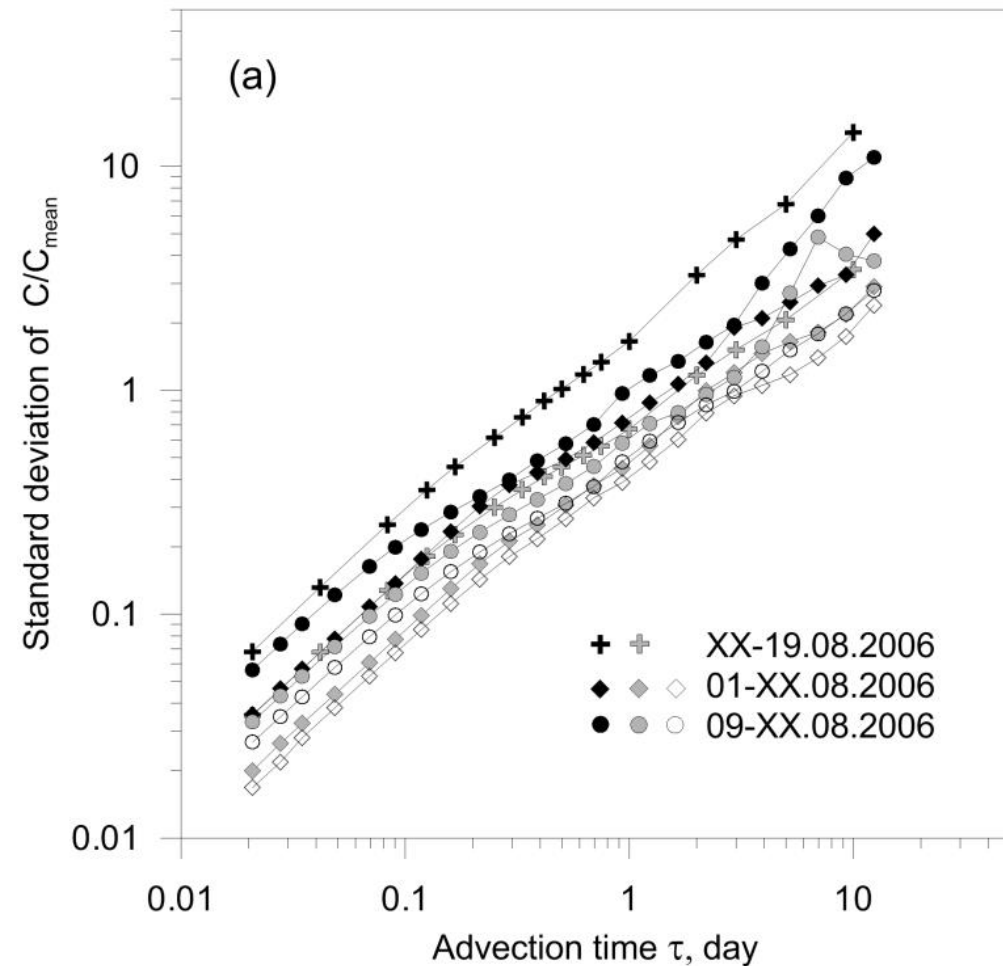
- Probability distribution of C / C_{mean} is characterized by large positive, time-growing values of *Skew* and *Excess*:

$Skew = 1.53$, $Excess = 15.1$, $\tau = 0.5$ h
 $Skew = 314.7$, $Excess = 1.3 \cdot 10^5$, $\tau = 10$ days

- Probability distribution of $\ln (C / C_{mean})$ is characterized by mostly negative, relatively close to zero values of *Skew*, while the kurtosis excess being positive approaches to zero with the growth of the advection time τ

- log-normality of normalized concentration C / C_{mean} at large τ

Results: statistics



Colors refer to model resolutions:

black – **0.125** n.m. resolution

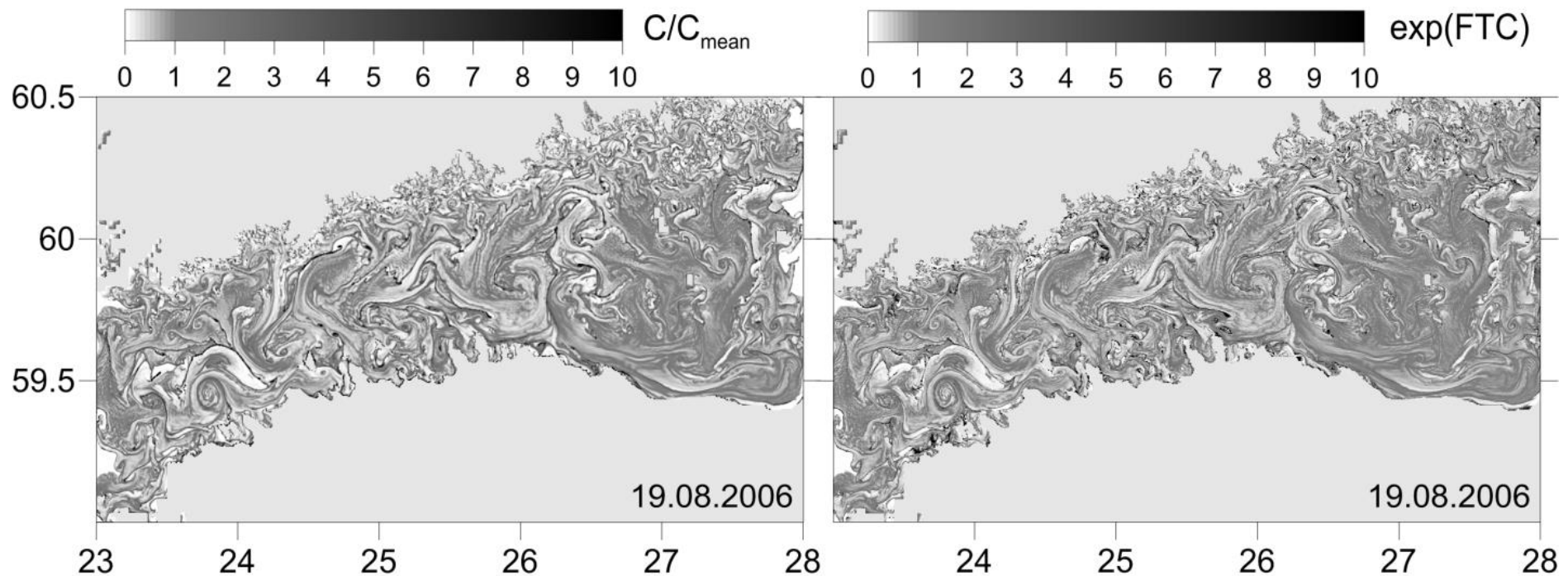
grey – **0.5** n.m. resolution

white – **1.0** n.m. resolution

- Nearly identical linear growth of standard deviation of particle concentrations in the log-log space for different resolutions
- Quadruple decrease in the grid size from 0.5 to 0.125 nautical miles results twofold increase of σ

Results: FTC

$$FTC(\mathbf{x}, t, \tau) = \int_t^{t-\tau} \text{div}(u(t'|\mathbf{x}, t)) dt'$$



- The maps of normalized concentration and finite-time clustering (FTC) almost identical for advection time $\tau = 1$ day

Conclusions

- Evolution of initially uniform particle concentration field with its probability density function and statistical moments depending on the advection time τ was studied.
- The synthetic particles gathered within narrow, elongated stripes within a relatively short advection time τ (of the order of one day). The cluster locations were characterized by extremely high, positive values of vorticity, Finite-Time Lyapunov Exponent and lateral thermohaline fronts.
- The clustering rate tended asymptotically at small τ to the standard deviation of flow divergence. The standard deviation of flow divergence depends strongly on the model resolution – standard deviation grows with the refinement of the model grid.
- At large τ , the probability function of floating particle concentration tend to lognormality.

Acknowledgements

This work was supported by institutional research funding IUT 19-6 of the Estonian Ministry of Education and Research.

Victor Zhurbas was supported by the Russian Science Foundation (Grant No 14-50-00095) and Russian Foundation for Basic Research (Grant No 15-05-01313).

The parallel implementation of the original POM was done by Dr. Antoni Jordi and is documented in Jordi & Wang (2012).

From small scales to large scales
–The Gulf of Finland Science Days 2017
9th-10th October 2017
Estonian Academy of Sciences, Tallinn

2nd Day



**Gulf of Finland
Co-operation**

J. Harff

What determines the dynamics of Baltic Sea coasts?

A topographic map of Europe and the Baltic Sea region. The map uses a color scale where green and yellow represent lower elevations, and brown and red represent higher elevations. The Baltic Sea is centrally located, surrounded by landmasses including Scandinavia to the north and west, and Eastern Europe to the east. The text "What determines the dynamics of Baltic Sea coasts?" is overlaid in large, bold, red letters with a black outline.

What determines the dynamics of Baltic Sea coasts?

Jan Harff

University of Szczecin, Poland

1. Introduction

2. Geology of the coast: framing the dynamics

3. Relative sea-level change and geological history

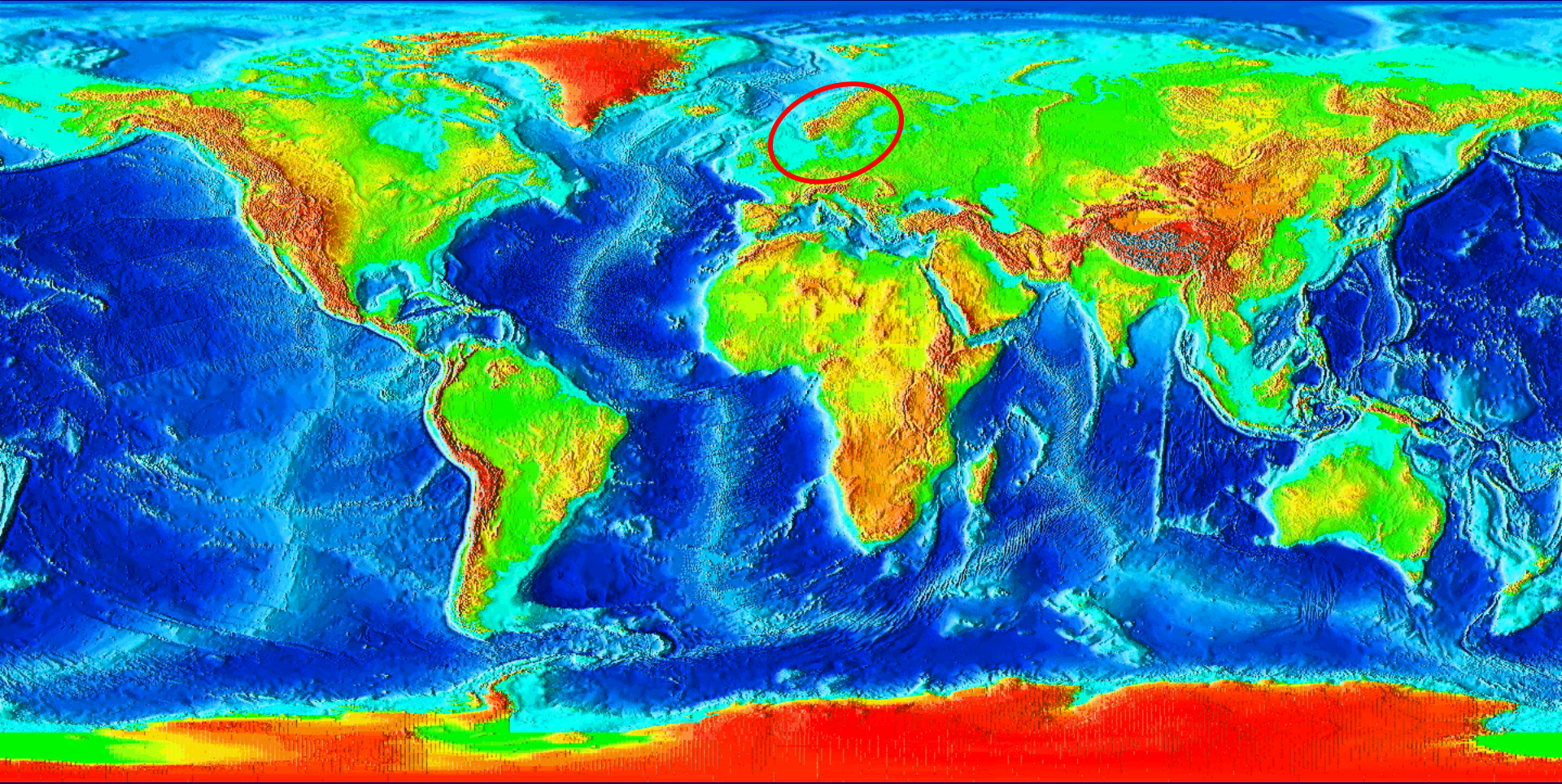
- the role of climate: water volume effect**
- vertical crustal movement (GIA) vs. eustasy**

4. Wind-driven waves – shaping the coast

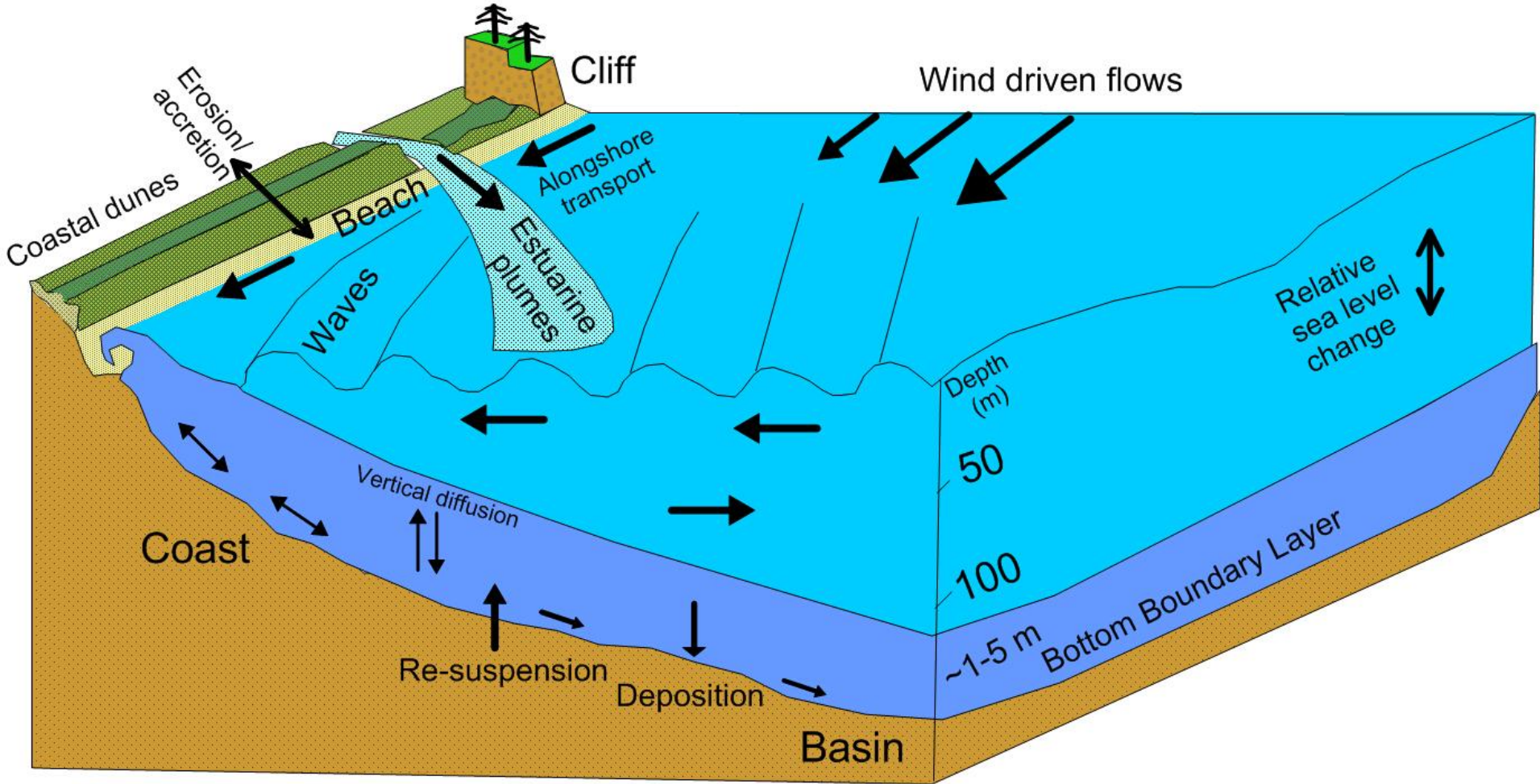
5. Estimation of future change at subsiding coasts

7. Conclusion

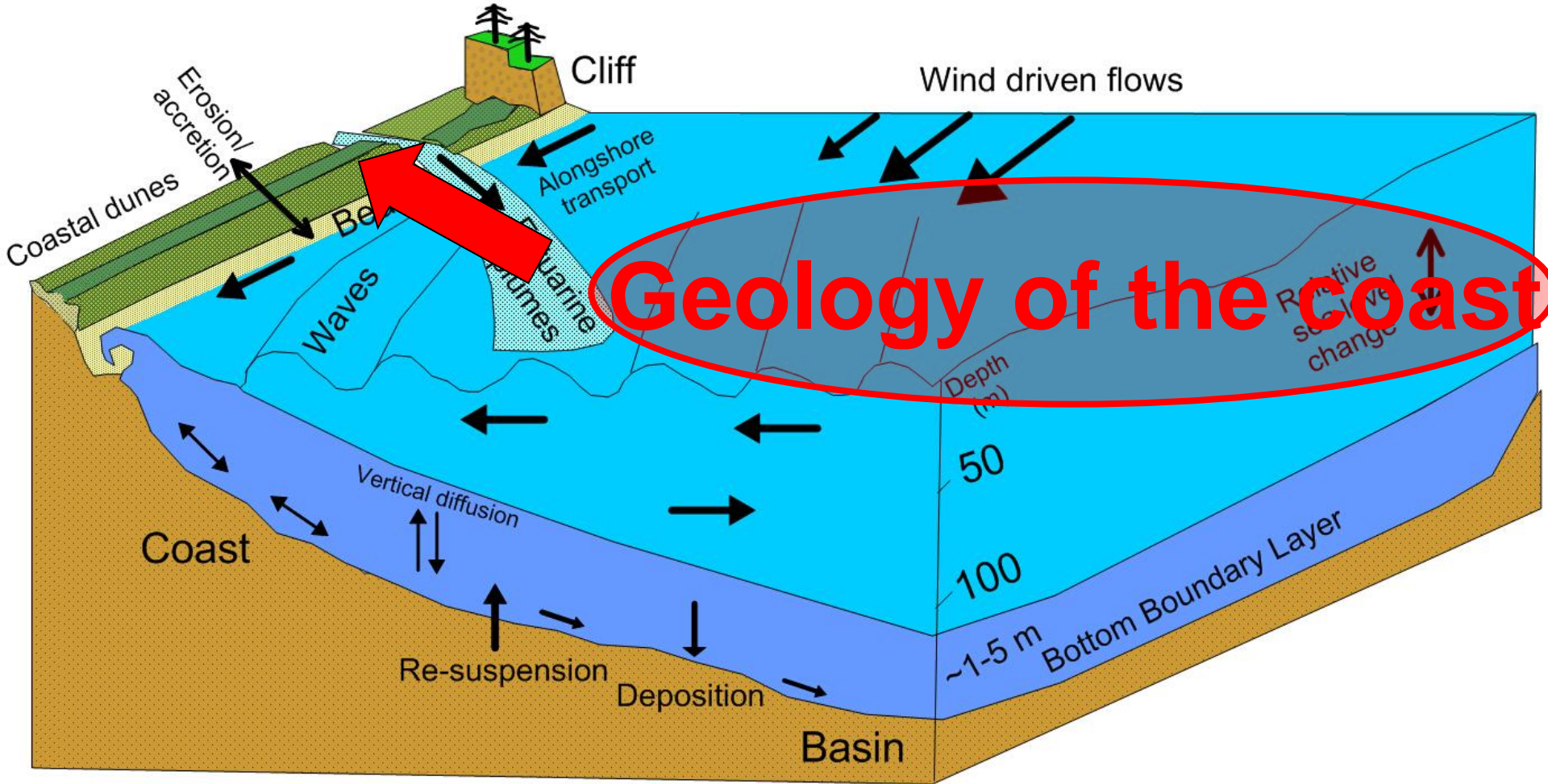
The Earth's Surface



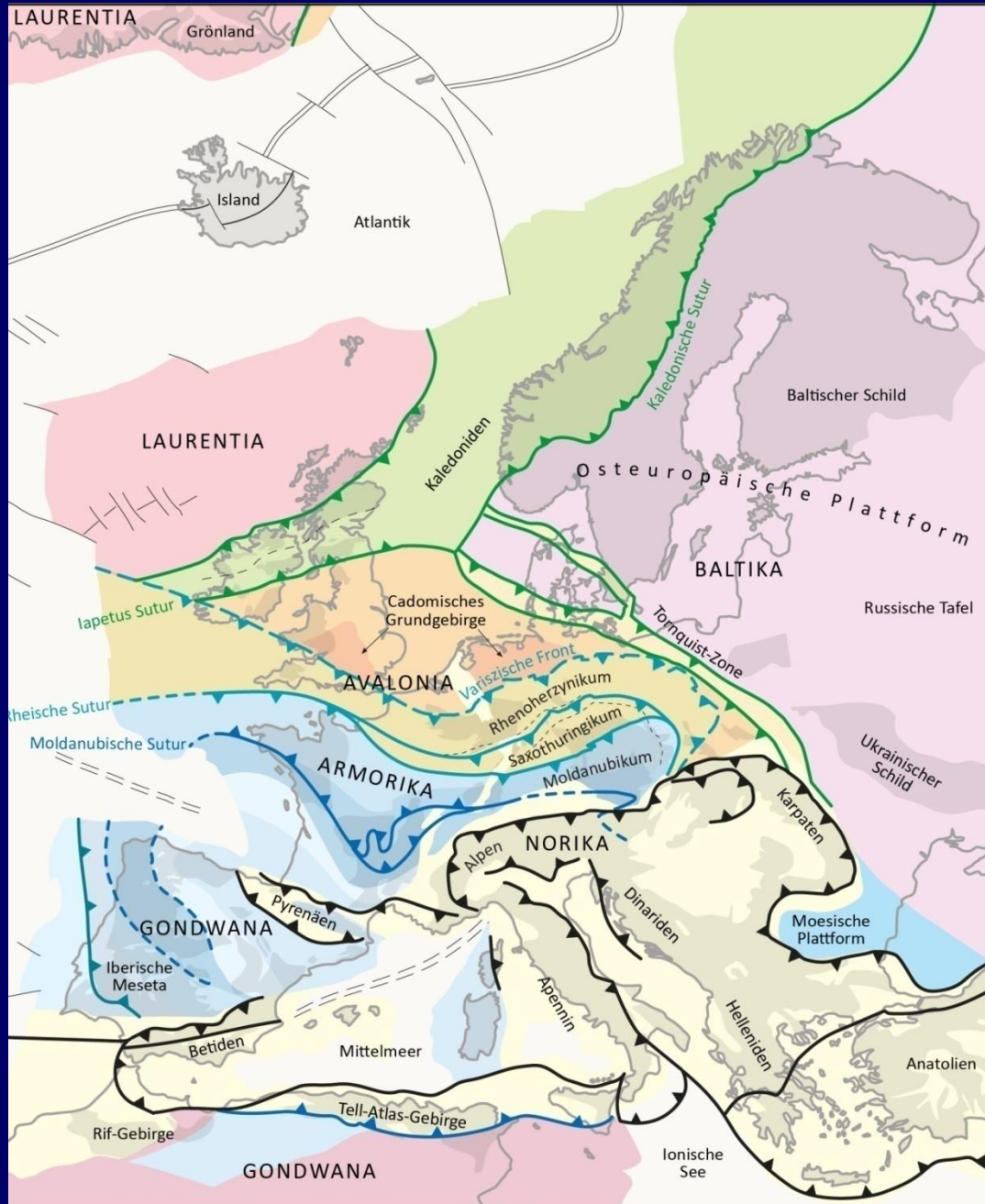
Summary of sedimenttransport mechanisms in the Baltic Sea



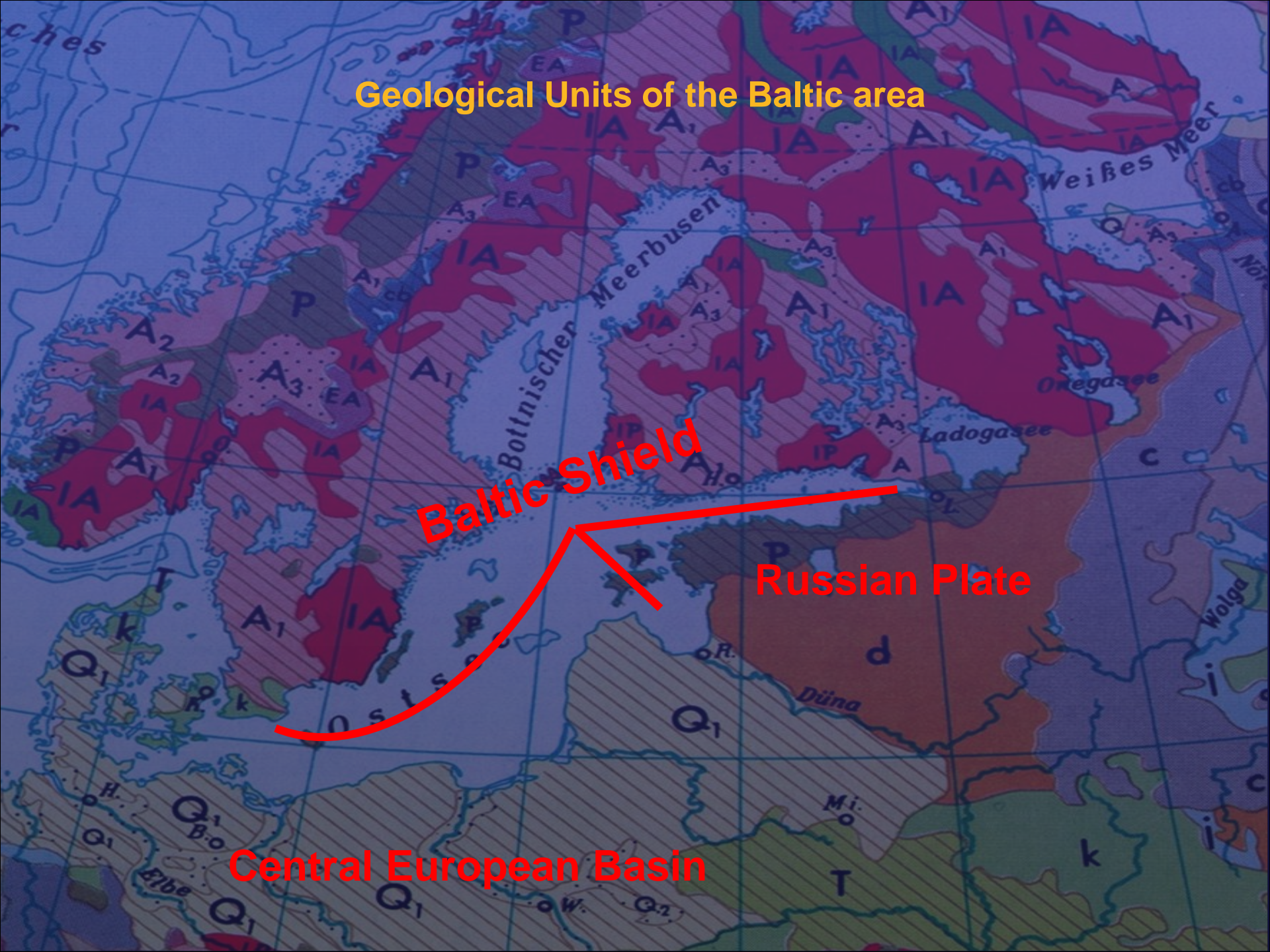
Summary of sediment transport mechanisms in the Baltic Sea



Regional tectonic structure of Europe



Geological Units of the Baltic area

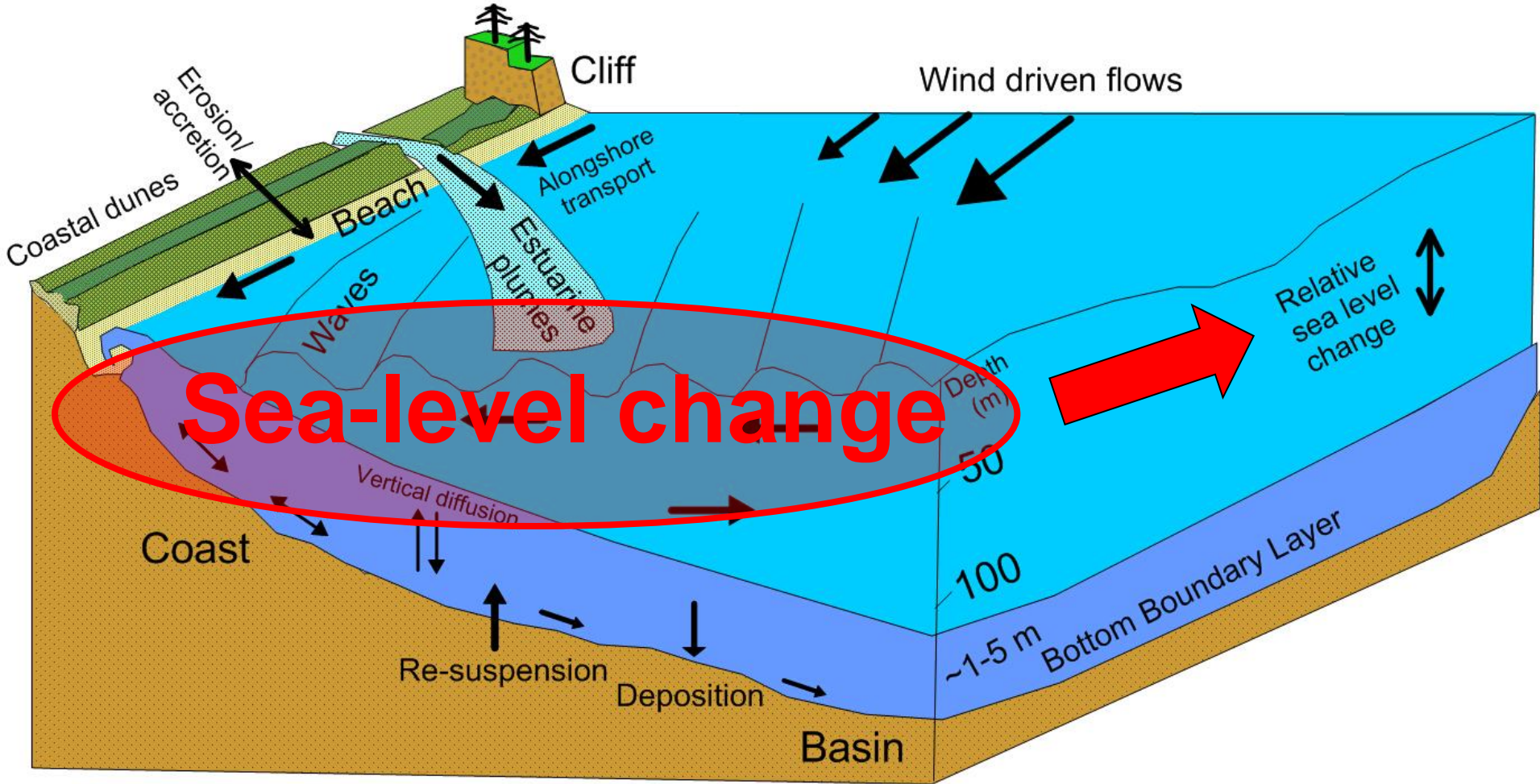


Baltic Shield

Russian Plate

Central European Basin

Summary of sediment transport mechanisms in the Baltic Sea



Relative sea level change and influencing factors

$$\Delta RSL = \Delta EC + \Delta GIA + \Delta G$$

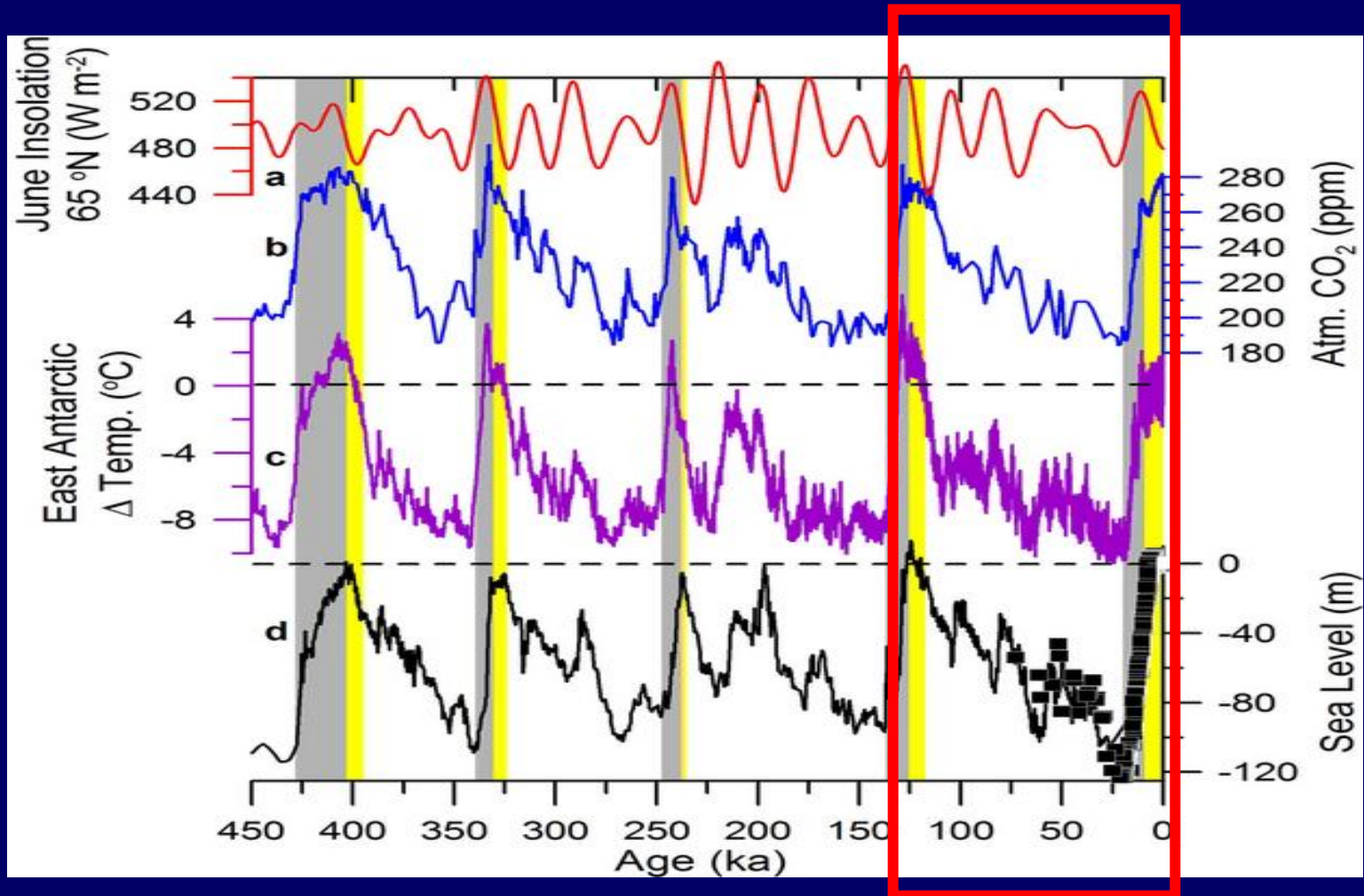
RSL relative sea level

EC eustatic (climatically controlled) component
(water volume effect)

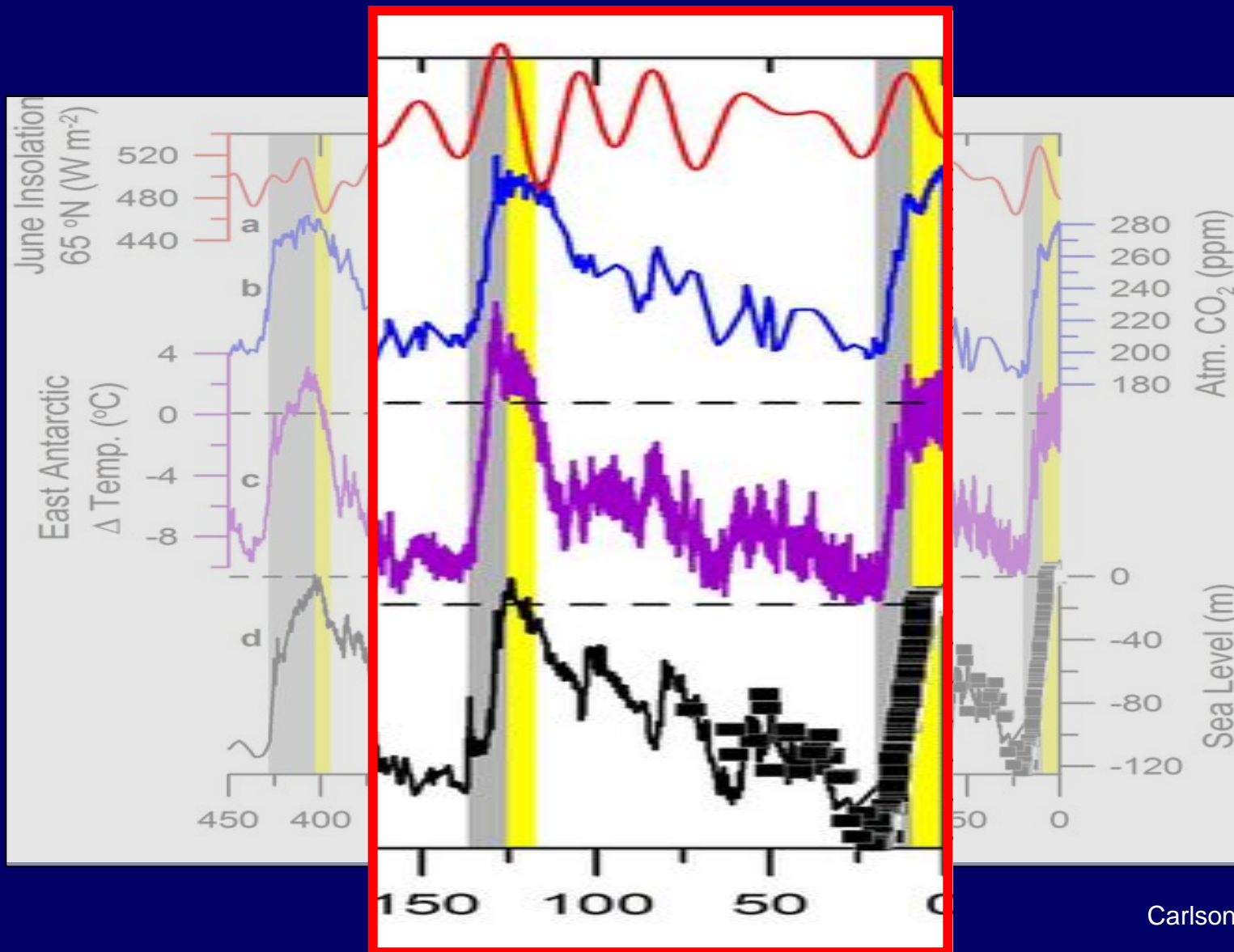
GIA glacio-isostatic adjustment

G gravitational (geoid) effects

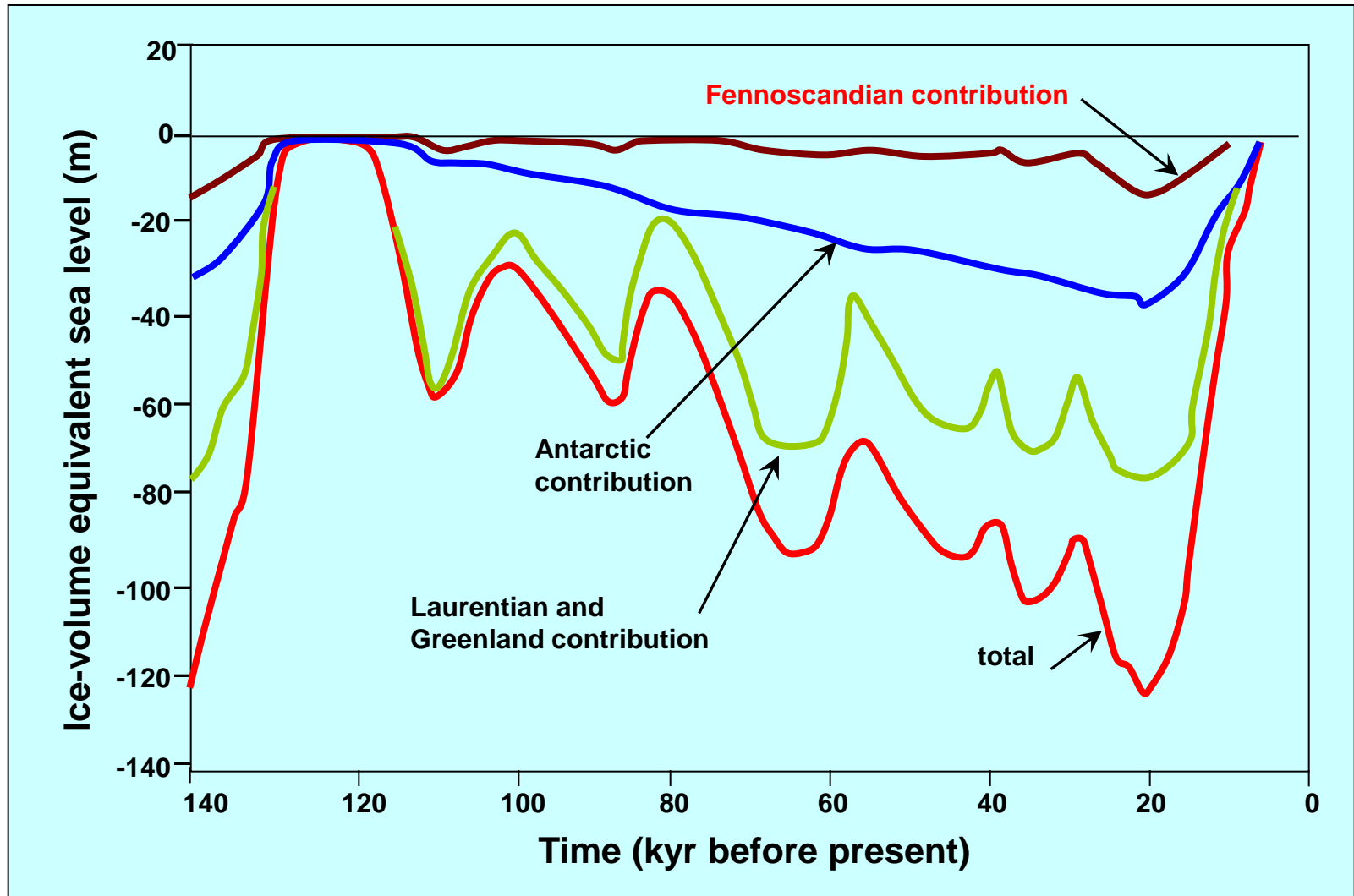
Climate and sea level of the last 450 kyrs



Climate and sea level of the Last Glacial Cycle



Global RSL Variation during the LGC (Ice volume effect)



Transgression / regression modelling

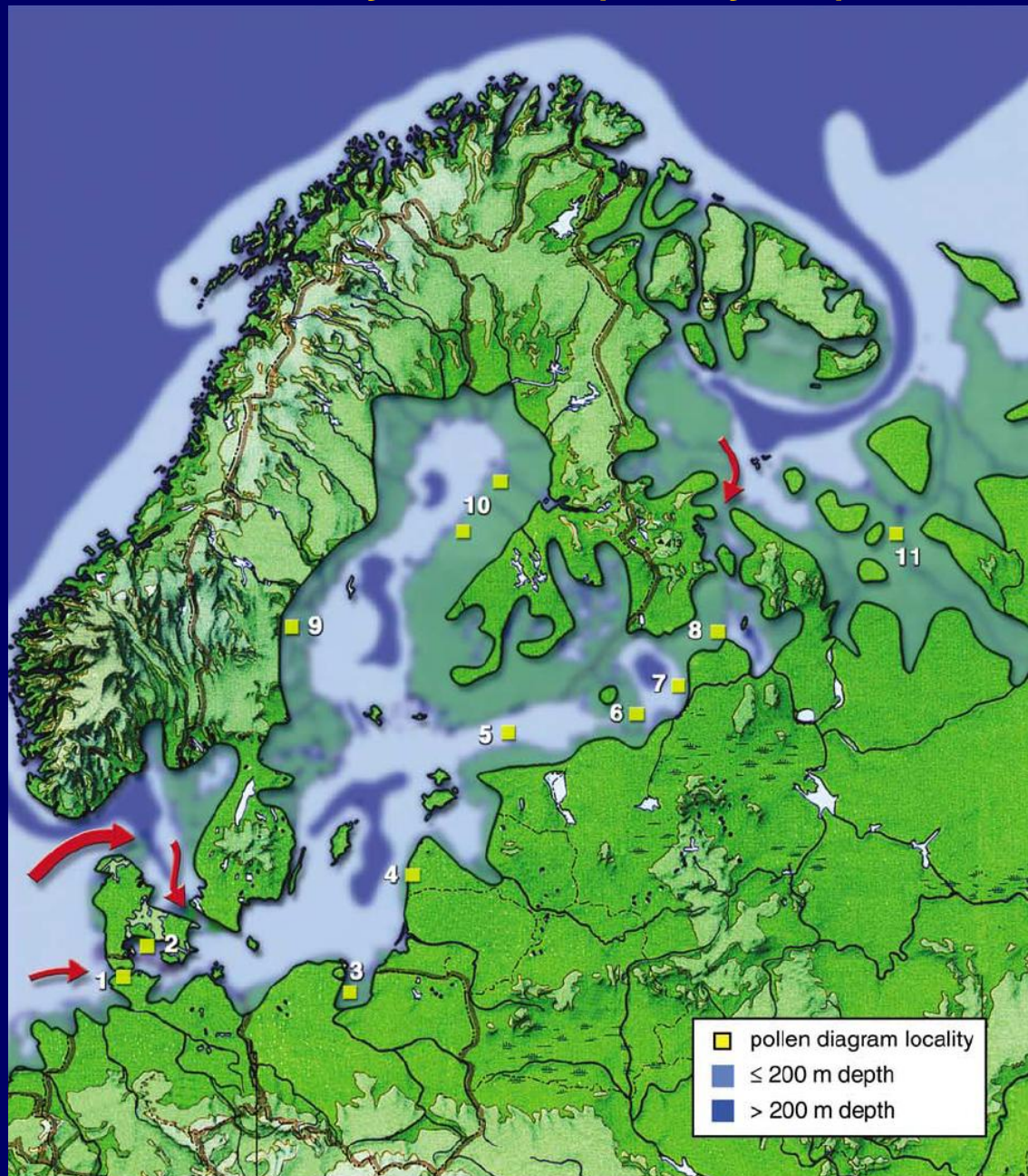
$$DEM_t = DEM_0 - \Delta RSL_t$$

DEM digital elevation model

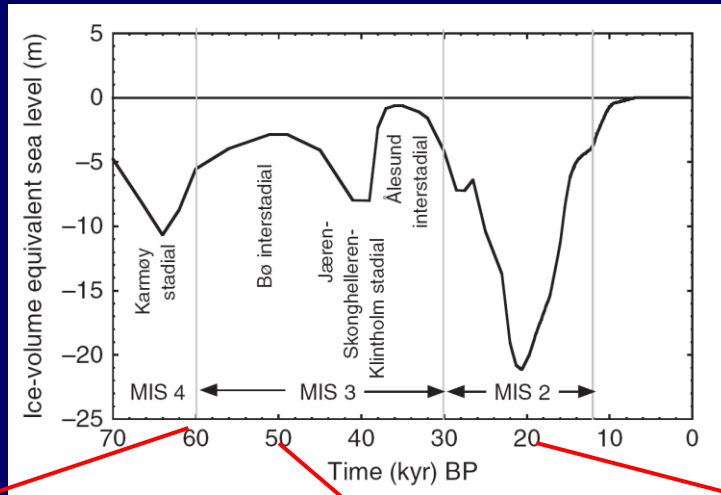
RSL = relative sea level

$t \in T$ time

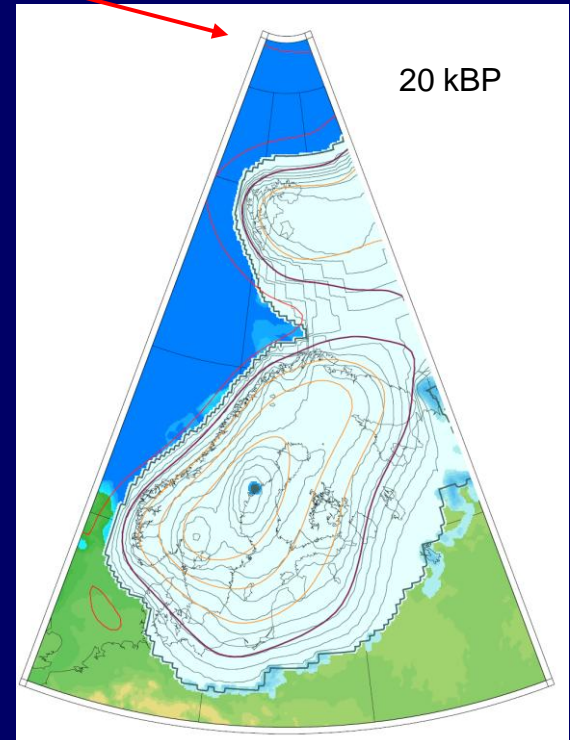
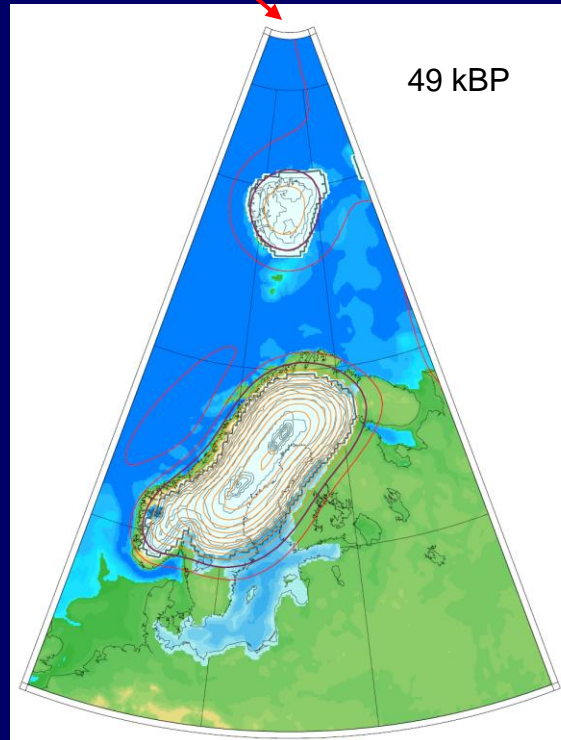
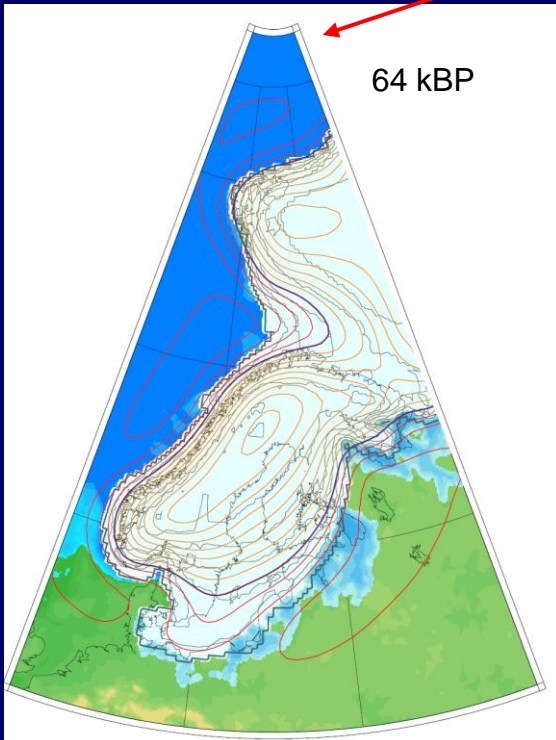
The Baltic-White Sea region at the peak of marine inundation in the Early Eemian (130 ky BP)



Ice-volume-equivalent sea-level (esl) function for the final Scandinavian–Barents ice model from MIS 3 to MIS 1 and paleogeographic models for the Baltic area



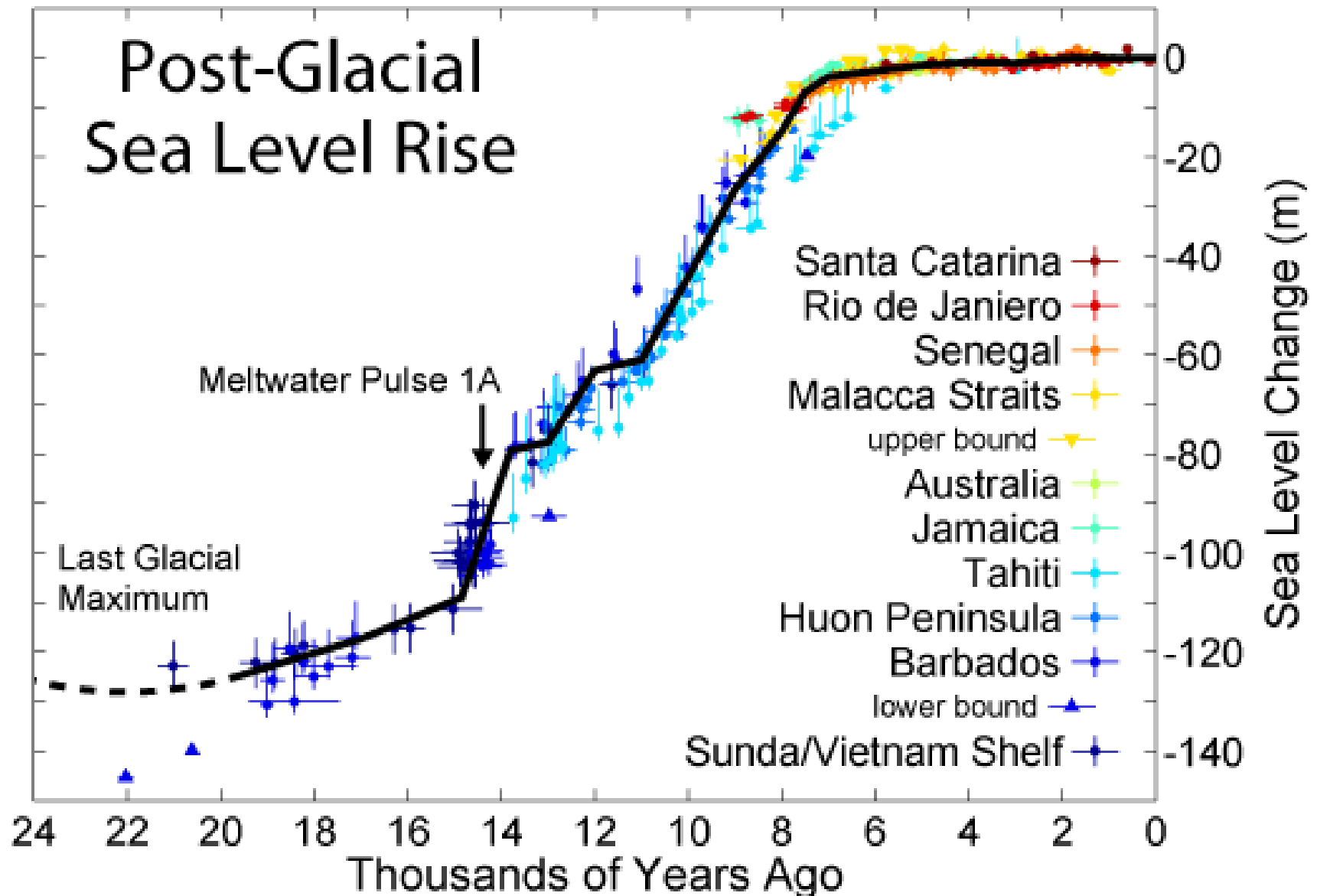
Lambeck et al. (2010)

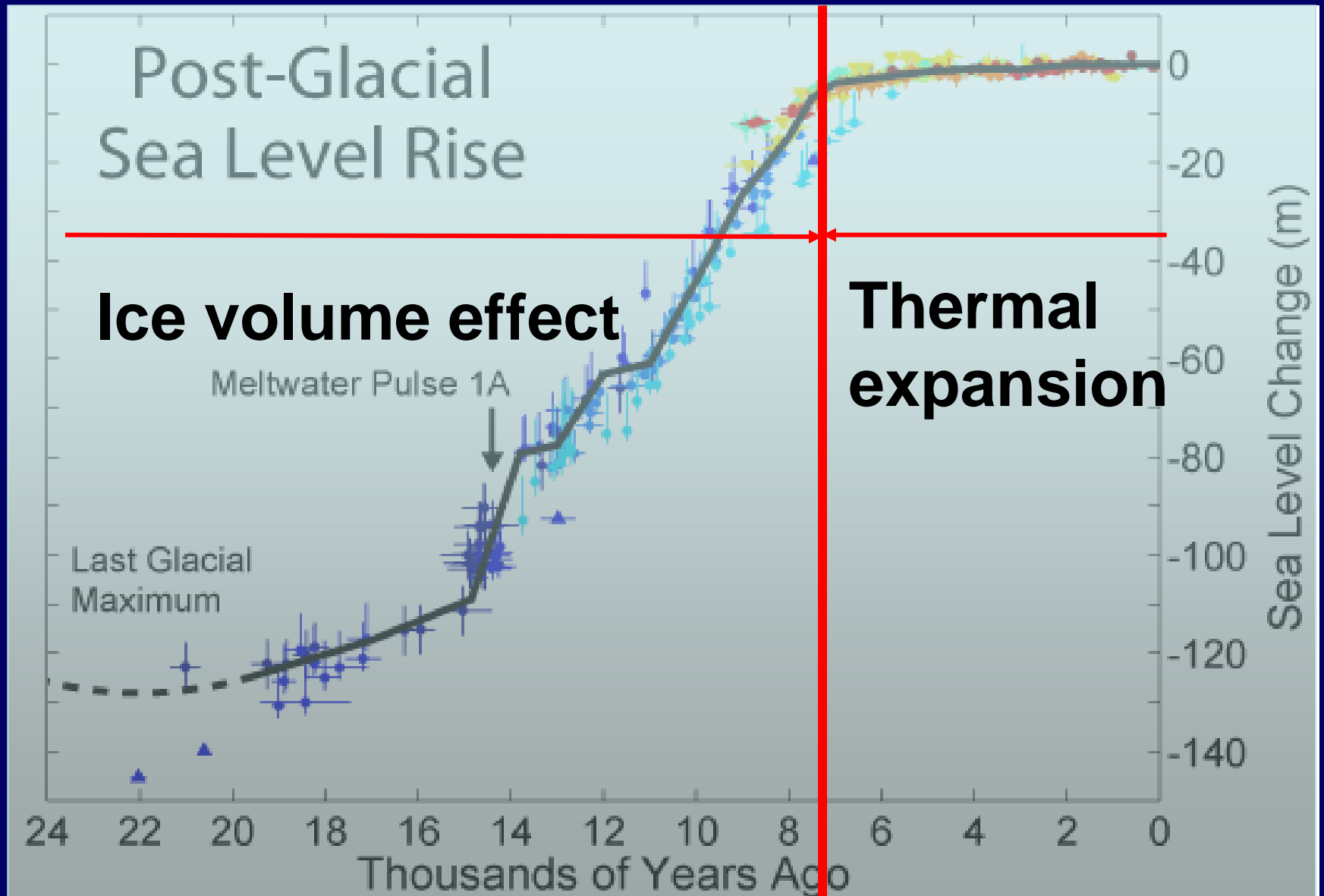


Extent of ice sheets and 120 m lower sea level in northern Europe during the LGM



Post-Glacial Sea Level Rise





Relative sea level change and influencing factors

$$\Delta RSL = \Delta EC + \Delta GIA + \Delta G$$

RSL relative sea level

EC eustatic (climatically controlled) component
(water volume effect)

GIA glacio-isostatic adjustment

G gravitational (geoid) effects

Sea level equation after Peltier (1998)

$$\begin{aligned}\delta rsl(\theta, \lambda, t) &= C(\theta, \lambda, t) \cdot \{ \delta G(\theta, \lambda, t) - \delta gia(\theta, \lambda, t) \} \\ &= C(\theta, \lambda, t) \cdot \left\{ \int \left[\iint (g^{-1} \Phi(\psi, t-t') - \Gamma(\psi, t-t')) \cdot \right. \right. \\ &\quad \left. \left. \cdot L(\theta', \lambda', t') \, d\sigma \right] dt' + g^{-1} \Delta \Phi(t) \right\}\end{aligned}$$

δrsl relative sea level change

δgia crustal deformation

δG gravity field

C ocean function

L load

Γ, Φ Green functions

Sea level equation after Peltier (1998)

$$\begin{aligned}\delta rsl(\theta, \lambda, t) &= C(\theta, \lambda, t) \cdot \{ \delta G(\theta, \lambda, t) - \delta gia(\theta, \lambda, t) \} \\ &= C(\theta, \lambda, t) \cdot \left\{ \int \left[\iint (g^{-1} \Phi(\psi, t-t') - \Gamma(\psi, t-t')) \cdot \right. \right. \\ &\quad \left. \left. \cdot L(\theta', \lambda', t') \, d\sigma \right] dt' + g^{-1} \Delta \Phi(t) \right\}\end{aligned}$$

δrsl relative sea level change

δgia crustal deformation

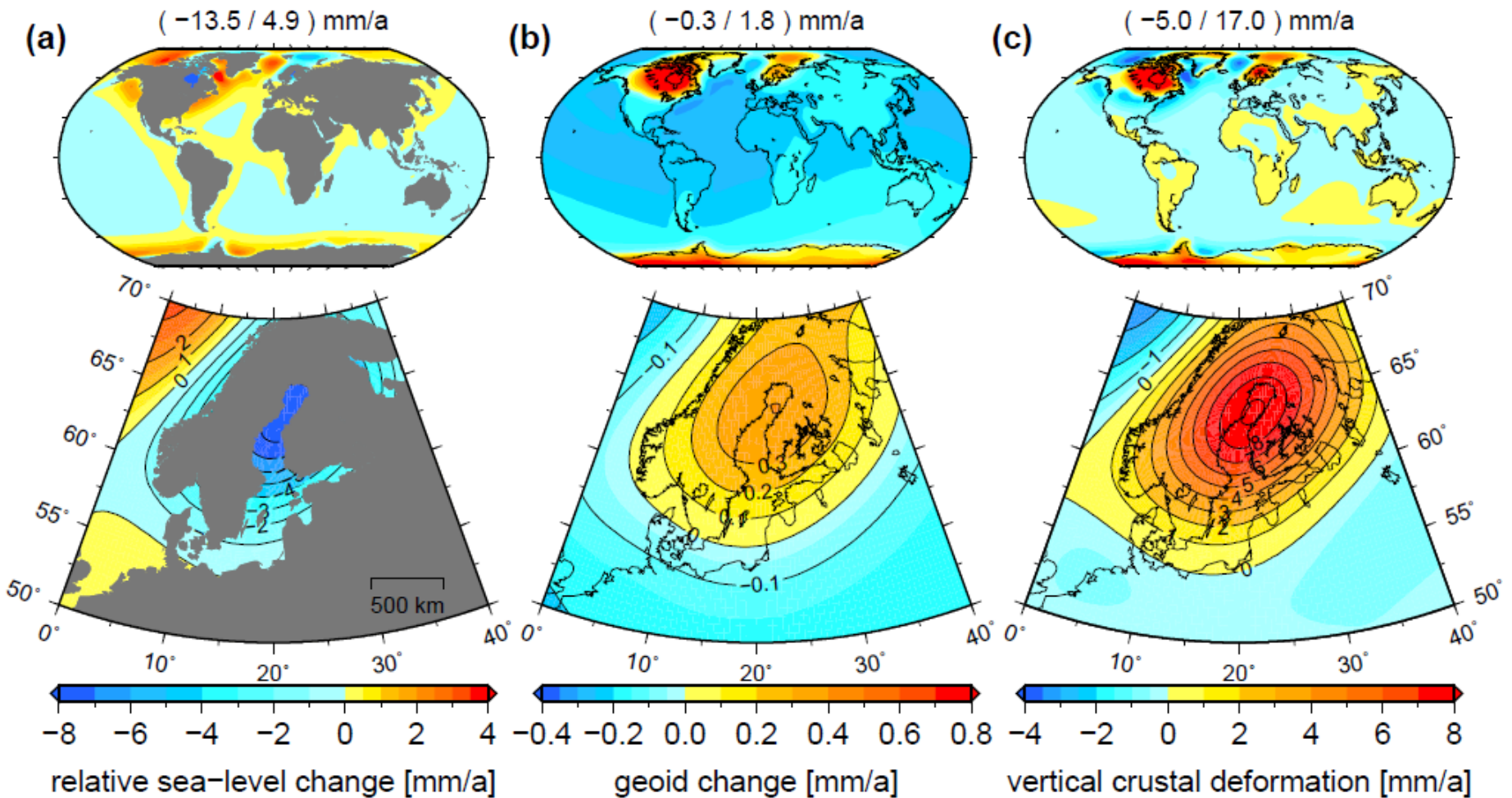
δG gravity field

C ocean function

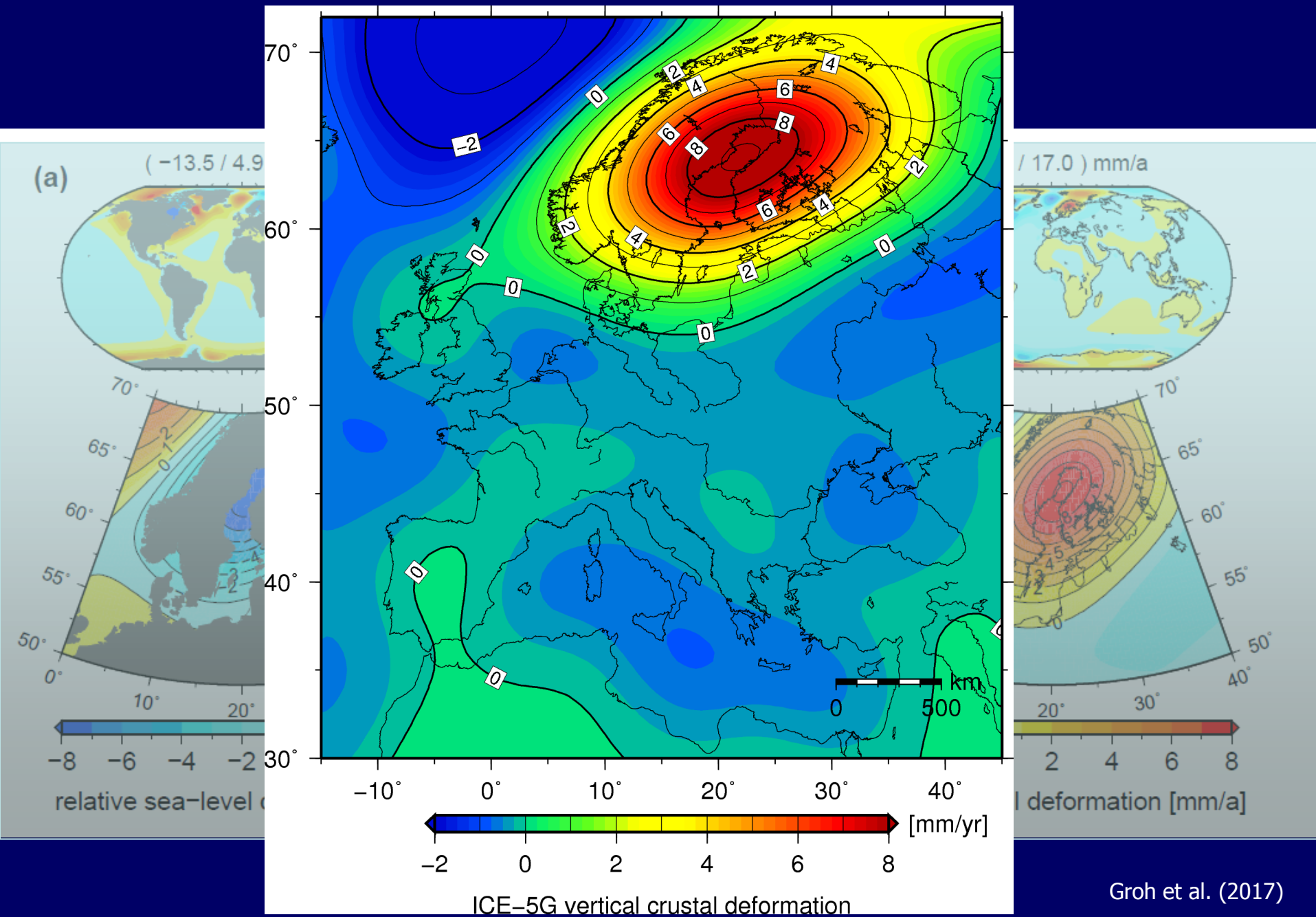
L load

Γ, Φ Green functions

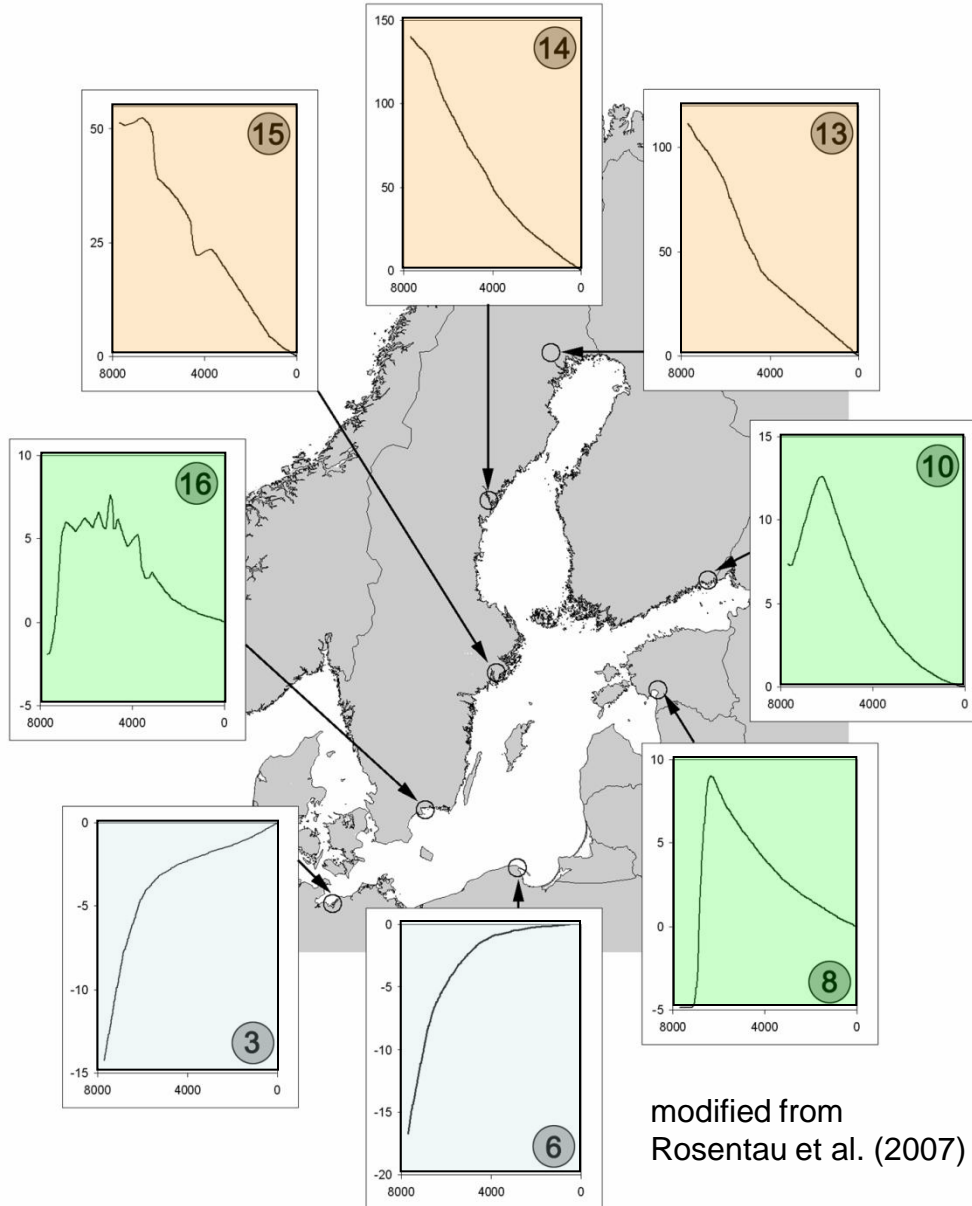
Predictions of GIA-induced mass signals according to the ICE-5G(VM2) model (Peltier, 2004)



Vertical crustal deformation



Selected Baltic Sea RSL curves



Regressive North: Åland –Islands



Foto: J. Harff (2003)

Kirchen-Ruine zu Hoff b. Horst

erbaut Mitte des 12. Jahrhunderts.

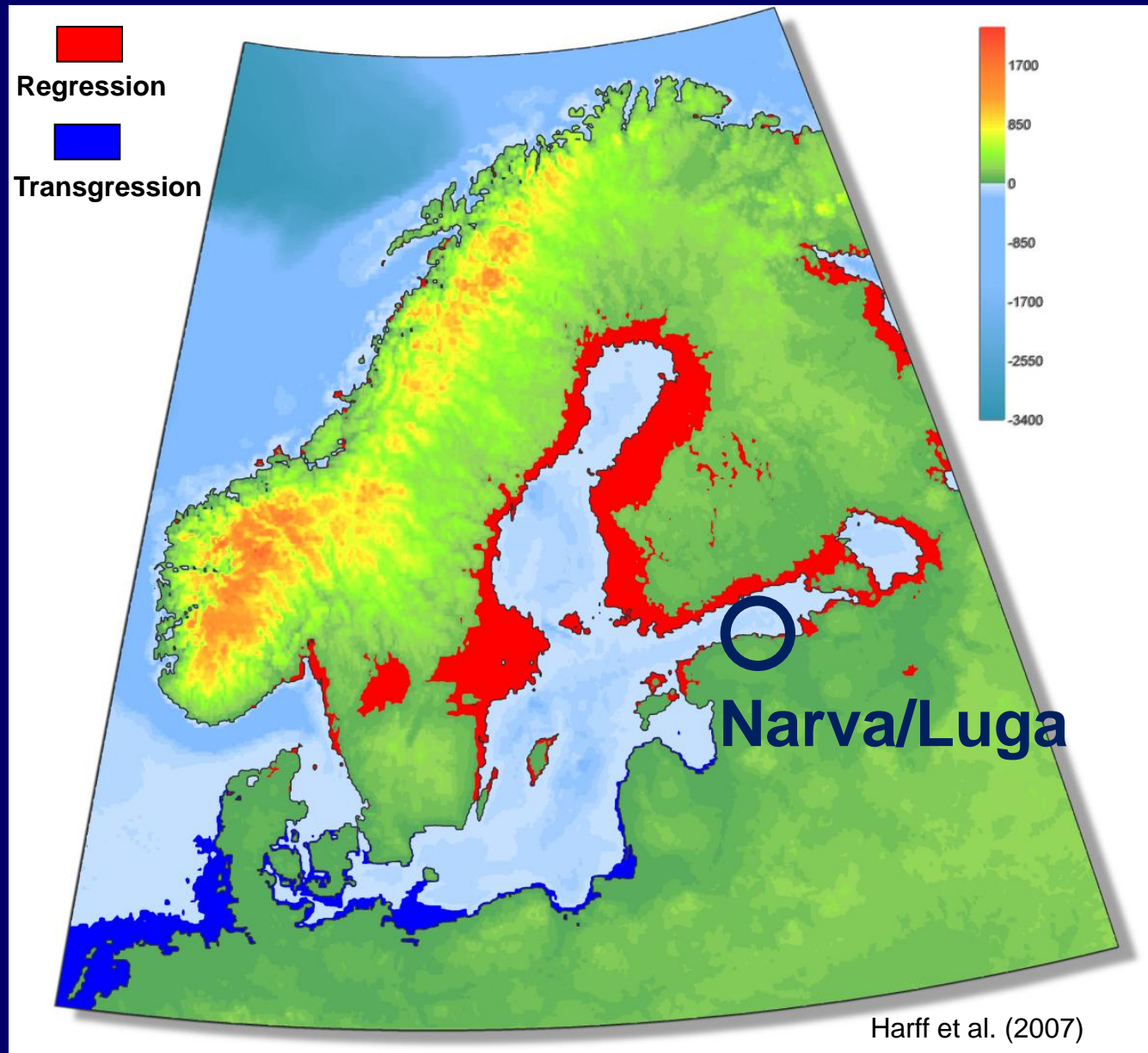
Die Wölbung stürzte am 14. Juli 1658
herunter

**Transgressive South:
Trzęsacz 1919**

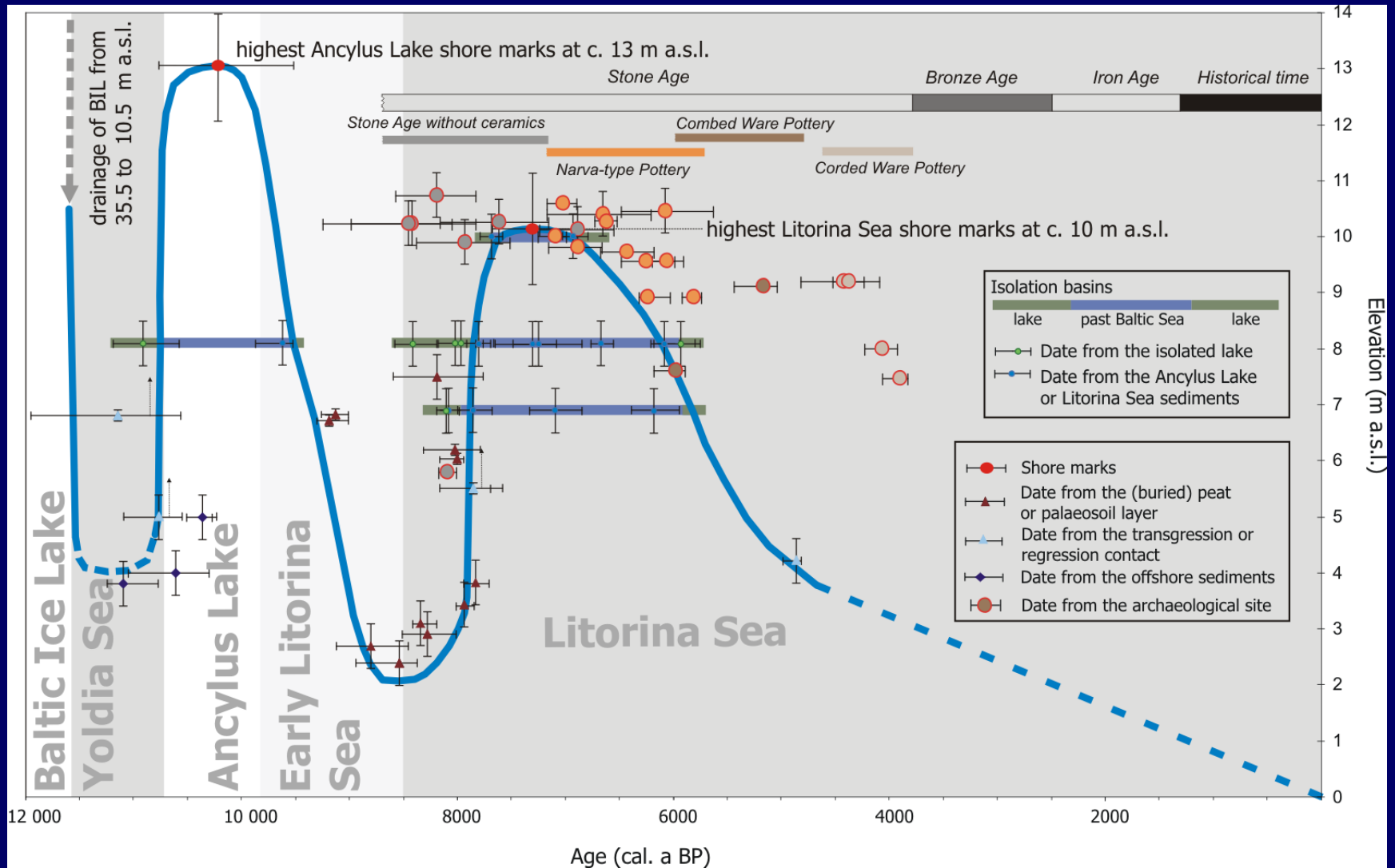


Trzesacz 1919

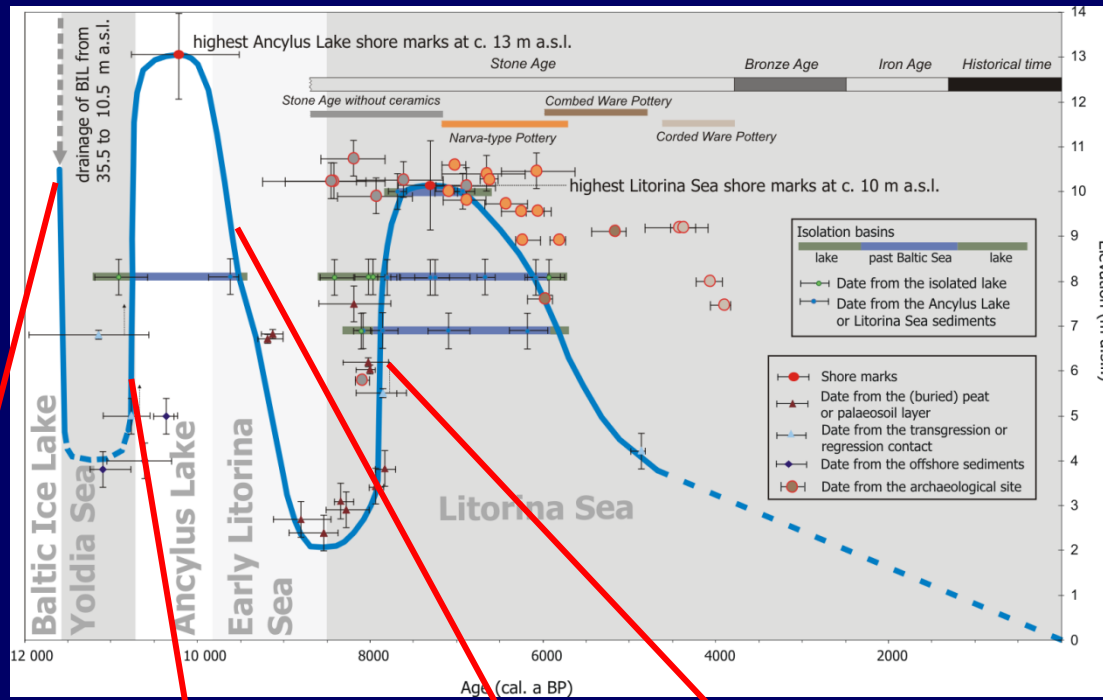
Areas of transgression and regression of the Baltic Sea since 8 cal. ka BP



Water-level curve for Narva-Luga



Water-level curve for Narva-Luga

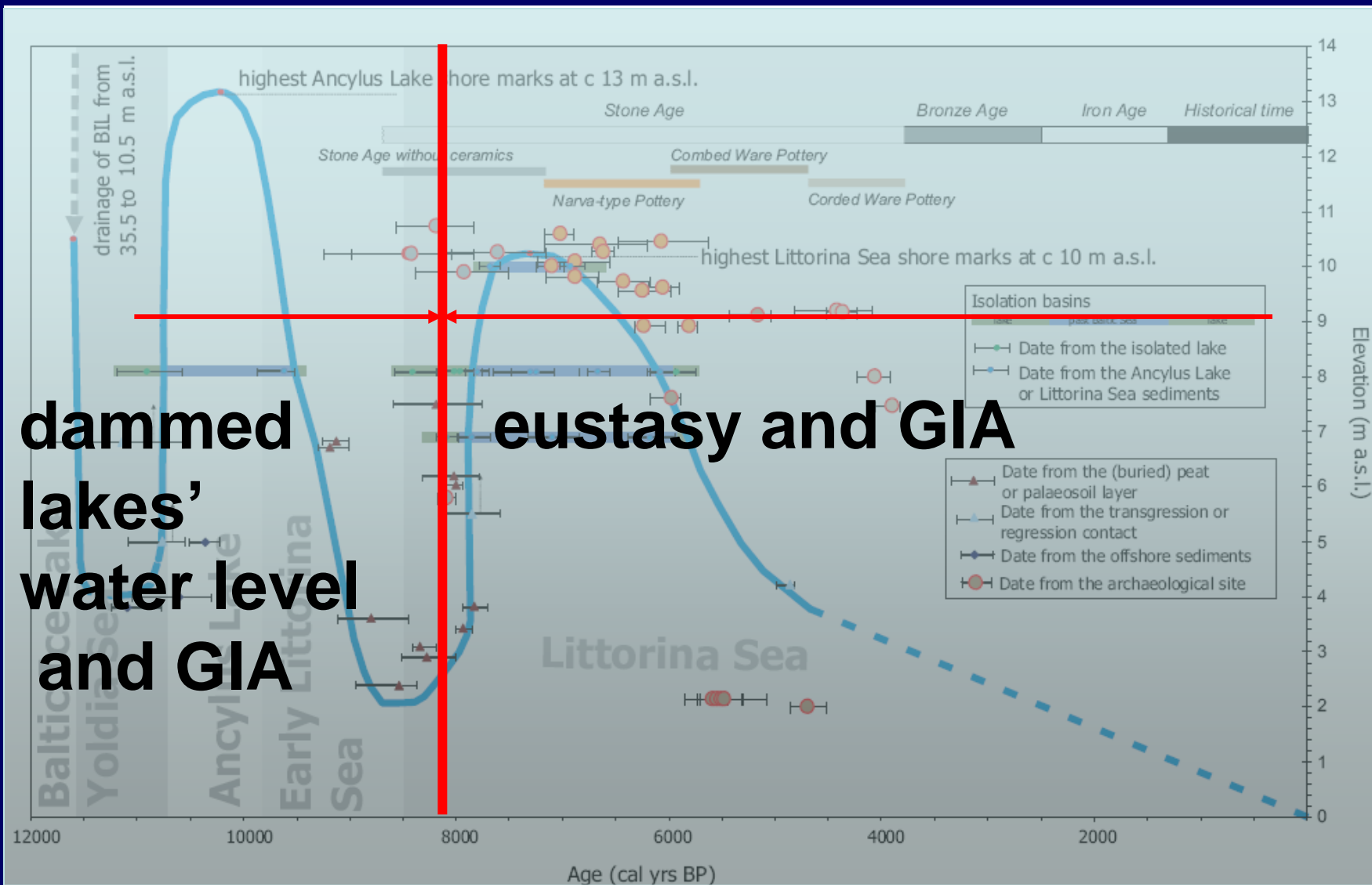


Rosentau et al. (2017)

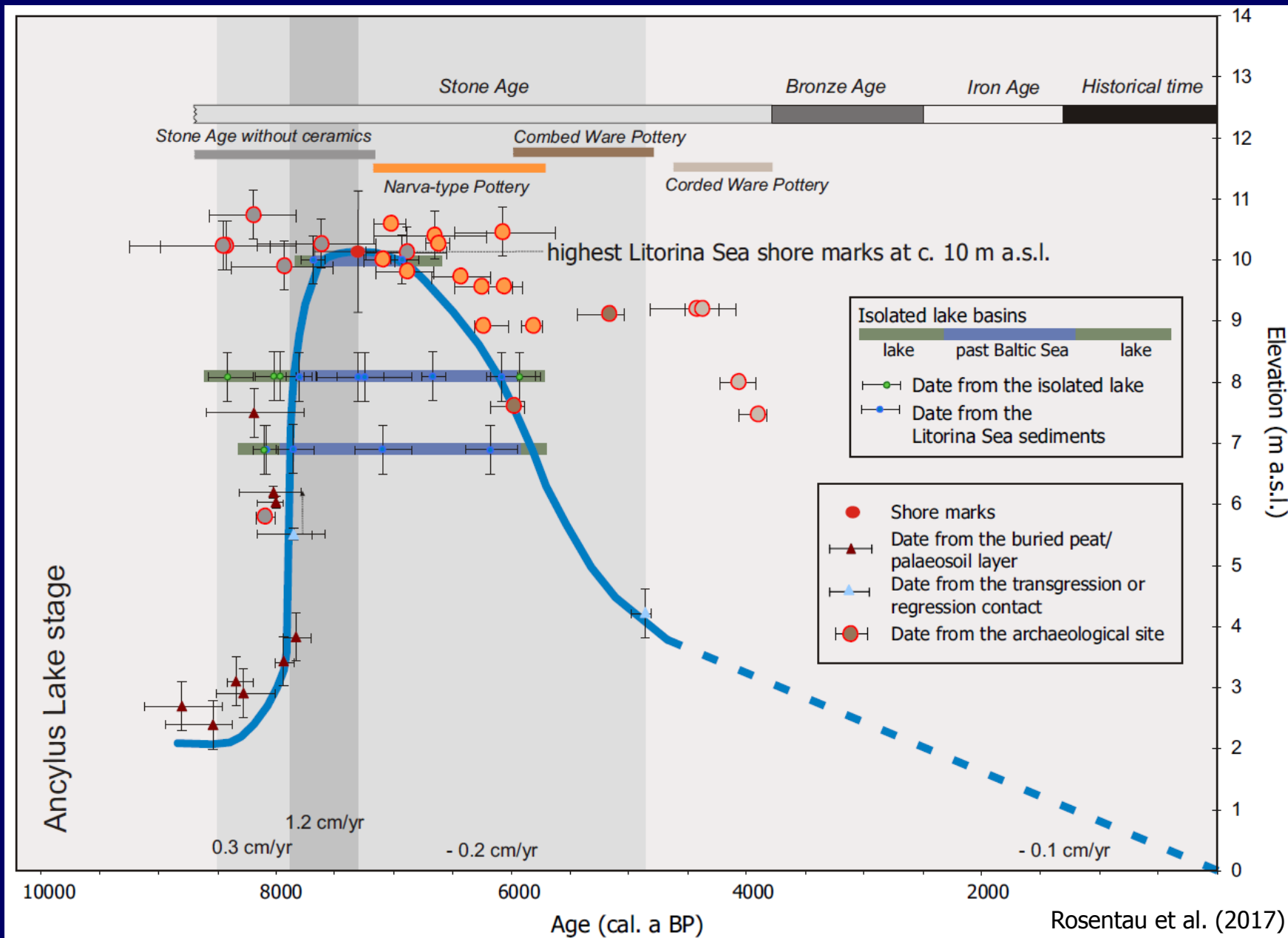


modified from Andren (2011)

Water-level curve for Narva-Luga and main influential factors for coastline change



^ RSL in Narva-Luga, E GoF



Littorina Sea at 8000 cal BP



Rosentau et al. (2011)

Littorina Sea at 7300 cal BP



Littorina Sea at 7000 cal BP



Littorina Sea at 6500 cal BP



Littorina Sea at 6000 cal BP



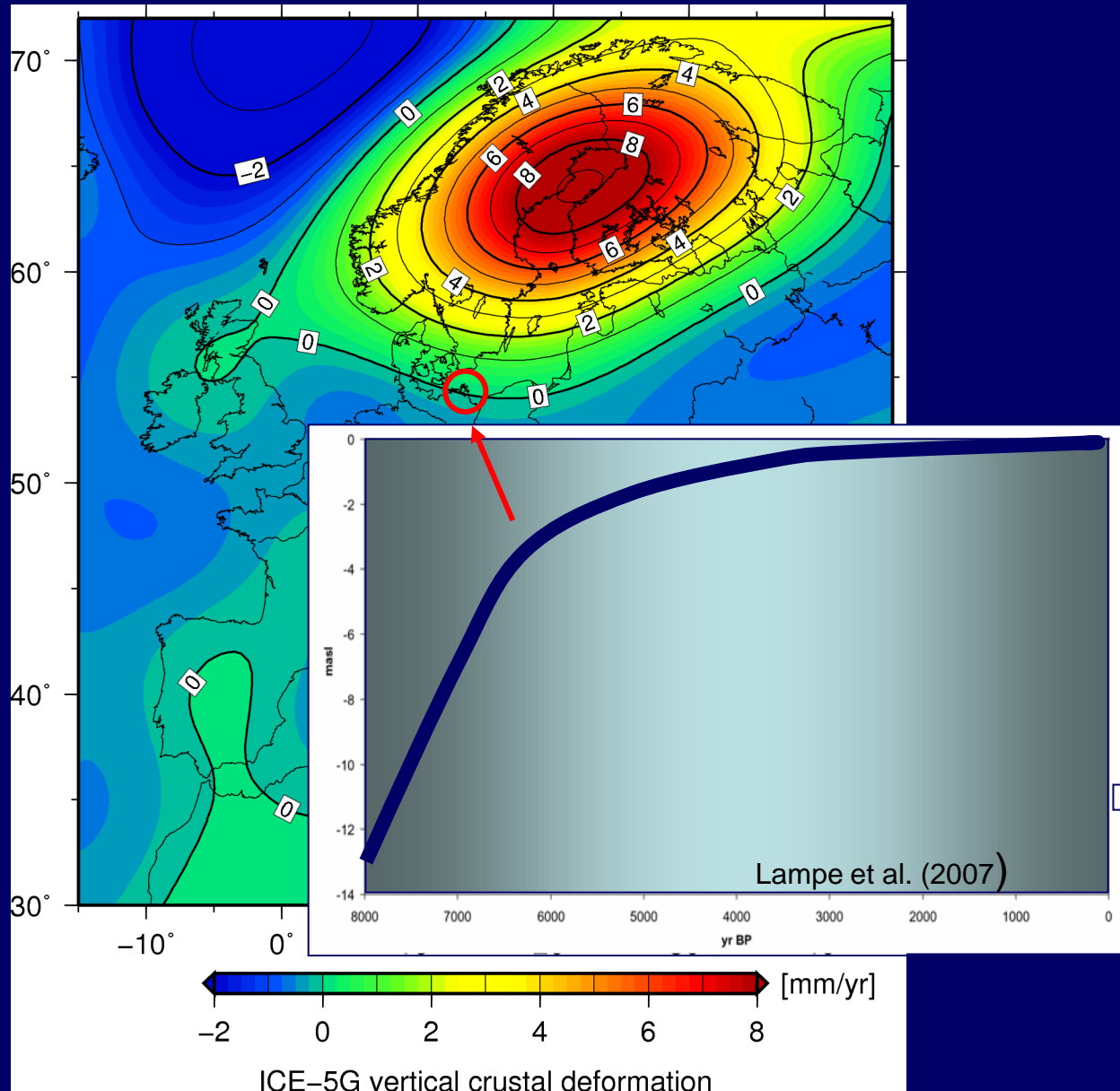
Littorina Sea at 5500 cal BP



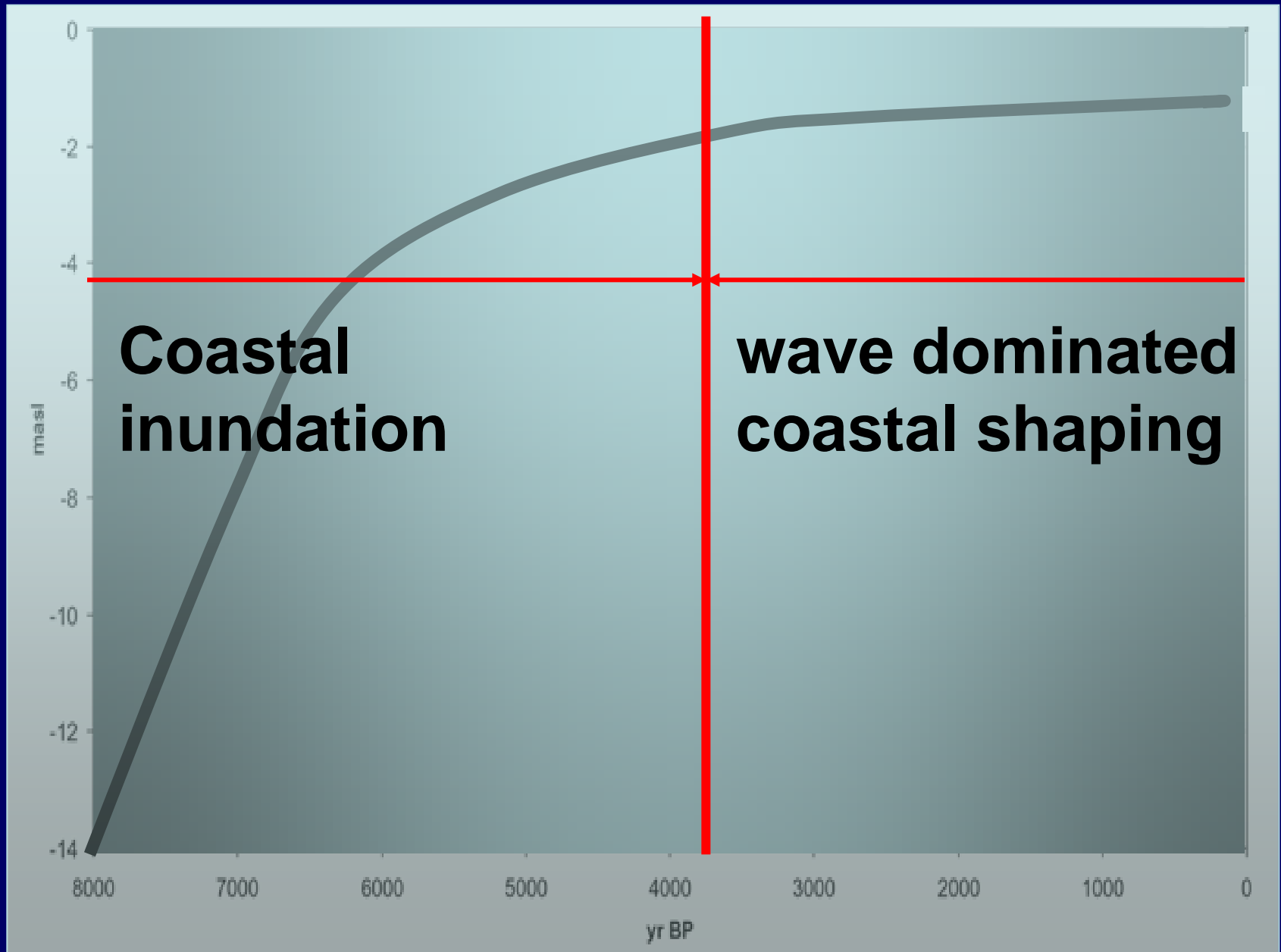
Littorina Sea at 4500 cal BP



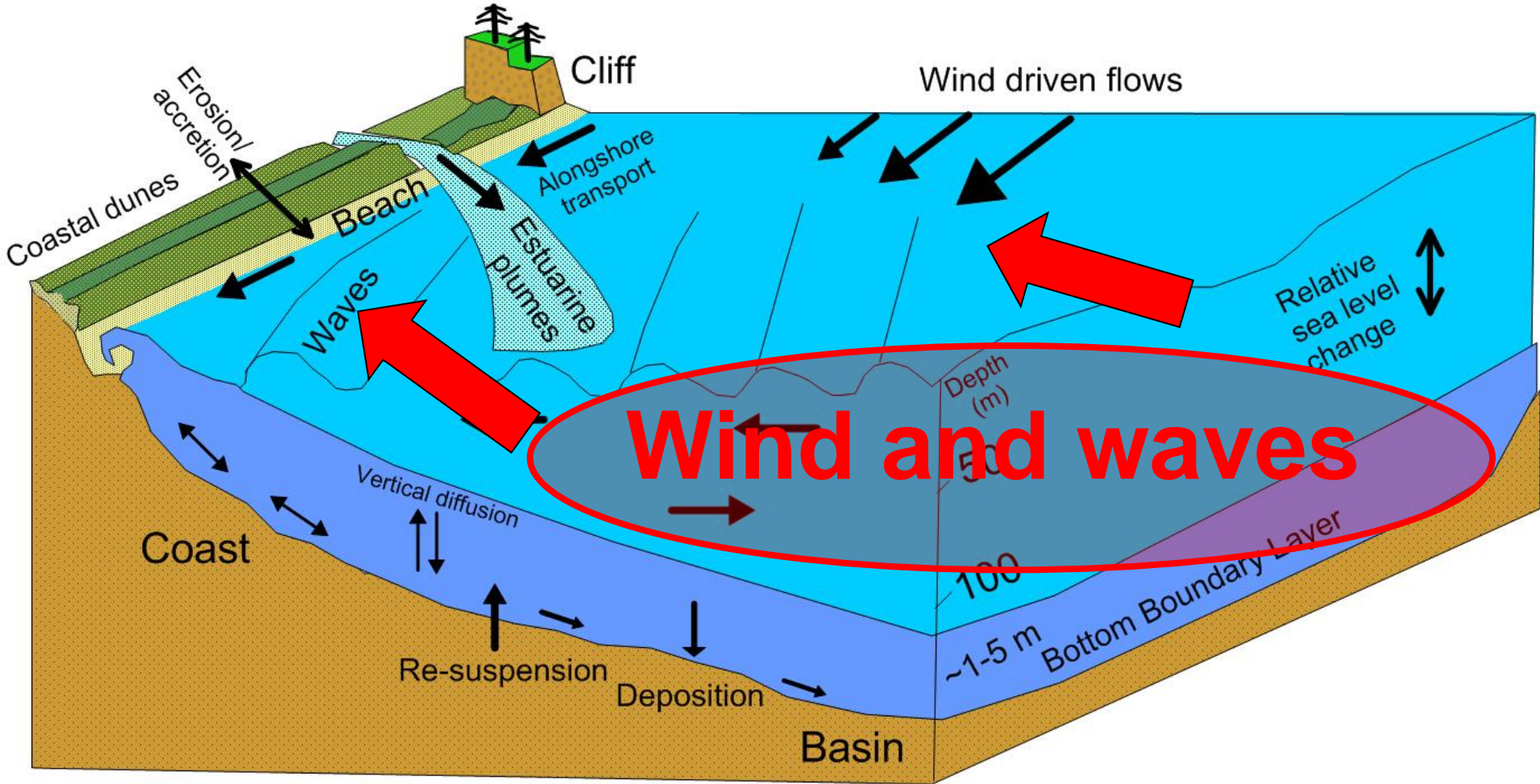
Relative sea level change in Europe



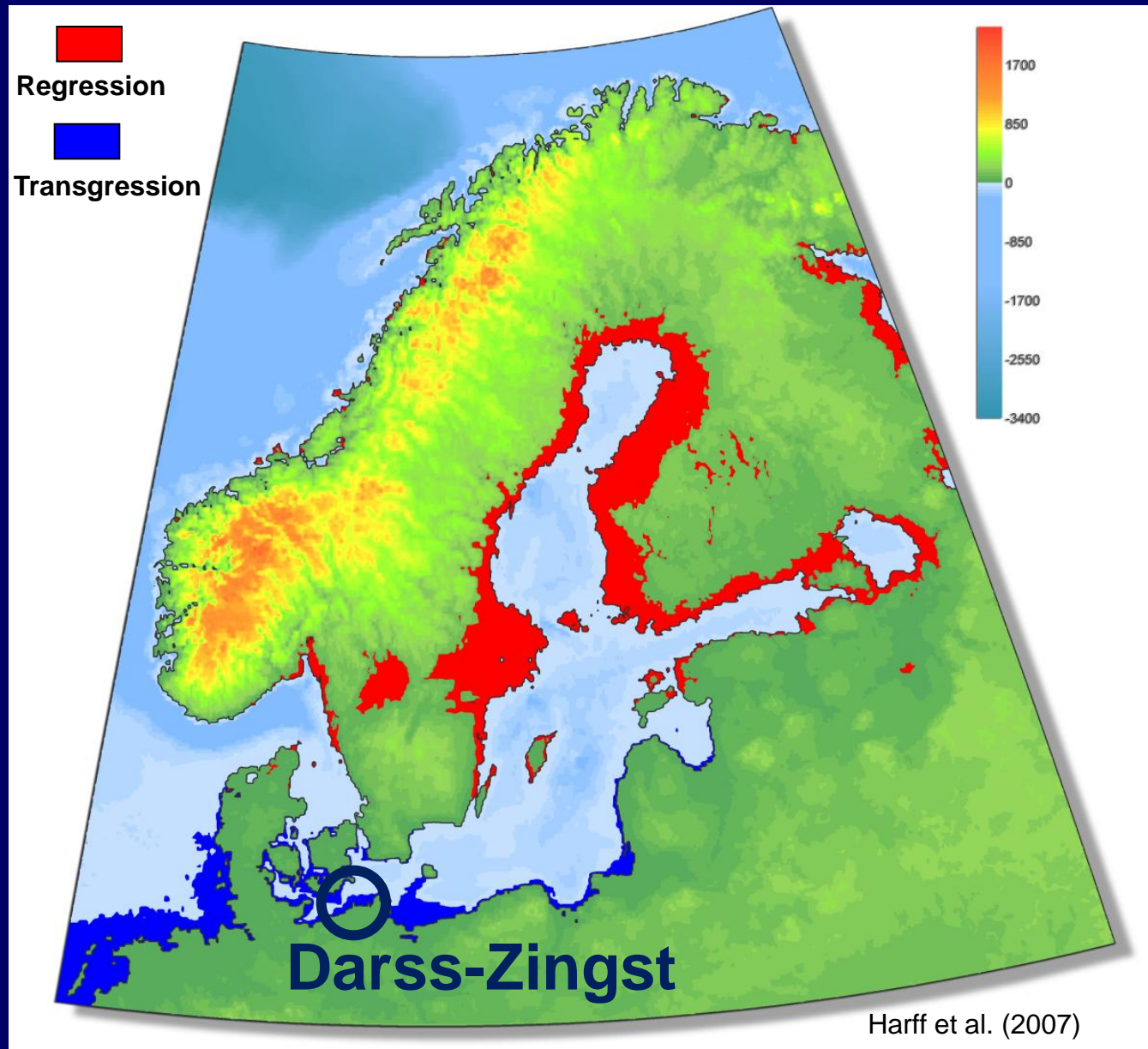
Effects of the sea-level rise on the southern Baltic Coast



Summary of sediment transport mechanisms in the Baltic Sea



Areas of transgression and regression of the Baltic Sea since 8 cal. ka BP



Morphodynamic modelling

$$DEM_t = DEM_0 - \Delta RSL_t + \Delta SED_t$$

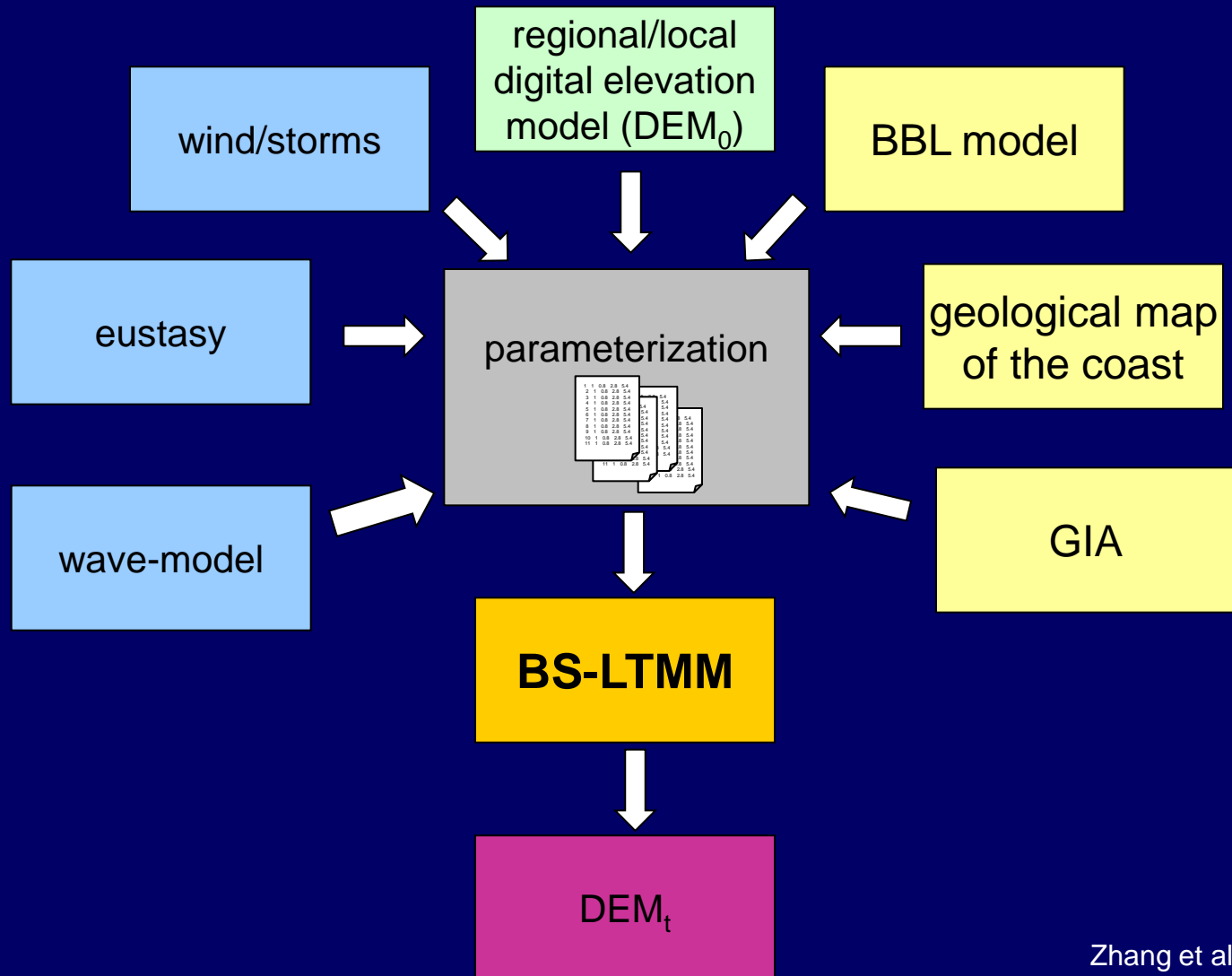
DEM digital elevation model

RSL = relative sea level

SED sediment thickness

$t \in T$ time

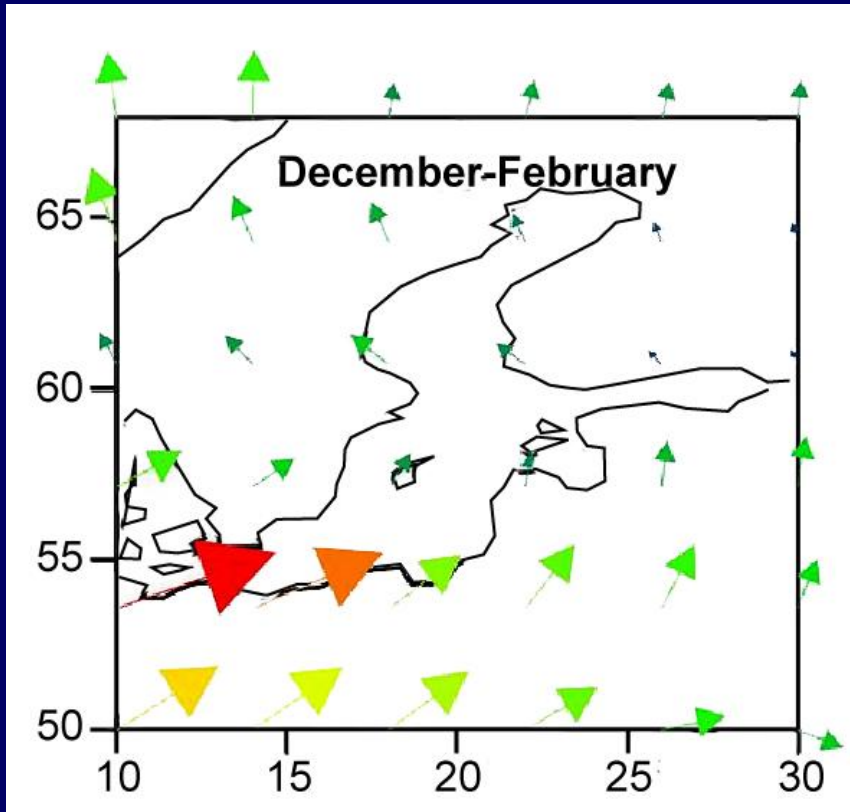
Sediment transport modelling with BS-LTMM: flow chart



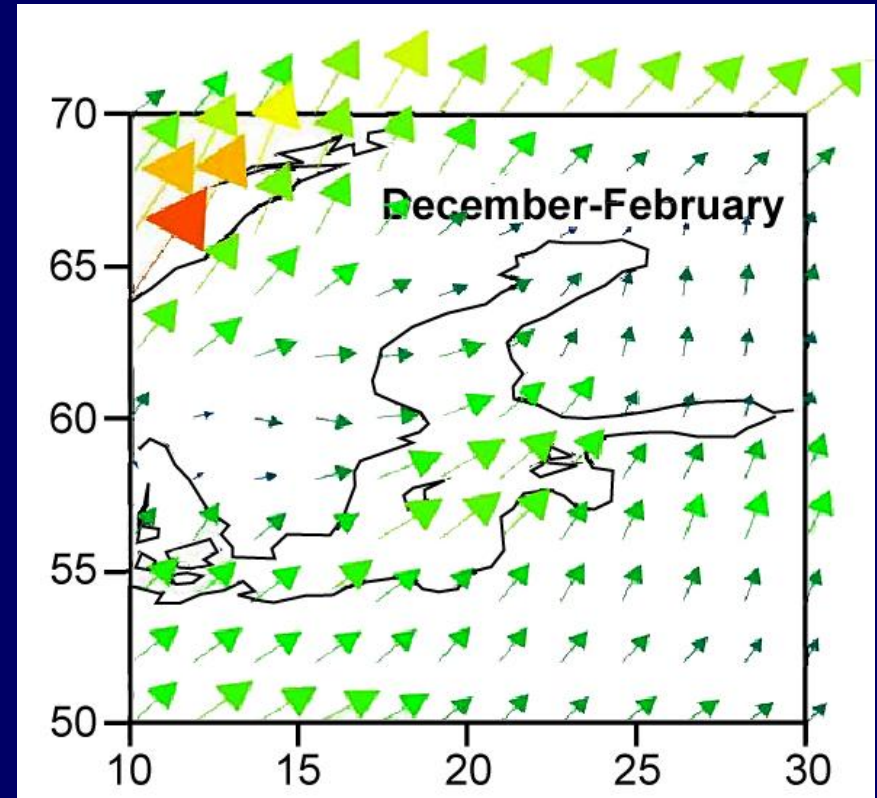
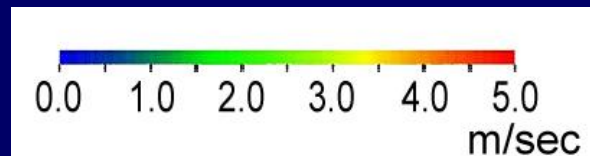
Major components of the global climate system.



Mean 10 m winds (annual)

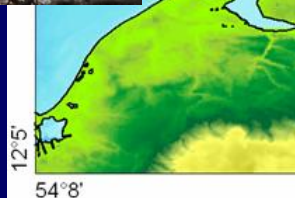
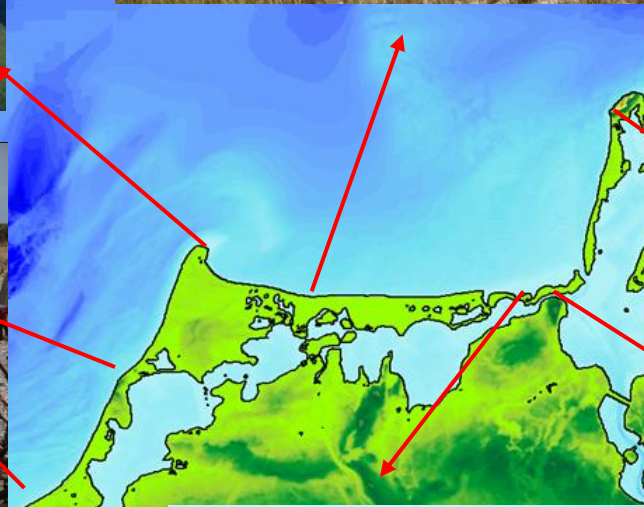


ECHO-G simulation
1000 – 1990 AD

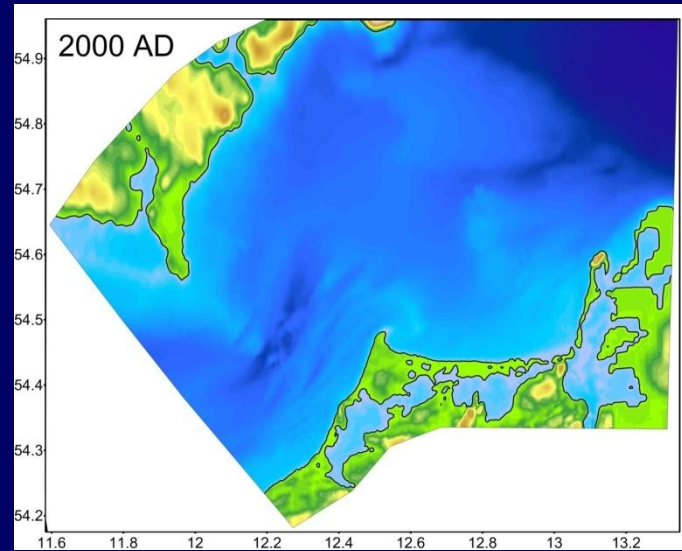
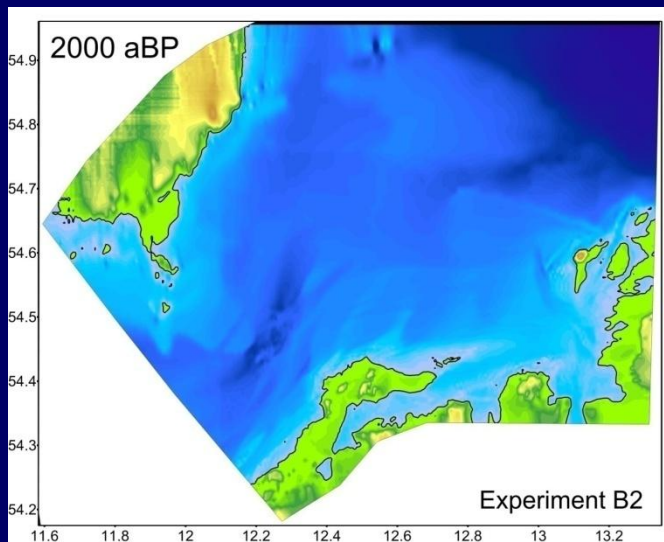
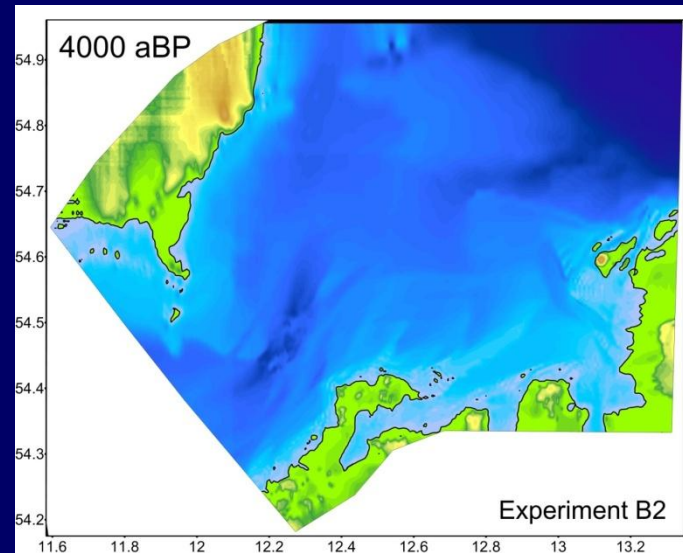
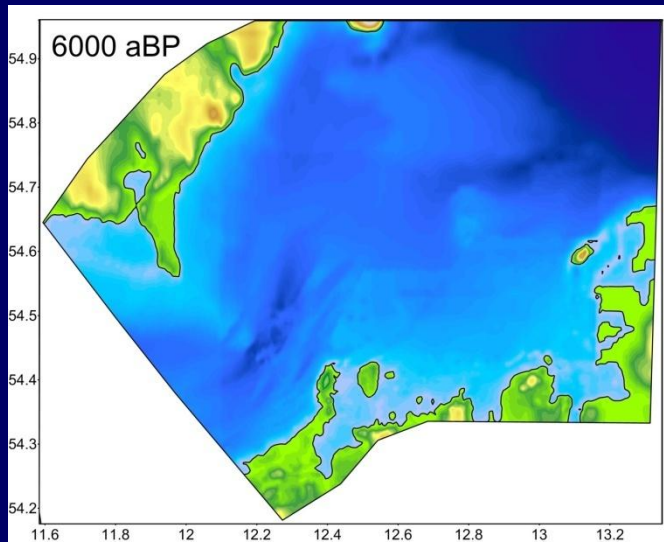


NCEP meteorological
reanalysis
1948 – 2005 AD

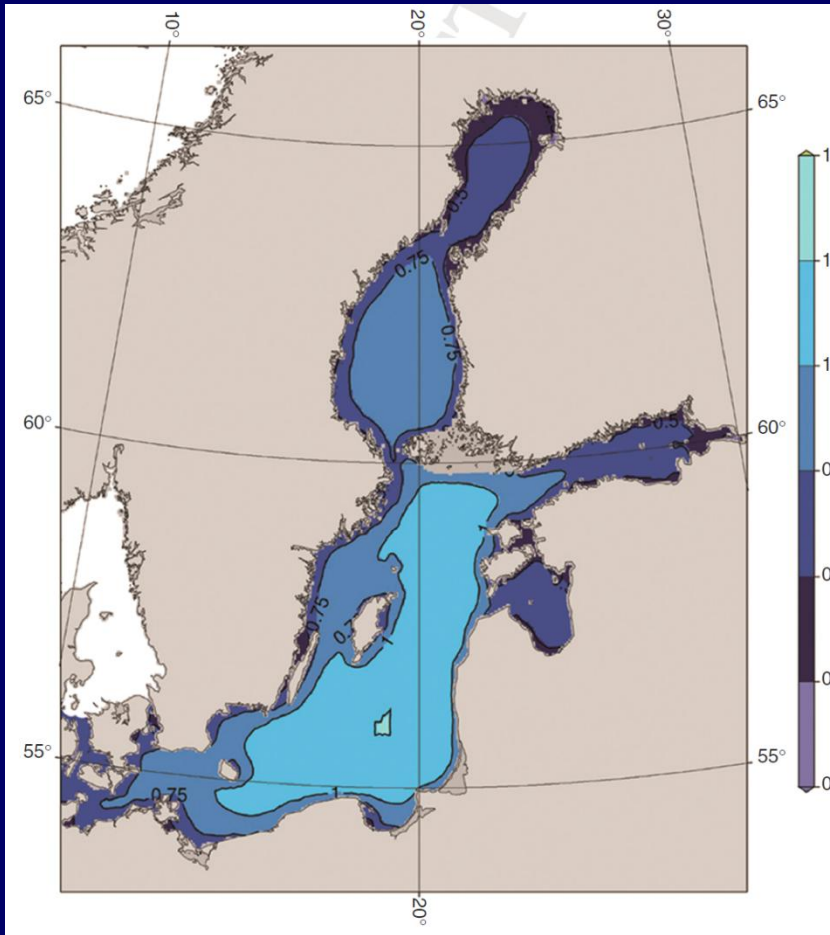
Darss-Zingst Peninsula: Topographic features



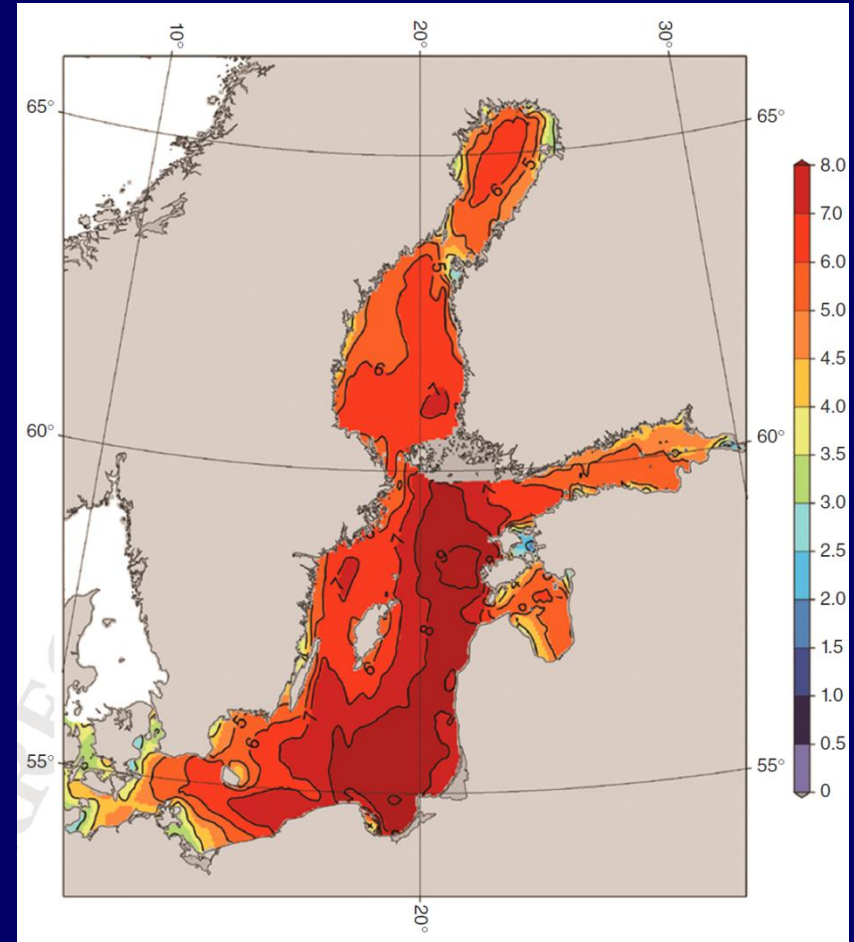
Model hindcast: 6000 aBP - present



Numerically simulated wave heights 2001 - 2007



Mean values (m)



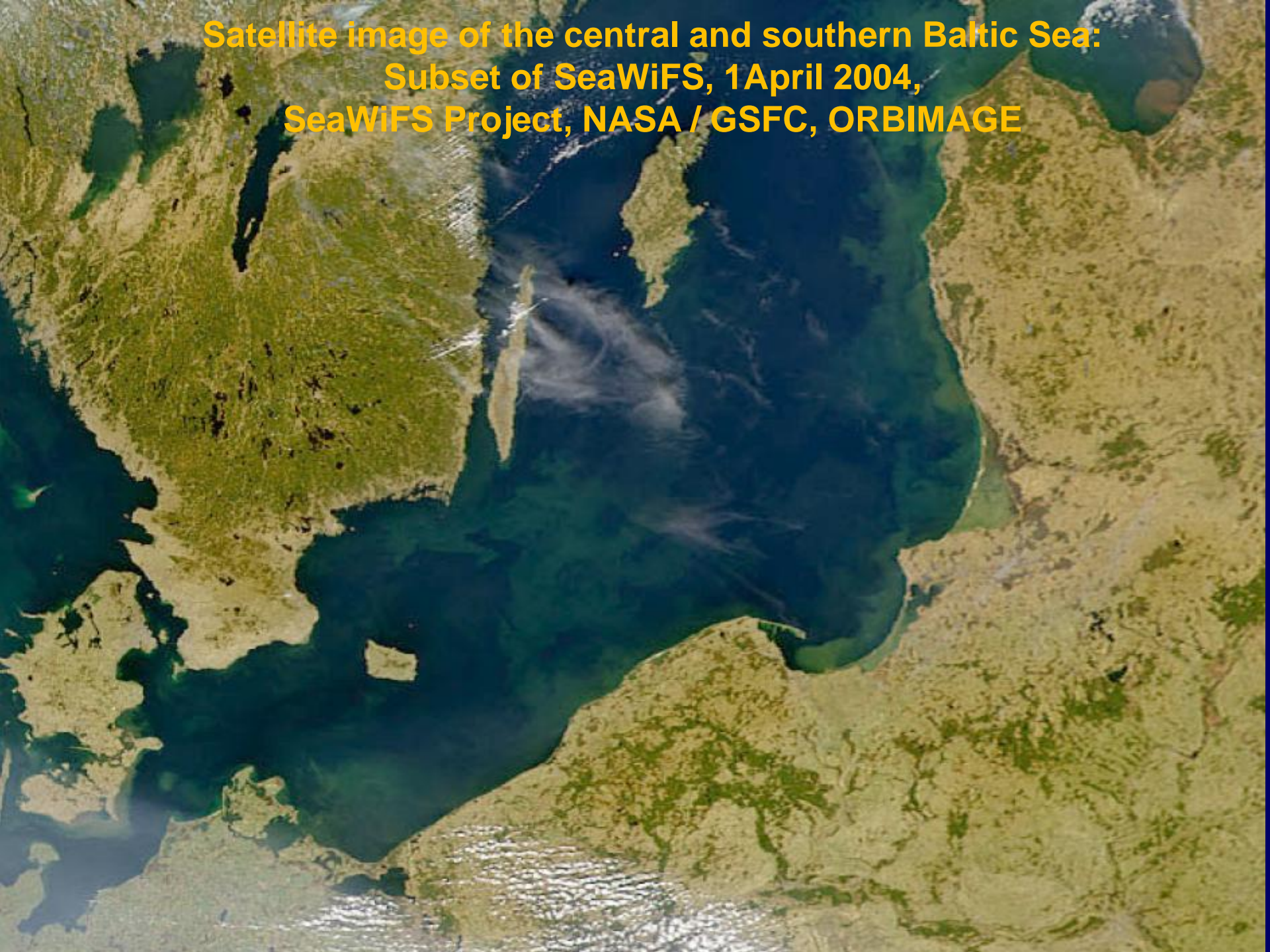
Extremes (m)


Long-shore sediment transport capacity Q [m³ /s] (CERC84 formula)

$$Q_{lst} = \frac{\rho K \sqrt{g / \lambda_b}}{16(\rho_s - \rho)(1 - p)} H_b^{2.5} \sin(2\Theta_b)$$

Q_{lst}	Long-shore sediment transport rate (m ³ /s)
K	empirical coefficient
g	gravitational acceleration
ρ_s	density of sand
ρ	density of water
p	sediment porosity
λ_s	breaker index
H_b	wave breaking height
Θ_b	incident wave angle at breaking

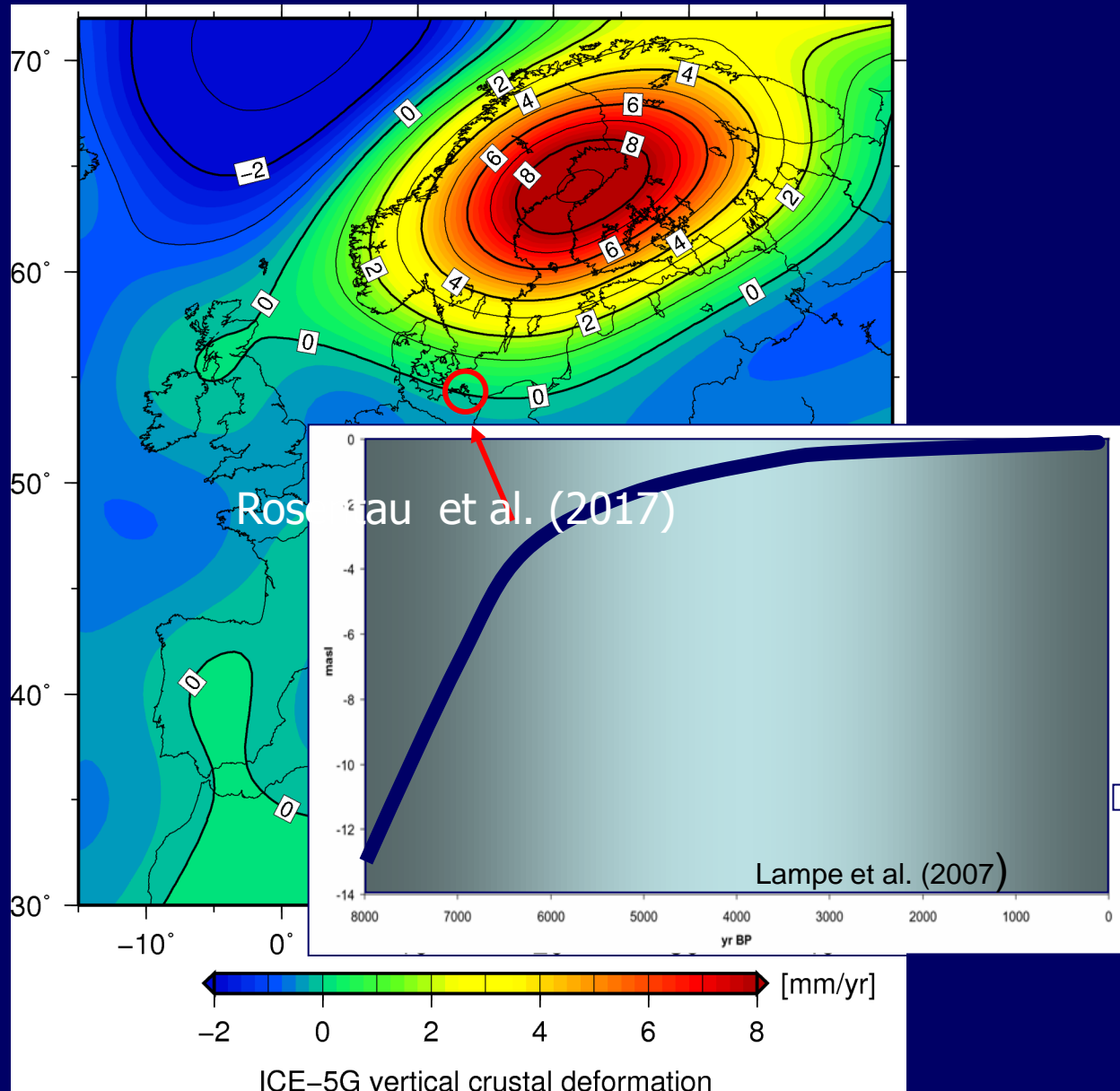
**Satellite image of the central and southern Baltic Sea:
Subset of SeaWiFS, 1 April 2004,
SeaWiFS Project, NASA / GSFC, ORBIMAGE**



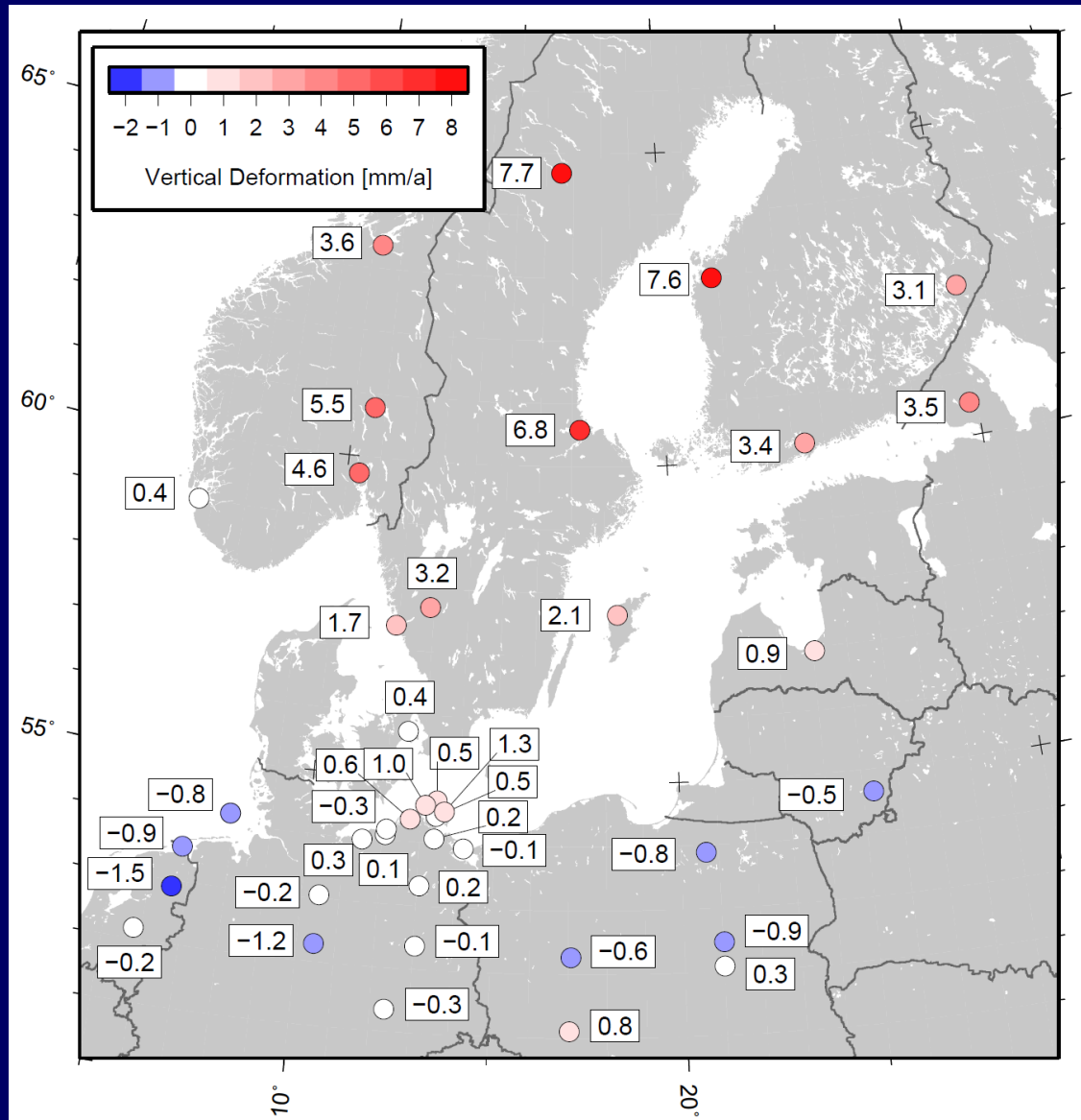


Future ?

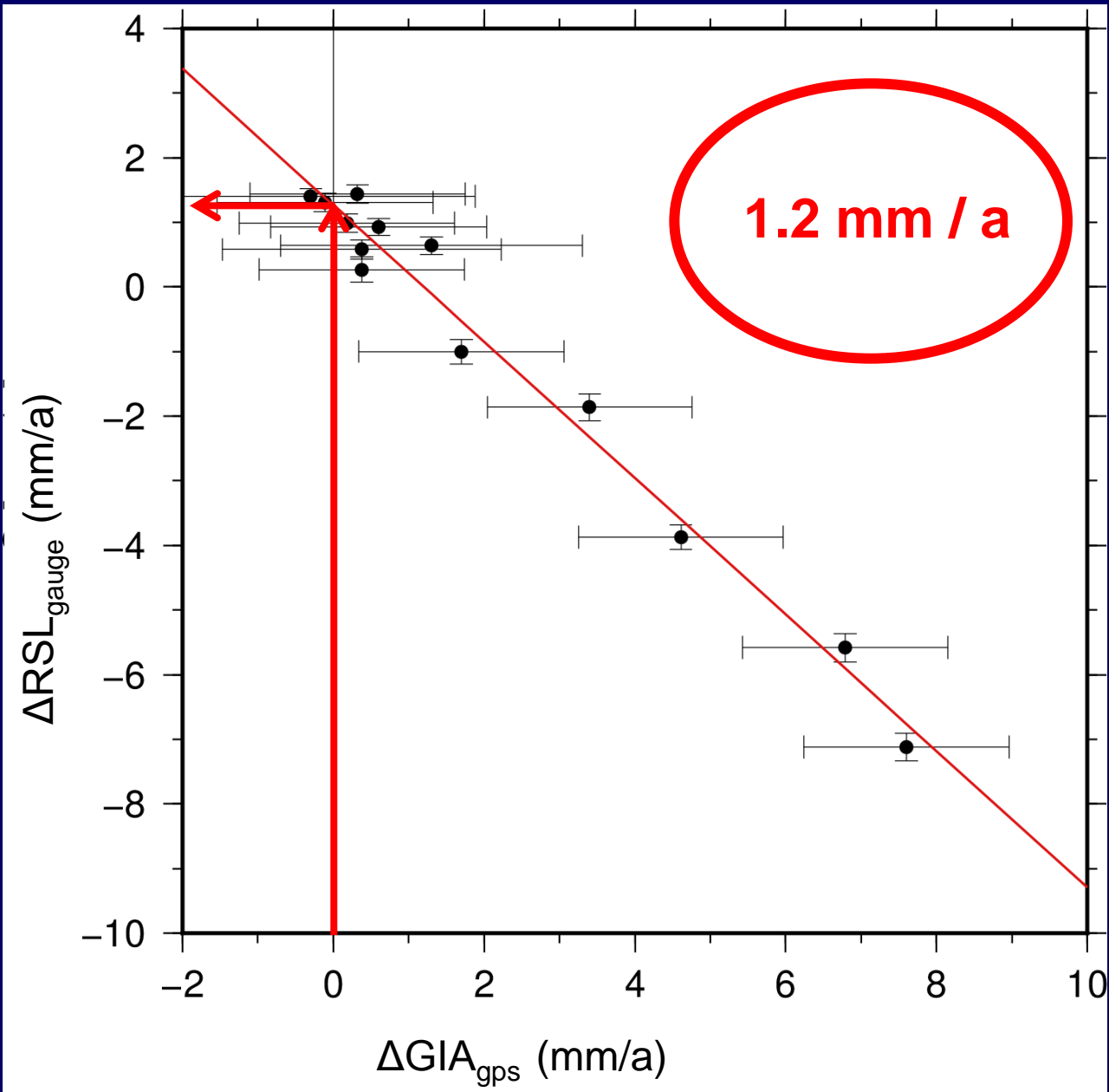
Relative sea level change in Europe



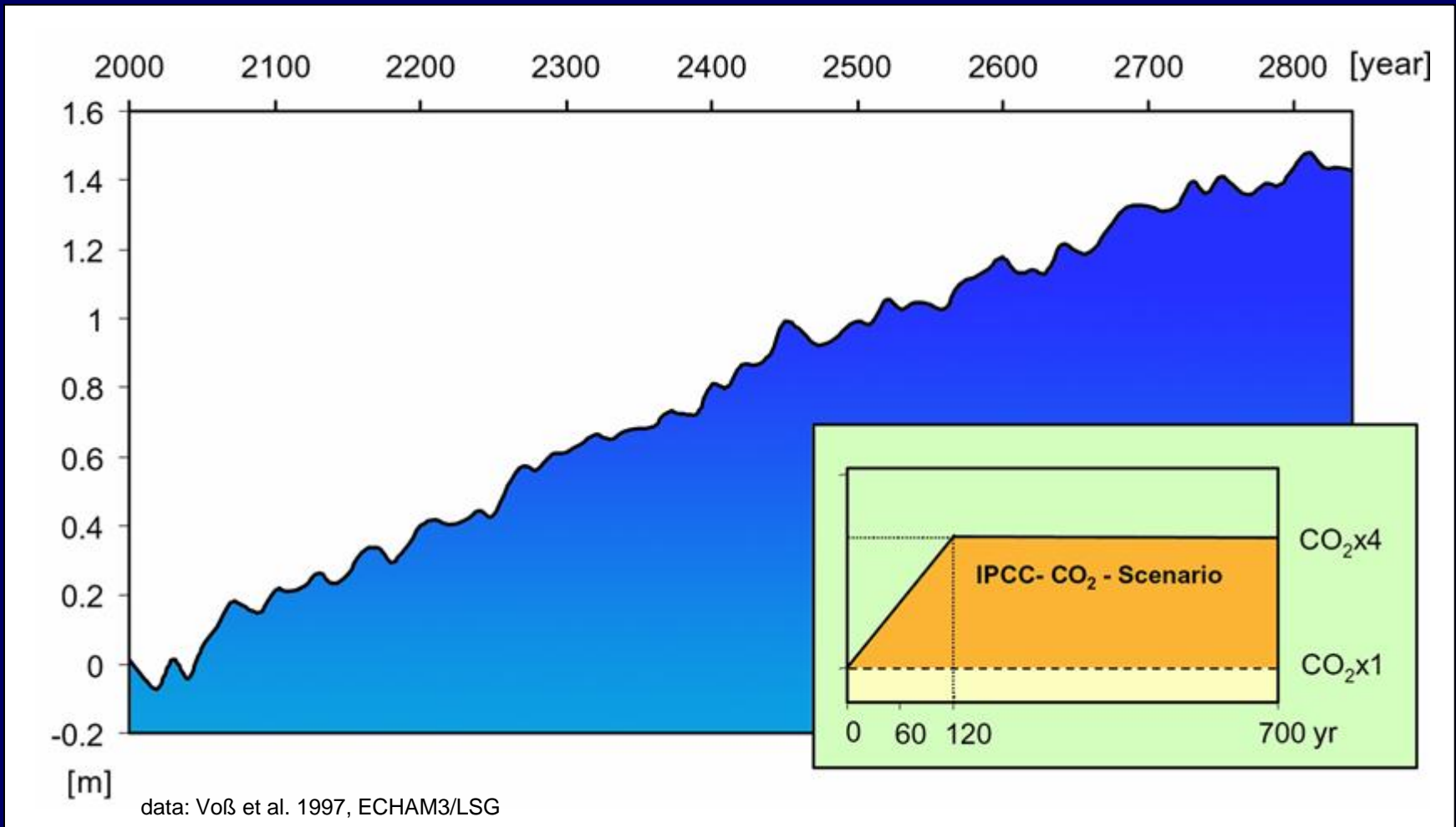
Vertical crustal deformation rates from the analysis of a regional GPS network (1994 – 2006)



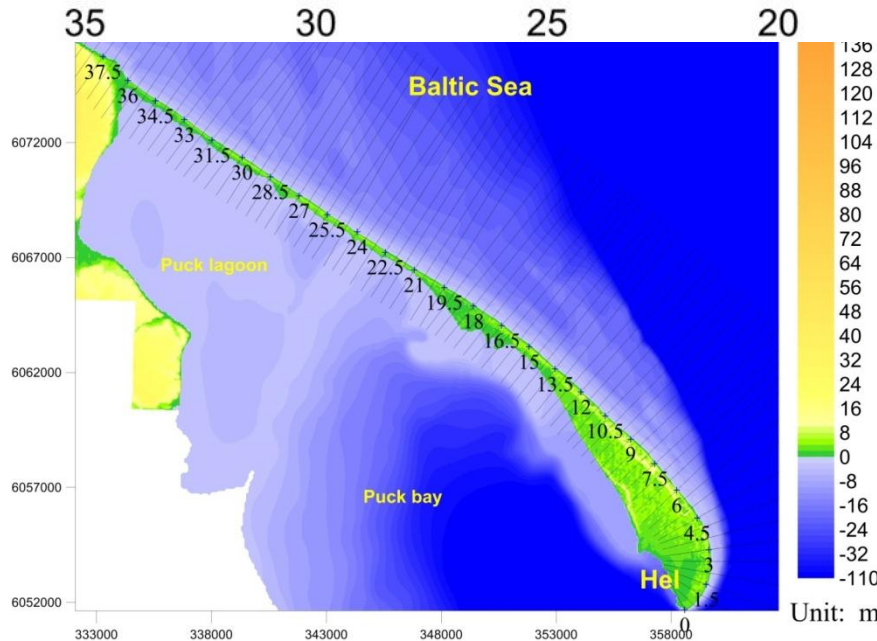
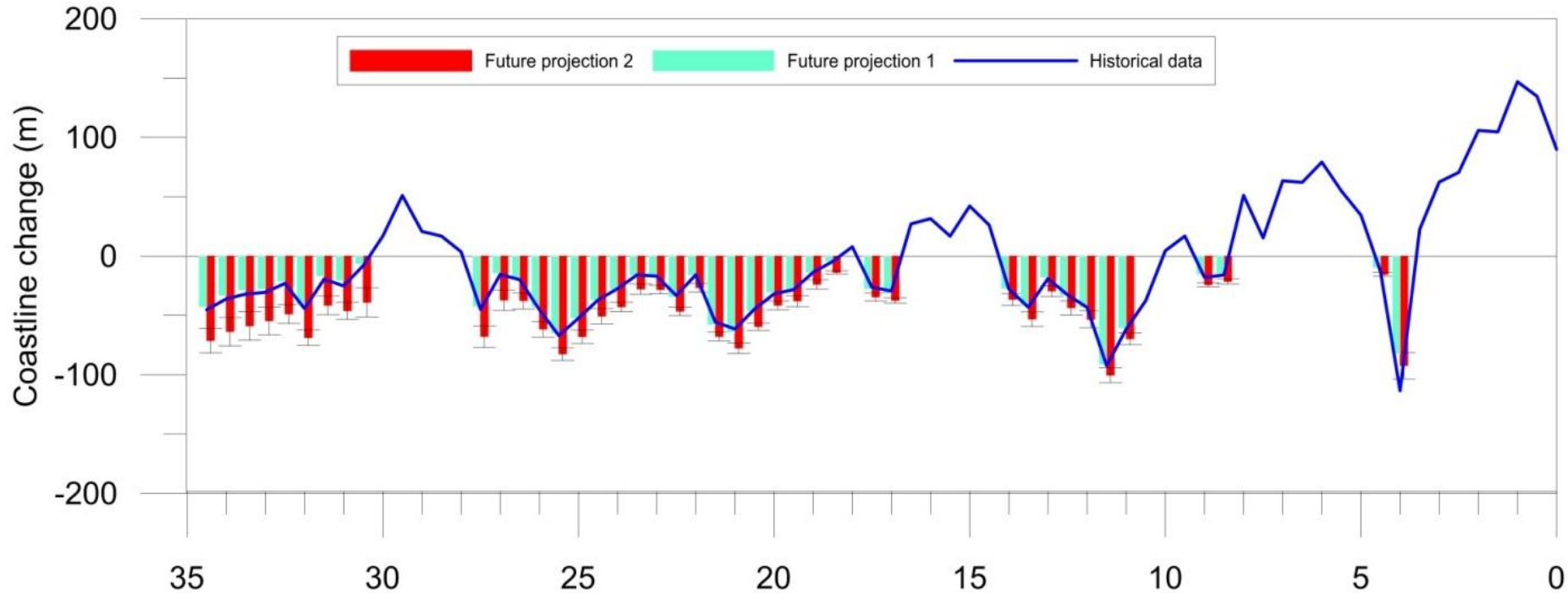
Vertical crustal deformation rates from GPS analysis versus relative sea-level change rates from tide gauge observations at 13 sites and mean eustatic change



Numerical modeling for future projection of Baltic eustatic sea-level change



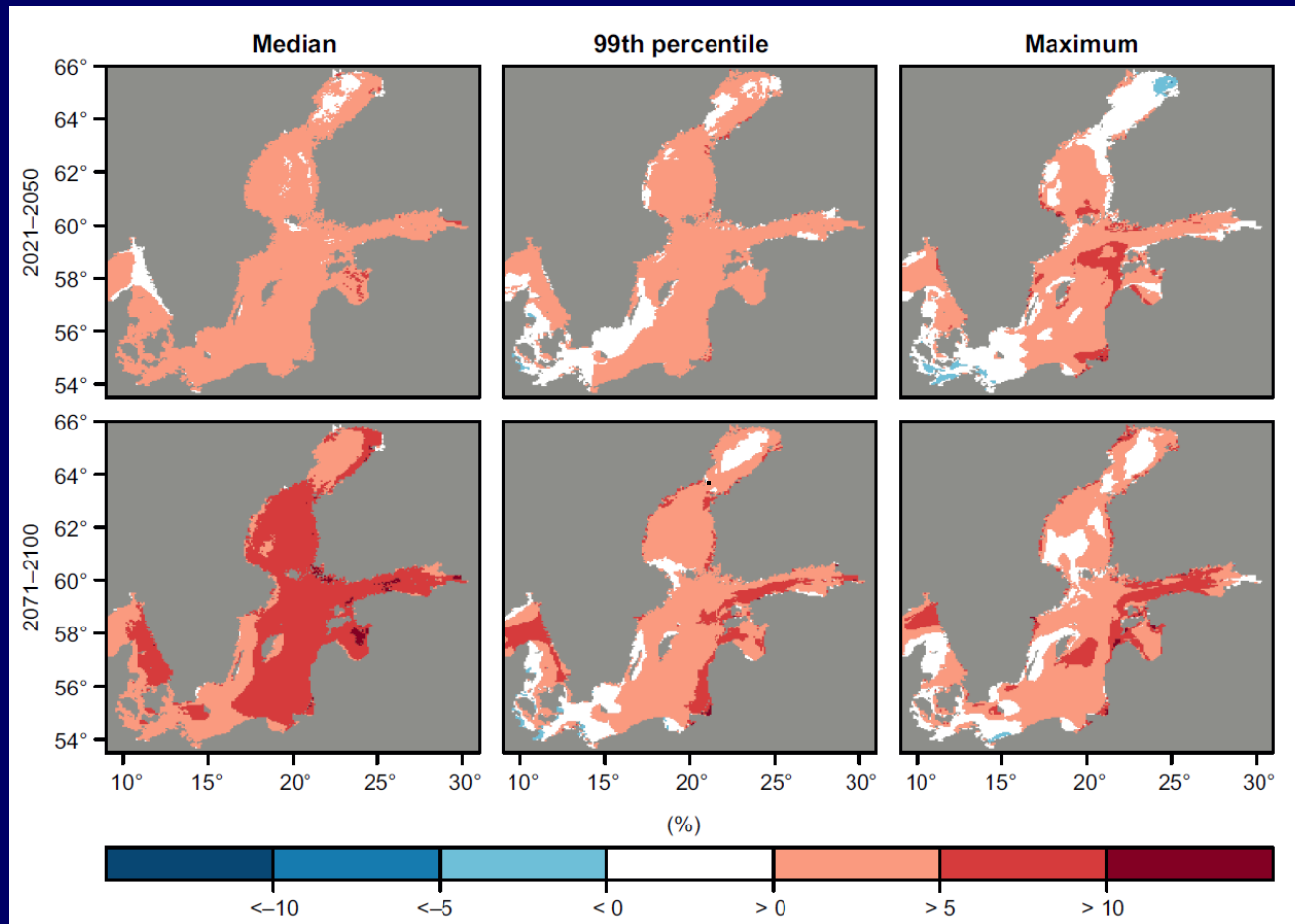
Future projection of coastline changes at Hel Peninsula 2000AD - 2100AD



Future projection 1:
eustatic sea-level rise of **1.2 mm/a**

Future projection 2:
eustatic sea-level rise of **2.4 mm/a**

Common changes in the four WAM realizations*) for 30-year means of annual median, 99th percentile and maximum significant wave height for the periods 2021–2050 and 2071–2100 relative to the period 1961–1990.

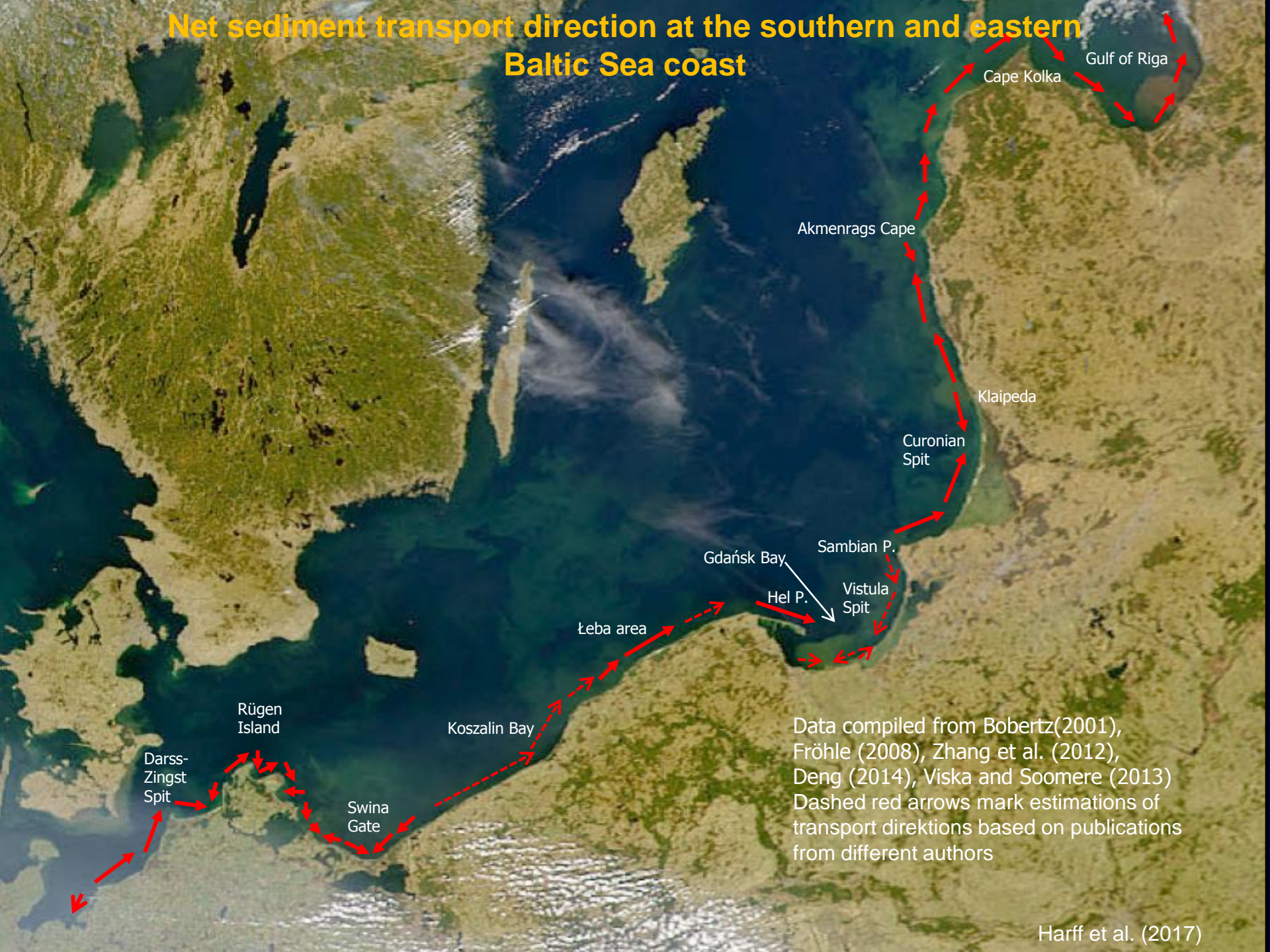


*) 3rd generation wave model WAM under two IPCC AR4 emission scenarios (A1B and B1) and two initial conditions of the forcing atmospheric fields

***) Colored areas indicate regions where all four realizations showed at least the same amount of relative change. White areas indicate regions where the four realizations did not show the same sign of change

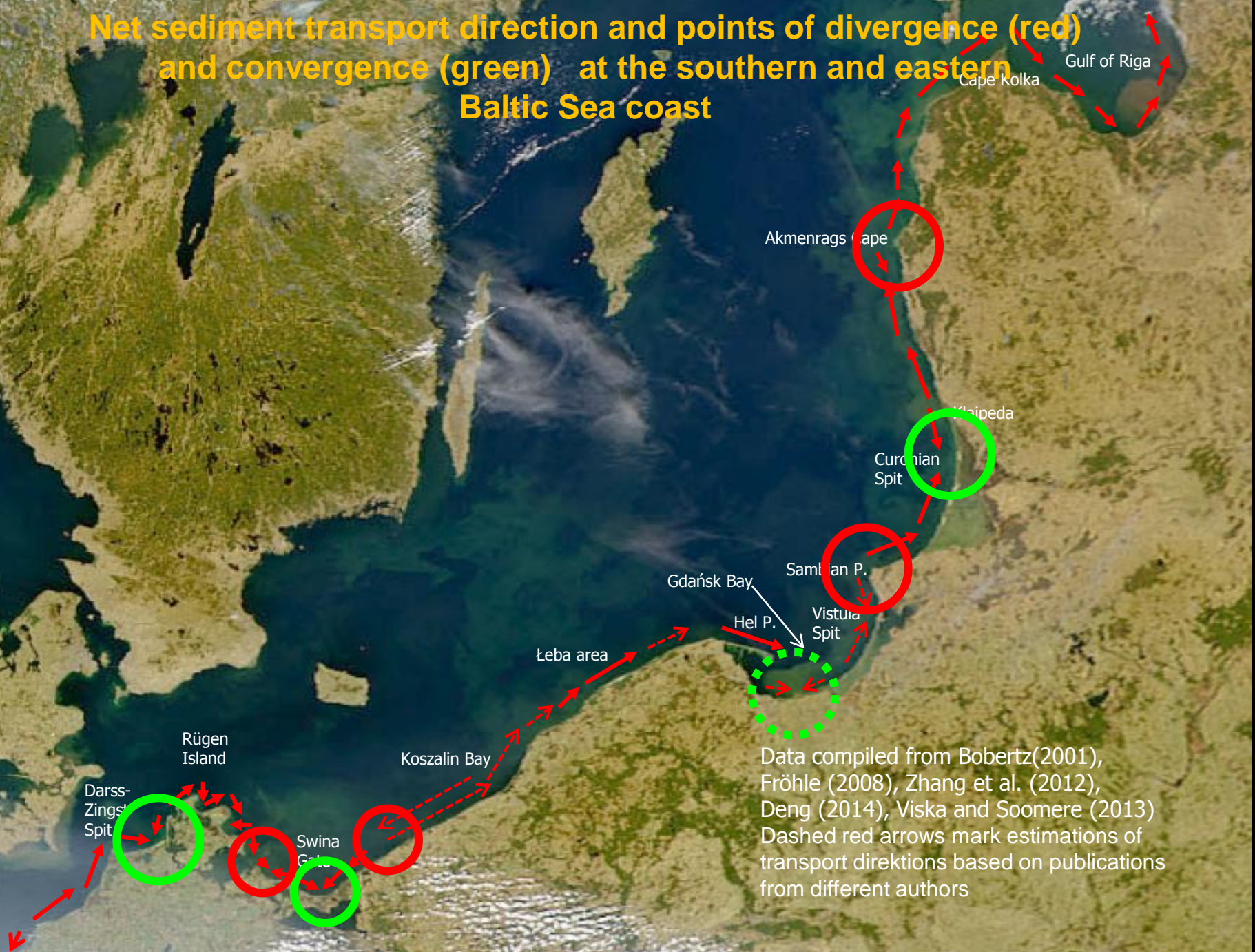
Groll et al. (2017)

Net sediment transport direction at the southern and eastern Baltic Sea coast



Data compiled from Bobertz(2001), Fröhle (2008), Zhang et al. (2012), Deng (2014), Viska and Soomere (2013)
Dashed red arrows mark estimations of transport direksions based on publications from different authors

Net sediment transport direction and points of divergence (red) and convergence (green) at the southern and eastern Baltic Sea coast



Data compiled from Bobertz(2001), Fröhle (2008), Zhang et al. (2012), Deng (2014), Viska and Soomere (2013)
Dashed red arrows mark estimations of transport direksions based on publications from different authors

Summary and conclusions

Driving forces of coastline changes act on different time- and spatial scales. The Baltic Sea coasts are subdivided into different entities shaped by special dynamics. At the Fennoscandian Shield GIA is compensating postglacial and modern eustatic rise and cause permanent regression of the sea. In southern an eastern Baltic after the Littorina transgression steric sea level rise together with wave dynamics shape the coast morphodynamically. Counterclockwise sediment transport dominates whereby marine and aeolian transport interact.

Sustainable coastal protection strategies have to reflect the regional environments. We need

- regional to local rsl-histories for neotectonic models
- integrated morphodynamic sediment models acting on different time scales
- regional (!) mass balance source-to-sink models
- regionalized future projections providing meteorological and hydrographical data.
- co-operation bridging between natural and engineering sciences
- environmental borders do not coincide with political borders. International co-operation between countries facing the same natural environment are indispensable for sustainable coastal management..

From small scales to large scales
–The Gulf of Finland Science Days 2017
9th-10th October 2017
Estonian Academy of Sciences, Tallinn

2nd Day



**Gulf of Finland
Co-operation**

K. Herkül, R. Aps

Spatial overlap of nature values, protected areas, and human uses in the Baltic Sea

Spatial overlap of nature values, protected areas, and human uses in the Baltic Sea



Coherent Linear Infrastructures
in Baltic Maritime Spatial Plans

Kristjan Herkül, Robert Aps
Estonian Marine Institute,
University of Tartu





Project's lifetime: March 2016 – February 2019

Total project budget: € 3 409 458;

European Regional Development Fund: € 2 674 451,50.

The overall objective of the Project: to increase transnational coherence of shipping routes and energy corridors in Maritime Spatial Plans (MSP) in the Baltic Sea Region (BSR). This prevents cross-border mismatches and secures transnational connectivity as well as efficient use of Baltic Sea space. Thereby Baltic LINES helps to develop the most appropriate framework conditions for Blue Growth activities (e.g. maritime transportation, offshore energy exploitation, coastal tourism etc.) for the coming 10-15 years increasing investors' security.

The main project activities include:

- Developing requirements for MSP in relation to the shipping and energy sector in BSR;
- Harmonizing BSR MSP data infrastructure for shipping routes and energy corridors, drafting guidelines for MSP data exchange and dissemination;
- Identifying and agreement on transnationally coherent planning of linear infrastructures;
- Providing recommendations for a formalized BSR agreement on transboundary consultations on linear infrastructure within the MSP process.

- **The extent and intensity of human uses of marine areas is increasing**
- **Conflicts between different interests for the space and marine resources and environmental sustainability**
- **Fishery, shipping, cables and pipelines, wind turbines, mineral extraction, tourism and recreation, nature conservation etc.**
- **EU legislation: Habitats Directive, Marine Strategy Framework Directive, Maritime Spatial Planning Framework Directive**
- **National legislation: maritime planning, protected areas**



Spatial overlap of seabed nature values, protected areas (PAs), shipping, fishing effort and cables and pipelines in the Baltic Sea

- Nature values vs PAs
- Cables, pipelines vs PAs
- Shipping vs PAs
- Fishing vs PAs
- Nature values vs cables, pipelines
- Shipping vs cables, pipelines
- Fishing vs cables, pipelines
- Shipping vs nature values
- Fishing vs nature values

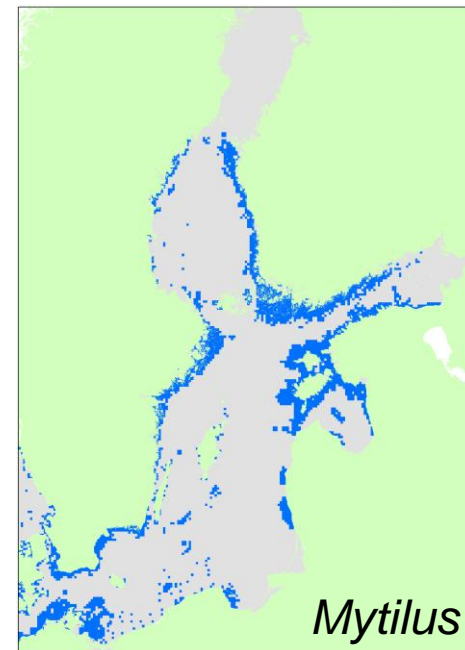
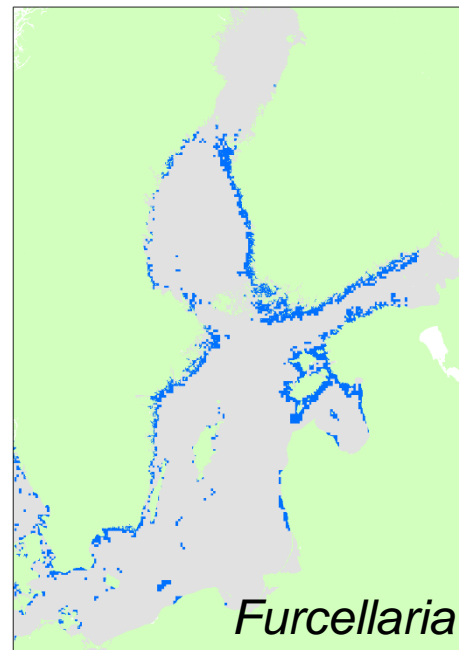
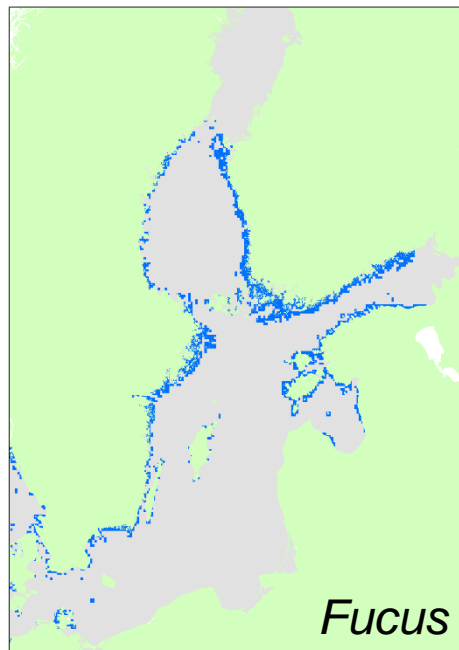
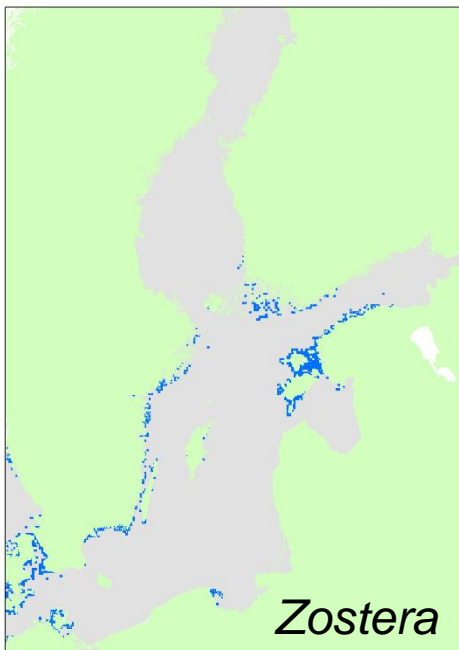
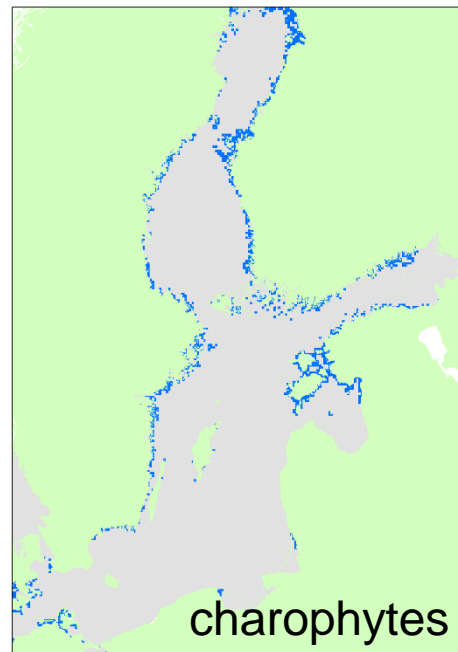
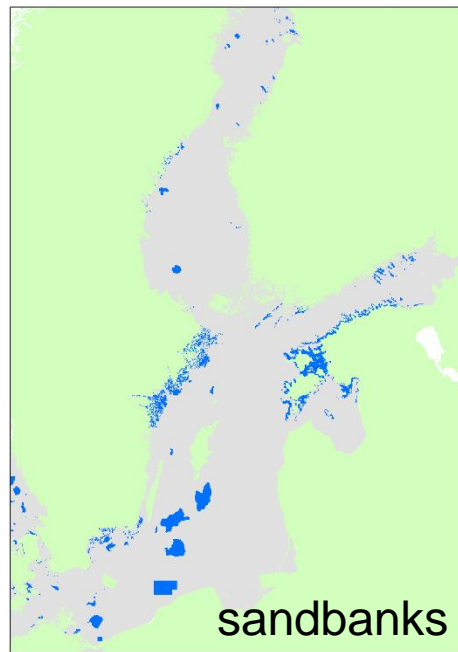
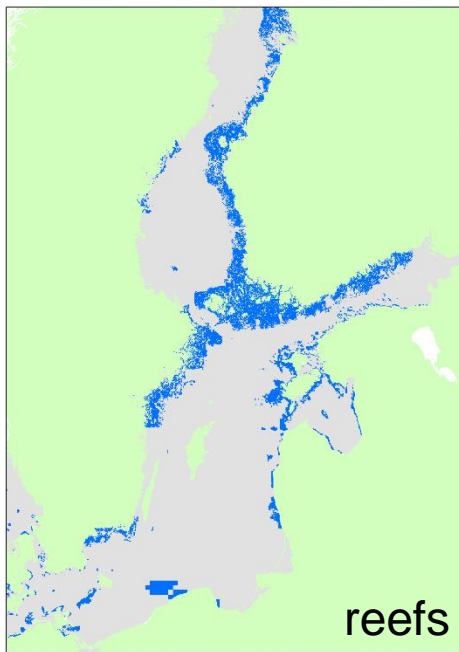


HELCOM map and data service <http://maps.helcom.fi/website/mapservice>

Nature values

- Habitats Directive habitats:
 - reefs (1170)
 - sandbanks (1110)
- Benthic key species/groups:
 - charophytes
 - *Zostera marina*
 - *Fucus vesiculosus*
 - *Furcellaria lumbricalis*
 - *Mytilus trossulus*



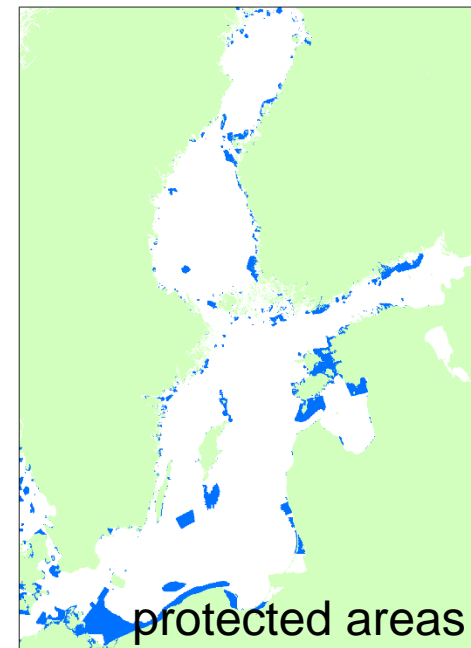
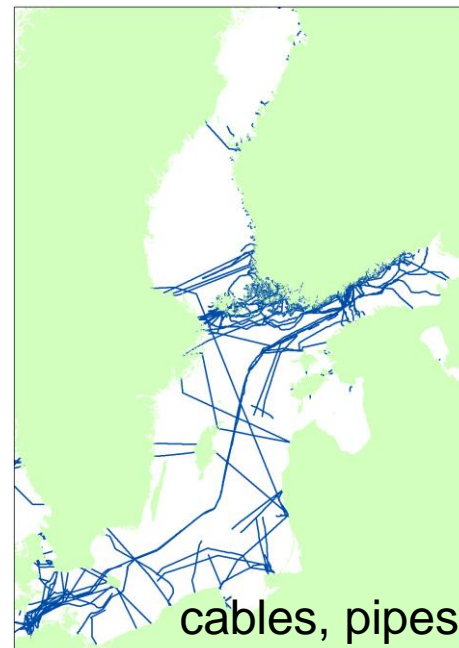
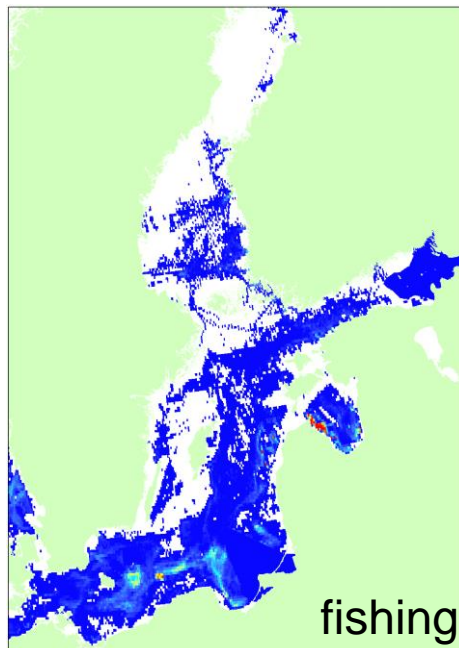
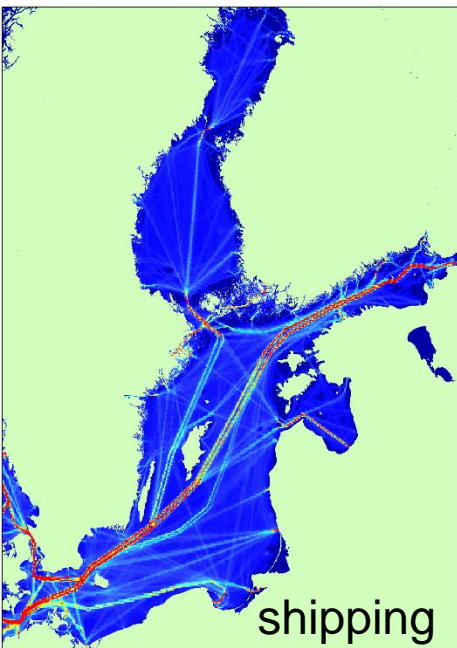
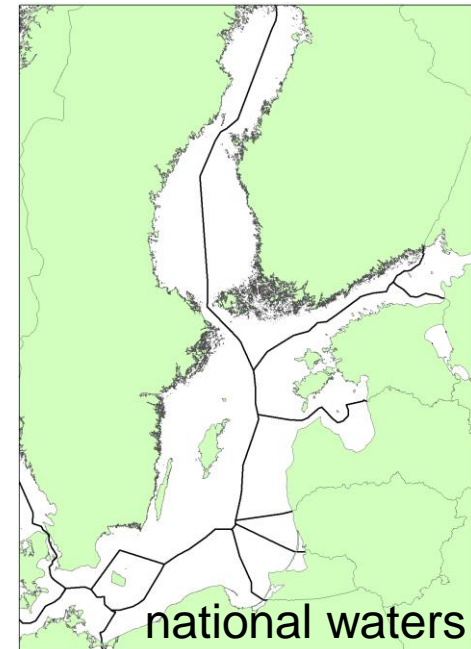


Human pressures

- Shipping (AIS density)
- Fishing (total effort of all gear types)
- Cables and pipelines

Protected areas

National waters (territorial + EEZ)*



Spatial resolution

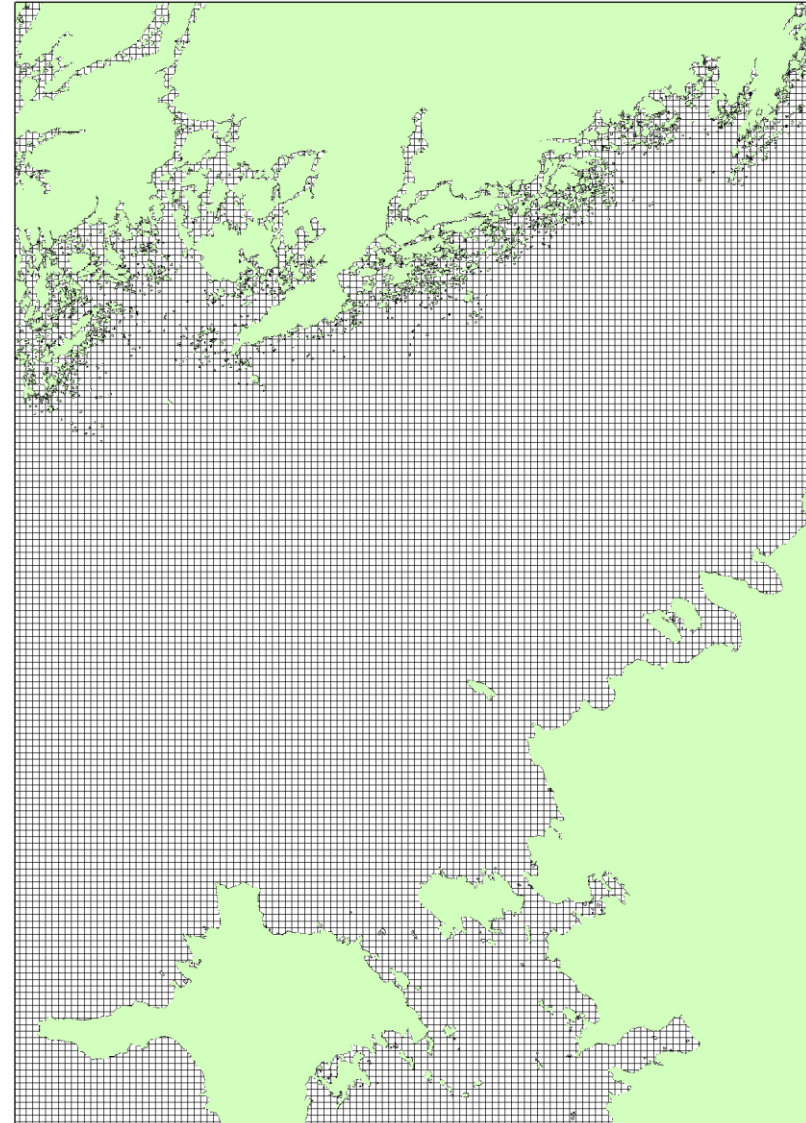
- 1 km EEA grid

Software

- ArcGIS
- R

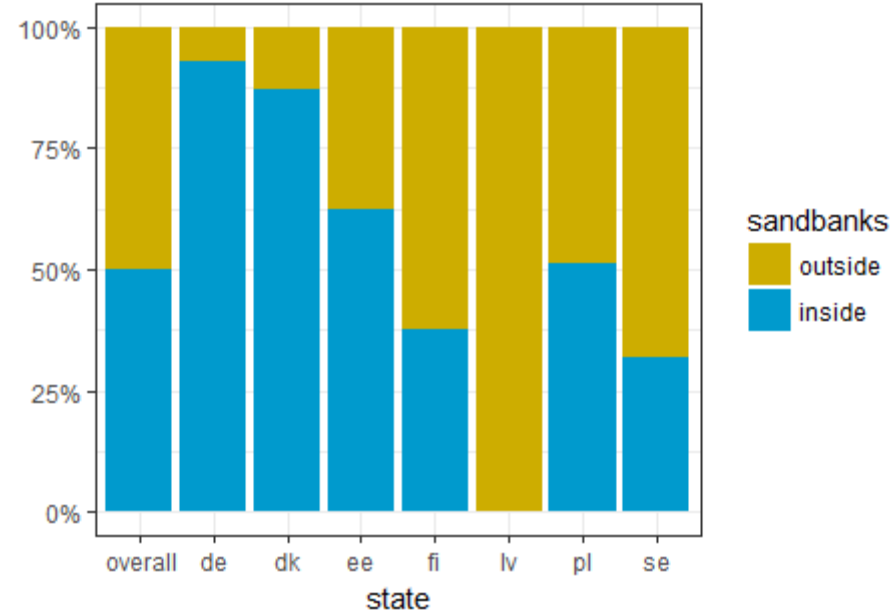
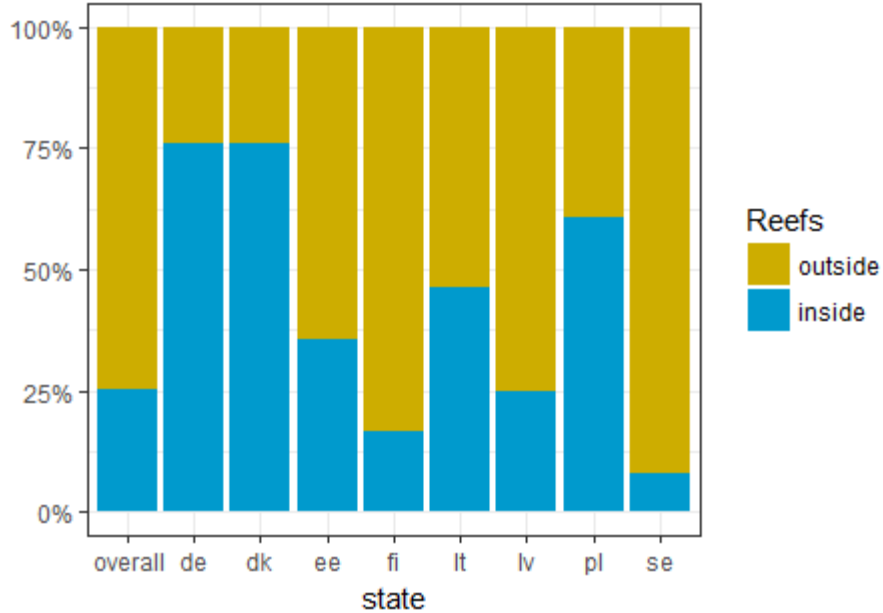
Spatial queries

- Presence/absence of nature values, PAs, cables and pipelines in each grid cell
- Mean AIS and fishing effort in each grid cell

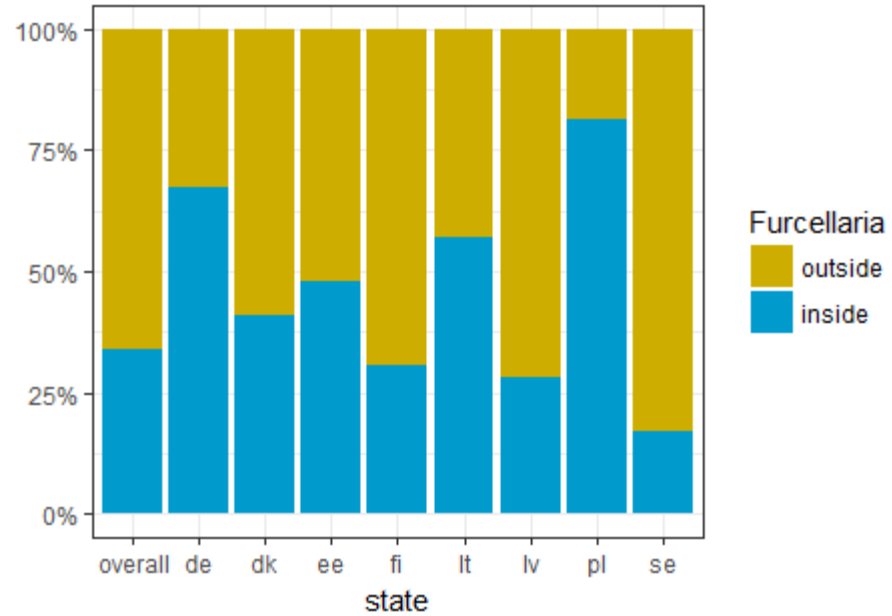
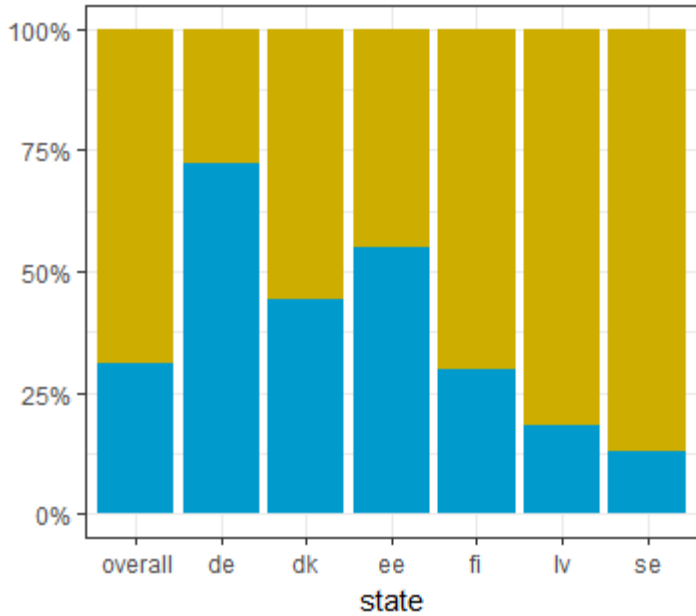
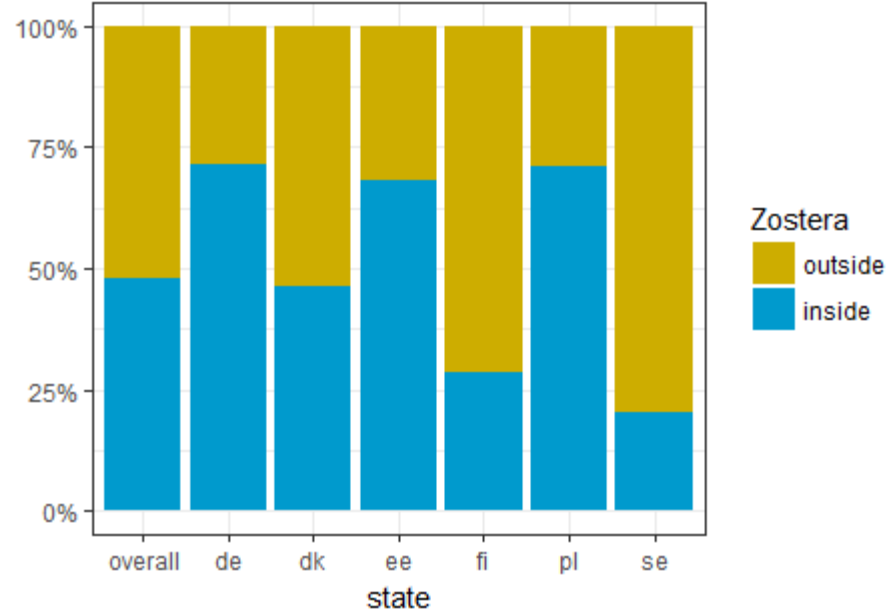
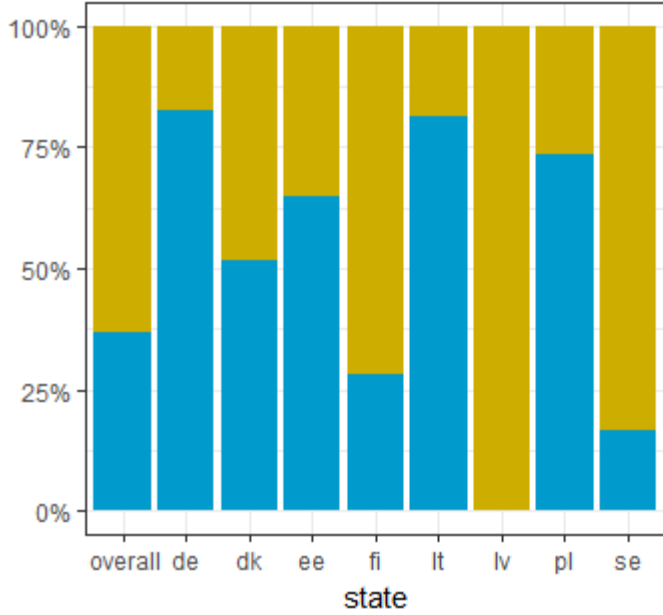


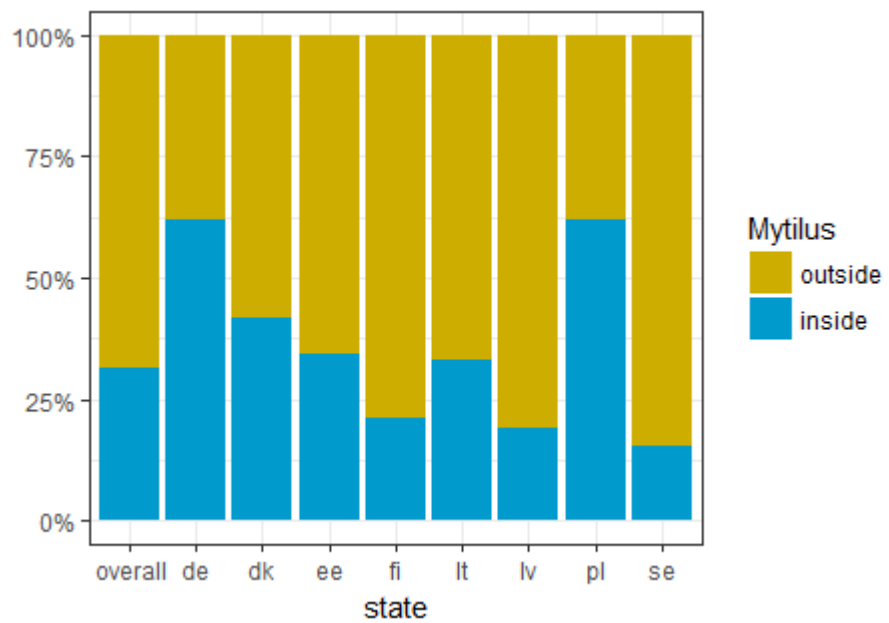
Overlap of nature values and PAs

Habitat Directive habitats



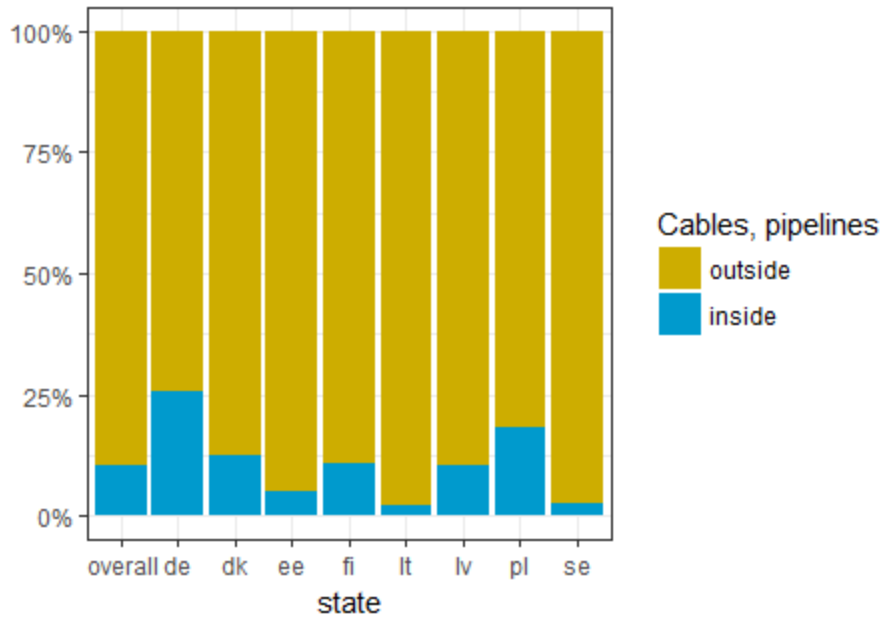
Benthic key species



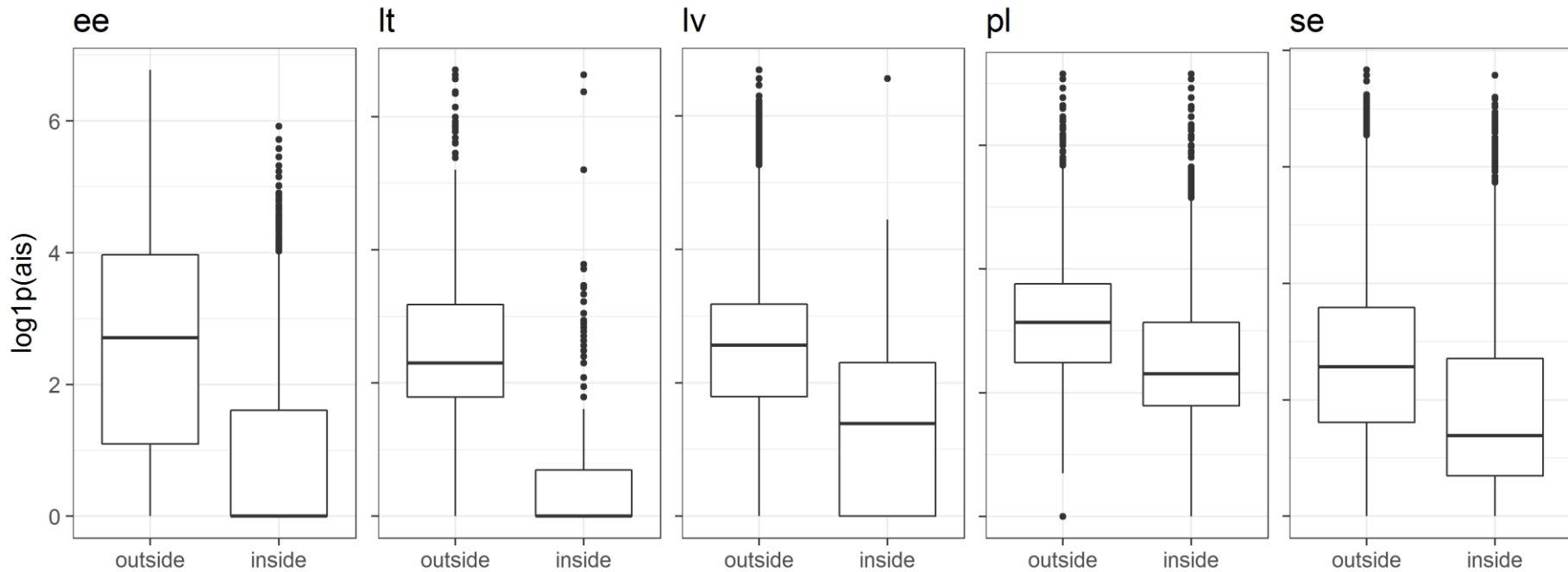
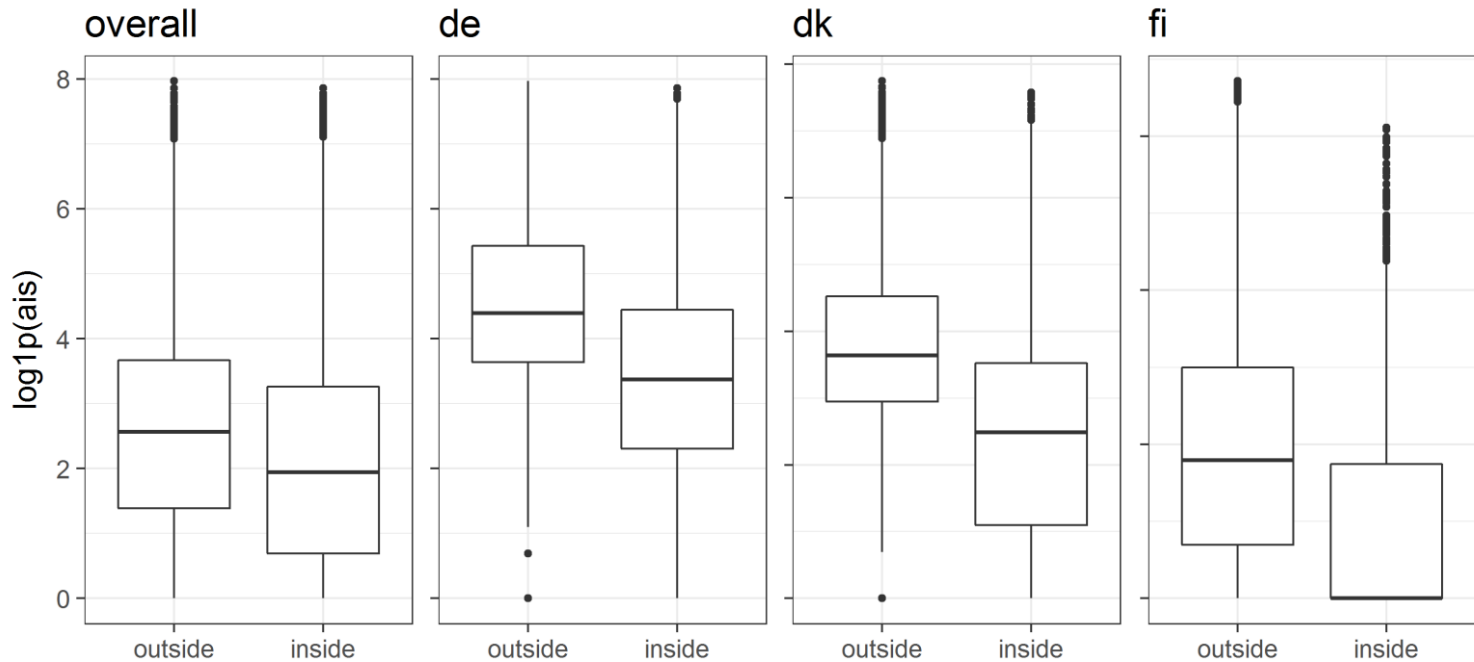


Overlap of cables-pipelines, shipping, fishing and PAs

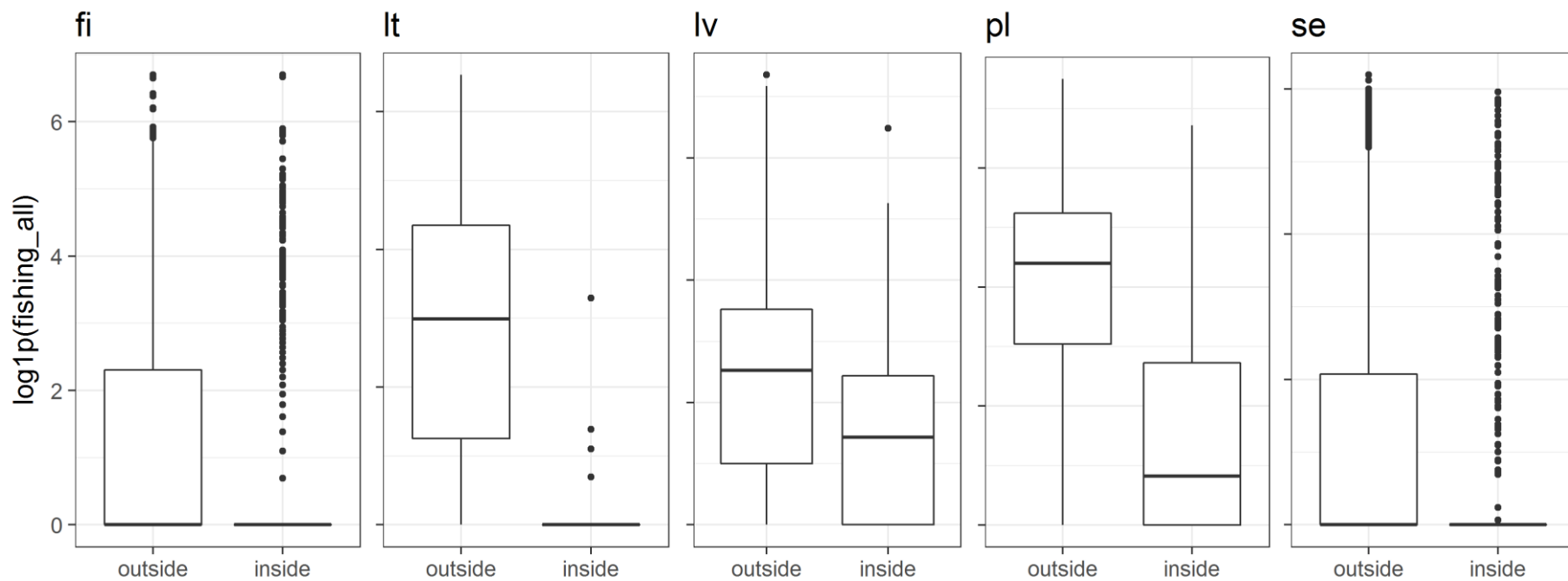
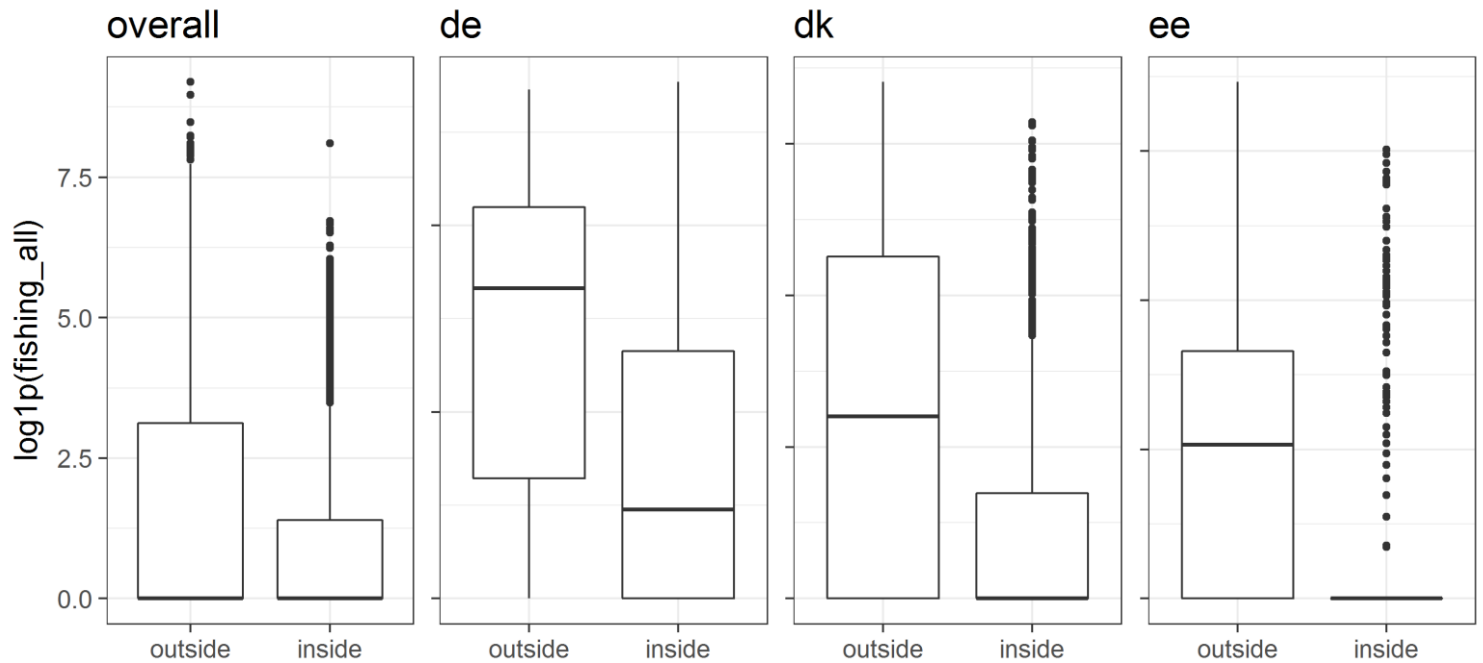
Cables, pipelines



Shipping

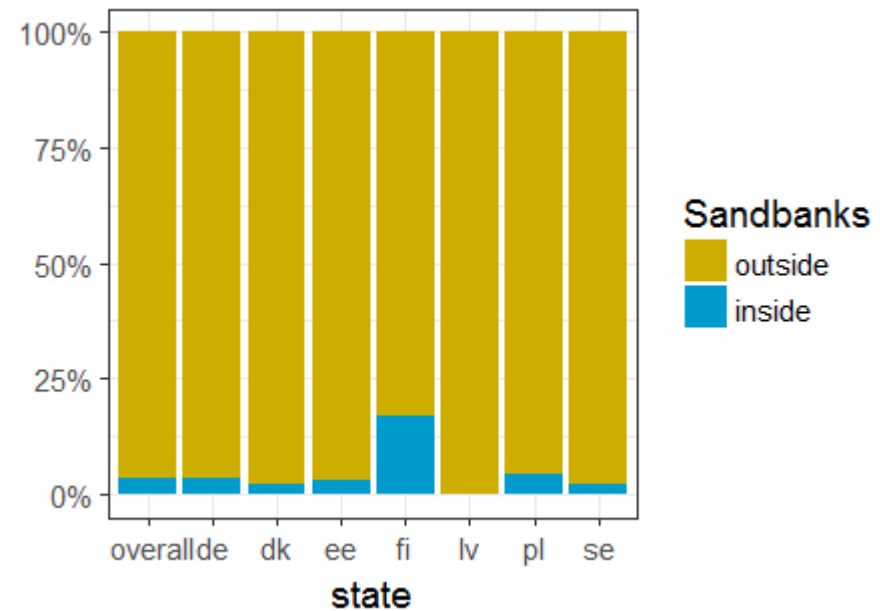
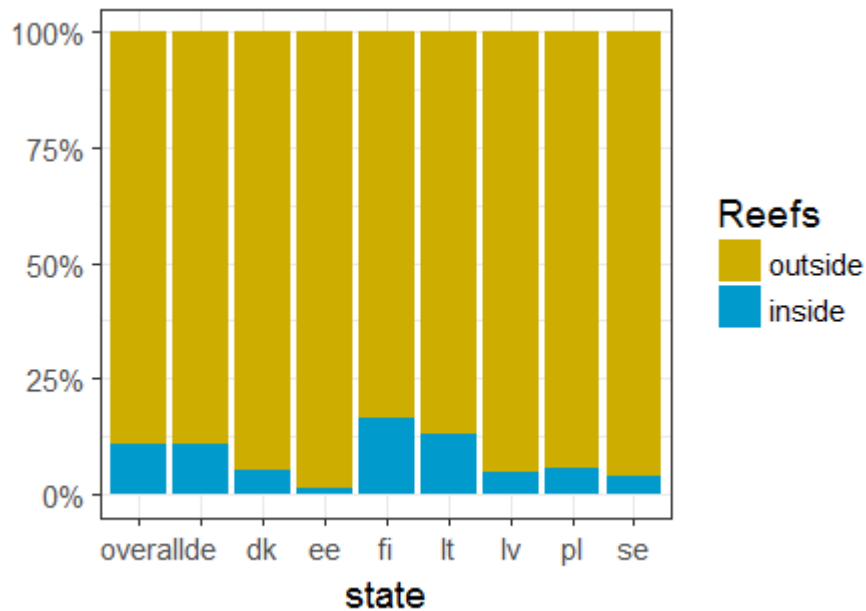


Fishing

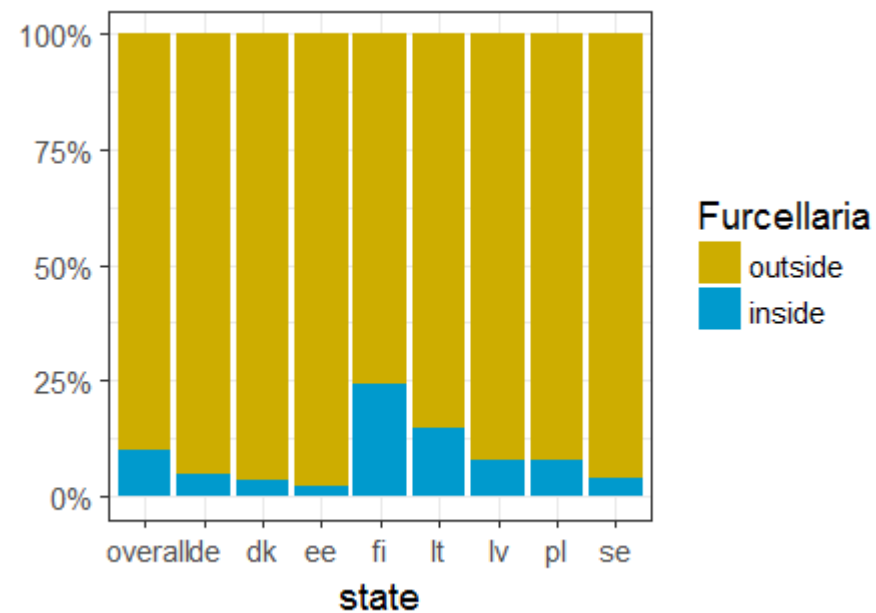
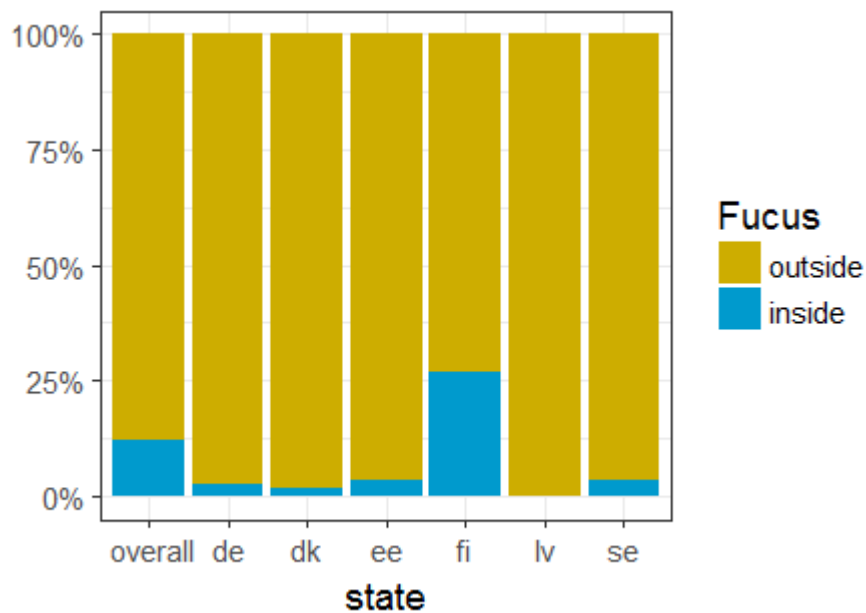
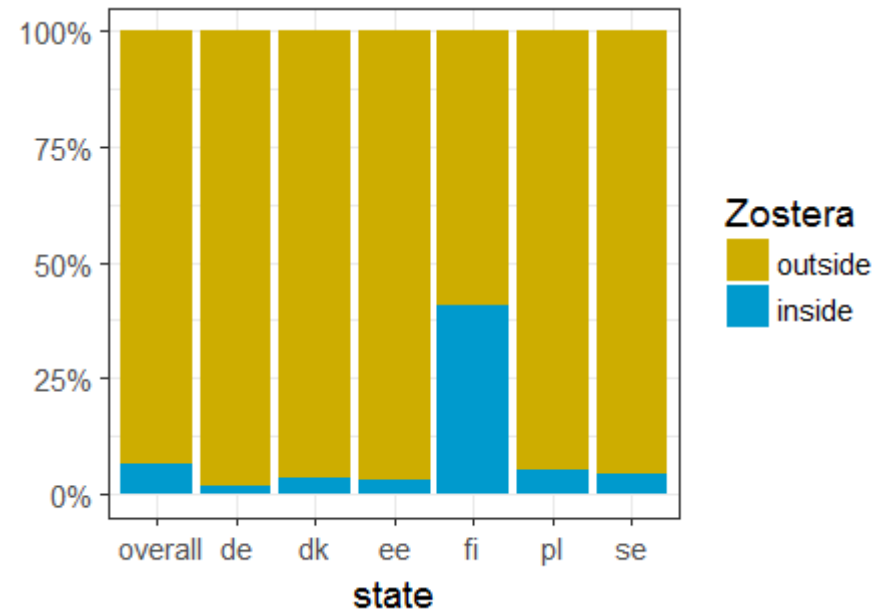
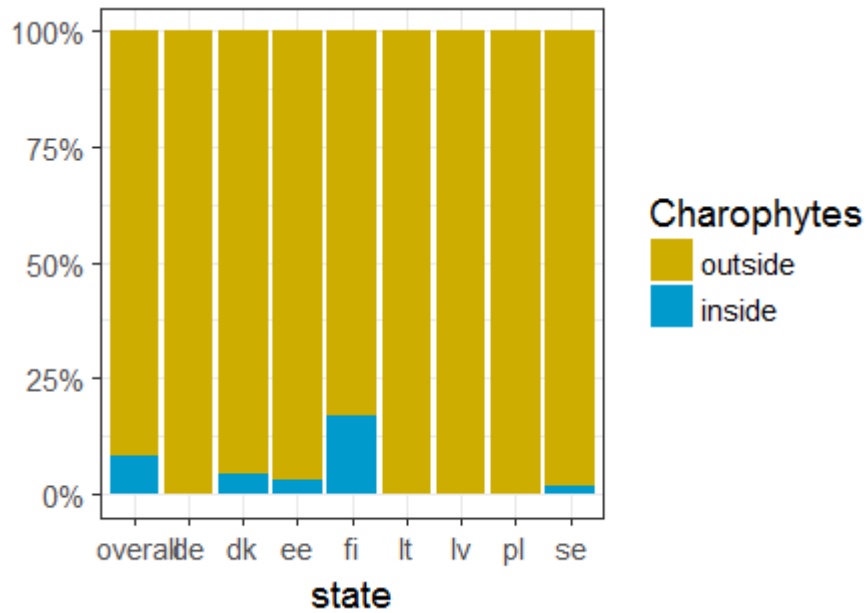


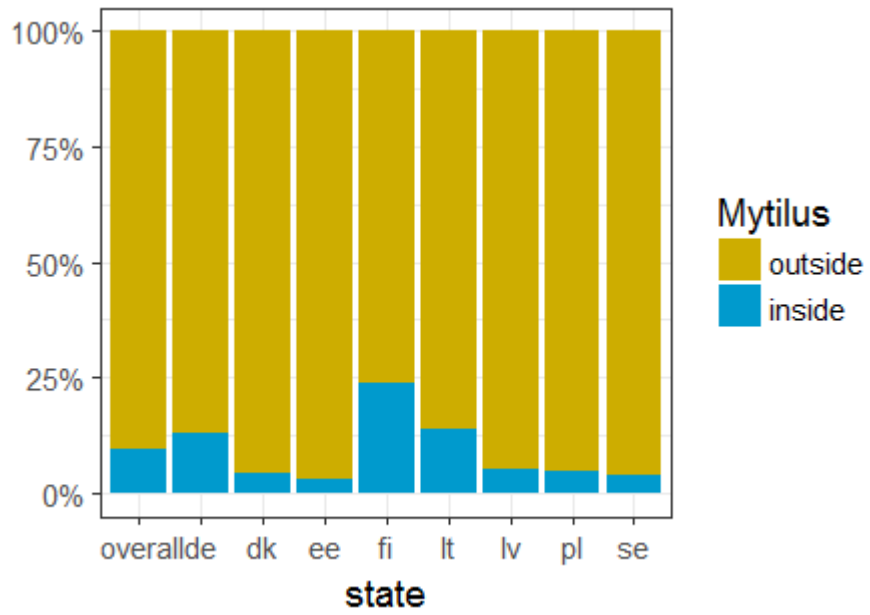
Overlap of nature values and cables-pipelines

Overlap of Habitat Directive habitats and cables-pipelines

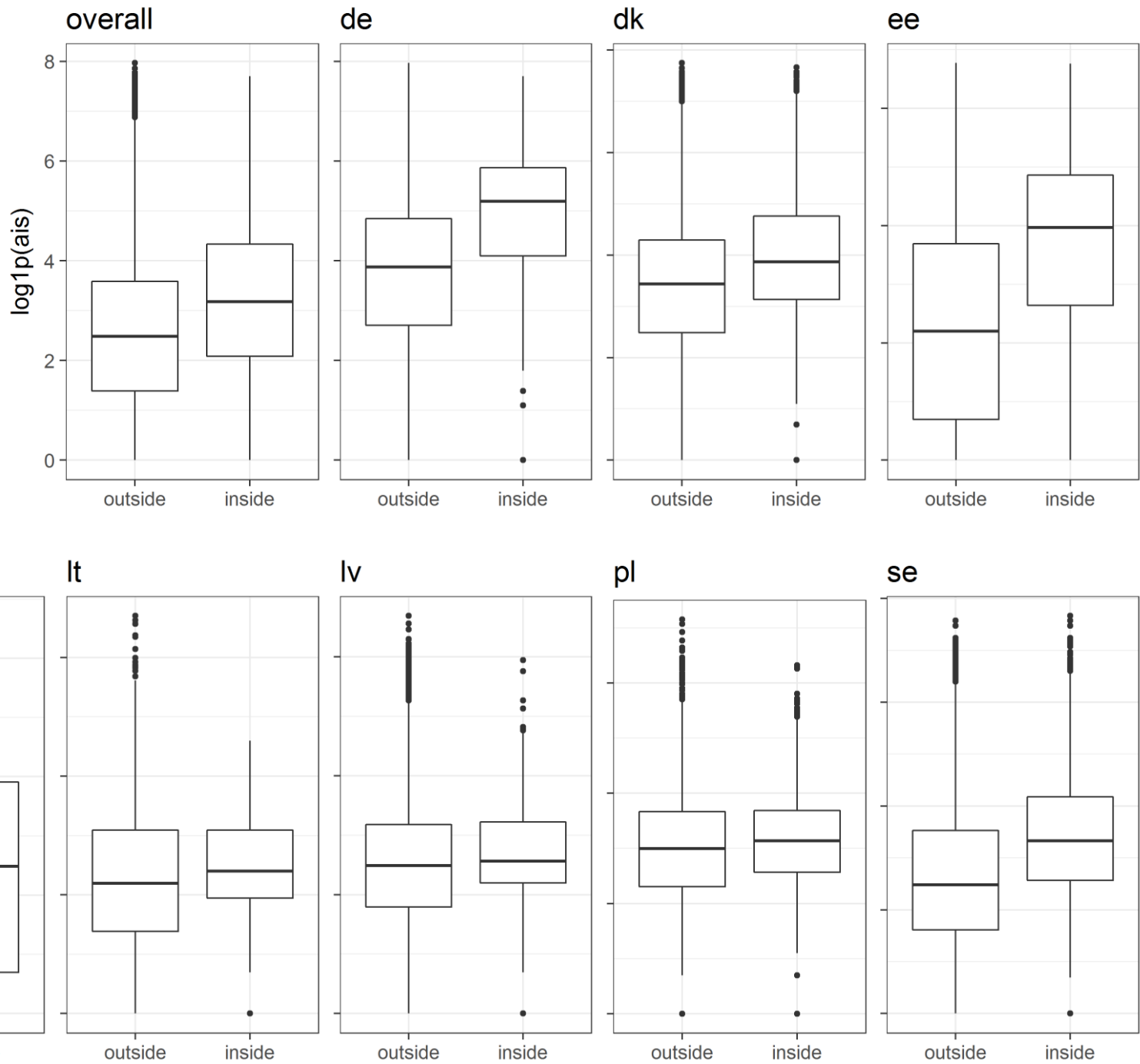


Overlap of benthic key species and cables-pipelines

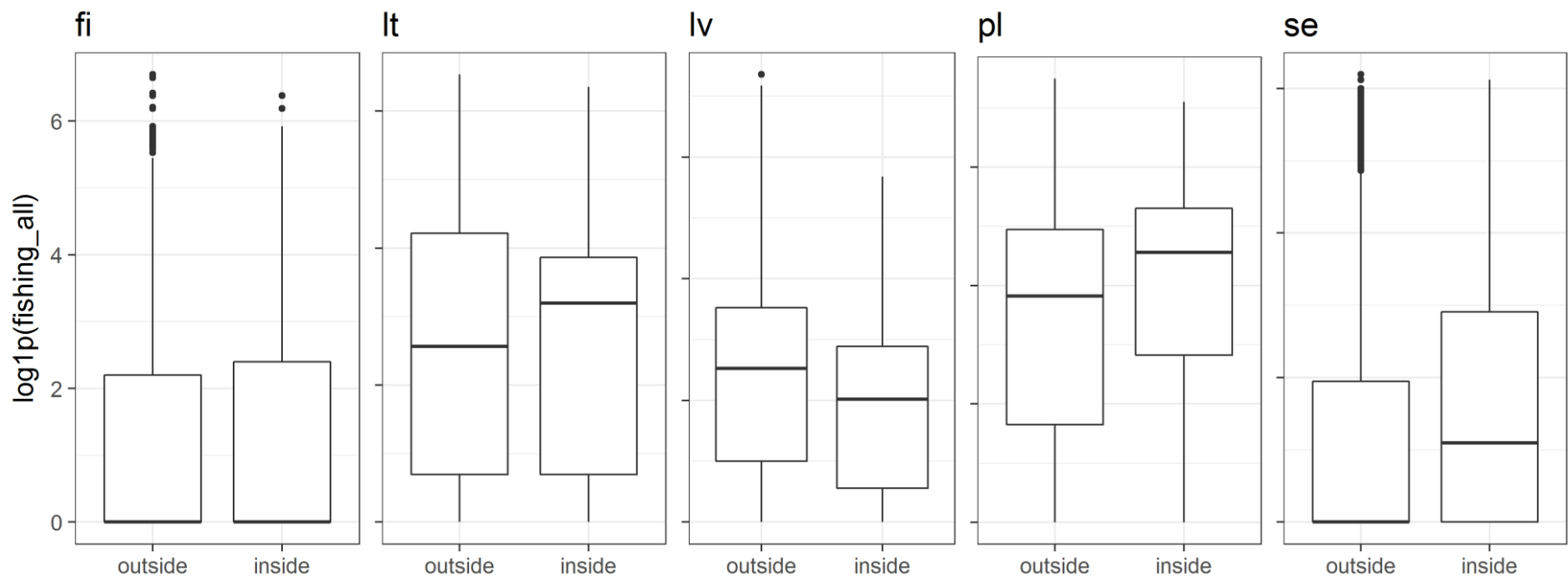
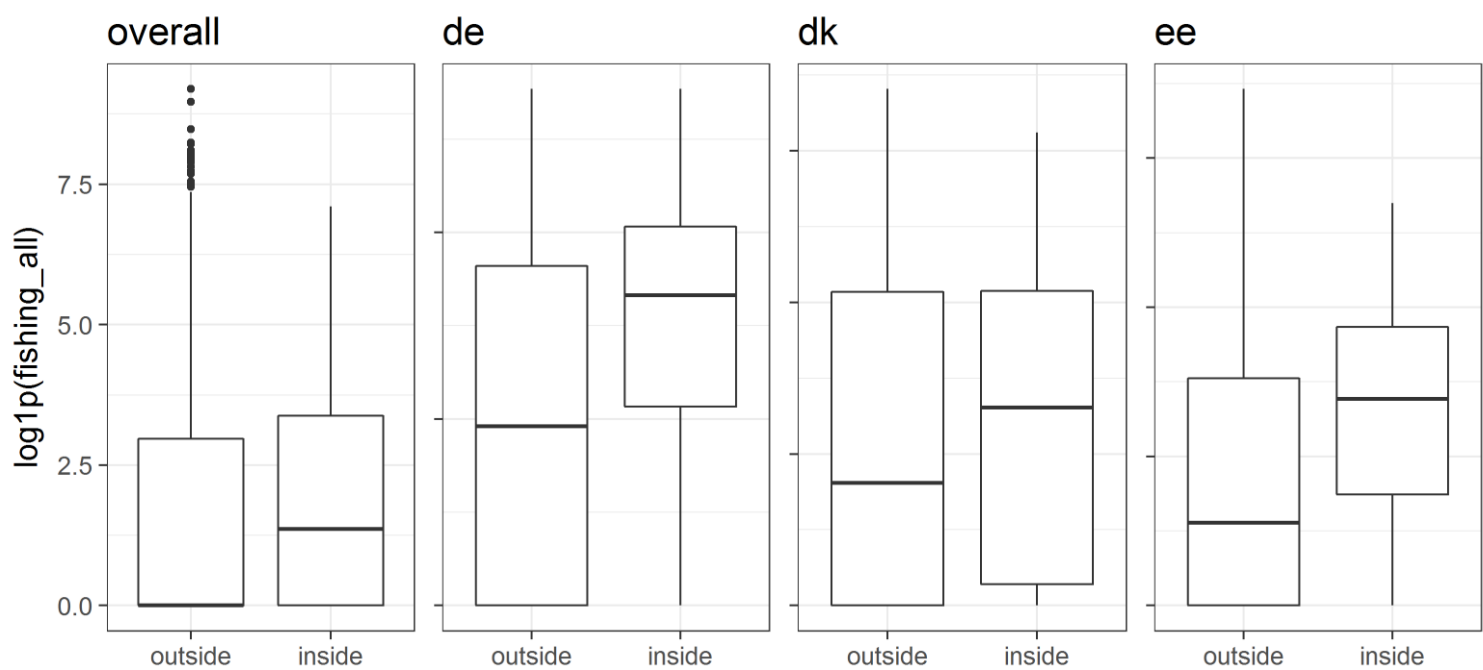




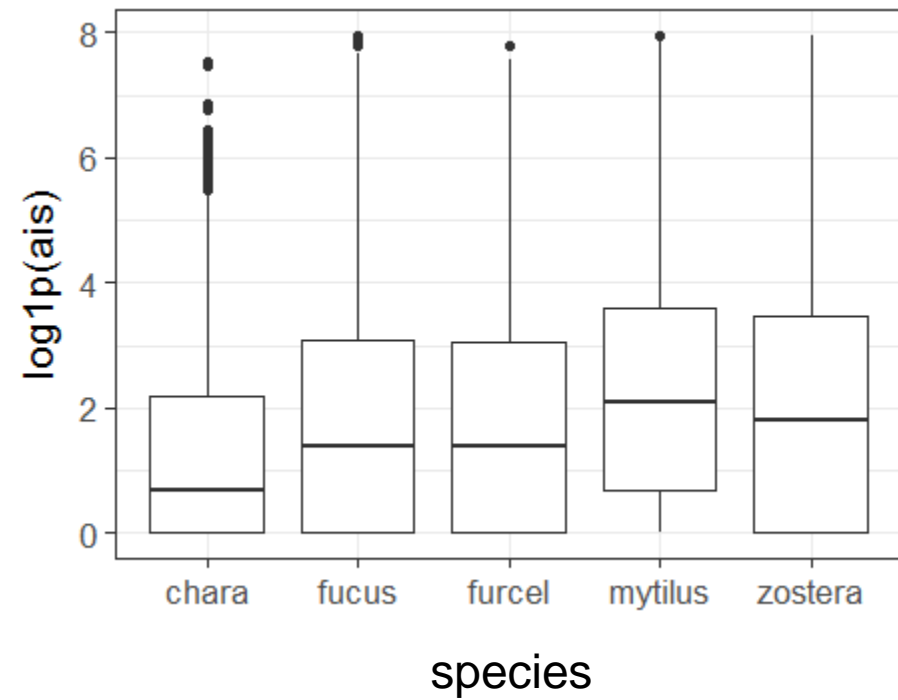
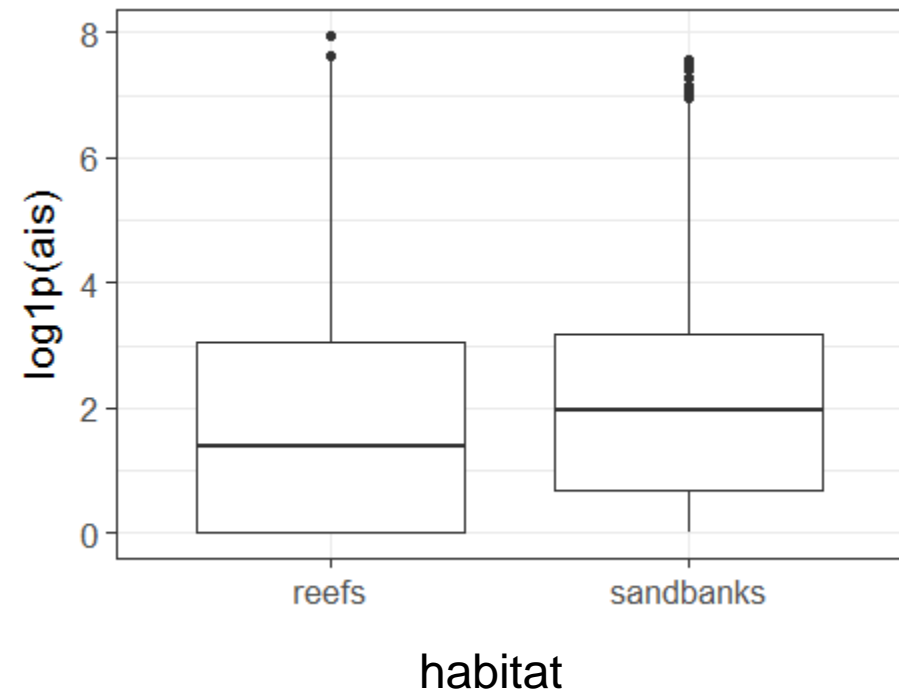
Overlap of shipping and cables-pipelines



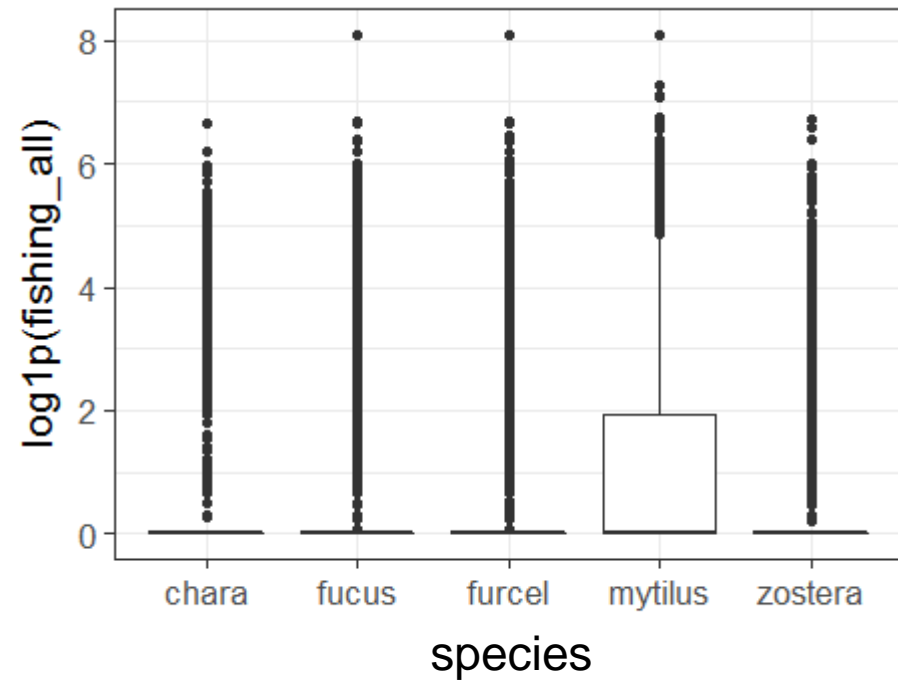
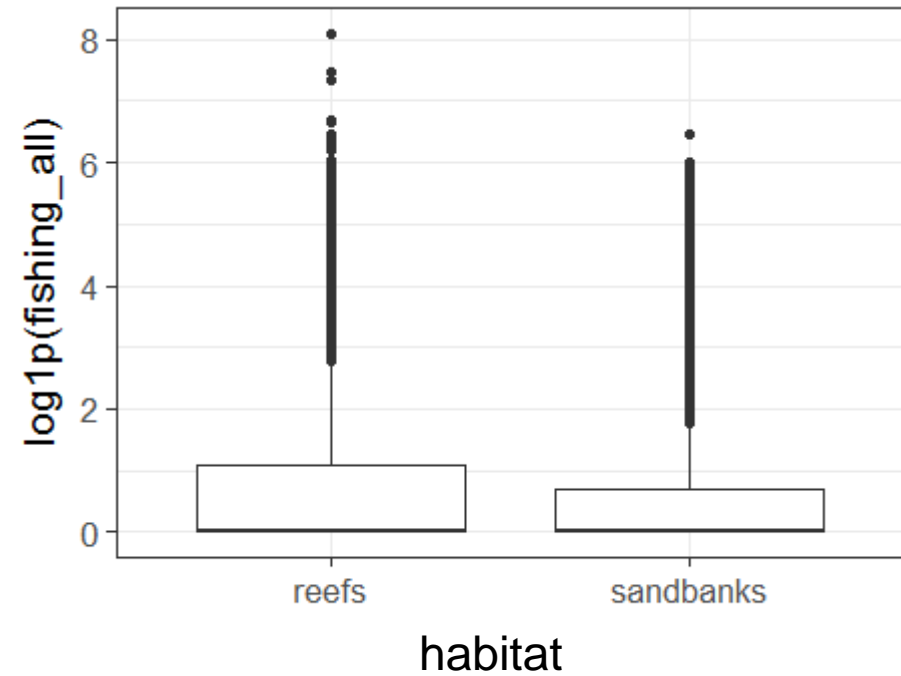
Overlap of fishing and cables-pipelines



Overlap of nature values and shipping



Overlap of nature values and fishing



- **Habitat Directive habitats**
 - sandbanks have two-fold higher overlap with PAs than reefs (reefs < sandbanks)
 - reefs have larger overlap with cables and pipelines than sandbanks (reefs > sandbanks)
 - ten-fold differences in the areal coverage by PAs between the countries
- **Benthic key species**
 - *Zostera marina* has highest overlap with PAs
 - *Mytilus trossulus* has the highest overlap with fishing
 - large differences in the areal coverage by PAs between the countries
- **Shipping and fishing intensity and occurrence of cables and pipelines is lower in PAs than outside of PAs**
- **Shipping and fishing intensity is higher inside cables-pipelines that outside**

Acknowledgements

This study is supported by European Regional Development Fund, INTERREG Baltic Sea Region project Baltic LINES “Coherent Linear Infrastructures in Baltic Maritime Spatial Plans”

Lead
partner

Partners



EUROPEAN UNION



BUNDESAMT FÜR
SEESCHIFFFAHRT
UND
HYDROGRAPHIE



Finnish Transport Agency

Swedish Agency
for Marine and
Water Management



S Y K E



Vides aizsardzības un
reģionālās attīstības
ministrija



From small scales to large scales
–The Gulf of Finland Science Days 2017
9th-10th October 2017
Estonian Academy of Sciences, Tallinn

2nd Day



**Gulf of Finland
Co-operation**

P. Ekholm, J. Riihimäki, J. Linjama, M. Ollikainen, E. Punttila, S. Puroila, A-K. Kosenius

Reducing agricultural phosphorus load by gypsum: results from the first year after amendment



REDUCING AGRICULTURAL PHOSPHORUS LOAD BY GYPSUM: RESULTS FROM THE FIRST YEAR AFTER AMENDMENT

Petri Ekholm, Juha Riihimäki, Jarmo Linjama
SYKE

Markku Ollikainen, Eliisa Punttila, Samuli Puroila, Anna-Kaisa Kosenius
University of Helsinki



Why gypsum ($\text{CaSO}_4 \cdot 2\text{H}_2\text{O}$)?

- **Baltic Sea Action Plan**
 - Finland has to reduce the load of P into the Gulf of Finland by **364 t y⁻¹**
 - Even if all the planned measures were fully implemented, the target would fall about **250 t y⁻¹** short (Knuuttila et al. 2017)
- **A need for efficient P abatement measures in agriculture**
- **A tentative estimate: gypsum amendment of agricultural fields could reduce the P load into**
 - the Gulf of Finland by **50 t y⁻¹**
 - the Archipelago Sea by **100 t y⁻¹**
- **Cost about 66 € kg⁻¹ P (gypsum, transportation, spreading)**
- **Reduces both dissolved and particulate P**
- **The SAVE project aims to**
 - **Study the performance of gypsum in a large pilot**
 - **Test gypsum transport and spreading**
 - **Survey farmers attitudes towards gypsum**
 - **Make a plan for gypsum treatment of all the potential fields in Finland**

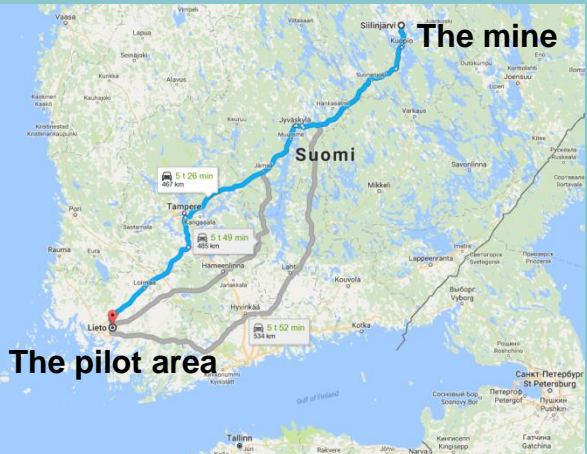
The apatite mine in Siilinjärvi



Gypsum formed as a side-product of phosphoric acid manufacturing



The pilot area: River Savijoki



The mine

The pilot area



>6 million kg of gypsum transported by 144 lorries



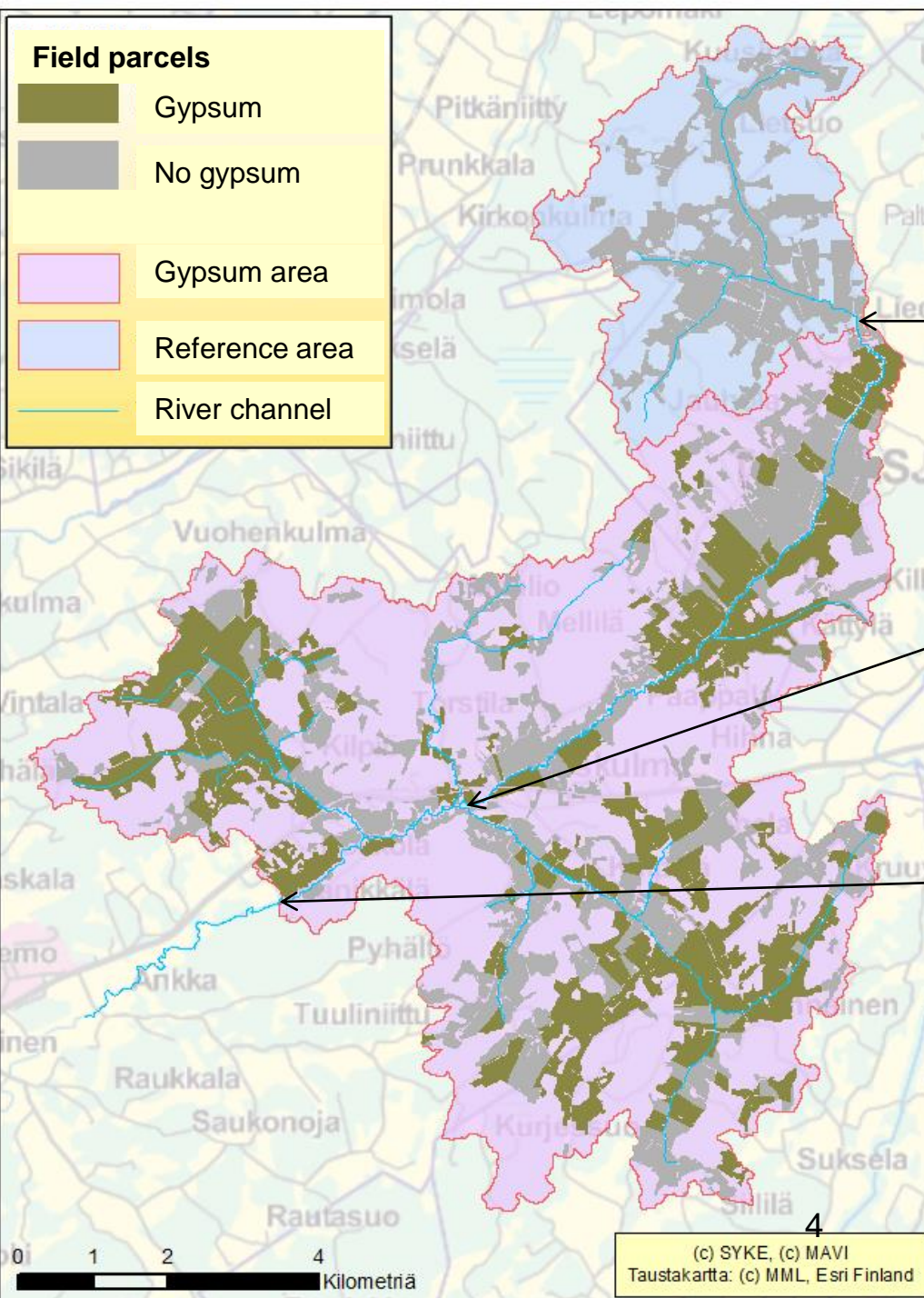
55 farms took part in the pilot



Gypsum was spread on 1530 hectares of fields in autumn 2016



A hint of gypsum (4000 kg/ha)



The River Savijoki (SW Finland) – Relatively homogeneous area in terms of

- Soil type of the fields (clay)
- Cultivation practices
- No other major loading sources

Control site

Catchment area 15 km²
No gypsum

Gypsum area, middle site

Catchment area 33 km²
28% upstream fields amended

Gypsum area, lower site

Catchment area 82 km²
43% upstream fields amended

Gypsum effect increases

All the sites equipped with online sensors and visited (quite) frequently for water quality sampling

Immediate effect

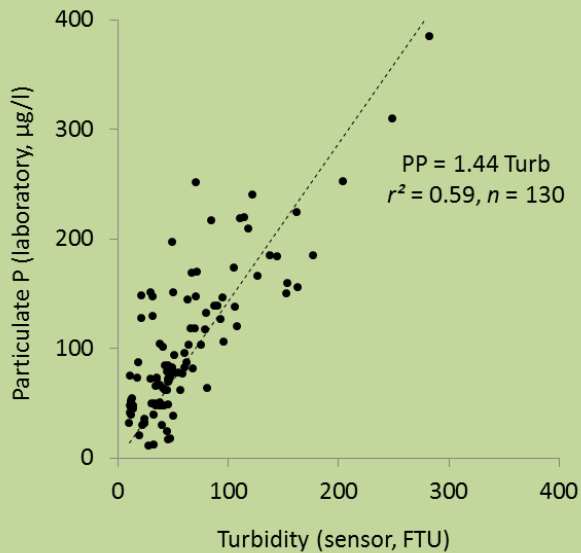
A field treated with gypsum



An untreated field



Estimation of the losses of particulate P



Estimation of the concentrations of particulate P

$$C_{PP} (\mu\text{g l}^{-1}) = 1.44 \text{ Turbidity}$$

Runoff measurements
 $q, (\text{l s}^{-1} \text{ km}^{-2})$



Calculation of hourly losses of particulate P

$$L_{PP} (\text{g km}^{-2} \text{ h}^{-1}) = q \cdot C_{PP} \cdot 3600/1000000$$

Summing up for daily losses



Comparison of pre- and post-gypsum losses in the control and gypsum areas



Loss of particulate P before, during and after the gypsum amendment

Area	Unit	Pre-gypsum 19.2.–31.7.2016 164 d
Runoff	mm	112
Control	g km ⁻² d ⁻¹	200
Gypsum area – middle	g km ⁻² d ⁻¹	267 (+33%)
Gypsum area – lower	g km ⁻² d ⁻¹	274 (+37%)

Before gypsum

- The loss of particulate P about one third higher in the gypsum area than in the control area

Loss of particulate P before, during and after the gypsum amendment

Area	Unit	Pre-gypsum 19.2.–31.7.2016 164 d	During gypsum 1.8.–31.10.2016 92 d
Runoff	mm	112	1.1
Control	g km ⁻² d ⁻¹	200	3.6
Gypsum area – middle	g km ⁻² d ⁻¹	267 (+33%)	2.7 (-25%)
Gypsum area – lower	g km ⁻² d ⁻¹	274 (+37%)	2.1 (-42%)

During the three months of gypsum spreading

- The loss of particulate P was smaller from the gypsum area
- The period was exceptionally dry

Loss of particulate P before, during and after the gypsum amendment

Area	Unit	Pre-gypsum 19.2.–31.7.2016 164 d	During gypsum 1.8.–31.10.2016 92 d	Post-gypsum 1.11.2016–26.9.2017 330 d
Runoff	mm	112	1.1	98
Control	g km ⁻² d ⁻¹	200	3.6	139
Gypsum area – middle	g km ⁻² d ⁻¹	267 (+33 %)	2.7 (-25%)	128 (-8.1%)
Gypsum area – lower	g km ⁻² d ⁻¹	274 (+37 %)	2.1 (-42%)	113 (-19%)

- **Note:** only 43% of fields upstream of the lower site were amended with gypsum
- To reach a 19% decrease in the overall loss of particulate P, the loss from gypsum amended fields has been
 - 43% smaller (lower site) than from non-treated fields
- The loss of particulate P reduced by 300 kg

Mean concentrations of dissolved P ($\mu\text{g l}^{-1}$)

Area	Pre-gypsum 19.2.–31.7.2016 164 d	During gypsum 1.8.–31.10.2016 92 d	Post-gypsum 1.11.2016–26.9.2017 330 d
<i>n</i>	14	6	20
Control	28	30	50
Gypsum area – middle	34	23	47
Gypsum area – lower	29	18	45

- Slight decrease (about 10%) in dissolved P
- Performance uncertain due to a low number of samples collected yet

Farmer survey

87% of the farmers responded to a questionnaire

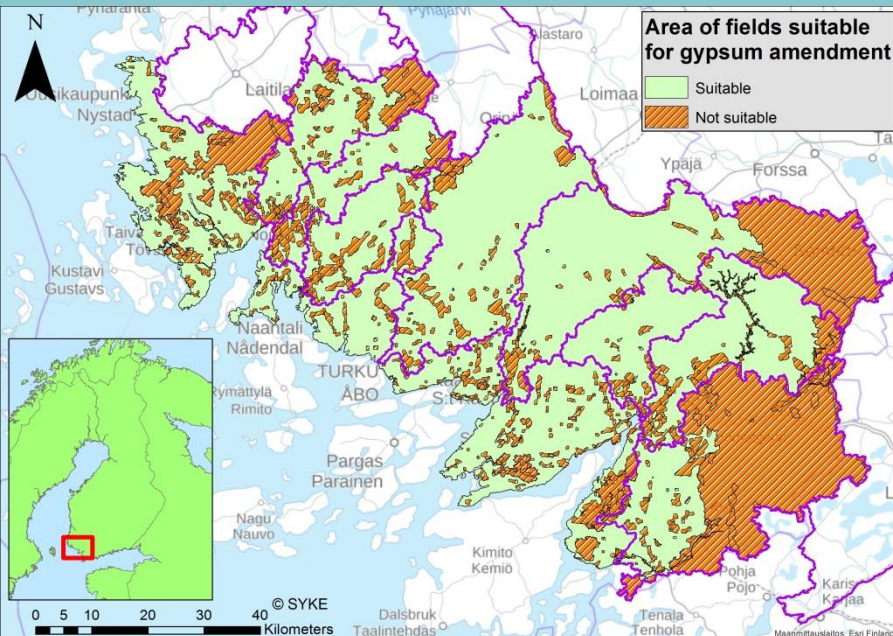
- **78% would use gypsum, if it were subsidized by the agri-environmental support scheme**
- **72% considered that local people sympathised with gypsum use**
- **70% would recommend gypsum to other farmers**
- **56% considered that gypsum is an easy agri-environmental measure**
- **6% experienced problems in gypsum spreading**

BUT: the autumn 2016 was perfect (= dry) for gypsum amendment

Tentative assessment of the potential of gypsum in the Archipelago sea catchment

- Catchment area 6580 km² (excluding islands)
- Field area 2020 km², of which not suitable the fields located
 - Upstream of lakes
 - On acid sulfate soils
 - On groundwater areas
 - Near Natura2000 sites

Area of suitable fields	Area (km ²)
All fields	1320
Fields on mineral soils	220
Fields on clay soils	1060
Fields on organic soils	40



Current P loss

$$2020 \text{ km}^2 \cdot 110 \text{ kg km}^{-2} \text{ y}^{-1} \text{ P} = 222 \text{ t y}^{-1}$$

$$1060 \text{ km}^2 \cdot 110 \text{ kg km}^{-2} \text{ y}^{-1} \text{ P} = 117 \text{ t y}^{-1}$$

After gypsum amendment (assuming a 40% reduction)

$$1060 \text{ km}^2 \cdot 0.6 \cdot 110 \text{ kg km}^{-2} \text{ y}^{-1} \text{ P} = 70 \text{ t y}^{-1}$$

A reduction of 47 t y⁻¹

Future tasks

- The Savijoki will be monitored (at least) till the end of 2018
 - So far 9% of the applied gypsum flushed away
 - Gypsum is anticipated to work for 4–5 years
- Soil and plant analysis
- Farmer survey repeated
- Effects of sulfate on fish assemblages and on trout spawn
 - No harmful effects found on thick-shelled river mussel (*Unio crassus*, adults and larvae) and common water moss (*Fontinalis antipyretica*)
- Effects of sulfate on the P release from river sediments
- Effects of gypsum on groundwater
- Plan for a larger scale gypsum treatment including the entire southern Finland...

... and other areas around the Baltic Sea

...any volunteers?

You may follow us on social media

FACEBOOK & TWITTER

[@nutritradebaltic](#) & [@NutriTradeEU](#)
[@savekipsihanke](#)

READ MORE

nutritradebaltic.eu
blogs.helsinki.fi/save-kipsihanke

From small scales to large scales
–The Gulf of Finland Science Days 2017
9th-10th October 2017
Estonian Academy of Sciences, Tallinn

2nd Day



**Gulf of Finland
Co-operation**

P.Yli-Hemminki, K. Jørgensen, J. Lehtoranta

Iron–manganese concretions contribute to benthic release of phosphorus and arsenic in anoxic conditions in the Gulf of Finland

*Iron–manganese concretions
contribute to benthic release of
phosphorus and arsenic in anoxic
conditions in the Gulf of Finland*

Pirjo Yli-Hemminki, Kirsten Jörgensen,
Jouni Lehtoranta

Pirjo
Yli-Hemminki

SYKE

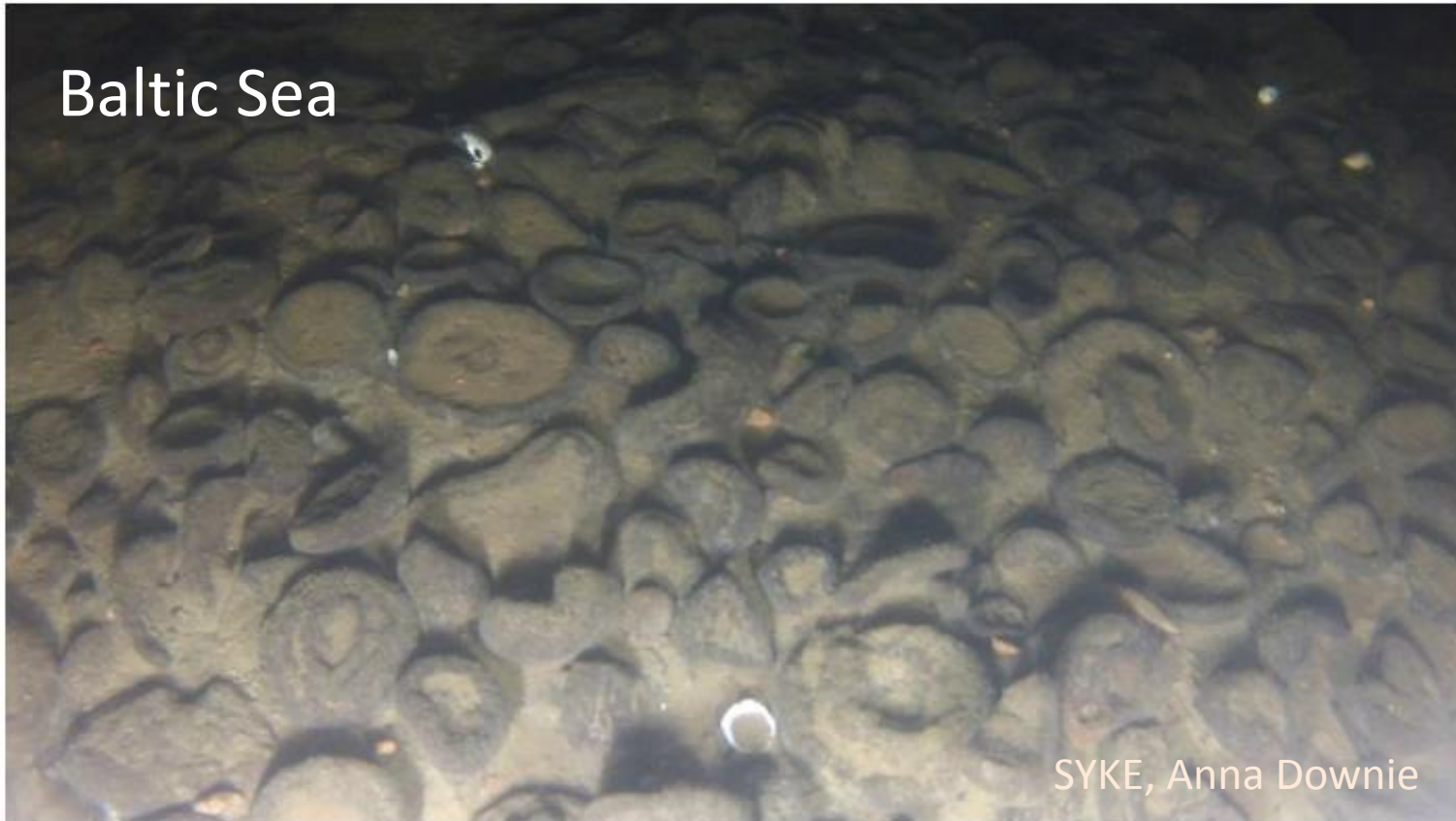
Marine research centre



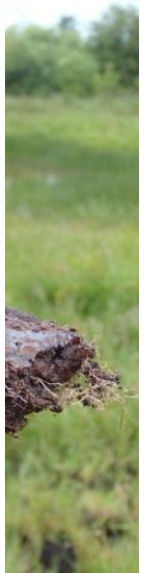
What and where?

- Concretions, nodules, lake ore, bog iron ore
 - Ggrowing minerals which have high concentrations of iron or manganese
- You may find them...

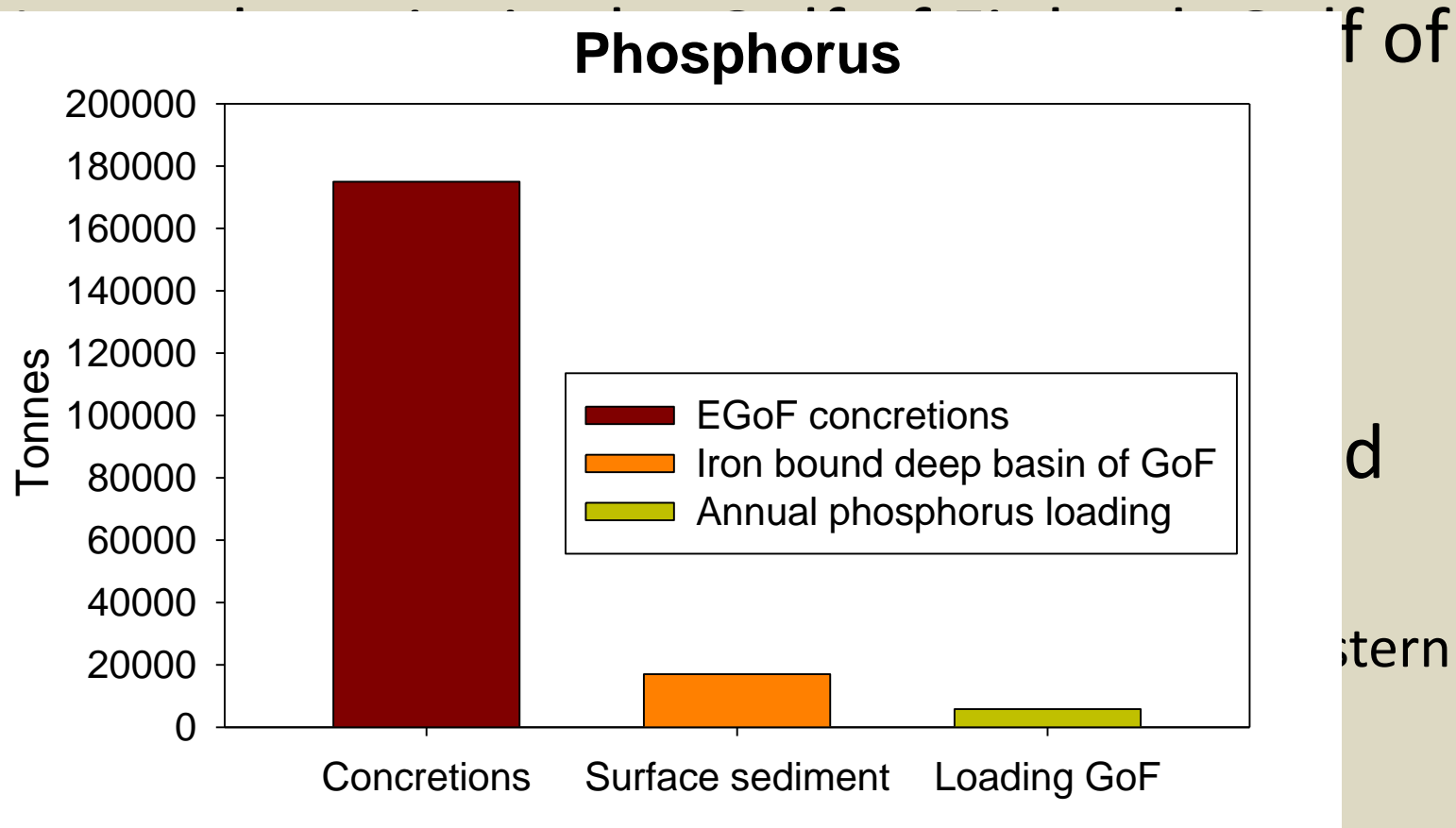
Baltic Sea



SYKE, Anna Downie



Concretions in the Baltic Sea



Glasby et al. 1997 Environments of formation of ferromanganese concretions in the Baltic sea: a critical review.

Geol Soc Spec Pub 119:213–237.

Vallius H, Zhamoïda V, Kotilainen A, Ryabchuk D (2011) Seafloor desertification— a future scenario for the Gulf of Finland? Central and Eastern European Development Studies 365–372.

Objective

Spherical concretions



- Concretions grow in oxic and dissolve in anoxic conditions
 - Oxic/anoxic conditions vary in the Gulf
- Microbes control directly or indirectly dissolution of concretions
- Our objective was to examine:
 - microbial community and oxidation of metals by microbes
 - effect of dissolution of concretions on release of phosphorus and arsenic
 - assess ecological significance of the concretions in the Gulf of Finland

Material and methods

- Microbial community
 - DNA extractions, PCR Clone library, RFLP analysis, and sequencing (Yli-Hemminki et al. 2014)
- Enrichment of Mn and Fe oxidizing bacteria
 - Liquid cultures and oxygen-Gradient tubes (Yli-Hemminki et al. 2014)
- Simulation of dissolution of concretions in anoxia
 - Incubations in artificial brackish water (Yli-Hemminki et al. 2016)

Yli-Hemminki et al. 2014. Iron–manganese concretions sustaining microbial life in the Baltic Sea: the structure of the bacterial community and enrichments in metal-oxidizing conditions. *Geomicrobiol J* 31:263–275

Yli-Hemminki P, Sara-Aho T, Jørgensen KS, Lehtoranta J. 2016. Ironmanganese concretions contribute to benthic release of phosphorus and arsenic in anoxic conditions in the Baltic Sea. *J Soils Sediments* 16: 2138-2152.

Results

- 1) Microbial communities
 - Overall community and manganese and iron oxidizers
- 2) Release of phosphorus and arsenic from concretions during anoxia

Microbial community

Bacteria inhabited surface and interior of concretions

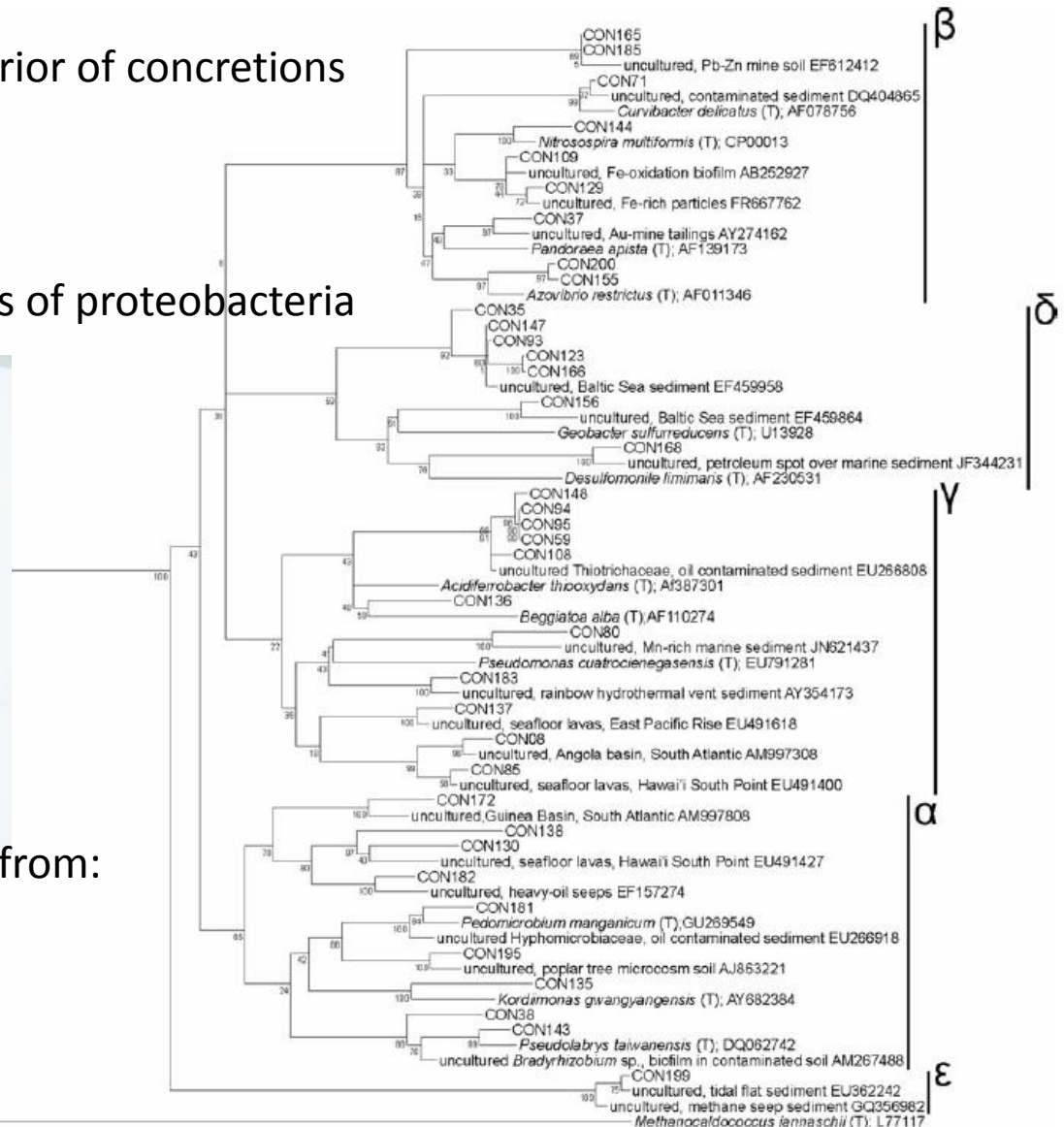
Diverse community:

- 12 phylas represented
- half of bacteria affiliated to classes of proteobacteria
- one third were unclassified

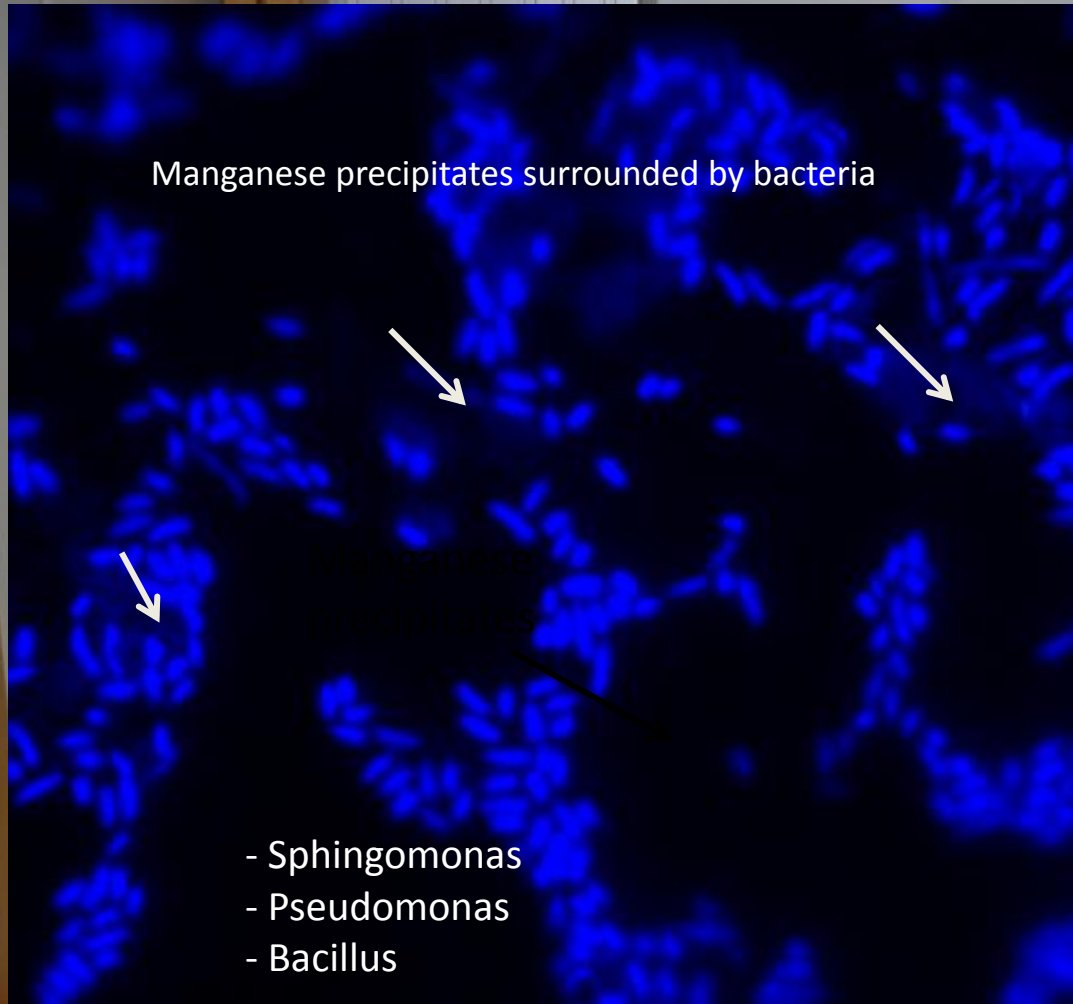


High similarity with bacteria found from:

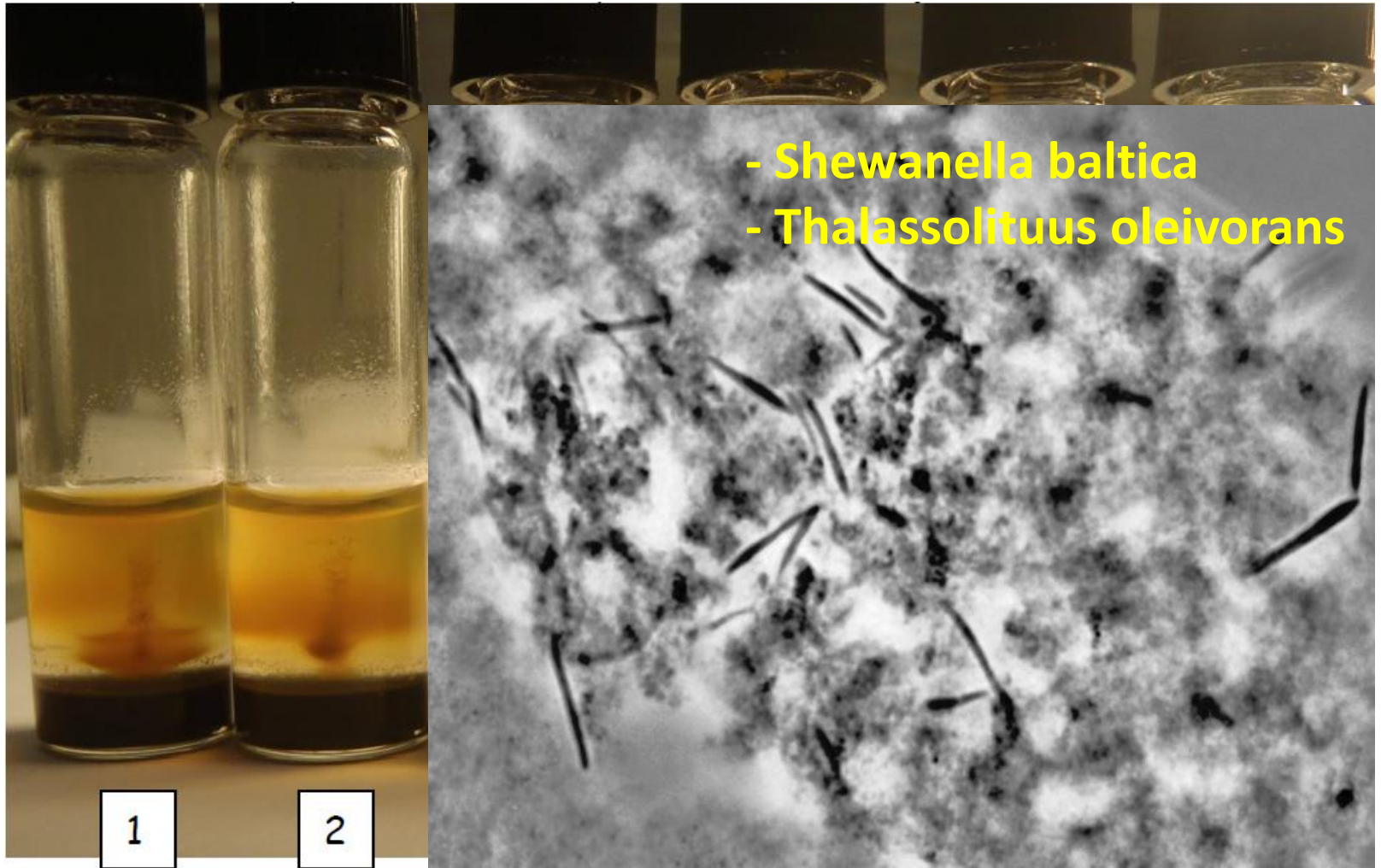
- Sea sediments
- ocean crust
- metal rich environments
- seafloor lavas from Hawaii



Manganese oxidizers in community



Iron bacteria



1

2

Inoculate
alive
+ orgC

Inoculate
alive

No
inoculate
+ orgC

No
inoculate

Killed
inoculate
+ orgC

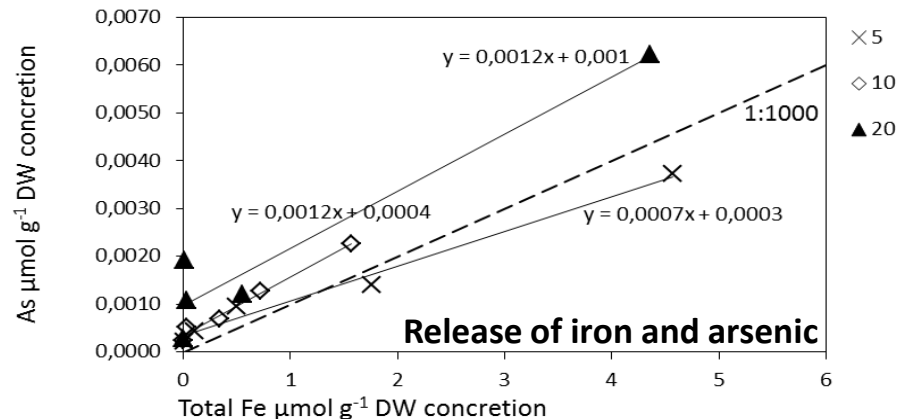
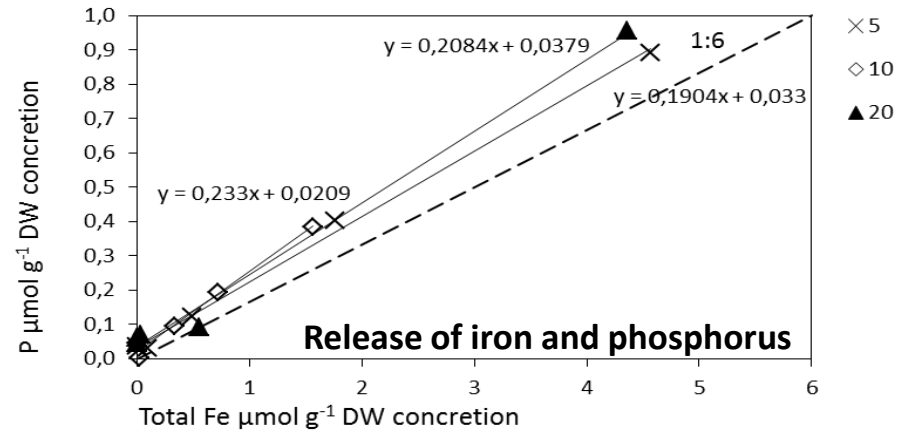
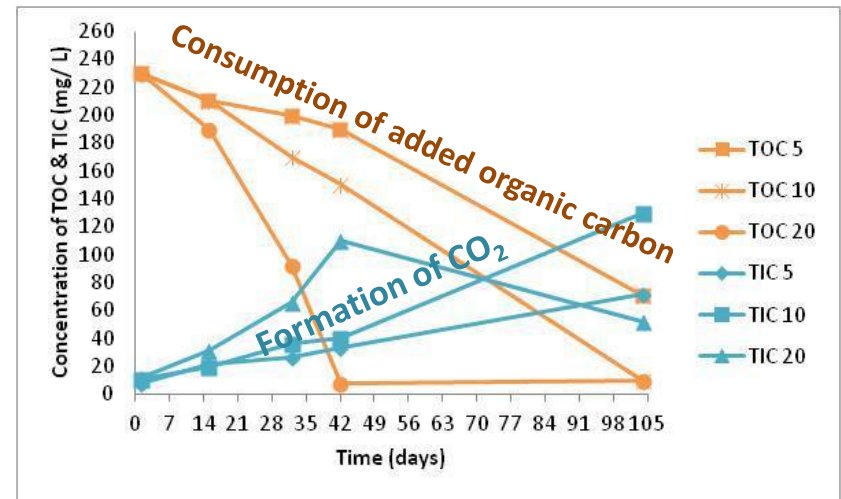
Killed
inoculate

Degradation in anoxia

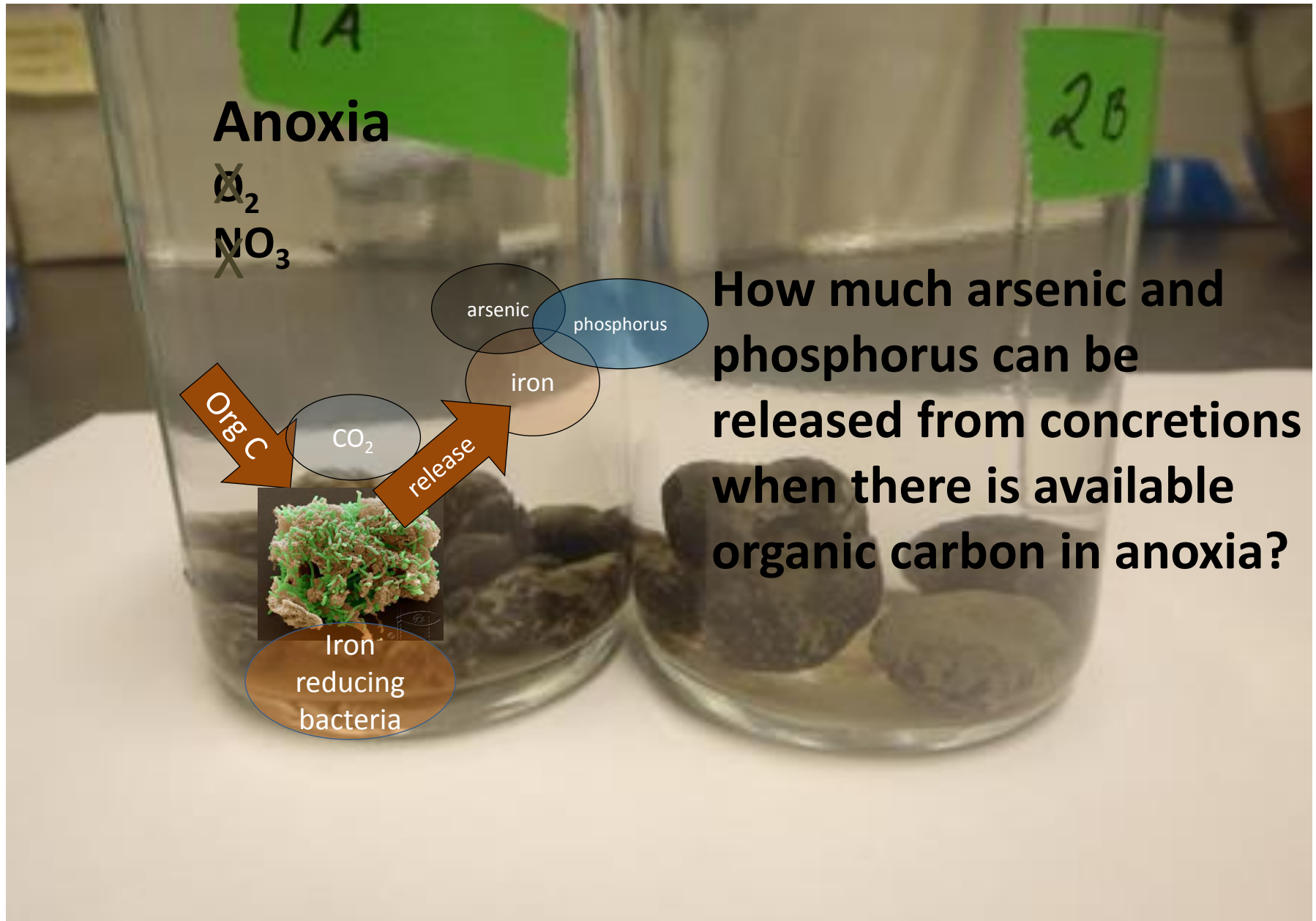


Bottle incubations in anoxic brackish water

- Yes/No added organic carbon
- Killed controls, insignificant release
- Temperature 5 °C



Degradation in anoxia



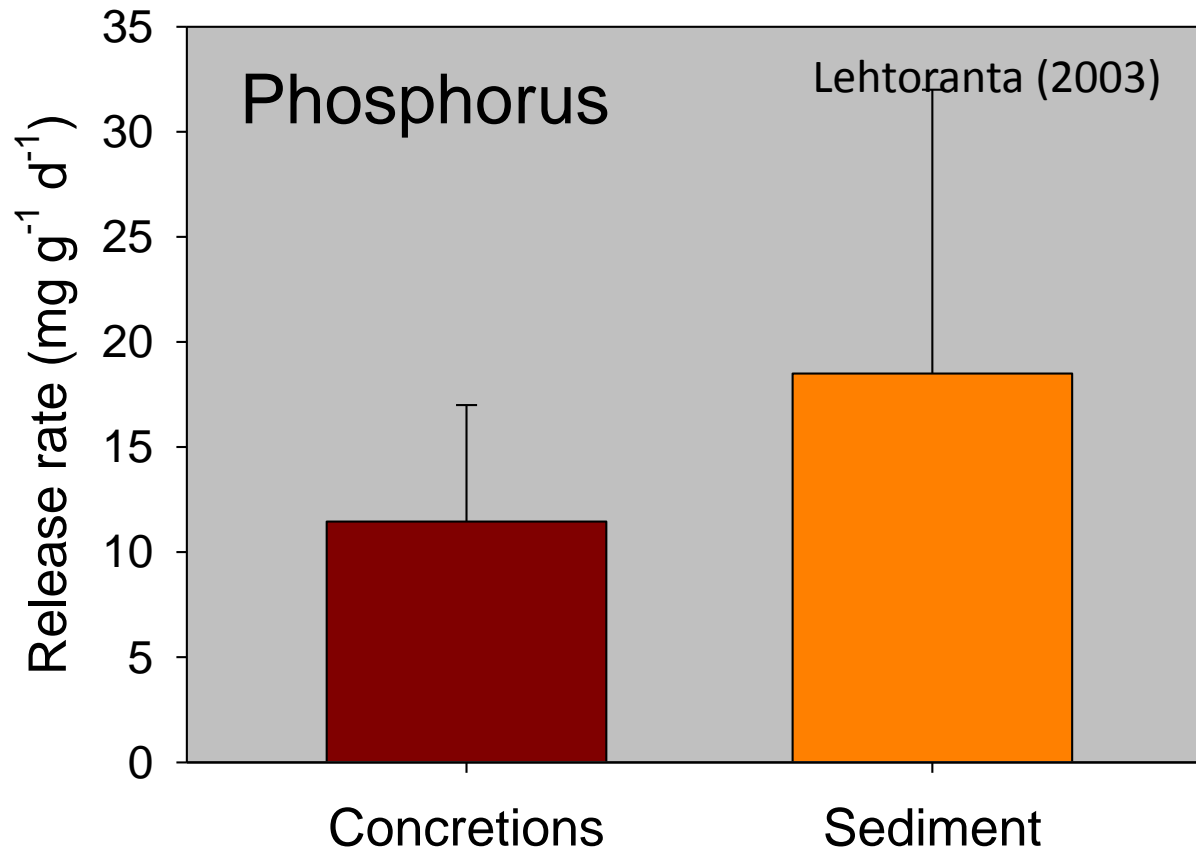
Calculation

- Only incubation with added carbon in cold temperature was considered
- Mean release rates from one gram of concretion:
 - Iron $6.7 \mu\text{g g}^{-1} \text{d}^{-1}$
 - Phosphorus $0.62 \mu\text{g g}^{-1} \text{d}^{-1}$
 - Arsenic $0.015 \mu\text{g g}^{-1} \text{d}^{-1}$
- Only 0.1 % of total iron and phosphorus, and 0.009% of total arsenic were released from concretions during 15 weeks incubation

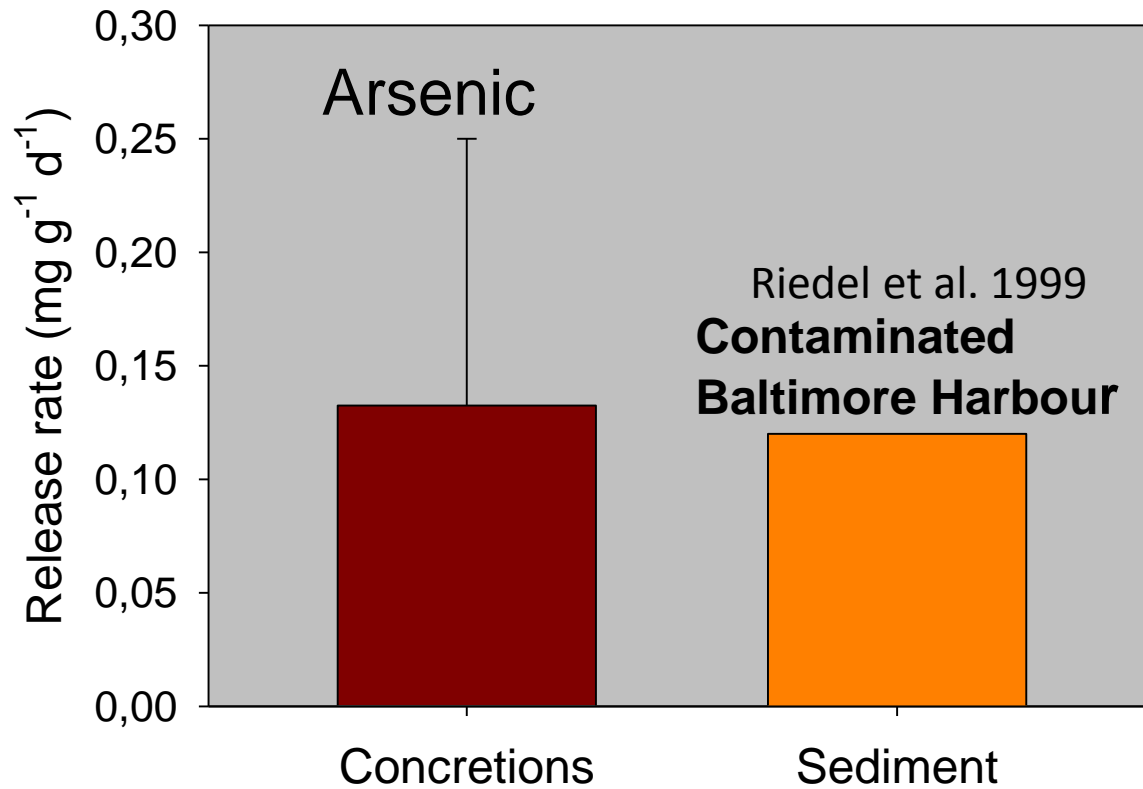
Release from concretion deposit

- Estimation:
 - Concretion deposit 15 kg m^{-2} (up to 24 kg m^{-2})
 - Mean release rates for phosphorus and arsenic
- Range for release
 - Phosphorus $5.9 - 17.0 \text{ mg m}^{-2} \text{ d}^{-1}$
 - Arsenic $0.015 - 0.25 \text{ mg m}^{-2} \text{ d}^{-1}$

Release from deposits vs sediment



Release from deposits vs sediment

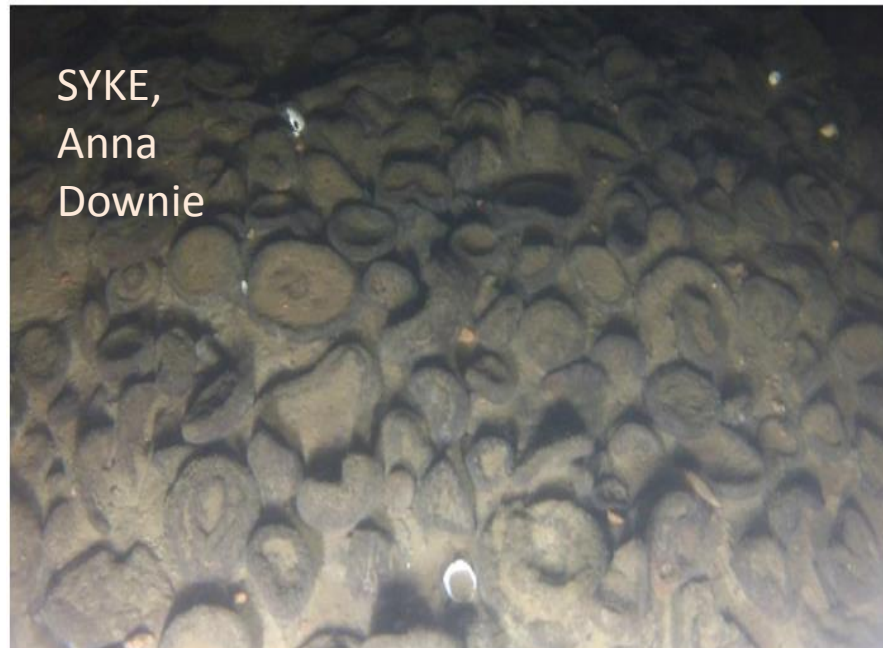


Conclusions



- An individual concretion forms a three-dimensional microcosm having a diverse microbial community
- Concretion microbes were capable to oxidize and reduce manganese and iron
 - i.e. participate in growth and degradation of concretions

Conclusions II



SYKE,
Anna
Downie

- Frequently occurring anoxia may release marked amounts of phosphorus and arsenic from deposits to water of the Gulf of Finland
- It is evident that only a minor proportion of total amount of phosphorus and arsenic in deposits is released during anoxia

References

- Yli-Hemminki P., Jørgensen K., and Lehtoranta J. 2014. Iron–manganese concretions sustaining microbial life in the Baltic Sea: the structure of the bacterial community and enrichments in metal-oxidizing conditions. *Geomicrobiol J* 31:263–275.
- Yli-Hemminki P, Sara-Aho T, Jørgensen KS, Lehtoranta J. 2016. Ironmanganese concretions contribute to benthic release of phosphorus and arsenic in anoxic conditions in the Baltic Sea. *J Soils Sediments* 16: 2138-2152.
- Anna Reunamo, Pirjo Yli-Hemminki, Jari Nuutinen, Jouni Lehtoranta & Kirsten S. Jørgensen 2017. Degradation of Crude Oil and PAHs in Iron–Manganese Concretions and Sediment from the Northern Baltic Sea. *Geomicrobiol J* 34: 385 – 399.
- Yli-Hemminki P. 2015. Microbes regulate metal and nutrient cycling in Fe-Mn concretions of the Gulf of Finland. Academic dissertation Helsinki 2015 ISBN 978-951-51-1623-9.

From small scales to large scales
–The Gulf of Finland Science Days 2017
9th-10th October 2017
Estonian Academy of Sciences, Tallinn

2nd Day



**Gulf of Finland
Co-operation**

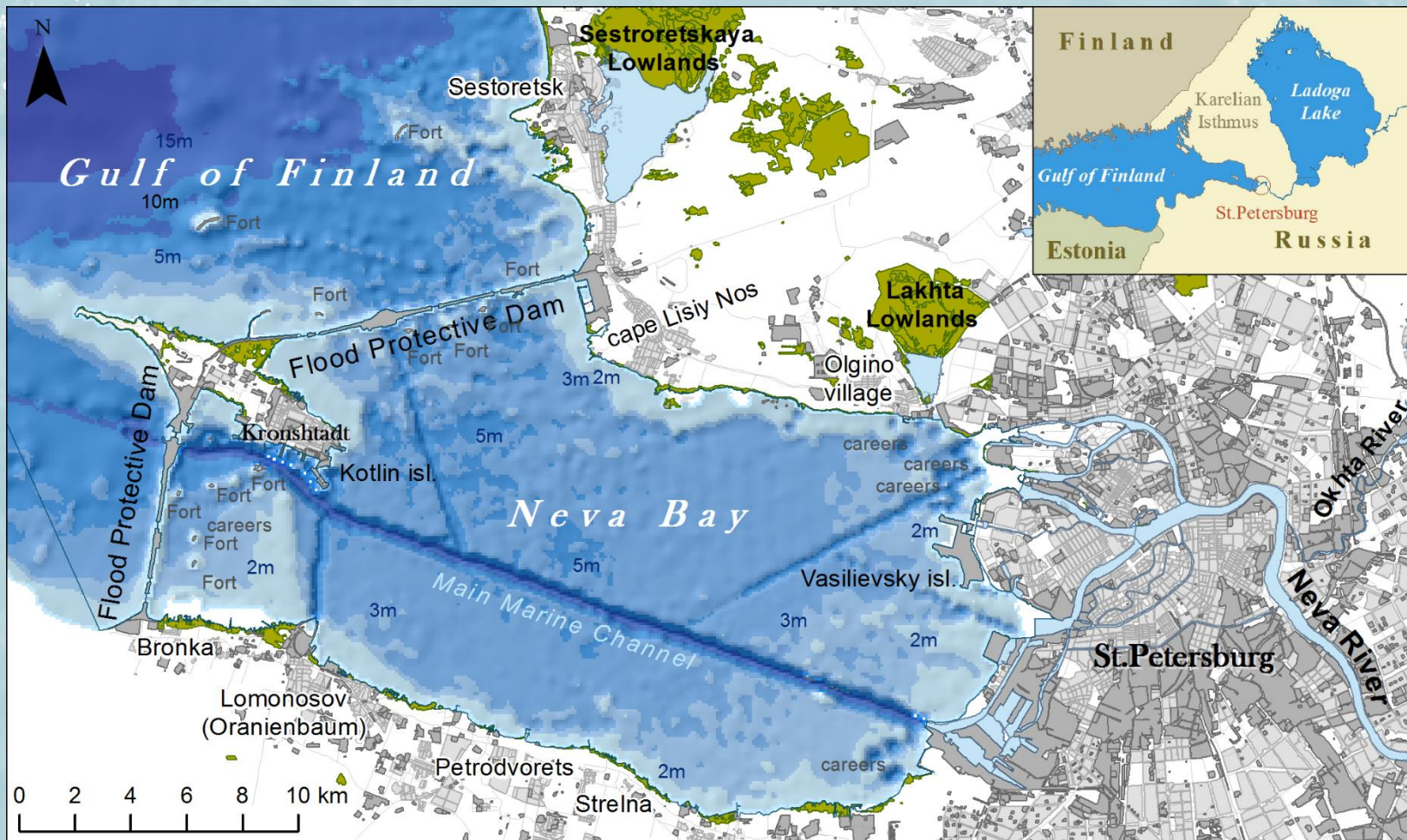
PD. Ryabchuk, H. Vallius, V. Zhamoida, A. Kotilainen, A. Rybalko, N. Malysheva, N. Deryugina, L. Sukhacheva

Sedimentary processes and pollution history of Neva Bay bottom sediments (eastern Gulf of Finland, Baltic Sea)

Sedimentary processes and pollution history of Neva Bay bottom sediments (eastern Gulf of Finland, Baltic Sea)

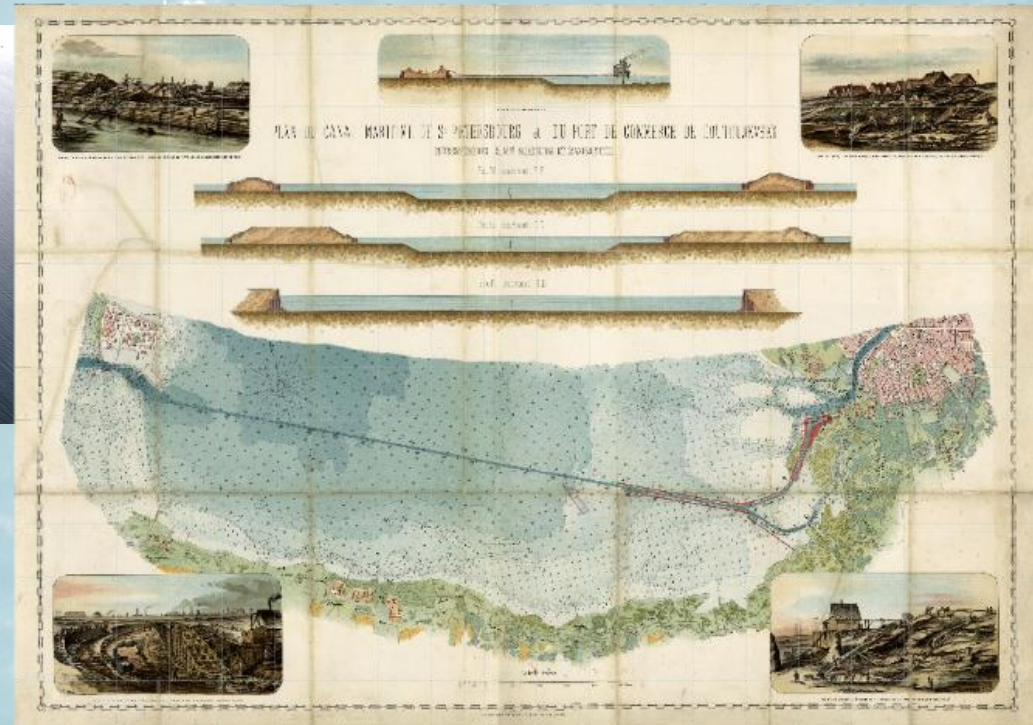
Daria Ryabchuk, Henry Vallius, Vladimir Zhamoida, Aarno Kotilainen, Alexander Rybalko, Nina Malysheva, Natalya Deryugina, Leontina Sukhacheva





Length - 21 km; maximal wideness - 15 km;
 water surface area - 329 km²; water mass volume - 1.2 km³ ;
 surface water current - up to 10 cm/sec; maximal natural
 depths – 5-6 meters; salinity - 0.3 – 1.0‰.

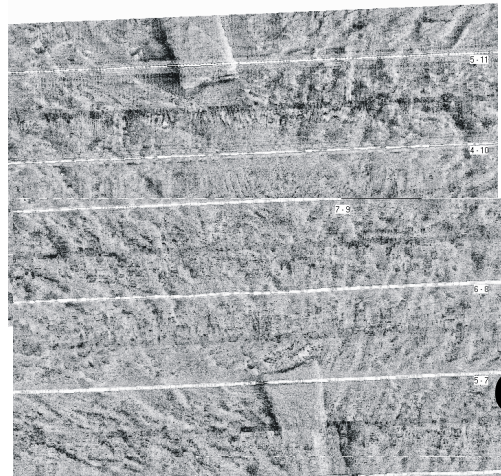
17 artificial islands (fortresses) have build since 1704. In 1885 the Marine Ship-Channel (12 m deep) was constructed.



Bottom relief of the eastern part of Neva Bay (former submarine sand mining carriers)



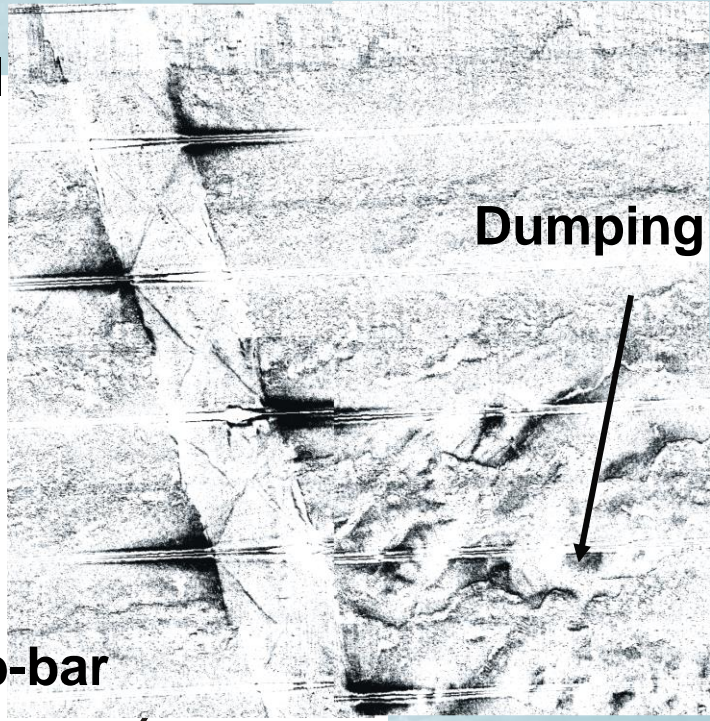
**Ship channel
filled with
sediments**



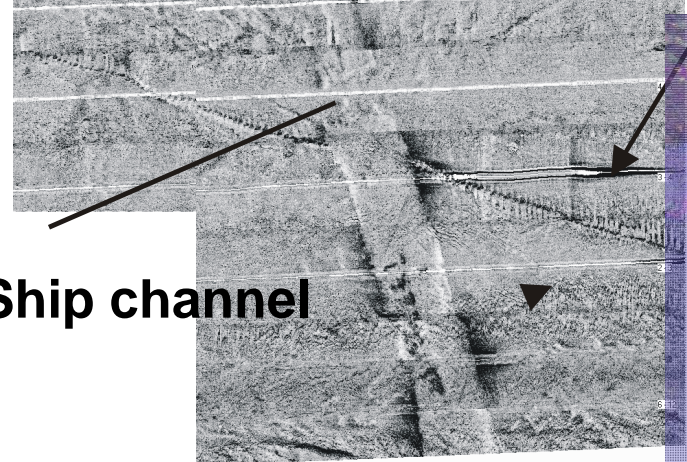
200 m

Crib-bar

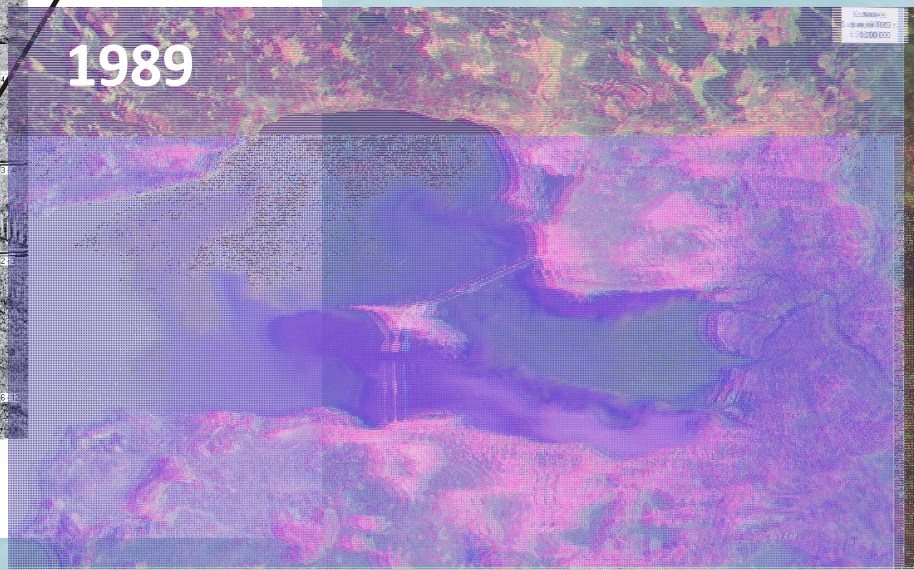
Dumping place

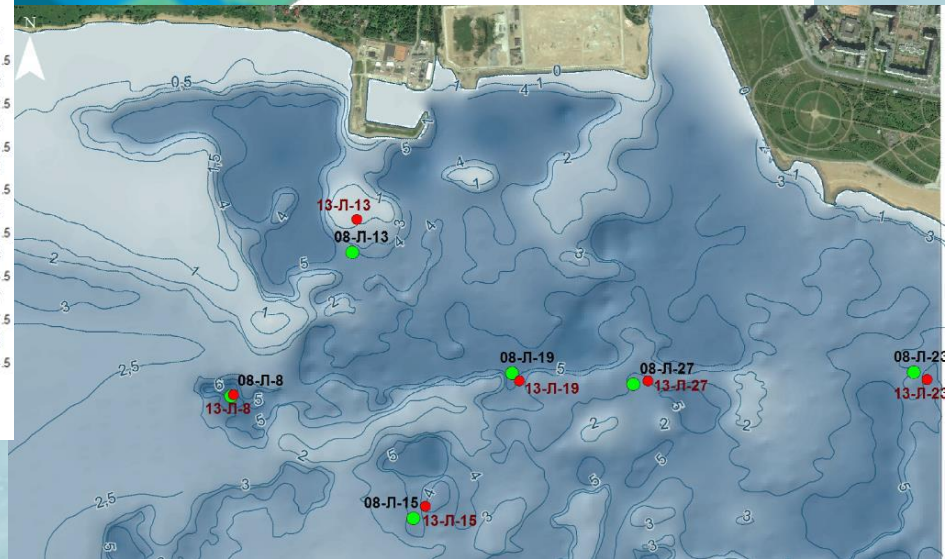
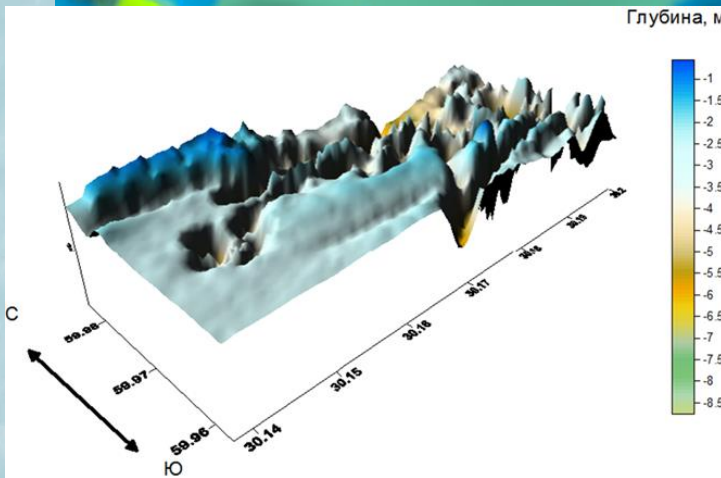
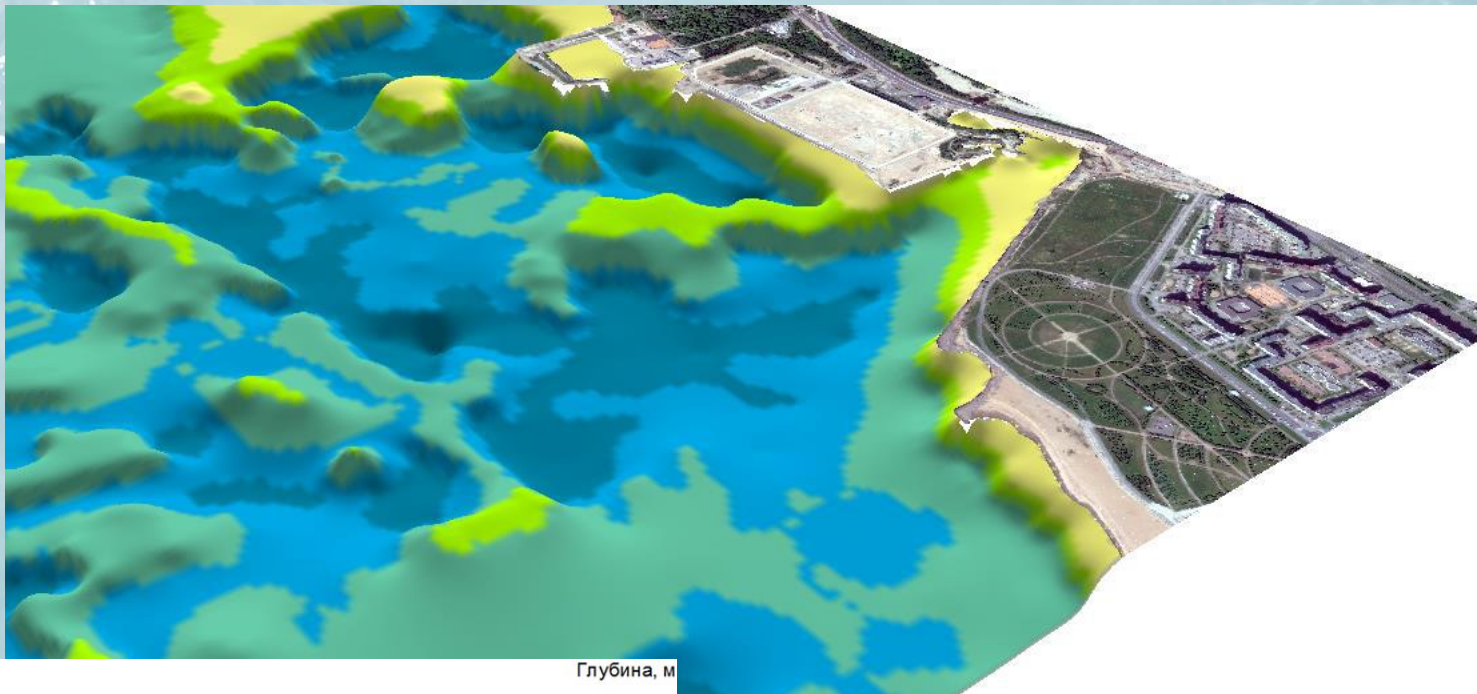


Ship channel



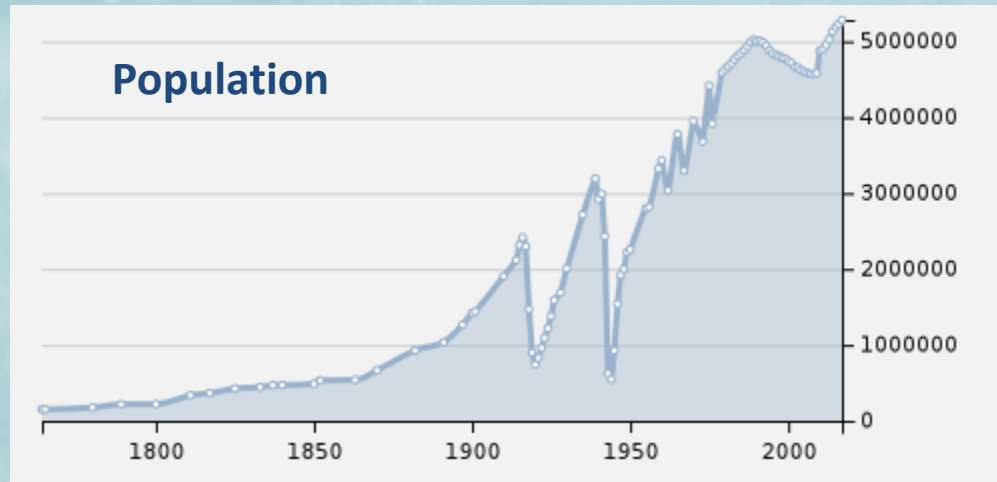
1989



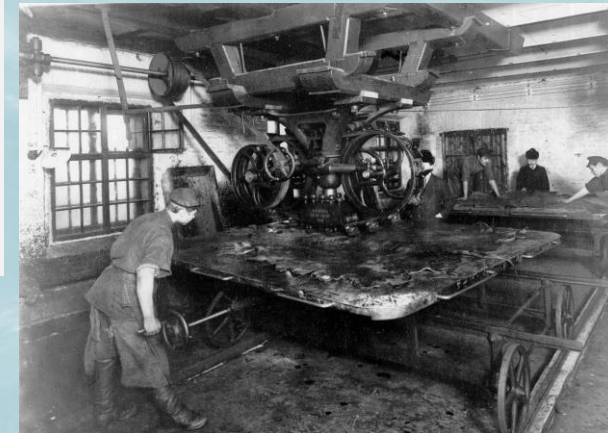


Submarine sand quarries

Dynamic of St. Petersburg population and industry



By 1914 – third city in Europe (after London and Paris)



St. Petersburg industry, 1913

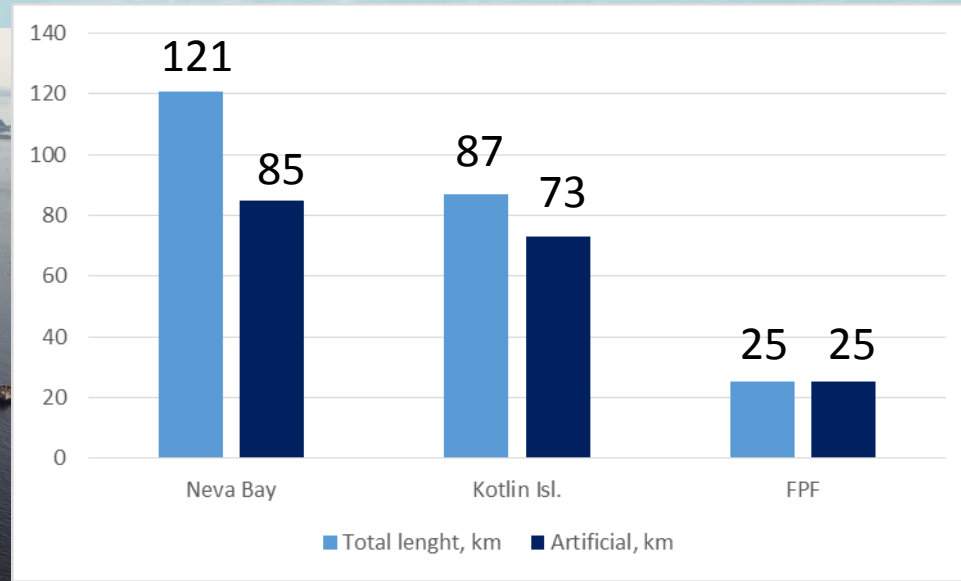
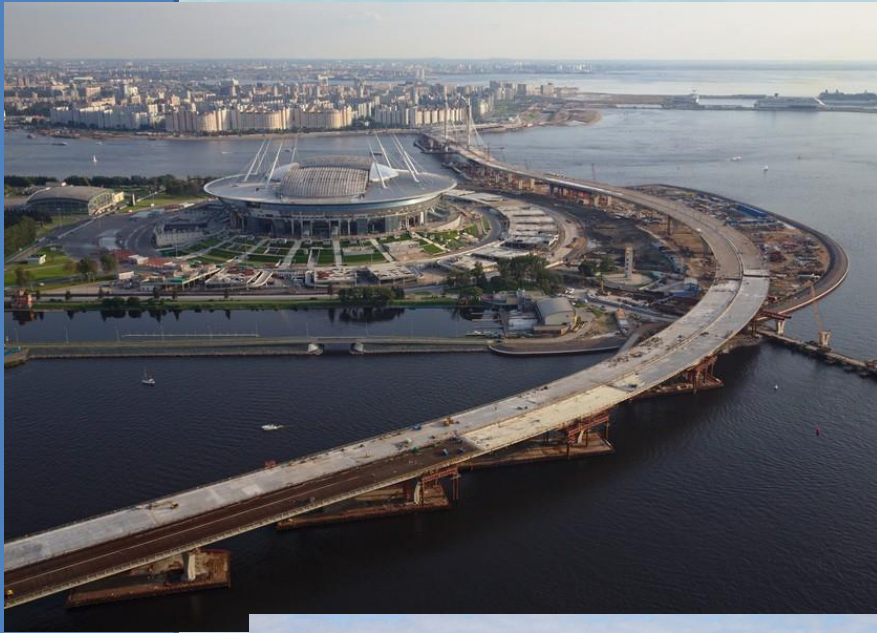
Number of enterprises - 1012

Number of employers - 242 600

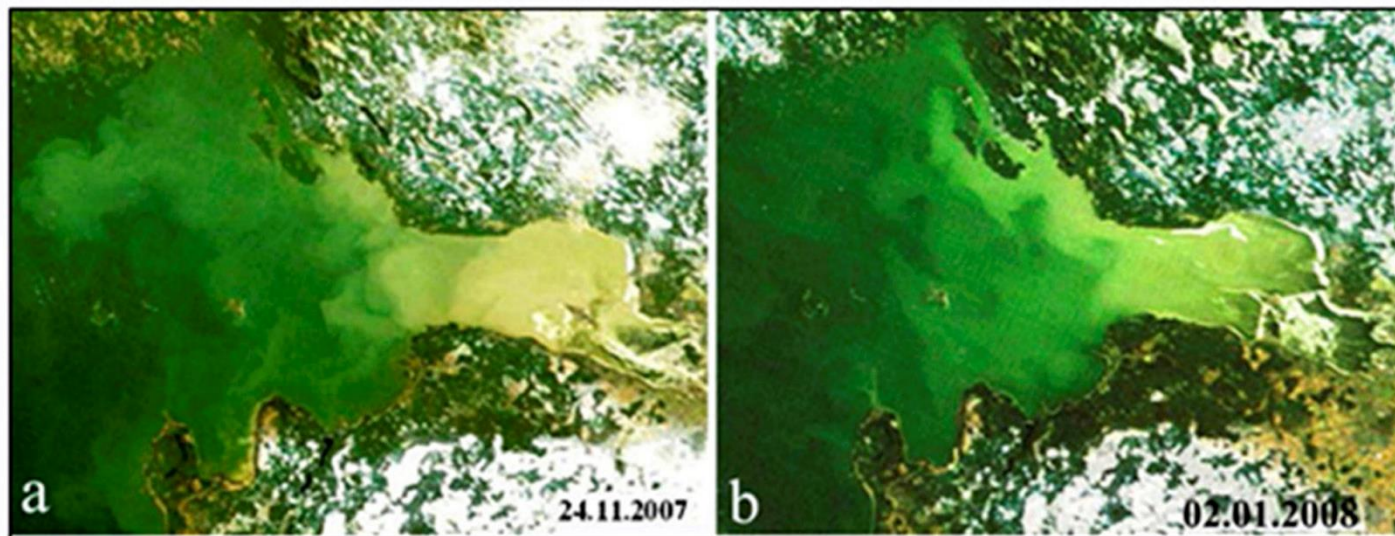
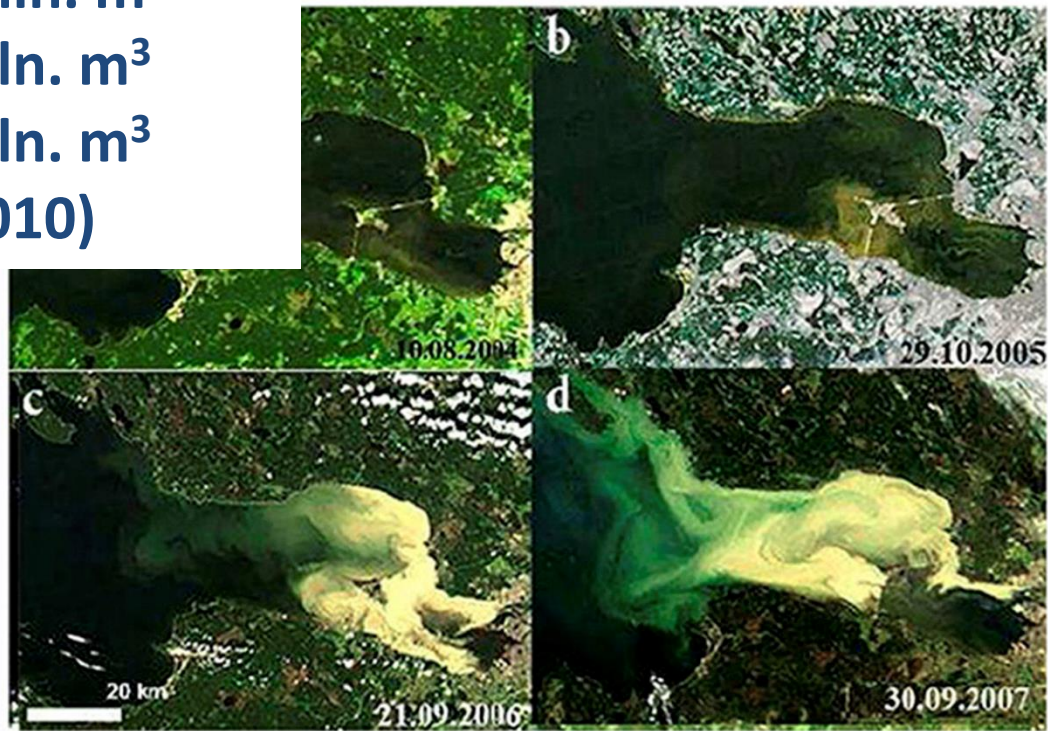
Letukchin, 2014



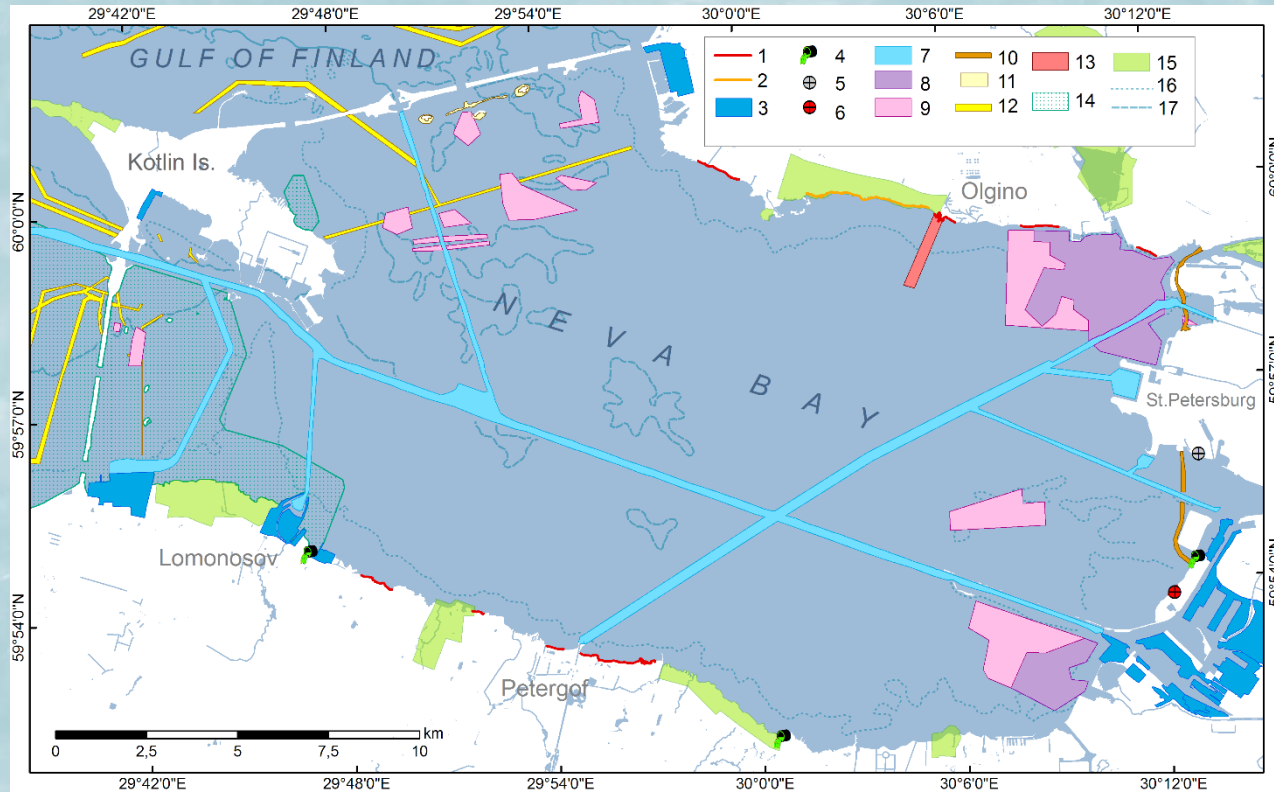
Coasts of Neva Bay are mostly artificial



2005 г. 1,233195 млн. m³
2006 г. 12,199286 млн. m³
2007 г. 7,533176 млн. m³
2008 г. 0,425794 млн. m³
(Zaitsev et al., 2010)

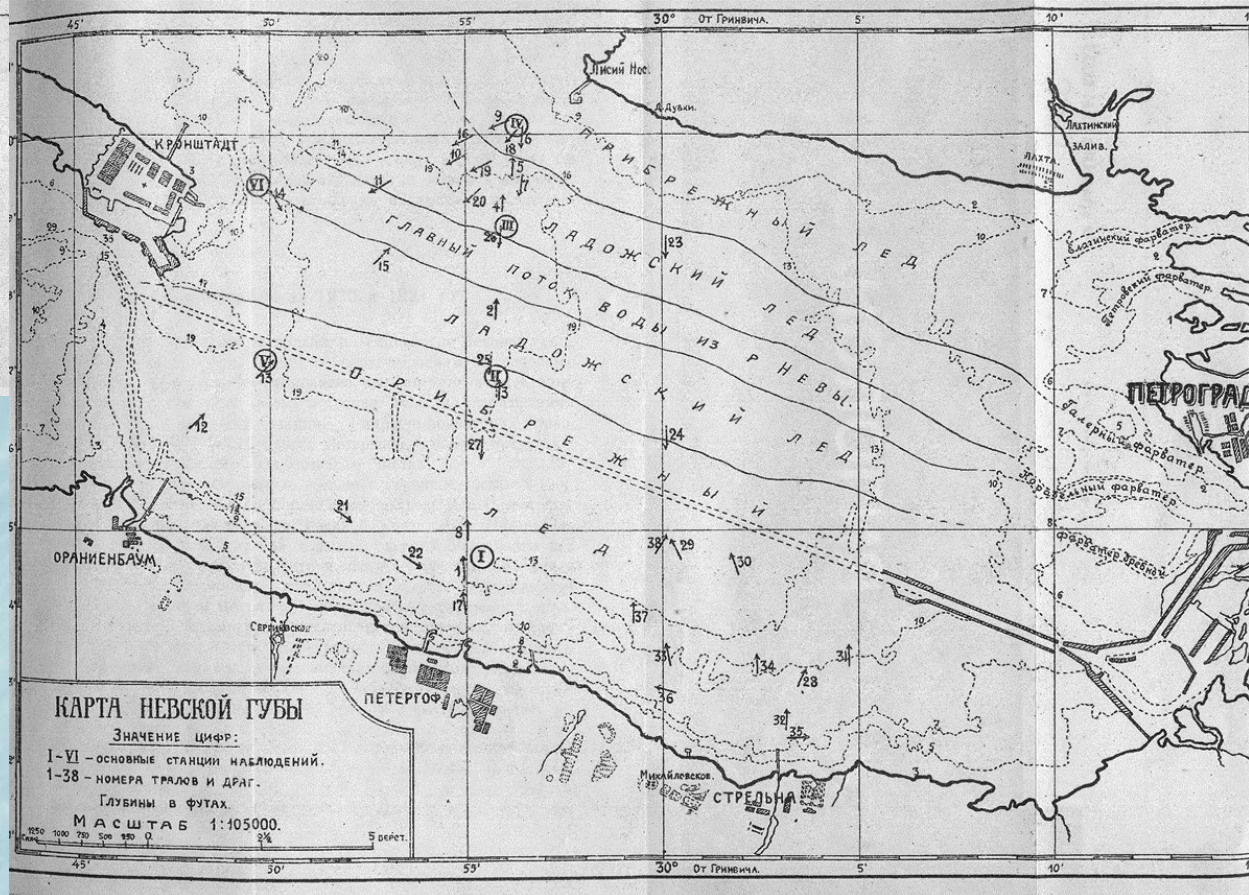
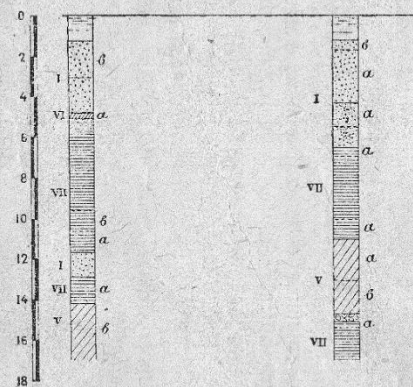
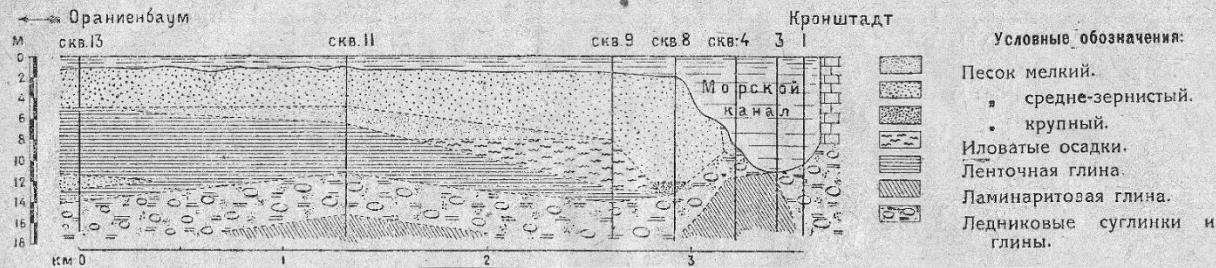


Map of technogenic load on Neva Bay bottom



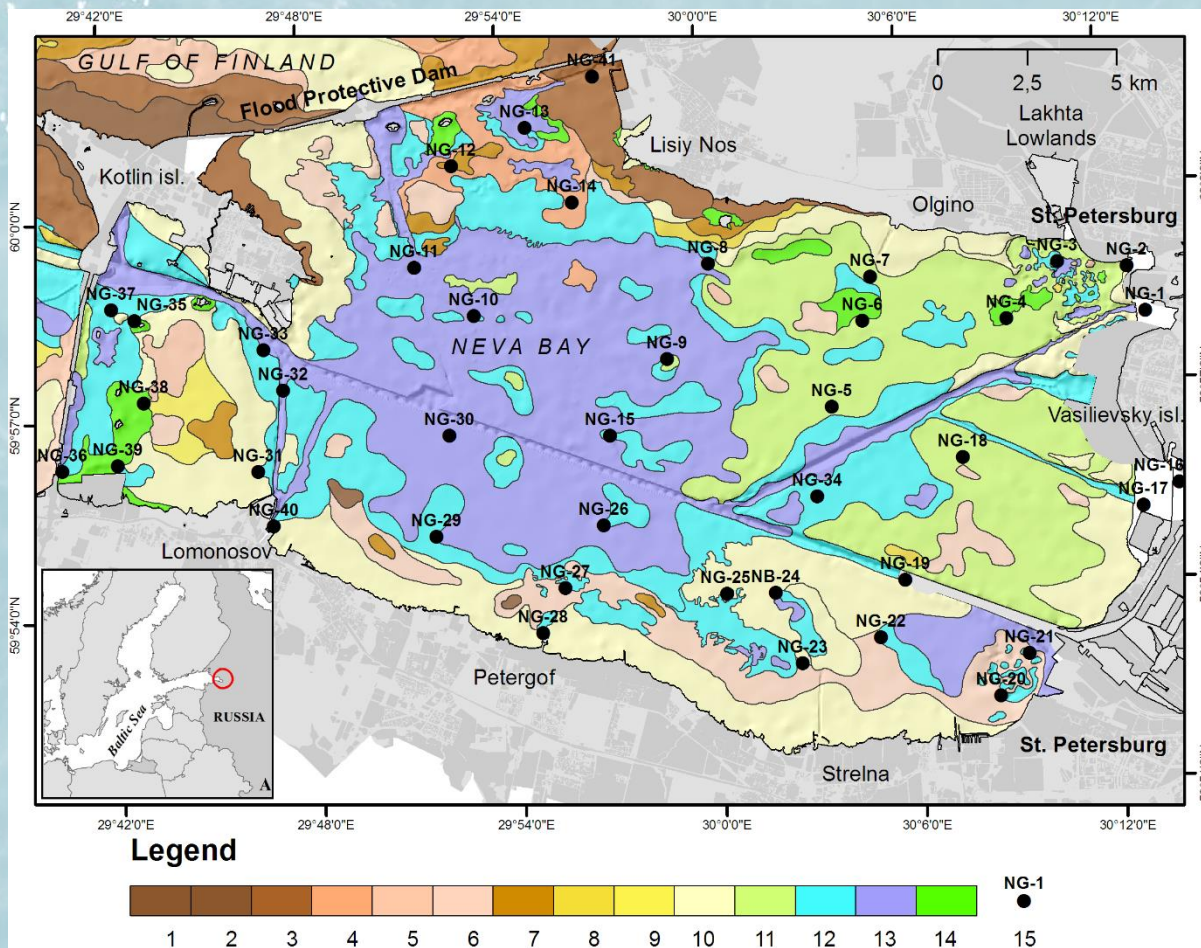
1 – areas of coastal erosion; 2 – areas of active Aeolian processes; technogenic objects onshore: 3 – area of cargo port; 4 – unauthorized wastewater discharge; 5 – dumping place of industrial and urban waste (with coast protection structures); 6 – dumping place of industrial and urban waste (without coast protection structures); technogenic objects onshore: 7 – navigation channels; 8 – area of former underwater sand excavation; 9 – dumping sites of dredged sediments; 10 – highway on pillar bridge (constructed in 2015-2016); 11 – stone crib-bars; 12 – wooden crib-bars; 13 – underwater pipeline; 14 – area of dredging; 15 – nature protection areas; 16 – isobaths.

Геологический профиль дна Финского залива по линии Ораниенбаум — Кронштадт.



Map of sampling sites by prof. K.Deryugin (1920-1923)



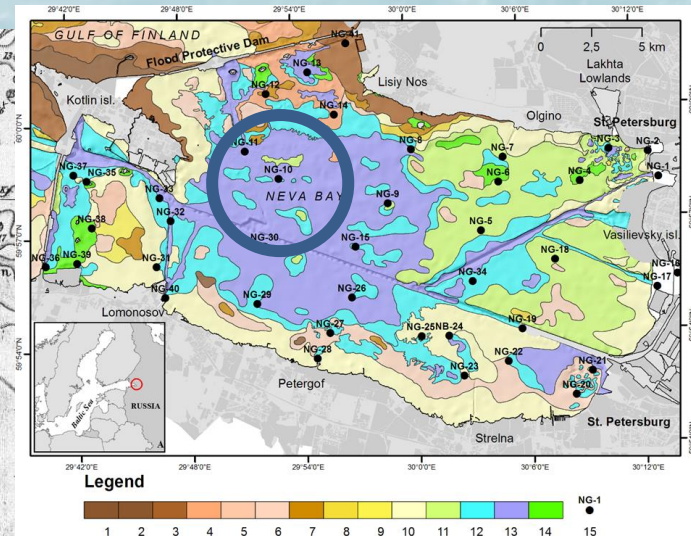
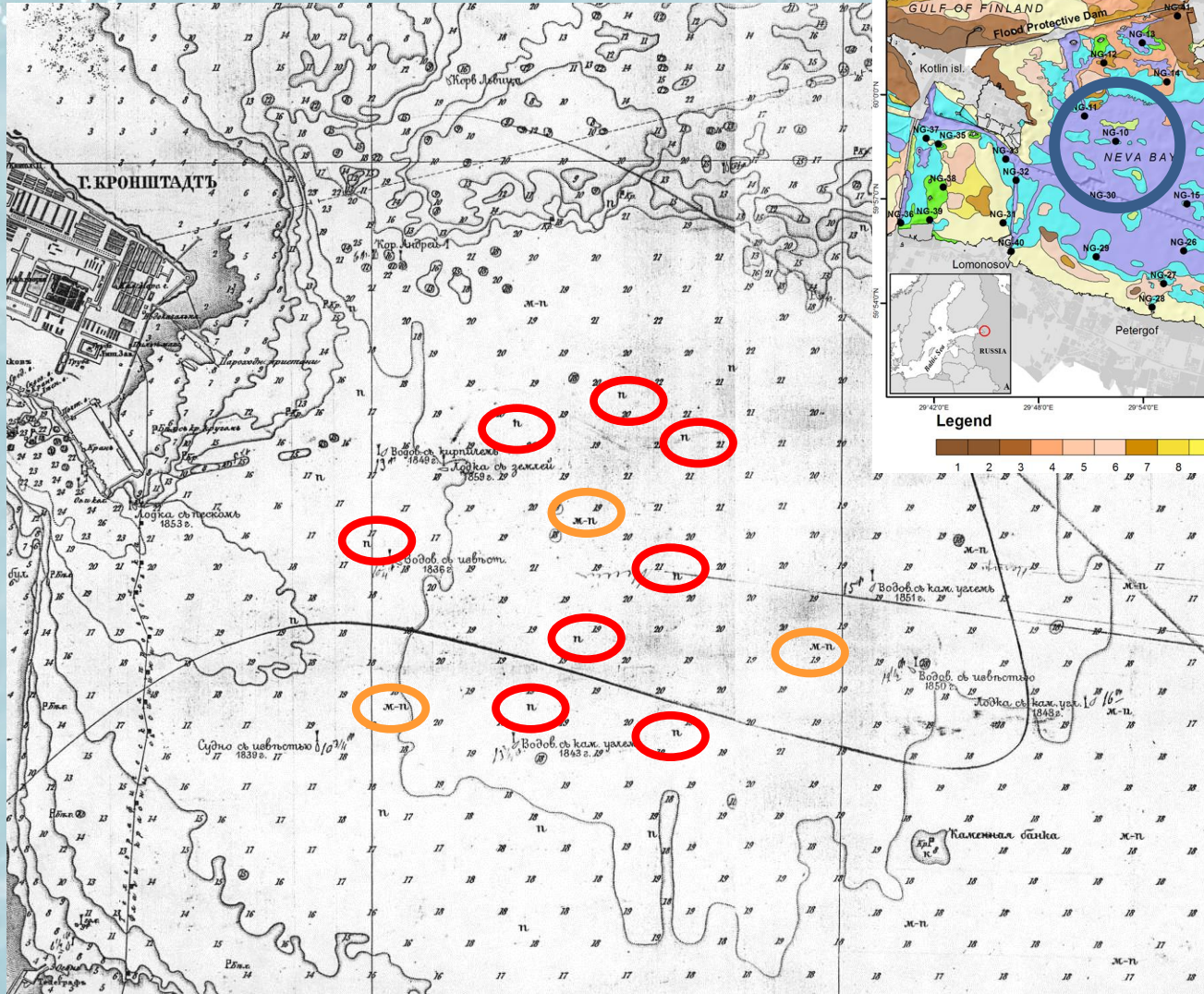


1989-1990 – state geological survey;
 1993-1995 – environmental geological study (VSEGEI);
 1999-2009 – geoenvironmental monitoring (SEVMORGEO);
 2004-2005 – geochemical research (GTK-VSEGEI);
 2011-2015 - geoenvironmental monitoring (VSEGEI)

Sea floor substrate map for Neva Bay and location of monitoring sampling sites.
 1 – boulders, pebbles; 2 – pebbles, gravel; 3 – boulders, pebbles, sand; 4 – unsorted sand; 5 – mainly coarse-grained sand; 6 – unsorted, mainly medium-grained sand; 7 – mainly fine-grained sand; 8 – sand with gravel; 9 – coarse-grained sand; 10 – medium-grained sand; 11 – fine-grained sand; 12 – silty sand; 13 – silt; 14 – silty clay-rich mud; 15 – mixed sediments; 15 – sediment sampling sites from the 2011-2015 survey.



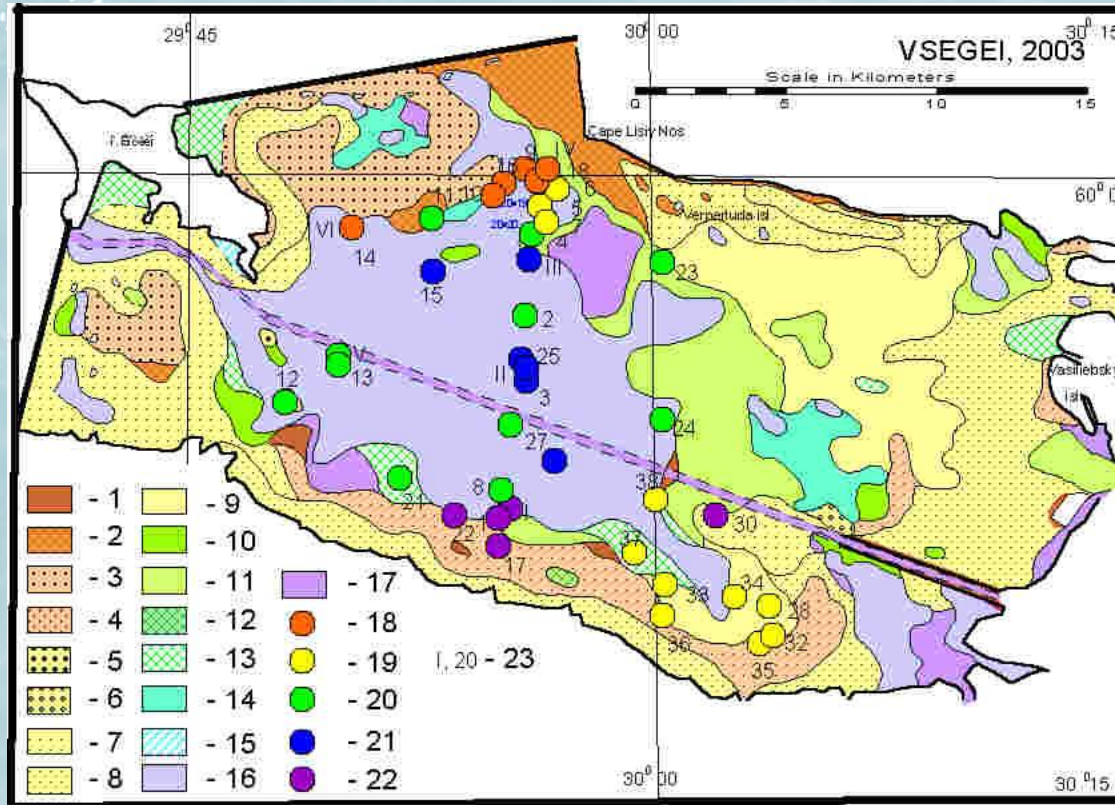
Comparison of 19th century nautical charts with modern data



 - sand
 - fine sand

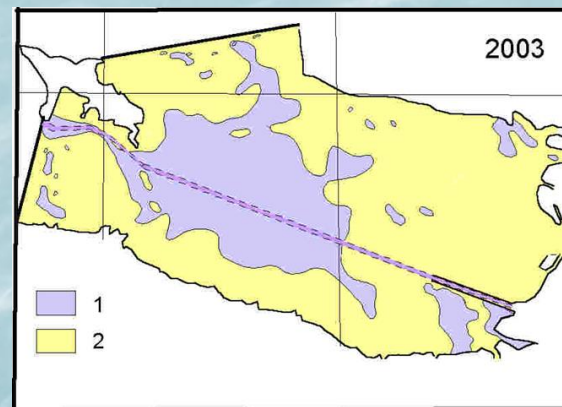
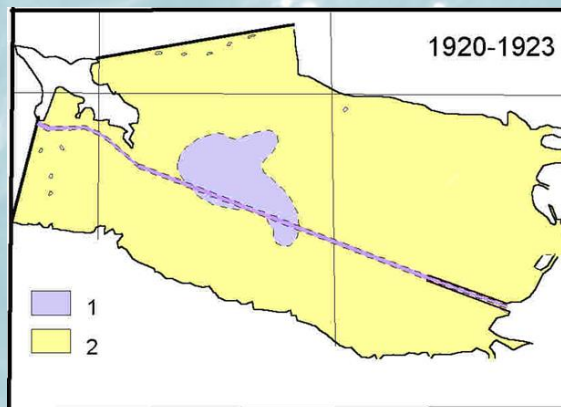
Fragment of the nautical chart of the Neva Bay, 1860.

Comparison of 1920-1923 expedition results with modern data

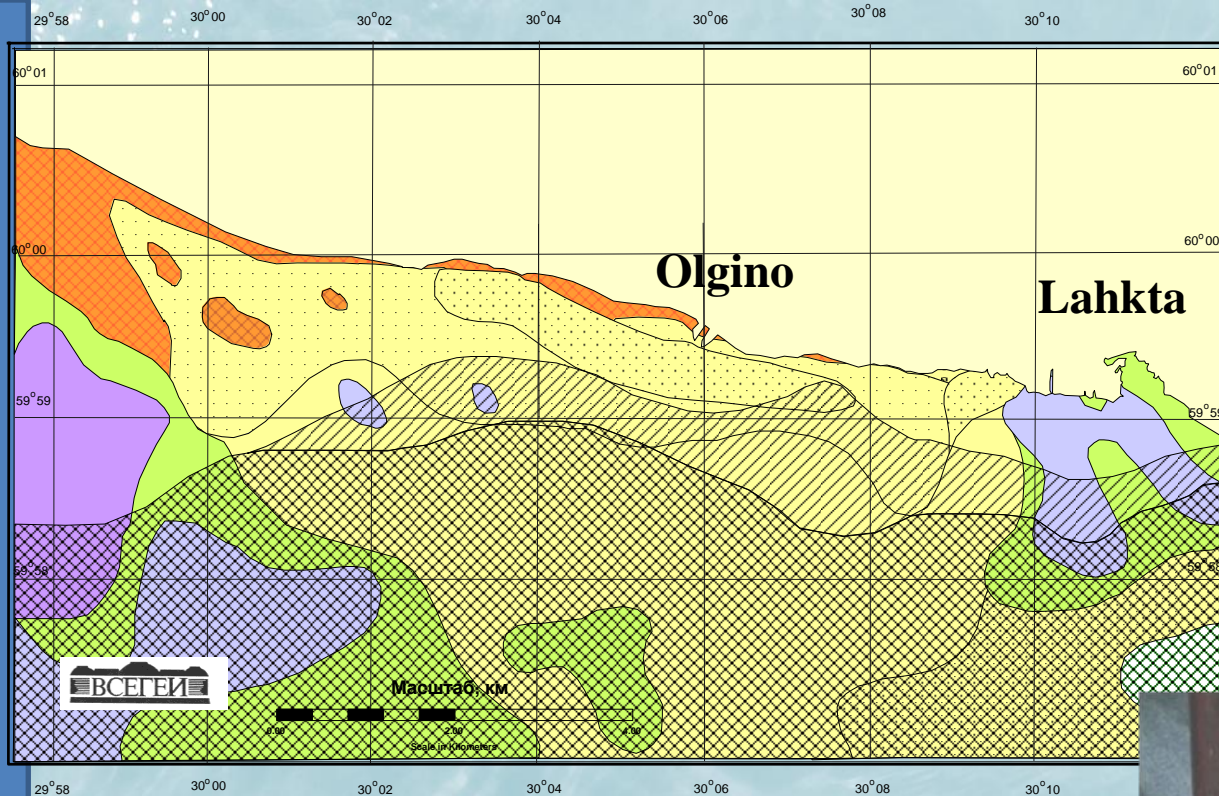


**Blue circles –
clayey mud
(1923)**

**Expansion of silty-clay
mud accumulation area
during 20th century
based on comparison
of prof. K.Derugin's
expedition (1923) and
results of geological
survey (1989-2003)**

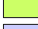


**1 – silty-clayey
mud;
2 – other sediment
types.**





Условные обозначения

Типы поверхностных осадков:

-  - пески с гравием и галькой
-  - пески средне-мелкозернистые
-  - пески мелкозернистые
-  - пески тонкозернистые
-  - алевриты песчаные
-  - алевриты пелитовые
-  - обнажения ледново-озерных глин

Поверхностные техногенные отложения, сформировавшиеся в 2006-2008 гг.:

-  - слой алевроглинистого наилка мощностью менее 5 мм
-  - слой алевроглинистого наилка мощностью от 5 мм до 5 см



07-Ляхта-14



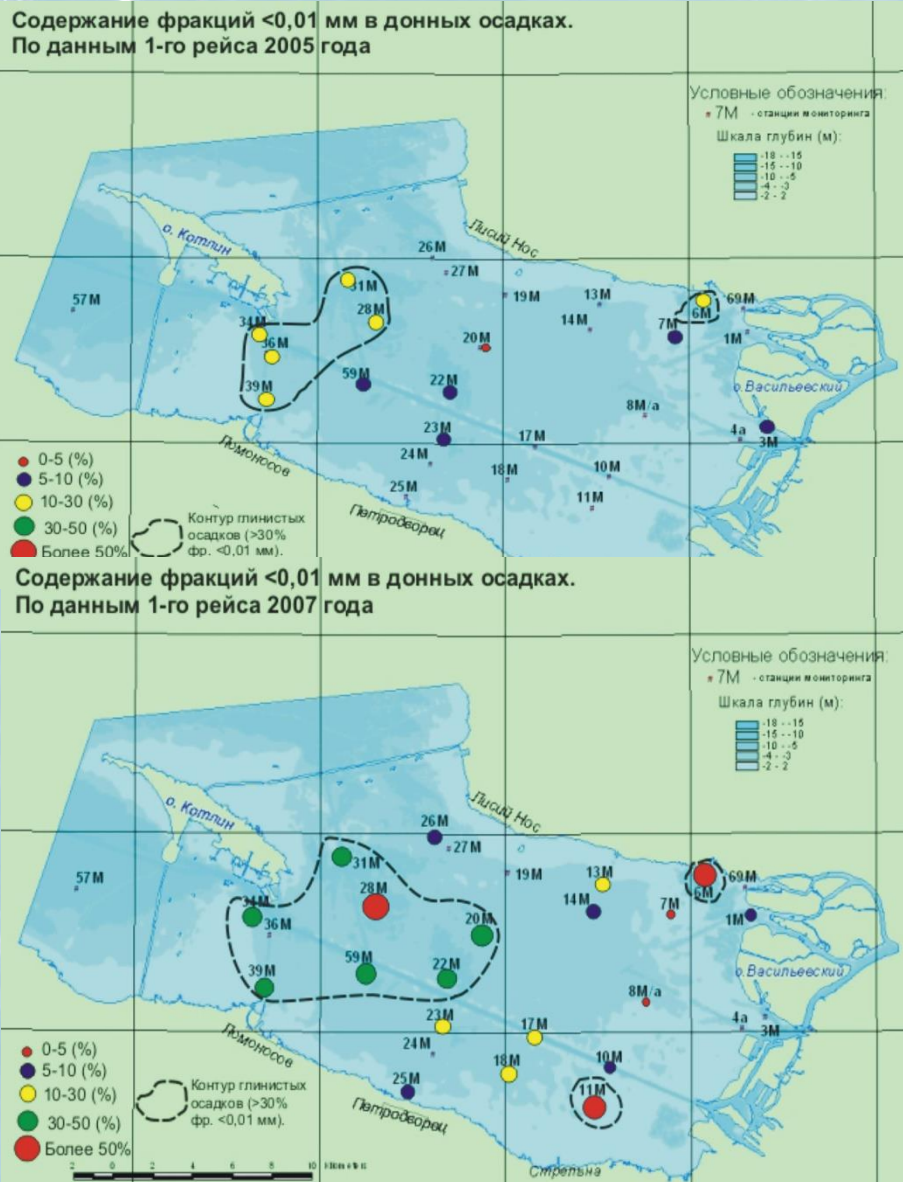
07-Ляхта-16



07-Ляхта-7

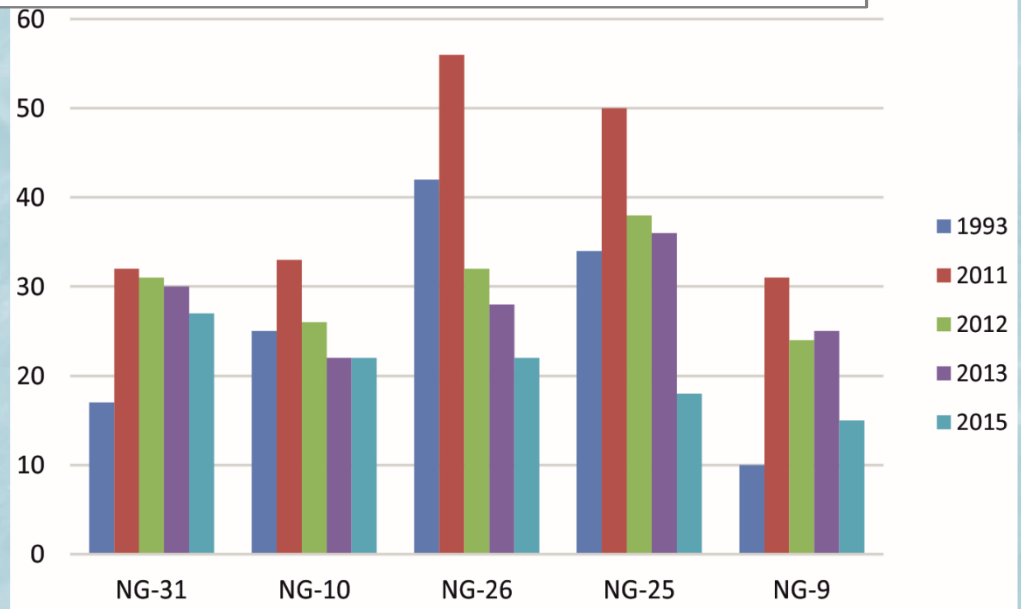
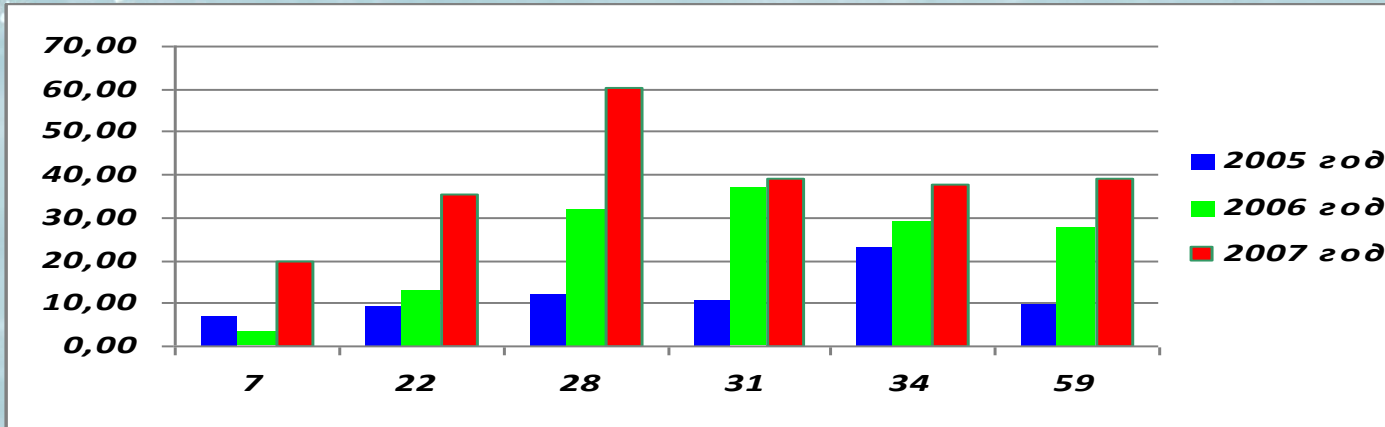


Changing the content of grain-size fractions $<0,01\text{ мм}$ in bottom sediments from 2005 to 2007



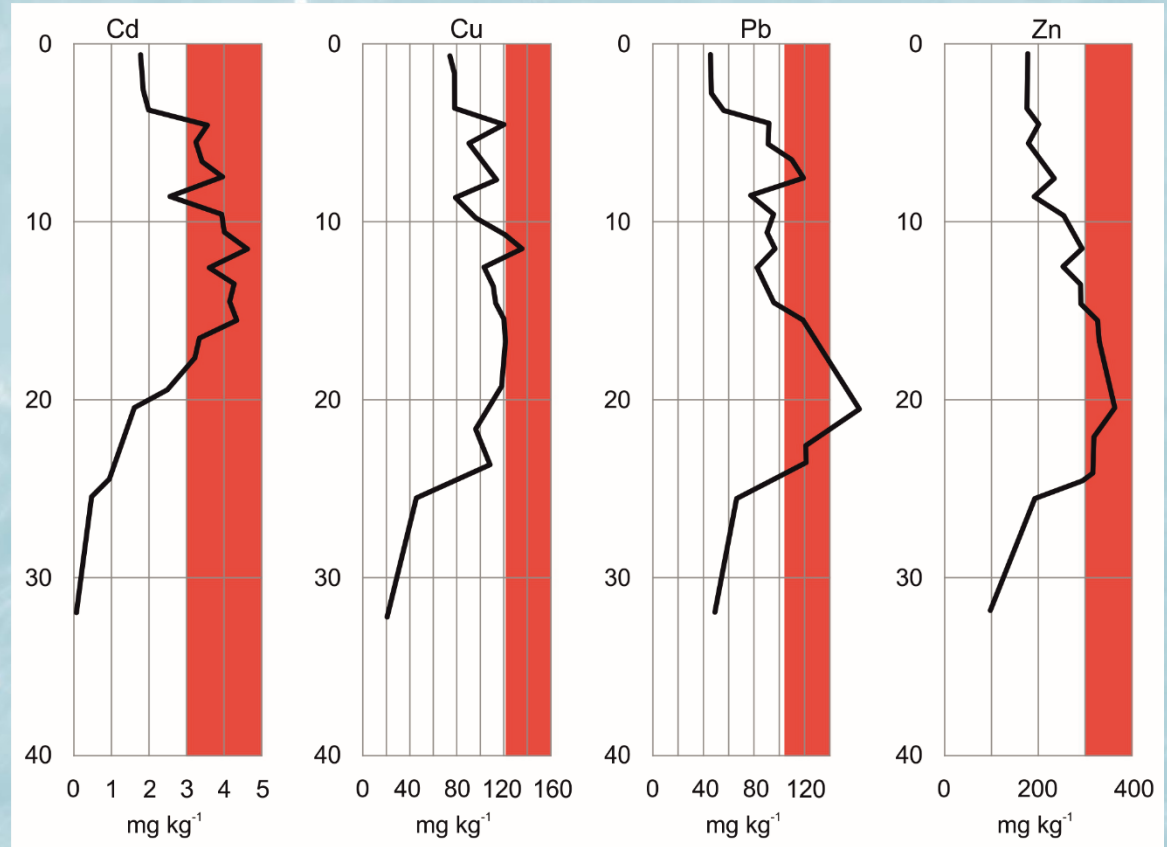
- In May 2005, the maximum content of the clay fraction was noted only in sediments in the western part of the Neva Bay, in 5-meter deep
- In May 2007, the area of clay sediments has expanded, and the content of pelitic fraction in some samples exceeded 50%

Relative abundance of <0.01 mm grain-size fraction in the upper 1 cm of Neva Bay benthic sediments (2005-2009)



Relative abundance of <0.01 mm grain-size fraction in the upper 1 cm of Neva Bay benthic sediments (1993-2015).

Concentration curves for cadmium (Cd), copper (Cu), lead (Pb), and zinc (Zn) in Neva Bay sediment cores (NG-2005-9).



Vertical axis shows core depth while red zone marks the “very high” contamination thresholds for respective metals in sediment according to Swedish EPA (2000) guidelines. Compiled by H.Vallius, 2006.

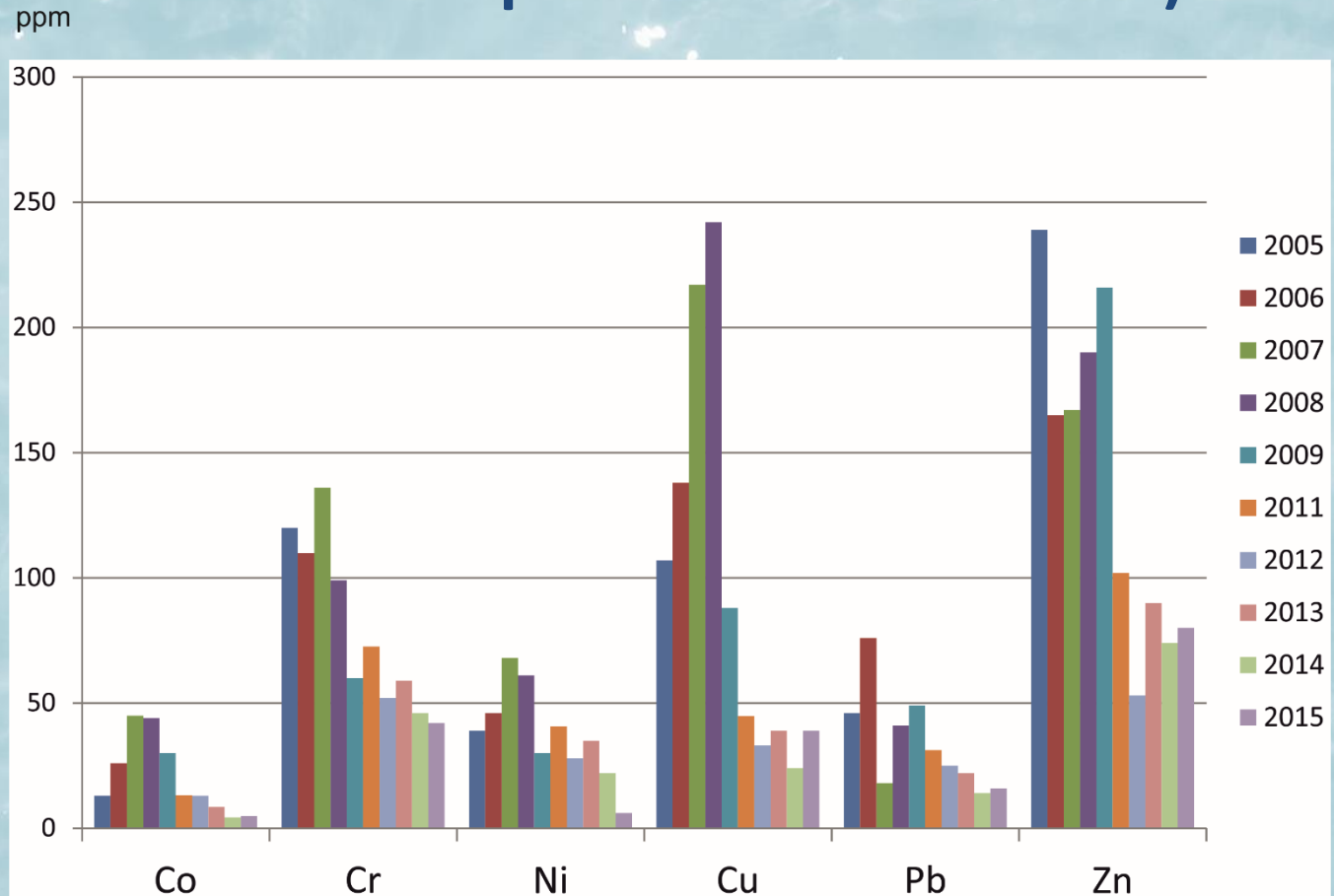
IKONOS, October 2, 2006
Concentrations of suspended matter: 1 –very high;
2 – high; 3 – medium; 4 –low;
5 –oil pollution; 6 –shallows;
7 – constructing harbor.



Aqua/MODIS 14 November 2007
Suspended matter concentrations:
1 –very high; 2 –high; 3 –medium;
4 –low; 5 –clouds; 6 –shadows of clouds.

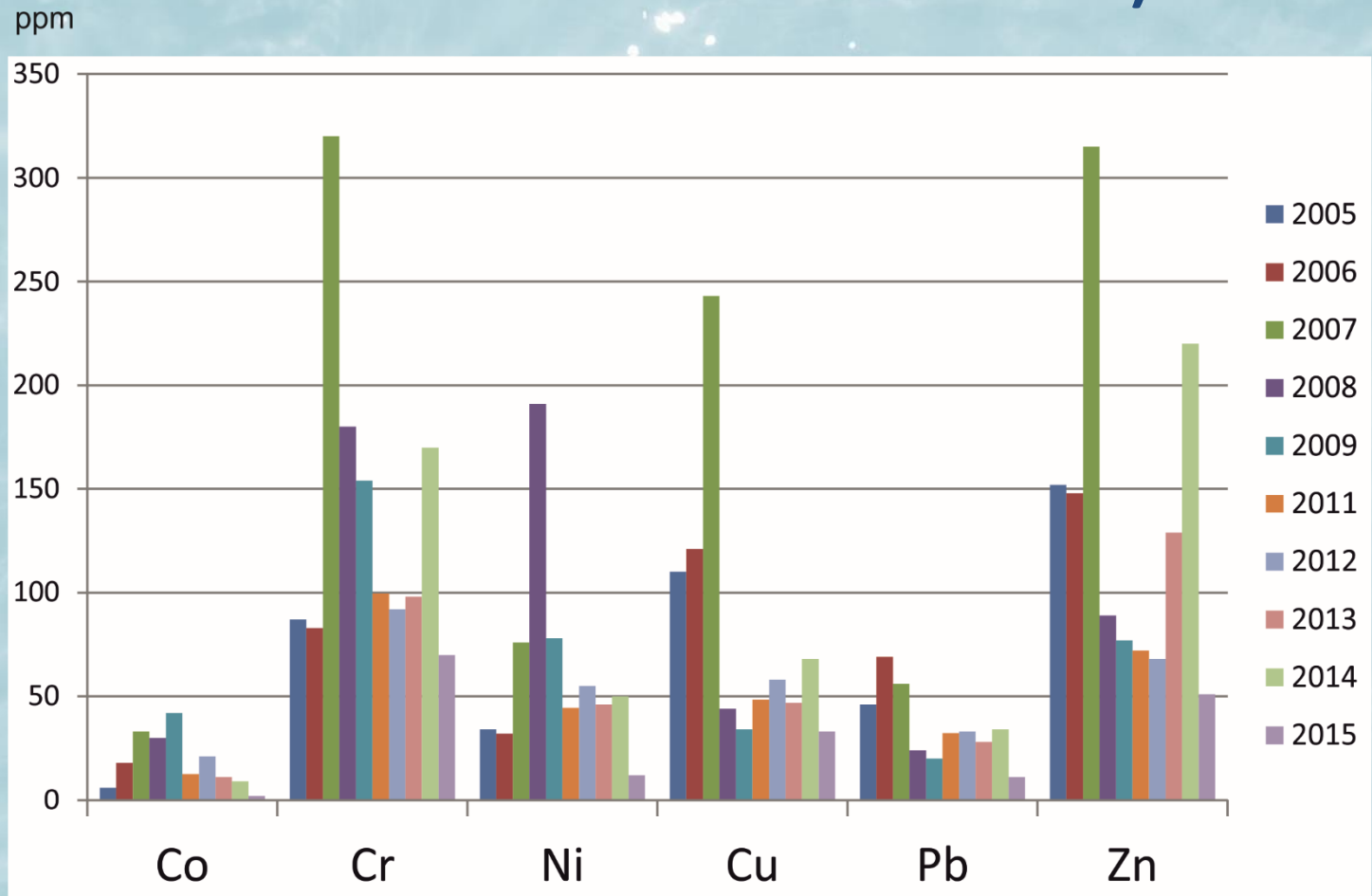


Heavy metal concentrations for Site NB-3 (from artificial depressions near Lakhta)



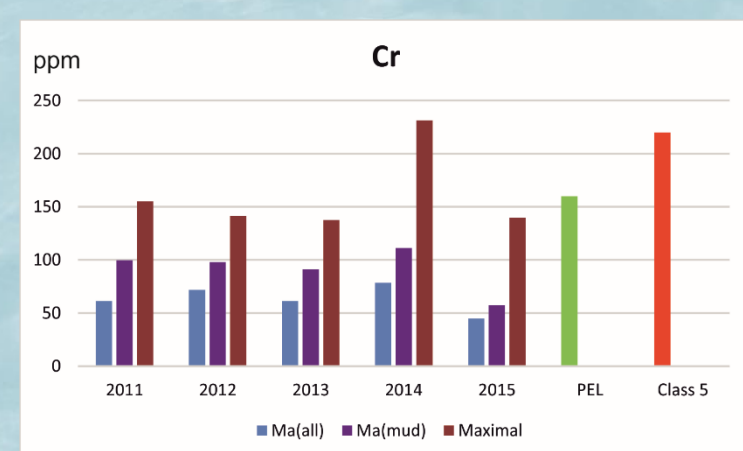
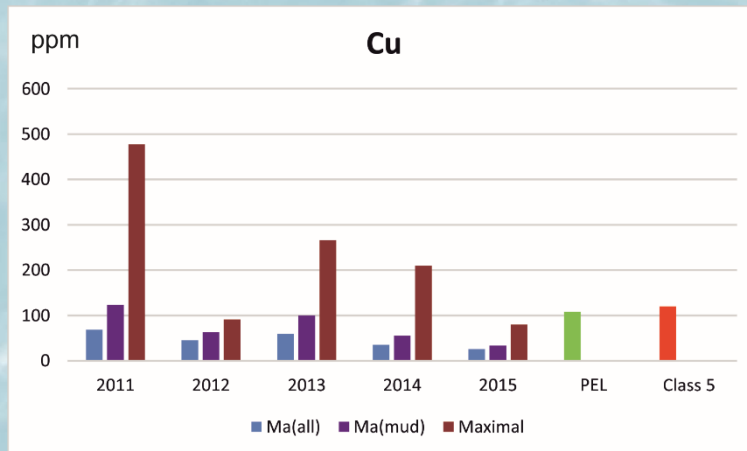
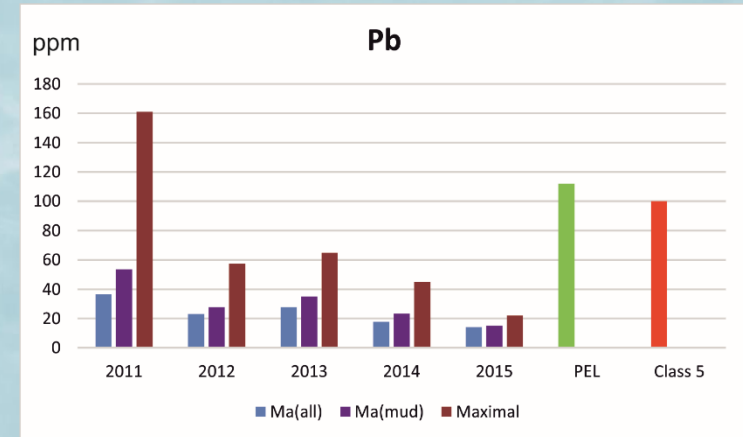
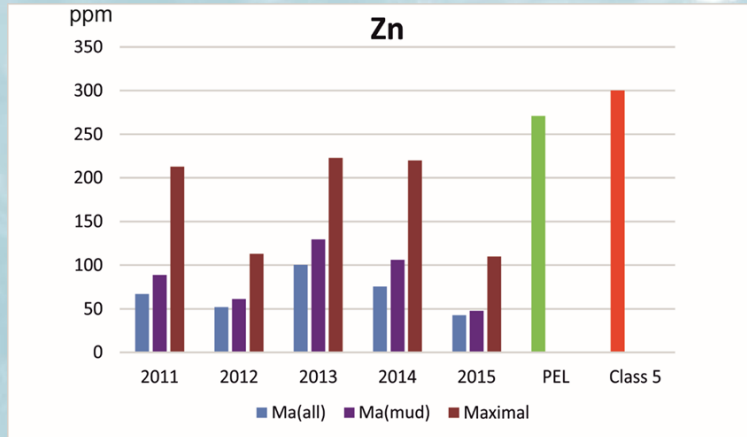
Data from 2005-2009 collected by Sevmorgeo and 2011-2015 data collected by VSEGEI.

Heavy metal concentrations for Site NB-10 (from the western sedimentation basin)



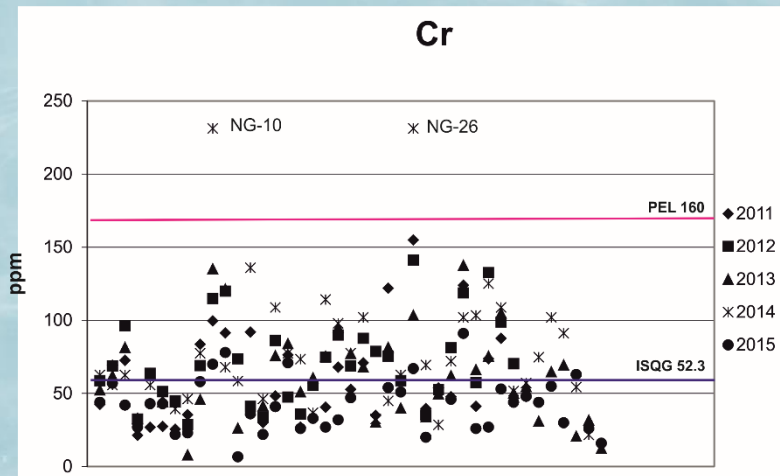
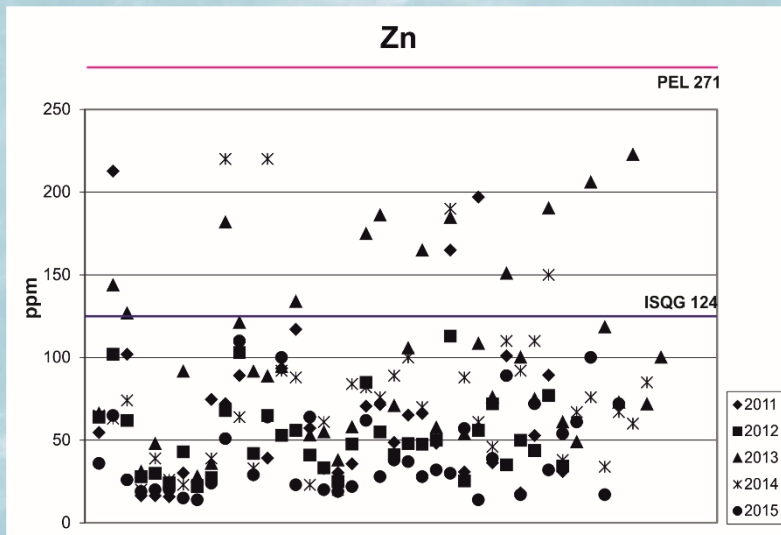
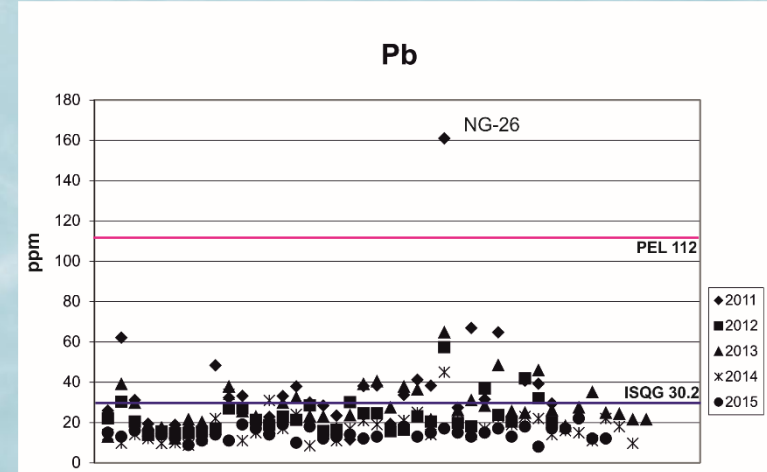
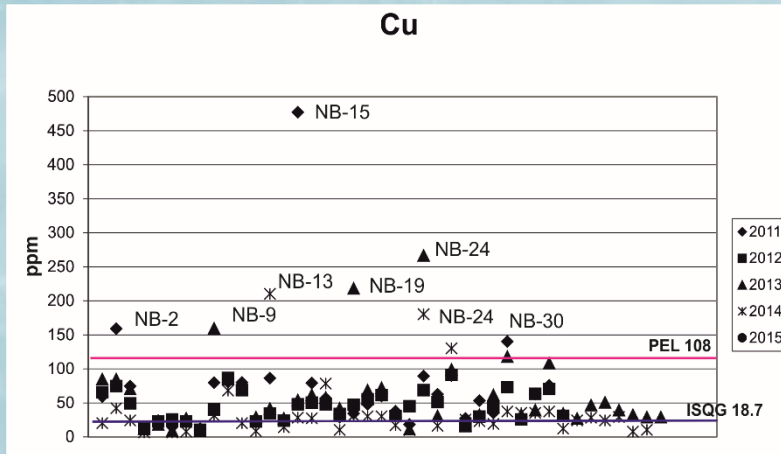
Data from 2005-2009 collected by Sevmorgeo and 2011-2015 data collected by VSEGEI.

Progression of mean and maximum heavy metal concentrations measured in Neva Bay benthic sediments from 2011-2015



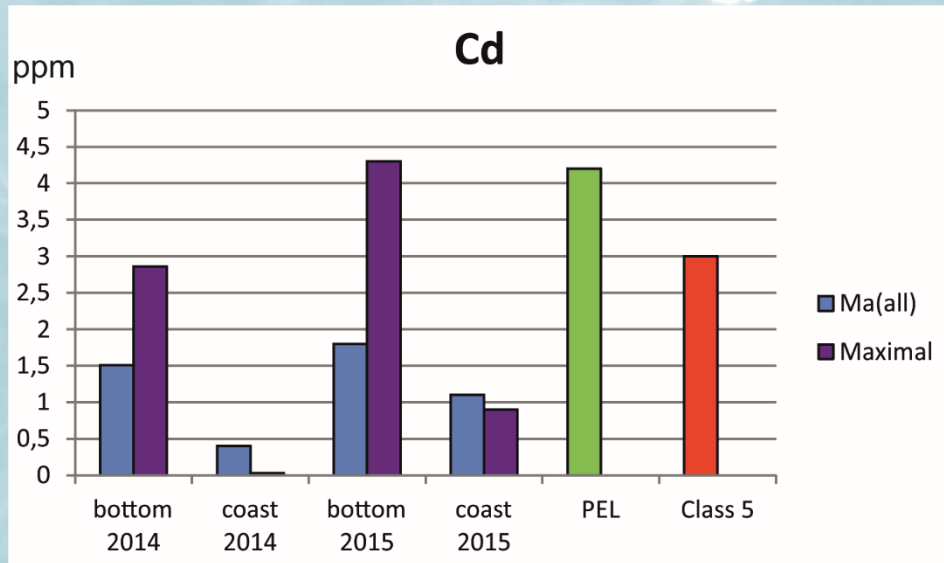
PEL= probable effect level, CCME, 2002; Class 5 = “very large” contamination, Swedish EPA, 2000. Ma(all) – arithmetic mean of concentrations across all grain-size fractions; Ma(mud) - arithmetic mean of concentrations in soft muddy sediments from areas of active accumulation.

Concentration of copper, lead, zinc and chromium (ppm) in Neva Bay benthic sediments



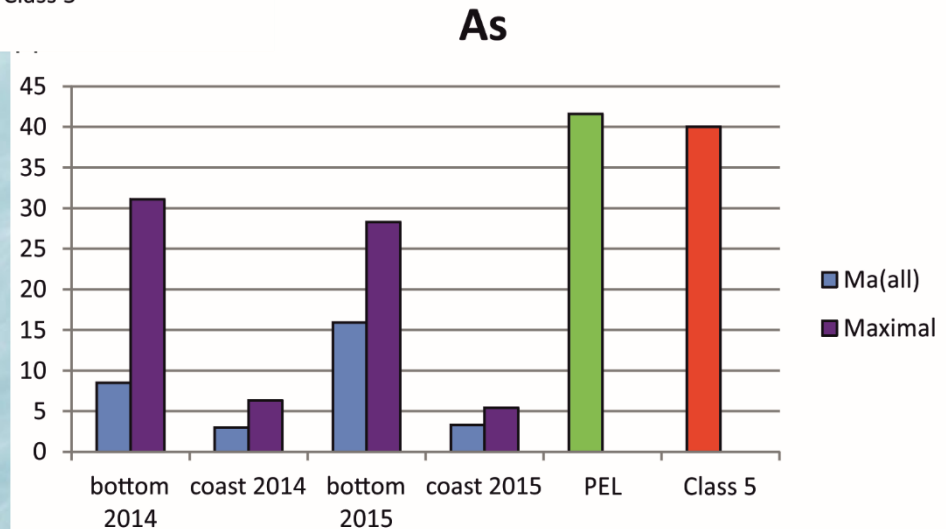
Horizontal lines; ISQG = interim sediment quality guideline and PEL = probable effect level; CCME, 2002

Mean (Ma) and maximum Cd and As concentrations (ppm) in Neva Bay benthic and backshore (coastal/beach) sediments

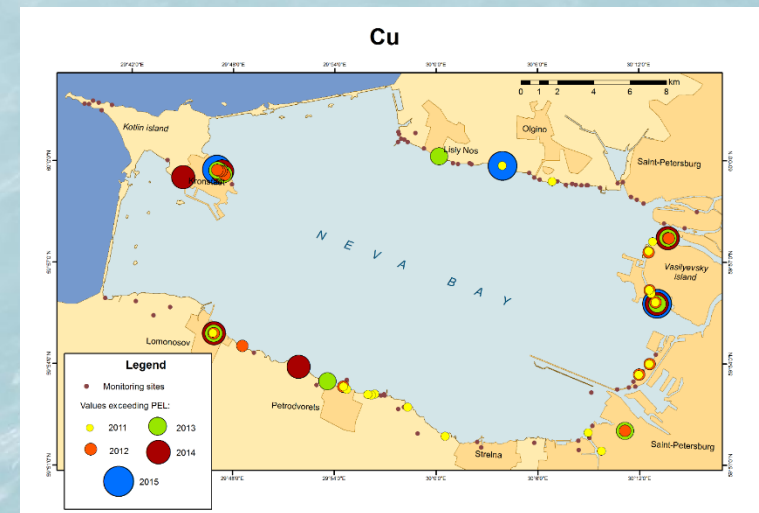
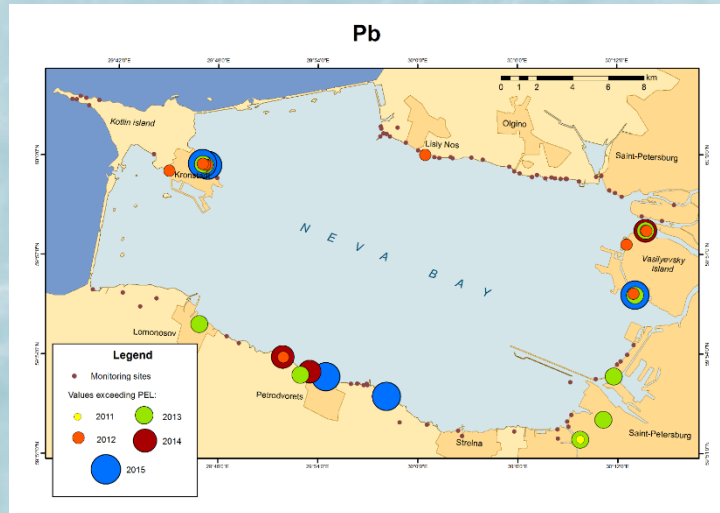
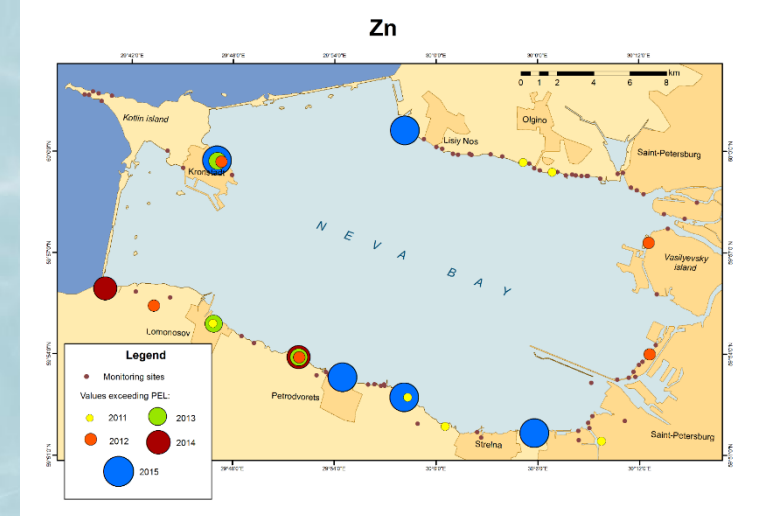
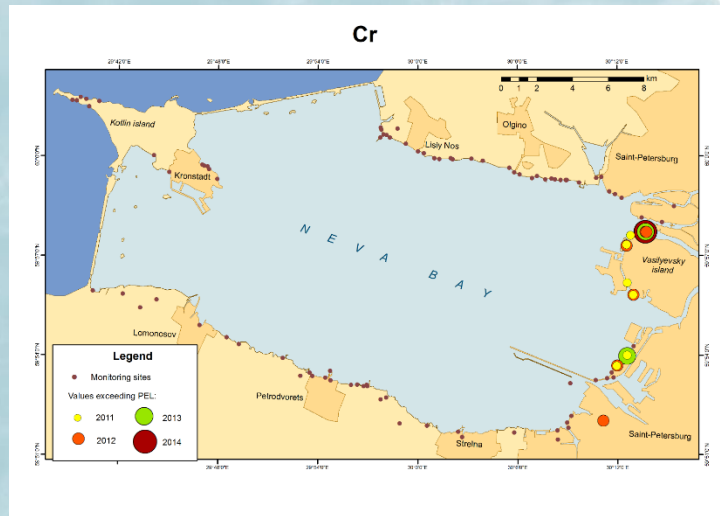


PEL= probable effect level, CCME, 2002; Class 5 = “very large” contamination, Swedish EPA, 2000

Ma(all) – arithmetic mean of concentrations across all grain-size fractions; **Ma(mud)** - arithmetic mean of concentrations in soft muddy sediments from areas of active accumulation.



Location of monitoring sites with heavy metal concentrations, exceeding PEL (PEL= probable effect level)



Conclusions

Coastal sedimentation basins around Neva Bay record a unique history of pollution. Metals began to accumulate rapidly in the first half of the 20th century. The highest concentrations occur in upper sections of sediment cores represent a time frame spanning from the 1950's to 1990's. Heavy metal concentrations subsequently decreased significantly from 1995 to 2005.

Intensive dredging in 2006-2007 resuspended and redistributed contaminated sediment around Neva Bay causing a dramatic increase in benthic sediment heavy metal concentrations.

Pollution history of Neva Bay bottom sediments is closely linked with changing of sedimentation conditions over the last three centuries causing the aerial extent of mud deposition expanding significantly during the 20th century.

Extremely high concentrations of heavy metals persist in backshore (coastal/beach) sediments around Neva Bay.

Future investigations

1. Continuation of monitoring ?
2. Development of Sediment Quality Standards for the EGoF
3. Study of background concentrations of harmful substances; natural and anthropogenic components in surface sediments
4. Modeling of sediment flows and possible secondary pollution of GoF environment

A sunset over a body of water with mountains in the distance. The sky is filled with soft, pink and orange clouds, and the water reflects the warm colors. A small, dark object is visible in the water on the right side.

Thank you for attention!

From small scales to large scales
–The Gulf of Finland Science Days 2017
9th-10th October 2017
Estonian Academy of Sciences, Tallinn

2nd Day



**Gulf of Finland
Co-operation**

S. Kholodkevich, T. Kuznetsova, A. Kurakin, A. Sharov

Development of a new approach in the assessment of biological effects of pollution in the Gulf of Finland

Development of a new approach in the assessment of biological effects of pollution in the Gulf of Finland

*Sergey Kholodkevich^{1,2}, Tatiana Kuznetsova¹,
Anton Kurakin¹, Andrey Sharov¹*



¹Institution of Russian Academy of Sciences Saint-Petersburg Scientific Research Center for Ecological Safety RAS;

² Saint-Petersburg State University



Now in the majority of the countries steady interest to on-line systems of monitoring environmental state using benthic invertebrates is observed.

Invertebrates have sufficient sensitivity for detection of chemical stress in the environment, e.g., aquatic ecosystems, including surficial, treated sewage and drinking water.

In our studies to assess ecosystem health (state) we use instrumental systems and technologies based on measurements of ecotoxicological biomarkers.

Ecotoxicological biomarker is a biochemical, cellular, physiological or behavioral variation that can be measured in tissue or body fluid samples or at the level of whole organisms that provides evidence of exposure to and/or effects of one or more pollutants (and/or radiation) (Depledge, 1993).

The biomarker concept, initially developed to form a basis for studies at the individual/population level, is extended to include community and ecosystem level studies. A strategy is outlined in which biomarkers might be used to assess chemical exposure and the cumulative, adverse effects of toxicants on biota *in situ* (Depledge et al., 1995).

«Healthy animals, healthy ecosystems»

MH Depledge and TS Galloway, 2005. *Front Ecol Environ* 3(5): 251–258

In a nutshell:

- To have a *healthy ecosystem*, the constituent animals, plants, and microbes must, on the whole, *be healthy*
- Recent technological advances have led to the *development of sensitive, robust, and environmentally relevant biological responses (biomarkers) that measure exposure to pollutants* and to give an assessment of the health status of individual animals
- By *measuring the health status* of a range of species representing different phylogenies and feeding types, we can use a weight of evidence approach to envisage *the ecological consequences of pollutant exposures*

Backgrounds of the method



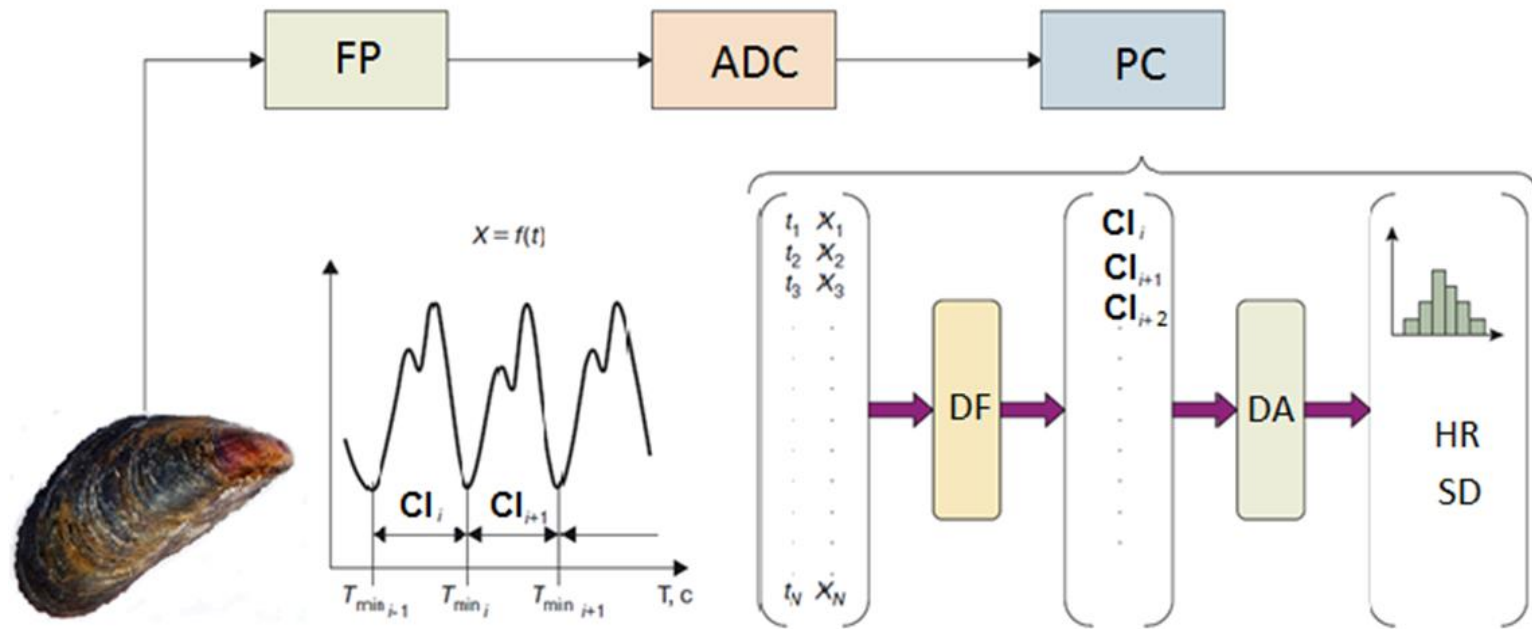
Chronic pollution of the aquatic ecosystems is reflected on the target invertebrates species *adaptive capacities*.

Health of organisms from sites different in anthropogenic pressure could be assessed *by standardized tests, based on analysis of recovery time of registered physiological and/or behavioural characteristics* of tested organisms after *a short-term functional loading* in the range of species tolerance.

In the frame of our studies it was shown that *mollusks and crustacean from clean sites differ from polluted areas by recovery time of their cardiac activity pattern and behaviour* after standardized test-treatment (Turja et al., 2014; Kholodkevich et al, 2017 J.Mar. System).

In 2010 at Winberg-2010 Conference for bioindication of ecosystem state in order to obtain accurate monitoring data on chemical stress in the invertebrates we proposed to use 2 new biomarkers:

- heart rate recovery time (Trec, mins) after rapid change of medium salinity - test used as functional load ;**
- coefficient of HR variation (CV, %) over the group of tested organisms after removal of load.**



Block-scheme of set up and automatic data processing. FP – photoplethysmograph, ADC – analog-to-digital converter, PC – portable computer, CI – cardiac interval, DF – digital filter, DA – distribution analysis, HR – heart rate, SD – standard deviation. Main mathematical characteristics of cardiac interval sample (no less 50-100).

Organisms we usually use for monitoring exposure to or the effects of environmental pollution in the sites of the Gulf of Finland:

Unionidae, *Mytilus* spp., *Macoma balthica*,

Astacus leptodactylus

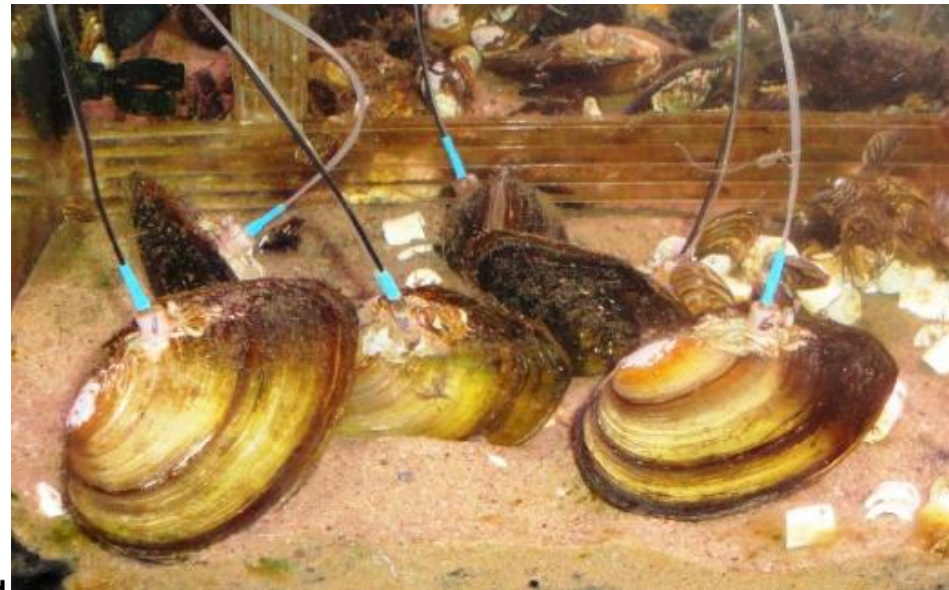
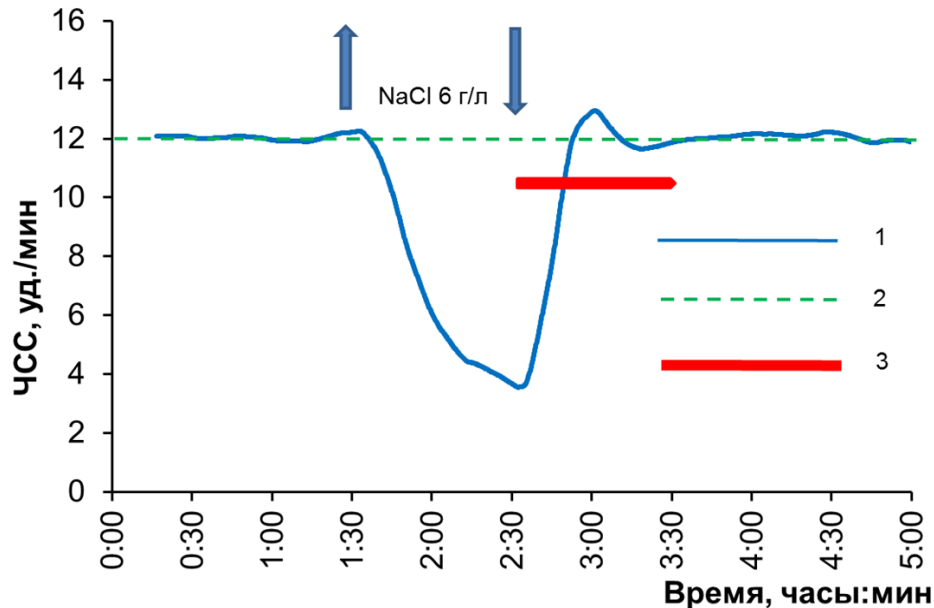


Method in use

Diagnostic of functional state of mollusks was done by analysis of characteristics of cardiac activity measured by non-invasive fiber-optic method and by the use of hyper- or hypo-osmotic treatment.

Biomarker **Trecov**:

Time of HR recovery to background level (after restoration of water salinity in tank)



- 1 – background pattern of HR of mollusk,
- 2 – mean value of HR,
- 3 – HR recovery time after removal of load.

Freshwater mussels from
the Eastern Gulf of Finland

In the recent report the examples of application of suggested biomarkers

in organisms from different aquatoria:

- the Gulf of Finland** (*Kholodkevich et al., 2017*),
- **the Bothnian Sea** (*Turja et al., 2014*),
- **the Gulf of Riga and a few lakes in Latvia** (*Kurakin et al., 2012*),
- **the Boka Kotorska Bay (Montenegro, Adriatic Sea),
and in rivers of the Yaroslavl Region.**

Examples of the caged mussels experiments in use



Assessment of biological effects of anthropogenic chemical stress:

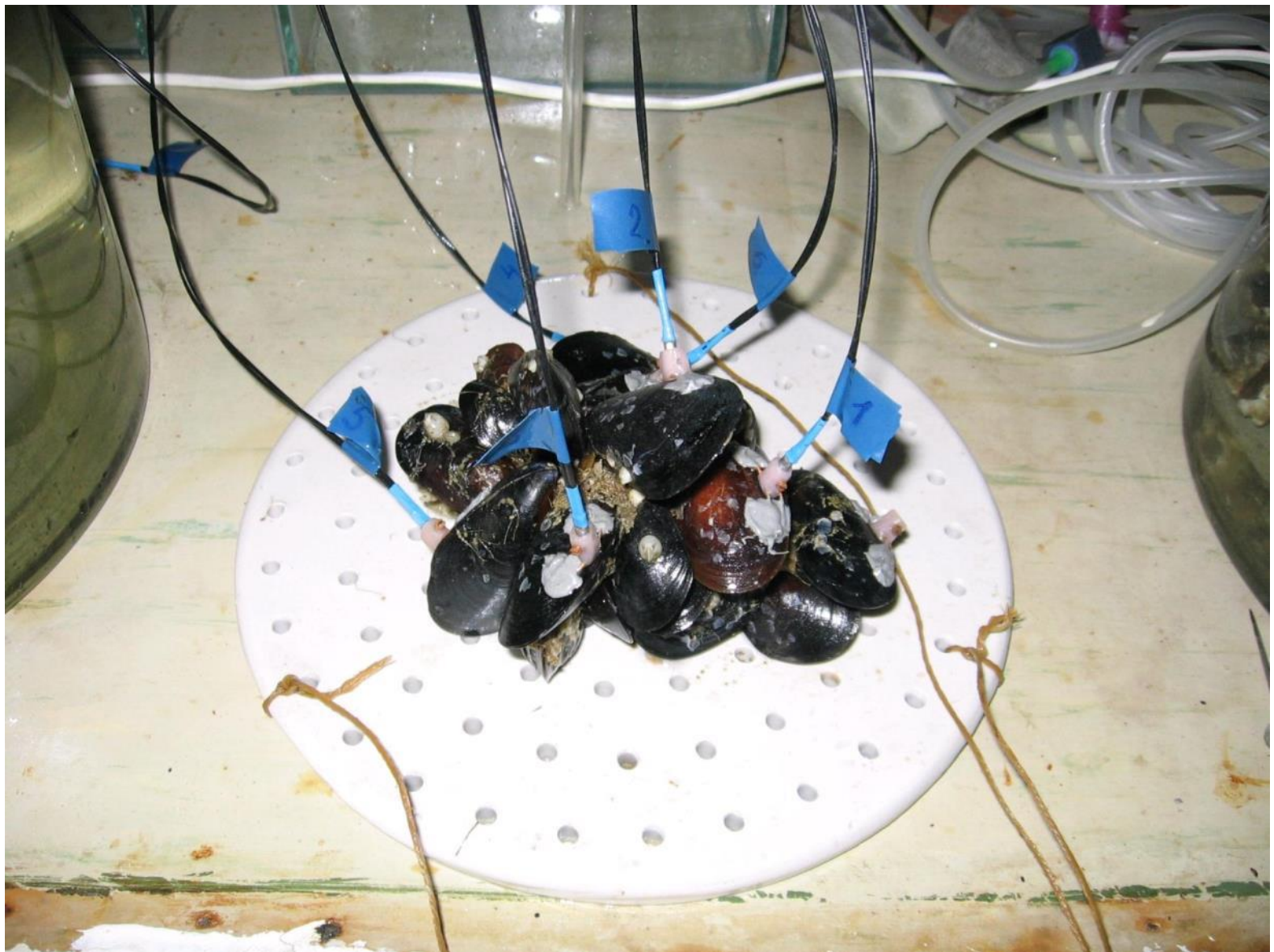
Method was approbated in the EU-funded projects for ecosystem health assessment of the Baltic Sea sub-regions :

- BONUS+BEAST Program (Biological Effects of Anthropogenic Chemical Stress: Tools for the Assessment of Ecosystem Health);
- HYDROTOX (Water Toxicity Estimation)

**Retrieving the cages
with the exposed
mussels on board of
the R/V "ARANDA"
of the Finnish
Environment
Institute
(SYKE,Helsinki)**

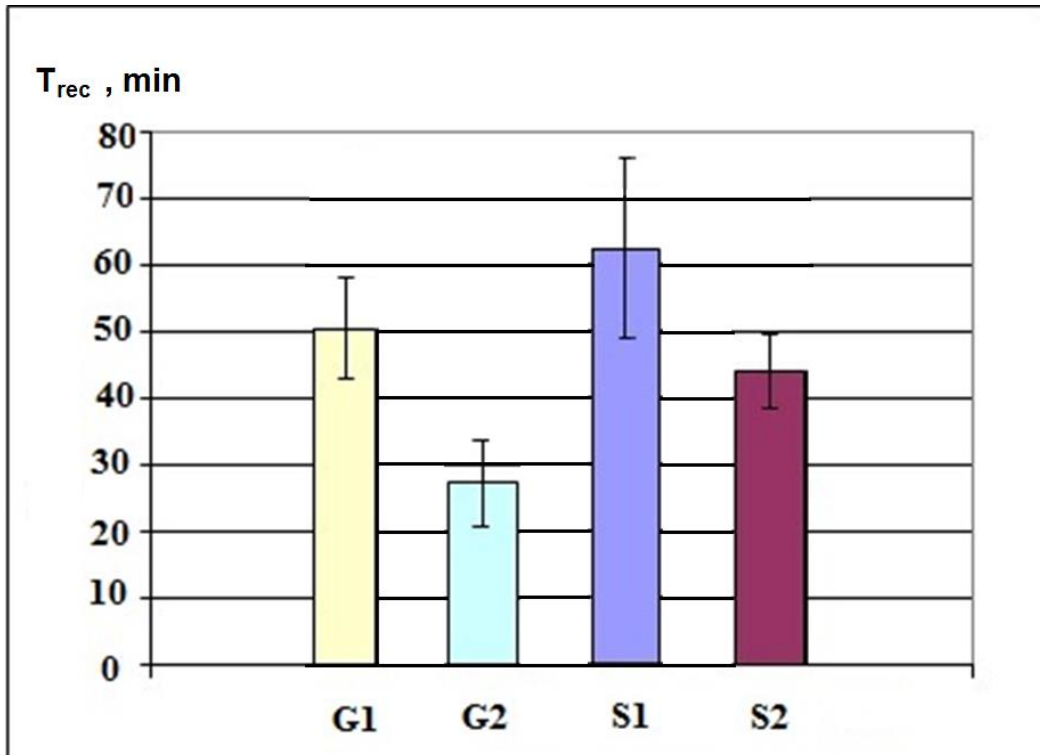
**BEAST Project
(2009-2011)**



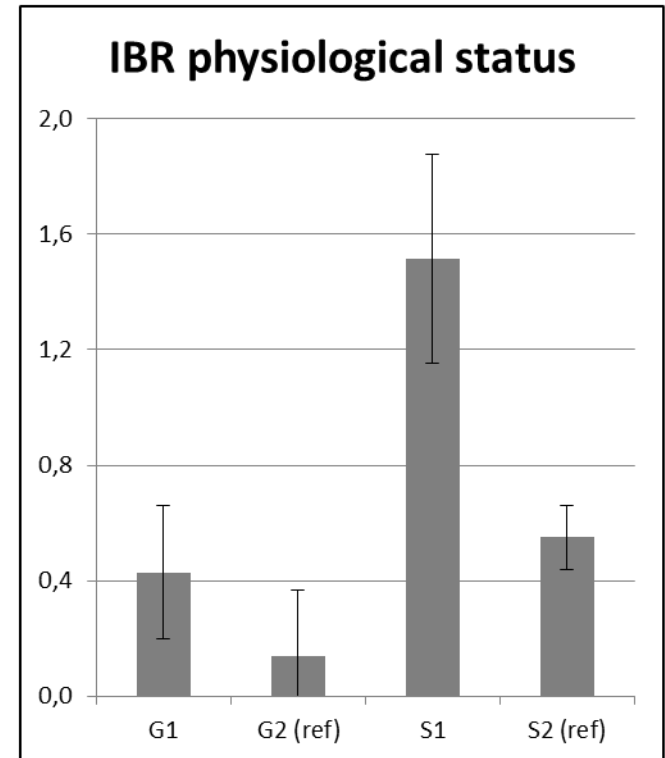


Batches of mussels with the optic-fiber sensors on their shells before deployment in cages at study sites

Integrated Biomarker Response

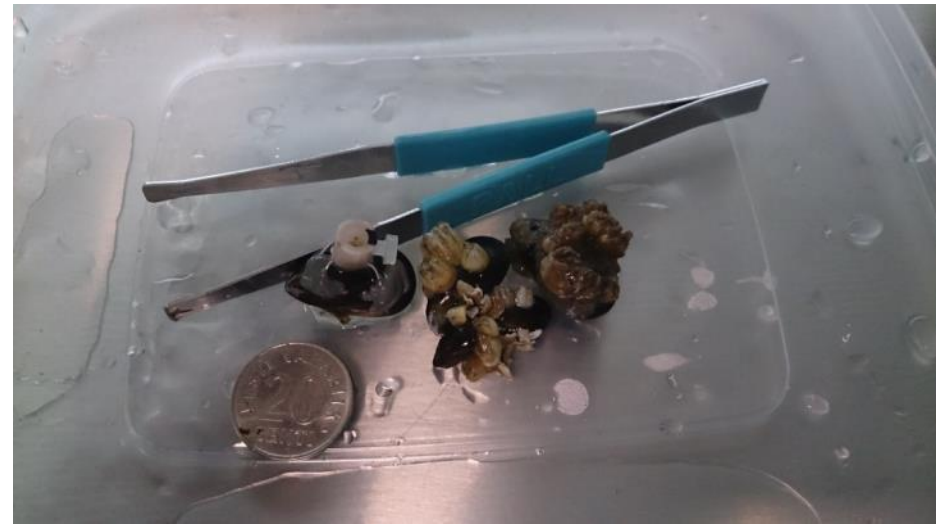


HR recovery time in mussels from stations S1, S2, G1, G2, located in the Gulf of Bothnia, Baltic Sea



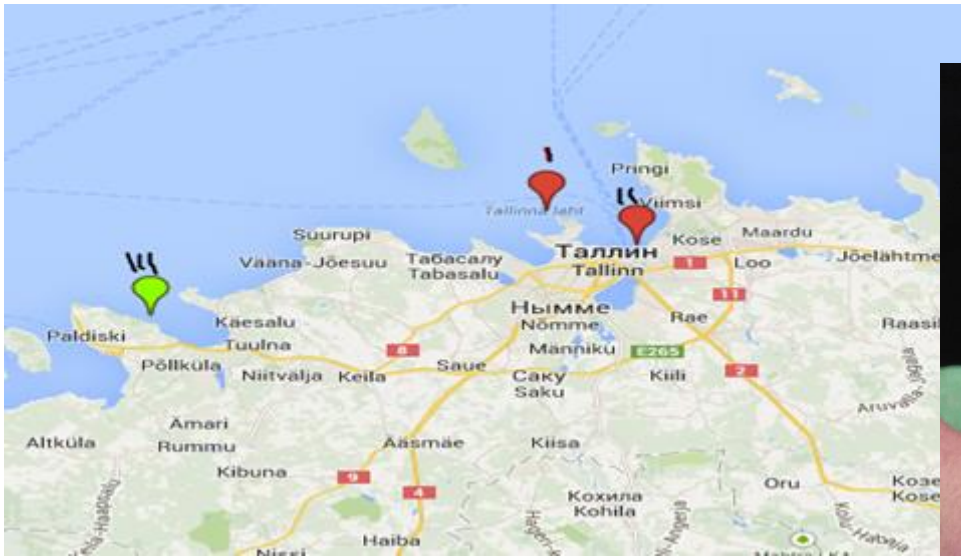
Parameters: LMS, Phagocytosis, Condition index, LPO, AChE

In laboratory testing physiological characteristics of the mussels exposed near TWWTPlant (Tallinn Bay expedition, 2014)



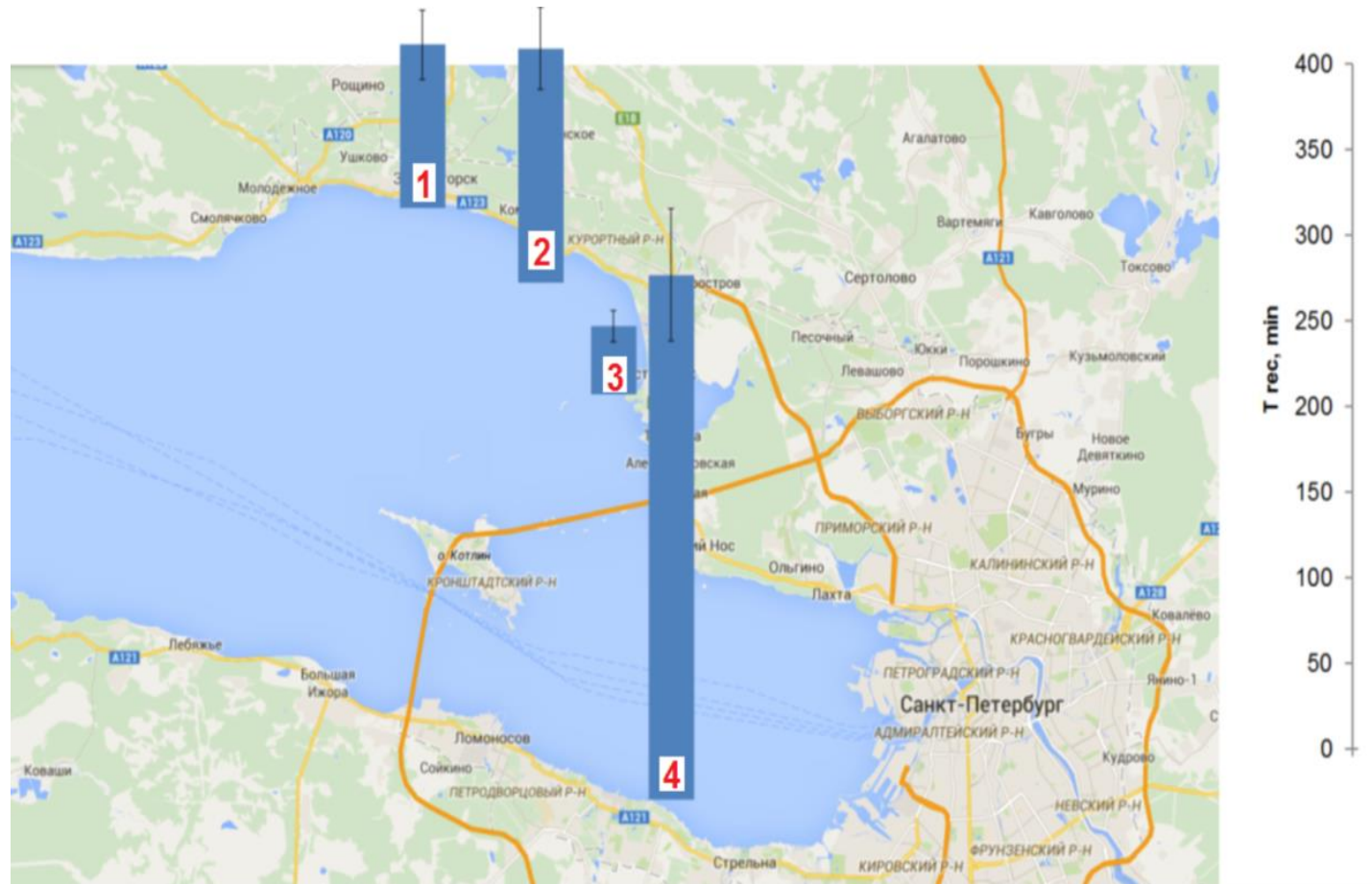
The map of study sites in the Tallinn Bay and the view of cages with mussels

green spot –reference site, red – study areas (near Pirita river and TallinnWasteWaterPlant tube)



Trec after 2 months of exposure near the TWWT tube increased from 45 min to 110min !!

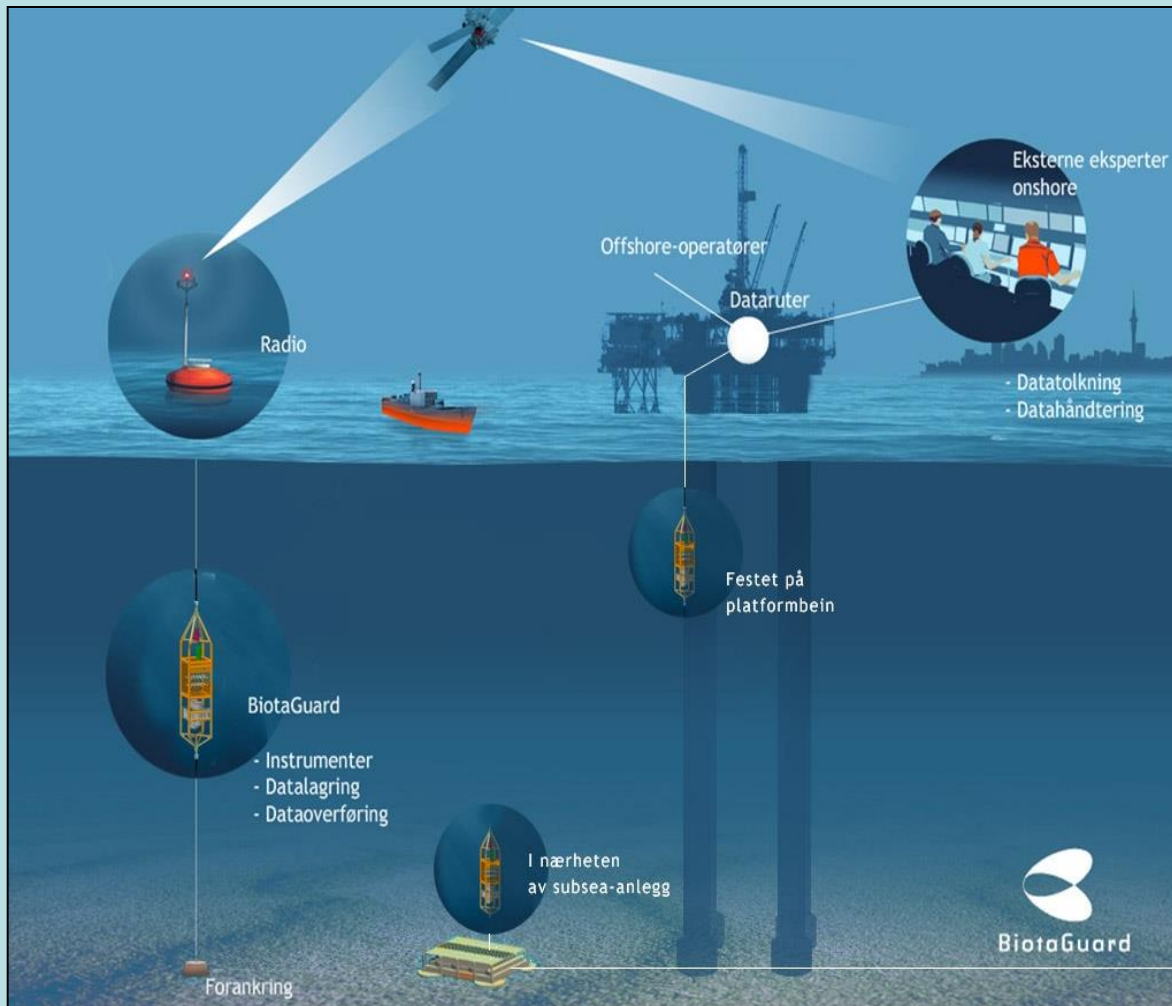
Heart rate recovery in Anodonta (n = 14) from different in pollution sites of the Eastern Gulf of Finland (2013-2014)



Mussels with valve gape sensor and with fiber optic cables attached to their valves (all non-invasive)



Bioelectronic systems of monitoring of functional state of benthic invertebrates could be useful for ecological monitoring of the sites of concern in the GoF



Implementation in:

- Ecological monitoring;
- Control of the quality of waters incoming to water supply;
- Control of the sewage waters quality;
- Aquaculture.

CONCLUSIONS

- *Monitoring of cardiac activity and behaviour* in benthic invertebrates are used as an *effective tools* in environmental pollution assessment.
- *Health of organisms* from different in anthropogenic pressure sites can be assessed by the use of bioelectronic system and *analysis heart rate recovery and behavior after a short-term functional load (salinity change)*.
- The methodological approach and method proposed could help the authorities *to discriminate sites different in ecological state and to make rapidly assessment of early signs of deterioration in biota state*.

Thank you
for your attention!

Äitah!
Kiitos!



From small scales to large scales
–The Gulf of Finland Science Days 2017
9th-10th October 2017
Estonian Academy of Sciences, Tallinn

2nd Day



**Gulf of Finland
Co-operation**

E. Mikhailova, L. Barabanova

Implication of genetic approaches for biosystem state and dynamics survey of the Gulf of Finland.

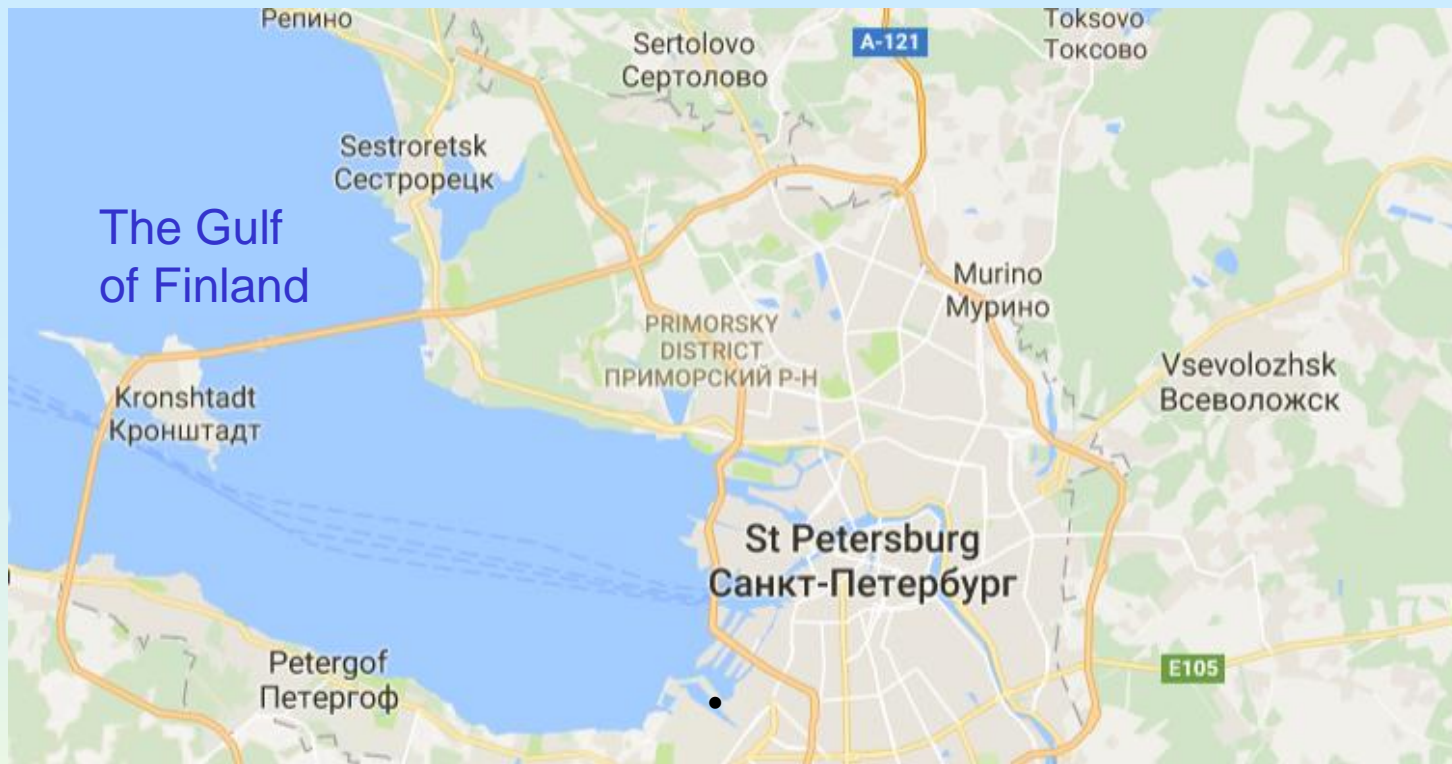


Implication of genetic approaches for biosystem state and dynamics survey of the Gulf of Finland.

Mikhailova E.I.* , Barabanova L.V.

Saint-Petersburg State University

9 - 10 October 2017



The Gulf of Finland has been subject to long-term significant anthropogenic pressure.

The latter is due to:

- heavy navigation activity and operation of seaport facilities;**
- Industrial and economic activities carried out to maintain sustainability of the coastal areas. The Dam of St.- Petersburg – one of the issues.**

Complex monitoring of ecological situation is needed, including:

- assessement of hydrological state
 - hydrochemical analyses
 - biological monitoring.
- } these studies are being carried out at regular basis

Biosystem dynamics of the Gulf of Finland has been studied by means of traditional hydrobiological methods using biodiversity criteria in particular.

This type of assessment allows for estimation of the current state of investigated biosystem at particular moment, but does not provide a long-term prognosis for possible changes.

Various genetic approaches are the source for a long-term forecast, therefore they **are indispensable for complex assessment of water system state including investigations on water organisms.**

Genetic methods give possibility:

- to estimate genotoxic effects of water pollution,
- to give a prognosis on the possible dynamics of a biosystem structure.

The Baykal amphipod *Gmelinoides fasciatus* is one of the most numerous species among alien organisms.



It became dominant in a number of water bodies of North-West of Russia – demonstration of significant influence of anthropogenic invasions on ecosystem.

The sideswimmer *Gmelinoides fasciatus* has not yet been subjected to substantial genetic studies, although

it has already been proposed as an indicator species to be used in long-term complex monitoring of the state of environmental conditions in various water bodies.

Cytogenetic characteristics of an individual species make it possible to expand data on biodiversity of biosystems.

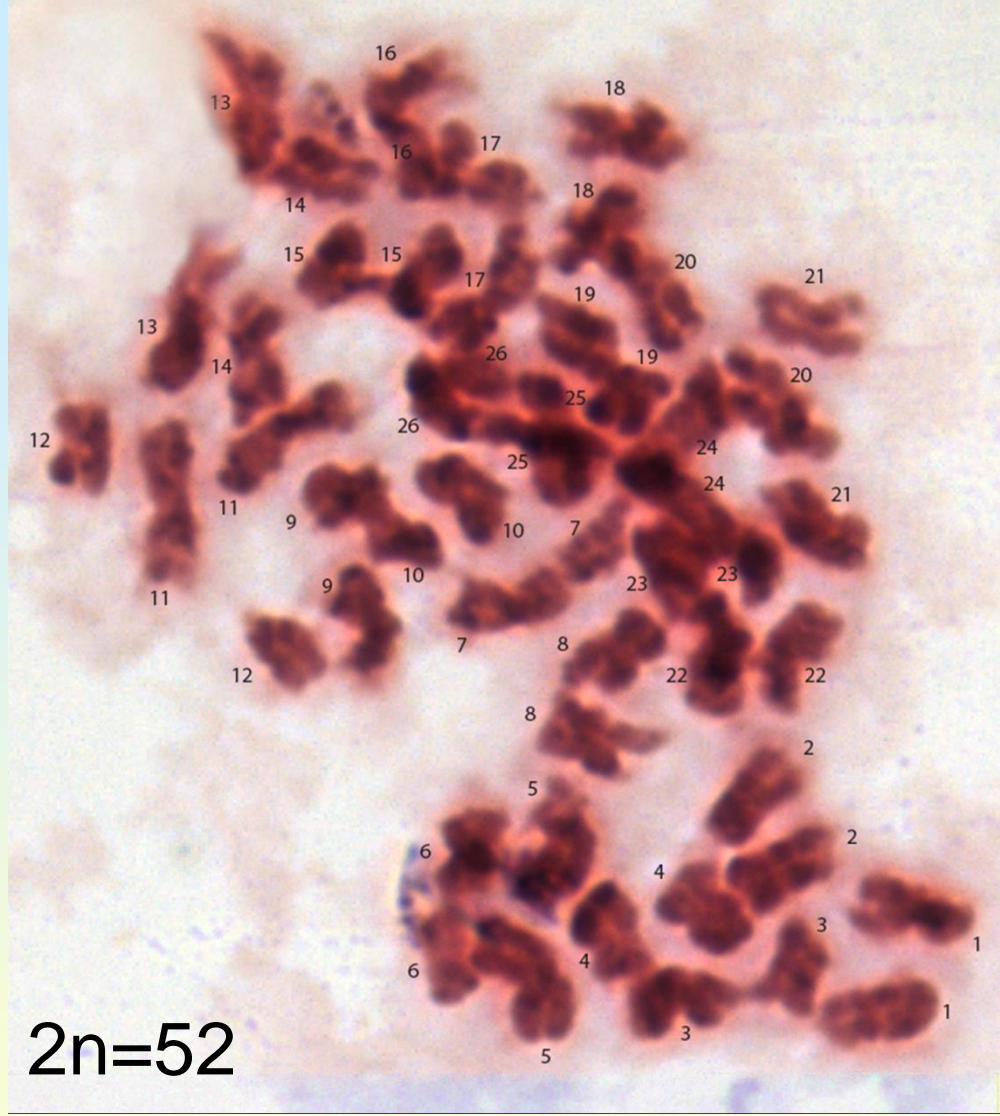
The analyses of chromosome structural features will allow:

- to establish phylogenetic links within the systematic category,
- to disclose genetic mechanisms underlying high degree of adaptation of this species to varying environmental conditions.



Karyotype analyses

is being performed using early embryos as the source of cells, nuclei and chromosomes.



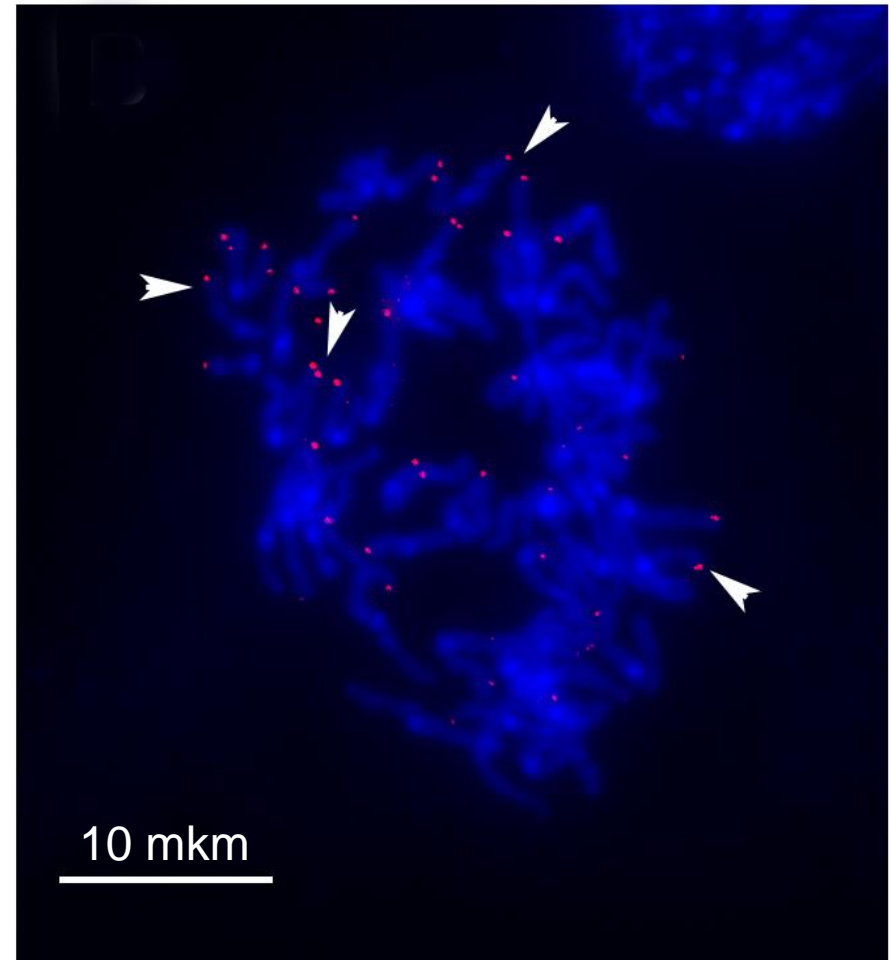
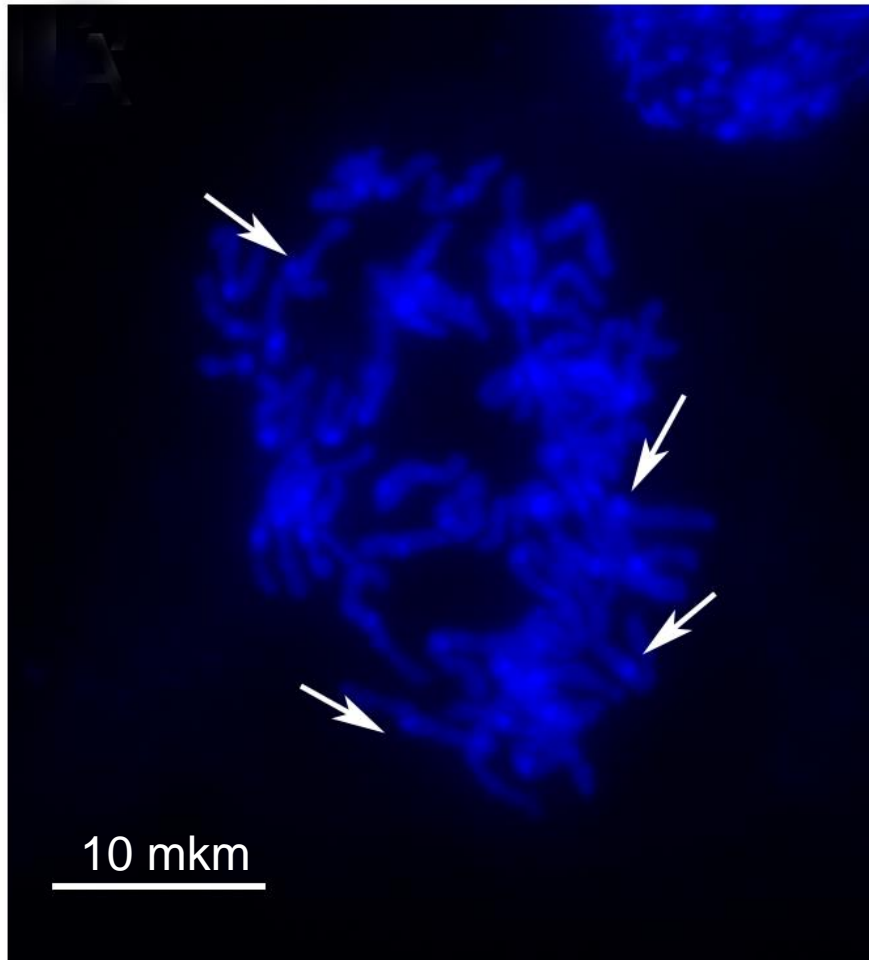
Analyses of conventionally stained metaphases of mitosis allowed us to determine the diploid chromosome number in *G. fasciatus*



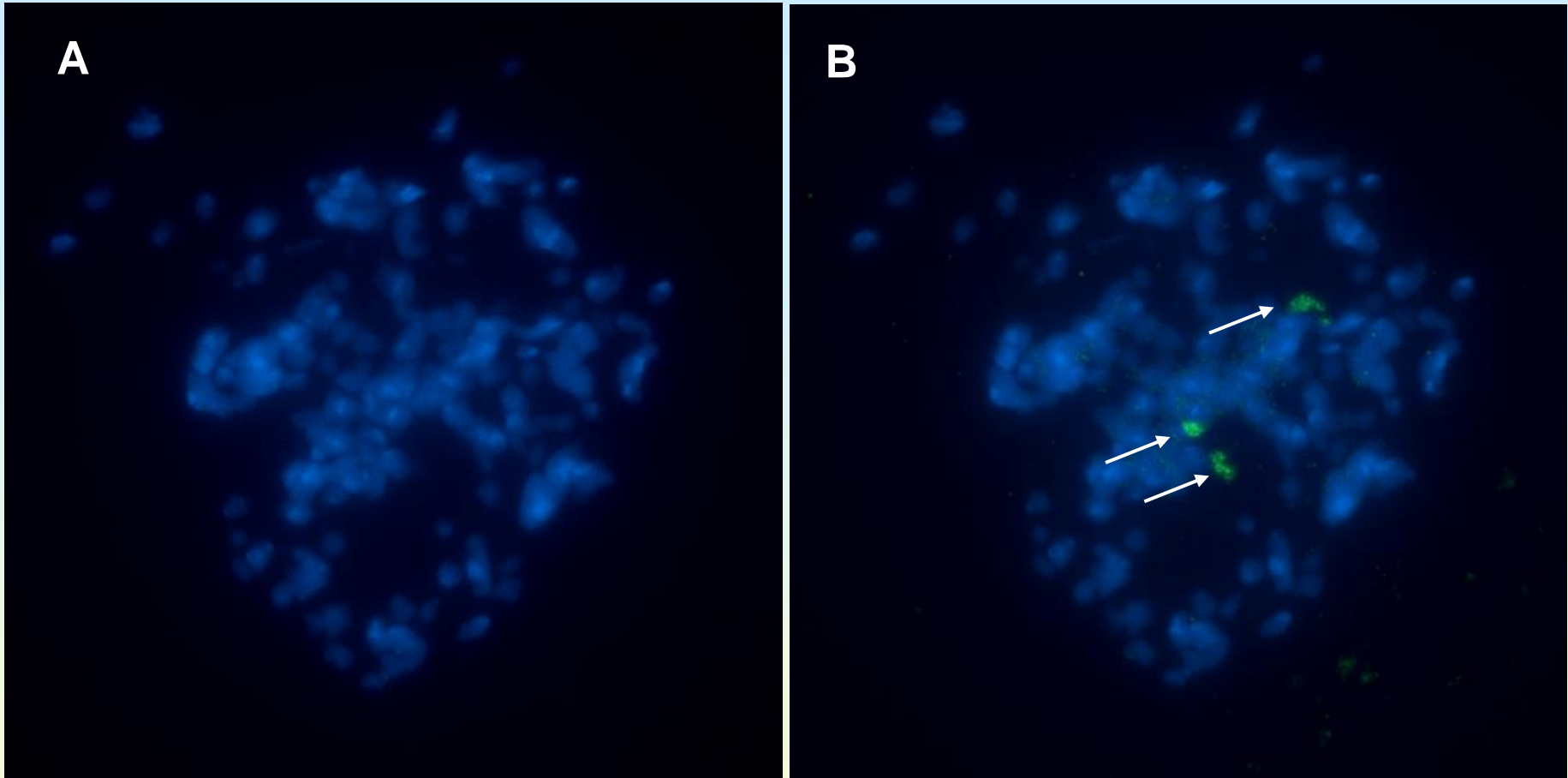
and to build the karyogram to
characterize the karyotype of
this amphipoda.



$2n=52$ or 26 pairs of chromosomes



The rDNA/FISH revealed that (TTAGG) $_n$ repeats hybridize to chromosome ends. A – DAPI-bright fluorescing Adenine-Thymine base-pair (A-T) rich pericentromeric regions (arrows); B – red telomeres (arrowheads).

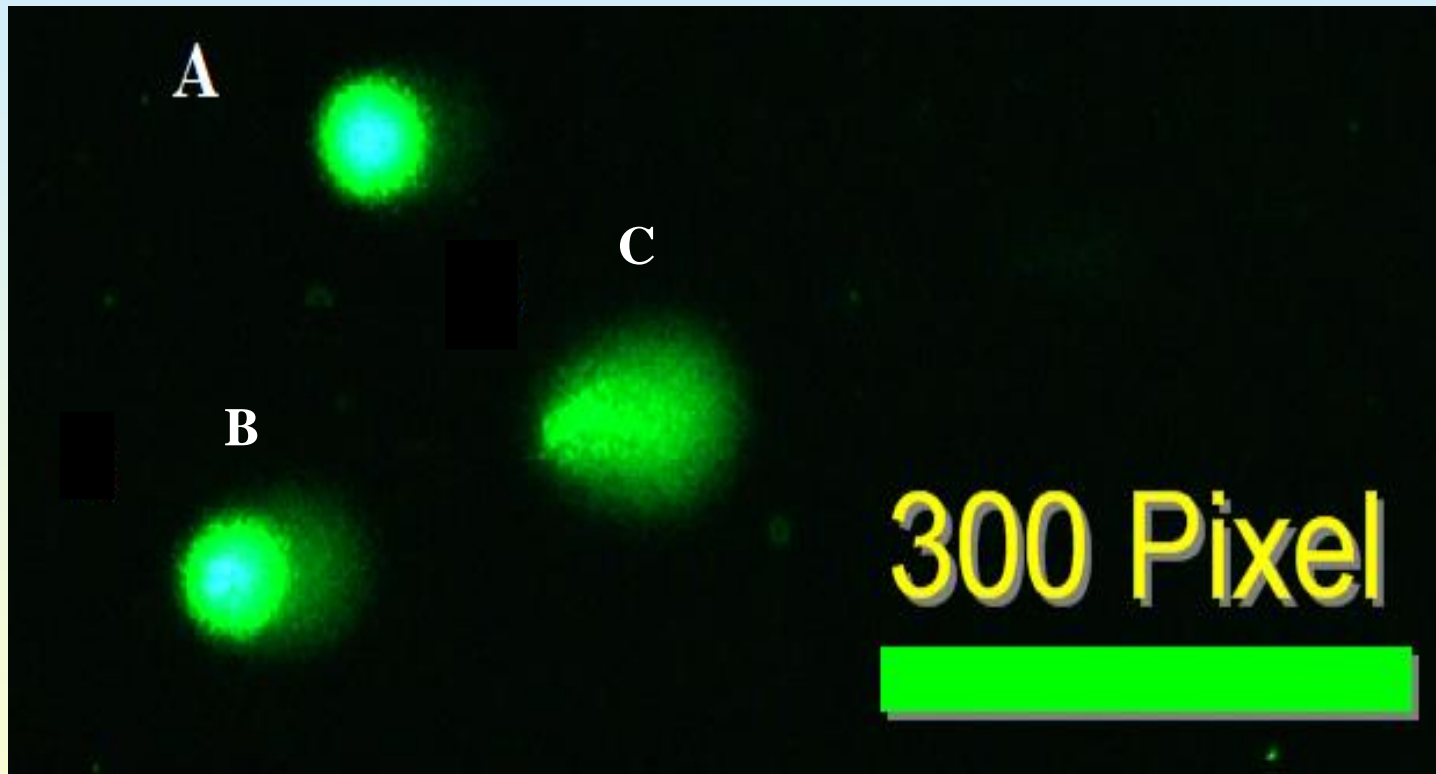


The 18S rDNA probe, amplified using a pair of primers specific for *G. fasciatus*, revealed from two to three (arrows) hybridization sites in the nuclei at different stages of the cell cycle.



Comet alkaline elctrophoresis

allows to assess frequencies of primary disturbances at DNA level, which might be prerequisites of chromosome abberations.



A – comets of embryonic nuclei with intact DNA, B – partial destruction of DNA, C – high level of distruction of DNA in the nucleus

Molecular biology approach

The traces of the adaptation process can remain as diverse micro-changes in the DNA (single nucleotide substitutions, micro-deletions, inversions, transpositions, *etc.*).

We've started the sequencing project and intend to compare the genomes of *G. fasciatus* from initial Baikal population and that of the non-native species from the Gulf of Finland, using rDNA and mtDNA cytochrome c oxidase subunit I (COI) gene as the first targets.

Comparative genome analyses could give an idea of whether ecological specialization took place along with invasion process.



The Team

Larisa Barabanova, Svetlana Galkina,
Elena Mikhailova, Eugene Potapenko

ACKNOWLEDGEMENTS

We are grateful to Maria Vishnevskaya for providing the probes for DNA-DNA *in situ* hybridization, to Maria Kulak, Timophei Glynin and Eugene Daev for their practical and theoretical contribution to this study. Fluorescence *in situ* hybridization procedures and microscopy was performed at the Research park of St.Petersburg State University “Chromas”.

FINANCIAL SUPPORT

Estonian and Finnish partners
for invitation and fantastic Forum 😊



The research was supported by RFBR grant 15-29-02526,
grant of the President of the Russian Federation in support of
Leading Scientific Schools 9513.2016.4

From small scales to large scales
–The Gulf of Finland Science Days 2017
9th-10th October 2017
Estonian Academy of Sciences, Tallinn

2nd Day



**Gulf of Finland
Co-operation**

A. Rybalko, O. Korneev, A. Pedchenko, D. Ryabchuk

Facies features (geodiversity) of sedimentation in the Eastern Gulf of Finland and their use for proper assessment of the results of geochemical monitoring of hazardous substances.

Facies features (geodiversity) of sedimentation in the Eastern Gulf of Finland and their use for proper assessment of the results of geochemical monitoring of hazardous substances.

Rybalko A., Korneev O., Pedchenko A., Ryabchuk D.

State Company VNII Okeanologija, SPSU, Federal State Budgetary Scientific Establishment "Berg State Research Institute on Lake and River Fisheries" VSEGEI



**Gulf of Finland
Co-operation**

what is what

Facies - sediments accumulating in a specific physiographic and hydrological environment and differing in composition and appearance from sediments that occurred under other conditions at the same time

Facies features or sedimentation situations - physico-geographical and hydrological conditions, under which sediments of a certain facies accumulate

Geodiversity is the replacement of some sediments by others at the seabed, which occurs as a result of a change in the facial conditions and facies.



Purpose of Presentation

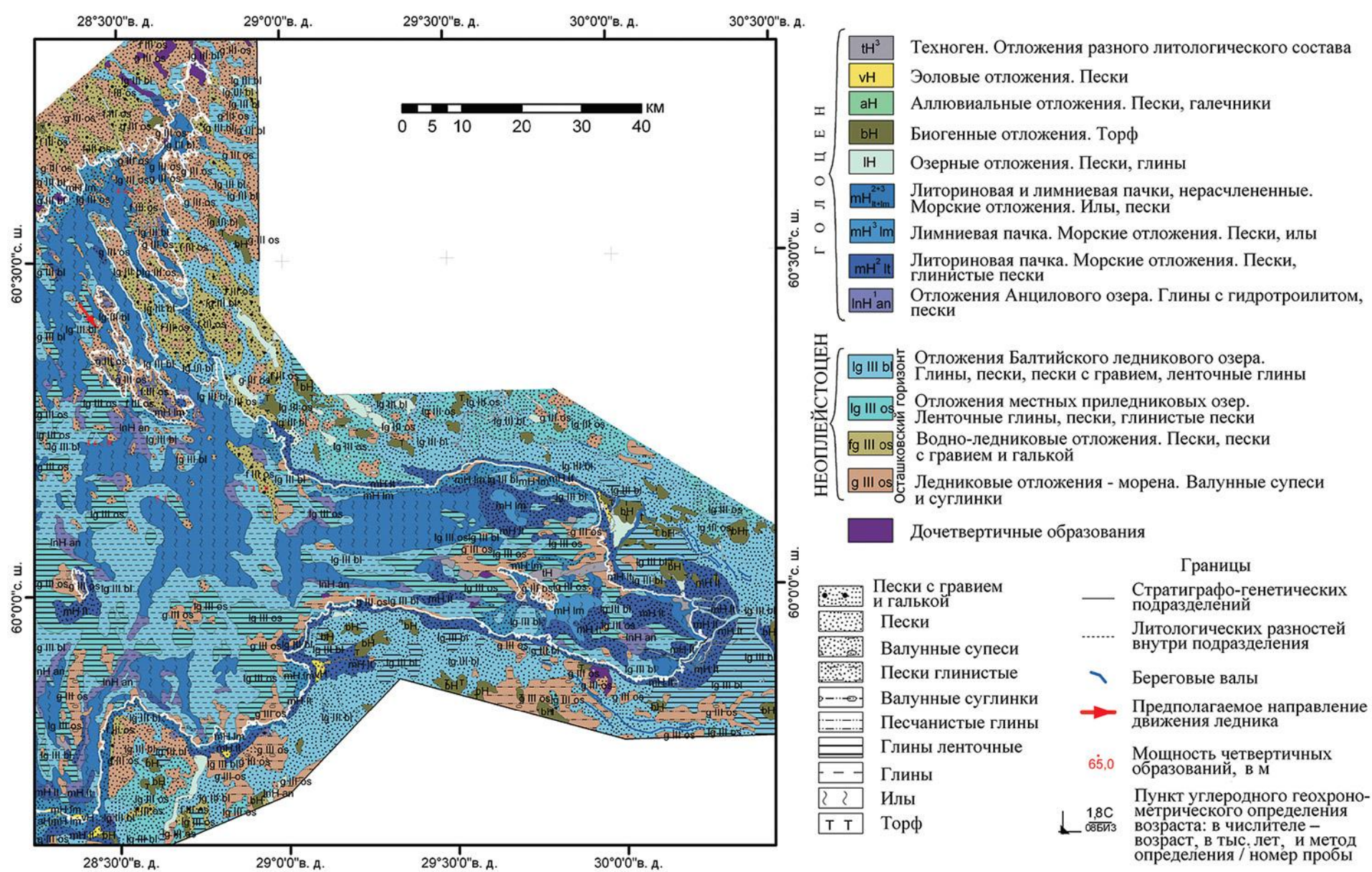
- Facies features of sedimentation largely determine the conditions of accumulation of hazardous pollutants, including heavy metals and hydrocarbons.
 - What facies are at the bottom of the Gulf of Finland?
 - How pollutants are associated with facies features?
 - What is the relationship between geo- and biodiversity?



MATERIALS

- The results of the geological survey of the shelf of the Gulf of Finland (VSEGEI since 1981)
- Results of geo monitoring of the Gulf of Finland (SEVMORGEO 2001-2014)

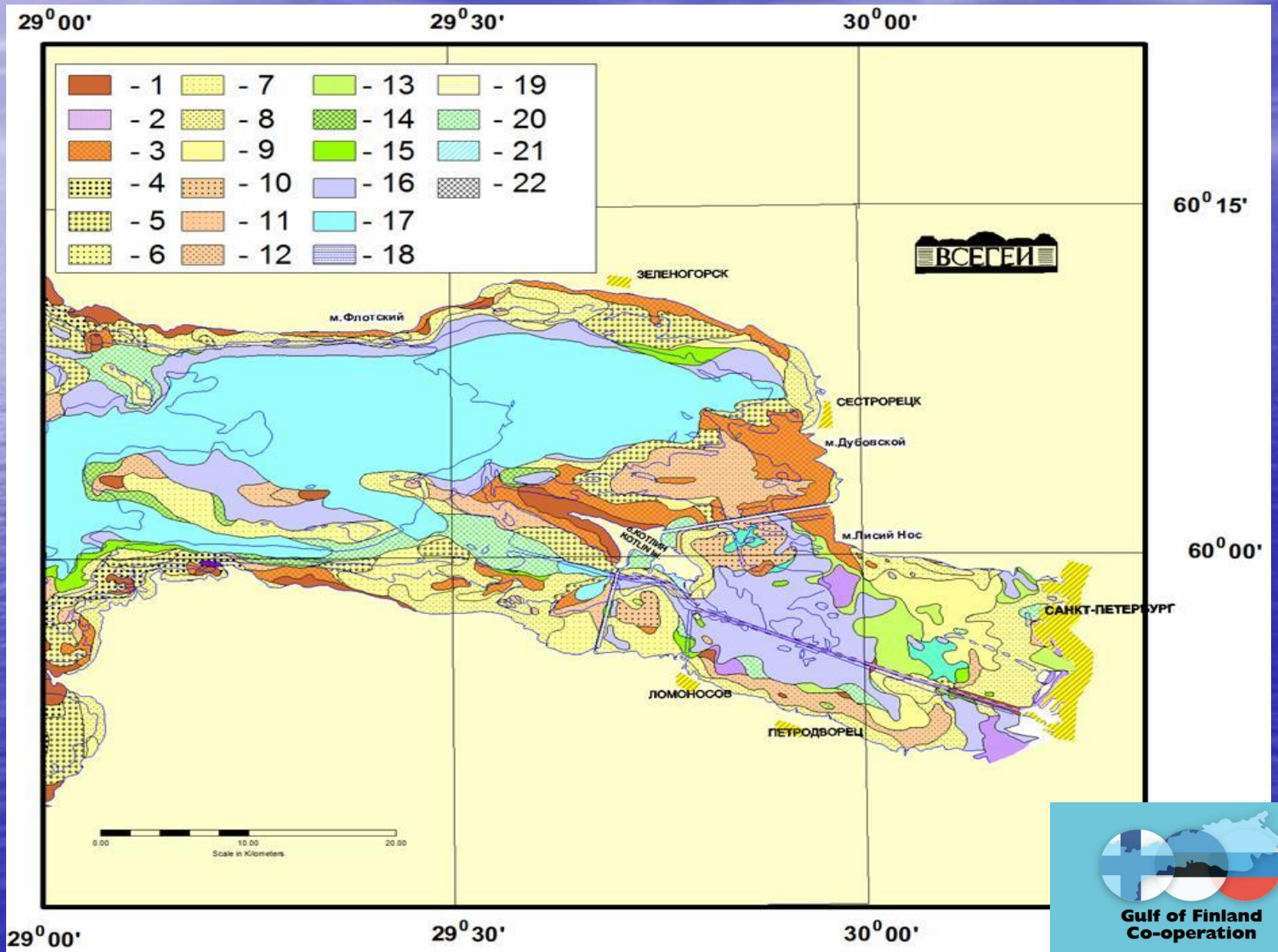




Quaternary map of the gulf of Finland (Russian part)(VSEGEI, 2005)



LITOLOGICAL MAP OF NEVA ESTUAZRY



Gulf of Finland
Co-operation

Facial features

- **The facies characteristic of bottom sediments depends on the hydrodynamics of the marine basin and the relief of the bottom. There are three groups of facial features: accumulative or sedimentogenic, erosive or destructive and transitory or transit.**

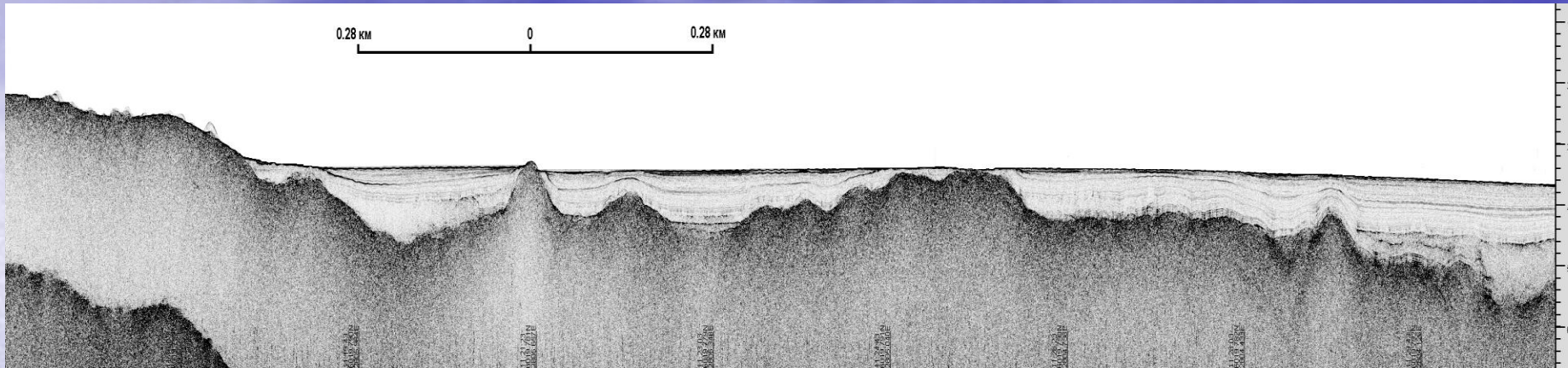


**Gulf of Finland
Co-operation**

Genetic series	Genetic type	Genetic subtype	Facies group
Underwater-Hypergenetic	Perluvium (underwater-eluvial)	Mechanogenic	Relict (residual) Condensate-eluvial
Hypergenetic-sedimento-genic	Palimpsest	Percuvial-wave Peruvial-fluvial	
Sedimento-genic	Wave	Seaside	Beach
		Coastal	Wave breaking Wave deformations
	Flowing (underwater-fluvial)	Tidal	sand bands sand waves sand ridges
		Bottom currents	rifels
Hepheloid	Shallow Transition Deep-water (stagnant)		



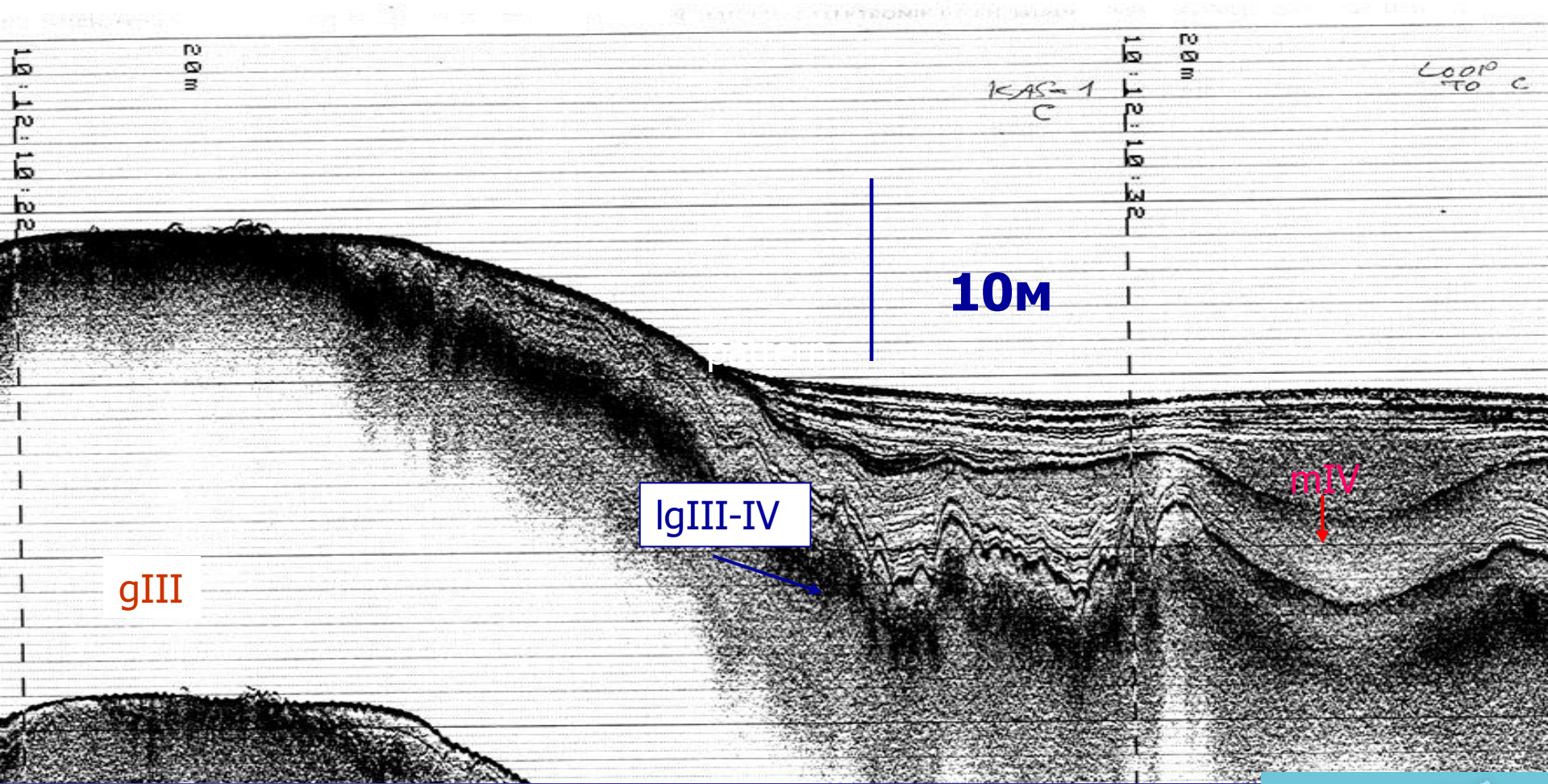
Nepheloidal sedimentary conditions



Финский залив 2007. Участок 1 (Выборгский залив), галс 1.

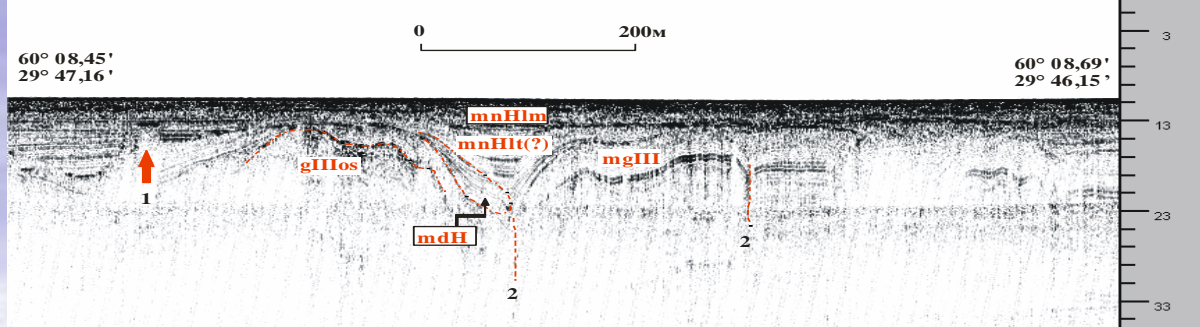
Nepheloid sedimentation conditions are confined to low relief areas and accumulate in the form of local sedimentary basins. They occupy about 50% of the seabed of the Russian part of the Gulf of Finland. They are mostly made

PATTERN OF SEISMIC RECORDING IN THE SEDIMENTING BASIN



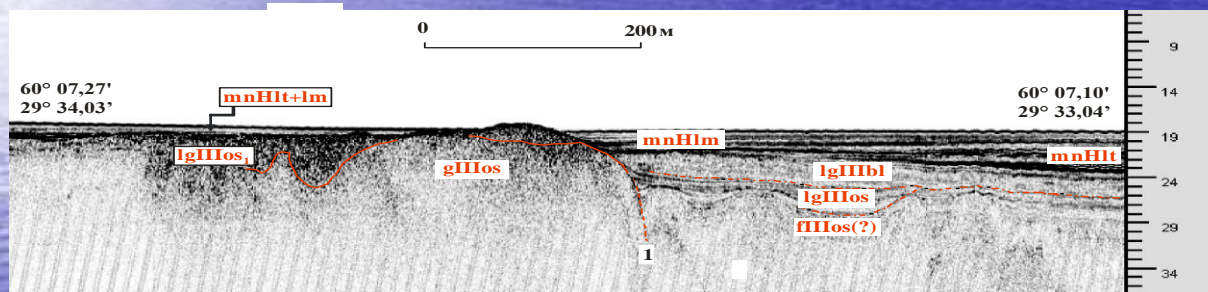
Sedimentation basins and their reflection on seismograms

PR2 Зона активного проявления современных геодинамических процессов



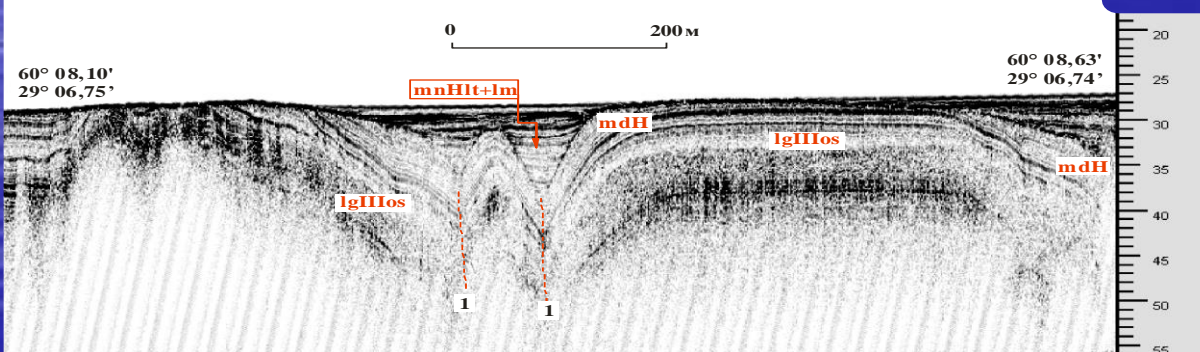
- 1 - предполагаемая зона прорыва газифлюидов
- 2 - предполагаемая зона геодинамических нарушений

PR3 Неравномерное развитие зон голоценовой седиментации, связанное с современными геодинамическими движениями



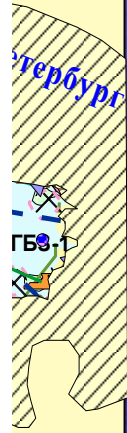
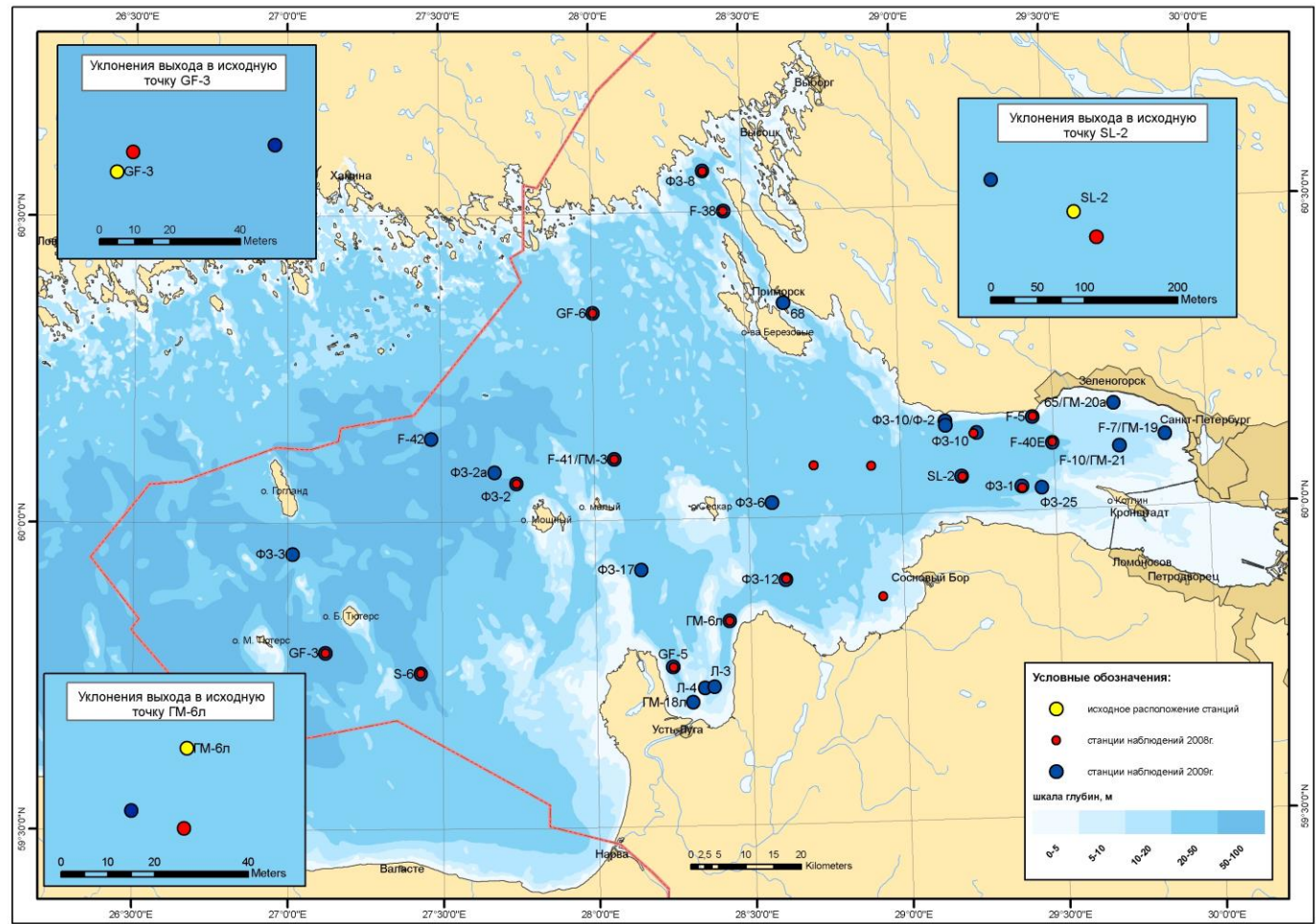
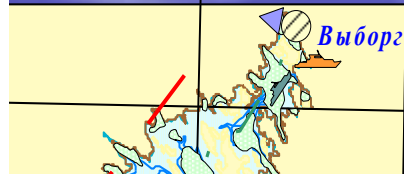
- 1 - предполагаемая зона геодинамических нарушений

PR4 Кратерные формы поймаков, сопровождаемые проявлением гравитационных процессов



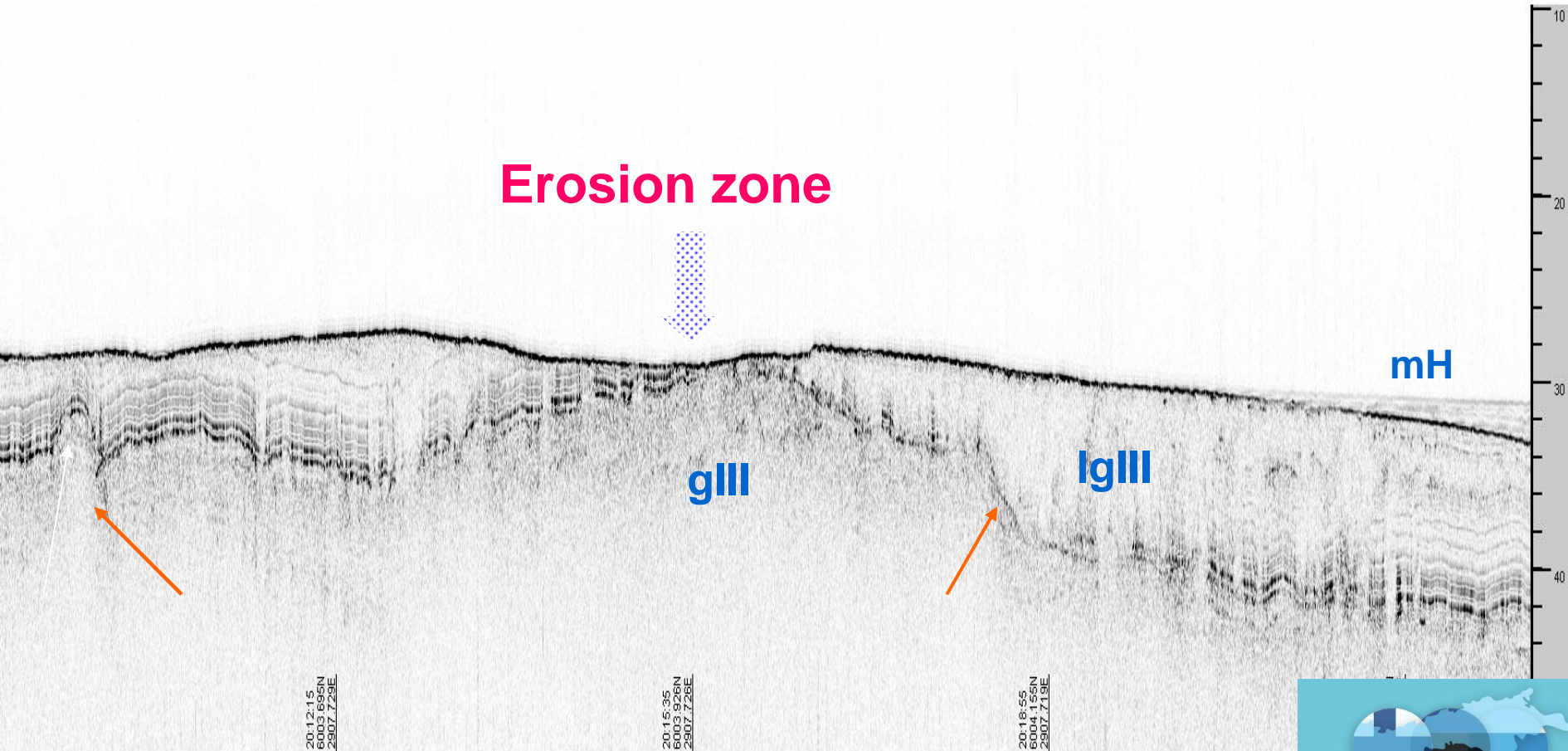
- 1 - предполагаемая зона геодинамических нарушений

POSITION OF SEDIMENTATION BASINS AND MONITORING STATIONS IN THE GULF OF FINLAND

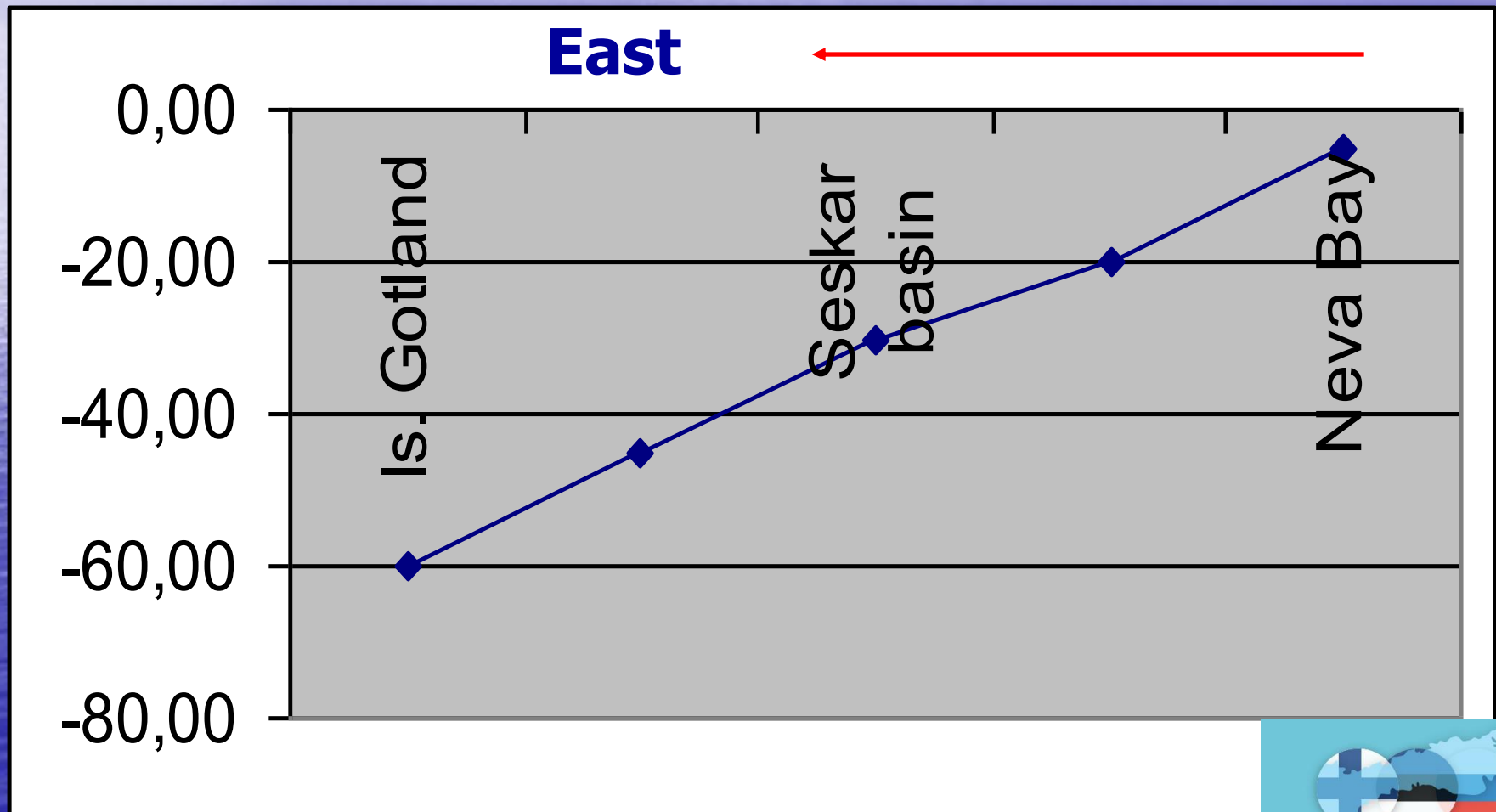


20 Kilometers

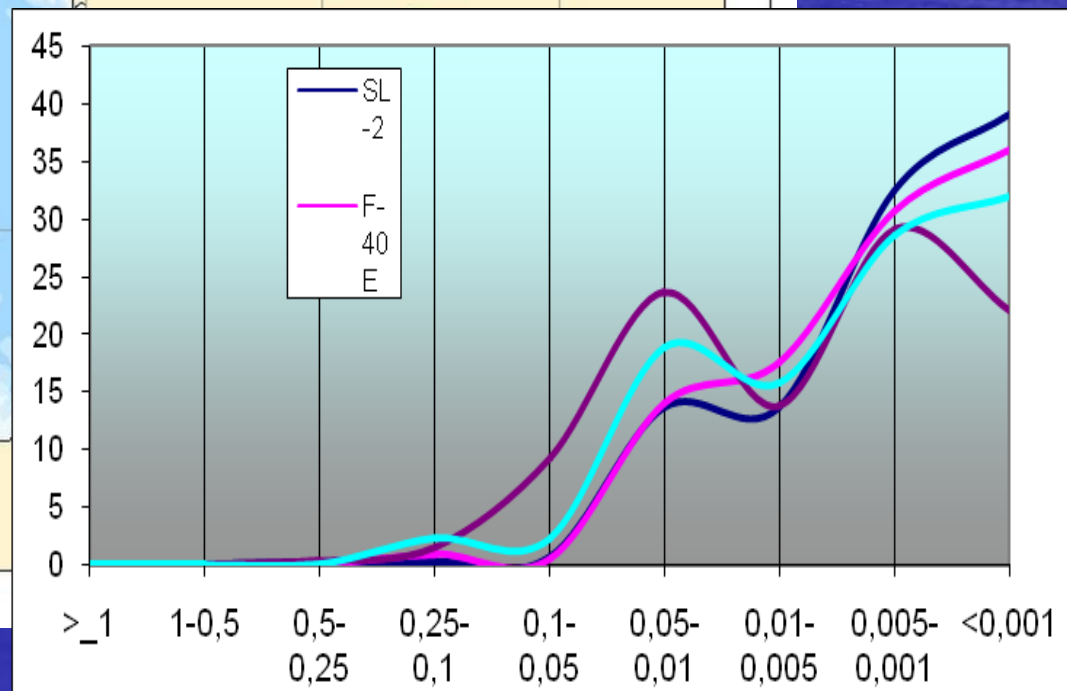
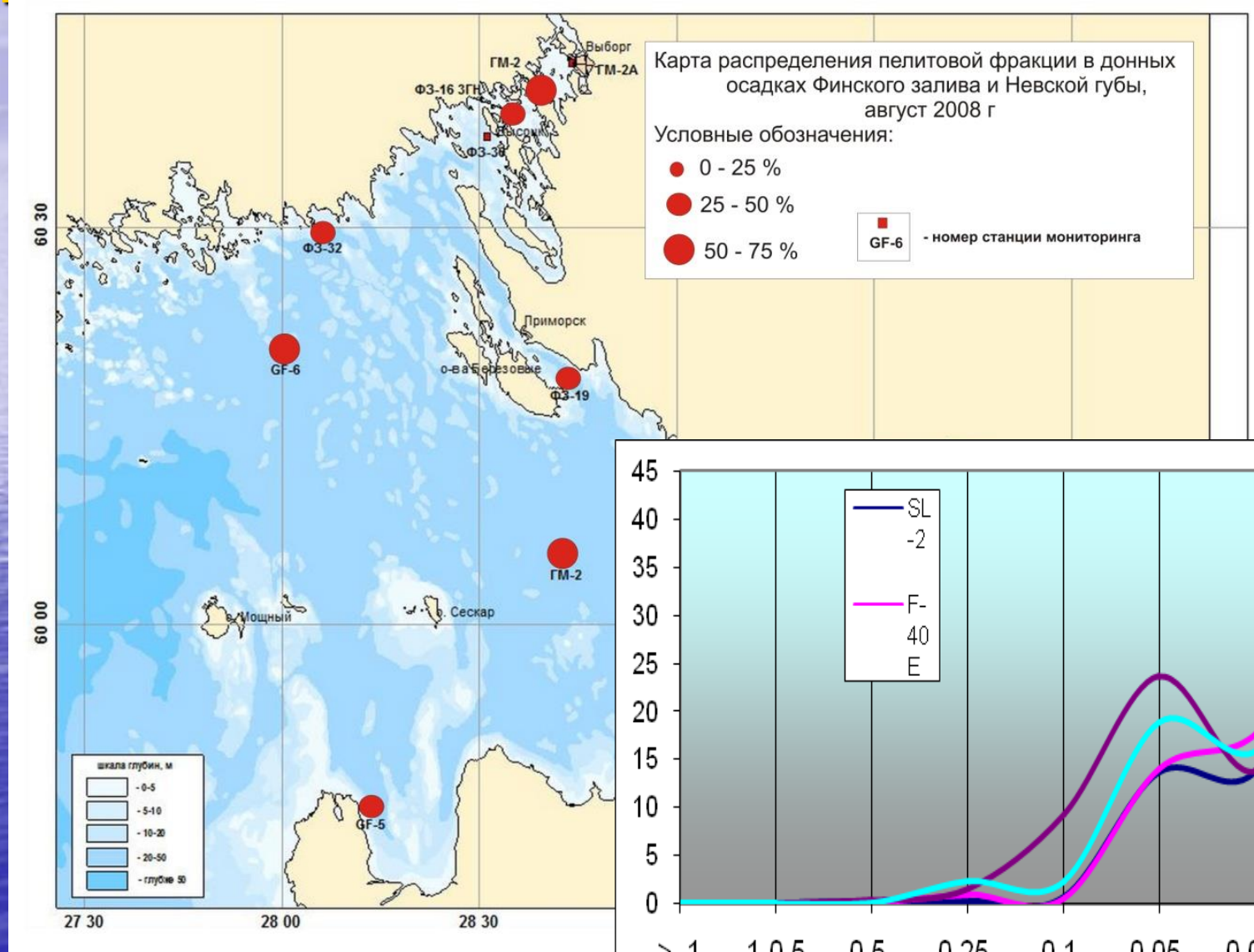
Not always depth is the decisive factor of localization of nepheloid sedimentation environments. Erosion window in the zone of considered neotectonic uplift



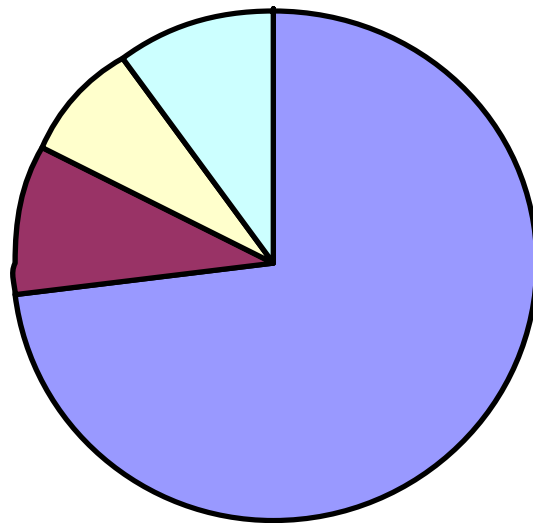
Changes in the depth of the surface of Holocene sediments from the Neva Bay to the Gotland sedimentary basins



Granulometric characteristic of nepheloid sediments



Clay minerals

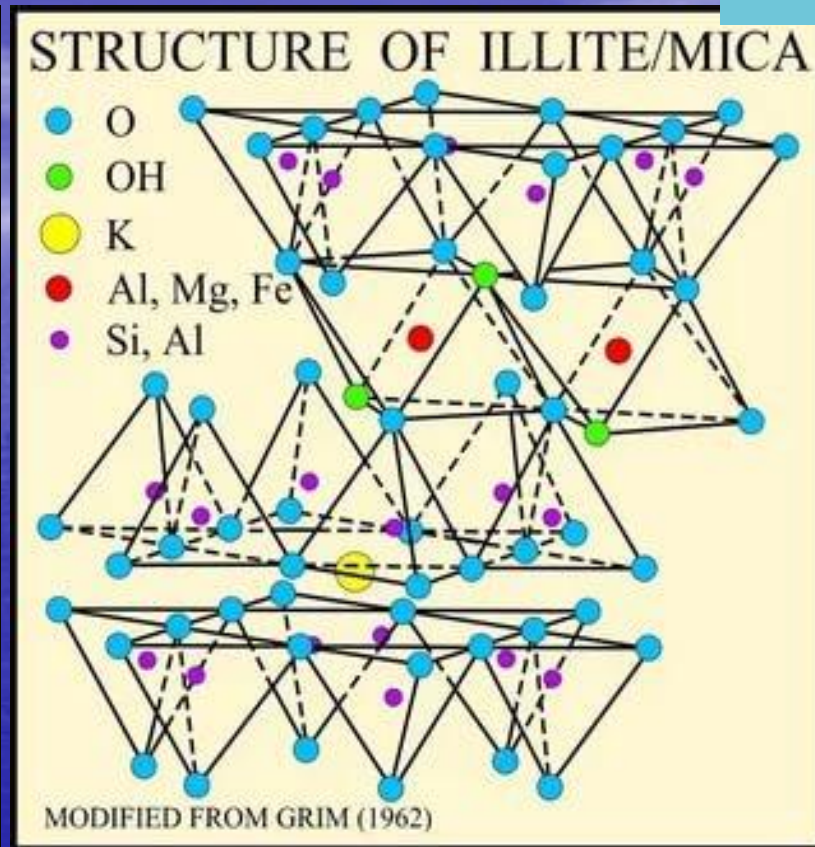
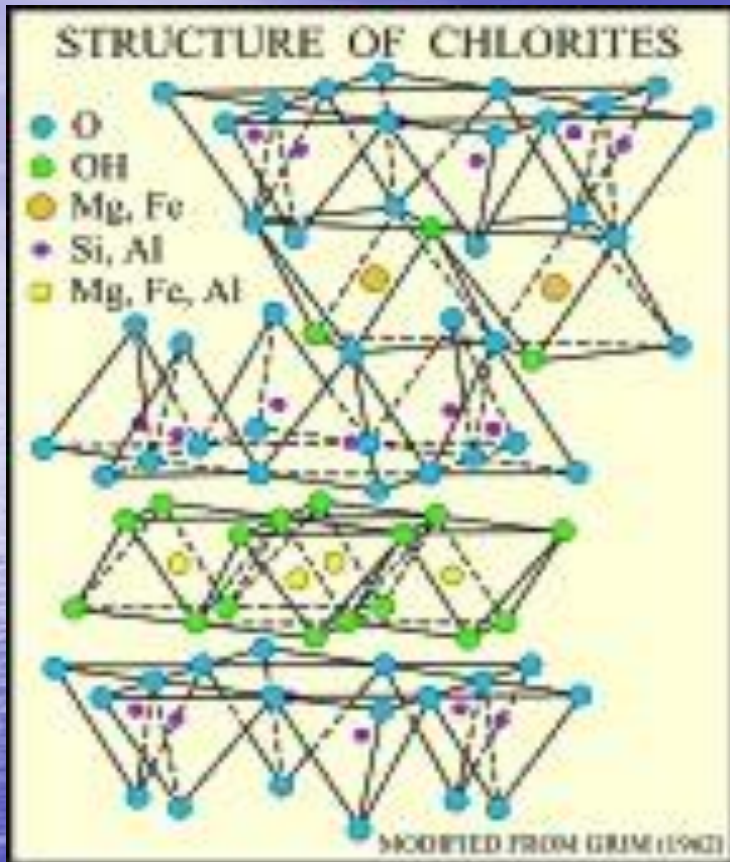


- illite
- chlorite
- kaolinite
- other

Clay minerals are represented by illite 70-85, chlorite 7-20%. kaolinite (up to 10%). Smectites are present in significant quantities. admixture of terrigenous minerals

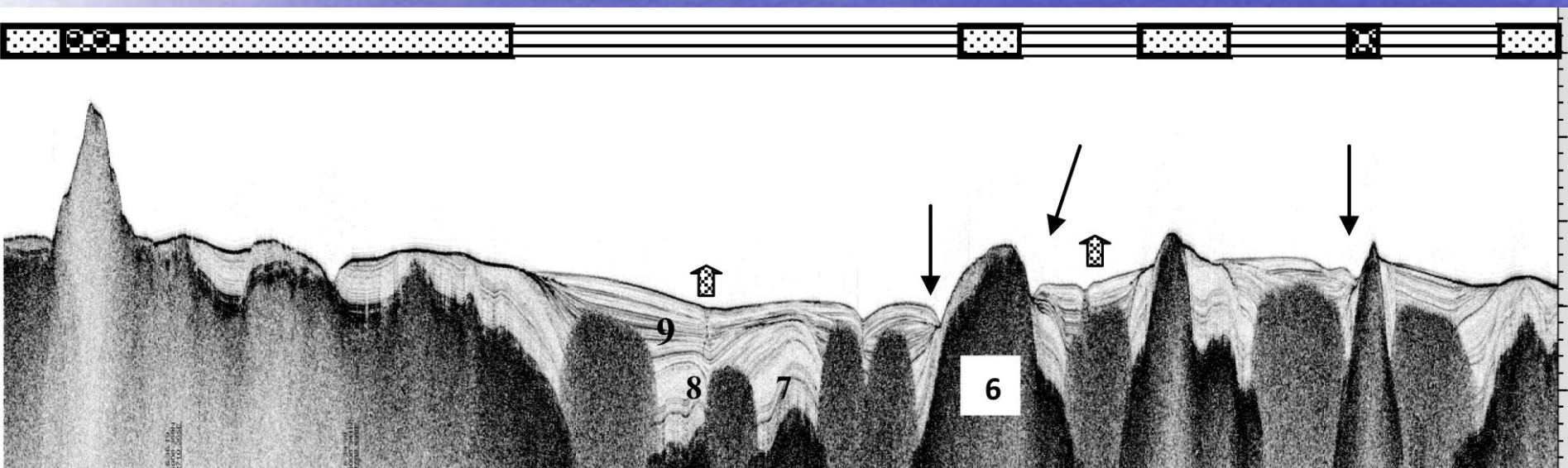


Crystal cell of clay minerals

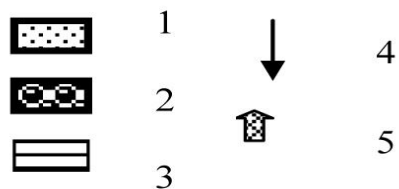


The sorption capacity of these minerals is medium
All pollutants (organic and inorganic) are located in interlayer spaces
Therefore, heavy metals in clay sediments are mobile forms

The remaining 40-50% of the seabed at depths from 3-5 to 40-50 m are occupied by sediments of the transit range (sea perlium) or zones of modern erosion. They are composed of sediments from clayey sands to boulder-pebble deposits.

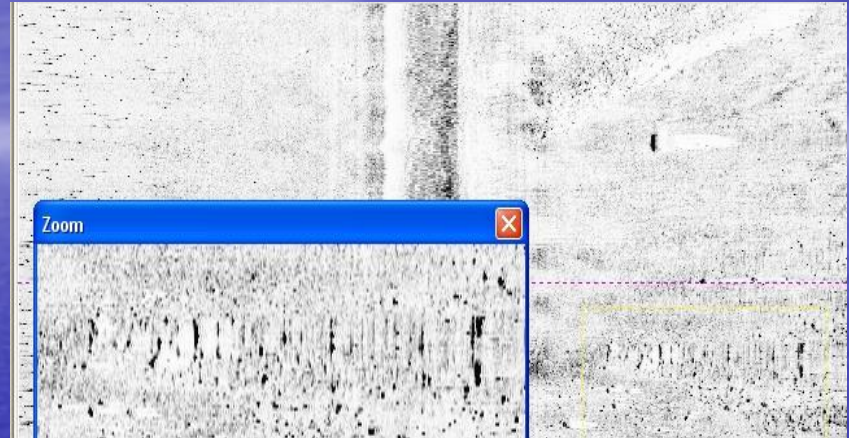
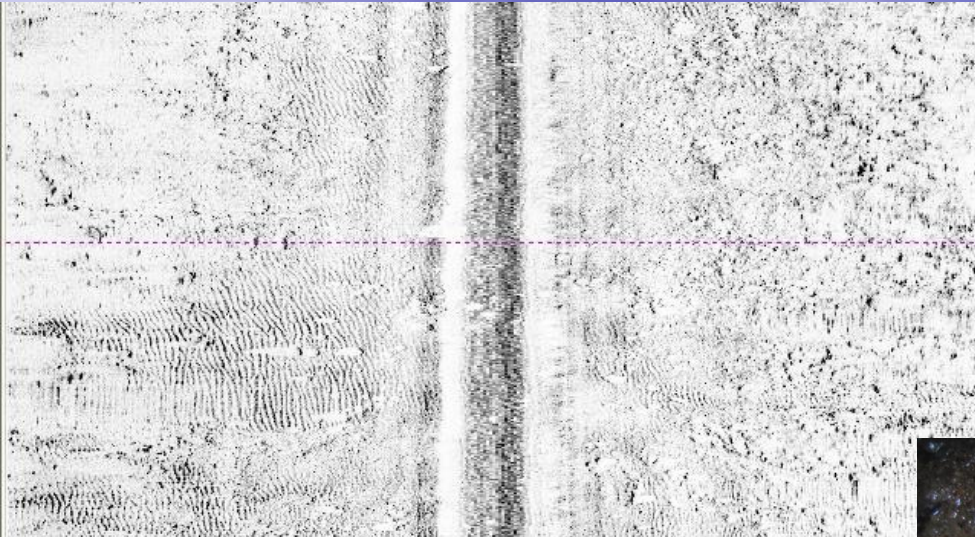


Условные обозначения:

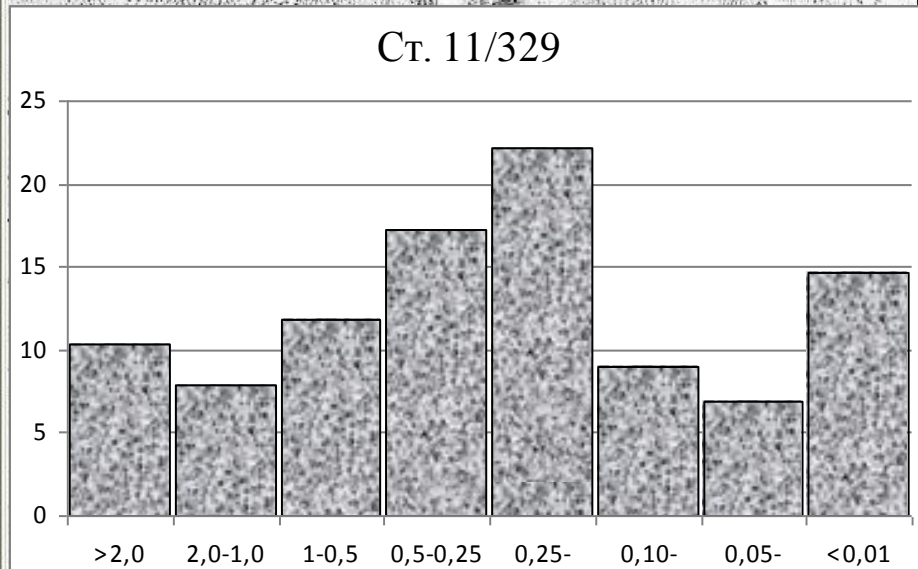


facies zones: 1-transit (sandy and sandy-silty with gravel); 2 - underwater perlium (bottom abrasion) (boulder-pebble and gravel-pebble sediments with sand); 3 - accumulative nepheloid (aleuropelites and pelites); 4 - zones of underwater erosion; 5 - pop stamps. Lithostratigraphic units: 6 - glacial deposits (moraine) - gIIIost; 7 - glacial-lacustrine deposits of the Valdai glaciation and BLO - lgIII ost + bl; 8 - lake sediments of the early stage of the Holocene - LH1; Marine littorine and postlitorin deposits - mIIIIt + Im

Perliviium



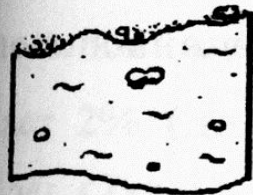
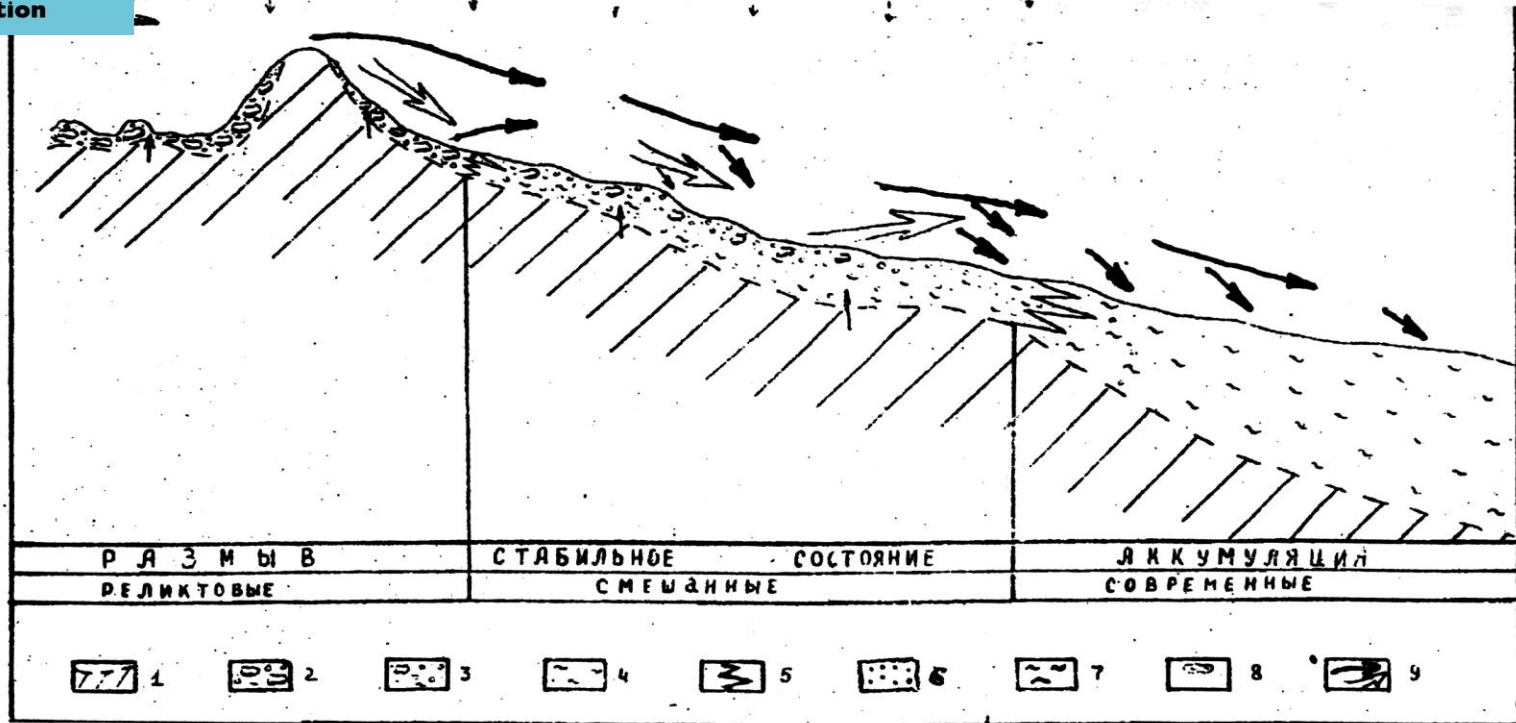
Ct. 11/329



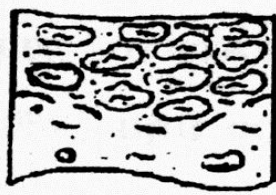


Gulf of Finland
Co-operation

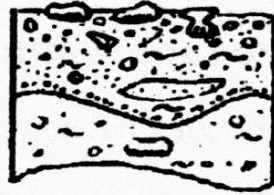
Perluvial series of sediments



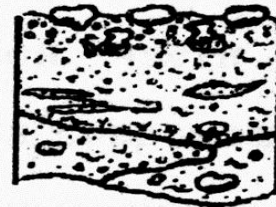
76-48
H = 176 м
2



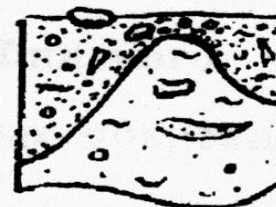
76-50
H = 151 м
3



77-20
H = 34 м
4



77-26
H = 62 м
5



77-39
H = 45 м
6

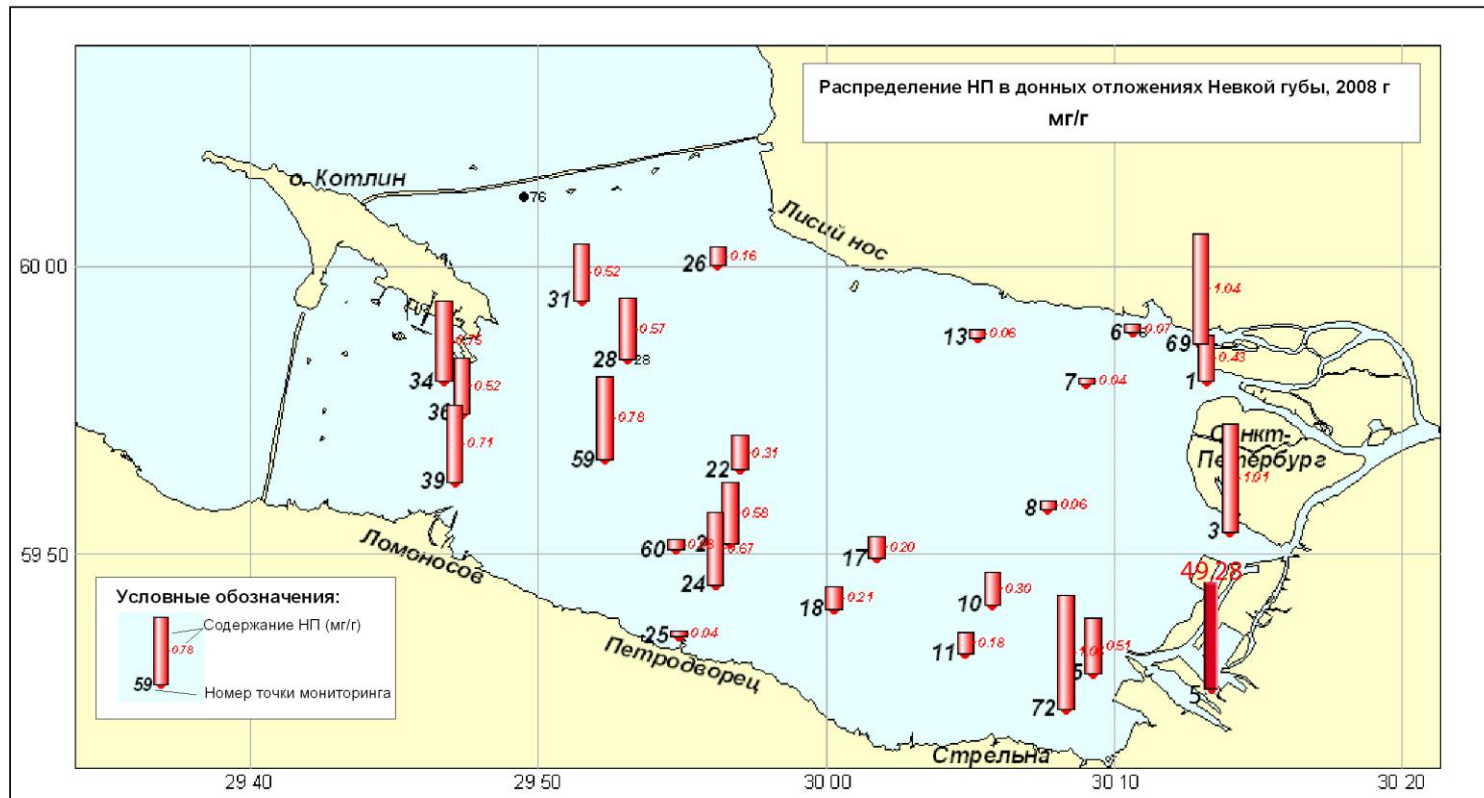


78-228
H = 31 м
7

Sandy sediments

- **Along the coast, in the zone of wave action, the undaluvial sands accumulate.**
- **Bottom currents arise in the narrows and sands are formed**

The difference in the granulometric composition and features of the sedimentation processes to a completely different level of concentration of microelements in them, including pollutants.

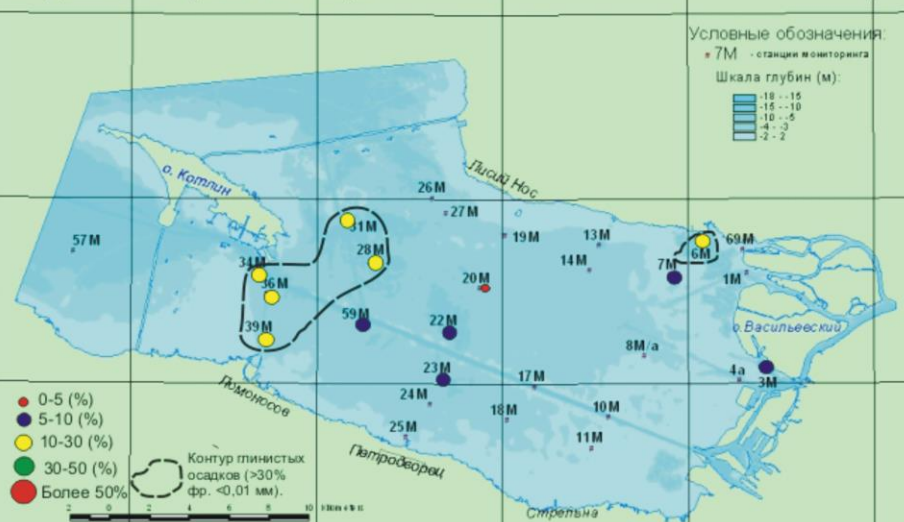


Distribution HC in bottom sediments in the Neva Bay in 2008 (mg/g)

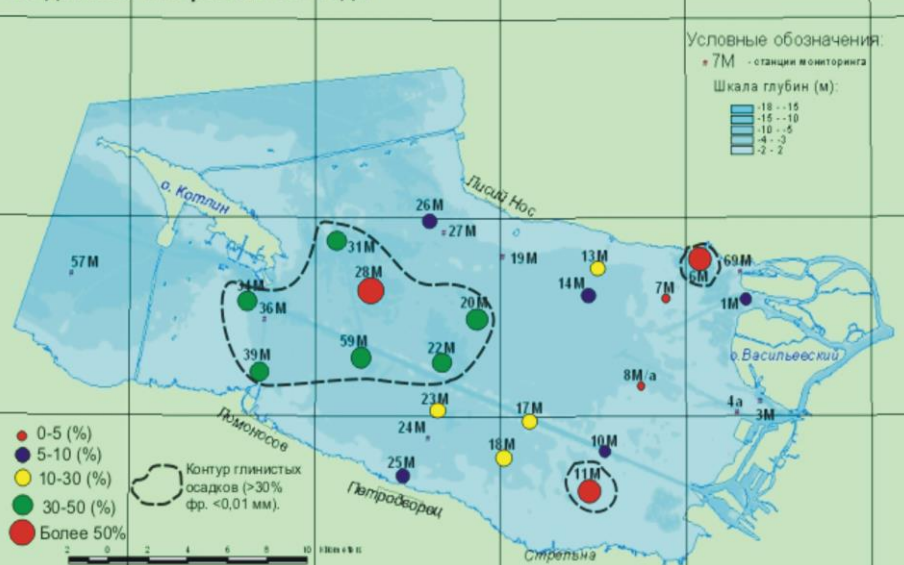
The change of fraction $<0,01\text{mm}$ in bottom sediments in May of 2005 and 2007



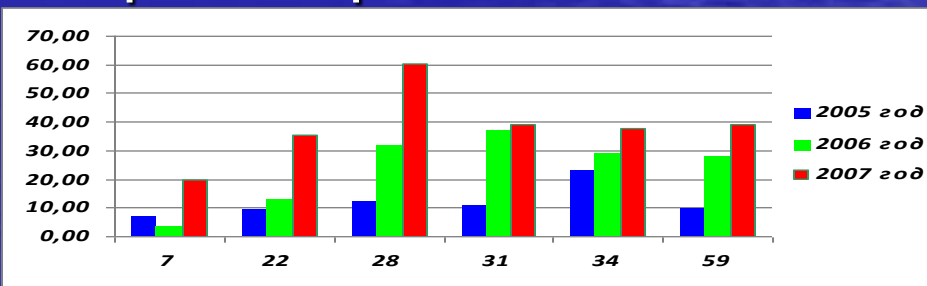
Содержание фракций $<0,01$ мм в донных осадках.
По данным 1-го рейса 2005 года



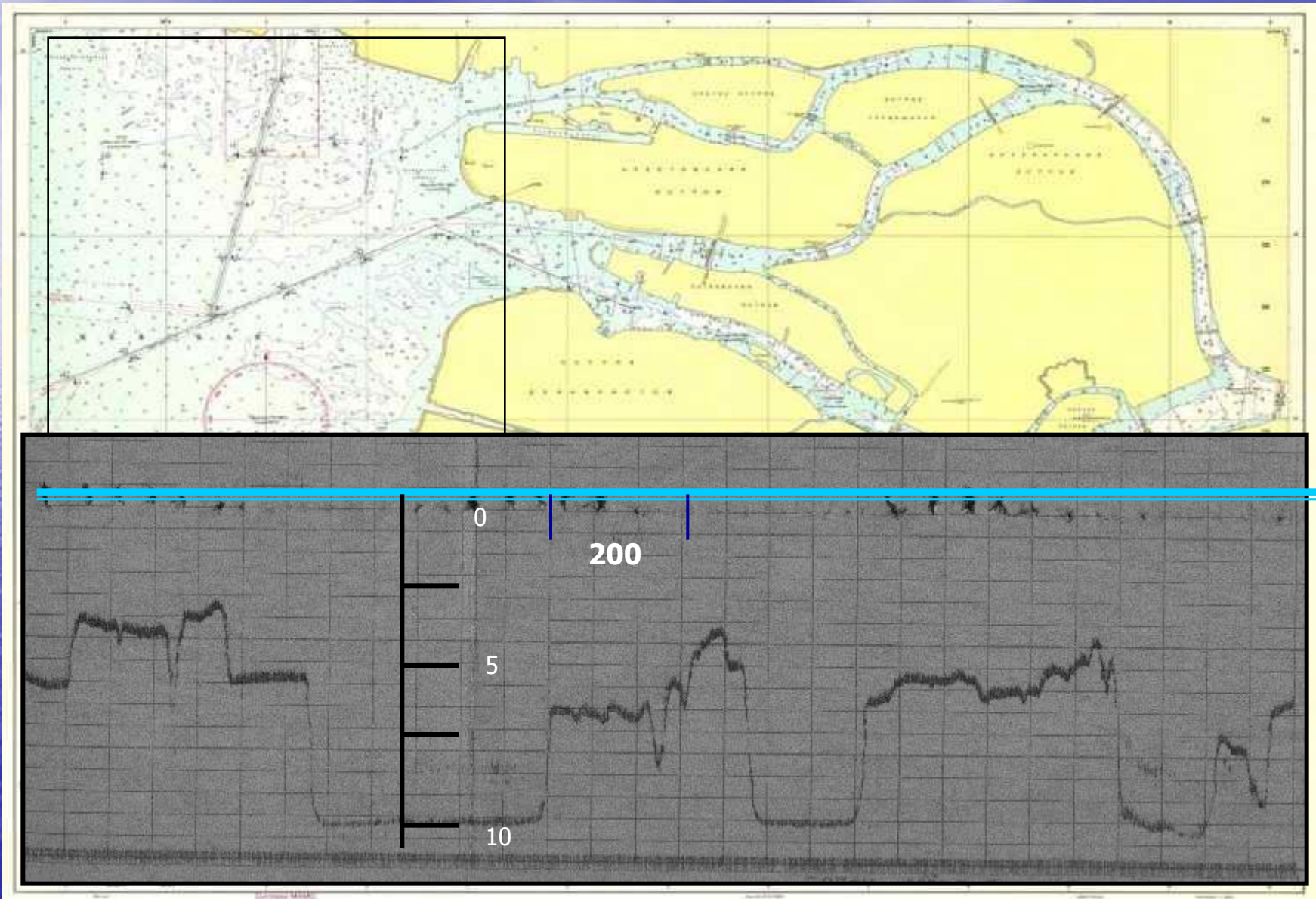
Содержание фракций $<0,01$ мм в донных осадках.
По данным 1-го рейса 2007 года



- В мае 2005 года максимальное содержание глинистой фракции отмечалось только у осадков в западной части губы, в 5-ти метровой впадине
- В мае 2007 года площадь глинистых осадков расширилась, а содержание пелитовой фракции в отдельных пробах превысило 50%

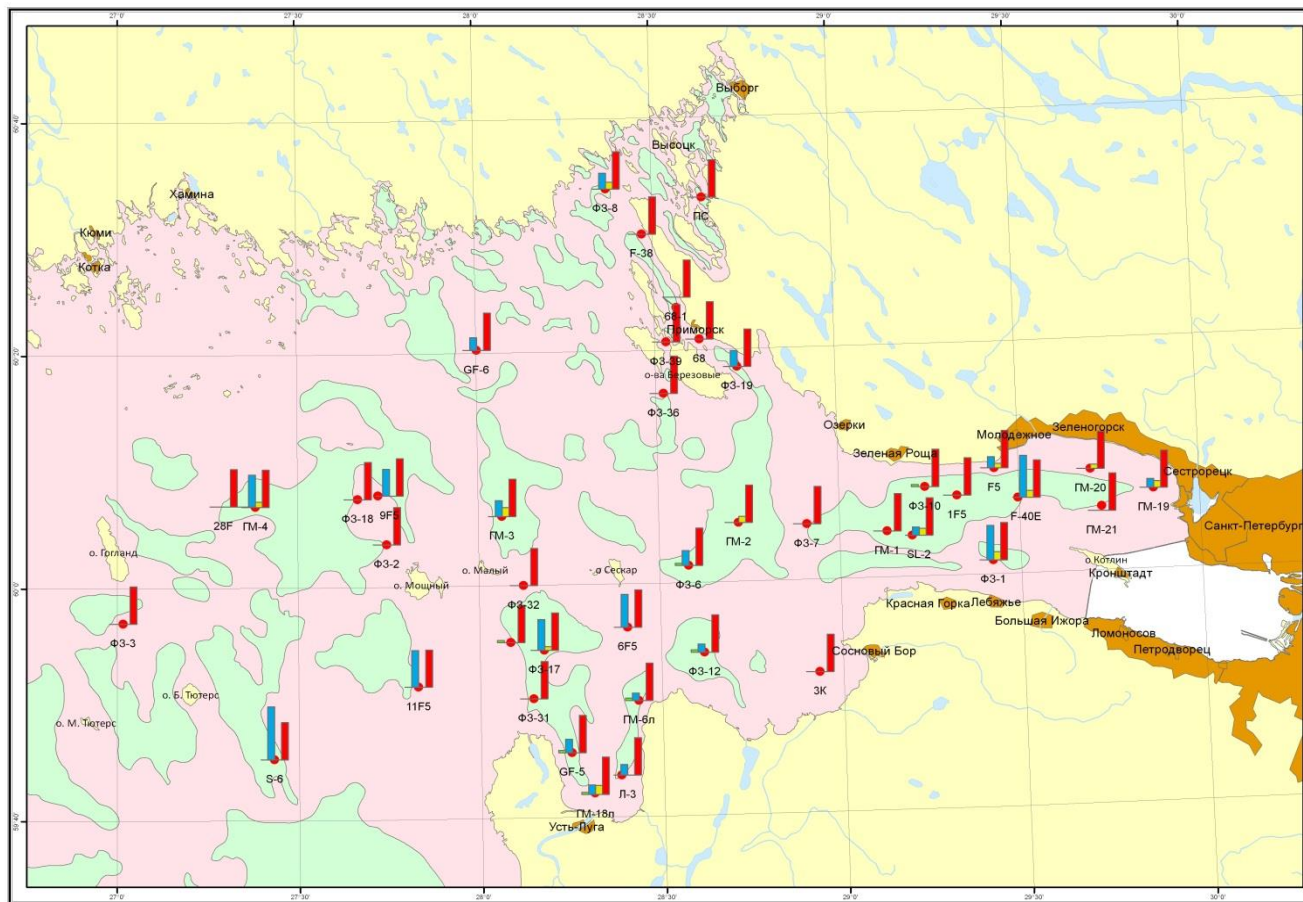


ПОДВОДНЫЕ КАРЬЕРЫ В НЕВСКОЙ ГУБЕ



The Map of hydrocarbons distribution in near-bottom waters (2012-2014)

Карта распределения нефтепродуктов в придонном слое воды.
(Центральный сектор восточной части Финского залива).
Масштаб 1: 500 000




УСЛОВНЫЕ ОБОЗНАЧЕНИЯ

- Станции мониторинга
- Распределение нефтепродуктов в придонном слое воды, мг/дм³:
 - 0.035
 - 2012 год
 - 2013 год
 - 2014 год
 - ПДК, 0.05 мг/дм³
- Зоны аккумуляции нефелюидных пелитовых осадков
- Зоны транзита осадочного материала и абразии морского дна
- Реки
- Озёра
- Города

ОАО "Севморнео"	Отчет о результатах работ по Договору 80/04/12: "Проведение Государственного мониторинга состояния недр прибрежно-шельфовой зоны Кандалакшского залива Белого моря, северного прибрежного шельфа Кольского полуострова-район Терiberka- Греника Баренцева моря и центрального сектора восточной части Финского залива Балтийского моря в связи с интенсивным хозяйственным освоением территории"	
	Ответственный исполнитель: Рыбалко А.Е.	2014 г.
	Ответственный исполнитель по листу: Рыбалко А.Е.	
Приложение 46 Лист 1	Карта распределения нефтепродуктов в придонном слое воды.	

Conclusions

- **When carrying out geochemical monitoring of bottom sediments, sampling should be carried out only in sediments that are uniform in the grain size**
- **The most suitable for monitoring stations are clayey silt, so the mineral composition of the minerals composing them does not contain analogues of pollutants**
- **When interpreting the results of the analyzes, attention should be paid to the median size of the bottom sediments**
- **It can be argued about the influence of the technogenic factor only when there is a sharp disparity between the concentrations of heavy metals and the average indices during several sampling cycles**

A sunset over the ocean. The sun is low on the horizon, creating a bright orange glow and a shimmering reflection on the water. A single bird is visible in flight in the upper left portion of the sky.

THANK YOU FOR YOUR ATTENTION!

From small scales to large scales
–The Gulf of Finland Science Days 2017
9th-10th October 2017
Estonian Academy of Sciences, Tallinn

2nd Day



**Gulf of Finland
Co-operation**

K. Rubtsova, T. Mironenko, E. Daev

Preliminary assessment of water and sediment pollutions in littoral zone of the Kotlin Island.

Preliminary assessment of water and sediment pollutions in littoral zone of the Kotlin Island.

Rubtsova K.D.^{1*}, Mironenko T.V.^{1}, Daev E.V.^{2***}**

¹School No 425, Kronstadt, Saint-Petersburg, Russia, 197760

²Dept. Genetics & Biotechnology, Saint-Petersburg State University, Saint-Petersburg, Russia, 199034

**- ksennru@mail.ru; **- tvmironenko@yandex.ru;*

****- mouse_gene@mail.ru*

The Kotlin Island Map



Red squares – sampling sites: “west”(recreation area) – “clean”
and “east” (city territory) – “dirty”

The west sampling site and the east sampling site



“West” sampling site

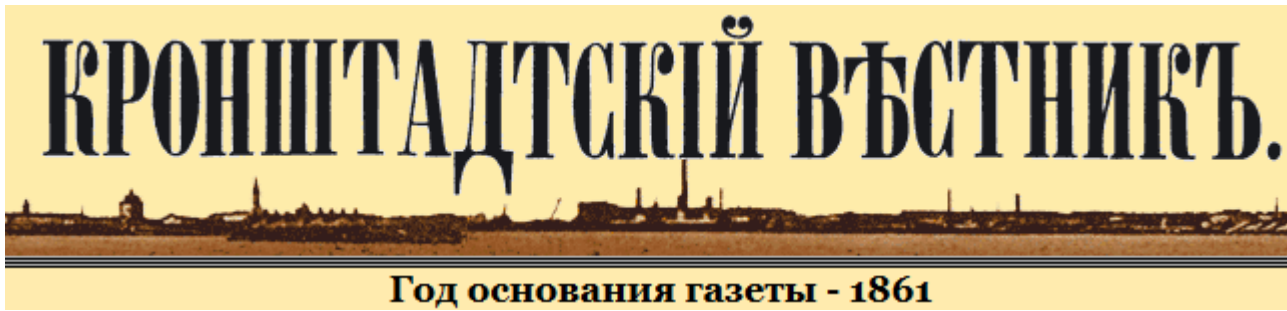
and

“East” sampling site



Relatively clean, officially protected recreation area. Wildlife sanctuary “Western Kotlin”.

Proximity (30-300 m) to the road, to car service station, to living facilities, garages etc. (unsaturated poly-hydrocarbons, diesel and gasoline fuel spots, garbage and other different pollutants).



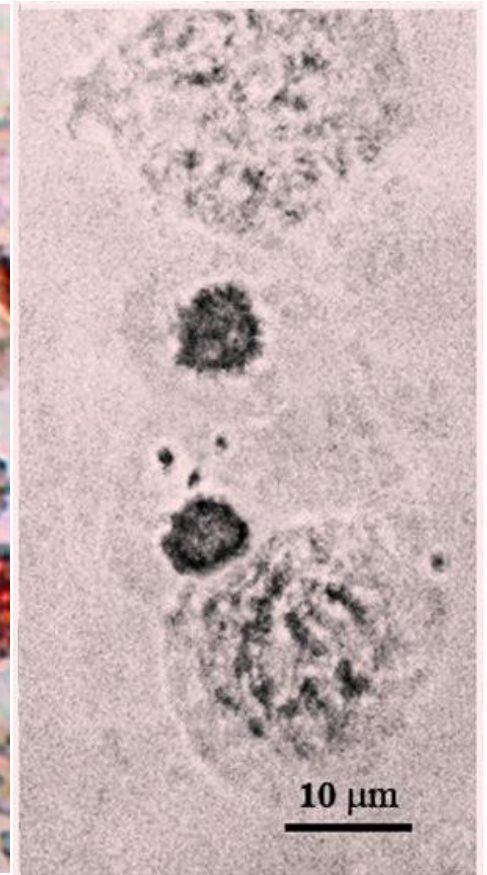
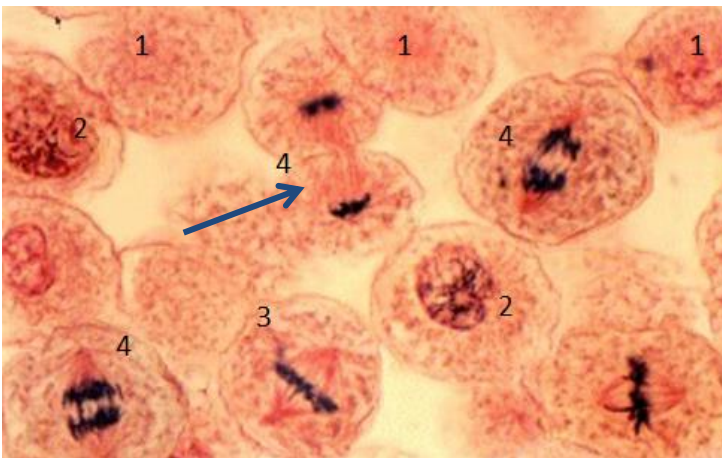
(The Kronstadt Herald newspaper, it was founded in 1861)



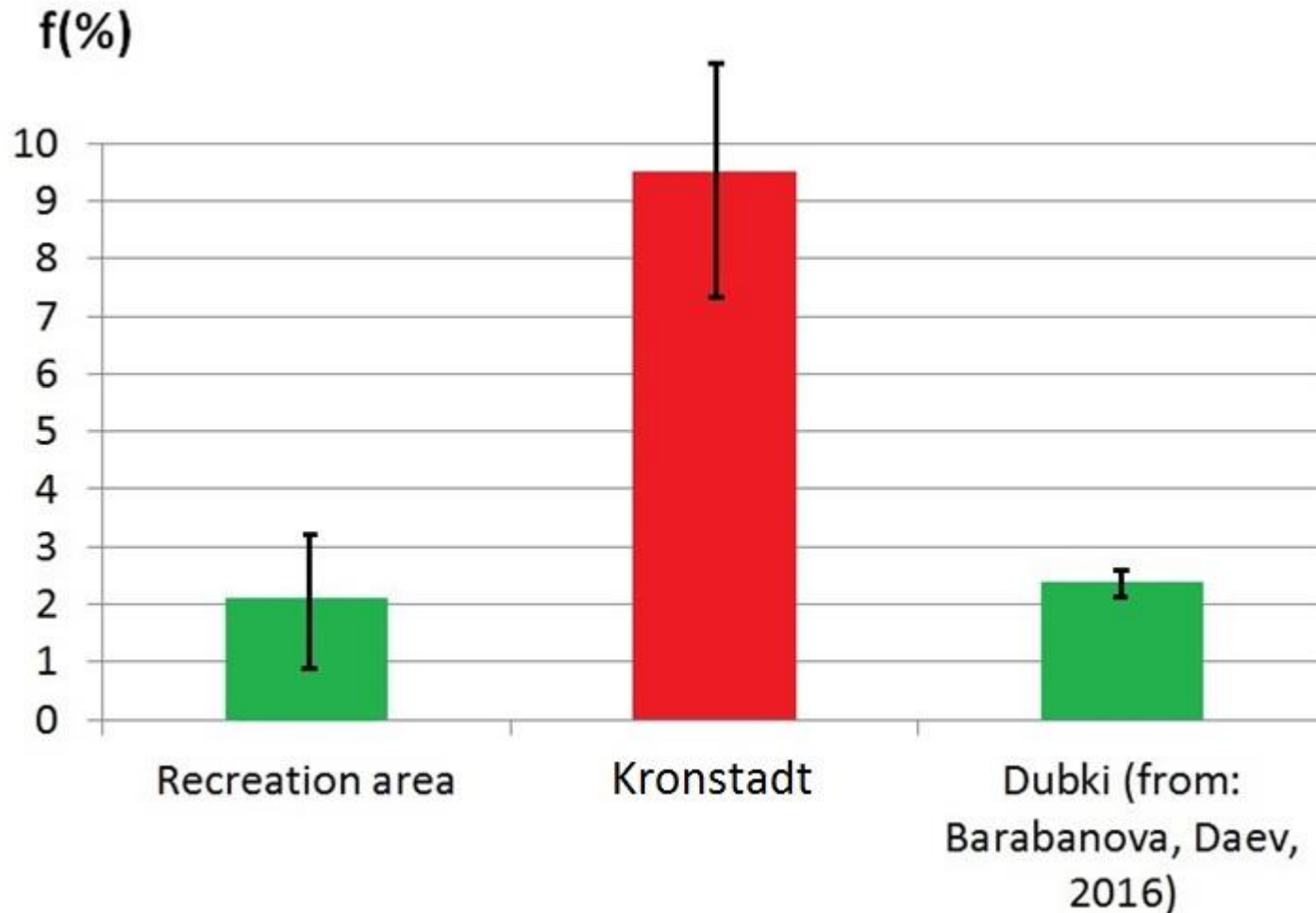
Just an example of several “spots” near coastline in Kronstadt

Gmelinoides fasciatus

as a cytogenetic bioindicator of water pollution



Total frequency of embryonic cells with chromosome aberrations ($f \pm m\%$) y in amphipods *Gmelinoides fasciatus* in the differently polluted sites of the Kotlin island.



**Spotty environment is needed to be
controlled!**

Thank you for your patience.

From small scales to large scales
–The Gulf of Finland Science Days 2017
9th-10th October 2017
Estonian Academy of Sciences, Tallinn

2nd Day



**Gulf of Finland
Co-operation**

G. Frumin, Y. Fetisova

Dynamics of water quality of the transboundary river Narva

"If you have an apple and I have an apple, and we exchange these apples, you and I will be left with one apple each. However, if you have an idea, and I have an idea, and we exchange these ideas, each one of us will have two ideas".

Bernard Shaw





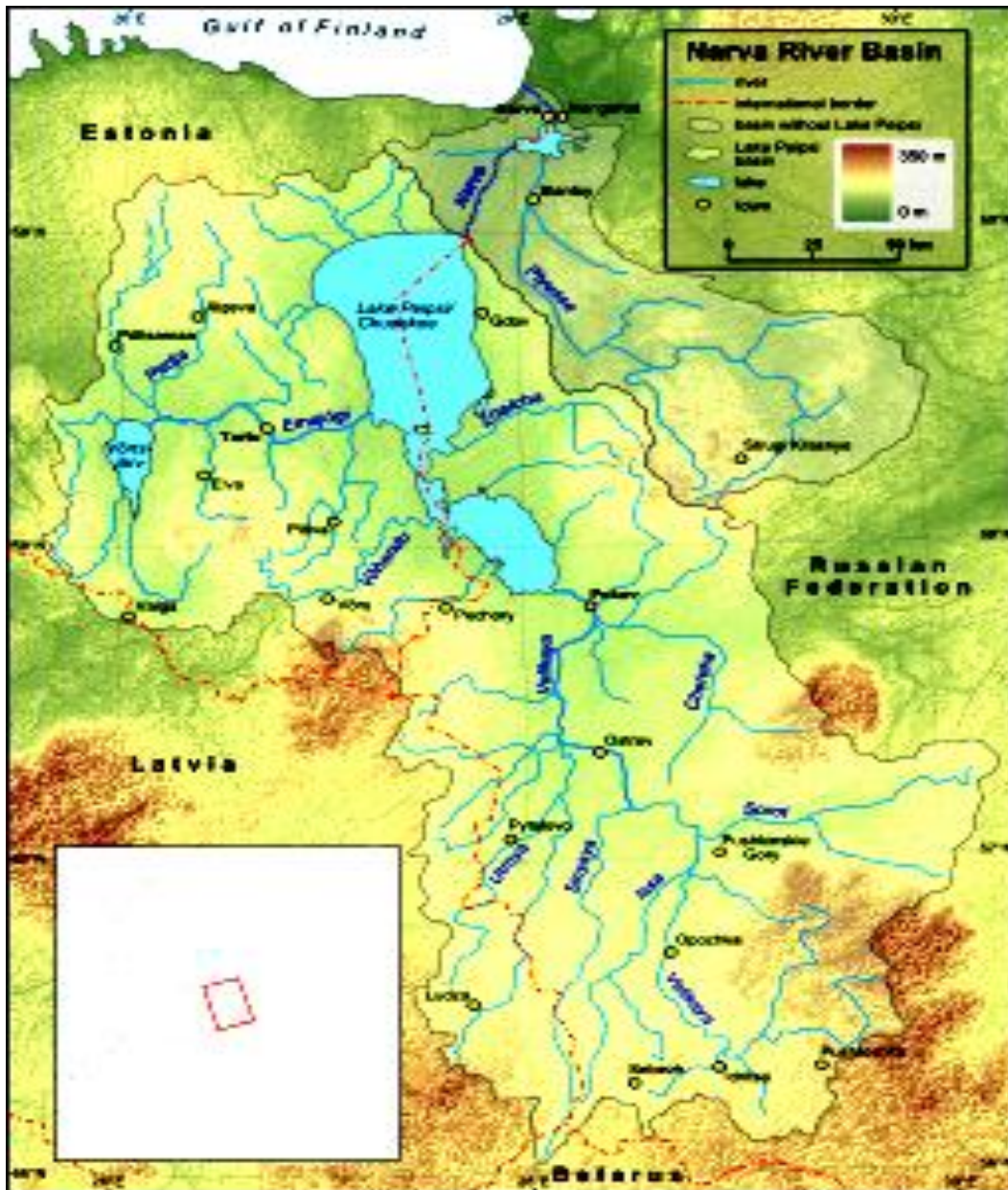
***Dynamics of Water
Quality of the
Transboundary River
Narva***

**Russian State Hydrometeorological
University**

Department of Ecology

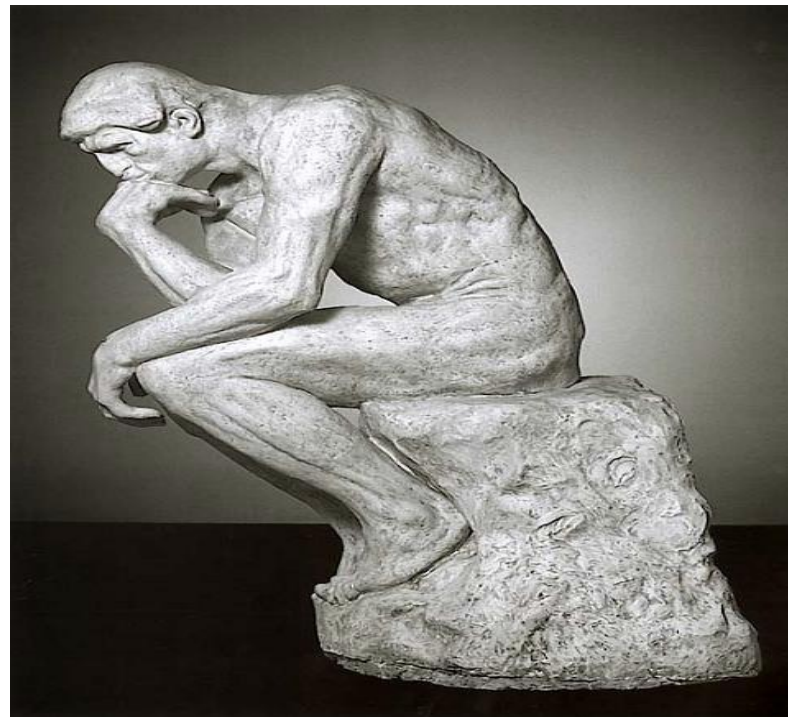
Grigory Frumin & Yu. Fetisova

gfrumin@mail.ru



Length	77 km
Width	0.15-1.2 km
Depth	5 m
Basin	56,225 km²
Average discharge	400 m³/s

Here there is a problem how to assess the quality of water for transboundary water bodies.



**The purpose of the study was
to assess the
interannual dynamics of the
water quality of
the Narva River**



Materials and methods of research

An attempt to assess the quality of river water based on chemical criteria was made in the Bavarian Water Use Service. This method is based on studies conducted earlier in the USA and Scotland. The method involves the measurement of a few chemical parameters in water samples followed by a representation of the resulting combination of results in the form of a single number (chemical index) which is the generalized water quality in a given sample. The chemical index is multiplicative and is expressed in the following form:

$$CJ = \prod_{i=1}^n q_i^{w_i} = q_1^{w_1} \cdot q_2^{w_2} \cdot \dots \cdot q_n^{w_n}$$

where CJ is the chemical index, the dimensionless value of the continuous scale is from 0 to 100

(here 0 is the worst and 100 is the best water quality);

n is the number of parameters; q_i – subindex;

W_i is the weight of the i -th parameter.

Parameters used to calculate the chemical index and their weights

Parameter	Weights, W
%O ₂	0,20
BOD ₅ , mgO ₂ /dm ³	0,20
Temperature, °C	0,08
NH ₄ ⁺ , mg/dm ³	0,15
NO ₃ ⁻ , mg/dm ³	0,10
PO ₄ ³⁻ , mg/dm ³	0,10
pH	0,10
Electrical conductivity, λ , $\mu\text{S}/\text{cm}$	0,07

$$\sum W = 1$$

Analytical dependencies between sub-indices and hydrochemical indicators

Parameter	Interval	Formula
%O ₂	72-100	$q = 1,14[\%O_2] - 12,06$
BOD ₅ , mgO ₂ /dm ³	0,7-2,8	$q = -8,61[BOD_5] + 106,06$
t, °C	14-20	$q = 0,128t^3 - 8,456t^2 + 173,4t - 1036$ at t < 15°C q = 100
NH ₄ ⁺ , mg/dm ³	0-0,9	$q = -62,41[NH_4^+] + 96,69$
NO ₃ ⁻ , mg/dm ³	0-32	$q = -2,51[NO_3^-] + 94,37$
PO ₄ ³⁻ , mg/dm ³	0,6-2,4	$q = -8,18[PO_4^{3-}] + 101,4$
pH	6,1-8,2	$q = -25,32(pH)^2 + 365,5pH - 1219,6$
Electrical conductivity, λ, μS/cm	175-425	$q = -0,1351\lambda + 125,1$

The model of the broken rod and Classification of water quality

Characteristics of water pollution	Value <i>CJ</i>	Quality class
Conditionally pure	98-100	1
Slightly contaminated	88-97	2
Contaminated	73-87	3
Dirty	46-72	4
Extremely dirty	0-45	5

Results and its discussion



Interannual dynamics of water quality of the Narva River (near the mouth)

Year	<i>CJ</i>	Quality of water	Quality class
2006	92.1	Slightly contaminated	2
2007	90.5	Slightly contaminated	2
2008	90.8	Slightly contaminated	2
2009	92.5	Slightly contaminated	2
2010	92.0	Slightly contaminated	2
2011	91.0	Slightly contaminated	2
2012	90.8	Slightly contaminated	2
2013	91.9	Slightly contaminated	2
2014	92.3	Slightly contaminated	2
2015	92.1	Slightly contaminated	2
2016	92.5	Slightly contaminated	2

Water quality of lakes (2000-2015 гг.)

Lake	<i>CJ</i>	Quality of water	Quality class
Peipsi	92.4	Slightly contaminated	2
Lämmijärv	90.8	Slightly contaminated	2
Pihkva	91.1	Slightly contaminated	2

The water quality of the rivers in the basin of the transboundary Narva River in 2015

River	<i>CJ</i>	Water quality	Quality class
Gdovka (Gdov)	59.1	Dirty	4
Zhelcha (Yamm)	85.4	Contaminated	3
Piusa (Pechory)	88.0	Slightly contaminated	2
Emajögi (Tartu)	88.0	Slightly contaminated	2
Rannapungerja (Lisaku-Avinurme mnt)	88.1	Slightly contaminated	2
Avijögi (Mulgi)	89.6	Slightly contaminated	2
Narva (Ivangorod)	93.3	Slightly contaminated	2
Plyussa (Slantsy)	93.4	Slightly contaminated	2

**Thank you for your
attention and patience**

